University of Alberta Library
0 1620 2918362 9

Digitized by the Internet Archive
in 2026 with funding from
University of Alberta Library

https://archive.org/details/0162029183629

**University of Alberta**

# Towards Carbyne: Synthesis and Study of Extremely Long Polyynes

by

Wesley A. Chalifoux

A thesis submitted to the Faculty of Graduate Studies and Research
in partial fulfillment of the requirements for the degree of

Doctor of Philosophy

Department of Chemistry

©Wesley A. Chalifoux
Spring 2010
Edmonton, Alberta

Permission is hereby granted to the University of Alberta Libraries to reproduce single copies of this thesis and to lend or sell such copies for private, scholarly or scientific research purposes only. Where the thesis is converted to, or otherwise made available in digital form, the University of Alberta will advise potential users of the thesis of these terms.

The author reserves all other publication and other rights in association with the copyright in the thesis and, except as herein before provided, neither the thesis nor any substantial portion thereof may be printed or otherwise reproduced in any material form whatsoever without the author's prior written permission.

UNIVERSITY LIBRARY
UNIVERSITY OF ALBERTA

## Examining Committee

Rik R. Tykwinski, Chemistry

Jeffrey M. Stryker, Chemistry

John C. Vederas, Chemistry

Josef Takats, Chemistry

Frank Marsiglio, Physics

Benjamin T. King, Chemistry, University of Nevada, Reno

**For my loving wife Krista.**

**Abstract**. This thesis focuses on the synthesis and characterization of oligoacetylenes (polyynes). There will be an introduction into the properties of polyconjugated materials, their potential usefulness and how polyynes fit into this category. After this will be a brief discussion of synthetic tools commonly employed in the assembly sp-hybridized carbon frameworks, which will include traditional methods as well as state-of-the-art procedures that have recently been developed. A more detailed discussion of polyynes that have been synthesized to date will follow. The construction of shorter polyynes, such as diynes to hexaynes, is a rather well developed area where conventional synthetic strategies are still typically useful, i.e., metal-catalyzed homo- or heterocoupling and exhaustive elimination reactions. The synthesis of longer polyynes (heptaynes, octaynes, etc.), on the other hand, can require more subtle synthetic approaches due to inherent problems of reagent compatibility and the reactive nature of many polyyne intermediates and products. A description of the innovative synthetic methods that have been used over the past decade to overcome some of these challenges will be presented. Furthermore, a review of all polyynes reported to date with a length of at least 16 sp-carbons is included, combined with an account of methods used for their characterization.

The chapters that follow the introduction will focus on various polyyne series that differ in endgroup used to impart stability into the polyyne. Each chapter, starting with the first, conveys the progression towards the design of a bulky, stable, and easily synthesized endgroup that provides for stable polyynes beyond a length of ten triple bonds (20 sp-carbons). These endgroups include the tris-(biphenyl-4-yl)silyl, adamantyl, *tert*-butyl, trityl and finally the "supertrityl", which is a hexa-*tert*-butyl functionalized trityl group. The polyynes were characterized by standard methods, which include but not limited to, $^{1}H$ and $^{13}C$ NMR, IR, and mass spectrometries. The optical properties were also examined through UV-Vis spectroscopic analysis, which showed a consistent lowering of the HOMO → LUMO band gap energy as a function of polyyne length. The trends in the UV-Vis data for the supertrityl polyynes has allowed for a more accurate prediction of this property of carbyne. The quantitative Raman analysis of the adamantyl series of polyynes was also carried out and provided very insightful data on the properties that polyynes possess. This includes a lowering of the $\mathcal{R}$–mode energy as a function of length, showing

that polyynes take on more of a cumulenic form as they get longer. X-ray crystallographic data on the *tert*-butyl polyyne series supports this premise by showing that there is indeed a reduction in bond-length alternation between single and triple bonds as a function of polyyne length. This trend ends, however, well before a cumulenic structure is achieved. Information about the third-order nonlinear optical properties of the adamantyl series was obtained from quantitative Raman spectroscopy. Finally, Raman and IR spectroscopies were used to document bending of adamantyl polyynes in the solid-state as well as the solution-state, and this trend becomes more pronounced as the polyynes become longer.

# Acknowledgments

I would first like to thank my wife Krista. Without her support, understanding, and patience, I could never have made it through this grueling eleven years at the U of A. Thanks to my parents and all my family for your support and encouragement throughout all my years of study.

I would also like to thank my fellow group members, past and present. To Erin Chernick and Katie Campbell for pointing me in the right direction: research in the Tykwinski group. To Thanh Luu, Erin Graham, Sharwatie Ramsaywack, Khalid Azyat, Sara Eisler, Amber Sadowy, Annabelle Shi Shun, Clement Osei Akoto, Mojtaba Gholami, Andreea Spantulescu, and Yasuhiro Morisaki for your assistance in preparation for my chem 401 talk, conferences, 502 seminar, candidacy exam and finally, my defense. Thanks to Paul Bichler, Dan Lehnherr, B. J. Medos and Adrian Murray for the great discussions, whether it was over coffee, or beers. You guys helped make all that time spent at the school more tolerable.

I express my gratitude to the Drs. Bob McDonald and Michael Ferguson for all their awesome work. To all the mass spec lab and Mrs. Lisa Nicolai, as well as spec services for going above and beyond when needed. A very big thanks to Diane Dowhaniuk for all your help with confusing claims and the tedious paperwork involved for sending samples across seas. I want to express my gratitude to my Italian collaborators for making my stay in Milan so great and for all the excellent Raman and IR data.

I especially thank my supervisor Rik. You have been a very gracious boss. Thanks for allowing us to be independent and think for ourselves while still being there when needed. Thanks for always bringing the spark back into the research when the chemistry starts getting stale.

# Table of Contents

**CHAPTER 1 INTRODUCTION TO POLYYNES** ..... **1**

1.1 INTRODUCTION TO POLYCONJUGATED MATERIALS ..... 1

1.2 THE LAST (MISSING?) ALLOTROPE OF CARBON ..... 3

1.3 POLYYNE SYNTHESIS ..... 5

*1.3.1 General synthetic considerations* ..... *5*

*1.3.2 Pentaynes* ..... *9*

*1.3.3 Hexaynes* ..... *11*

*1.3.4 Heptaynes.* ..... *15*

*1.3.5 Octaynes* ..... *17*

*1.3.6 Nonaynes* ..... *20*

*1.3.7 Decaynes, and beyond* ..... *21*

1.4 INTERESTING AND POTENTIALLY USEFUL PROPERTIES OF POLYYNES ..... 26

*1.4.1 UV-Vis Spectroscopy* ..... *26*

*1.4.2 Nonlinear Optics* ..... *27*

1.5 CONCLUSIONS ..... 28

1.6 REFERENCES ..... 29

**CHAPTER 2 SYNTHESIS OF TRIS(4-BIPHENYL-4-YL)SILYL-ENDCAPPED POLYYNES** ..... **36**

2.1 INTRODUCTION ..... 36

2.2 RESULTS AND DISCUSSION ..... 37

*2.2.1 Large Triarylsilyl Endgroup for the Stabilization of Polyynes, Initial Design* ..... *37*

*2.2.2 Large Triarylsilyl Endgroup for the Stabilization of Polyynes, Revised Design* ..... *40*

*2.2.3 TBPS Polyynes: A Model System for Larger Triarylsilyl Endgroups* ..... *41*

2.3 CONCLUSIONS AND PARTING THOUGHTS ..... 46

2.4 REFERENCES ..... 48

**CHAPTER 3 SYNTHESIS AND PROPERTIES OF ADAMANTYL-ENDCAPPED POLYYNES ..... 50**

3.1 INTRODUCTION ..... 50

3.2 SYNTHESIS OF ADAMANTYL-ENDCAPPED POLYYNES ..... 51

3.3 PHYSICAL AND SPECTROSCOPIC PROPERTIES OF ADAMANTYL POLYYNES ..... 60

*3.3.1 UV-Vis Spectroscopic Analysis ..... 60*

*3.3.2 IR and Raman Spectroscopic Analysis of Adamantyl Polyynes ..... 64*

*3.3.3 Computational Analysis of Polyynes ..... 69*

*3.3.4 X-ray crystallography ..... 76*

*3.3.5 Electrochemistry of Adamantyl-Endcapped Polyynes ..... 78*

3.4 CONCLUSIONS ..... 80

3.5 REFERENCES ..... 81

**CHAPTER 4 SYNTHESIS AND PROPERTIES OF *t*-BUTYL-ENDCAPPED POLYYNES ..... 85**

4.1 INTRODUCTION ..... 85

4.2 SYNTHESIS OF *t*-BUTYL-ENDCAPPED POLYYNES ..... 86

4.3 PHYSICAL AND SPECTROSCOPIC PROPERTIES OF *t*-BUTYL-ENDCAPPED POLYYNES ..... 89

*4.3.1 UV-Vis Spectroscopic Analysis of t-Butyl Polyynes ..... 89*

*4.3.2 NMR Spectroscopic Analysis of t-Butyl Polyynes ..... 90*

*4.3.3 X-Ray Crystallographic Analysis of t-Butyl Polyynes ..... 91*

4.4 CONCLUSIONS ..... 98

4.5 REFERENCES ..... 99

**CHAPTER 5 BUILDING STABILITY INTO POLYYNES USING LARGE ENDGROUPS ..... 102**

5.1 INTRODUCTION ..... 102

5.2 SYNTHESIS OF SUPERTRITYL POLYYNES ..... 103

*5.2.1 Synthesis of a Feedstock Starting Material Towards Supertrityl Polyynes ..... 103*

*5.2.2 Synthesis of Supertrityldiyne ..... 104*

*5.2.3 Friedel-Craft Approach Towards Ketones as Polyyne Intermediates ..... 105*

*5.2.4 Alcohol Formation and Oxidation Towards Ketones as Polyyne Intermediates ..... 108*

*5.2.5 Mild Removal of a TIPS Group ..... 109*

*5.2.6 Traditional Crosscoupling Methods as a Means to Longer Polyynes ..... 111*

*5.2.7 Using a Modified Homocoupling Protocol to Generate Crosscoupled Products ..... 115*

5.3 PHYSICAL PROPERTIES OF SUPERTRITYLPOLYYNES ..... 117

*5.3.1 UV-Vis Spectroscopic Analysis ..... 117*

*5.3.2 NMR Spectroscopic Analysis ..... 131*

*5.3.3 DSC Analysis ..... 138*

*5.3.4 X-Ray Crystallographic Data ..... 141*

5.4 CONCLUSIONS ..... 147

5.5 REFERENCES ..... 149

**CHAPTER 6 GENERAL DISCUSSION AND CONCLUSIONS ..... 152**

6.1 REFERENCES ..... 157

**CHAPTER 7 EXPERIMENTAL SECTION ..... 159**

7.1 TBPS-ENDCAPPED POLYYNES (CHAPTER 2 DATA) ..... 161

7.2 ADAMANTYL-ENDCAPPED POLYYNES (CHAPTER 3 DATA) ..... 170

7.3 *t*-BUTYL-ENDCAPPED POLYYNES (CHAPTER 4 DATA) ..... 189

7.4 SUPERTRITYL-ENDCAPPED POLYYNES (CHAPTER 5 DATA) ..... 200

7.5 REFERENCES ..... 234

**APPENDIX A SYNTHESIS OF TRITYL-ENDCAPPED POLYYNES ..... 237**

A.1 CONCLUSIONS ..... 241

A.2 EXPERIMENTAL SECTION ..... 242

A.3 REFERENCES ..... 249

**APPENDIX B DFT SIMULATION DATA ..... 250**

**APPENDIX C SELECTED SPECTRA ..... 253**

# List of Tables

**Table 1-1.** Known, characterized 1,3,5,7,9,11,13,15-hexadecaoctaynes. ..... **18**

**Table 1-2.** Known, characterized polyynes with >10 acetylene units. ..... **24**

**Table 2-1.** Synthesis of **2.10** via Pd-catalyzed crosscoupling. ..... **44**

**Table 3-1.** UV-Vis absorbance data for adamantyl polyynes **3.1c-k** ..... **63**

**Table 3-2.** Raman and IR frequencies for the Σ-lines in the solid- and solution-states. ..... **66**

**Table 3-3.** List of vibrational frequencies, IR and Raman intensities of linear ($D_{\infty h}$) and bent ($C_{2v}$) conformations of hydrogen-capped polyyne H–$(C{\equiv}C)_5$–H. Data obtained through DFT calculations carried out at PBEPBE/cc-pVQZ level. Data for the strongest Raman line are bolded. .**74**

**Table 3-4.** Vibrational Frequencies as well as IR and Raman Intensities for Polyynes **3.1e**, **3.1f**, and **3.1h** ..... **75**

**Table 3-5.** Peak potentials of the first reduction and oxidation steps of hexayne **3.1e** and octayne **3.1f** ..... **80**

**Table 4-1.** UV-Vis absorbance data for *t*-butyl polyynes in hexanes. ..... **90**

**Table 4-2.** $^{13}C$ NMR spectroscopic data for polyynes **4.1a-h**. ..... **90**

**Table 4-3.** Summary of experimental and theoretical BLA data. ..... **95**

**Table 4-4.** Selected bond lengths (Å) for polyynes **4.1a-c**, **4.1f**, and **4.1h**. ..... **96**

**Table 5-1.** Crosscoupling conditions toward the synthesis of diyne **5.7**. ..... **105**

**Table 5-2.** Synthesis of $n$ = 12 precursors by screening various crosscoupling conditions. ..... **114**

**Table 5-3.** Synthesis of supertrityl polyynes **5.33**, **5.40**–**5.43**, and **5.53** using a modified Glaser–Eglinton-Hay coupling protocol. ..... **115**

**Table 5-4.** Data for the longest wavelength absorbance ($\lambda_{max}$). ..... **121**

**Table 5-5.** Data for the second longest wavelength absorbance ($\lambda_{peak2}$). ..... **122**

**Table 5-6.** Alkyne carbon signals for polyynes **5.1a-j**. ..... **132**

**Table 5-7.** $^{13}C$ NMR chemical shift data for the terminal polyyne series. ..... **138**

**Table 5-8.** Comparison of thermal decomposition points of known polyynes by DSC analysis. ..... **139**

**Table B-1.** The full list of harmonic frequencies, IR and Raman intensities, irreproducible representations of the normal modes for bent H-(C≡C)$_5$-H (the A1 Я–mode and B1 IR mode are highlighted, see Figure B-1). Data from DFT calculations (PBEPBE/cc-pVQZ).....**251**

# List of Figures

**Figure 1-1.** Common oligo- and/or polymeric systems based on acetylenic building blocks. .....2

**Figure 1-2.** Pictures of diamond ($sp^3$-carbon), graphite/graphene ($sp^2$-carbon) and fullerene/nanotubes ($sp^2$-carbon), the known allotropes of carbon along with 3-D molecular representations. .....4

**Figure 1-3.** The structure of carbyne. .....4

**Figure 1-4.** Structures of the tri- and tetrayne isolated by Bryce and coworkers. .....12

**Figure 2-1.** Approximate size relationship of common silyl endgroups. .....37

**Figure 2-2.** Tris(hexaphenylbenzene)silyl (THPBS) endgroup. .....38

**Figure 2-3.** a) THPBS endgroup showing the ortho phenyl groups (shown in red) in close proximity with each other making it difficult to place three of these on one silicon atom. b) Tris(triphenylbenzene)silyl (TTPBS) endgroup. .....40

**Figure 2-4.** a) X-ray crystal structure of **2.8** showing the radius of the TBPS endgroup. b) Crystal packing of **2.8**, with the red arrow showing a distance of 8 Å between neighboring molecules (all shown at 20% probability, hydrogen atoms removed for clarity). .....43

**Figure 2-5.** Space-filling models based on the X-ray structure of **2.10** (non-hydrogen atoms represented at the 20% probability level) shown as the a) side view, b) end-on view with TMS in front, and c) end-on view with TBPS in front, displaying the size difference of the TBPS endgroup versus the TMS endgroup. The carbons and hydrogens on the TMS group are colored blue and red, respectively, to contrast the different endgroups. .....47

**Figure 3-1.** Adamantyl endcapped polyynes **3.1a-k**. .....51

**Figure 3-2.** UV-Vis spectra of adamantyl polyynes **3.1c-k** in THF. Quantitative data was obtained for **3.1c-f**. Quantitative UV-Vis absorption of the deca- (**3.1h**) and dodecayne **3.1k** (dotted lines) could not be obtained due to decomposition. Relative intensities have been adjusted based on the trend to show their spectra in relation to the shorter polyynes. .....61

**Figure 3-3.** UV-Vis spectra of adamantyl polyynes **3.1c-h** in hexanes. Quantitative data was obtained for **3.1c-f**. Quantitative UV-Vis absorption of the decayne (**3.1h**, dotted line) could not be

obtained due to decomposition. Relative intensity has been adjusted based on the trend to show their spectra in relation to the shorter polyynes. ..... 62

**Figure 3-4.** Plot of log ($E_g$) versus log ($n$) for the adamantyl series in THF (red) and hexanes (blue). The solid line in each case represents a line-of-best-fit to the data ($E_g$ is the $\lambda_{max}$ in eV). ..... 64

**Figure 3-5.** Experimental Raman (•••) and IR (—) spectra (2500-1800 $cm^{-1}$) of a) solid samples and b) THF solutions of polyynes **3.1a-h**. The arrows indicate violations of the mutual exclusion in the IR spectra. ..... 65

**Figure 3-6.** a) Experimental frequency dispersion of Raman and IR lines as a function of the number of carbon atoms $N_C$ (from spectroscopic data in the solid state). (b) Theoretical vibrational displacements (bond-length changes) for decayne **3.1h** associated with the three branches of the plot in (a) shown by the double-headed arrows (from PBEPBE/cc-pVDZ calculations). Unscaled theoretical vibrational frequencies are also given. The central bond of the chain is indicated by the bond index of zero. Green bars denote C≡C bonds and red bars C–C bonds. Sinusoidal lines are superimposed onto the stick plots to ease the recognition of the number of nodes. ..... 67

**Figure 3-7.** a) Ball and stick model of the optimized bent structure of **3.1e** calculated from first principles (PBEPBE/cc-pVDZ). b) Experimental IR and Raman spectra of **3.1e** (THF solution). c) Simulated IR and Raman spectra of **3.1e** based on first principles calculations at the PBEPBE/cc-pVDZ level (the arrows denote a Raman mode activated in the IR as predicted by the calculations). ..... 70

**Figure 3-8.** Simulated Raman and IR spectra of the bent (top) and linear (bottom) conformations of H–$(C≡C)_5$–H calculated at the PBEPBE/cc-pVQZ level (simulated structures are shown as insets). The thin black curve is the Raman spectrum enhanced by a factor of 10. Activation of the strong IR line is observed as a shoulder of the strong Raman line (arrow **2**). The activation in the IR of the strong Raman line is more evident (arrow **1**). Simulated peaks are Lorentzian functions with a FWHM = 4 $cm^{-1}$. ..... 72

**Figure 3-9.** Simulations of the IR and Raman spectra of H–$(C≡C)_6$–H at the PBEPBE/cc-pVQZ level in the linear and bent structures (the inset pictures show the optimized structures). For the

bent structure, both of the Raman peaks located between 2000 and 2100 $cm^{-1}$ are visible in the IR (shown by arrows). ..... 73

**Figure 3-10.** a) ORTEP drawing of **3.10** where only the major part (60%) of the disordered adamantane group is shown (non-hydrogen atoms represented at the 20% probability level), and b) space-filling model of **3.10** as derived from X-ray diffraction studies showing the similar diameter of the adamantyl and TMS endgroups (disordered adamantane shown). ..... 76

**Figure 3-11.** ORTEP representations at the 20% probability level for a) tetrayne **3.1c** and b) hexayne **3.1e**..... 77

**Figure 3-12.** Hirsch and coworkers aryl hexaynes. ..... 79

**Figure 3-13.** Cyclic voltammograms measured in $CH_2Cl_2$ containing 0.1M $Bu_4NPF_6$ of a) hexayne **3.1e** (scan rate = 100 $mVs^{-1}$), b) hexayne **3.1e** at different scan rates (scan rate = 100, 200, 500 and 1000 $mVs^{-1}$), and c) octayne **3.1f** (scan rate = 100 $mVs^{-1}$). Fc = ferrocenium/ferrocene couple. ..... 79

**Figure 4-1.** Triisopropylsilyl (**S1**), 1-adamantyl (**3.1**) and *t*-butyl (**4.1**) endcapped polyynes..... 86

**Figure 4-2.** Quantitative UV-Vis spectra of *t*-butyl triyne **4.1b**, tetrayne **4.1c**, hexayne **4.1e**, octayne **4.1f**, and decayne **4.1h** in hexanes..... 89

**Figure 4-3.** A comparison of $^{13}C$ NMR spectra of polyynes **4.1a-f** and **4.1h** ($CDCl_3$)..... 91

**Figure 4-4.** ORTEP drawings (20% probability level) for **4.1a-c**, **4.1f**, **4.1h-A** and **4.1h-B**..... 93

**Figure 4-5.** End-on view of **4.1h-A** and **4.1h-B** highlighting nonlinearity of each molecule (hydrogen atoms removed for clarity)..... 93

**Figure 4-6.** Plot of BLA (blue) and $BLA_{avg}$ (red) versus the number of triple bonds ($n$). The line is provided as a guide to the eye..... 97

**Figure 4-7.** Plot of BLA and $BLA_{avg}$ versus $1/n$, where $n$ is the number of triple bonds. A line of best fit is shown for BLA (blue) and $BLA_{avg}$ (red). An extrapolation of the octa- and decayne (black line) shows BLA = 0.135 Å for infinite polyyne. ..... 97

**Figure 5-1.** Supertrityl polyynes **5.1a-j**..... 103

**Figure 5-2.** UV-Vis spectra of supertrityl polyyne series **5.1a-j** in hexanes..... 119

**Figure 5-3.** Overlaid UV-Vis spectra of **5.1j** ($n$ = 20) in hexanes (black), $CH_2Cl_2$ (red), and THF (blue) showing a blue-shift and sharper absorbances for the solution of **5.1j** in hexanes. The

spectrum recorded in THF has been scaled to the approximate expected extinction coefficient for the longest absorbance wavelength. ..... 121

**Figure 5-4.** Plot of band gap energy ($E_g$) vs. $1/n$ (where $n$ is the number of triple bonds). Linear regression line fitted for $n$ = 8-20 (red squares) suggests a band gap energy for infinite polyyne (carbyne) of 2.18 eV ($\lambda$ = 569 nm). ..... 123

**Figure 5-5.** Expansion of the region $n$ = 10-20 with an extrapolation using a polynomial fit that results in an intercept of 2.37 eV, which corresponds to $\lambda$ = 523 nm for infinite polyyne (black dotted line inserted to show the linear regression line). ..... 124

**Figure 5-6.** Plot of $E_g$ vs. number of triple bonds ($n$) showing the dramatic change in slope as a function of length. The dotted line is inserted as a guide to the eye to show that the ECL should occur at around 30 triple bonds in length. ..... 125

**Figure 5-7.** Plot of the longest wavelength ($\lambda_{max}$, blue line) and the second longest absorbance ($\lambda_{peak2}$, red line) wavelength. The dotted line is inserted as an approximate extrapolation to show that saturation is clearly occurring well before $\lambda$ = 569 nm, as predicted in Figure 5-4. $\Delta E(\nu^*_{0\text{-}1})$ = difference in energy between the first and second excited state vibrational levels. ..... 126

**Figure 5-8.** Lewis-Calvin plot ($\lambda^2 = kn$) of supertritýl polyyne series. ..... 127

**Figure 5-9.** Power-law plot of $E_g$ vs. $n$ (inset in red) The solid line represents the line-of-best-fit for $n$ = 4-12. ..... 128

**Figure 5-10.** UV-Vis spectra of unsymmetrical Tr*-TIPS polyynes from tetrayne **5.32** to decayne **5.53** in hexanes. The y-axis represents arbitrary absorbance units. ..... 129

**Figure 5-11.** Overlay plot of hexaynes **5.1j** and **5.40** in hexanes showing the extinction coefficient and change in the absorbance spectrum for the unsymmetrical TIPS-protected hexayne **5.40**. The area under the curve was approximated in Excel using the equation 'SUMPRODUCT(A2:A30–A1:A29,(B2:B30+B1:B29)/2)', where the x-values are in cells A1 to A30, and y-values are in cells B1 to B30. This is an approximate method for finding the area under the curve by summing the area of the trapezoids generated from points on the y-axis (B1:B30) and point on the x-axis (A1:A30). ..... 130

**Figure 5-12.** Overlay of UV-Vis spectra of supertrityl terminal polyynes from tetrayne **5.34** to decayne **5.54** in hexanes. The y-axis represents arbitrary absorbance units. ..... **131**

**Figure 5-13.** Expanded $^{13}C$ NMR spectra showing the alkyne resonances for **5.1j**. ..... **132**

**Figure 5-14.** Plot of alkyne chemical shift versus the number of triple bonds ($n$). ..... **133**

**Figure 5-15.** Plot of most downfield $^{13}C$ NMR carbon signal as a function of polyyne length ($n$) showing that the second endgroups influence on the chemical shift is nonexistent by $n \approx 10$. ..... **134**

**Figure 5-16.** Plot of the most upfield alkyne $^{13}C$ NMR carbon signals as a function of polyyne length ($n$) showing that the second endgroups influence on the chemical shift is nonexistent by $n \approx 10$. ..... **135**

**Figure 5-17.** Plot of the $^{13}C$ NMR carbon signals of the internal alkynes of the polyyne as a function of polyyne length ($n$). ..... **136**

**Figure 5-18.** Plot of $^{1}H$ NMR chemical shift of the terminal acetylene hydrogen as a function of polyyne length ($n$). ..... **137**

**Figure 5-19.** Plot of thermal decomposition ($T_{max}$) as a function of polyyne length. ..... **140**

**Figure 5-20.** Comparison of various tetrayne endgroup sizes based on X-ray crystallographic data. The blue line is drawn along the C(1)-C(2) and C(7')-C(8) bonds to show how much the supertrityl endgroups overlap the polyyne core. ..... **142**

**Figure 5-21.** Space-filling model of hexaynes **5.40** and **5.1b** based on X-ray crystallographic data. ..... **143**

**Figure 5-22.** Crystal packing of hexayne **5.1b**, as viewed along the a) crystallographic $a$-axis and b) crystallographic $b$-axis (hydrogens removed for clarity, 20% probability level). c) Cartoon representation of the solid-state packing of **5.1b**. ..... **145**

**Figure 5-23.** Space-filling models of monoyne **5.6**, diyne **5.7** and triyne **5.25** based on the X-ray crystallographic data (20% probability level). ..... **147**

**Figure 6-1.** Structures of a) previously synthesized bent tetraynes (**1**) and b) proposed hexayne targets (**2**) using various lengths of alkyl linker. ..... **153**

**Figure 6-2.** Generic encapsulation of an aryl endcapped polyyne functionalized with electron donating groups (EDG) and electron withdrawing groups (EWG) as well as bulky groups to keep rotaxane from slipping off. ..... **155**

**Figure A-1.** Trityl (Tr) acetylene **A1**. ..... 238

**Figure B-1.** Simulated Raman and IR spectra of the linear and bent conformations of H-$(C\equiv C)_{10}$-H (according to PBEPBE/cc-pVQZ). The thinner black curve is the Raman spectrum enhanced by a factor of 10. Activation of the strong IR line is observed as a shoulder of the strong Raman line (arrow 2). The activation in the IR of the strong Raman line is by converse more evident (arrow 1). Simulated peaks are Lorentzian functions with a FWHM = 4 $cm^{-1}$ ..... 252

**Figure C-1.** $^{1}H$ NMR spectrum of **2.5**. ..... 254

**Figure C-2.** $^{13}C$ NMR spectrum of **2.5**. ..... 254

**Figure C-3.** $^{1}H$ NMR spectrum of **2.6**. ..... 255

**Figure C-4.** $^{13}C$ NMR spectrum of **2.6**. ..... 255

**Figure C-5.** $^{1}H$ NMR spectrum of **2.7**. ..... 256

**Figure C-6.** $^{13}C$ NMR spectrum of **2.7**. ..... 256

**Figure C-7.** $^{1}H$ NMR spectrum of **2.8**. ..... 257

**Figure C-8.** $^{13}C$ NMR spectrum of **2.8**. ..... 257

**Figure C-9.** $^{1}H$ NMR spectrum of **2.9**. ..... 258

**Figure C-10.** $^{13}C$ NMR spectrum of **2.9**. ..... 258

**Figure C-11.** $^{1}H$ NMR spectrum of **2.10**. ..... 259

**Figure C-12.** $^{13}C$ NMR spectrum of **2.10**. ..... 259

**Figure C-13.** $^{1}H$ NMR spectrum of **2.13**. ..... 260

**Figure C-14.** $^{13}C$ NMR spectrum of **2.13**. ..... 260

**Figure C-15.** $^{1}H$ NMR spectrum of **2.14**. ..... 261

**Figure C-16.** $^{13}C$ NMR spectrum of **2.14**. ..... 261

**Figure C-17.** $^{1}H$ NMR spectrum of **2.15**. ..... 262

**Figure C-18.** $^{13}C$ NMR spectrum of **2.15**. ..... 262

**Figure C-19.** $^{1}H$ NMR spectrum of **2.16**. ..... 263

**Figure C-20.** $^{13}C$ NMR spectrum of **2.16**. ..... 263

**Figure C-21.** $^{1}H$ NMR spectrum of **3.3**. ..... 264

**Figure C-22.** $^{13}C$ NMR spectrum of **3.3**. ..... 264

**Figure C-23.** $^{1}$H NMR spectrum of **3.8**.....265

**Figure C-24.** $^{13}$C NMR spectrum or **3.8**.....265

**Figure C-25.** $^{1}$H NMR spectrum of **3.15**.....266

**Figure C-26.** $^{13}$C NMR spectrum of **3.15**.....266

**Figure C-27.** $^{1}$H NMR spectrum of **3.17**.....267

**Figure C-28.** $^{13}$C NMR spectrum of **3.17**.....267

**Figure C-29.** $^{1}$H NMR spectrum of **3.18**.....268

**Figure C-30.** $^{13}$C NMR spectrum of **3.18**.....268

**Figure C-31.** $^{1}$H NMR spectrum of **3.19**.....269

**Figure C-32.** $^{13}$C NMR spectrum of **3.19**.....269

**Figure C-33.** $^{1}$H NMR spectrum of **3.20**.....270

**Figure C-34.** $^{13}$C NMR spectrum of **3.20**.....270

**Figure C-35.** $^{1}$H NMR spectrum of **3.21**.....271

**Figure C-36.** $^{13}$C NMR spectrum of **3.21**.....271

**Figure C-37.** $^{1}$H NMR spectrum of **3.22**.....272

**Figure C-38.** $^{13}$C NMR spectrum of **3.22**.....272

**Figure C-39.** $^{1}$H NMR spectrum of **3.23**.....273

**Figure C-40.** $^{13}$C NMR spectrum of **3.23**.....273

**Figure C-41.** $^{1}$H NMR spectrum of **3.24**.....274

**Figure C-42.** $^{13}$C NMR spectrum of **3.24**.....274

**Figure C-43.** $^{1}$H NMR spectrum of **3.27**.....275

**Figure C-44.** $^{13}$C NMR spectrum of **3.27**.....275

**Figure C-45.** $^{1}$H NMR spectrum of **3.28**.....276

**Figure C-46.** $^{13}$C NMR spectrum of **3.28**.....276

**Figure C-47.** $^{1}$H NMR spectrum of **3.29**.....277

**Figure C-48.** $^{13}$C NMR spectrum of **3.29**.....277

**Figure C-49.** $^{1}$H NMR spectrum of **7.3**.....278

**Figure C-50.** $^{13}$C NMR spectrum of **7.3**.....278

**Figure C-51.** $^{1}$H NMR spectrum of **3.32**.....279

**Figure C-52.** $^{13}$C NMR spectrum of **3.32**.....279

**Figure C-53.** $^{1}$H NMR spectrum of **3.34**.....280

**Figure C-54.** $^{13}$C NMR spectrum of **3.34**.....280

**Figure C-55.** $^{1}$H NMR spectrum of **3.35**.....281

**Figure C-56.** $^{13}$C NMR spectrum of **3.35**.....281

**Figure C-57.** $^{1}$H NMR spectrum of **7.4**.....282

**Figure C-58.** $^{13}$C NMR spectrum of **7.4**.....282

**Figure C-59.** $^{1}$H NMR spectrum of **7.5**.....283

**Figure C-60.** $^{13}$C NMR spectrum of **7.5**.....283

**Figure C-61.** $^{13}$C NMR spectrum of **3.36**.....284

**Figure C-62.** $^{1}$H NMR spectrum o **3.1a**.....284

**Figure C-63.** $^{13}$C NMR spectrum of **3.1a**.....285

**Figure C-64.** $^{13}$C NMR spectrum of **3.1b**.....285

**Figure C-65.** $^{13}$C NMR spectrum of **3.1c**.....286

**Figure C-66.** $^{13}$C NMR spectrum of **3.1d**.....286

**Figure C-67.** $^{13}$C NMR spectrum of **3.1e**.....287

**Figure C-68.** $^{13}$C NMR spectrum of **3.1f**.....287

**Figure C-69.** $^{13}$C NMR spectrum of **3.1h**.....288

**Figure C-70.** $^{1}$H NMR spectrum of **4.2**.....289

**Figure C-71.** $^{13}$C NMR spectrum of **4.2**.....289

**Figure C-72.** $^{1}$H NMR spectrum of **4.3**.....290

**Figure C-73.** $^{13}$C NMR spectrum for **4.3**.....290

**Figure C-74.** $^{1}$H NMR spectrum of **4.4**.....291

**Figure C-75.** $^{13}$C NMR spectrum of **4.4**.....291

**Figure C-76.** $^{1}$H NMR spectrum of **4.5**.....292

**Figure C-77.** $^{13}$C NMR spectrum of **4.5**.....292

**Figure C-78.** $^{1}$H NMR spectrum of **4.6**.....293

**Figure C-79.** $^{13}$C NMR spectrum of **4.6**. ..... 293

**Figure C-80.** $^{1}$H NMR spectrum of **4.7**. ..... 294

**Figure C-81.** $^{13}$C NMR spectrum of **4.7**. ..... 294

**Figure C-82.** $^{1}$H NMR spectrum of **4.9**. ..... 295

**Figure C-83.** $^{13}$C NMR spectrum of **4.9**. ..... 295

**Figure C-84.** $^{1}$H NMR spectrum of **4.13**. ..... 296

**Figure C-85.** $^{13}$C NMR spectrum of **4.13**. ..... 296

**Figure C-86.** $^{1}$H NMR spectrum of **4.14**. ..... 297

**Figure C-87.** $^{13}$C NMR spectrum of **4.14**. ..... 297

**Figure C-88.** $^{1}$H NMR spectrum of **4.15**. ..... 298

**Figure C-89.** $^{13}$C NMR spectrum of **4.15**. ..... 298

**Figure C-90.** $^{1}$H NMR spectrum of **4.1a**. ..... 299

**Figure C-91.** $^{13}$C NMR spectrum of **4.1a**. ..... 299

**Figure C-92.** $^{13}$C NMR spectrum of **4.1b**. ..... 300

**Figure C-93.** $^{13}$C NMR spectrum of **4.1c**. ..... 300

**Figure C-94.** $^{13}$C NMR spectrum of **4.1d**. ..... 301

**Figure C-95.** $^{13}$C NMR spectrum of **4.1e**. ..... 301

**Figure C-96.** $^{13}$C NMR spectrum of **4.1f**. ..... 302

**Figure C-97.** $^{13}$C NMR spectrum of **4.1h**. ..... 302

**Figure C-98.** $^{1}$H NMR spectrum of **5.6**. ..... 303

**Figure C-99.** $^{13}$C NMR spectrum of **5.6**. ..... 303

**Figure C-100.** $^{13}$C NMR spectrum of **7.6**. ..... 304

**Figure C-101.** $^{1}$H NMR spectrum of **7.7**. ..... 304

**Figure C-102.** $^{13}$C NMR spectrum of **7.7**. ..... 305

**Figure C-103.** $^{1}$H NMR spectrum of **7.8**. ..... 305

**Figure C-104.** $^{13}$C NMR spectrum of **7.8**. ..... 306

**Figure C-105.** $^{1}$H NMR spectrum of **5.8**. ..... 306

**Figure C-106.** $^{13}$C NMR spectrum of **5.8**. ..... 307

**Figure C-107.** $^{1}$H NMR spectrum of 5.9 ..... 307

**Figure C-108.** $^{13}$C NMR spectrum of 5.9 ..... 308

**Figure C-109.** $^{1}$H NMR spectrum of 5.7 ..... 309

**Figure C-110.** $^{13}$C NMR spectrum of 5.7 ..... 309

**Figure C-111.** $^{1}$H NMR spectrum of 5.10 ..... 309

**Figure C-112.** $^{13}$C NMR spectrum of 5.10 ..... 310

**Figure C-113.** $^{13}$C NMR spectrum of 5.11 ..... 310

**Figure C-114.** $^{1}$H NMR spectrum of 5.12 ..... 311

**Figure C-115.** $^{13}$C NMR spectrum of 5.12 ..... 311

**Figure C-116.** $^{1}$H NMR spectrum of 5.15 ..... 312

**Figure C-117.** $^{13}$C NMR spectrum of 5.15 ..... 312

**Figure C-118.** $^{1}$H NMR spectrum of 5.16 ..... 313

**Figure C-119.** $^{13}$C NMR spectrum of 5.16 ..... 313

**Figure C-120.** $^{1}$H NMR spectrum of 5.17 ..... 314

**Figure C-121.** $^{13}$C NMR spectrum of 5.17 ..... 314

**Figure C-122.** $^{1}$H NMR spectrum of 5.18 ..... 315

**Figure C-123.** $^{13}$C NMR spectrum of 5.18 ..... 315

**Figure C-124.** $^{1}$H NMR spectrum of 5.21 ..... 316

**Figure C-125.** $^{13}$C NMR spectrum of 5.21 ..... 316

**Figure C-126.** $^{1}$H NMR spectrum of 5.22 ..... 317

**Figure C-127.** $^{13}$C NMR spectrum of 5.22 ..... 317

**Figure C-128.** $^{1}$H NMR spectrum of 5.23 ..... 318

**Figure C-129.** $^{13}$C NMR spectrum of 5.23 ..... 318

**Figure C-130.** $^{1}$H NMR spectrum of 5.24 ..... 319

**Figure C-131.** $^{13}$C NMR spectrum of 5.24 ..... 319

**Figure C-132.** $^{1}$H NMR spectrum of 5.25 ..... 320

**Figure C-133.** $^{13}$C NMR spectrum of 5.25 ..... 320

**Figure C-134.** $^{1}$H NMR spectrum of 5.26 ..... 321

**Figure C-135.** $^{13}$C NMR spectrum of **5.26**.....321

**Figure C-136.** $^{1}$H NMR spectrum of **5.27**.....322

**Figure C-137.** $^{13}$C NMR spectrum of **5.27**.....322

**Figure C-138.** $^{1}$H NMR spectrum of **5.28**.....323

**Figure C-139.** $^{13}$C NMR spectrum of **5.28**.....323

**Figure C-140.** $^{1}$H NMR spectrum of **5.30**.....324

**Figure C-141.** $^{13}$C NMR spectrum of **5.30**.....324

**Figure C-142.** $^{1}$H NMR spectrum of **5.31**.....325

**Figure C-143.** $^{13}$C NMR spectrum of **5.31**.....325

**Figure C-144.** $^{13}$C NMR spectrum of **5.32**.....326

**Figure C-145.** $^{13}$C NMR spectrum of **5.33**.....326

**Figure C-146.** $^{1}$H NMR spectrum of **5.34**.....327

**Figure C-147.** $^{13}$C NMR spectrum of **5.34**.....327

**Figure C-148.** $^{1}$H NMR spectrum of **5.35**.....328

**Figure C-149.** $^{13}$C NMR spectrum of **5.35**.....328

**Figure C-150.** $^{13}$C NMR spectrum of **5.36**.....329

**Figure C-151.** $^{13}$C NMR spectrum of **5.37**.....329

**Figure C-152.** $^{13}$C NMR spectrum of **5.38**.....330

**Figure C-153.** $^{13}$C NMR spectrum of **5.39**.....330

**Figure C-154.** $^{13}$C NMR spectrum of **5.40**.....331

**Figure C-155.** $^{13}$C NMR spectrum of **5.41**.....331

**Figure C-156.** $^{13}$C NMR spectrum of **5.42**.....332

**Figure C-157.** $^{13}$C NMR spectrum of **5.43**.....332

**Figure C-158.** $^{1}$H NMR spectrum of **5.44**.....333

**Figure C-159.** $^{13}$C NMR spectrum of **5.44**.....333

**Figure C-160.** $^{1}$H NMR spectrum of **5.45**.....334

**Figure C-161.** $^{13}$C NMR spectrum of **5.45**.....334

**Figure C-162.** $^{1}$H NMR spectrum of **5.48**.....335

**Figure C-163.** $^{13}C$ NMR spectrum of **5.48**.....335

**Figure C-164.** $^{13}C$ NMR spectrum of **5.49**.....336

**Figure C-165.** $^{1}H$ NMR spectrum of **5.50**.....336

**Figure C-166.** $^{13}C$ NMR spectrum of **5.50**.....337

**Figure C-167.** $^{1}H$ NMR spectrum of **5.51**.....337

**Figure C-168.** $^{13}C$ NMR spectrum of **5.51**.....338

**Figure C-169.** $^{1}H$ NMR spectrum of **5.52**.....338

**Figure C-170.** $^{13}C$ NMR spectrum of **5.52**.....339

**Figure C-171.** $^{1}H$ NMR spectrum of **5.1a**.....339

**Figure C-172.** $^{13}C$ NMR spectrum of **5.1a**.....340

**Figure C-173.** $^{13}C$ NMR spectrum of **5.1b**.....340

**Figure C-174.** $^{13}C$ NMR spectrum of **5.1c**.....341

**Figure C-175.** $^{13}C$ NMR spectrum of **5.1d**.....341

**Figure C-176.** $^{13}C$ NMR spectrum of **5.1e**.....342

**Figure C-177.** $^{13}C$ NMR spectrum of **5.1f** (fully decoupled).....342

**Figure C-178.** $^{13}C$ NMR spectrum of **5.1f** ($^{1}H$–$^{13}C$ coupling observed).....343

**Figure C-179.** $^{13}C$ NMR expanded spectrum of **5.f**.....343

**Figure C-180.** $^{13}C$ NMR spectrum of **5.1g**.....344

**Figure C-181.** $^{13}C$ NMR expanded spectrum of **5.1g**.....344

**Figure C-182.** $^{13}C$ NMR spectrum of **5.1h**.....345

**Figure C-183.** $^{13}C$ NMR expanded spectrum of **5.1h**.....345

**Figure C-184.** $^{13}C$ NMR spectrum of **5.1j**.....346

**Figure C-185.** $^{13}C$ NMR expanded spectrum of **5.1j**.....346

# List of Schemes

**Scheme 1-1.** Commonly used homocoupling conditions for the synthesis of symmetrical polyynes. 6

**Scheme 1-2.** Bohlmann's attempted crosscoupling under Eglinton conditions. 7

**Scheme 1-3.** Cadiot-Chodkiewicz crosscoupling. 7

**Scheme 1-4.** Polyyne formation using the FBW rearrangement. 8

**Scheme 1-5.** In situ desilylation/dimerization protocols for the synthesis of polyynes. 9

**Scheme 1-6.** Tobe and coworker's [2+1] chelotropic fragmentation and alkylidene carbene rearrangement. 10

**Scheme 1-7.** Diederich and coworker's SS–FVP route to pentaynes. 10

**Scheme 1-8.** Tykwinski and coworker's use of the FBW rearrangement to synthesize a pentayne. 10

**Scheme 1-9.** Negishi and coworker's pair selective protocol. 11

**Scheme 1-10.** Formation of diarylhexaynes via oxidative homocoupling. 12

**Scheme 1-11.** A one-pot approach to hexayne formation based on a FBW rearrangement. 12

**Scheme 1-12.** Synthesis of hexaynes through a) two-fold FBW rearrangement and b) SS-FVP. 13

**Scheme 1-13.** Cox and coworker's synthesis of diphenyl hexayne via a fluoride catalyzed elimination reaction. 13

**Scheme 1-14.** The formation of insulated hexaynes by a) Hirsch and coworkers and b,c) Gladysz and coworkers. 14

**Scheme 1-15.** Bohlmann's synthesis of the first isolated heptayne. 15

**Scheme 1-16.** Heptayne synthesis via chain length extension by a) Walton and coworkers and b) Gladysz and coworkers. 16

**Scheme 1-17.** Hirsch's heptayne synthesis. 16

**Scheme 1-18.** Heptayne syntheses from Bruce and coworkers. 17

**Scheme 1-19.** The FBW approach towards the synthesis of octaynes. 19

**Scheme 1-20.** Frauenrath and Hoheisel`s Negishi protocol toward octaynes. 20

**Scheme 1-21.** Eastmond and coworkers synthesis of a nonayne via a mixed Hay coupling. 21

**Scheme 1-22.** Synthesis of a TIPS-endcapped decayne. 22

**Scheme 1-23.** Walton and Johnson's synthesis of the *t*-butyl-endcapped dodecayne. ..... 23

**Scheme 1-24.** Cox and coworkers synthesis of an aryl-endcapped dodecayne. ..... 23

**Scheme 1-25.** Dodecayne synthesis by Bruce and coworkers. ..... 25

**Scheme 1-26.** Synthesis of a tetradecayne by Gladysz and coworkers. ..... 25

**Scheme 2-1.** Synthesis of bromo-HPB (**2.2**). ..... 38

**Scheme 2-2.** Synthesis of dypnone (**2.3**) and bromotriphenylbenzene (**2.4**). ..... 40

**Scheme 2-3.** Synthesis of **2.5** as a model system for larger triarylsilyl polyynes. ..... 41

**Scheme 2-4.** "One-pot" synthesis of unsymmetrical acetylene **2.6**. ..... 42

**Scheme 2 5.** Selective protiodesilylation of **2.6** followed by Pd-catalyzed homocoupling to give diyne **2.8**. ..... 42

**Scheme 2-6.** Desilylation of **2.10** using mild basic conditions followed by Hay coupling to give tetrayne **2.14**. ..... 44

**Scheme 2-7.** The in situ desilylation/bromination of **2.10** followed by Pd-catalyzed crosscoupling to give unsymmetrical triyne **2.16**. ..... 45

**Scheme 2-8.** Attempted selective desilylation of **2.16** using mild basic conditions followed by Hay coupling to give hexayne **2.17**. ..... 46

**Scheme 3-1.** Synthesis of 1-ethynyladamantane **3.2** and acid **3.3**. ..... 52

**Scheme 3-2.** Synthesis of diyne **3.1a** using Hay (**path A**) or Pd-catalyzed homocoupling (**path B**) conditions. ..... 53

**Scheme 3-3.** Synthesis of triyne **3.1b** via a FBW rearrangement. ..... 53

**Scheme 3-4.** Synthesis of tetrayne **3.1c**. ..... 54

**Scheme 3-5.** Attempted synthesis of alcohol **3.12** towards the formation of pentayne **3.1d**. ..... 55

**Scheme 3-6.** Divergent strategy towards the synthesis of pentayne **3.1d**. ..... 55

**Scheme 3-7.** Synthesis of dibromoolefins **3.21**, **3.22** and **3.23**. ..... 56

**Scheme 3-8.** Synthesis of hexa- (**3.1e**), octa- (**3.1f**) and decayne (**3.1h**) via 1) a dimerization reaction followed by a two-fold FBW rearrangement (**route A**); or 2) a FBW rearrangement followed by dimerization (**route B**). ..... 58

**Scheme 3-9.** Synthesis of hexayne **3.35**. ..... 59

**Scheme 3-10.** Desilylation of hexayne **3.35** using a mild fluoride source followed by dimerization under Pd-catalysis to give dodecayne **3.1k**. ..... **60**

**Scheme 4-1.** Synthesis of triyne **4.1b** via a FBW rearrangement. ..... **86**

**Scheme 4-2.** Synthesis of tetrayne **4.1c**. ..... **87**

**Scheme 4-3.** Synthesis of pentayne **4.1d**. ..... **87**

**Scheme 4-4.** Synthesis of hexayne **4.1e**, octayne **4.1f**, and decayne **4.1h**. ..... **88**

**Scheme 5-1.** Synthesis of supertritylacetylene **5.6**. ..... **104**

**Scheme 5-2.** Synthesis of supertrityldiyne **5.7**. ..... **105**

**Scheme 5-3.** Synthesis of acid **5.10**. ..... **106**

**Scheme 5-4.** Synthesis of ketones **5.12–5.14** via Friedel-Crafts acylation. ..... **107**

**Scheme 5-5.** Synthesis of hexa-, octa-, and decaynes (**5.1b-d**) via a dibromoolefination, FBW rearrangement, and finally a homocoupling reaction. ..... **107**

**Scheme 5-6.** Synthesis of supertrityl triyne **5-25**. ..... **108**

**Scheme 5-7.** Toward the synthesis of deprotected supertrityl tetrayne **5.34** and pentayne **5.35**. ..... **109**

**Scheme 5-8.** Mild desilylation conditions developed to generate terminal tetrayne **5.34**. ..... **111**

**Scheme 5-9.** Synthesis of longer unsymmetrical polyynes utilizing Sonogashira and Negishi crosscoupling conditions. BRSM - based on recovered starting material ..... **112**

**Scheme 5-10.** Desilylation of **5.23** to give **5.48** followed by formation of terminal bromide **5.49**. ..... **113**

**Scheme 5-11.** Synthesis of polyynes **5.1a-c** using the Hay homocoupling protocol, **5.1d** and **5.1e** using the Eglinton protocol, and **5.1d-j** using a modified Glaser-Eglinton-Hay homocoupling protocol. ..... **117**

**Scheme 6-1.** Proposed synthesis of even longer supertrityl polyynes. ..... **152**

**Scheme A-1.** Synthesis of acid **A2** and acid chloride **A3**. ..... **239**

**Scheme A-2.** Synthesis of dibromoolefins **A7-A9** via a Friedel-Crafts reaction followed by dibromoolefination. Compound **A8** was subjected to a FBW rearrangement followed by dimerization under modified Eglinton conditions to give octayne **A11**. ..... **239**

**Scheme A-3.** Synthesis of triyne **A14** via a FBW rearrangement. ..... **240**

## List of Symbols

| | |
|---|---|
| Å | Angstrom |
| $[\alpha]_D$ | optical rotation of 589 nm light (sodium D line) |
| $\delta$ | chemical shift |
| $\varepsilon$ | molar extinction coefficient |
| $\lambda_{max}$ | wavelength of maximum absorbance |
| $\mu$ | micro |
| $\gamma$ | molecular second hyperpolarizability |
| $\Delta$ | heat |
| $E_g$ | band gap energy |
| $T_{max}$ | DSC decomposition temperature |
| $Я$ | symmetric (Raman active) stretching mode |
| $J$ | coupling constant |
| $M_r$ | formula weight |

## List of Abbreviations

| | |
|---|---|
| APPI | atmospheric pressure photoionization |
| APT | attached proton test |
| aq | aqueous |
| Arb. | arbitrary |
| BLA | bond length alternation |
| Bu | butyl |
| calcd. | calculated |
| CCDC | Cambridge Crystallographic Data Centre |
| CD | cyclo dextrins |
| cm | centimeter(s) |
| CV | cyclic voltammetry |
| d | doublet |
| DCTB | trans-2-[3-{4-tert-butylphenyl}-2-methyl-2-propenylidene]malononitrile |
| DFT | density functional theory |
| DMF | *N,N*-dimethylformamide |
| DMSO | dimethylsulfoxide |
| DP | decomposition point |
| DSC | differential scanning calorimetry |
| EA | elemental analysis |
| ECC | Effective Conjugation Coordinate |
| ECL | effective conjugation length |
| EI MS | electron impact mass spectroscopy |
| ESI | electrospray ionization |
| Et | ethyl |
| equiv. | equivalent(s) |
| eV | electron volts |

| | |
|---|---|
| FAB MS | fast atom bombardment mass spectroscopy |
| FBW | Fritsch-Buttenberg-Wiechell |
| FTIR | Fourier transform infrared spectroscopy |
| FWHM | full-width half-maximum |
| g | gram(s) |
| h | hour(s) |
| HMPA | hexamethylphosphoramide |
| HMQC | heteronuclear multiple quantum coherence |
| HOMO | highest occupied molecular orbital |
| HPB | hexaphenylbenzene |
| HPLC | high performance liquid chromatography |
| HRMS | high resolution mass spectrometry |
| Hz | Hertz |
| *i* | iso |
| IR | infrared |
| L | liter |
| LDA | lithium diisopropylamine |
| LED | light emitting diode |
| LUMO | lowest unoccupied molecular orbital |
| m | multiplet |
| M | molar |
| MALDI | matrix-assisted laser desorption ionization |
| Me | methyl |
| mg | milligram(s) |
| MHz | megaHertz |
| mL | milliliter(s) |
| mmol | millimole(s) |
| mol | mole(s) |

| | |
|---|---|
| Mp | melting point |
| MS | mass spectroscopy |
| mV | millivolts |
| *m/z* | mass-to-charge ratio |
| *n*-BuLi | *n*-butyllithium |
| NBS | *N*-bromosuccinimide |
| NLO | nonlinear optical (optics) |
| nm | nanometer(s) |
| NMR | nuclear magnetic resonance |
| OLED | organic light-emitting diode |
| ORTEP | Oak Ridge thermal ellipsoid plot |
| *p* | *para* |
| PBE | Perdew-Burke-Ernzerhof |
| PCC | pyridinium chlorochromate |
| Ph | phenyl |
| PMA | phosphomolybdic acid |
| ppm | parts per million |
| Pr | propyl |
| q | quartet |
| $R_f$ | retention factor |
| rt | room temperature |
| s | singlet |
| satd. | saturated |
| sh | shoulder |
| SS-FVP | solution-spray flash-vacuum-pyrolysis |
| t | triplet |
| *t* | tertiary |
| TBAF | tetrabutyl ammonium fluoride |

| | |
|---|---|
| TBPS | tris(biphenyl-4-yl)silyl |
| TBS | *t*-butyldimethylsilyl |
| TBDMS | *t*-butyldimethylsilyl |
| TES | triethyldilyl |
| TFT | thin-film transistor |
| TGA | thermogravimetric analysis |
| THF | tetraydrofuran |
| THPBS | tris(hexaphenylbenzene)silyl |
| TIPS | triisopropylsilyl |
| TLC | thin layer chromatography |
| TMEDA | *N,N,N′,N′*-tetramethylethylenediamine |
| TMS | trimethylsilyl |
| TOF | time-of-flight |
| tol | tolyl |
| TPS | triphenylsilyl |
| Tr* | supertrityl [tris(3,5-di-*t*-butylphenyl)methyl] |
| TTPBS | tris(triphenylbenzene)silyl |
| UV | ultraviolet |
| UV-Vis | ultraviolet-visible |
| vw | very weak |
| w | weak |

# Chapter 1 Introduction to Polyynes[‡]

## 1.1 Introduction to Polyconjugated Materials

Throughout history, human kind has made several advancements in technology and new discoveries that have shaped the way we live today. These advancements have propelled us forward towards new ideas and achievements that allow us to do what was thought to be unimaginable. In particular is the area of organic materials, where several synthetic achievements have been made that include polymers,[1-3] synthetic diamond,[4-6] graphite,[5-8] and fullerenes,[7] just to name a few. These materials have properties that allow for improved and even unique new designs for devices.[3,7,9-11] Currently we live in a world where computers are relied upon for many of our daily tasks, and the tasks become increasingly complex; thus, improvements in computer speed and power are constantly required. The electronics industry has seen impressive advancements in computer chip technology, with the ability to miniaturize the architecture to sub-micron sizes. However, we are reaching the limit in our ability to advance these devices. Therefore, new materials are being sought out, such as semiconducting organic materials, in order to continue to improve upon this technology.

With the electronics field starting to look to new materials for devices, the area of organic-electronic devices is beginning to emerge. Semiconducting organic materials have the potential to be used in a variety of these emerging technologies such as organic thin-film transistors (TFTs),[10] organic light-emitting diodes (OLEDs),[9] and nonlinear optical media.[11] The potential to fabricate new and interesting devices from organic molecules, oligomers, and polymers has subsequently led to a significant effort in exploratory research in these areas.[12-20] The appeal of organic materials typically lies in their ability to harness light (photons) to be used in energy transfer processes, requiring no heat transfer. Also, it is relatively easy to synthetically tune

---

[‡] A version of this chapter has been published. Chalifoux, W. A.; Tykwinski, R. R. *C. R. Chimie* **2009**, *12*, 341.

electronic and optical properties merely by systematically changing either the size or the constitution of the molecular skeleton. To this end, one approach toward optimizing organic materials is through the formation and study of a series of structurally related molecules, known as oligomers, in which the degree of conjugation is controlled by the number of repeat units. Using this so-called oligomer approach,[21] the electronic make-up of the molecules can be probed and correlated to, for example, optical properties (HOMO-LUMO transition energies).[18,19,22] This strategy has been applied to a plethora of different structural motifs, including, for example, partially acetylenic systems such as polydiacetylenes,[23-25] polytriacetylenes,[18,25,26] and poly(phenylene ethynylene)s (Figure 1-1).[14,27-32] What is interesting is that there is relatively little information known about a series of oligomers known as polyynes, that are arguably the most efficiently conjugated organic materials.[33-35]

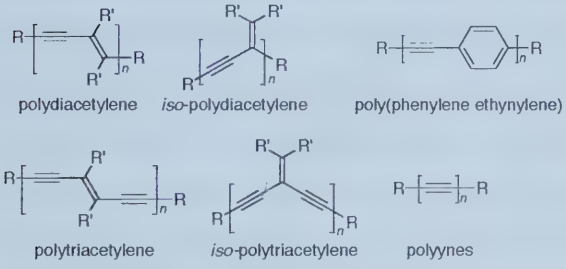


**Figure 1-1.** Common oligo- and/or polymeric systems based on acetylenic building blocks.

Polyynes, which are made up of alternating triple and single bonds, possess a very efficiently conjugated system because there is very little or no loss in this conjugation due to conformational effects (bond rotation), something that is possible with double bonds. Polyynes are one-dimensional, linear molecules, and it is because of this structural feature that they are often referred to as "molecular wires." Efficient conjugation and rigid linearity are substantial assets that polyynes possess making these materials potentially useful in many optical and electronic applications.

## 1.2 The Last (Missing?) Allotrope of Carbon

In the realm of all-carbon and carbon-rich materials, one hardly needs to be reminded of the significance of diamond and graphite and the impact they have made on society.[4-6,8] While certainly obvious, it is worth noting that these two very important allotropes are both composed almost entirely of carbon, yet they show inherently different materials properties due to the difference in their hybridization, i.e., diamond is derived from $sp^3$-hybridized carbon while graphite (as well as graphene, fullerenes, and carbon nanotubes, Figure 1-2) is made up of $sp^2$-hybridized carbon. The $sp^3$-hybridized carbon atoms of diamond are organized into a rigid 3-dimentional network of 6-membered rings as a result of the tetrahedral arrangement of bonds. Graphite on the other hand, is comprised of layers of 2-dimetional sheets of $sp^2$-carbon atoms that are bonded in a manner that produces a hexagonal (honeycomb) lattice. Individual sheets of graphite, referred to as graphene, can be produced by synthesis,[36] oxidation of graphite,[37] plasma etching of carbon nanotubes,[38] opening of multiwalled carbon nanotubes,[39] or exfoliated from bulk graphite;[40-44] all have interesting properties apart from the bulk graphite. The next logical allotrope in this series would be comprised of sp-hybridized carbon, a material commonly referred to as "carbyne." The existence of carbyne, however, has been a controversial topic for decades (Figure 1-3).[45-49] This material would consist of a linear array of bonded carbon atoms that could potentially act as wires the thickness of only a single sp-hybridized carbon atom.

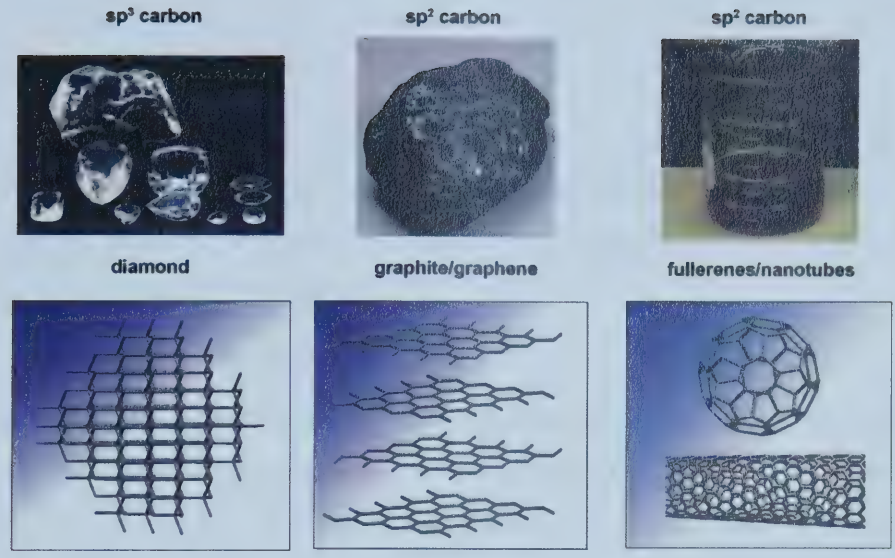


**Figure 1-2.** Pictures of diamond ($sp^3$-carbon), graphite/graphene ($sp^2$-carbon) and fullerene/nanotubes ($sp^2$-carbon), the known allotropes of carbon along with 3-D molecular representations.[50]

While naturally occurring carbyne may or may not exist, defined length oligomers (polyynes) based on the contiguous connection of acetylenic units have become desirable synthetic targets over the past decade.[33-35,51] The current renaissance in polyyne chemistry is not, however, the first era in which exploration of both the synthesis and characterization of polyynes has been popular. Between the 1950s and 70s, the study of such molecules attracted the interest of pioneers such as Jones,[52,53] Bohlmann,[54-56] Walton,[57-59] and Nakagawa.[60] The work done pertaining to polyynes over the past half-century continues to provide scientists with an unprecedented opportunity to gain insight into the properties of carbyne, as well as compare it to other allotropic forms of carbon.

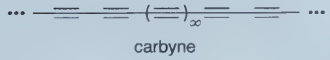

carbyne

**Figure 1-3.** The structure of carbyne.

## 1.3 Polyyne Synthesis

Currently, there are a number of techniques that are commonly used to synthesize polyynes. Many of these methods rely on the homo- or heterocoupling (Equation 1) of preformed acetylenic precursors,[61] while others use an elimination event to form the polyyne in the last

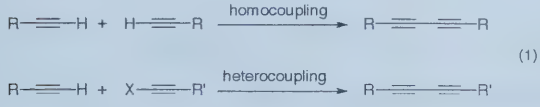


(1)

step.[62,63] A handful of methods have also been developed that rely on the extrusion of a molecular subunit as a means to assemble the polyyne framework.[64] Highlighted examples of each synthetic strategy will be presented in this chapter, concentrating primarily on the synthesis of polyynes with a length of at least five triple bonds (i.e., pentaynes). This introductory section will conclude with a more thorough description of known polyynes with a length of at least 16 carbons, given that there are relatively few such molecules. Finally, as a brief look into the properties of these materials will be outlined.

### 1.3.1 General synthetic considerations

The first reported polyyne synthesis arguably dates back to the year 1869 when Carl Glaser reported that copper(I) phenylacetylide underwent an oxidative dimerization in the presence of air to produce diphenylbutadiyne (Scheme 1-1a).[65]

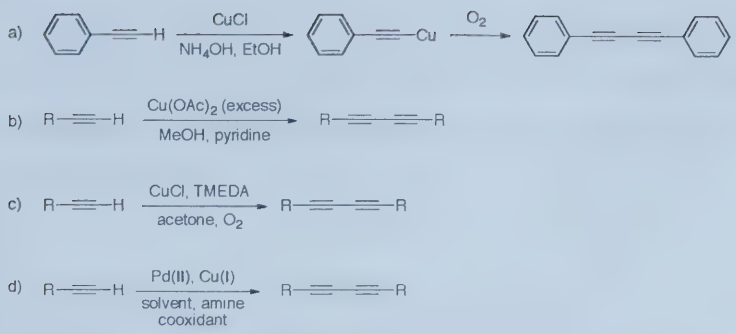


**Scheme 1-1.** Commonly used homocoupling conditions for the synthesis of symmetrical polyynes.

A variety of improvements have been made to the copper-catalyzed homocoupling method reported by Glaser that do not require the isolation of a potentially explosive copper(I) acetylide. For example, the oxidative coupling of acetylenes using $Cu(OAc)_2$ in the presence of MeOH and pyridine was reported in 1956 by Eglinton and Galbraith (Scheme 1-1b).[66] Another breakthrough in the oxidative dimerization of acetylenes was reported by Hay in 1962, who reported that CuCl in the presence of TMEDA and $O_2$ is an exceptionally effective system (Scheme 1-1c).[67] The solvents commonly used in this reaction include acetone or $CH_2Cl_2$, and the procedures enhanced effectiveness stems from the remarkable solubility of the Cu catalyst as a result of the TMEDA ligand. Other refinements of the typical homocoupling reactions have been invoked such as the use of Pd catalysis instead of the traditional Cu(I)/Cu(II) system (Scheme 1-1d).[61,68] Pd catalysis can often lead to excellent yields of desired product when Cu catalysis is sluggish or ineffective.[69,70] Recently, it has also been reported that Pd-catalyzed homocoupling of acetylenes can also occur under aerobic conditions where oxygen in the air acts as the co-oxidant to regenerate the active Pd(II) catalyst.[71]

Although Cu(I)/Cu(II) mediated homocoupling reactions are typically an excellent choice for the synthesis of symmetrical polyynes, they are often unsuitable for the formation of unsymmetrical derivatives such as, for example, triynes. This has been demonstrated by the excellent work done by Bohlmann and coworkers,[72] where the reaction of phenylbutadiyne with

pent-2-ene-4-yn-1-ol produced almost exclusively the α,ω-tetrayne, with only small amount of the unsymmetrical triyne obtained from the reaction (Scheme 1-2). This was explained through a mechanistic investigation that shows that the relative acidity of the acetylenic precursors plays an important role in the reaction rate and thus, the more acidic diyne reacts faster, leading primarily to the tetrayne product.

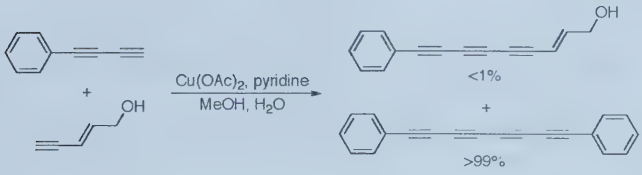


**Scheme 1-2.** Bohlmann's attempted crosscoupling under Eglinton conditions.

The problem of forming unsymmetrical diynes, triynes and in some cases tetraynes has been addressed through the crosscoupling method developed by Cadiot and Chodkiewicz (Scheme 1-3).[61,73-75] In this case, a terminal alkyne (or polyyne) is allowed to react with a bromo-, iodo-, or chloroalkyne derivative, leading to the unsymmetrical product. This reaction can, however, be complicated by the competing homocoupling reaction of the alkynyl halide, leading to a product mixture that is often difficult to separate. Pd-catalyzed versions of this protocol have also recently been developed as well.[69,76]

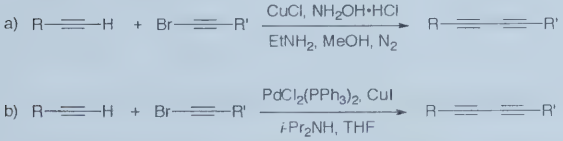


**Scheme 1-3.** Cadiot-Chodkiewicz crosscoupling.

A more recent development in the formation of polyynes in known as the Fritsch-Buttenberg-Wiechell (FBW) rearrangement[77-82] in which an alkylidene carbene/carbenoid is formed in situ and then undergoes a 1,2-migration of a pendent alkyl, aryl or alkynyl group to

generate a carbon-carbon triple bond (Scheme 1-4). While the conditions of the original FBW rearrangement are quite harsh (i.e., strong base and high temperatures), a fact that renders it incompatible with many functional groups, milder variations of the FBW rearrangement have subsequently been developed and provide a route to access symmetrical and unsymmetrical polyynes.[34,64,83-96]

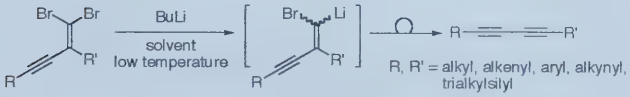


**Scheme 1-4.** Polyyne formation using the FBW rearrangement.

Typically the penultimate step towards the synthesis of a polyyne is the removal of a silyl protecting group of the immediate precursor prior to dimerization. Desilylation to produce terminal acetylenes is usually not typically a problem, other than adding a step to the polyyne synthesis. Terminal diynes, however, have a tendency to be less stable to isolation, making isolation less desirable. Mori and coworkers have pioneered the concept of an oxidative acetylenic homocoupling directly from a trialkylsilyl-protected acetylene, thus forming a diyne without the need for isolation the terminal alkyne precursor (Scheme 1-5a).[97] This concept has also been applied to the synthesis of tetraynes by the in situ desilylation of a TMS group followed by dimerization by simply adding $K_2CO_3$ to standard Eglinton conditions (Scheme 1-5b).[98] A procedure designed for the in situ removal of a TIPS group towards the synthesis of diynes and tetraynes involves the use of TBAF in the presence of a $Cu(OAc)_2$ catalyst (Scheme 1-5c).[95] For TES-protected triyne derivatives, a one-pot reaction has been achieved using a sequence of TBAF mediated desilylation, in situ quenching with $ClSiMe_3$ (used as a fluoride scavenger), and Hay homocoupling to yield the desired product (Scheme 1-5d).[99]

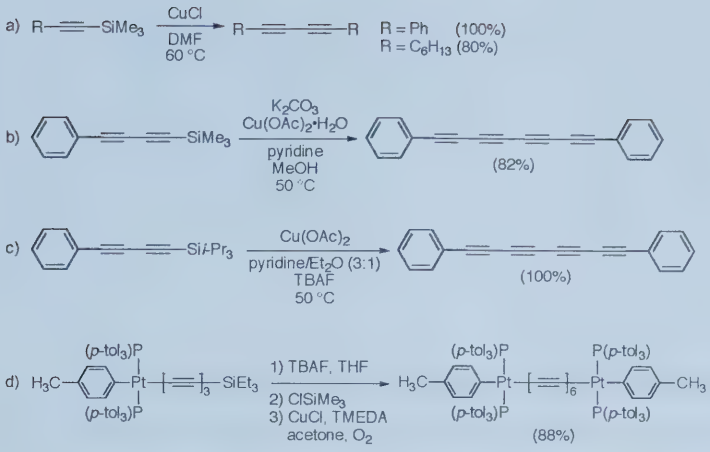


**Scheme 1-5.** In situ desilylation/dimerization protocols for the synthesis of polyynes.

### 1.3.2 Pentaynes

Pentaynes present a rather unique synthetic challenge due to their odd number of acetylene units. There has been successful formation of a pentayne skeleton through the use of an exhaustive elimination reaction.[100] Also, more "traditional" methods can be used such as the Cadiot-Chodkiewicz reaction[101] or a mixed Hay coupling reaction.[59,99,102] To avoid the need for potentially unstable triyne precursors, however, several innovative synthetic techniques have been recently developed.

Tobe and coworkers reported an interesting procedure for the synthesis of symmetrical triynes and pentaynes utilizing a [2+1] chelotropic fragmentation (Scheme 1-6).[64] In this case, a suitably functionalized enyne is irradiated with high energy UV light (254 nm), inducing an electrocyclic ring closure followed by the chelotropic extrusion of indane to give a free alkylidene carbene intermediate. The intermediate then undergoes a Fritsch-Buttenberg-Wiechell rearrangement via migration of one of the pendent butadiynyl groups affording the desired pentayne. Tobe and coworkers have also used this method to form cyclic polyynes known as the cyclo-$C_n$ series.[64]

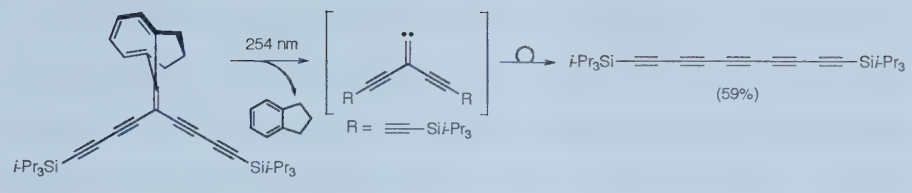


**Scheme 1-6.** Tobe and coworker's [2+1] chelotropic fragmentation and alkylidene carbene rearrangement.

Diederich and coworkers have used solution-spray flash-vacuum-pyrolysis (SS-FVP) to tackle the problem of pentayne, as well as hexayne, formation (Scheme 1-7).[13,103] In this case, readily available 3,4-dialkynyl-3-cyclobutene-1,2-diones can be converted to the desired polyynes on a multi-gram scale, as demonstrated by formation of the diphenyl- and bis(triisopropylsilyl)-terminated pentaynes.

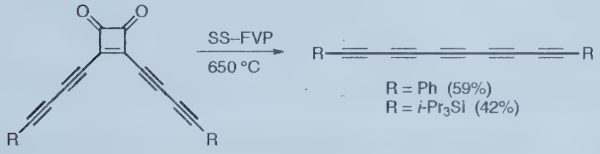


**Scheme 1-7.** Diederich and coworker's SS–FVP route to pentaynes.

Pentaynes can be formed via the FBW rearrangement starting from the appropriate dibromoolefinic precursor.[104] In the case shown in Scheme 1-8, a two-fold rearrangement leads to the polyyne product in 45% yield.[84]

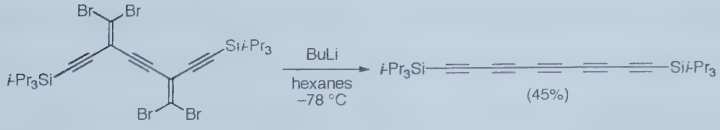


**Scheme 1-8.** Tykwinski and coworker's use of the FBW rearrangement to synthesize a pentayne.

Polyynes have been formed by Cataldo through the vaporization of graphite by electric arc and by the hydrolysis of calcium carbide ($CaC_2$) in an aqueous solution of $NH_4Cl$ containing Cu(I)/Cu(II) salts.[105-107] Both methods lead to a mixture of hydrogen-terminated polyynes that can be separated by HPLC using a C-18 column. The pentayne H–(C≡C)$_5$–H is typically the longest of the series to be formed in a reasonable quantity in this manner.

To date, there have been limited reports of unsymmetrical syntheses of pentaynes. Negishi and coworkers have applied their pair selective protocol to the formation of polyyne derivatives (Scheme 1-9).[108] In this case, a Zn-acetylide, formed in situ from the corresponding *E*-1-chloro-1-hexen-3,5-hexadiyne precursor (not shown), is coupled with a 4-aryl-1,1-dibromo-1-buten-3-yne partner, followed by elimination to the desired pentaynes. As well, the FBW rearrangement has been used to synthesize unsymmetrical pentaynes.[84,104,109]

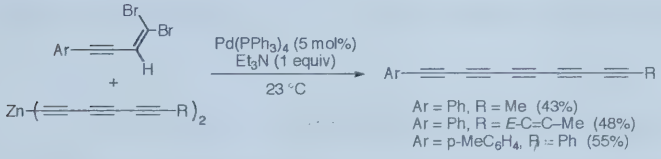


**Scheme 1-9.** Negishi and coworker's pair selective protocol.

### 1.3.3 Hexaynes

There are quite a few examples of hexayne syntheses, most of which involve the initial formation a trialkylsilyl-protected triyne precursor, followed by removal of the silyl group and a subsequent oxidative homocoupling reaction. While the stability of the terminal triyne precursor can be a determining factor in the success of such reactions, if kept in solution following removal of the silyl protecting group, reactions to form hexaynes typically proceed in reasonable to good yields, such as the examples shown in Scheme 1-10.[85,86] It is worth noting that recent work by Bryce and coworkers has demonstrated that terminal triynes, and even tetraynes, can show

surprising stability in the solid-state through the use of a large, sterically demanding endgroups (Figure 1-4).[110-112]

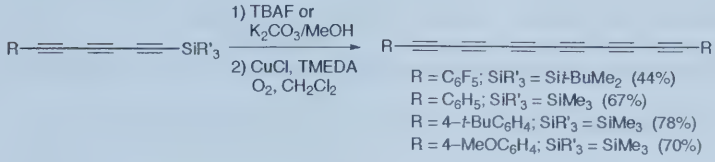
1) TBAF or
$K_2CO_3$/MeOH
2) CuCl, TMEDA
$O_2$, $CH_2Cl_2$
R = $C_6F_5$; SiR'$_3$ = Si*t*-BuMe$_2$ (44%)
R = $C_6H_5$; SiR'$_3$ = SiMe$_3$ (67%)
R = 4–*t*-Bu$C_6H_4$; SiR'$_3$ = SiMe$_3$ (78%)
R = 4–MeO$C_6H_4$; SiR'$_3$ = SiMe$_3$ (70%)

**Scheme 1-10.** Formation of diarylhexaynes via oxidative homocoupling.

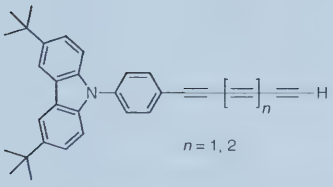


**Figure 1-4.** Structures of the tri- and tetrayne isolated by Bryce and coworkers.

A one-pot procedure using a FBW rearrangement has been utilized as an alternative route towards hexayne formation (Scheme 1-11).[87] In this case, formation of a Li-acetylide from a FBW rearrangement of a previously desilylated dibromoolefinic precursor has been accomplished through reaction with two equivalents of BuLi in toluene. To this mixture is added CuBr and TMEDA to give an intermediate Cu-acetylide,[113] and oxygen gas is then bubbled into the mixture to ultimately afford the desired hexayne in good yield.

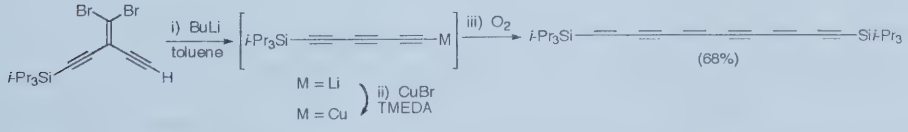


**Scheme 1-11.** A one-pot approach to hexayne formation based on a FBW rearrangement.

The need to synthesize a triyne intermediate prior to homocoupling can be circumvented through formation of the complete carbon framework prior to introducing the final acetylene units. As with pentaynes described above, this has been done with both the FBW rearrangement[13,34,84,103] and the SS-FVP technique of Diederich (Scheme 1-12).[13,34,84,103] In each case, a two-fold elimination process is accomplished, such as dual FBW rearrangements or the pyrolytic openings of two cyclobutenediones resulting in the loss of carbon monoxide. The hexaynes have been obtained in moderate to good yields.

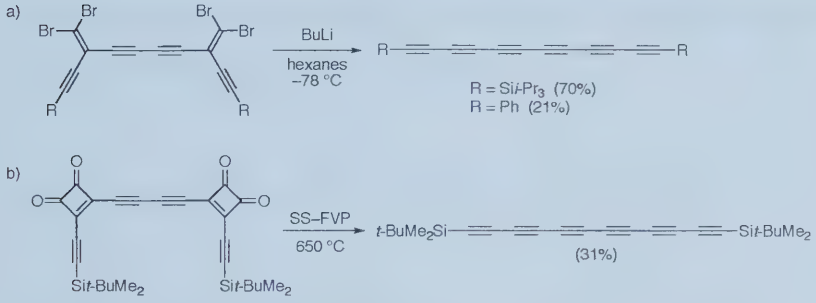


**Scheme 1-12.** Synthesis of hexaynes through a) two-fold FBW rearrangement and b) SS-FVP.

An alternative route that does not require oxidative homocoupling as the final step for polyyne formation has been reported by Cox and workers.[114] This route establishes the 12 carbon framework of the incipient polyyne via an oxidative homocoupling of the two enediyne "halves", followed by a fluoride-catalyzed elimination reaction to form the acetylenic skeleton (Scheme 1-13).

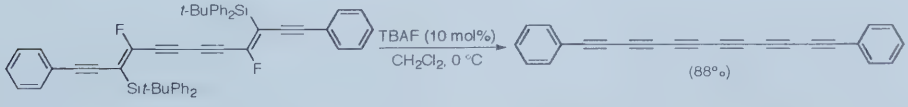


**Scheme 1-13.** Cox and coworker's synthesis of diphenyl hexayne via a fluoride catalyzed elimination reaction.

Numerous approaches have been made in order to insulate the polyyne core with alkyl chains that are tethered to the two termini for the purpose of improving polyyne stability. For example, Hirsch and coworkers have used phenyloxy endgroups that are connected via a flexible alkyl chain. The tethered triynes are first desilylated and then subjected to Hay conditions to form the hexayne core (Scheme 1-14a).[115] Gladysz and coworkers, pioneers in this area, used long-chain alkyl diphosphine ligands that span the two Pt endgroups for their insulation strategy of hexaynes.[116,117] The bridging tether could be introduced in one of two ways, either through ligand exchange at the platinum centers using a bidentate diphosphine ligand (Scheme 1-14b) or through the use of ring-closing metathesis with the Grubbs I catalyst to tether the two halves together, followed by reduction of the resulting alkene (Scheme 1-14c).

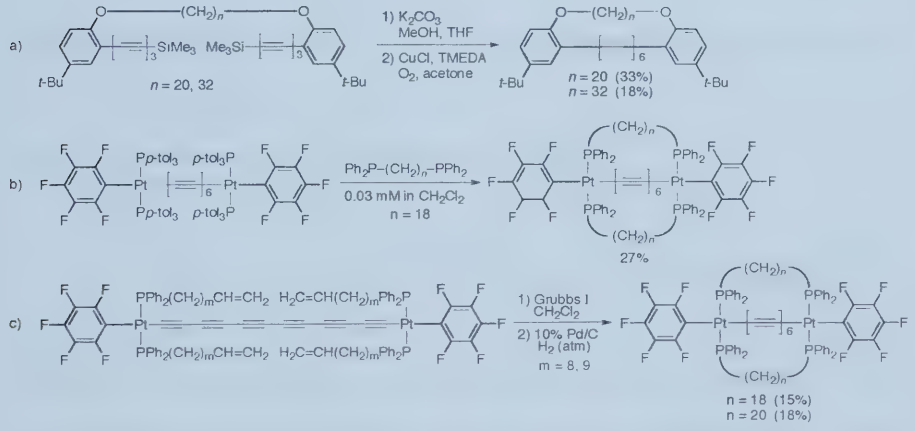


**Scheme 1-14.** The formation of insulated hexaynes by a) Hirsch and coworkers and b,c) Gladysz and coworkers.

Finally, Tomita and Sugiyama have approached the problem of hexayne stabilization through rotaxane formation using cyclodextrins (CDs). They observed, using time-course UV-Vis spectroscopic studies, that there is substantial stabilization of bis(phenanthryl)hexayne while encapsulated within one or two CD molecules, as compared to the free hexayne.[118]

### 1.3.4 Heptaynes.

As was mentioned earlier with triynes and pentaynes, odd numbered polyynes are more challenging targets. Though not obvious, heptaynes, as well as longer odd numbered polyynes, are quite formidable synthetic targets in that they cannot be assembled by a simple dimerization reaction. Furthermore, beyond hexaynes, kinetic stability of the product becomes a more serious issue as well. Bohlmann and coworkers have been the first to report the synthesis and characterization of a heptayne, which is achieved by carrying out an exhaustive elimination of a suitably functionalized *t*-butyl-endcapped precursor (Scheme 1-15).[119] The heptayne product is reported to have crystallized from a mixture of petroleum ether and MeOH, giving a yellow crystalline solid that slowly turned black upon heating to ca. 150 °C.

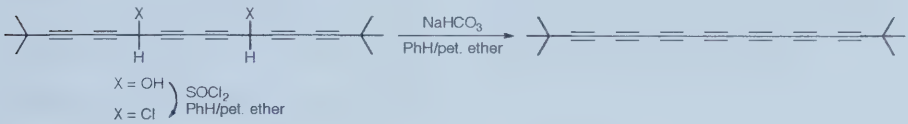


**Scheme 1-15.** Bohlmann's synthesis of the first isolated heptayne.

Walton and coworkers have reported the synthesis of a triethylsilyl-endcapped heptayne using Hay coupling to extend a hexayne framework by one acetylene unit through a reaction with excess $Et_3SiC{\equiv}CH$ (Scheme 1-16a).[59] Although no yield is given, this product is characterized by UV-Vis spectroscopy and then desilylated to give the di-deprotected polyyne product, which is also characterized by UV-Vis spectroscopy. Gladysz and coworkers have used a conceptually analogous chain length extension protocol toward a Pt-endcapped heptayne. This one-pot reaction, analogous to the synthesis of the symmetrical hexayne, involves desilylation of the pentayne precursor with TBAF, followed by the addition of trimethylchlorosilane which acts as a fluoride scavenger (Scheme 1-16b).[99,102] The resulting deprotected polyyne is then subjected to Hay coupling in the presence of excess triethylsilylbutadiyne to yield the unsymmetrical heptayne in a modest 20% yield as a red solid after chromatographic purification.

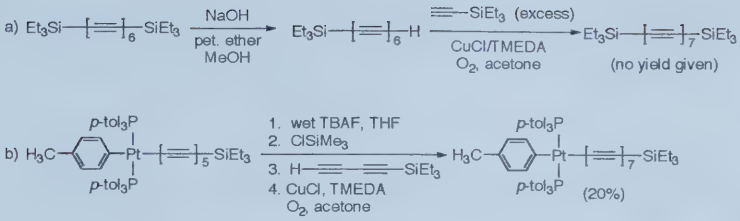


**Scheme 1-16.** Heptayne synthesis via chain length extension by a) Walton and coworkers and b) Gladysz and coworkers.

As a part of their efforts towards encasing polyynes within an insulating sheath provided by an alkyl tether (as also described in the previous section), Hirsch and coworkers reported a rather unique mode of heptayne formation (Scheme 1-17). Subjecting a tethered triyne to Pd-catalyzed Sonogashira coupling conditions in the presence of diiodoacetylene provided the desired heptayne in 11% yield as an orange solid that could be characterized by $^{1}$H NMR and UV-Vis spectroscopies, as well as FAB MS analysis.[115]

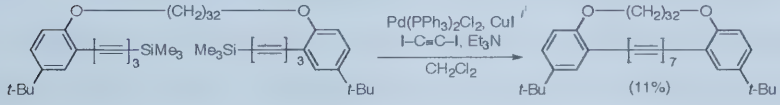


**Scheme 1-17.** Hirsch's heptayne synthesis.

Bruce and coworkers have elegantly developed the chemistry of gold acetylides toward the formation of both Ru- and Co-endcapped heptaynes (Scheme 1-18).[120,121] In both cases, the Pd-catalyzed reaction of the Au-diyne with I–(C≡C)$_3$–I led to the desired heptayne product, and in the case of the cobalt species a remarkable 86% yield has been obtained. Both species have been characterized crystallographically, and these are the only X-ray structures reported to date for heptaynes.[120]

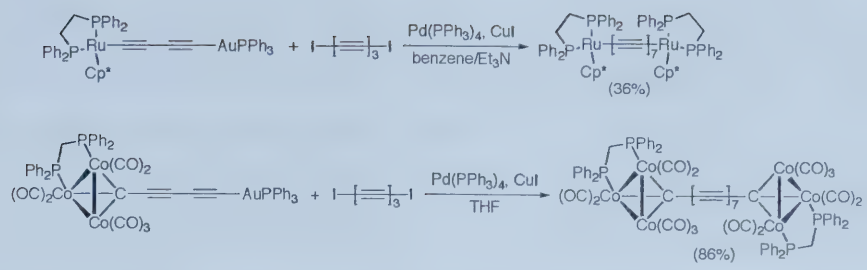

**Scheme 1-18.** Heptayne syntheses from Bruce and coworkers.

In addition to those described above, the parent heptayne, H–(C≡C)$_7$–H,[59,107,122] has been formed by a number of methods, and both H–(C≡C)$_7$–CN[107] and NC–(C≡C)$_7$–CN[123,124] have also be synthesized and studied. In most cases, the heptayne is formed as part of a mixture of polyynes with varying length and is subsequently separated chromatographically.

### 1.3.5 Octaynes

Octaynes are much less commonly seen in the literature, and this is primarily due to the fact that they, as well as the intermediates to make them, show considerably lower kinetic stability under ambient conditions. Although a substantial amount of work has been done over the past 40 years in this area, mostly within the last decade, few polyynes of 16 carbons or longer have been synthesized and characterized (Table 1-1). Given that there are obvious challenges associated with the synthesis and isolation of octaynes and even longer polyynes, stabilization of the reactive polyyne framework has become the main goal in order to provide macroscopic quantities of these materials for subsequent characterization.[33,34] Through recent work, empirical evidence supports the idea that extended polyynes can be stabilized through the incorporation of bulky substituents on the polyyne termini. Hirsch and coworkers have demonstrated that the use of large dendrimeric endgroups provides bench-stable octaynes (Table 1-1, entry 8).[125] Gladysz and coworkers have successfully used bulky Pt endgroups to achieve the stability needed to isolate these precious materials (Table 1-1, entry 16 and 18).[90] In both cases, the final octayne product is formed through Cu-catalyzed oxidative dimerization of the tetrayne "halves". Other notable octayne systems

formed through oxidative dimerization include the stable ferrocene derivative (Table 1-1, entry 12), and a porphyrin-endcapped species, both of which would be expected to have interesting electronic and optical properties (Table 1-1, entry 13).

Hirsch and coworkers, with their work towards the encapsulation of polyynes, have also put forth efforts toward to an octayne. Unfortunately, unlike their experience with heptayne synthesis using a $-O(CH_2)_{32}O-$ tether (Scheme 1-17), only a trace amount of the desired octayne product could be isolated using a slightly longer $-O(CH_2)_{40}O-$ tether (Table 1-1, entry 9).[115]

**Table 1-1.** Known, characterized 1,3,5,7,9,11,13,15-hexadecaoctaynes.

| Entry | Octayne | Characterization | Reference(s) |
|---|---|---|---|
| 1 |  | UV-Vis | 59,107,122 |
| 2 |  | $^1$H and $^{13}$C NMR, IR, UV-Vis, DSC, EI HRMS, EA, X-ray, DP | 104,126 |
| 3 |  | IR, UV-Vis, EI MS | 123,124 |
| 4 |  | $^1$H and $^{13}$C NMR, IR, UV-Vis, EA, DSC, NLO | 86,127 |
| 5 | 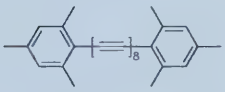 | IR, UV-Vis, EA, DP | 57 |
| 6 | 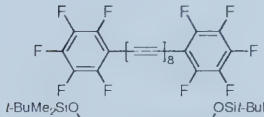 | $^{19}$F and $^{13}$C NMR, IR, MALDI-TOF HRMS, DP | 85 |
| 7 | 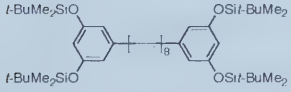 | $^1$H and $^{13}$C NMR, IR, Raman, UV-Vis, FAB MS, CV | 125 |
| 8 |  | $^1$H and $^{13}$C NMR, Raman, UV-Vis, FAB MS | 125 |
| 9 | 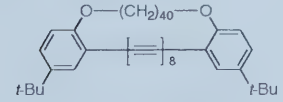 | UV-Vis, FAB MS | 115 |
| 10 |  | UV-Vis | 59 |
| 11 | | $^1$H and $^{13}$C NMR, IR, UV-Vis, EI HRMS, DSC, X-ray, NLO | 84 |
| 12 | 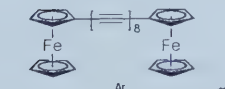 | IR, UV-Vis, DP | 128 |
| 13 | 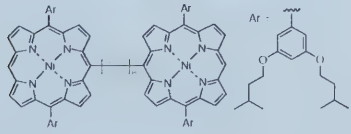 | $^1$H NMR, IR, UV-Vis, MALDI-TOF MS | 129 |

| | | | |
|---|---|---|---|
| 14 | 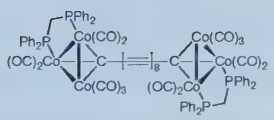 | $^1$H and $^{31}$P NMR, IR, ESI MS, EA | 121 |
| 15 | 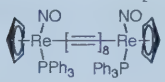 | $^1$H, $^{13}$C, and $^{31}$P NMR, IR, Raman, UV-Vis, FAB MS, CV, DSC, EA | 101,130 |
| 16 | 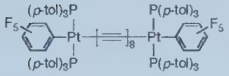 | $^1$H, $^{13}$C, and $^{31}$P NMR, IR, UV-Vis, FAB MS, CV, EA, TGA, DP, X-ray | 131 |
| 17 | 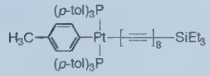 | $^1$H, $^{13}$C, and $^{31}$P NMR, IR, UV-Vis, MS[b], EA, DP | 99,102 |
| 18 | 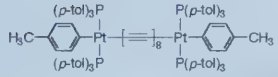 | $^1$H, $^{13}$C, and $^{31}$P NMR, IR, UV-Vis, CV, MS[b], EA, DSC, TGA, NLO | 99,102,132 |
| 19 | 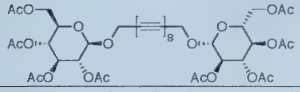 | $^1$H and $^{13}$C NMR, IR, $[\alpha]_D$, UV-Vis, ESI HRMS, EA, DP | 133 |

[a]Ar = Fréchet's aromatic polyether [G–3] dendrimer. [b]Ionization method not reported.

A two-fold FBW rearrangement has been used to synthesize TIPS- and phenyl-endcapped octaynes, giving the desired products in 10% and 13% yields, respectively (Scheme 1-19 and Table 1-1, entries 4 and 11).[34,84,86] The TIPS-endcapped octayne can be stored as a solid indefinitely under refrigeration without appreciable decomposition. Armitage reported that the phenyl-endcapped octayne was isolated as an unstable copper colored solid that tended to explode upon heating when crystallized from ether/EtOH.[127] However, when crystallized from THF, the resulting rust-colored solid shows surprisingly enhanced stability, surviving years if kept under refrigeration.[134] It is unclear whether the improved stability derives from a more stable polymorph or from a change in purity.[86]

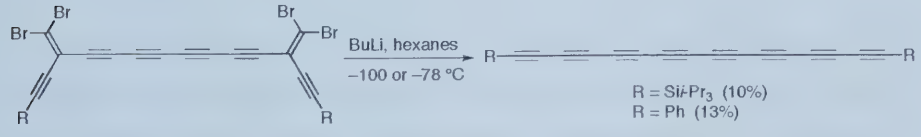


**Scheme 1-19.** The FBW approach towards the synthesis of octaynes.

Recently, Frauenrath and Hoheisel reported a new Negishi protocol toward the synthesis of glycosylated polyynes (Scheme 1-20 and Table 1-1, entry 19).[133] The formation of the Zn-

acetylide was carried out by monodesilylation using MeLi•LiBr followed by treatment with $ZnCl_2$. This Zn-acetylide intermediate was subjected to Pd-catalyzed crosscoupling conditions with the brominated diyne coupling partner to generate the unsymmetrical glycosylated tetrayne in a 45% yield. Desilylation was achieved using silver nitrate and the resulting tetrayne intermediate subjected to oxidative dimerization under Hay conditions to give the glycosylated octayne in 58% yield over two steps.

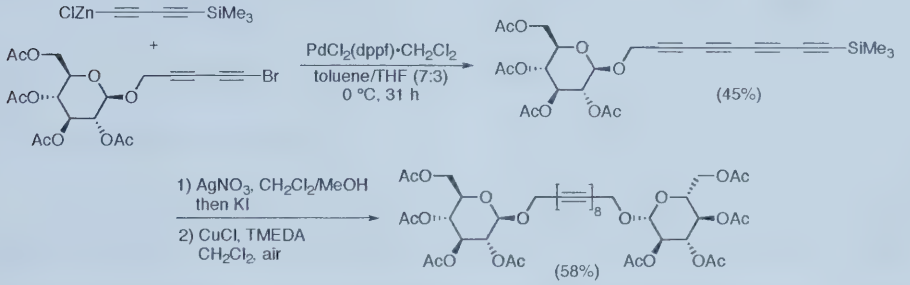


**Scheme 1-20.** Frauenrath and Hoheisel's Negishi protocol toward octaynes.

It is worth noting that X-ray crystallographic analyses of octaynes are scarce, and only three structures have been reported to date. These include the *t*-butyl-endcapped species (Table 1-1, entry 2),[104] the TIPS-endcapped species (Table 1-1, entry 11),[84] and the Pt-endcapped species (Table 1-1, entry 16).[131]

### 1.3.6 Nonaynes

Nonaynes are rare and to the best of our knowledge there are only two intended syntheses of a nonayne. The first includes the early work of Eastmond where a monodeprotected octayne is first obtained through a carefully controlled kinetic desilylation and this is followed by a crosscoupling reaction with excess triethylsilylacetylene in order to obtain the bis(TES)nonayne (Scheme 1-21).[59] From the same work by Eastmond, the protected nonayne was desilylated to generate H–(C≡C)$_9$–H, which is a compound that has also been observed as a product of electric

arc discharge between graphite electrodes.[107] Although their syntheses were not intended, three other nonaynes have been reported as byproducts of the Hay coupling reaction towards decaynes, albeit in these cases characterization is limited to MS and/or UV-Vis spectroscopic analysis.[84,104,125]

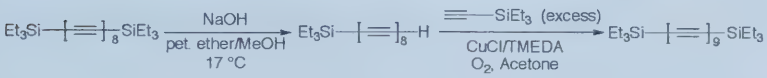


**Scheme 1-21.** Eastmond and coworkers synthesis of a nonayne via a mixed Hay coupling.

### 1.3.7 Decaynes, and beyond

Decaynes (Table 1-2) have been realized as early as 1960 but their isolation and characterization has proven to be difficult.[126] The length of 20 carbons seems to typically be the upper limit of polyyne stability for most series of polyynes. This is particularly true for early work that has been reported for the *t*-Bu and Ph derivatives (Table 1-2, entries 3 and 5). Likewise, the decayne has been formed for the $Et_3Si$ series (entry 9), as well as longer derivatives (vide infra), but even the octayne is already unstable to isolation in its neat form. Despite this seemingly upper limit of 20 carbons, work done by a few groups has recently shown that the issue of stability can be overcome, and these studies have provided decaynes in macroscopic quantities. Of particular note, both the Gladysz and Hirsch groups have successfully formed and isolated stable decaynes that are terminated with either metals (Re and Pt) or dendrimeric endgroups, respectively (Table 1-2, entries 14, 15, 17 and entry 8, respectively).[99,125]

One of the most studied series of polyynes is that with terminal TIPS groups, which was done by the Tykwinski group, and includes polyynes up to the decayne (Table 1-2, entry 12). Their efforts toward making the bis(TIPS)decayne include an attempted four-fold FBW rearrangement, which proved to be futile, with no desired product being isolated (Scheme 1-22).[34,84] The decayne has been synthesized, however, by reorganizing the steps and implementing a two-fold FBW rearrangement on the tetrabromoolefin first to produce the

unsymmetrical pentayne (Scheme 1-22). The pentayne is then subjected to standard protiodesilylation conditions to give the unstable deprotected pentayne, which is subjected directly to oxidative homocoupling conditions, without isolation, to yield the decayne in an overall yield of 30%. The third-order nonlinear optical characteristics of this series of polyynes, including the decayne, have been explored and the data show an impressive increase in molecular second hyperpolarizability as a function of increasing conjugation length.[135]

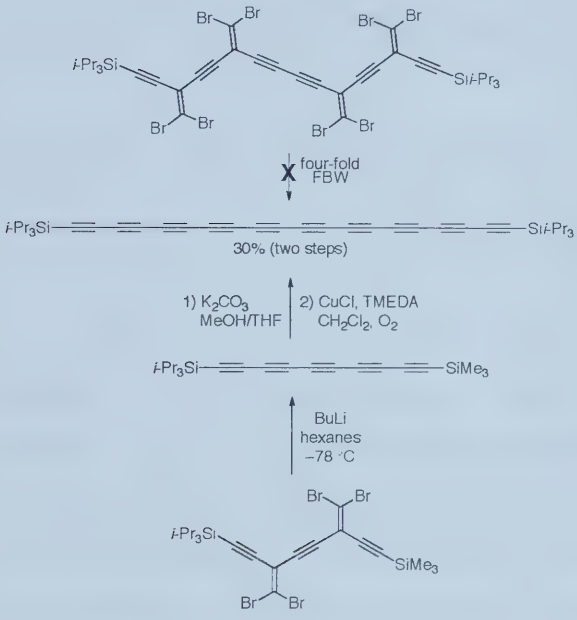


**Scheme 1-22.** Synthesis of a TIPS-endcapped decayne.

The synthesis of polyynes beyond 20 carbons in length has been nothing less then a monumental synthetic challenge, for which there still remains no simple or general solution. The earliest evidence for the formation of a dodecayne was reported in 1972.[57,59] This work, by Walton and Johnson, reports the synthesis of *t*-Bu–(C≡C)$_{12}$–*t*-Bu (Scheme 1-23).[57] This comes from the mixed Hay coupling of Et$_3$Si–(C≡C)$_4$–H and H–(C≡C)$_2$–*t*-Bu to give the desired hexayne, which is carefully desilylated with NaOH to give the terminal hexayne. Attempted Hay coupling of this compound resulted in a black solid from which a trace amount of the desired dodecayne could be

observed spectroscopically, but not fully characterized. However, when the terminal hexayne is subjected to Eglinton-Galbraith coupling conditions, also forming a black solid, reddish-brown needles of desired product are isolated after extraction of the black solid with $CHCl_3$ and purification by column chromatography. The product is reported to be very unstable and decomposes in less than 10 min under ambient conditions. Walton and coworkers have formed $Et_3Si–(C{\equiv}C)_{12}–SiEt_3$ and characterized it by UV-visible spectroscopy (Table 1-2, entry 10). This same report provides evidence of $Et_3Si–(C{\equiv}C)_{16}–SiEt_3$ (Table 1-2, entry 11), although characterization was limited to UV-Vis spectroscopic analysis of an impure sample.

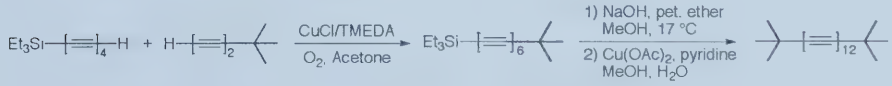


**Scheme 1-23.** Walton and Johnson's synthesis of the *t*-butyl-endcapped dodecayne.

Recently, Cox and coworkers have reported the synthesis of the first aryl-endcapped dodecayne using a very interesting and innovative strategy of $\beta$-chlorovinylsilane elimination (Scheme 1-24).[136] In this case, the 24 carbon skeleton is assembled in the form of a masked dodecayne, which has been constructed through a series of oxidative homocoupling steps using a modified Eglinton–Glaser–Hay coupling condition ($Cu(OTf)_2$, TMEDA, $CH_2Cl_2$, $O_2$). Final polyyne formation is accomplished through exhaustive elimination using TBAF. Unfortunately, they have been unable to isolate this prized material but report analysis by UV-visible spectroscopy and 'matrix free' MALDI-TOF mass spectrometry, confirming its identity.

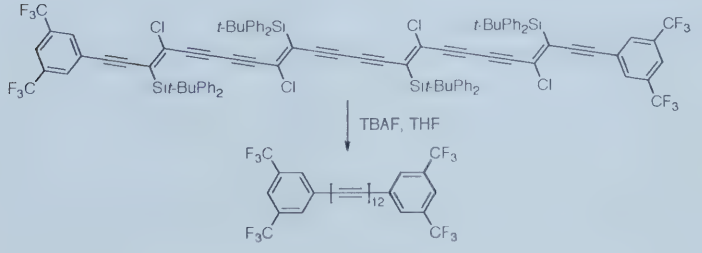


**Scheme 1-24.** Cox and coworkers synthesis of an aryl-endcapped dodecayne.

**Table 1-2.** Known, characterized polyynes with ≥10 acetylene units.

| Entry | Decayne | Characterization | Reference |
|---|---|---|---|
| 1 | | UV-Vis | 59 |
| 2 | | UV-Vis | 59 |
| 3 | 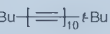 | $^1$H and $^{13}$C NMR, IR, EI HRMS, UV-Vis, DSC, EA, X-ray, DP | 57,104,126 |
| 4 | | UV-Vis, DP | 57 |
| 5 | 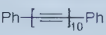 | UV-Vis, IR, DP | 57 |
| 6 | 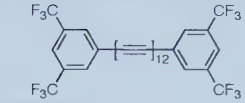 | UV-Vis, MALDI-TOF MS | 136 |
| 7 | 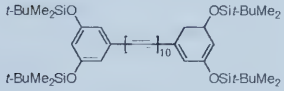 | FAB MS | 125 |
| 8 | 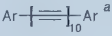 [a] | $^1$H and $^{13}$C NMR, Raman, UV-Vis, FAB MS, CV | 125 |
| 9 | | UV-Vis | 59 |
| 10 | 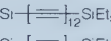 | UV-Vis | 59 |
| 11 | 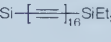 | UV-Vis[b] | 59 |
| 12 | 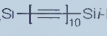 | $^1$H and $^{13}$C NMR, IR, UV-Vis, MALDI MS, DSC, NLO | 84 |
| 13 | 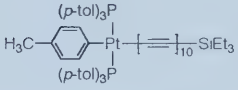 | UV-Vis | 99,102 |
| 14 | 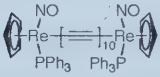 | $^1$H, $^{13}$C, and $^{31}$P NMR, IR, Raman, UV-Vis, FAB MS, CV, DSC | 130 |
| 15 | 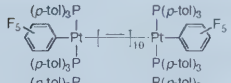 | $^1$H and $^{31}$P NMR[b], IR[b], UV-Vis, FAB MS[b] | 137 |
| 16 | | $^1$H and $^{31}$P NMR[b], IR[b], UV-Vis | 137 |
| 17 | 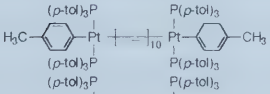 | $^1$H, $^{13}$C, and $^{31}$P NMR, IR, UV-Vis, CV, MS[c], EA, DSC, TGA, NLO | 99,102,132 |
| 18 | 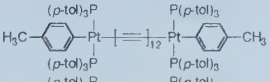 | $^1$H, $^{13}$C, and $^{31}$P NMR, IR, UV-Vis, MS[c], EA, DSC, TGA, NLO | 99,102,132 |
| 19 | 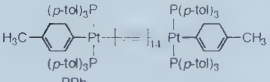 | $^1$H, $^{13}$C, and $^{31}$P NMR, IR, UV-Vis, MS[c], EA, DSC, TGA | 99,102 |
| 20 | 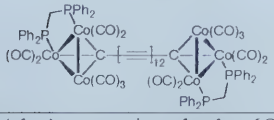 | $^1$H and $^{31}$P NMR, IR, ESI MS | 121 |

[a]Ar = Fréchet's aromatic polyether [G–3] dendrimer. [b]Analysis of an impure sample. [c]Ionization method not reported.

Using the same general protocol as described earlier for metal-endcapped heptaynes (Scheme 1-18), Bruce and coworkers have reported the Pd-catalyzed formation of a dodecayne that is endcapped with carbon-tricobalt clusters (Scheme 1-25). This same reaction gives a lesser amount of the octayne (Table 1-1, entry 14), the result of oxidative homocoupling of two equivalents of the gold-acetylide. While the dodecayne product is reported to be insufficiently soluble for $^{13}C$ NMR spectroscopic analysis, the constitution of the product was confirmed by ESI MS analysis and also characterized by $^{1}H$ NMR, $^{31}P$ NMR, and IR spectroscopies.

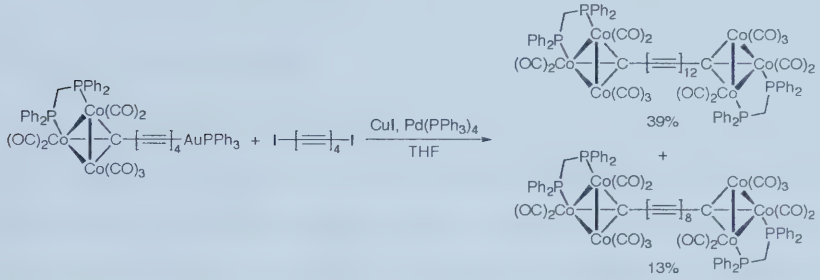


**Scheme 1-25.** Dodecayne synthesis by Bruce and coworkers.

Using a chain length extension protocol, Gladysz and coworkers have successfully achieved stable polyynes well beyond 20 sp-carbons in length (Table 1-2, entries 17-19).[99] This achievement is a breakthrough in the field, proving that polyyne molecules of 24 and even 28 (Scheme 1-26) contiguous sp-hybridized carbons can be synthesized and, perhaps even more importantly, that they are stable. Most remarkable is the fact that they have been able to provide an entire suite of spectroscopic and physical characterization for this series, providing exciting insight into some of the properties of carbyne.

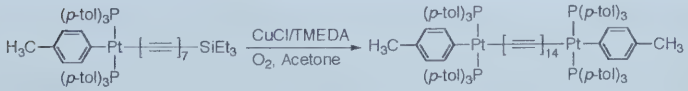


**Scheme 1-26.** Synthesis of a tetradecayne by Gladysz and coworkers.

## 1.4 Interesting and Potentially Useful Properties of Polyynes

The synthesis of molecules containing multiple triple bonds in conjugation, and making them stable, is an impressive feat in its own. Apart from breaking records in conjugation and length, these molecules also possess unique and interesting properties. By making these molecules stable we are now able to realistically utilize these materials for advanced applications. The properties that pose the most interest seem to be that of optics and electronics, which will be discussed briefly in this chapter with detailed analyses to follow in subsequent chapters.

### 1.4.1 UV-Vis Spectroscopy

One of the most diagnostic tools for the characterization of polyynes is UV-Vis spectroscopy. The reason is that the spectra associated with polyynes typically consist of relatively sharp bands (vibrational fine structure). In cases where the endgroup has minimal effect on the polyyne (i.e., through conjugation), the longest wavelength is typically the most intense.[57,59,84,99,104,122,123,126,128,132,133] However, when the endgroup can influence the electronic nature of the polyyne core through conjugation, such as aryl or metal endgroups, this is no longer the case and the longest wavelength may or may not be the most intense.[57,86,115,125,127] All series of polyynes share two common traits: as they get longer there is a bathochromic shift as well as an increase in the absorbtivity. What is also interesting, and potentially useful, is that the longer polyynes become nearly transparent in the high-energy region of the UV-Visible spectrum.

There is a wealth of information that is obtained from UV-Vis data and with the ability to prepare a series of analogous oligomers one can examine structure-function trends as a function of length. The ability to predict the properties of the ultimate polyyne known as carbyne is perhaps one of the biggest reasons to synthesize polyynes. Being able to provide structures that approach or reach saturation of their UV-Vis properties would give a good idea of the optical properties of the sp-carbon allotrope. To date there has been a handful of predictions for this material that include Hirsch and coworkers, whose dendritic polyyne series predicts an absorbance for carbyne at 569 nm.[125] Gladysz and coworkers have also predicted values that are similar such as 565 nm

for their Re-endcapped polyyne series[101] and 573 nm for the Pt-endcapped polyyne series.[99] For a series of TIPS-endcapped polyynes reported by Tykwinski and coworkers, an absorbance of 570 nm was predicted for carbyne.[84] Although these results appear quite consistent a question naturally arises: have we synthesized polyynes long enough to get an accurate prediction of the optical properties of carbyne? In many of the cases where $\lambda_{max}$ is predicted for carbyne, only the data points from the longest polyynes are taken into account and extrapolated to an asymptotic limit. This approach assumes, however, that saturation will occur quickly as one nears the Effective Conjugation Length (ECL). Thus, previous estimates have always placed significant "trust" in the last few points in each analysis, i.e., the longest polyynes in each study. What if this trust is misplaced and the ECL is not yet near? These are the questions that still need to be answered, which is why longer polyynes are still being sought.

### 1.4.2 Nonlinear Optics

Another interesting aspect of polyyne chemistry is their potential as nonlinear optical (NLO) materials.[84,135] Their NLO properties stem from high second hyperpolarizabilities ($\gamma$) which has been measured using a differential optical Kerr effect (DOKE) detection setup.[135] What is interesting is that there is not only an increase in $\gamma$ as a function of length, but that this increase is superlinear with very sizable increases in $\gamma \sim n^c \sim L^c$, where $L$ is the length of the molecule, $n$ is the number of repeat units and $c$ or $c'$ is the power-law exponent. The exponent $c$ is commonly used as a figure of merit on third-order nonlinearities between different conjugated oligomers. Once saturation is approached, exponent $c$ should begin to diminish to a value of $c = 1$, and any increases in conjugation length should no longer have an effect.

For the TIPS polyyne series a value of $c = 4.28$ was obtained which is the largest exponent observed for a series of conjugated oligomers.[84] The phenyl series has also been studied resulting in $c = 3.79$.[86] Both of these molecules display nonlinearities that are far higher than the predicted values of $c = 1.26–3.3$,[138-140] however, saturation has not yet been achieved and thus longer derivatives should result in even larger γ-values.

## 1.5 Conclusions

Polyynes certainly have a place at the table when it comes to new, advanced organic materials for optic, electronic and optoelectronic applications. This is because these molecules display unique optical and nonlinear optical properties that change and even enhance as a function of length. Varying the polyyne length is a simple and efficient method for tuning the electronics to suit our need. Also, polyynes are the frontrunners when it comes to mapping out the properties of the elusive allotrope known as carbyne, because as polyynes become longer, they should begin to resemble this material. However, there is still a lot of work to be done, not only in developing new strategies towards the synthesis of polyynes, especially longer ones (> 20 sp-carbons), but also imparting stability into the molecules to allow for their isolation, purification, characterization and maybe even application. The following chapters of this thesis will touch on old and new tactics towards polyyne synthesis and a story that details the progression of polyyne endgroup development that allowed for the synthesis of really long polyynes.

## 1.6 References


[1] Bunz, U. H. F. *Macromol. Rapid Commun.* **2009**, *30*, 772.

[2] Yang, S.-H.; Hsu, C.-S. *J. Polym. Sci., Part A: Polym. Chem.* **2009**, *47*, 2713.

[3] Cho, M. J.; Choi, D. H.; Sullivan, P. A.; Akelaitis, A. J. P.; Dalton, L. R. *Prog. Polym. Sci.* **2008**, *33*, 1013.

[4] *The Properties of Natural and Synthetic Diamond*; Field, J. E., Ed; Academic Press: London, 1992.

[5] Kirk, R. E.; Othmer, D. F.; Grayson, M.; Eckroth, D. In *Kirk-Othmer Encyclopedia of Chemical Technology*; 3 ed.; Wiley: New York, 1978; Vol. 4, pp 556.

[6] Falcao, E. H. L.; Wudl, F. *J. Chem. Technol. Biotechnol.* **2007**, *82*, 524.

[7] *Carbon Materials for Advances Technologies*; Burchell, T. D., Ed; Pergamon: New York, 1999.

[8] Kelly, B. T. *Physics of Graphite*; Applied Science Publishers: London, 1981.

[9] Shirota, Y.; Kageyama, H. *Chem. Rev.* **2007**, *107*, 953.

[10] Murphy, A. R.; Fréchet, J. M. J. *Chem. Rev.* **2007**, *107*, 1066.

[11] He, G. S.; Tan, L.-S.; Zheng, Q.; Prasad, P. N. *Chem. Rev.* **2008**, *108*, 1245.

[12] Bunz, U. H. F.; Rubin, Y.; Tobe, Y. *Chem. Soc. Rev.* **1999**, *28*, 107.

[13] Diederich, F.; Rubin, Y. *Angew. Chem. Int. Ed.* **1992**, *31*, 1101.

[14] Hoeben, F. J. M.; Jonkheijm, P.; Meijer, E. W.; Schenning, A. P. H. J. *Chem. Rev.* **2005**, *105*, 1491.

[15] Anthony, J. E. *Chem. Rev.* **2006**, *106*, 5028.

[16] *Acetylene Chemistry*; Diederich, F.; Stang, P. J.; Tykwinski, R. R., Eds; Wiley-VCH: Weinheim, 2005; p 508.

[17] *Modern Acetylene Chemistry*; Stang, P. J.; Diederich, F., Eds; VCH: Weinheim, 1995.

[18] Martin, R. E.; Diederich, F. *Angew. Chem. Int. Ed.* **1999**, *38*, 1350.

[19] Meier, H. *Angew. Chem. Int. Ed.* **2005**, *44*, 2482.

[20] *Carbon-Rich Compounds: From Molecules to Materials*; Haley, M. M.; Tykwinski, R. R., Eds; Wiley-VCH: Weinheim, 2006.

[21] *Electronic Materials: The Oligomer Approach*; Müllen, K.; Wegner, G., Eds; Wiley-VCH: Weinheim, 1998.

[22] Meier, H. In *Carbon-Rich Compounds: From Molecules to Materials*; Haley, M. M.; Tykwinski, R. R., Eds; Wiley-VCH: Weinheim, 2006; pp 476.

[23] Nielsen, M. B.; Diederich, F. *Chem. Rev.* **2005**, *105*, 1837.

[24] Pilzak, G. S.; van Lagen, B.; Hendrikx, C. C. J.; Sudhölter, E. J. R.; Zuilhof, H. *Chem. Eur. J.* **2008**.

[25] Gholami, M.; Tykwinski, R. R. *Chem. Rev.* **2006**, *106*, 4997.

[26] Martin, R. E.; Gubler, U.; Cornil, J.; Balakina, M.; Boudon, C.; Bosshard, C.; Gisselbrecht, J.-P.; Diederich, F.; Günter, P.; Gross, M.; Brédas, J.-L. *Chem. Eur. J.* **2000**, *6*, 3622.

[27] Bunz, U. H. F. *Chem. Rev.* **2000**, *100*, 1605.

[28] McQuade, D. T.; Pullen, A. E.; Swager, T. M. *Chem. Rev.* **2000**, *100*, 2537.

[29] Frampton, M. J.; Anderson, H. L. *Angew. Chem. Int. Ed.* **2007**, *46*, 1028.

[30] Tahara, K.; Tobe, Y. *Chem. Rev.* **2006**, *106*, 5274.

[31] Kawase, T.; Kurata, H. *Chem. Rev.* **2006**, *106*, 5250.

[32] Swager, T. In *Acetylene Chemistry - Chemistry, Biology and Material Science*; Diederich, F.; Stang, P. J.; Tykwinski, R. R., Eds; Wiley-VCH: Weinheim, 2005; pp 233.

[33] Tobe, Y.; Wakabayashi, T. In *Acetylene Chemistry - Chemistry, Biology and Material Science*; Diederich, F.; Stang, P. J.; Tykwinski, R. R., Eds; Wiley-VCH: Weinheim, 2005; pp 387.

[34] Chalifoux, W. A.; Tykwinski, R. R. *Chem. Rec.* **2006**, *6*, 169.

[35] Yam, V. W. W.; Tao, C. H. In *Carbon-Rich Compounds: From Molecules to Materials*; Haley, M. M.; Tykwinski, R. R., Eds; Wiley-VCH: Weinheim, 2006; pp 421.

[36] Wei, D.; Liu, Y.; Zhang, H.; Huang, L.; Wu, B.; Chen, J.; Yu, G. *J. Am. Chem. Soc.* **2009**, *131*, 11147.

[37] Dikin, D. A.; Stankovich, S.; Zimney, E. J.; Piner, R. D.; Dommett, G. H. B.; Evmenenko, G.; Nguyen, S. T.; Ruoff, R. S. *Nature* **2007**, *448*, 457.

[38] Jiao, L. Y.; Zhang, L.; Wang, X. R.; Diankov, G.; Dai, H. J. *Nature* **2009**, *458*, 877.

[39] Kosynkin, D. V.; Higginbotham, A. L.; Sinitskii, A.; Lomeda, J. R.; Dimiev, A.; Price, B. K.; Tour, J. M. *Nature* **2009**, *458*, 872.

[40] Novoselov, K. S.; Geim, A. K.; Morozov, S. V.; Jiang, D.; Zhang, Y.; Dubonos, S. V.; Grigorieva, I. V.; Firsov, A. A. *Science* **2004**, *306*, 666.

[41] Li, X. L.; Wang, X. R.; Zhang, L.; Lee, S. W.; Dai, H. J. *Science* **2008**, *319*, 1229.

[42] Li, X. L.; Zhang, G. Y.; Bai, X. D.; Sun, X. M.; Wang, X. R.; Wang, E. G.; Dai, H. J. *Nature Nanotechnology* **2008**, *3*, 538.

[43] Hernandez, Y. *Nature Nanotechnology* **2008**, *3*, 563.

[44] Choucair, M.; Thordarson, P.; Stride, J. A. *Nature Nanotechnology* **2009**, *4*, 30.

[45] Cataldo, F. *Polym. Int.* **1997**, *44*, 191.

[46] *Polyynes: Synthesis, Properies, and Applications*; Cataldo, F., Ed; CRC Press: Boca Raton, 2006.

[47] Kudryavtsev, Y. P.; Evsyukoc, S.; Gusevca, M.; Babaev, C.; Khvistov, C. In *Chemistry and Physics of Carbon*; Thrower, P. A., Ed; Dekker: New York, 1997; Vol. 25, pp 1.

[48] Lagow, R. J.; Kampa, J. J.; Wei, H.-C.; Battle, S. L.; Genge, J. W.; Laude, D. A.; Harper, C. J.; Bau, R.; Stevens, R. C.; Haw, J. F.; Munson, E. *Science* **1995**, *267*, 362.

[49] Smith, P. P. K.; Buseck, P. R. *Science* **1982**, *216*, 984.

[50] www.theodoregray.com and www.seilnacht.com

[51] Bunz, U. H. F. *Angew. Chem. Int. Ed.* **1996**, *35*, 969.

[52] Jones, E. R. H.; Thaller, V. In *The Chemistry of the Carbon-Carbon Triple Bond*; Patai, S., Ed; Wiley: New York, 1978; Vol. 2, pp 621.

[53] Jones, E. R. H. *Proc. Chem. Soc. Lond.* **1960**, 199.

[54] Bohlmann, F. *Angew. Chem.* **1953**, *65*, 385.

[55] Bohlmann, F. *Fortschr. Chem. Forsch.* **1966**, *6*, 65.

[56] Bohlmann, F.; Bornowski, H.; Arndt, C. *Fortschr. Chem. Forsch.* **1962**, *4*, 138.

[57] Johnson, T. R.; Walton, D. R. M. *Tetrahedron* **1972**, *28*, 5221.

[58] Eastmond, R.; Johnson, T. R.; Walton, D. R. M. *J. Organomet. Chem.* **1973**, *50*, 87.

[59] Eastmond, R.; Johnson, T. R.; Walton, D. R. M. *Tetrahedron* **1972**, *28*, 4601.

[60] Nakagawa, M.; Akiyama, S.; Nakasuji, K.; Nishimoto, K. *Tetrahedron* **1971**, *27*, 5401.

[61] Siemsen, P.; Livingston, R. C.; Diederich, F. *Angew. Chem. Int. Ed.* **2000**, *39*, 2632.

[62] Weller, M. D.; Cox, L. R. *C. R. Chimie* **2009**, *12*, 366.

[63] Orita, A.; Otera, J. *Chem. Rev.* **2006**, *106*, 5387.

[64] Tobe, Y.; Umeda, R.; Iwasa, N.; Sonoda, M. *Chem. Eur. J.* **2003**, *9*, 5549.

[65] Glaser, C. *Ber. Dtsch. Chem. Ges.* **1869**, *2*, 422.

[66] Eglinton, G.; Galbraith, A. R. *Chem. Ind. (London)* **1956**, 737.

[67] Hay, A. S. *J. Org. Chem.* **1962**, *27*, 3320.

[68] Lei, A.; Srivastava, M.; Zhang, X. *J. Org. Chem.* **2002**, *67*, 1969.

[69] Chalifoux, W. A.; Ferguson, M. J.; Tykwinski, R. R. *Eur. J. Org. Chem.* **2007**, 1101.

[70] Marsden, J. A.; Miller, J. J.; Haley, M. M. *Angew. Chem. Int. Ed.* **2004**, *43*, 1694.

[71] Li, J.-H.; Liang, Y.; Xie, Y.-X. *J. Org. Chem.* **2005**, *70*, 4393.

[72] Bohlmann, F.; Schönowsky, H.; Inhoffen, E.; Grau, G. *Chem. Ber.* **1964**, *97*, 794.

[73] Cadiot, P.; Chodkiewicz, W. In *Chemistry of Acetylenes*; Viehe, H. G., Ed; Dekker: New York, 1969; pp 597.

[74] Marino, J. P.; Nguyen, H. N. *J. Org. Chem.* **2002**, *67*, 6841.

[75] Nishihara, Y.; Ikegashira, K.; Hirabayashi, K.; Ando, J.-i.; Mori, A.; Hiyama, T. *J. Org. Chem.* **2000**, *65*, 1780.

[76] Kim, S.; Kim, S.; Lee, T.; Ko, H.; Kim, D. *Org. Lett.* **2004**, *6*, 3601.

[77] Buttenberg, W. P. *Liebigs Ann. Chem.* **1894**, *279*, 324.

[78] Fritsch, P. *Liebigs Ann. Chem.* **1894**, *279*, 319.

[79] Wiechell, H. *Liebigs Ann. Chem.* **1894**, *279*, 337.

[80] Stang, P. J. *Chem. Rev.* **1978**, *78*, 383.

[81] Knorr, R. *Chem. Rev.* **2004**, *104*, 3795.

[82] Kirmse, W. *Angew. Chem. Int. Ed.* **1997**, *36*, 1164.

[83] Eisler, S.; Chahal, N.; McDonald, R.; Tykwinski, R. R. *Chem. Eur. J.* **2003**, *9*, 2542.

[84] Eisler, S.; Slepkov, A. D.; Elliott, E.; Luu, T.; McDonald, R.; Hegmann, F. A.; Tykwinski, R. R. *J. Am. Chem. Soc.* **2005**, *127*, 2666.

[85] Kendall, J.; McDonald, R.; Ferguson, M. J.; Tykwinski, R. R. *Org. Lett.* **2008**, *10*, 2163.

[86] Luu, T.; Elliott, E.; Slepkov, A. D.; Eisler, S.; McDonald, R.; Hegmann, F. A.; Tykwinski, R. R. *Org. Lett.* **2005**, *7*, 51.

[87] Luu, T.; Morisaki, Y.; Cunningham, N.; Tykwinski, R. R. *J. Org. Chem.* **2007**, *72*, 9622.

[88] Luu, T.; Shi, W.; Lowary, T. L.; Tykwinski, R. R. *Synthesis* **2005**, 3167.

[89] Spantulescu, A.; Luu, T.; Zhao, Y.; McDonald, R.; Tykwinski, R. R. *Org. Lett.* **2008**, *10*, 609.

[90] Ochiai, M.; Nishi, Y.; Goto, S.; Frohn, H. J. *Angew. Chem. Int. Ed.* **2005**, *44*, 406.

[91] Ochiai, M. *Synlett* **2009**, 159.

[92] Li, J.; Park, S.; Miller, R. L.; Lee, D. *Org. Lett.* **2009**, *11*, 571.

[93] Robertson, J.; Naud, S. *Org. Lett.* **2008**, *10*, 5445.

[94] Xu, G.-L.; Xi, B.; Updegraff, J. B.; Protasiewicz, J. D.; Ren, T. *Organometallics* **2006**, *25*, 5213.

[95] Heuft, M. A.; Collins, S. K.; Yap, G. P. A.; Fallis, A. G. *Org. Lett.* **2001**, *3*, 2883.

[96] Mukai, C.; Miyakoshi, N.; Hanaoka, M. *J. Org. Chem.* **2001**, *66*, 5875.

[97] Ikegashira, K.; Nishihara, Y.; Hirabayashi, K.; Mori, A.; Hiyama, T. *Chem. Comm.* **1997**, 1039.

[98] Haley, M. M.; Bell, M. L.; Brand, S. C.; Kimball, D. B.; Pak, J. J.; Wan, W. B. *Tetrahedron Lett.* **1997**, *38*, 7483.

[99] Zheng, Q.; Bohling, J. C.; Peters, T. B.; Frisch, A. C.; Hampel, F.; Gladysz, J. A. *Chem. Eur. J.* **2006**, *12*, 6486.

[100] Cook, C. L.; Jones, E. R. H.; Whiting, M. C. *J. Chem. Soc.* **1952**, 2883.

[101] Dembinski, R.; Bartik, T.; Bartik, B.; Jaeger, M.; Gladysz, J. A. *J. Am. Chem. Soc.* **2000**, *122*, 810.

[102] Zheng, Q.; Gladysz, J. A. *J. Am. Chem. Soc.* **2005**, *127*, 10508.

[103] Rubin, Y.; Lin, S. S.; Knobler, C. B.; Anthony, J.; Boldi, A. M.; Diederich, F. *J. Am. Chem. Soc.* **1991**, *113*, 6943.

[104] Chalifoux, W. A.; McDonald, R.; Ferguson, M. J.; Tykwinski, R. R. *Angew. Chem. Int. Ed.* **2009**, *48*, 7915.

[105] Cataldo, F. *Tetrahedron* **2004**, *60*, 4265.

[106] Cataldo, F. *Carbon* **2003**, *41*, 2671.

[107] Cataldo, F. *Tetrahedron Lett.* **2004**, *45*, 141.

[108] Métay, E.; Hu, Q.; Negishi, E.-i. *Org. Lett.* **2006**, *8*, 5773.

[109] Lucotti, A.; Tommasini, M.; Fazzi, D.; Del Zoppo, M.; Chalifoux, W. A.; Ferguson, M. J.; Zerbi, G.; Tykwinski, R. R. *J. Am. Chem. Soc.* **2009**, *131*, 4239.

[110] Wang, C.; Batsanov, A. S.; West, K.; Bryce, M. R. *Org. Lett.* **2008**, *10*, 3069.

[111] West, K.; Wang, C.; Batsanov, A. S.; Bryce, M. R. *Org. Biomol. Chem.* **2008**, *6*, 1934.

[112] West, K.; Wang, C.; Batsanov, A. S.; Bryce, M. R. *J. Org. Chem.* **2006**, *71*, 8541.

[113] Ruitenberg, K.; Kleijn, H.; Westmijze, H.; Meijer, J.; Vermeer, P. *J. R. Neth. Chem. Soc.* **1982**, *101*, 405.

[114] Weller, M. D.; Kariuki, B. M.; Cox, L. R. *Tetrahedron Lett.* **2008**, *49*, 4596.

[115] Klinger, C.; Vostrowsky, O.; Hirsch, A. *Eur. J. Org. Chem.* **2006**, 1508.

[116] de Quadras, L.; Bauer, E. B.; Mohr, W.; Bohling, J. C.; Peters, T. B.; Martín-Alvarez, J. M.; Hampel, F.; Gladysz, J. A. *J. Am. Chem. Soc.* **2007**, *129*, 8296.

[117] Stahl, J.; Mohr, W.; de Quadras, L.; Peters, T. B.; Bohling, J. C.; Martín-Alvarez, J. M.; Owen, G. R.; Hampel, F.; Gladysz, J. A. *J. Am. Chem. Soc.* **2007**, *129*, 8282.

[118] Sugiyama, J.; Tomita, I. *Eur. J. Org. Chem.* **2007**, 4651.

[119] Bohlmann, F. *Chem. Ber.* **1953**, *86*, 657.

[120] Antonova, A. B.; Bruce, M. I.; Ellis, B. G.; Gaudio, M.; Humphrey, P. A.; Jevric, M.; Melino, G.; Nicholson, B. K.; Perkins, G. J.; Skelton, B. W.; Stapleton, B.; White, A. H.; Zaitseva, N. N. *Chem. Comm.* **2004**, 960.

[121] Bruce, M. I.; Zaitseva, N. N.; Nicholson, B. K.; Skelton, B. W.; White, A. H. *J. Organomet. Chem.* **2008**, *693*, 2887.

[122] Tsuji, M.; Tsuji, T.; Kuboyama, S.; Yoon, S.-H.; Korai, Y.; Tsujimoto, T.; Kubo, K.; Mori, A.; Mochida, I. *Chem. Phys. Lett.* **2002**, *355*, 101.

[123] Schermann, G.; Grösser, T.; Hampel, F.; Hirsch, A. *Chem. Eur. J.* **1997**, *3*, 1105.

[124] Grösser, T.; Hirsch, A. *Angew. Chem. Int. Ed.* **1993**, *32*, 1340.

[125] Gibtner, T.; Hampel, F.; Gisselbrecht, J.-P.; Hirsch, A. *Chem. Eur. J.* **2002**, *8*, 408.

[126] Jones, E. R. H.; Lee, H. H.; Whiting, M. C. *J. Chem. Soc.* **1960**, 3483.

[127] Armitage, J. B.; Entwistle, N.; Jones, E. R. H.; Whiting, M. C. *J. Chem. Soc.* **1954**, 147.

[128] Schlögl, K.; Steyrer, W. *J. Organomet. Chem.* **1966**, *6*, 399.

[129] Nakamura, K.; Fujimoto, T.; Takara, S.; Sugiura, K.-i.; Miyasaka, H.; Ishii, T.; Yamashita, M.; Sakata, Y. *Chem. Lett.* **2003**, *32*, 694.

[130] Bartik, T.; Bartik, B.; Brady, M.; Dembinski, R.; Gladysz, J. A. *Angew. Chem. Int. Ed.* **1996**, *35*, 414.

[131] Mohr, W.; Stahl, J.; Hampel, F.; Gladysz, J. A. *Inorg. Chem.* **2001**, *40*, 3263.

[132] Samoc, M.; Dalton, G. T.; Gladysz, J. A.; Zheng, Q.; Velkov, Y.; Ågren, H.; Norman, P.; Humphrey, M. G. *Inorg. Chem.* **2008**, *47*, 9946.

[133] Hoheisel, T. N.; Frauenrath, H. *Org. Lett.* **2008**, *10*, 4525.

[134] Elliot, E.; Tykwinski, R. R. *unpublished results.*

[135] Slepkov, A. D.; Hegmann, F. A.; Eisler, S.; Elliott, E.; Tykwinski, R. R. *J. Chem. Phys.* **2004**, *120*, 6807.

[136] Simpkins, S. M. E.; Weller, M. D.; Cox, L. R. *Chem. Comm.* **2007**, 4035.

[137] Mohr, W.; Stahl, J.; Hampel, F.; Gladysz, J. A. *Chem. Eur. J.* **2003**, *9*, 3324.

[138] Nalwa, H. S.; Mukai, J.; Kakuta, A. *J. Phys. Chem.* **1995**, *99*, 10766.

[139] Buma, W. J.; Fanti, M.; Zerbetto, F. *Chem. Phys. Lett.* **1999**, *313*, 426.

[140] Archibong, E. F.; Thakkar, A. J. *J. Chem. Phys.* **1993**, *98*, 8324.

# Chapter 2 Synthesis of Tris(4-biphenyl-4-yl)silyl-Endcapped Polyynes[‡]

## 2.1 Introduction

One of the biggest hurdles with regards to the synthesis of polyynes is the fact that stability decreases substantially as a function of length.[1] This decreased stability leads to decomposition of the polyyne as a result of indiscriminate intermolecular reactions (polymerization). It is because of this that there are very few reports of polyyne syntheses beyond 20 sp-carbons (decayne) in length[2-7] and of these polyynes only one has reportedly been isolated and sufficiently characterized.[2,7] It has been shown that the stability of a polyyne can be enhanced by placing bulky endgroups at the termini of the polyyne, which act to shield the reactive polyyne core from decomposition.[8,9] Excellent examples of this were recently reported by Hirsch and coworkers,[10] as well as Gladysz and coworkers.[11]

The bulky nature of the triisopropylsilyl (TIPS) endgroup has been utilized to increase the stability of polyynes, allowing for the successful synthesis of a series of polyynes up to 20 carbons in length.[8] It was envisioned that utilizing an even larger silyl endgroup would serve to increase the stability of the polyyne and allow for the formation of stable polyynes beyond 20 carbons in length. Thus, the tris(biphenyl-4-yl)silyl (TBPS) endgroup was ultimately designed, and it shows a diameter over twice that of the TIPS group (Figure 2-1).[12] It was predicted that the large size of this endgroup should prevent approach of extended polyyne molecules to within the 4 Å distance required for intermolecular cross-linking to occur (decomposition from polymerization).[13,14] Because this endgroup was also reasonably easy to access, its potential as a polyyne protecting group was explored.

---

[‡] Portions of this chapter have been published. Chalifoux, W. A.; Ferguson, M. J.; Tykwinski, R. R. *Eur. J. Org. Chem.* **2007**, 1101.

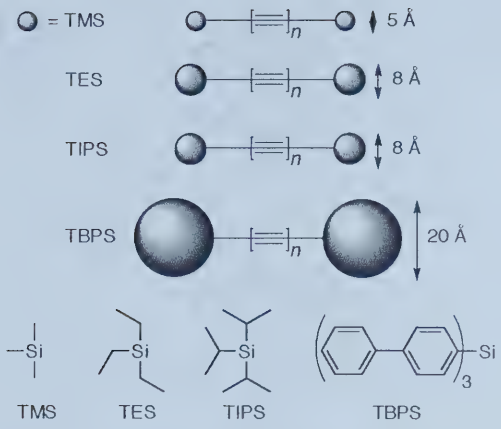


**Figure 2-1.** Approximate size relationship of common silyl endgroups.

## 2.2 Results and Discussion

### 2.2.1 Large Triarylsilyl Endgroup for the Stabilization of Polyynes, Initial Design

Before going into the details that ultimately led to the tris(4-biphenyl-4-yl)silyl (TBPS) polyyne series it would be prudent to explain the series of events that led up to the synthesis of these molecules. First, the hypothesis that bulky endgroups inherently stabilize polyynes directed this project. Therefore, an endgroup was sought that was similar in nature to the TIPS endgroup (i.e., $SiR_3$) but with a much larger size. A "shoot for the stars" approach was followed by dreaming up a silyl group that contained three hexaphenylbenzene (HPB) groups (Figure 2-2). The resulting tris(hexaphenylbenzene)silyl (THPBS) endgroup was modeled and showed to be approximately 30 Å in diameter.[12] This is over four times larger than a TIPS group and gave confidence that polyynes derived from this endgroup would be much more stable than the TIPS analogues, allowing for longer derivatives to be synthesized and isolated.

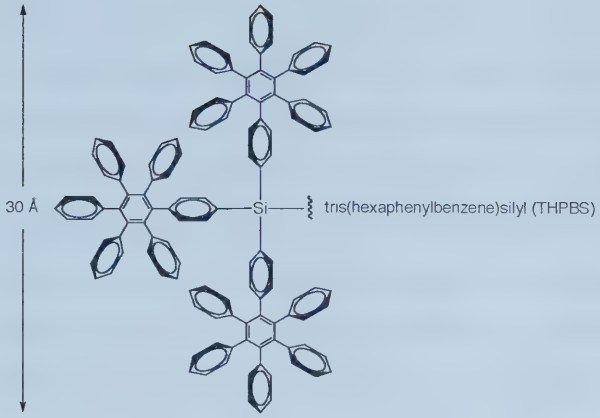


**Figure 2-2.** Tris(hexaphenylbenzene)silyl (THPBS) endgroup.

The attempted synthesis of the THPBS endgroup started with the synthesis of bromotolan (**2.1**), which was obtained from the Pd-catalyzed crosscoupling of 4-bromo-1-iodobenzene and phenylacetylene in good yield (Scheme 1).[15] The bromotolan (**2.1**) underwent a [4+2] cycloaddition reaction with 2,3,4,5-tetraphenylcyclopenta-2,4-dien-1-one at high temperature to give bromo-HPB in excellent yield (**2.2**).[15]

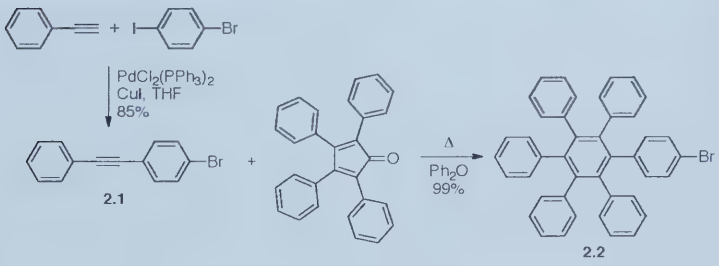


**Scheme 2-1.** Synthesis of bromo-HPB (**2.2**).

The formation of the Grignard reagent was attempted by the reaction of **2.2** with freshly ground Mg turnings. None of the Grignard reagent formed, even with addition of a catalytic amount of $I_2$ crystals. Lithium-halogen exchange was thus effected on **2.2** using *n*-BuLi. The

lithium-halogen exchange was not successful when carried out in diethyl ether due to solubility issues, but the reaction did work in THF. The addition of the lithiated **2.2** intermediate to $SiCl_4$, however, resulted in no desired product, with 98% isolation of HPB resulting from protonation of the intermediate upon workup. The higher boiling toluene was attempted as the solvent but, again, no lithium-halogen exchange occurred. However, when a small amount of diethyl ether was added, the lithium-halogen exchange proceeded smoothly. Once again, the addition of the lithiated **2.2** intermediate to $SiCl_4$ and heating to reflux led to no desired product. It is possible that the lithiated intermediate is too sterically hindered to add to $SiCl_4$. It is somewhat strange that not even one equivalent of the nucleophile added to $SiCl_4$, even after three days with heating. Realizing how difficult is to add one equivalent to $SiCl_4$ suggested that the addition of three equivalents to $SiCl_4$ would be impossible. After further evaluation of the structure it seemed plausible that the *ortho* phenyl groups would cause a steric problem for the addition of three equivalents of lithiated **2.2** (labeled in red, Figure 2-3a). Removal of these phenyl groups from THPBS results in an endgroup that is approximately the same diameter as THPBS, however, the synthesis of this derivative seemed unnecessarily difficult. Upon searching the literature, a similar derivative was discovered, the synthesis of which seemed relatively straightforward using readily available and inexpensive starting materials, thus, the tris(triphenylbenzene)silyl (TTPBS) group was targeted (Figure 2-3b).

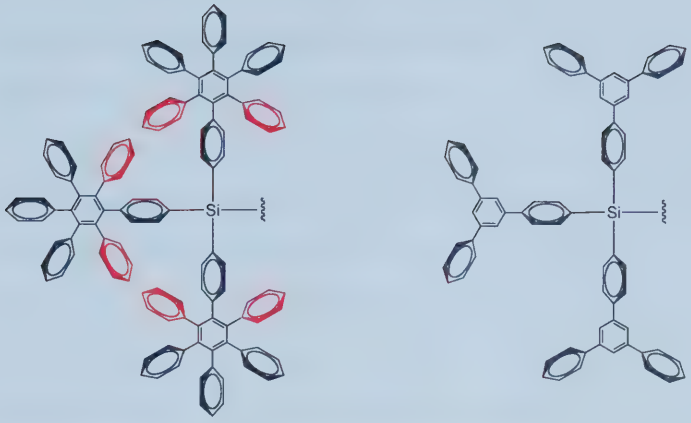


**Figure 2-3.** a) THPBS endgroup showing the ortho phenyl groups (shown in red) in close proximity with each other making it difficult to place three of these on one silicon atom. b) Tris(triphenylbenzene)silyl (TTPBS) endgroup.

### 2.2.2 Large Triarylsilyl Endgroup for the Stabilization of Polyynes, Revised Design

The synthesis of the TTPBS endgroup was initiated by the synthesis of dypnone (**2.3**). Dypnone (**2.3**) was easily synthesized in moderate yield by the self-aldol condensation reaction of acetophenone in the presence of $SiCl_4$ followed by dehydration (Scheme 2-2). Dypnone (**2.3**) was then allowed to react with 4′-bromoacetophenone in the presence of $SiCl_4$ to form bromotriphenylbenzene (**2.4**).[16] This step presumably goes through [4+2] cycloaddition/dehydration to afford the desired product.

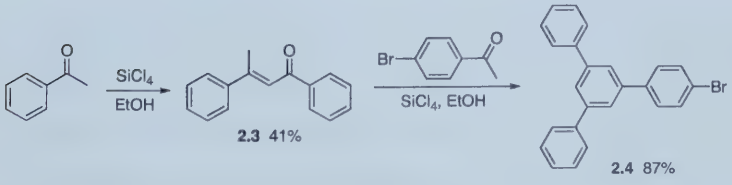


**Scheme 2-2.** Synthesis of dypnone (**2.3**) and bromotriphenylbenzene (**2.4**).

With **2.4** in hand, it was presumed that lithiation or Grignard formation from **2.4**, followed by addition to $SiCl_4$, would yield the desired TTPBS endgroup. Before any attempt was made using **2.4** it was decided to first carry out a few test reactions for the formation of a triarylsilyl group. This was done as a one-pot addition of three equivalents of phenyllithium to $SiCl_4$ followed by the addition of one equivalent of lithiated trimethylsilylacetylene to generate 2-trimethylsilyl-1-triphenylsilylethyne **2.5** (Scheme 2-3). While the one-pot synthesis of a tetraarylsilane containing at least two different functional groups has been demonstrated,[17] to our knowledge this is the first example of a multi-component reaction to obtain an ethynyltriarylsilane. While this has shown that this route was possible on the simple phenyl system in good yield (74%), it was unclear as to whether it would be transferable to a polyphenyl system and another model system, the TBPS, was devised.

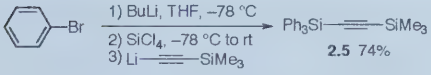


**Scheme 2-3.** Synthesis of **2.5** as a model system for larger triarylsilyl polyynes.

### 2.2.3 TBPS Polyynes: A Model System for Larger Triarylsilyl Endgroups

Before jumping into synthesizing large amounts of compound **2.4** in order to make the TTPBS-endcapped polyynes, the very similar, yet simple model system, i.e., the TBPS endgroup, was chosen to test reaction condition compatibility and the resulting product stability. The TBPS endgroup is easily made from readily available 4-halogenated biphenyl derivatives. The synthesis of the protected TBPS target, **2.6**, was optimized and achieved in one-pot with yields up to 76% by the sequential addition of three equivalents of lithiated biphenyl and one equivalent of lithiated TMS acetylene to $SiCl_4$ (Scheme 2-4). The synthesis of **2.6** was also successful using the corresponding biphenyl Grignard reagent, however, yields were lower (ca. 30%). Modeling of this compound showed that this endgroup is quite large on its own being ca. 20 Å in diameter.[12] Since the TBPS endgroup was similar in size to the TTPBS endgroup, and bulk quantities could be

synthesized easily without any prior synthetic steps, the synthesis of polyynes utilizing this endgroup was attempted. If successful, the TTPBS endgroup would be revisited using the same strategy after optimization of the conditions.

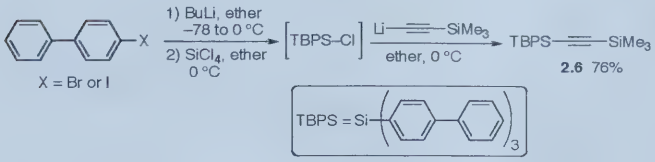


**Scheme 2-4.** "One-pot" synthesis of unsymmetrical acetylene **2.6**.

Under protiodesilylation conditions at 0 °C, the TMS group of **2.6** could be selectively removed to yield **2.7** in excellent yield (Scheme 2-5). It should be noted that at higher temperatures, or prolonged exposure to these conditions, the TBPS group was also cleaved leading to decreased yield of **2.7**. The attempted synthesis of **2.8** using Hay[18,19] conditions was unsuccessful, leading to poor yields. However, the synthesis of **2.8** has been carried out in good yield under Pd-catalyzed homocoupling conditions reported by Zhang and coworkers.[20]

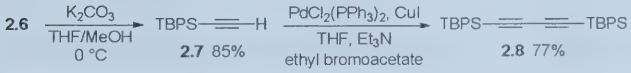


**Scheme 2-5.** Selective protiodesilylation of **2.6** followed by Pd-catalyzed homocoupling to give diyne **2.8**.

X-ray crystallographic characterization of **2.8** showed a radius of approximately 10 Å for the TBPS group, consistent with the modeling study, and clearly demonstrates its larger size in comparison to the TIPS group (Figure 2-4a).[8,12] This sterically demanding endgroup places each polyyne core a distance of 8 Å from its nearest neighbor in the crystal lattice, double the maximum allowable separation distance required for an intermolecular reaction to occur (Figure 2-4b).[13,14,21]

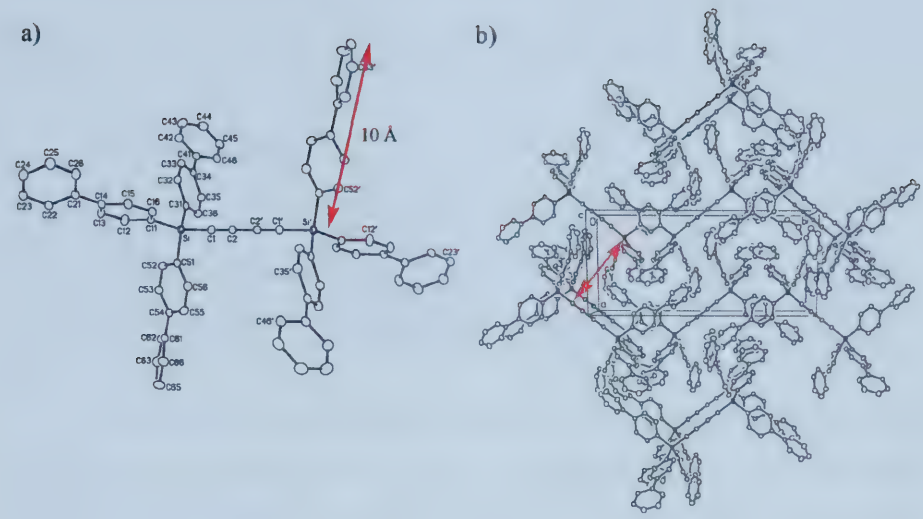


**Figure 2-4.** a) X-ray crystal structure of **2.8** showing the radius of the TBPS endgroup. b) Crystal packing of **2.8**, with the red arrow showing a distance of 8 Å between neighboring molecules (all shown at 20% probability, hydrogen atoms removed for clarity).

Treatment of **2.6** with *N*-bromosuccinimide in the presence of catalytic silver nitrate gave bromide **2.9** directly in excellent yield without the need for prior desilylation (Equation 1).[22] The synthesis of **2.9** could also be carried out from **2.7** under the same conditions.[23] The subsequent synthesis of differentially protected **2.10** was accomplished under Pd-catalyzed crosscoupling

condition between **2.7** (or **2.9**) and **2.11** (or **2.12**) in moderate yield (Table 1).[19] The main side products from this reaction were the homocoupled product (**2.8**) and bis(TMS)butadiyne, which could be separated chromatographically. Many variants of this reaction were attempted with surprisingly little effect on the yield. The best yield was ultimately obtained by coupling both terminal acetylenes (**2.7** and **2.11**) in the presence of ethyl bromoacetate as the oxidant (Entry 6).

**Table 2-1.** Synthesis of **2.10** via Pd-catalyzed crosscoupling.

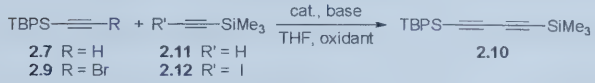


| Entry | Substrate 1 | Substrate 2 | Catalyst system | Base | Oxidant | Yield |
|---|---|---|---|---|---|---|
| 1 | **2.9** | **2.11** | $PdCl_2(PPh_3)_2$/CuI | *i*-$Pr_2NH$ | N/A | 45% |
| 2 | **2.9** | **2.11** | $Pd(PPh_3)_4$/CuI | *i*-$Pr_2NH$ | N/A | 39% |
| 3 | **2.9** | **2.11** | $PdCl_2(PPh_3)_2$/CuCl | *i*-$Pr_2NH$ | N/A | 54% |
| 4 | **2.7** | **2.12** | $PdCl_2(PPh_3)_2$/CuI | $Et_3N$ | N/A | 44% |
| 5 | **2.7** | **2.12** | $PdCl_2(PPh_3)_2$/CuI | *i*-$Pr_2NH$ | N/A | 48% |
| 6 | **2.7** | **2.11** | $PdCl_2(PPh_3)_2$/CuI | *i*-$Pr_2NH$ | ethyl bromoacetate | 57% |

The selective deprotection of **2.10** proved to be more problematic than anticipated. When the conditions that were used for the deprotection of **2.6** were applied, the chemoselectivity for the TMS group over the TBPS group diminished considerably, even at low temperature. Desilylation with one equivalent of TBAF was attempted at 0 °C, but led only to a modest 27% yield of desired product. These results suggested that an even milder desilylation procedure needed to be established. It was found that by adding $Et_3N$ to **2.10** in a solution of wet THF, desilylation did occur with better selectivity. Yields of ca. 55% were consistently obtained when the reaction was carefully monitored and immediately stopped when complete. Ultimately, it was determined that $NaHCO_3$ in a 1:1 mixture of THF/MeOH at low temperature gave **2.13** in excellent yield (Scheme 2-6). Unlike the synthesis of diyne **2.8**, standard Hay coupling conditions gave tetrayne **2.14** in good yield. Tetrayne **2.14** shows exceptional stability in the solid state, decomposing only at temperatures above 250 °C, as determined by capillary thermolysis.

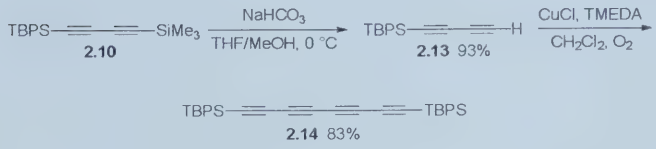


**Scheme 2-6.** Desilylation of **2.10** using mild basic conditions followed by Hay coupling to give tetrayne **2.14**.

The in situ desilylation/bromination of **2.10** giving **2.15** was achieved in excellent yield by cooling the reaction to 0 °C (Scheme 2-7). An unfortunate problem with this reaction was that it was very slow, requiring 3-6 days to reach completion. Higher temperatures, however, led to a decrease in selectivity. The rate of the reaction could be enhanced by adding five times the amount of silver nitrate, allowing for the complete reaction in 24 hours. An interesting spectral feature for **2.15** occurs in the $^{13}C$ NMR spectrum, where the C(1) carbon resonates upfield at 42.4 ppm in $CDCl_3$ due to the presence of bromine (presumably due to the heavy atom effect).[24] Crosscoupling of **2.15** with TMS acetylene gave the unsymmetrical triyne **2.16** in moderate yield.

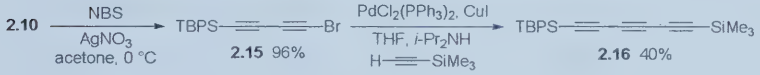


**Scheme 2-7.** The in situ desilylation/bromination of **2.10** followed by Pd-catalyzed crosscoupling to give unsymmetrical triyne **2.16**.

The synthesis of hexayne **2.17** from triyne **2.16** proved to be frustratingly difficult due to the complete lack of chemoselectivity in the desilylation step using the conditions developed for diyne **2.10** (Scheme 2-8). Using these mild conditions, only a trace amount of **2.18** was detected by thin-layer chromatography. The crude reaction mixture was nonetheless subjected to Hay coupling conditions without prior purification in the hopes of obtaining sufficient quantities of hexayne **2.17** for characterization. Only a trace amount of **2.17** was obtained, which proved to be difficult to purify and characterize. Due to the apparent chemical instability of the TBPS group, no further attempts were made to isolate or synthesize hexayne **2.17**.

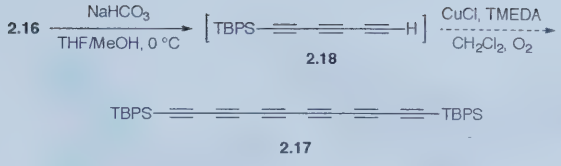


**Scheme 2-8.** Attempted selective desilylation of **2.16** using mild basic conditions followed by Hay coupling to give hexayne **2.17**.

## 2.3 Conclusions and Parting Thoughts

A new and efficient one-pot procedure was developed for the formation of ethynyl silanes, where the silyl group can be either a triphenylsilyl (TPS, **2.5**) or a tris(biphenyl-4-yl)silyl (TBPS, **2.6**). Starting from alkyne **2.6**, the synthesis of unsymmetrical mono-, di-, and triynes differentially protected with the TBPS and either TMS, H or Br endgroups has been achieved in good yields. Symmetrical di- and tetraynes substituted with the TBPS group have also been synthesized via oxidative homocoupling. The large size of the TBPS endgroup has been demonstrated by X-ray crystallography of diyne **2.8**. Unfortunately, the inability to selectively remove a TMS group in the presence of the TBPS endgroup in longer precursors such as triyne **2.18** has, to date, prevented the synthesis of longer derivatives.

It was clear that the propensity of the TBPS group to cleave increased as a function of polyyne length making longer derivatives difficult to synthesize. The lability of the TBPS endgroup is a result of electronic effect between silicon and carbon, which stems from the well-known fact that carbon-silicon bonds are polarized due to the higher electronegativity of carbon versus silicon. One can imagine that as the number of electronegative groups on silicon increases, such as three aryl groups, the Lewis acidity of silicon is thus increased, making it more prone to nucleophilic attack. This would explain why the TBPS endgroup is almost as easy to cleave as a TMS group, even though the TBPS group is clearly much larger (see Figure 2-5). Despite the larger size of the TBPS group, one can see that there is not much more protection from nucleophilic attack ($S_N2$) compared to the TMS group.

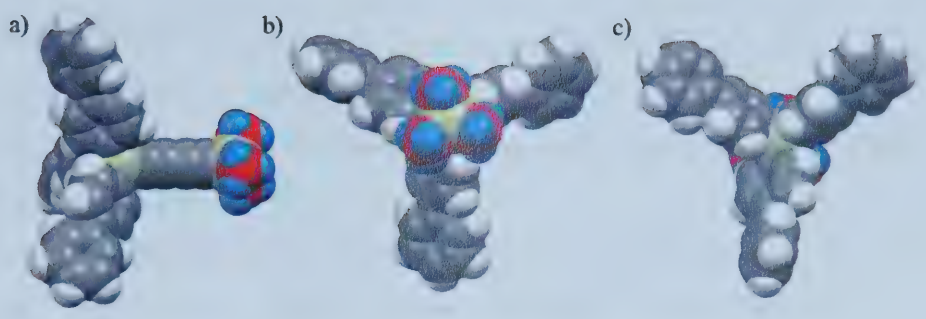


**Figure 2-5.** Space-filling models based on the X-ray structure of **2.10** (non-hydrogen atoms represented at the 20% probability level) shown as the a) side view, b) end-on view with TMS in front, and c) end-on view with TBPS in front, displaying the size difference of the TBPS endgroup versus the TMS endgroup. The carbons and hydrogens on the TMS group are colored blue and red, respectively, to contrast the different endgroups.

Another interesting observation is that the ability to cleave the TBPS increases as a function of polyyne length, resulting in poor selectivity in desilylation. A study done by Walton and coworkers has shown that the acidity of terminal polyyne hydrogen increases as a function of polyyne length due to the increasing electronegativity of the polyyne as it becomes longer.[25] This would have two effects: 1) the increased electronegativity of the alkynyl substituent would make the silicon even more electrophilic, and 2) the alkyne becomes a better leaving group in the course of the desilylation process. Both factors likely contribute to the greater tendency for desilylation of the TBPS group as a function of polyyne length. With this analysis in mind, it was concluded that triarylsilyl endgroups were not the best answer for the synthesis of long, stable polyynes.

## 2.4 References


[1] Chalifoux, W. A.; Tykwinski, R. R. *C. R. Chimie* **2009**, *12*, 341.

[2] Zheng, Q.; Bohling, J. C.; Peters, T. B.; Frisch, A. C.; Hampel, F.; Gladysz, J. A. *Chem. Eur. J.* **2006**, *12*, 6486.

[3] Simpkins, S. M. E.; Weller, M. D.; Cox, L. R. *Chem. Comm.* **2007**, 4035.

[4] Mohr, W.; Stahl, J.; Hampel, F.; Gladysz, J. A. *Chem. Eur. J.* **2003**, *9*, 3324.

[5] Johnson, T. R.; Walton, D. R. M. *Tetrahedron* **1972**, *28*, 5221.

[6] Eastmond, R.; Johnson, T. R.; Walton, D. R. M. *Tetrahedron* **1972**, *28*, 4601.

[7] Bruce, M. I.; Zaitseva, N. N.; Nicholson, B. K.; Skelton, B. W.; White, A. H. *J. Organomet. Chem.* **2008**, *693*, 2887.

[8] Eisler, S.; Slepkov, A. D.; Elliott, E.; Luu, T.; McDonald, R.; Hegmann, F. A.; Tykwinski, R. R. *J. Am. Chem. Soc.* **2005**, *127*, 2666.

[9] Stahl, J.; Bohling, J. C.; Bauer, E. B.; Peters, T. B.; Mohr, W.; Martin-Alvarez, J. M.; Hampel, F.; Gladysz, J. A. *Angew. Chem. Int. Ed.* **2002**, *41*, 1872.

[10] Gibtner, T.; Hampel, F.; Gisselbrecht, J.-P.; Hirsch, A. *Chem. Eur. J.* **2002**, *8*, 408.

[11] Zheng, Q.; Gladysz, J. A. *J. Am. Chem. Soc.* **2005**, *127*, 10508.

[12] The approximate diameter was calculated from the radius, measured from silicon to the proton in the 4'-position of the furthest phenyl group. The distance was measured using Spartan'02 v.1.0.6 after performing a molecular mechanics minimization using an MMFF94 force field.

[13] Baughman, R. H.; Yee, K. C. *J. Polym. Sci. Macromol. Rev.* **1978**, *13*, 219.

[14] Enkelmann, V. *Chem. Mater.* **1994**, *6*, 1337.

[15] Kübel, C.; Chen, S.-L.; Müllen, K. *Macromolecules* **1998**, *31*, 6014.

[16] Elmorsy, S. S.; Khalil, A. G. M.; Girges, M. M.; Salama, T. A. *Tetrahedron Lett.* **1997**, *38*, 1071.

[17] Gilman, H.; Plunkett, M. A.; Dunn, G. E. *J. Am. Chem. Soc.* **1951**, *73*, 1686.

[18] Hay, A. S. *J. Org. Chem.* **1962**, *27*, 3320.

[19] Siemsen, P.; Livingston, R. C.; Diederich, F. *Angew. Chem. Int. Ed.* **2000**, *39*, 2632.

[20] Lei, A.; Srivastava, M.; Zhang, X. *J. Org. Chem.* **2002**, *67*, 1969.

[21] Carré, F.; Devylder, N.; Dutremez, S. G.; Guérin, C.; Henner, B. J. L.; Jolivet, A.; Tomberli, W.; Dahan, F. *Organometallics* **2003**, *22*, 2014.

[22] Nishikawa, T.; Shibuya, S.; Hosokawa, S.; Isobe, M. *Synlett* **1994**, 485.

[23] Hofmeister, H.; Annen, K.; Laurent, H.; Wiechert, R. *Angew. Chem. Int. Ed.* **1984**, *23*, 727.

[24] Lin, S.-T.; Lee, C.-C.; Liang, D. W. *Tetrahedron* **2000**, *56*, 9619.

[25] Eastmond, R.; Johnson, T. R.; Walton, D. R. M. *J. Organomet. Chem.* **1973**, *50*, 87.

# Chapter 3 Synthesis and Properties of Adamantyl-Endcapped Polyynes[‡]

## 3.1 Introduction

The synthesis of polyynes not only has its place with respect to new and interesting materials but also to help provide insight into the properties of the material known as carbyne.[1-4] This material would represent the all sp-carbon allotrope, but whose properties remain unknown due to the lack of an authentic sample or suitable model compounds. The comparison of the properties of this allotrope to the currently known allotropes (i.e., diamond, graphite, etc.) is of considerable interest because one need not be reminded of the immense impact that these known allotropes have on society today.

The synthesis of a series of polyynes whose endgroups minimize the perturbation of the π-system should result in a material with considerable resemblance to that of the carbyne in terms of physical properties. By incorporating an $sp^3$-carbon at each terminus, it is predicted that there would be little influence on the electronics of the polyyne chain itself. As well, the possibility of unwanted endgroup cleavage (a problem discussed in Chapter 2) is removed, or at least greatly reduced. Adamantyl groups were incorporated at the termini to achieve this goal while at the same time providing a rather robust endgroup that could be easily incorporated from inexpensive and easily accessible starting materials. As an interesting side note, the adamantyl endgroup represents the simplest monomeric unit of the $sp^3$-carbon allotrope, diamond, so in a way one can look at this as merging the two allotropes to make new and interesting materials.

---

[‡] Portions of this chapter have been published. Lucotti, A.; Tommasini, M.; Fazzi, D.; Del Zoppo, M.; Chalifoux, W. A.; Ferguson, M. J.; Zerbi, G.; Tykwinski, R. R. *J. Am. Chem. Soc.* **2009**, *131*, 4239. The Raman spectroscopy and theoretical calculations were done by our collaborators (A. Lucotti, M. Tommasini, D. Fazzi, M. Del Zoppo and G. Zerbi).

## 3.2 Synthesis of Adamantyl-Endcapped Polyynes

The synthesis of adamantyl polyynes **3.1a-k** was successful up to 12 triple bonds in length (Figure 3-1). Their syntheses were all carried out using a divergent approach from either ethynyl adamantane **3.2**[5] or acid **3.3**,[5] both of which were easily synthesized from

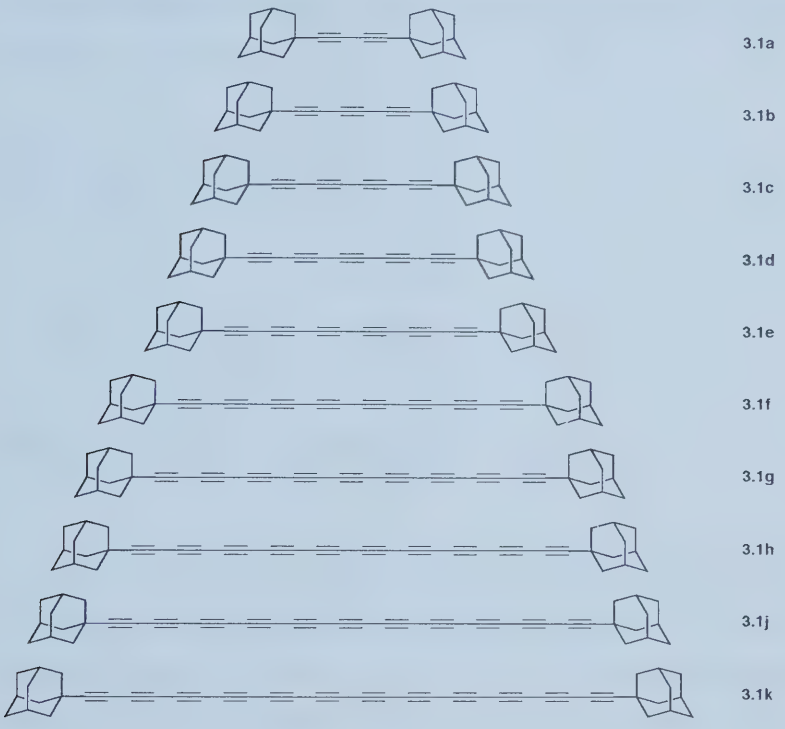


**Figure 3-1.** Adamantyl-endcapped polyynes **3.1a-k**.

readily available starting materials by using, or slightly modifying, reported procedures (Scheme 3-1). The first step was the synthesis of 1-bromoadamantane **3.4** by the treatment of adamantane with neat $Br_2$ at reflux giving the desired product in good yield.[6] Alternatively, 1-bromoadamantane **3.4** could be purchased from commercial suppliers rather inexpensively. The next step involved the Friedel-Craft reaction of **3.4** with neat vinyl bromide at low temperature to yield intermediate **3.5**. The original literature procedure reported the use of rather expensive $AlBr_3$

as the Lewis acid.[5] It was found that this could be substituted with reagent grade $AlCl_3$, which worked rather efficiently, giving intermediate **3.5** as a mixture of halogenated isomers. This crude mixture was taken through a two-fold elimination reaction in the presence of base at high temperature resulting in the formation of 1-ethynyladamantane **3.2** in moderate to good yield over two steps from **3.4**. The lithiated acetylene was formed upon treatment of **3.2** with BuLi, and the subsequent nucleophilic addition to $CO_2$ and acidic workup resulted in acid **3.3** in nearly quantitative yield every time.[5,7]

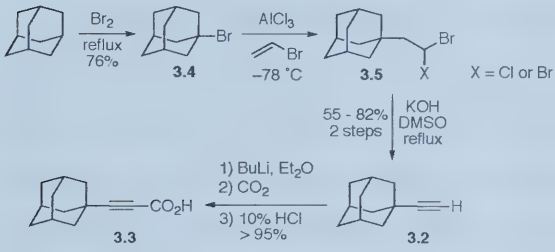


**Scheme 3-1.** Synthesis of 1-ethynyladamantane **3.2** and acid **3.3**.

The synthesis of diyne **3.1a**[8] was first attempted under Hay coupling conditions,[9,10] which proved rather difficult, giving only a moderate yield of the desired product (**path A**, Scheme 3-2). It has been reported that the synthesis of diynes containing bulky endgroups is typically sluggish under Cu-catalyzed homocoupling conditions.[11] Is was previously shown[11] that by using Pd-catalyzed conditions reported by Zhang and coworkers,[12] diynes that incorporate bulky endgroups could be obtained in good yields (**path B**, Scheme 3-2).

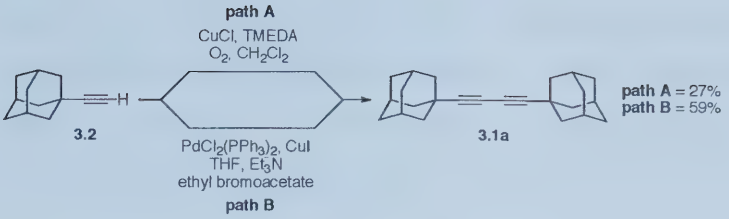


**Scheme 3-2.** Synthesis of diyne **3.1a** using Hay (**path A**) or Pd-catalyzed homocoupling (**path B**) conditions.

Following a previously reported procedure for the synthesis of analogous triynes,[13] two equivalents of lithiated **3.2** with ethyl formate resulted in alcohol **3.6** (Scheme 3-3). This diynol was not isolated due to low stability, but carried forward through an oxidation using PCC to give ketone **3.7**. Ketone **3.7** was also not isolated because of stability issues and was thus subjected to conditions first reported by Ramirez and coworkers[14] which was later made famous by Corey and Fuchs,[15] generating dibromoolefin **3.8** in good yield. Dibromoolefin **3.8** was subjected to a Fritsch-Buttenberg-Wiechell (FBW) rearrangement to generate triyne **3.1b** in good yield.[16-18]

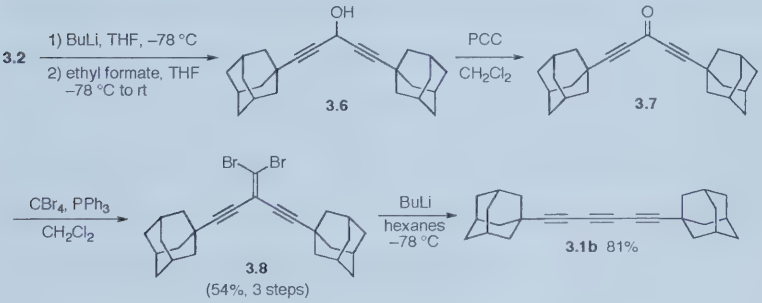


**Scheme 3-3.** Synthesis of triyne **3.1b** via a FBW rearrangement.

The synthesis of tetrayne **3.1c** was initiated by converting 1-ethynyladamantane **3.2** to alkynyl bromide **3.9**[19] in the presence of NBS and $AgNO_3$ in excellent yield (Scheme 3-4).[20] Crosscoupling of **3.9** with 2-methyl-3-butyn-2-ol under Cadiot-Chodkiewicz[10,21] conditions led to

protected diyne **3.10**[19] in good yield. Removal of the acetone protecting group was effected by treatment with KOH at high temperature yielding adamantyl diyne **3.11** in good yield.[19] Although dimerization of monoyne **3.2** under Hay conditions proved difficult, the dimerization of diyne **3.1c** proceeded efficiently, giving tetrayne **3.1c**[8] in quantitative yield.

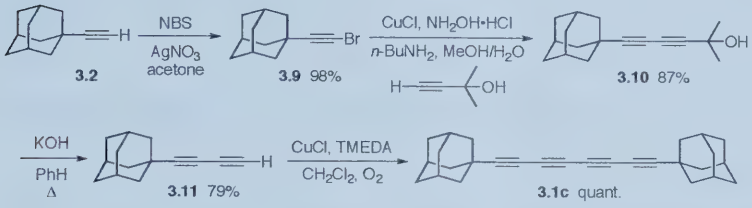


**Scheme 3-4.** Synthesis of tetrayne **3.1c**.

The synthesis of pentayne **3.1d** presented a unique challenge since there is a paucity of synthetic tools at a chemist's disposal for the synthesis of long, odd numbered polyynes. Crosscoupling reactions were ruled out early due to the tendency for a lack of selectivity when attempting to crosscouple longer polyynes.[22] It was thought that the carbon backbone could be installed in a manner similar to the procedure used for triyne **3.1b**. An attempt was made to form alcohol **3.12** by the addition of two equivalents of lithiated diyne **3.11** to ethyl formate (Scheme 3-5). Oxidation and formation of the dibromoolefin (**3.12**) would be expected to provide a precursor that would undergo a FBW rearrangement, leading to pentayne **3.1d**. This route unfortunately failed in the early stages of alcohol formation, presumably due to the instability of the exposed alcohol, flanked by polyconjugated systems.

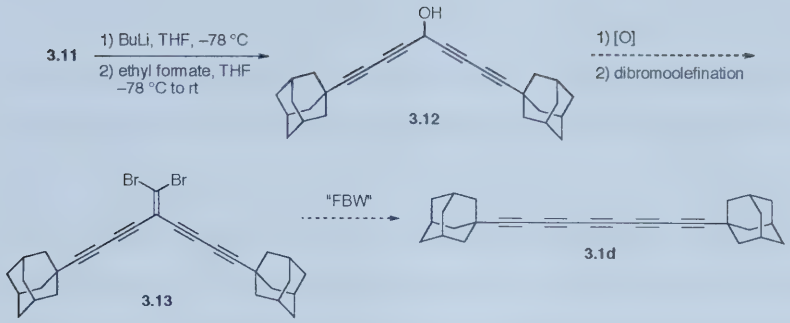


**Scheme 3-5.** Attempted synthesis of alcohol **3.12** towards the formation of pentayne **3.1d**.

A new approach was taken toward the synthesis of symmetrical pentayne **3.1d** that mimicked the method used in the Tykwinski group toward the synthesis of unsymmetrical pentaynes.[23-25] Using a divergent strategy, the Friedel-Crafts acylation reaction[26] between acid chloride **3.14**, made by treatment of acid **3.3** with thionyl chloride, and the adamantyl-TMS-triyne **3.15** (the synthesis of **3.15** is shown in Scheme 3-7 and Scheme 3-8), gave ketone **3.16** (Scheme 3-6). Ketone **3.16** was not isolated but was crudely purified by passing through a plug of silica gel, followed by reaction under dibromoolefination conditions to give **3.17** in 40% over 2 steps. The FBW rearrangement of **3.17** proceeded in good yield to give pentayne **3.1d**.

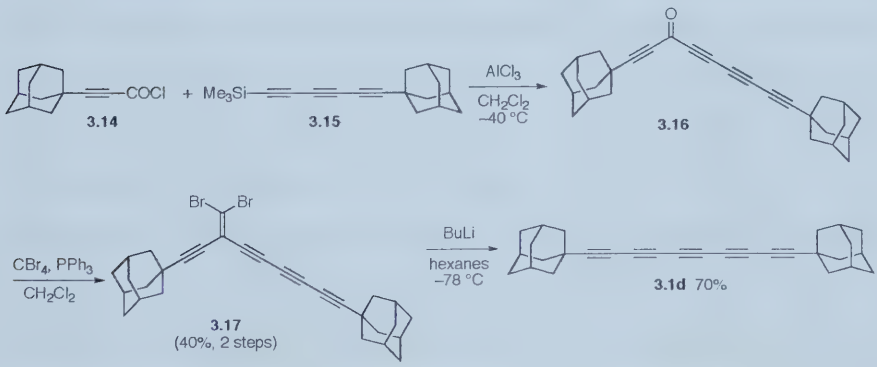


**Scheme 3-6.** Divergent strategy towards the synthesis of pentayne **3.1d**.

Following the synthesis of **3.1d**, the synthesis of longer adamantyl polyynes were all initiated from acid **3.3**, via conversion to acid chloride **3.14**. Friedel-Crafts reaction of **3.14** with an α,ω-bis(trimethylsilyl) polyyne in the presence of $AlCl_3$ formed ketones **3.18**, **3.19** and **3.20** in 53%, 42% and 38% yield, respectively (Scheme 3-7).[26] These ketones are not very stable to isolation and tend to decompose to form an insoluble black residue, especially **3.20**. This factor explains the poor yields upon attempted isolation of these ynone products. It should be noted that due to this instability the ketones were typically not isolated, but carried forward to the next step immediately after purification through a short plug of silica gel. The dibromoolefination reaction on the solutions of **3.18**, **3.19**, and **3.20** gave dibromoolefins **3.21**, **3.22** and **3.23** in moderate to good yields over the three steps from **3.3**.

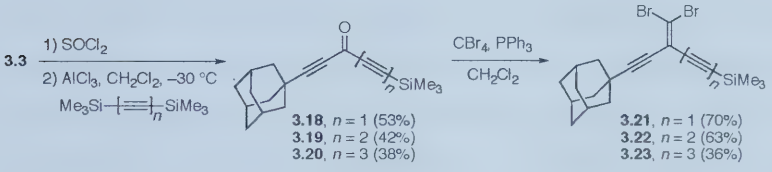


**Scheme 3-7.** Synthesis of dibromoolefins **3.21**, **3.22** and **3.23**.

At this stage, it was initially intended that dibromoolefins **3.21**, **3.22** and **3.23** would be used to pre-construct the carbon backbone and utilize a FBW rearrangement in the final step to obtain the corresponding polyynes (**route A**, Scheme 3-8). This indeed worked and desilylation of dibromoolefins **3.21**, **3.22** and **3.23** proceeded under protiodesilylation conditions to give **3.24**-**3.26**. Desilylated dibromoolefin **3.24** was isolated as a stable solid and was thus fully characterized. Stability dropped off rapidly, however, and thus dibromoolefins **3.25** and **3.26** were carried forward in solution without isolation. Dimerization under Hay conditions worked well, forming tetrabromoolefins **3.27**, **3.28** and **3.29** in moderate to good yield. A two-fold FBW rearrangement was performed giving hexa- (**3.1e**), octa- (**3.1f**), and decaynes (**3.1h**) in 74%, 38% and 3% yields, respectively. Thus, a two-fold FBW rearrangement is a viable method for the synthesis of hexayne **3.1e** and even for the octayne **3.1f**. Although this is the first reported

successful synthesis of a decayne (**3.1h**) using an FBW rearrangement, the low yield clearly shows that this route would not be suitable for providing large quantities of material needed for further studies. The problem is believed to arise from the substantial decrease in solubility of the tetrabromoolefins in the nonpolar solvents required for the FBW rearrangement. Other solvent conditions were tried (toluene, HMPA, or mixtures thereof), however, none led to the isolation of the desired product. A slight alteration to the protocol was implemented where the order of the steps was changed. Carrying out the FBW rearrangement on dibromoolefins **3.21**, **3.22** and **3.23** led to unsymmetrical polyynes **3.15**, **3.30** and **3.31** (**route B**, Scheme 3-8). Triyne **3.15** could be isolated as a stable solid and was fully characterized. Tetrayne **3.30**, however, was considerably less stable as a neat solid, immediately turning black upon isolation. Due to the instability of tetrayne **3.30** and pentayne **3.31**, neither could be isolated or characterized. They could, however, be kept in solution without considerable degradation and were thus carried forward as such to the next step. As an interesting side note, partial desilylation of pentayne **3.31** was observed after passing through silica gel, something that has also been reported in other systems.[24] By subjecting tetra- (**3.30**) and pentayne (**3.31**) to the modified Hay conditions reported, in situ desilylation and dimerization was observed leading to the octa- (**3.1f**) and decayne (**3.1h**) in yields of 75% and 29%, respectively, over the two steps.[27] There was a significant improvement in overall yield when going from dibromoolefins **3.22** and **3.23** to octayne **3.1f** (**route A** = 28% vs. **route B** = 75%) and decayne **3.1h** (**route A** = 2% vs. **route B** = 29%) allowing for bulk quantities of material to be synthesized. It should be noted that under Hay conditions, along with the decayne **3.1h**, a small amount of the nonayne **3.1g** side product was produced, even when the reaction was cooled to 0 °C. Pure **3.1h** was obtained in 29% yield after recrystallization from $CH_2Cl_2$. The problem of nonayne **3.1g** side product formation was circumvented using a modified Eglinton-Glaser protocol developed by Haley and coworkers,[28] giving the desired decayne **3.1h**, again, in 29% yield.

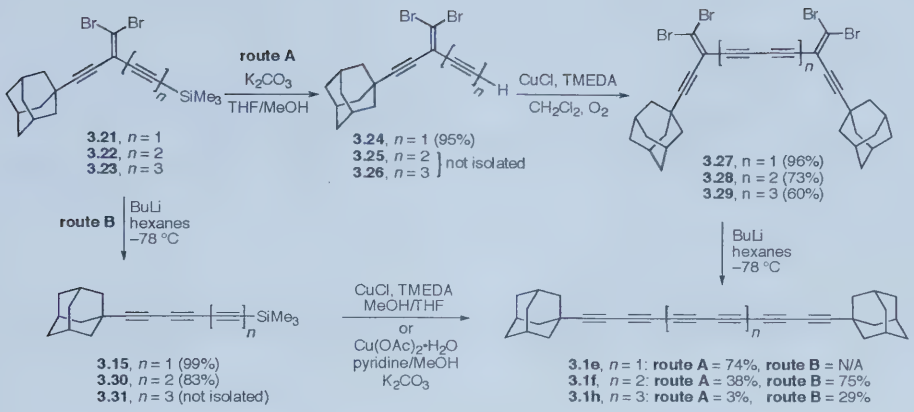


**Scheme 3-8.** Synthesis of hexa- (**3.1e**), octa- (**3.1f**) and decayne (**3.1h**) via 1) a dimerization reaction followed by a two-fold FBW rearrangement (**route A**); or 2) a FBW rearrangement followed by dimerization (**route B**).

As part of the campaign to synthesize polyynes beyond ten triple bonds, an attempt was made to synthesize dodecayne **3.1k** using a similar strategy. The larger *t*-butyldimethylsilyl (TBS) protecting group was incorporated. It was presumed that this more robust and larger silyl group would improve stability of intermediates, allow for easier handling, purification, and thus improve the odds of isolating **3.1k**. One strategy involved the Friedel-Crafts reaction of **3.14** with tetrayne **3.32** to give the TBS protected ketone **3.33** (**route A**, Scheme 3-9). This ketone was passed through a plug of silica gel and reacted under dibromoolefination conditions to yield **3.34** in 14% yield over two steps. An FBW rearrangement of dibromoolefin **3.34** to generate unsymmetrical hexayne **3.35** was successful in a modest 29% yield. As an alternate attempt to make hexayne **3.35** in bulk quantities, a mixed Hay coupling was attempted with the expectation of a statistical mixture of coupled products. Upon treatment of triynes **3.15** and **3.36** with CuCl and TMEDA in a solvent mixture of MeOH and THF, in situ desilylation of the TMS groups followed by dimerization led to a modest yield of 18% (**route B**, Scheme 3-9). The low yield is possibly, in part, due to different desilylation rates for the two starting triynes as well as similar solubilities and retention factors (chromatography) of products, which made purification difficult.

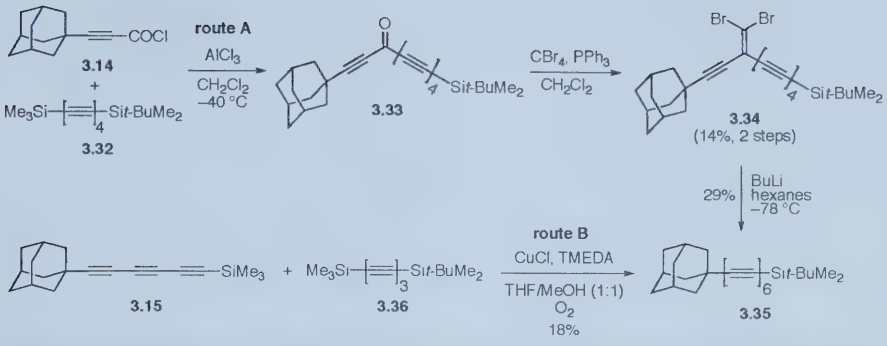


**Scheme 3-9.** Synthesis of hexayne **3.35**.

Although disappointing yields of **3.35** were obtained following either route, there was sufficient material to attempt the synthesis of dodecayne **3.1k**. The first step involved removal of the TBS group. The desilylation was unsuccessful using the traditional technique of TBAF in wet THF and led only to black insoluble material in the reaction. The TBS group was thus removed using a milder approach of potassium fluoride in wet THF (Scheme 3-10). The presumably unstable deprotected hexayne intermediate was reacted immediately, after a quick workup and purification through a plug of silica gel, under Hay homocoupling conditions at –40 °C. Unfortunately, this led to formation of dodecayne **3.1k** as well as a considerable amount of undecayne **3.1j** product, a result, again, of losing one acetylene unit. The products of this reaction underwent considerable decomposition upon isolation, leading to the formation of a black solid. Pd-catalysis was then attempted, which led to substantial decomposition in the form of a black insoluble solid. However, after filtering through a plug of silica gel, an orange-red solution was obtained that showed the presence of dodecayne **3.1k**, as well as the undecayne **3.1j** side product. A slurry wash in hot toluene, followed by cooling and filtration gave pure dodecayne **3.1k**. The product proved to be very unstable to isolation as a solid, leading to rapid formation of a black, insoluble solid almost immediately. This made characterization by standard methods very difficult. The formation of **3.1k**, however, was confirmed by its very characteristic UV-Vis absorption spectrum.

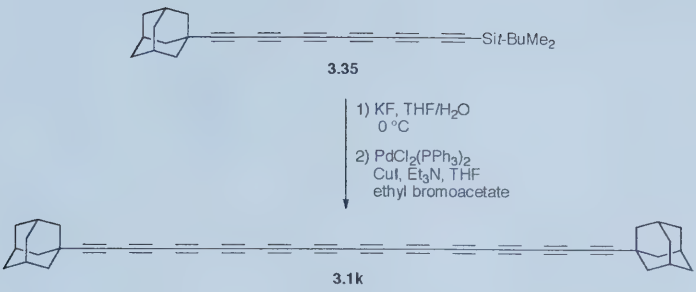


**Scheme 3-10**. Desilylation of hexayne **3.35** using a mild fluoride source followed by dimerization under Pd-catalysis to give dodecayne **3.1k**.

## 3.3 Physical and Spectroscopic Properties of Adamantyl Polyynes

### 3.3.1 UV-Vis Spectroscopic Analysis

The UV-Vis spectra of adamantyl polyynes **3.1a-k** have been acquired in THF (Figure 3-2) as well as in hexanes (Figure 3-3, except for **3.1k**). The spectra show a consistent red shift in absorbance as a function of polyyne length that reflects the expected lowering of the HOMO → LUMO band gap energy. Another attribute of the UV-Vis absorbance of these polyynes is that they display fine structure in their spectra, making UV-Vis analysis a powerful tool for characterization. Quantitative UV-Vis analysis was obtained in THF and in hexanes for the tetrayne **3.1c** up to the octayne **3.1f**. One can clearly see that there is a consistent increase in the extinction coefficient as a function of length. Quantitative analysis of decayne **3.1h** was attempted, but showed low extinction coefficients due to rapid decomposition of the sample before spectra could be acquired. Qualitative UV-Vis analysis of the dodecayne **3.1k** was also obtained, providing evidence that it was, in fact, successfully synthesized.

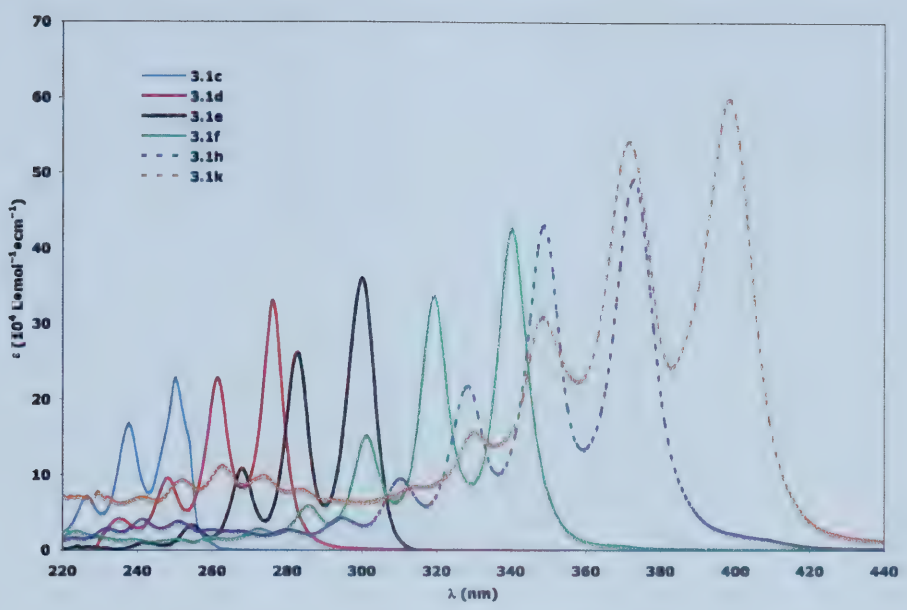


**Figure 3-2.** UV-Vis spectra of adamantyl polyynes **3.1c-k** in THF. Quantitative data was obtained for **3.1c-f**. Quantitative UV-Vis absorption of the deca- (**3.1h**) and dodecayne **3.1k** (dotted lines) could not be obtained due to decomposition. Relative intensities have been adjusted based on the trend to show their spectra in relation to the shorter polyynes.

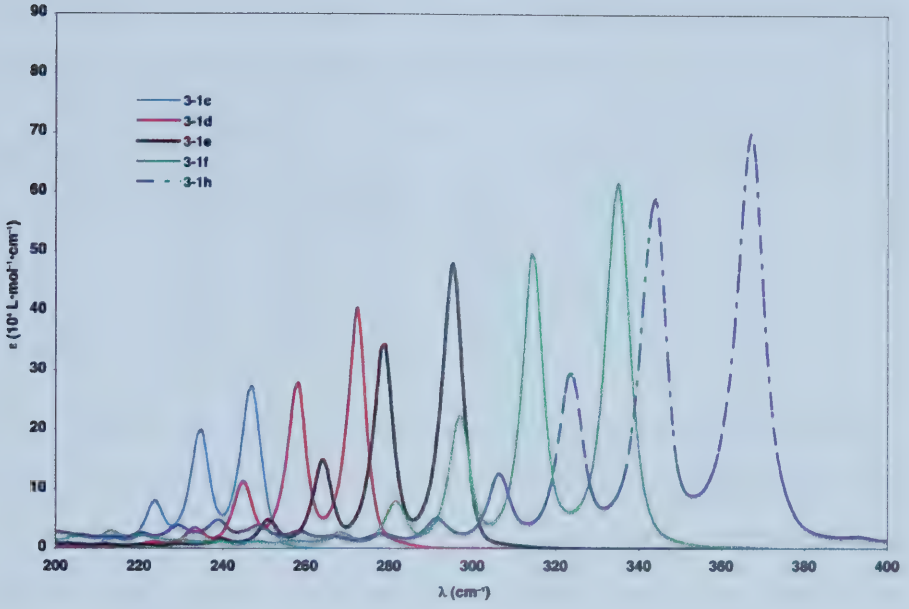


**Figure 3-3.** UV-Vis spectra of adamantyl polyynes **3.1c-h** in hexanes. Quantitative data was obtained for **3.1c-f**. Quantitative UV-Vis absorption of the decayne (**3.1h**, dotted line) could not be obtained due to decomposition. Relative intensity has been adjusted based on the trend to show their spectra in relation to the shorter polyynes.

There are several observed differences in the UV-Vis absorbances of polyynes when measured in hexanes versus THF. In the less polar hexanes solvent, there is a hypsochromic shift observed for $\lambda_{max}$, as well as larger extinction coefficients (Table 3-1). Extinction coefficients are as high as 617000 $L \cdot mol^{-1} \cdot cm^{-1}$ in hexanes for **3.1f** and are steadily increasing as a function of polyyne length. One would expect impressive values that begin to approach a million for polyynes beyond $n = 10$, if only these compounds were sufficiently stable to isolate and analyze.

**Table 3-1.** UV-Vis absorbance data for adamantyl polyynes **3.1c-k**.

| Compound | $n$ | hexanes | | THF | |
|---|---|---|---|---|---|
| | | $\lambda_{max}$ (nm) | $\varepsilon$ ($M^{-1}cm^{-1}$) | $\lambda_{max}$ (nm) | $\varepsilon$ ($M^{-1}cm^{-1}$) |
| **3.1c** | 4 | 247 | 273000 | 250 | 229000 |
| **3.1d** | 5 | 272 | 405000 | 276 | 332000 |
| **3.1e** | 6 | 295 | 480000 | 300 | 361000 |
| **3.1f** | 8 | 335 | 617000 | 340 | 428000 |
| **3.1h** | 10 | 367 | N/A | 373 | N/A |
| **3.1k** | 12 | N/A | N/A | 398 | N/A |

While trends in $\varepsilon$ are not obvious, analysis of $\lambda_{max}$ values can be accomplished in a more methodical fashion. Considering electron correlation effects, the empirical power-law $E_g = 1/\lambda_{max} \sim n^{-x}$ describes the relationship between $E_g$, $\lambda_{max}$ and $n$ (where $E_g$ is the energy of the HOMO → LUMO transition).[29-31] There is a consistent power-law decrease in $E_g$ through $n = 10$ in hexanes ($E_{g\ (hexanes)} \sim n^{-0.434}$) and $n = 12$ in THF ($E_{g\ (THF)} \sim n^{-0.427}$) shown in Figure 3-4. The values obtained from hexanes and THF are close to the well-established "Lewis-Calvin Law" of $E_g \sim n^{-0.5}$ that has been documented for many conjugated materials.[32] When saturation occurs within a series, the band gap becomes constant and therefore log $E_g$ becomes constant. One can see from Figure 3-4 that saturation of the HOMO–LUMO gap has clearly not yet been achieved by the stage of the dodecayne **3.1k**.

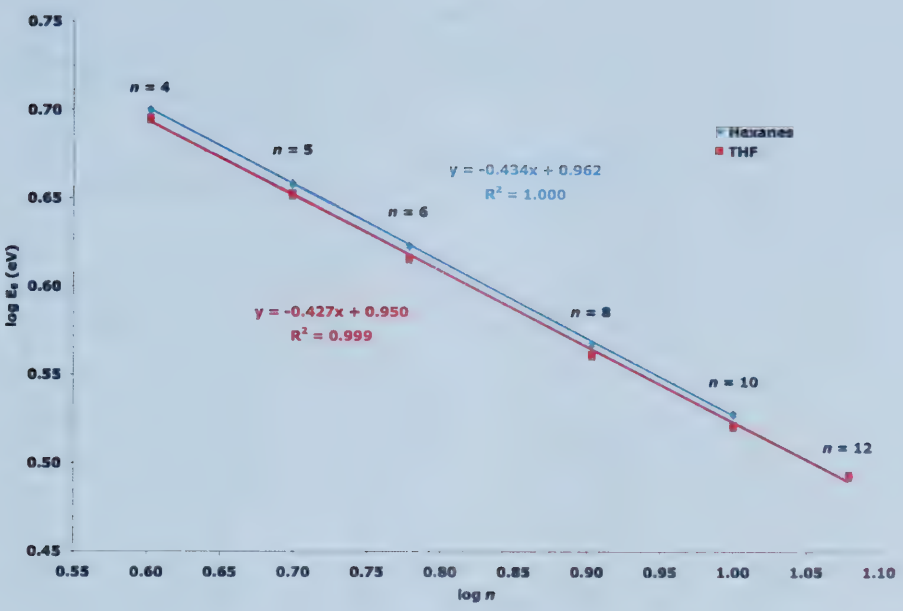


**Figure 3-4.** Plot of log ($E_g$) versus log ($n$) for the adamantyl series in THF (red) and hexanes (blue). The solid line in each case represents a line-of-best-fit to the data ($E_g$ is the $\lambda_{max}$ in eV).

### 3.3.2 IR and Raman Spectroscopic Analysis of Adamantyl Polyynes

The analysis of adamantyl polyynes **3.1a-h** by Raman and IR spectroscopies has been done in collaboration with Professor Dr. Giuseppe Zerbi and coworkers (Milan, Italy), in both the solid- and solution-states (Figure 3-5). The spectra show that the samples are very clean, and the strongest lines observed in the 1950–2300 $cm^{-1}$ range are unquestionably assigned[33-35] to the Я–mode based on the Effective Conjugation Coordinate (ECC) theory[36,37] of polyconjugated chains.[38] Most of the other lines in the spectra (not shown) can be assigned to the adamantyl groups,[39] with the exception of a few minor lines below 600 $cm^{-1}$ that are assigned to transversal and/or longitudinal vibrational modes of the polyyne chains.[40,41] As expected from the ECC model, a decrease in the Raman frequency of the Я–mode is observed as the number of C≡C bonds increases from **3.1a** (2250 $cm^{-1}$) to **3.1h** (1950 $cm^{-1}$), as shown in Table 3-2.[34,42]

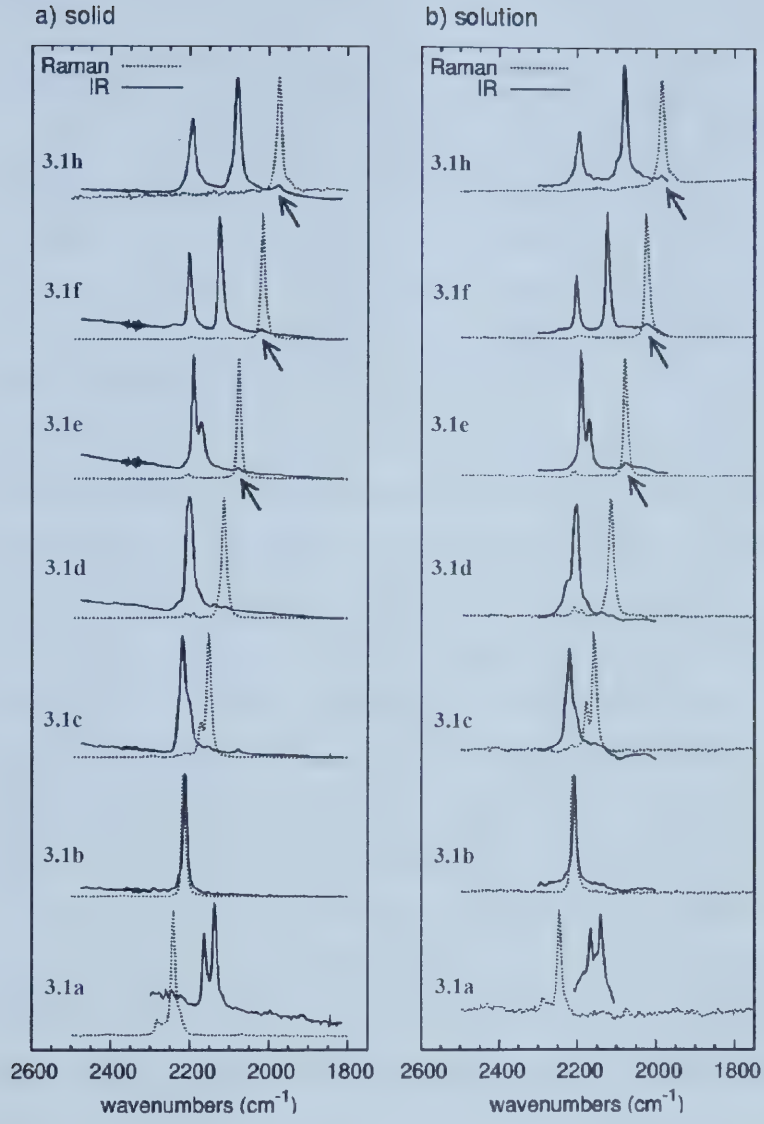


**Figure 3-5.** Experimental Raman (•••) and IR (—) spectra (2500-1800 $cm^{-1}$) of a) solid samples and b) THF solutions of polyynes **3.1a-h**. The arrows indicate violations of the mutual exclusion in the IR spectra.

**Table 3-2.** Raman and IR frequencies for the Я-lines in the solid- and solution-states.[a]

| Compound | Raman (solid, $cm^{-1}$) | IR (solid, $cm^{-1}$) | Raman (soln, $cm^{-1}$) | IR (soln, $cm^{-1}$) |
|---|---|---|---|---|
| **3.1a** | 2241 s | 2163 s, 2137 s | 2246 s | 2166 s, 2141 s |
| **3.1b** | 2216 s | 2212 s | 2211 s | 2208 s |
| **3.1c** | 2171 m, 2151 s | 2218 s | 2177 m, 2158 s | 2220 s |
| **3.1d** | 2113 s | 2201 s | 2115 s | 2204 s |
| **3.1e** | 2075 s | 2191 s, 2171 s 2078 w | 2078 s | 2191 s, 2170 s 2078 w |
| **3.1f** | 2014 s | 2202 s, 2125 s 2018 w | 2024 s | 2203 s, 2124 s 2024 w |
| **3.1h** | 1974 s | 2194 s, 2080 s 1976 w | 1985 s | 2195 s, 2081 s 1985 w |

[a]Intensities labeled as: s – strong; m – medium; w – weak

The solution and solid-state IR spectra of **3.1a** both show a doublet in the C≡C triple bond stretching region. This is unexpected since **3.1a** has only two triple bonds, therefore one mode should be symmetric (Raman active) and the other should be antisymmetric (IR active). The frequency for the solid-state Raman active mode (2241 $cm^{-1}$) is well separated from the IR doublet (2163 and 2137 $cm^{-1}$) (see Figure 3-5). The occurrence of only one IR active mode has also been predicted by DFT calculations so one might suspect contaminants in the sample. The possibility of impurities (i.e., contaminations from alkynes), however, can be ruled out for **3.1a** since no other signals that could be attributed to polyynes was observed in either the IR and Raman. It is also unlikely that **3.1a** underwent degradation during analysis, since this is the most stable compound of the series, not to mention, no degradation was observed for any other derivative during analysis. Therefore, it is suspected that the doublet of **3.1a** in the IR is due to a Fermi resonance from a collective CH bending mode of the adamantyl groups located at approximately 1075 $cm^{-1}$. The existence of this vibration is predicted by DFT calculations (IR fundamental 2179 $cm^{-1}$ /2 ≅ 1090 $cm^{-1}$).

The IR spectra of polyynes **3.1b-d** display only a single absorbance, while the longer polyynes **3.1e-h** show two significant IR absorptions in the spectral region ascribed to C≡C stretching. Calculations show that the two observed IR bands can be assigned to Я–modes, each mode differing in the number of nodes of the vibrational displacements of the chain (longitudinal, one-dimensional confined phonons, see Figure 3-6). The spectra also show frequency dispersion for one of the IR active Я–modes, which decreases in energy as the chain length increases (Figures

3-5 and 3-6). The other IR band maintains approximately the same frequency irrespective of the polyyne length.

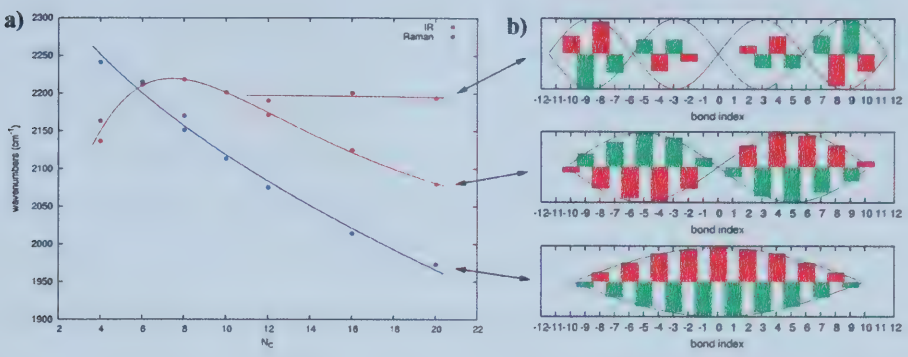


**Figure 3-6.** a) Experimental frequency dispersion of Raman and IR lines as a function of the number of carbon atoms $N_C$ (from spectroscopic data in the solid state). (b) Theoretical vibrational displacements (bond-length changes) for decayne **3.1h** associated with the three branches of the plot in (a) shown by the double-headed arrows (from PBEPBE/cc-pVDZ calculations). Unscaled theoretical vibrational frequencies are also given. The central bond of the chain is indicated by the bond index of zero. Green bars denote C≡C bonds and red bars C–C bonds. Sinusoidal lines are superimposed onto the stick plots to ease the recognition of the number of nodes.

According to group theory, for centrosymmetric systems the Raman active Я–vibrations are totally symmetric (g, gerade), while the IR active lines are anti-symmetric (u, ungerade) with respect to the center of symmetry of the molecule. From a comparison of the solid-state spectra in Figure 3-5a (see arrows), it is clear that perfect mutual exclusion between Raman and IR lines is not upheld, particularly for the longer polyynes **3.1e-h**. The totally symmetric, Raman active Я–mode at 2075, 2014, and 1974 $cm^{-1}$ for **3.1e**, **3.1f** and **3.1h**, respectively, is also conspicuously present as a weak feature in each of the respective IR spectra. It can thus be concluded that the longer polyynes have an equilibrium structure in the solid-state such that the molecule lacks inversion symmetry.

In the search for a rationalization of these experimental observations, it may be argued that the centrosymmetric structure of the adamantyl polyynes is most easily destroyed if the terminal adamantyl groups adopt an eclipsed conformation, which might then give rise to the weak IR bands observed in the Raman spectra. This premise is not, however, consistent with the observed data. Specifically, the adamantyl-adamantyl interaction of the eclipsed conformation should be stronger in the shorter polyynes, due to the smaller separation of the end-groups. On the contrary, experimentally the longer polyyne chains **3.1e-h** show a more definite activation of the Raman mode in the IR. Moreover, the first principles calculations for the parent molecule of **3.1d**, the hydrogen terminated pentayne H–$(C\equiv C)_5$–H, demonstrate the analogous violation of mutual exclusion. This suggests that the nature of the endgroup is seemingly irrelevant.

Unfortunately, no structural information is readily available for the carbon chains in solution. The observation of the lack of the mutual exclusion principle between Raman and IR spectra recorded on solutions represents the first reported attempt, outside of gas phase analyses,[43,44] to characterize the shape of polyyne chains in the absence of crystal field effects and/or effects due to the packing of endgroups.

The gross features of the IR and Raman spectra for **3.1a-h** measured in solution (THF) are remarkably similar in nearly all respects to those measured in the solid-state (Figure 3-5b). This includes strong Raman active Я–lines that decrease in frequency as the length is increased from **3.1a** (2246 $cm^{-1}$) to **3.1h** (1985 $cm^{-1}$), and two IR active transitions, one of which shifts to lower frequency as the polyyne length is increased. The only major difference between solution- and solid-state spectra is a non-systematic, small frequency shift between the values recorded on solution- and solid-state samples, both in the IR and Raman. These small variances between phases are commonly encountered in spectroscopy and arise from effects of the molecular environment.

The analysis of the solution spectra shows that for polyynes **3.1e-h**, mutual exclusion between Raman and IR spectra is not upheld. In particular, the totally symmetric Raman Я–line at 2078, 2024, and 1985 $cm^{-1}$ for **3.1e**, **3.1f** and **3.1h**, respectively, is also present in the IR spectra at essentially identical frequencies. This data thus confirms that: a) at least locally, a non-

centrosymmetric polyyne chain is present in solution, and b) the nonlinear geometry is related to the intrinsic nature of polyynes, i.e., it is determined by the shallowness of the intramolecular potential along C–C≡C bending coordinates.

### 3.3.3 Computational Analysis of Polyynes

On the basis of the above discussion, the following questions still need further consideration: (a) Is the static equilibrium geometry of polyynes bent or linear? (b) Is the polyyne bending potential indeed very shallow? (c) Can only a slightly bent polyyne framework account for the spectroscopic observations of incomplete mutual exclusion (i.e., Raman modes activated in the IR)? (d) Do endgroups (e.g., adamantyl) significantly affect the experimental symmetry considerations presented? (e) Is it possible that the IR signals ascribed to the violation of mutual exclusion arise from an ungerade IR active vibration of similar frequency? DFT calculations can help with the answers to these questions, and several sets of calculations have been undertaken. First, DFT simulations were carried out on **3.1a-f** and **3.1h** to model the structure, bond lengths, and bond angles of these molecules, using the pure PBE,[45] functional and Dunning's double split correlation-consistent cc-pVDZ basis set.[46] The computational procedure started from an initially bent polyyne skeleton, and for longer chains (i.e., **3.1e-h**), the geometry optimization converged to a slightly bent structure as a minimum. Previous experimental[43,44] and theoretical[47-49] studies clearly agree that the bending potential of related linear carbon structures is shallow. As for the presence of stable minima for bent structures, recent work has shown that this seems to be the case in carbon suboxide[44,49] and Pt-endcapped polyynes.[50] Thus, the overall bent shape calculated for the adamantyl-endcapped polyynes could result from either a very flat minimum corresponding to the linear structure or a stable minimum for a bent geometry.

To more fully assess the prospect of a nonlinear ground state structure for the adamantyl polyynes and the associated vibrational analysis, additional first principles calculations (PBEPBE/cc-pVDZ) for **3.1e** were carried out (Figure 3-7a). This analysis supports a bent structure for **3.1e**. Furthermore, the calculated IR and Raman spectra compare fairly well with the

experimental observations in the C≡C stretching region (Figures 3-7b and 3-7c). An analysis of the simulations of Raman and IR spectra show that the mutual exclusion principle is violated not only in the IR spectrum, but also in the Raman, albeit much less prominently. Moreover, the violation of mutual exclusion is predicted in the IR spectrum for a second band (arrow, Figure 3-7c) in addition to the ECC band. These calculations support the assignment of the observed shoulder in the IR to a Raman mode activated in the IR (see corresponding arrow in the experimental spectrum, Figure 3-7b).

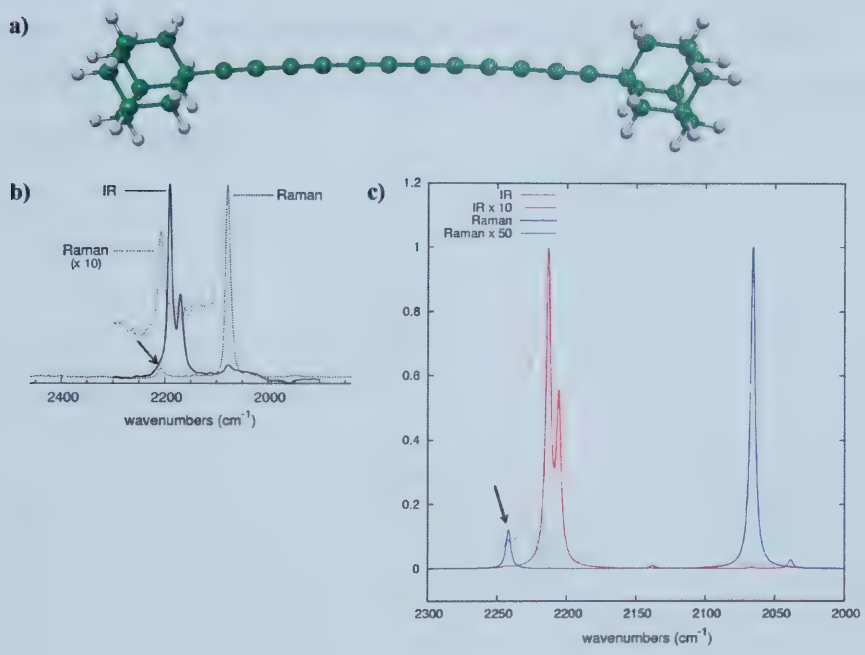


**Figure 3-7.** a) Ball and stick model of the optimized bent structure of **3.1e** calculated from first principles (PBEPBE/cc-pVDZ). b) Experimental IR and Raman spectra of **3.1e** (THF solution). c) Simulated IR and Raman spectra of **3.1e** based on first principles calculations at the PBEPBE/cc-pVDZ level (the arrows denote a Raman mode activated in the IR as predicted by the calculations).

To confirm that the results of polyynes **3.1a-h** did not arise due to an endgroup effect generated by the adamantyl groups, first principles calculations were carried out at the PBEPBE/cc-pVQZ level for the parent pentayne H–$(C{\equiv}C)_5$–H and hexayne H–$(C{\equiv}C)_6$–H with both a linear and bent conformation (Figures 3-8 and 3-9, respectively).[51] It is worth noting that in this case, a more extended basis set (quadruple zeta as opposed to double zeta) was applied due to the simpler molecular structure (i.e., no terminal adamantyl groups). These results confirm a detectable activation in the IR spectrum of the strong Raman band, as well as the converse (i.e., activation in the Raman spectrum of the strong IR band). These calculations nicely demonstrate that the violation of mutual exclusion does not depend on the endgroup (i.e., adamantyl versus hydrogen), and they are also consistent with the results obtained when the less expensive basis set (cc-pVDZ) was applied.

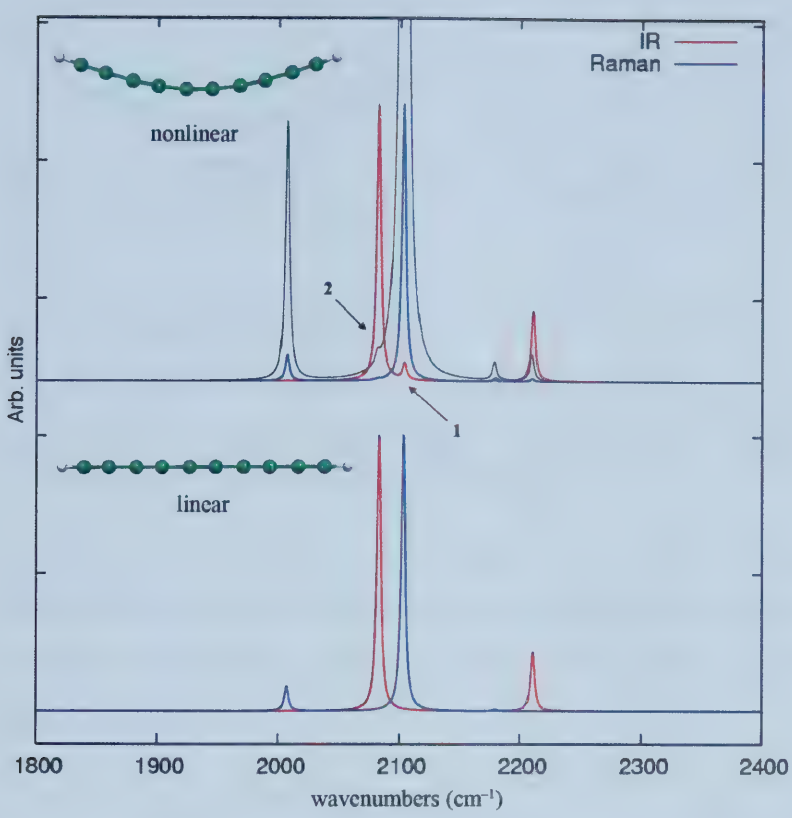


**Figure 3-8.** Simulated Raman and IR spectra of the bent (top) and linear (bottom) conformations of H–(C≡C)$_5$–H calculated at the PBEPBE/cc-pVQZ level (simulated structures are shown as insets). The thin black curve is the Raman spectrum enhanced by a factor of 10. Activation of the strong IR line is observed as a shoulder of the strong Raman line (arrow **2**). The activation in the IR of the strong Raman line is more evident (arrow **1**). Simulated peaks are Lorentzian functions with a FWHM = 4 cm$^{-1}$.

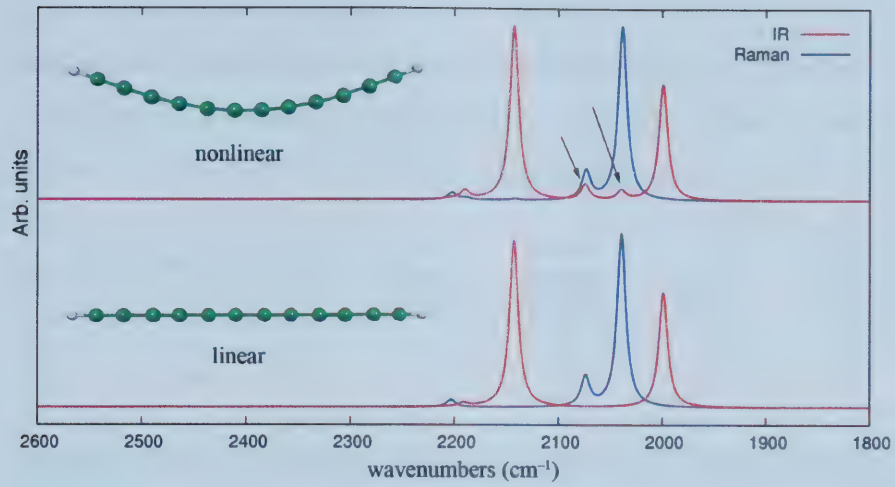


**Figure 3-9.** Simulations of the IR and Raman spectra of H–$(C\equiv C)_6$–H at the PBEPBE/cc-pVQZ level in the linear and bent structures (the inset pictures show the optimized structures). For the bent structure, both of the Raman peaks located between 2000 and 2100 cm$^{-1}$ are visible in the IR (shown by arrows).

Finally, DFT calculations were used to ensure that the weak band observed in the IR spectra (corresponding to the strong Raman line, see Figure 3-5) should not be assigned to an ungerade IR active vibration with a similar frequency, but to the same normal mode observed in the Raman at the same frequency. The results of DFT calculations at the cc-pVQZ level for H–$(C\equiv C)_5$–H (linear and bent polyyne geometries, Table 3-3) and the cc-pVDZ level for adamantyl-endcapped polyynes **3.1e**, **3.1f** and **3.1h** (bent geometries, Table 3-4) were examined. The frequencies falling in the region of interest of the present study (1900–2200 cm$^{-1}$) were considered; for **3.1f** and **3.1h** the first mode with a frequency smaller than the strong Raman line has also been included. It should be noted that these modes consistently show a large C–C stretching character and the strong Raman line in these molecules can be always described as a collective in-phase C≡C stretching coupled with the in-phase C–C shrinking (Я–mode, Figure 3-6 and ref [34]).

**Table 3-3.** List of vibrational frequencies, IR and Raman intensities of linear ($D_{\infty h}$) and bent ($C_{2v}$) conformations of hydrogen-capped polyyne H–(C≡C)$_5$–H. Data obtained through DFT calculations carried out at PBEPBE/cc-pVQZ level. Data for the strongest Raman line are bolded.

| irrep[a] | irrep[a] | Frequency ($cm^{-1}$) | Frequency ($cm^{-1}$) | Raman intensity ($A^4$/amu) | Raman intensity ($A^4$/amu) | IR intensity (km/mol) | IR intensity (km/mol) |
|---|---|---|---|---|---|---|---|
| $D_{\infty h}$ | $C_{2v}$ | $D_{\infty h}$ | $C_{2v}$ | $D_{\infty h}$ | $C_{2v}$ | $D_{\infty h}$ | $C_{2v}$ |
| $\Sigma_g^+$ | $A_1$ | 2008 | 2008 | 3579 | 3423 | 0.0 | 0.0 |
| $\Sigma_u^+$ | $B_2$ | 2083 | 2082 | 0.0 | 133 | 17 | 17 |
| **$\Sigma_g^+$** | **$A_1$** | **2104** | **2104** | **39552** | **36432** | **0.0** | **1.0** |
| $\Sigma_g^+$ | $A_1$ | 2180 | 2179 | 248 | 240 | 0.0 | 0.2 |
| $\Sigma_u^+$ | $B_2$ | 2210 | 2210 | 0.0 | 348 | 4 | 4 |

[a] Irreproducible representation

**Table 3-4.** Vibrational Frequencies as well as IR and Raman Intensities for Polyynes **3.1e**, **3.1f**, and **3.1h**.[a]

| irrep[b] | frequency ($cm^{-1}$) | Raman intensity ($A^4$/amu) | IR intensity (km/mol) |
|---|---|---|---|
| | **3.1e** | | |
| u | 2038 | 12 | 16 |
| **g** | **2066** | **351598** | **2** |
| g | 2138 | 3176 | 0.3 |
| u | 2205 | 239 | 279 |
| u | 2212 | 356 | 549 |
| g | 2242 | 42662 | 2 |
| | **3.1f** | | |
| g | 1587 | 1007 | 0.001 |
| **g** | **1977** | **1078980** | **0.2** |
| u | 2007 | 1 | 14 |
| g | 2092 | 4297 | 0.02 |
| u | 2142 | 99 | 1138 |
| u | 2163 | 2 | 57 |
| g | 2210 | 4881 | 0 |
| g | 2221 | 160367 | 0.3 |
| u | 2235 | 33 | 617 |
| | **3.1h** | | |
| g | 1619 | 1171 | 0.01 |
| **g** | **1902** | **2670098** | **4** |
| u | 1987 | 18 | 12 |
| g | 2059 | 5391 | 0.2 |
| u | 2079 | 3863 | 1693 |
| u | 2124 | 53 | 62 |
| g | 2174 | 300530 | 5 |
| g | 2177 | 1568 | 0.04 |
| u | 2210 | 4 | 0.01 |
| u | 2224 | 1581 | 1380 |
| g | 2232 | 140834 | 4 |

[a] Data obtained through DFT calculations carried out at PBEPBE/cc-pVDZ level. Data for the strongest Raman line are highlighted. Calculations have been carried out on slightly bent optimized structures at the same level of theory as above. [b] Irreproducible representations deduced by approximating the symmetry of the chain to the $C_i$ group (i.e., by neglecting the bending of the chain).

As shown in Table 3-3, none of the C≡C vibrational frequencies are affected upon moving from the linear ($D_{\infty h}$) to bent ($C_{2v}$) conformation for the carbon chain H–(C≡C)$_5$–H. Furthermore, this data clearly shows that no IR active ungerade vibrations are found in close proximity of the gerade strong Raman active vibration at 2104 cm$^{-1}$. An inspection of the data reported in Table 3-4 confirms that this is also the case for polyynes **3.1e**, **3.1f** and **3.1h**, i.e., there are no IR active ungerade vibrations found in close proximity to the gerade strong Raman active vibrations at 2066, 1977, and 1902 cm$^{-1}$, respectively. Thus, the DFT results confirm that in all cases considered, irrespective of basis set size and chain termination, the signals observed experimentally in the solid- and solution-state IR spectra for **3.1e-h** must be ascribed to a violation of mutual exclusion rather than to an ungerade IR vibration.

### 3.3.4 X-ray crystallography

Part of the reason for utilizing the adamantyl endgroup was to impart steric bulk on the terminus of the polyyne and thus improve stability. This endgroup was successful in stabilizing polyynes up to six triple bonds (**3.1e**), although stability decreased significantly by the length of the octayne **3.1f**. It is not surprising when one compares the diameter of the adamantyl endgroup to that of a TMS group. The X-ray structure **3.10** clearly shows that the size of these two endgroups are quite similar (Figure 3-10) and since the TMS group is only moderately effective in stabilizing polyynes, one would expect a similar case for the adamantyl, which is indeed the case.

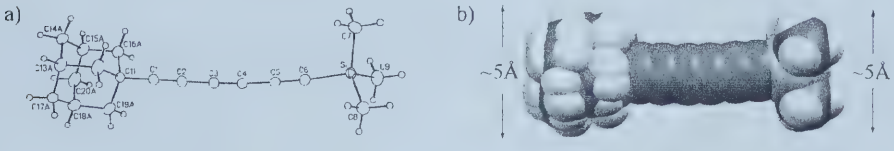


**Figure 3-10.** a) ORTEP drawing of **3.10** where only the major part (60%) of the disordered adamantane group is shown (non-hydrogen atoms represented at the 20% probability level), and b) space-filling model of **3.10** as derived from X-ray diffraction studies showing the similar diameter of the adamantyl and TMS endgroups (disordered adamantane shown).

It has been well documented that polyynes are flexible and do in fact bend in the solid-state,[52] as shown in the previous sections. This is also the case with the tetrayne **3.1c**, which is bent centrosymmetrically in a gentle S-shape with C–C≡C bond angles ranging from 176.84(15)° – 178.24(13)° (Figure 3-11a). The structure of hexayne **3.1e** is non-centrosymmetric with a bent bow-like shape and C–C≡C bond angles in the range 175.4(2) – 178.8(2)° with an average of 177.2° (Figure 3-11b). With hexayne **3.1e** being bent in this manner in the solid-state, the inversion symmetry of the linear chain is lost. Thus, the lack of an inversion center accounts for the experimental IR and Raman observations pertaining to a violation of mutual exclusion.

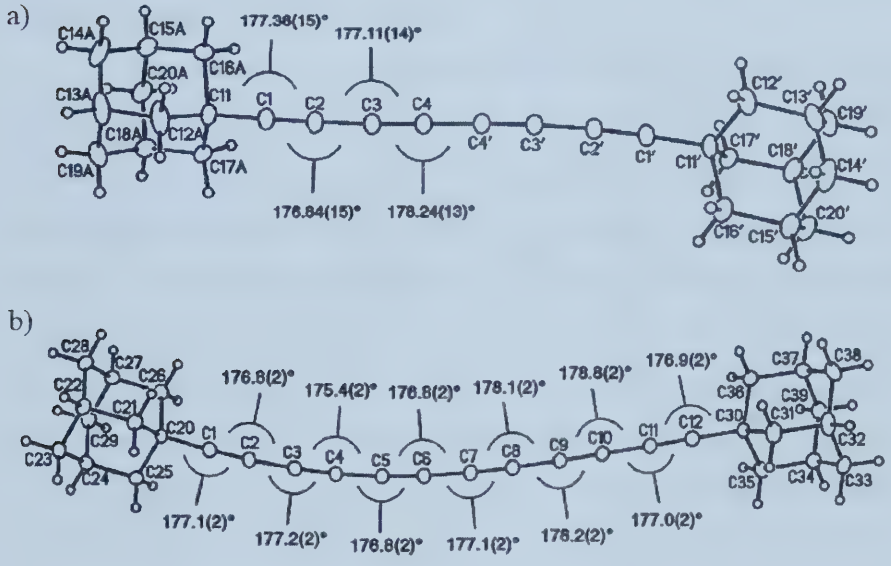


**Figure 3-11.** ORTEP representations at the 20% probability level for a) tetrayne **3.1c** and b) hexayne **3.1e**.

### 3.3.5 Electrochemistry of Adamantyl-Endcapped Polyynes

Electrochemical studies of polyynes have previously been done, which include aryl[53] and metal-endcapped[42b,54,55] polyynes. In the case of aryl-endcapped polyynes, oxidation is unsuccessful, however, these molecules can be reduced and under high sweep rates this reduction becomes more reversible.[53] Also, the reduction of these polyynes becomes easier as a function of polyyne length. Electrochemical studies of polyynes that contain metal endgroups, such as Re-endcapped[42b] or Pt-endcapped,[54,55] have been done. In these cases, it is observed that the polyynes have a reversible oxidation step with no observable reduction step, contrary to the aryl systems. Although these studies show that polyynes as a whole can be studied electrochemically, it does not give a clear insight into the redox behavior of a polyyne chain itself, as these systems are conjugated with endgroups that perturb the π-system.

The redox properties of alkyl-endcapped polyynes has yet to be determined. These systems do not suffer from endgroups that can seriously affect the redox properties of the polyyne and would thus provide a better picture of their redox behavior. The electrochemical properties of the adamantyl-endcapped tetrayne **3.1c**, hexayne **3.1e**, and octayne **3.1f** have been explored in collaboration with Professor Luis Echegoyen and coworkers (Clemson University, South Carolina) as summarized in Figure 3-13 and Table 3-5. All experiments have been carried out in $CH_2Cl_2$ containing 0.1M $Bu_4NPF_6$ with a conventional three-electrode cell. A glassy carbon disc (3 mm diameter) serves as the working electrode. A small amount of ferrocene (Fc) is added at the end of the experiments and used as an internal reference for potentials. In the case of tetrayne **3.1c**, no signal is observed within the available potential range. The hexayne **3.1e**, on the other hand, shows one reversible oxidation and one irreversible reduction step (Figure 3-13a). Unlike the aryl hexayne reported by Hirsch and coworkers (see Figure 3-12),[53] compound **3.1e** does not become more reversible when the scan rate was increased (Figure 3-13b). This indicates that the radical anion of **3.1e** is even more reactive than Hirsch's compound. This also likely explains the formation of an insoluble brown-black solid during analysis. Octayne **3.1f** also shows irreversible reduction steps with no oxidation step (Figure 3-13c). The reduction occurred at a potential 200 mV lower than **3.1e** as a result of the longer π-system.

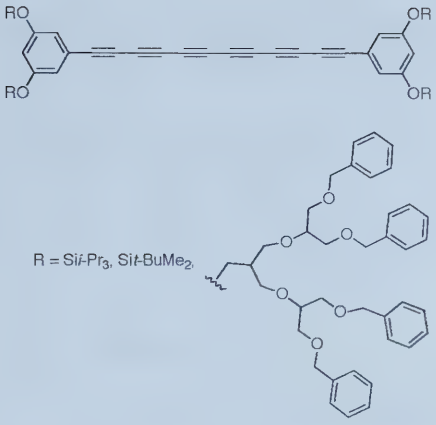


**Figure 3-12.** Hirsch and coworkers aryl hexaynes.

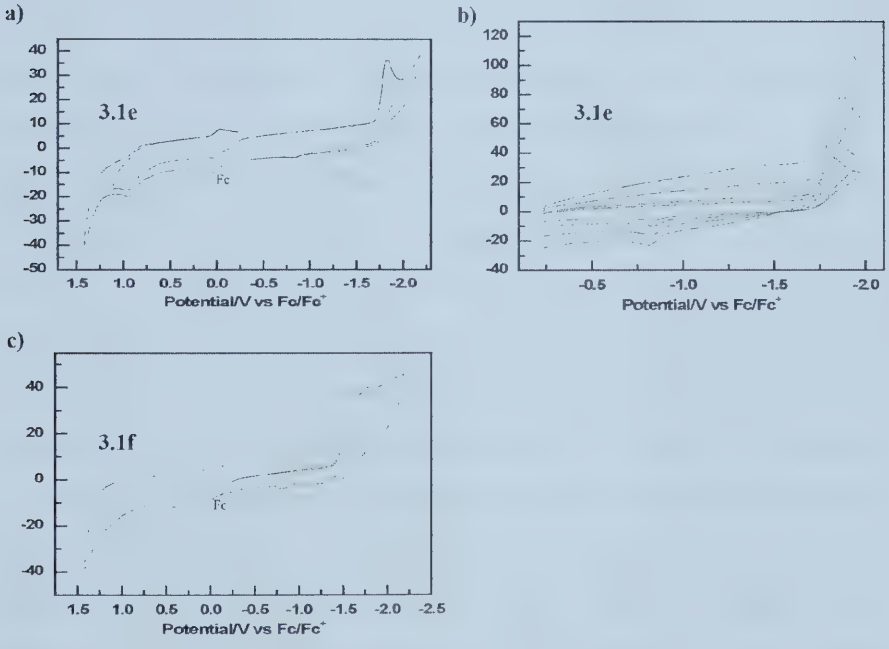


**Figure 3-13.** Cyclic voltammograms measured in $CH_2Cl_2$ containing 0.1M $Bu_4NPF_6$ of a) hexayne **3.1e** (scan rate = 100 $mVs^{-1}$), b) hexayne **3.1e** at different scan rates (scan rate = 100, 200, 500 and 1000 $mVs^{-1}$), and c) octayne **3.1f** (scan rate = 100 $mVs^{-1}$). Fc = ferrocenium/ferrocene couple.

**Table 3-5.** Peak potentials of the first reduction and oxidation steps of hexayne **3.1e** and octayne **3.1f**.

| Compound | $Ep_c\ red_1$ | $Ep_a\ ox_1$ |
|---|---|---|
| **3.1d** | - | - |
| **3.1e** | -1.83 | 0.94 |
| **3.1f** | -1.63 | - |

## 3.4 Conclusions

The synthesis of a series of polyynes utilizing an adamantyl endgroup has successfully been achieved using a Friedel-Crafts/FBW rearrangement protocol. Polyynes of this series are stable up to the hexayne (**3.1e**), however, the stability decreases with the octayne **3.1f** and by the decayne **3.1h**, isolation and characterization is difficult due to rapid decomposition. The UV-Vis spectral data show a lowering of the HOMO–LUMO band gap as a function of polyyne length, which is displayed by a red shift of $\lambda_{max}$ for each successively longer polyyne in the series. Raman and IR spectroscopic analyses have been carried out and, with the help of X-ray crystallography and DFT calculations, the analyses showed that adamantyl-endcapped polyynes adopt a nonlinear (bent) structure in both the solid- and solution-states. This hypothesis is supported by the observation that the Raman-active Я-mode line appears in the IR absorption spectra for compounds **3.1e-h**, and is thus a violation of the mutual-exclusion principle. This experimental evidence is noteworthy in the case of solution-state analysis, since it suggests that a bent shape in the polyynes is a characteristic of the molecule itself rather than the result of external influences such as crystal packing effects. It is necessary to point out, however, that the solution-state IR and Raman data presented here cannot establish the underlying cause of the violation of mutual exclusion, so the following questions remain: does the violation derive from a nonlinear equilibrium conformation(s) (static symmetry breaking), large-amplitude bending vibrations (dynamic symmetry breaking), or both? Further theoretical and experimental studies are underway to shed light on the answer to this question.

## 3.5 References


[1] Smith, P. P. K.; Buseck, P. R. *Science* **1982**, *216*, 984.

[2] Lagow, R. J.; Kampa, J. J.; Wei, H.-C.; Battle, S. L.; Genge, J. W.; Laude, D. A.; Harper, C. J.; Bau, R.; Stevens, R. C.; Haw, J. F.; Munson, E. *Science* **1995**, *267*, 362.

[3] Kudryavtsev, Y. P.; Evsyukoc, S.; Gusevca, M.; Babaev, C.; Khvistov, C. In *Chemistry and Physics of Carbon*; Thrower, P. A., Ed; Dekker: New York, 1997; Vol. 25, pp 1.

[4] Cataldo, F. *Polym. Int.* **1997**, *44*, 191.

[5] Stetter, H.; Goebel, P. *Chem. Ber.* **1962**, *95*, 1039.

[6] Stetter, H. *Chem. Ber.* **1959**, *92*, 1629.

[7] Zhang, B.; Breslow, R. *J. Am. Chem. Soc.* **1997**, *119*, 1676.

[8] Müller, T.; Hullinger, J.; Seichter, W.; Weber, E.; Weber, T.; Wübbenhorst, M. *Chem. Eur. J.* **2000**, *6*, 54.

[9] Hay, A. S. *J. Org. Chem.* **1962**, *27*, 3320.

[10] Siemsen, P.; Livingston, R. C.; Diederich, F. *Angew. Chem. Int. Ed.* **2000**, *39*, 2632.

[11] Chalifoux, W. A.; Ferguson, M. J.; Tykwinski, R. R. *Eur. J. Org. Chem.* **2007**, 1101.

[12] Lei, A.; Srivastava, M.; Zhang, X. *J. Org. Chem.* **2002**, *67*, 1969.

[13] Eisler, S.; Chahal, N.; McDonald, R.; Tykwinski, R. R. *Chem. Eur. J.* **2003**, *9*, 2542.

[14] Ramirez, F.; Desai, N. B.; McKelvie, N. *J. Am. Chem. Soc.* **1962**, *84*, 1745.

[15] Corey, E. J.; Fuchs, P. L. *Tetrahedron Lett.* **1972**, *13*, 3769.

[16] Fritsch, P. *Liebigs Ann. Chem.* **1894**, *279*, 319.

[17] Buttenberg, W. P. *Liebigs Ann. Chem.* **1894**, *279*, 324.

[18] Wiechell, H. *Liebigs Ann. Chem.* **1894**, *279*, 337.

[19] Jiang, M. X.-W.; Rawat, M.; Wulff, W. D. *J. Am. Chem. Soc.* **2004**, *126*, 5970.

[20] Nishikawa, T.; Shibuya, S.; Hosokawa, S.; Isobe, M. *Synlett* **1994**, 485.

[21] Cadiot, P.; Chodkiewicz, W. In *Chemistry of Acetylenes*; Viehe, H. G., Ed; Dekker: New York, 1969; pp 597.

[22] Bohlmann, F.; Schönowsky, H.; Inhoffen, E.; Grau, G. *Chem. Ber.* **1964**, *97*, 794.

[23] Chalifoux, W. A.; McDonald, R.; Ferguson, M. J.; Tykwinski, R. R. *Angew. Chem. Int. Ed.* **2009**, *48*, 7915.

[24] Eisler, S.; Slepkov, A. D.; Elliott, E.; Luu, T.; McDonald, R.; Hegmann, F. A.; Tykwinski, R. R. *J. Am. Chem. Soc.* **2005**, *127*, 2666.

[25] Chalifoux, W. A.; Tykwinski, R. R. *C. R. Chimie* **2009**, *12*, 341.

[26] Walton, D. R. M.; Waugh, F. *J. Organomet. Chem.* **1972**, *37*, 45.

[27] Since hexayne **3.1e** was successfully synthesized following **route A** it was not synthesized following **route B** from triyne **3.15**.

[28] Haley, M. M.; Bell, M. L.; Brand, S. C.; Kimball, D. B.; Pak, J. J.; Wan, W. B. *Tetrahedron Lett.* **1997**, *38*, 7483.

[29] Bubeck, C. In *Electronic Materials – the Oligomer Approach*; Müllen, K.; Wegner, G., Eds; Wiley-VCH: Weinheim, 1998; Chapter 8.

[30] Luo, Y.; Norman, P.; Ruud, K.; Agren, H. *Chem. Phys. Lett.* **1998**, *285*, 160.

[31] Mathy, A.; Ueberhofen, K.; Schenk, R.; Gregorius, H.; Garay, R.; Müllen, K.; Bubeck, C. *Phys. Rev. B* **1996**, *53*, 4367.

[32] Lewis, G. N.; Calvin, M. *Chem. Rev.* **1939**, *25*, 273.

[33] Milani, A.; Tommasini, M.; Del Zoppo, M.; Castiglioni, C.; Zerbi, G. *Phys. Rev. B* **2006**, *74*, 153418.

[34] Tommasini, M.; Fazzi, D.; Milani, A.; Del Zoppo, M.; Castiglioni, C.; Zerbi, G. *J. Phys. Chem. A* **2007**, *111*, 11645.

[35] Tommasini, M.; Milani, A.; Fazzi, D.; Del Zoppo, M.; Castiglioni, C.; Zerbi, G. *Physica E* **2008**, *40*, 2570.

[36] Castiglioni, C.; Zerbi, G.; Gussoni, M.; Lopez Navarrete, J. T. *Solid State Commun.* **1988**, *65*, 625.

[37] Castiglioni, C.; Tommasini, M.; Zerbi, G. *Philos. Trans. R. Soc. London, A* **2004**, *362*, 2425.

[38] Extensive theoretical work and first-principles calculations support the premise that the strong Raman band (Я-mode) considered here (and activated in the IR spectrum) is

certainly a fundamental vibration rather than a combination or Fermi resonance band (see refs 33-37).

[39] Jensen, J. O. *Spectrochim. Acta, Part A* **2004**, *60*, 1895.

[40] Casari, C. S.; Li Bassi, A.; Baserga, A.; Ravagnan, L.; Piseri, P.; Lenardi, C.; Tommasini, M.; Milani, A.; Fazzi, D.; Bottani, C. E.; Milani, P. *Phys. Rev. B* **2008**, *77*, 195444.

[41] Anharmonicity is expected to play a major role in the description of low-frequency bending vibrations but should not affect the selection rules for the fundamental vibrations (Я-band) discussed here. More specifically, anharmonicity certainly changes the vibrational wave function, but it cannot change the irreproducible representation to which it belongs. In other words, selection rules for fundamentals are not expected to be broken if anharmonicity is taken into account; only the value of the transition probabilities would be affected. While anharmonicity is considered to be weak and negligible for the high frequency C≡C stretching vibrations explored in this study, it is expected to play a major role in the description of the low-frequency bending vibrations. This discussion is, however, outside the scope of the current investigation. For a theoretical description of anharmonicity effects in polyynes, see Neugebauer, J.; Reiher, M. *J. Phys. Chem. A* **2004**, *108*, 2053.

[42] For exemplary studies of polyynes by Raman spectroscopy, see: (a) Schermann, G.; Grösser, T.; Hampel, F.; Hirsch, A. *Chem. Eur. J.* **1997**, *3*, 1105. (b) Dembinski, R.; Bartik, T.; Bartik, B.; Jaeger, M.; Gladysz, J. A. *J. Am. Chem. Soc.* **2000**, *122*, 810. (c) Tabata, H.; Fujii, M.; Hayashi, S.; Doi, T.; Wakabayashi, T. *Carbon* **2006**, *44*, 3168. (d) Lucotti, A.; Tommasini, M.; Del Zoppo, M.; Castiglioni, C.; Zerbi, G.; Cataldo, F.; Casari, C. S.; Li Bassi, A.; Russo, V.; Bogana, M.; Bottani, C. E. *Chem. Phys. Lett.* **2006**, *417*, 78. (e) Yang, S.; Kertesz, M.; Zólyomi, V.; Kürti, J. J. *Phys. Chem. A* **2007**, *111*, 2434. (f) Casari, C. S.; Russo, V.; Li Bassi, A.; Bottani, C. E.; Cataldo, F.; Lucotti, A.; Tommasini, M.; Del Zoppo, M.; Castiglioni, C.; Zerbi, G. *Appl. Phys. Lett.* **2007**, *90*, 013111. (g) Milani, A.; Tommasini, M.; Fazzi, D.; Castiglioni, C.; Del Zoppo, M.; Zerbi, G. *J. Raman Spectrosc.* **2008**, *39*, 164.

[43] Van Orden, A.; Saykally, R. J. *Chem. Rev.* **1998**, *98*, 2313.

[44] Masiello, T.; Voorhees, A. J.; Abel, M. J.; Nibler, J. W. *J. Phys. Chem. A* **2005**, *109*, 3139.

[45] Perdew, J. P.; Burke, K.; Ernzerhof, M. *Phys. Rev. Lett.* **1996**, *77*, 3865.

[46] Woon, D. E.; Dunning, T. H. *J. Chem. Phys.* **1993**, *98*, 1358.

[47] Liang, C.; Allen, L. C. *J. Am. Chem. Soc.* **1991**, *113*, 1873.

[48] Botschwina, P. *J. Phys. Chem. A* **2007**, *111*, 7431.

[49] Koput, J. *Chem. Phys. Lett.* **2000**, *320*, 237.

[50] Zhuravlev, F.; Gladysz, J. A. *Chem. Eur. J.* **2004**, *10*, 6510.

[51] See Appendix B for a full list of harmonic frequencies, IR and Raman intensities, and irreproducible representations of the normal modes for H-(C≡C)$_5$-H.

[52] Szafert, S.; Gladysz, J. A. *Chem. Rev.* **2006**, *106*, PR1.

[53] Gibtner, T.; Hampel, F.; Gisselbrecht, J.-P.; Hirsch, A. *Chem. Eur. J.* **2002**, *8*, 408.

[54] Mohr, W.; Stahl, J.; Hampel, F.; Gladysz, J. A. *Chem. Eur. J.* **2003**, *9*, 3324.

[55] Zheng, Q.; Bohling, J. C.; Peters, T. B.; Frisch, A. C.; Hampel, F.; Gladysz, J. A. *Chem. Eur. J.* **2006**, *12*, 6486.

# Chapter 4 Synthesis and Properties of *t*-Butyl-Endcapped Polyynes[‡]

## 4.1 Introduction

The synthesis of polyynes for the purposes of gaining insight into the material known as carbyne has been an ongoing task for the Tykwinksi group[1-5] and others.[6] The synthesis of a series of polyynes that minimizes endgroup effects on the polyyne π-system, while imparting stability to the polyyne, is one of the main goals of this research.[7] Ideally, the use of hydrogen[8-10] or even methyl[11] groups would achieve this goal, but the instability of such molecules often complicates their synthesis, purification, and analysis. Thus, other relatively benign endgroups have also been utilized, such as the adamantyl endgroup (**3.1**),[7] as well as the triisopropylsilyl endgroup (**S1**),[3] each providing a series of polyynes up to ten triple bonds and allowed for their physical properties to be studied (Figure 4-1). In one of these studies, the adamantyl polyynes were investigated experimentally via analysis of electronic absorption spectra of radical ions generated by radiolysis.[12] Unfortunately, the molecules proved difficult to study effectively via computational methods due to the size of the adamantyl groups, making the comparisons between theoretical and experimental data challenging. Thus, polyynes bearing the structurally similar, albeit smaller, *t*-Bu endgroup were investigated.[13-15] On the basis of this earlier work, it was hypothesized that the *t*-Bu polyynes would be sufficiently stable and chemically well-behaved for subsequent study. Thus, the synthesis of this series of polyynes was attempted using the methods developed for adamantyl derivatives **3.1**.

---

[‡] Portions of this chapter have been published. Chalifoux, W. A.; MacDonald, R.; Ferguson, M. J.; Tykwinski, R. R. *Angew. Chem. Int. Ed.* **2009**, *48*, 7915.

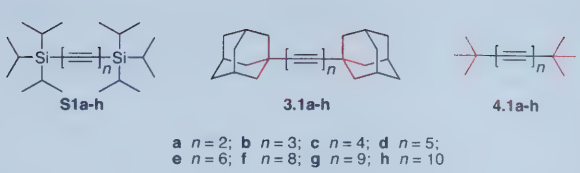


**Figure 4-1.** Triisopropylsilyl- (**S1**), 1-adamantyl- (**3.1**) and *t*-butyl-endcapped (**4.1**) polyynes.

## 4.2 Synthesis of *t*-Butyl-Endcapped Polyynes

The synthesis of diyne **4.1a** was accomplished following a procedure previously reported.[16] Triyne **4.1b** has been easily assembled via a Fritsch-Buttenberg-Wiechell (FBW) rearrangement in a manner reported for other symmetrical triynes.[17] This method involved addition of lithiated *t*-butylacetylene to ethyl formate to give alcohol **4.2** in excellent yield (Scheme 4-1). The alcohol **4.2** was oxidized using PCC to obtain ketone **4.3** in good yield. Dibromoolefination of ketone **4.3**, using the protocol reported by Ramirez,[18] gave **4.4** in excellent yield. The final step was the FBW rearrangement, which resulted in nearly quantitative yield of triyne **4.1b**, albeit the isolated yield by crystallization was only 42%.

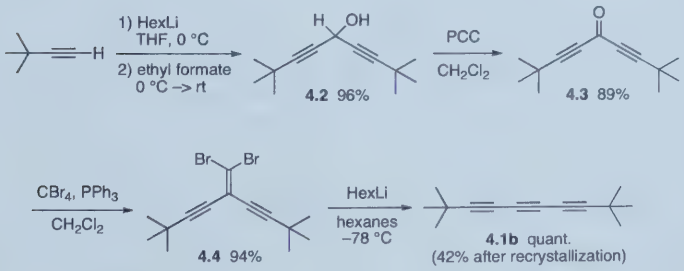


**Scheme 4-1.** Synthesis of triyne **4.1b** via a FBW rearrangement.

The synthesis of tetrayne **4.1c** was carried out in a manner analogous to that reported for the adamantyl tetrayne (Chapter 3). The reaction of *t*-butylacetylene and 1-bromo-3-methyl-1-butyn-3-ol under Cadiot-Chodkiewicz[19,20] heterocoupling conditions gave diyne **4.5** in good yield

(Scheme 4-2).[21] Deprotection followed by homocoupling under Hay[19,22] conditions gave tetrayne **4.1c** in good yield over two steps.

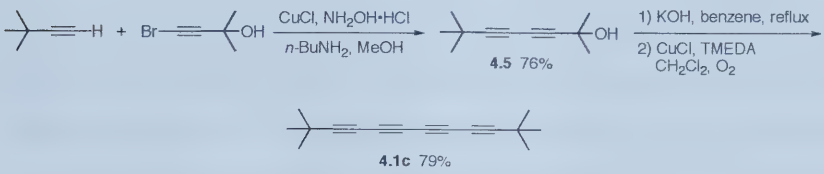


**Scheme 4-2.** Synthesis of tetrayne **4.1c**.

Pentayne **4.1d** was a more significant synthetic challenge since oxidative dimerization reactions are not particularly applicable.[6] Following the protocol shown for the adamantyl pentayne (see Chapter 3, compound **3.1e**), a Friedel-Crafts reaction[23] between triyne **4.6**[24,25] and the acid chloride derived from **4.7** resulted in ketone **4.8** (Scheme 4-3). Since **4.8** is not stable to isolation, it was carried on directly to the dibromoolefination step, which gave **4.9** in 45% yield over the two steps. In the final step, pentayne **4.1d** was produced in 75% yield from **4.9** via a FBW rearrangement.

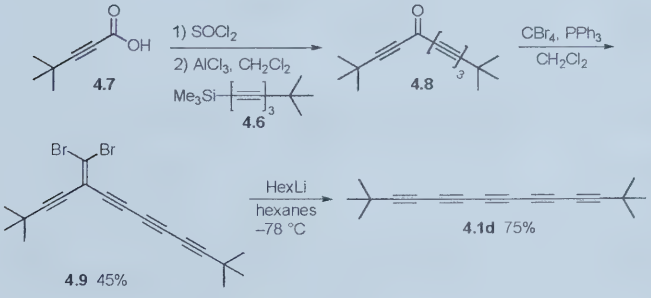


**Scheme 4-3.** Synthesis of pentayne **4.1d**.

The construction of hexa-, octa-, and decaynes **4.1e**, **4.1f**, and **4.1h** each followed a comparable sequence of steps starting from the common precursor, acid **4.7**. Thus, reaction of **4.7**

with thionyl chloride followed by a Friedel-Crafts acylation reaction with the appropriate α,ω-bis(trimethylsilyl)polyyne gave the corresponding ketone intermediates **4.10**–**4.12** (Scheme 4-4). Given their instability, the crude products (**4.10**–**4.12**) were purified by passing through a short column of silica gel and then carried on directly to the dibromoolefination step. This gave dibromoolefins **4.13**–**4.15** in yields that ranged from 29% (**4.15**) to 80% (**4.13**) over the two steps. A FBW rearrangement of **4.13** resulted in unsymmetrical triyne **4.6** in good yield. A FBW rearrangement of **4.14** and **4.15** produced tetrayne **4.16** and pentayne **4.17**, both of which were not stable and therefore not isolated. Triyne **4.6** and tetrayne **4.16** were subjected to slightly modified Hay oxidative homocoupling conditions (THF, MeOH, CuCl, TMEDA, $O_2$).[22] Under these conditions, the trimethylsilyl-protecting group was effectively removed, and homocoupling afforded **4.1e** or **4.1f** in acceptable yield. Attempts to use this same procedure with pentayne **4.17** led not only to the desired product **4.1h**, but also nonayne **4.1g**.[26] Changing the catalyst system to that of Eglinton-Glaser[19,27-29] ($Cu(OAc)_2 \cdot H_2O$, THF, MeOH, pyridine) circumvented this problem and gave decayne **4.1h** in a respectable yield of 54%.

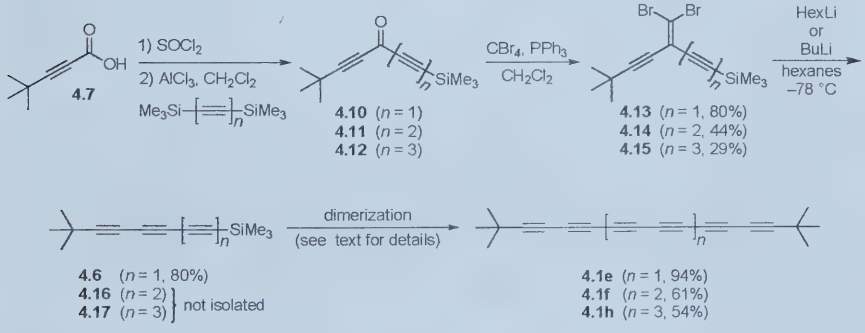


**Scheme 4-4.** Synthesis of hexayne **4.1e**, octayne **4.1f**, and decayne **4.1h**.

## 4.3 Physical and Spectroscopic Properties of *t*-Butyl-Endcapped Polyynes

### 4.3.1 UV-Vis Spectroscopic Analysis of *t*-Butyl Polyynes

Polyynes **4.1a-f** and **4.1h** have been characterized by EI (**4.1a-f**) and MALDI (**4.1h**) MS analysis to confirm their constitution. Their UV–Vis spectra are consistent with those previously published by Bohlmann[30] and Jones,[31] showing considerable vibrational fine structure for the HOMO → LUMO transition, accompanied by a consistent lowering of $\lambda_{max}$ energy as a function of polyyne length (Figure 4-2 and Table 4-1).

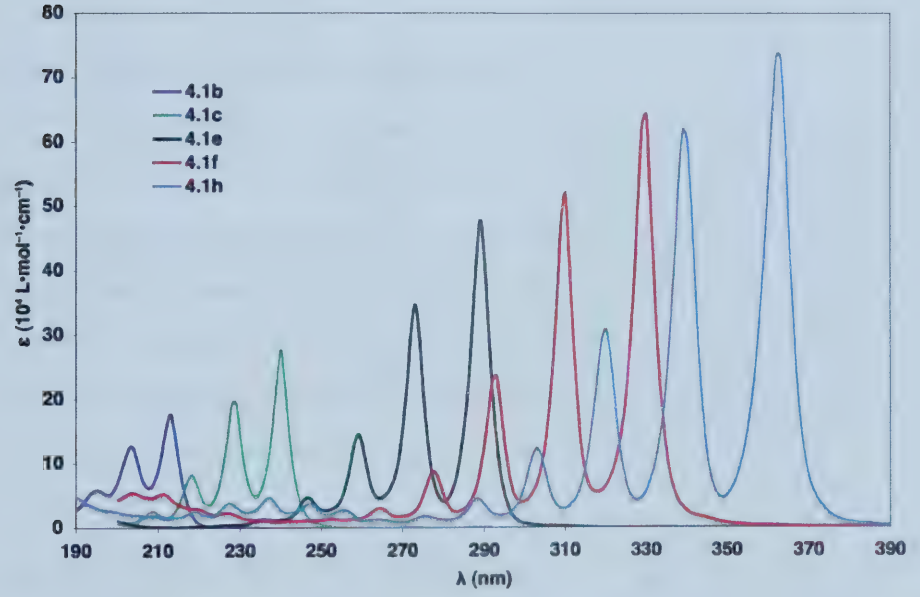


**Figure 4-2.** Quantitative UV-Vis spectra of *t*-butyl triyne **4.1b**, tetrayne **4.1c**, hexayne **4.1e**, octayne **4.1f**, and decayne **4.1h** in hexanes.

As seen with the adamantyl polyyne series (Chapter 3), there is a hypsochromic shift as well as higher extinction coefficients (ε) when the UV-Vis spectroscopic analysis is done in hexanes versus THF (Table 4-1). As the polyynes become longer there is not only a consistent red

shift of $\lambda_{max}$, but also an increase in ε value. This trend culminates in a $\lambda_{max}$ value for **4.1h** at 362 nm (in hexanes), with a significant molar absorptivity (ε = 736000 $L \cdot mol^{-1} \cdot cm^{-1}$).

**Table 4-1.** UV-Vis absorbance data for *t*-butyl polyynes in hexanes.

| Compound | *n* | hexanes | | THF | |
|---|---|---|---|---|---|
| | | $\lambda_{max}$ (nm) | ε ($M^{-1} \cdot cm^{-1}$) | $\lambda_{max}$ (nm) | ε ($M^{-1} \cdot cm^{-1}$) |
| **4.1b** | 3 | 213 | 178000 | - | - |
| **4.1c** | 4 | 240 | 277000 | 243 | 274000 |
| **4.1d** | 5 | 266 | - | - | - |
| **4.1e** | 6 | 289 | 478000 | 293 | 401000 |
| **4.1f** | 8 | 330 | 643000 | 335 | 519000 |
| **4.1h** | 10 | 362 | 736000 | 368 | 530000 |

### 4.3.2 NMR Spectroscopic Analysis of *t*-Butyl Polyynes

While the $^{1}H$ NMR spectra are obviously of little interest, the $^{13}C$ NMR spectra of these simple hydrocarbons are worth discussing. As has been observed for other homologous series of polyynes,[3] there are consistent trends in the observed chemical shifts as a function of length (Table 4-2). The most deshielded acetylenic resonance moves consistently downfield from δ 86.3 (**4.1a**) to δ 89.6 (**4.1h**), while the most upfield resonance of each polyyne is found in a narrow range of δ 61.7–61.4 (for **4.1a** it is observed at δ 63.7). The remaining resonances converge toward a value of ca. 63 ppm as the length is increased (see Figure 4-3).

**Table 4-2.** $^{13}C$ NMR spectroscopic data for polyynes **4.1a-h**.

| Polyyne | $^{13}C$ NMR spectroscopic data in $CDCl_3$ (ppm) |
|---|---|
| **3a** | 86.3, 63.7, 30.6, 28.0 |
| **3b** | 87.0, 64.4, 61.4, 30.4, 28.1 |
| **3c** | 87.7, 64.5, 61.8, 61.5, 30.3, 28.2 |
| **3d** | 88.4, 64.4, 62.1, 62.0, 61.7, 30.2, 28.3 |
| **3e** | 88.8, 64.4, 62.5, 62.5, 61.9, 61.6, 30.2, 28.3 |
| **3f** | 89.4, 64.4, 63.4, 63.2, 62.9, 62.3, 61.7, 61.4, 30.1, 28.4 |
| **3h** | 89.6, 64.3, 63.8, 63.5, 63.5, 63.0, 62.6, 62.1, 61.6, 61.4, 30.1, 28.4 |

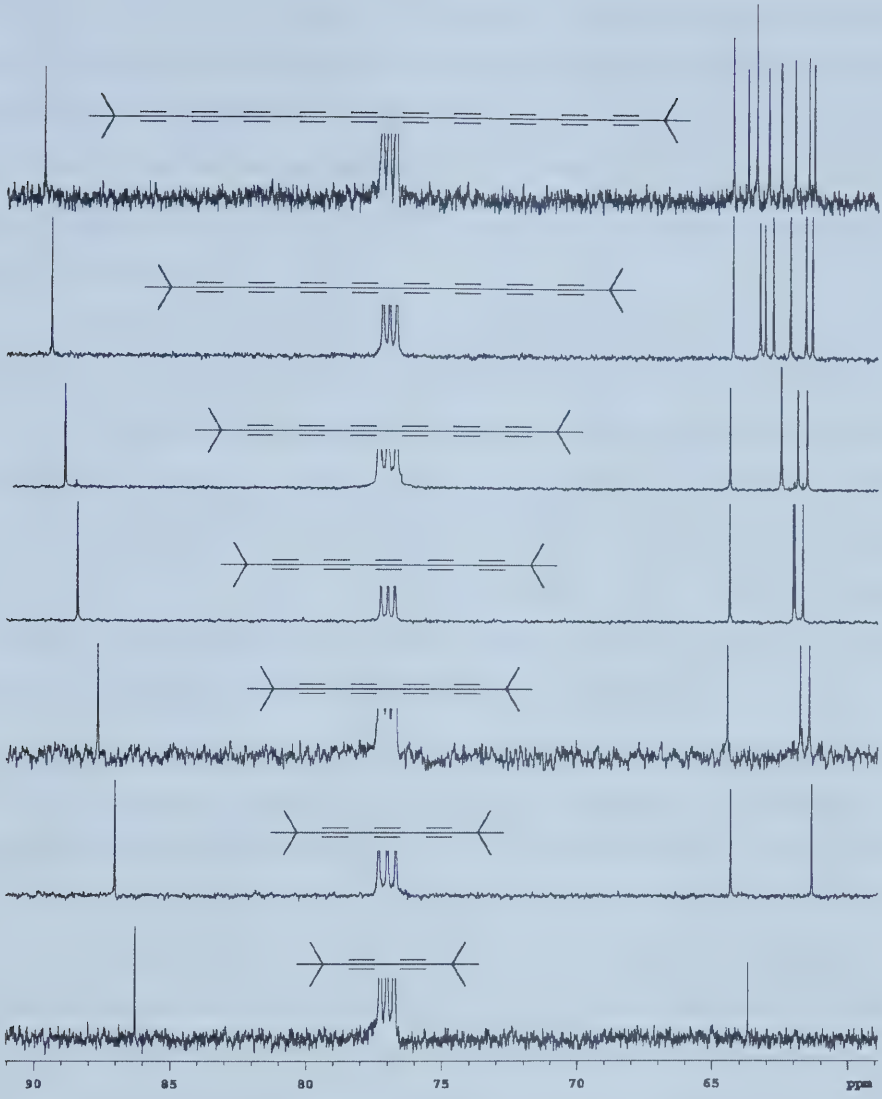


**Figure 4-3.** A comparison of $^{13}C$ NMR spectra of polyynes **4.1a-f** and **4.1h** ($CDCl_3$).

### 4.3.3 X-Ray Crystallographic Analysis of *t*-Butyl Polyynes

Whereas trends in data from NMR and UV-Vis spectroscopic analysis for polyynes have become almost routine in recent years,[1,3,7,32-37] one particular question has remained unanswered:

Do extended polyynes show experimental evidence of reduced bond length alternation (BLA = the bond length difference between the central single and triple bonds) as a function of increasing length? With X-ray crystallographic data for extended polyynes being essentially nonexistent, an answer to this query has remained open until recently. To convey this lack of experimental data, prior to octayne **4.1f**,[4] there are only two published reports solid-state structures of polyynes with at least 16 sp-carbons.[3,38]

Given that polyynes are essentially a 1-D conjugated system, the changes in HOMO – LUMO gap versus length should be intricately dependent on the degree of BLA in the polyyne structure.[39,40] Recent theoretical studies have upheld the prediction that neither the HOMO – LUMO gap nor the BLA for polyynes will go to a value of zero,[41-44] a phenomena commonly referred to as Peierls distortion.[45] Experimentally, it should be possible to explore trends in BLA as a function of polyyne length via X-ray crystallographic analysis. As polyynes become increasingly longer, however, stability decreases significantly and obtaining single crystals for analysis of polyynes beyond the length of a hexayne has been a difficult task.[46]

For polyyne series **4.1**, useful diffraction patterns have been obtained for diyne **4.1a**, triyne **4.1b**, tetrayne **4.1c**, octayne **4.1f**, and decayne **4.1h** (Figure 4-4).[4,47] The structure of decayne **4.1h** deserves extra attention, given that it is the only successful crystallographic analysis of a polyyne of longer than 16 contiguous sp-hybridized carbons.[48] Crystals of **4.1h** were grown by slow evaporation of a $CH_2Cl_2$ solution at 4 °C. The structure contains two crystallographically independent molecules in the unit cell (labeled as molecule **4.1h-A** and **4.1h-B** in Figure 4-4 and Figure 4-5). Molecule **4.1h-A** is unsymmetrical, adopting a semi-helical conformation with C–C≡C bond angles that range from 174.4(6)° to 179.3(5)° (Figure 4-5). Molecule **4.1h-B**, on the other hand, is centrosymmetric, adopting a gentle S-shape, with a slightly smaller deviation from linearity having C–C≡C bond angles that range from 176.1(6)° to 179.5(8)°. One of the most impressive aspects of decayne **4.1h** is its length with the molecule spanning an amazing 2.7 nm from end-to-end (i.e., C2A to C23A or C2B to C2B').

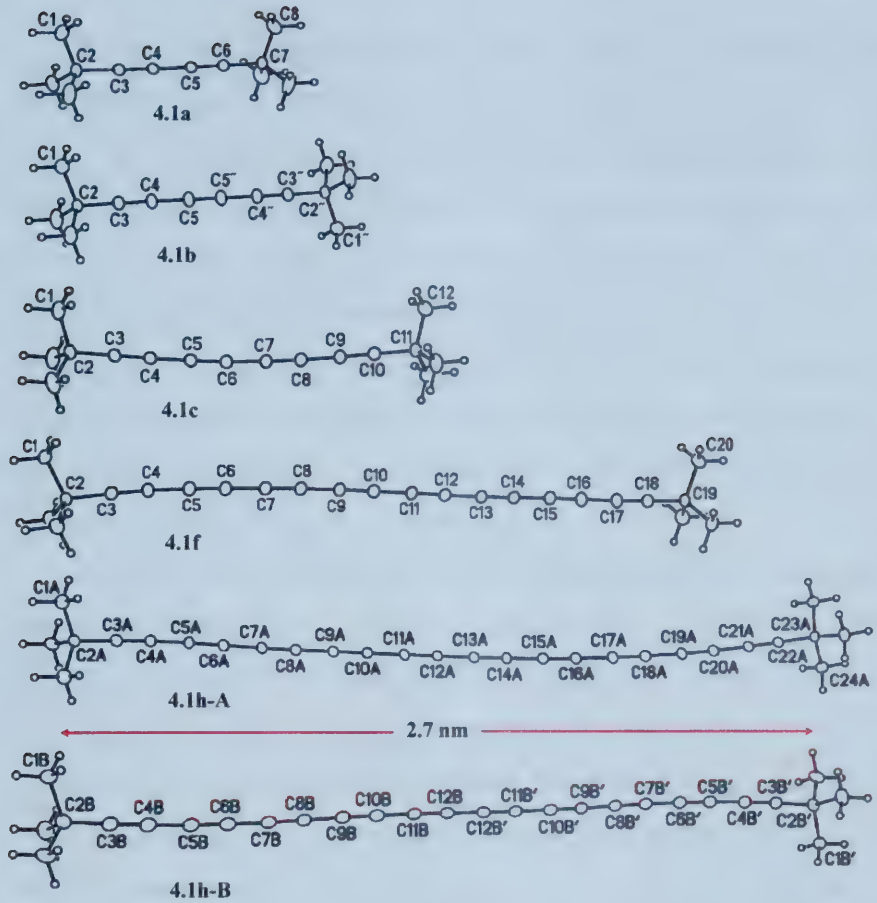


**Figure 4-4.** ORTEP drawings (20% probability level) for **4.1a-c**, **4.1f**, **4.1h-A** and **4.1h-B**.

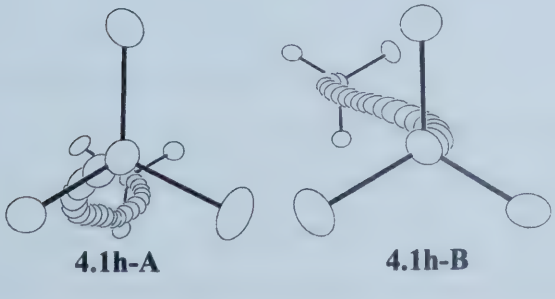


**Figure 4-5.** End-on view of **4.1h-A** and **4.1h-B** highlighting nonlinearity of each molecule (hydrogen atoms removed for clarity).

A recent review by Szafert and Gladysz estimates a BLA of ca. 0.07-0.08 Å for an infinite polyyne system, a prediction made from the comprehensive analysis of X-ray crystallographic data for polyyne structures of at least 8 contiguous sp-hybridized carbons.[48] This estimate is potentially complicated by "endgroup effects" because many of the polyynes in this analysis are endcapped with groups that are strongly conjugated with the polyyne core. Computational chemists have also frequently addressed BLA in polyynes, due, at least in part, to the relative structural simplicity of these molecules.[41,43,44,49] From these theoretical studies, it is clear that the choice of basis set and electron correlations can have a dramatic effect on results.[50-53] Nevertheless, a consistent trend has emerged from recent investigations that predict that BLA values converge to a value of ca. 0.13 Å (Table 4-3, entries 13-17).[41,42,44]

An analysis of the solid-state structure for polyynes **4.1a-c**, **4.1f** and **4.1h** reveals a distinct trend in reduced BLA as a function of polyyne length, similar to that predicted theoretically.[41,42,44] The analysis of BLA from the X-ray data of **4.1a-c**, **4.1f**, and **4.1h-A/B** was conducted in two ways. First, as reported for computed structures (Table 4-3, entries 13-17), BLA was calculated as the bond length difference between the central single and triple bonds in each structure (selected bond lengths given in Table 4-4). This leads to a consistent reduction in BLA values from a maximum of 0.184 Å for dimer **4.1a** to a minimum of 0.139 Å (average of **4.1h-A** and **4.1h-B**). This analysis also suggests that the reduction in BLA is approaching saturation by the stage of the decayne, similar to that predicted by theory.[41,43,44,49] This is clearly displayed when BLA is plotted versus the number of triple bonds ($n$) (blue line, Figure 4-6). A plot of BLA versus the inverse of the number of triple bonds ($1/n$) also displays a reduction in BLA that is approaching saturation by the decayne (Figure 4-7). A line-of-best-fit for BLA predicts limiting values of 0.126 Å. When one looks at the data points for the octa- (**4.1f**) and decayne (**4.1h**), it appears that the values are leveling off and therefore an extrapolation based on these points predict a limiting value of BLA = 0.135 Å at the asymptotic limit.[43] One potential issue with this BLA analysis, however, is that it relies on the difference of two specific bonds, where small errors in either of these bond lengths might be overemphasized in comparison with other bond

**Table 4-3.** Summary of experimental and theoretical BLA data.

| Entry | Polyyne | BLA[a] (Å) | ESD[b] (BLA) | C–Cavg (Å) | C≡C$_{avg}$ (Å) | BLA$_{avg}$[c] (Å) | ESD (BLA$_{avg}$) | Ref |
|---|---|---|---|---|---|---|---|---|
| 1 | **4.1a** | 0.184 | 0.004 | 1.382 | 1.199 | 0.183 | 0.004 | 4 |
| 2 | **4.1b** | 0.164 | 0.006 | 1.368 | 1.202 | 0.166 | 0.004 | 4 |
| 3 | **4.1c** | 0.151 | 0.002 | 1.365 | 1.204 | 0.161 | 0.001 | 4,47 |
| 4 | **4.1f** | 0.140 | 0.002 | 1.356 | 1.209 | 0.147 | 0.001 | 4 |
| 5 | **4.1h-A** | 0.144 | 0.007 | 1.350 | 1.207 | 0.143 | 0.003 | 4 |
| 6 | **4.1h-B** | 0.134 | 0.015 | 1.354 | 1.206 | 0.148 | 0.006 | 4 |
| 7 | **4.1h-A/B$_{avg}$** | 0.139 | 0.008 | 1.352 | 1.206 | 0.146 | 0.003 | 4 |
| 8 | **S1a** | 0.169 | 0.004 | 1.373 | 1.204 | 0.169 | 0.004 | 54 |
| 9 | **S1c** | 0.157 | 0.003 | 1.366 | 1.209 | 0.157 | 0.002 | 3 |
| 10 | **S1d** | 0.148 | 0.004 | 1.362 | 1.209 | 0.153 | 0.002 | 3 |
| 11 | **S1e** | 0.149 | 0.004 | 1.361 | 1.208 | 0.153 | 0.002 | 3 |
| 12 | **S1f** | 0.153 | 0.006 | 1.361 | 1.200 | 0.161 | 0.006 | 3 |
| 13 | H-(C≡C)$_9$-H | 0.1291[d] | – | 1.36175 | 1.2254 | 0.13675 | – | 41 |
| 14 | H-(C≡C)$_\infty$-H | 0.1276[d] | – | – | – | – | – | 41 |
| 15 | H-(C≡C)$_\infty$-H | 0.133[e] | – | – | – | – | – | 44 |
| 16 | H-(C≡C)$_\infty$-H | 0.131[f] | – | – | – | – | – | 44 |
| 17 | H-(C≡C)$_\infty$-H | 0.134[g] | – | – | – | – | – | 42 |

[a] See text (Note: for non-centrosymmetric structures, BLA was calculated using the average of positionally equivalent bonds {i.e., BLA (**4.1a**) = (C4–C5) – [(C3≡C4) + (C5≡C6)]/2}). [b] ESD = estimated standard deviation. [c] [C–C$_{avg}$] – [C≡C$_{avg}$]; note: calculation does not include terminal C–C bond (e.g., C2–C3). [d] Calculated at CCSD(T)/cc-PVTZ level of theory. [e] Results from BHHLYP functional. [f] Results from CAM-B3LYP functional. [g] Results from B3LYP//BH&HLYP functional.

length values. In an attempt to minimize such an error, the difference between the average of all single and triple bonds, BLA$_{avg}$, has also been examined and plotted versus $n$ (red line, Figure 4-6) and $1/n$ (red line, Figure 4-7). Similar to the pure BLA values, BLA$_{avg}$ values also decrease consistently as a function of length for **4.1a-c**, **4.1f**, and **4.1h**, and the onset of saturation is also suggested by the stage of the decayne. A comparison of BLA and BLA$_{avg}$ for **4.1f** and **4.1h** versus those predicted theoretically for H-(C≡C)$_9$-H (Table 4-3, entry 13) shows that the experimental values are greater by only ca. 0.01 Å.

**Table 4-4.** Selected bond lengths (Å) for polyynes **4.1a-c**, **4.1f**, and **4.1h**.

| Bond | 4.1a | 4.1b | 4.1c | 4.1f | 4.1h-A | 4.1h-B |
|---|---|---|---|---|---|---|
| C3-C4 | 1.200(3) | 1.201(4) | 1.1989(18) | 1.201(2) | 1.198(6) | 1.192(8) |
| C4-C5 | 1.382(3) | 1.368(3) | 1.3683(19) | 1.367(2) | 1.360(6) | 1.365(8) |
| C5-C6 | 1.198(3) | 1.204(5) | 1.2095(18) | 1.210(2) | 1.213(6) | 1.200(8) |
| C6-C7 | | | 1.3597(19) | 1.352(2) | 1.354(6) | 1.354(9) |
| C7-C8 | | | 1.2083(19) | 1.218(2) | 1.211(6) | 1.216(8) |
| C8-C9 | | | 1.3679(19) | 1.349(2) | 1.340(6) | 1.356(9) |
| C9-C10 | | | 1.1993(19) | 1.213(2) | 1.218(6) | 1.210(9) |
| C10-C11 | | | | 1.353(2) | 1.342(6) | 1.347(9) |
| C11-C12 | | | | 1.213(2) | 1.207(6) | 1.212(8) |
| C12-C13 | | | | 1.352(2) | 1.351(6) | 1.346(13) |
| C13-C14 | | | | 1.214(2) | 1.208(6) | |
| C14-C15 | | | | 1.355(2) | 1.340(6) | |
| C15-C16 | | | | 1.207(2) | 1.208(6) | |
| C16-C17 | | | | 1.366(2) | 1.352(7) | |
| C17-C18 | | | | 1.196(2) | 1.204(6) | |
| C18-C19 | | | | | 1.356(6) | |
| C19-C20 | | | | | 1.206(6) | |
| C20-C21 | | | | | 1.354(6) | |
| C21-C22 | | | | | 1.194(6) | |

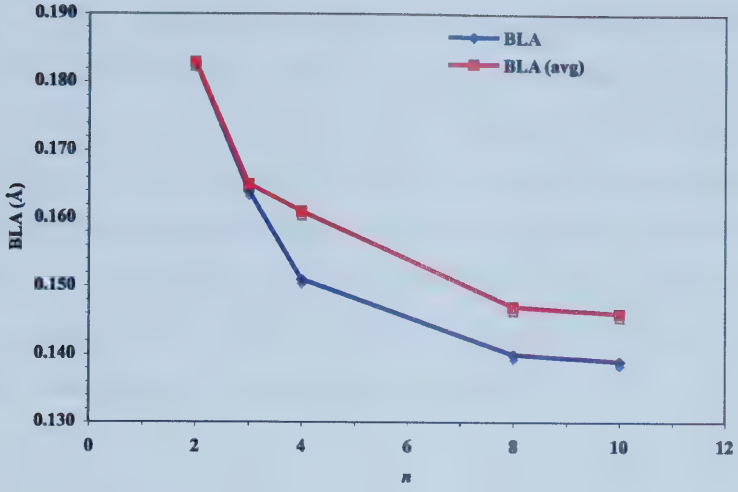


**Figure 4-6.** Plot of BLA (blue) and $BLA_{avg}$ (red) versus the number of triple bonds ($n$). The line is provided as a guide to the eye.

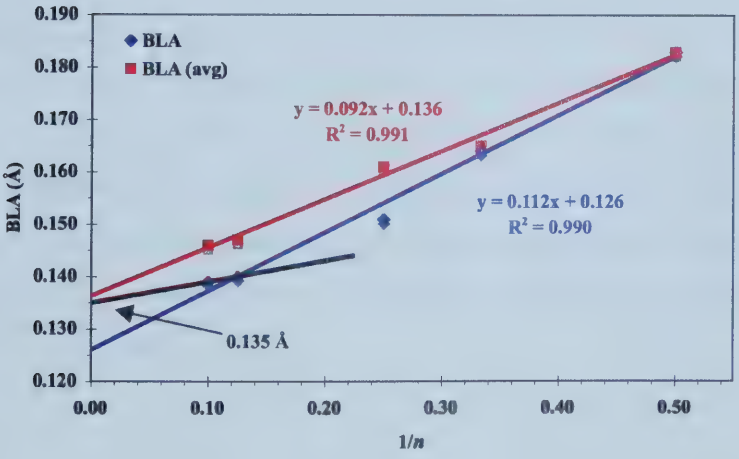


**Figure 4-7.** Plot of BLA and $BLA_{avg}$ versus $1/n$, where $n$ is the number of triple bonds. A line of best fit is shown for BLA (blue) and $BLA_{avg}$ (red). An extrapolation of the octa- and decayne (black line) shows BLA = 0.135 Å for infinite polyyne.

The TIPS-endcapped polyynes **S1** provide for the only substantive comparison of similar experimental BLA and $BLA_{avg}$ analyses, as shown in Table 4-3 entries 8-12. While there is an overall reduction in both BLA and $BLA_{avg}$ values as one moves from diyne **S1a** to octayne **S1f**, neither the individual values nor the overall trend compare well with the data for molecules in the *t*-Bu-endcapped series. It is particularly interesting that $BLA_{avg}$ data for molecules **S1** show no real trend. It seems plausible that this would result from an endgroup effect in which the silane moiety reduces BLA toward each terminus of the polyyne, which effectively negates any apparent overall BLA that might be present toward the center of the molecule.

## 4.4 Conclusions

In summary, a series of *t*-Bu-endcapped polyynes, analogous to the adamantyl series (**3.1**), has been synthesized to explore the properties of conjugated oligomers composed of sp-hybridized carbon. The resulting polyynes exhibit reasonable stability under ambient conditions, which has allowed for X-ray analysis of several derivatives, including the first crystallographic analysis of a decayne. Analysis of bond length alternation provides the first experimental evidence for reduced BLA as a function of polyyne length and predicts a limiting BLA value of ca. 0.135 Å.

With the successful synthesis of $sp^3$-carbon endcapped polyynes, such as the adamantyl and *t*-butyl derivatives, it appeared to be a good idea to continue with this strategy. With the limit of stability for the adamantyl and the *t*-butyl polyynes stopping at approximately the decayne, however, a new endgroup design was clearly needed in order to provide stable polyynes beyond 20 sp-carbons in length.

## 4.5 References


[1] Luu, T.; Elliott, E.; Slepkov, A. D.; Eisler, S.; McDonald, R.; Hegmann, F. A.; Tykwinski, R. R. *Org. Lett.* **2005**, *7*, 51.

[2] Kendall, J.; McDonald, R.; Ferguson, M. J.; Tykwinski, R. R. *Org. Lett.* **2008**, *10*, 2163.

[3] Eisler, S.; Slepkov, A. D.; Elliott, E.; Luu, T.; McDonald, R.; Hegmann, F. A.; Tykwinski, R. R. *J. Am. Chem. Soc.* **2005**, *127*, 2666.

[4] Chalifoux, W. A.; McDonald, R.; Ferguson, M. J.; Tykwinski, R. R. *Angew. Chem. Int. Ed.* **2009**, *48*, 7915.

[5] Chalifoux, W. A.; Ferguson, M. J.; Tykwinski, R. R. *Eur. J. Org. Chem.* **2007**, 1101.

[6] For an extensive review on polyynes beyond six contiguous triple bonds; see Chalifoux, W. A.; Tykwinski, R. R. *C. R. Chimie* **2009**, *12*, 341.

[7] Lucotti, A.; Tommasini, M.; Fazzi, D.; Del Zoppo, M.; Chalifoux, W. A.; Ferguson, M. J.; Zerbi, G.; Tykwinski, R. R. *J. Am. Chem. Soc.* **2009**, *131*, 4239.

[8] Tsuji, M.; Tsuji, T.; Kuboyama, S.; Yoon, S.-H.; Korai, Y.; Tsujimoto, T.; Kubo, K.; Mori, A.; Mochida, I. *Chem. Phys. Lett.* **2002**, *355*, 101.

[9] Cataldo, F. *Tetrahedron Lett.* **2004**, *45*, 141.

[10] Eastmond, R.; Johnson, T. R.; Walton, D. R. M. *Tetrahedron* **1972**, *28*, 4601.

[11] Cook, C. L.; Jones, E. R. H.; Whiting, M. C. *J. Chem. Soc.* **1952**, 2883.

[12] Aboulfadl, H.; Chalifoux, W. A.; Tykwinski, R. R.; Bally, T., unpublished results.

[13] Polyynes terminated with *t*-Bu groups are of the earliest homologous series to be synthesized and examined, first reported by Bohlmann in 1953 for polyynes up to the heptamer (**4.1a-f**); see Bohlmann, F. *Chem. Ber.* **1953**, *86*, 657.

[14] Jones and Whiting subsequently extended the *t*-butyl series to include octayne **4.1f** and decayne **4.1h**; see Jones, E. R. H.; Lee, H. H.; Whiting, M. C. *J. Chem. Soc.* **1960**, 3483.

[15] In the 1972, Johnson and Walton reported the synthesis of dodecayne ($n$ = 12), but this polyyne decomposed rapidly at ambient temperature; see Johnson, T. R.; Walton, D. R. M. *Tetrahedron* **1972**, *28*, 5221.

[16] Li, J.-H.; Liang, Y.; Xie, Y.-X. *J. Org. Chem.* **2005**, *70*, 4393.

[17] Eisler, S.; Chahal, N.; McDonald, R.; Tykwinski, R. R. *Chem. Eur. J.* **2003**, *9*, 2542.

[18] Ramirez, F.; Desai, N. B.; McKelvie, N. *J. Am. Chem. Soc.* **1962**, *84*, 1745.

[19] Siemsen, P.; Livingston, R. C.; Diederich, F. *Angew. Chem. Int. Ed.* **2000**, *39*, 2632.

[20] Cadiot, P.; Chodkiewicz, W. In *Chemistry of Acetylenes*; Viehe, H. G., Ed; Dekker: New York, 1969; pp 597.

[21] Rösner, M.; Köbrich, G. *Angew. Chem.* **1975**, *87*, 715.

[22] Hay, A. S. *J. Org. Chem.* **1962**, *27*, 3320.

[23] Walton, D. R. M.; Waugh, F. *J. Organomet. Chem.* **1972**, *37*, 45.

[24] Lewis, M. D.; Duffy, J. P.; Heck, J. V.; Menes, R. *Tetrahedron Lett.* **1988**, *29*, 2279.

[25] Ladika, M.; Stang, P. J. *J. Chem. Soc., Chem. Commun.* **1981**, 459.

[26] The analogous formation of nonaynes has been observed before under Hay conditions; see refs 3 and 35.

[27] Glaser, C. *Ann. Chem.* **1870**, *154*, 137.

[28] Glaser, C. *Ber. Dtsch. Chem. Ges.* **1869**, *2*, 422.

[29] Eglinton, G.; Galbraith, A. R. *Chem. Ind. (London)* **1956**, 737.

[30] Bohlmann, F. *Chem. Ber.* **1953**, *86*, 657.

[31] Jones, E. R. H.; Lee, H. H.; Whiting, M. C. *J. Chem. Soc.* **1960**, 3483.

[32] Zheng, Q.; Bohling, J. C.; Peters, T. B.; Frisch, A. C.; Hampel, F.; Gladysz, J. A. *Chem. Eur. J.* **2006**, *12*, 6486.

[33] Schermann, G.; Grösser, T.; Hampel, F.; Hirsch, A. *Chem. Eur. J.* **1997**, *3*, 1105.

[34] Klinger, C.; Vostrowsky, O.; Hirsch, A. *Eur. J. Org. Chem.* **2006**, 1508.

[35] Gibtner, T.; Hampel, F.; Gisselbrecht, J.-P.; Hirsch, A. *Chem. Eur. J.* **2002**, *8*, 408.

[36] Dembinski, R.; Bartik, T.; Bartik, B.; Jaeger, M.; Gladysz, J. A. *J. Am. Chem. Soc.* **2000**, *122*, 810.

[37] Mohr, W.; Stahl, J.; Hampel, F.; Gladysz, J. A. *Chem. Eur. J.* **2003**, *9*, 3324.

[38] Mohr, W.; Stahl, J.; Hampel, F.; Gladysz, J. A. *Inorg. Chem.* **2001**, *40*, 3263.

[39] Kertesz, M.; Choi, C. H.; Yang, S. *Chem. Rev.* **2005**, *105*, 3448.

[40] Milani, A.; Tommasini, M.; Zerbi, G. *J. Raman Spectrosc.* **2009**, in press.

[41] Zeinalipour-Yazdi, C. D.; Pullman, D. P. *J. Phys. Chem. B* **2008**, *112*, 7377.

[42] Yang, S. J.; Kertesz, M. *J. Phys. Chem. A* **2006**, *110*, 9771.

[43] Yang, S.; Kertesz, M. *J. Phys. Chem. A* **2008**, *112*, 146.

[44] Peach, M. J. G.; Tellgrent, E. I.; Salek, P.; Helgaker, T.; Tozer, D. J. *J. Phys. Chem. A* **2007**, *111*, 11930.

[45] Hoffmann, R. *Angew. Chem. Int. Ed. Engl.* **1987**, *26*, 846.

[46] To the best of our knowledge, before this work only two octayne X-ray crystal structures have been reported. See: ref 3 and ref 38.

[47] The crystallographic analysis of tetrayne **4.1c** has previously been reported but no coordinates were made available to the CCDC; see Lagow, R. J.; Kampa, J. J.; Wei, H.-C.; Battle, S. L.; Genge, J. W.; Laude, D. A.; Harper, C. J.; Bau, R.; Stevens, R. C.; Haw, J. F.; Munson, E. *Science* **1995**, *267*, 362.

[48] Szafert, S.; Gladysz, J. A. *Chem. Rev.* **2006**, *106*, PR1.

[49] Yang, S. J.; Kertesz, M.; Zolyomi, V.; Kurti, J. *J. Phys. Chem. A* **2007**, *111*, 2434.

[50] Zhang, C. J.; Cao, Z. X.; Wu, H. S.; Zhang, Q. R. *Int. J. Quantum Chem.* **2004**, *98*, 299.

[51] Weimer, M.; Hieringer, W.; Della Sala, F.; Gorling, A. *Chem. Phys.* **2005**, *309*, 77.

[52] Scemama, A.; Chaquin, P.; Gazeau, M. C.; Benilan, Y. *J. Phys. Chem. A* **2002**, *106*, 3828.

[53] Horny, L.; Petraco, N. D. K.; Pak, C.; Schaefer, H. F. *J. Am. Chem. Soc.* **2002**, *124*, 5861.

[54] Constable, E. C.; Gusmeroli, D.; Housecroft, C. E.; Neuburger, M.; Schaffner, S. *Acta Crystallogr., Sect. C: Cryst. Struct. Commun.* **2006**, *C62*, o505.

# Chapter 5 Building Stability into Polyynes Using Large Endgroups

## 5.1 Introduction

One of the problems associated with polyynes is their highly reactive nature due to the number of triple bonds in conjugation. These materials can readily decompose through polymerization[1] and even, in some reported cases, explode.[2] It is this instability that makes their synthesis and isolation difficult and it is partly because of this challenge that chemists find these compounds alluring targets. Chemists have designed a variety of innovative synthetic protocols in order to impart stability into polyynes. These include encasing the polyyne core inside a sheath such as alkyl chains that span the endgroups,[3-5] rotaxanes,[6-8] and even rotaxanes using cyclodextrins.[9] Another way to impart stability is to use sterically demanding endgroups.[10-17] Large endgroups prevent the approach of the polyynes toward one another in a way that might lead to polymerization via crosslinking. Stable polyynes have indeed been synthesized and the limit of their synthesis often seems to reside around ten triple bonds in length.[18,19] In one case, stable polyynes were made by Gladysz and coworkers up to 14 triple bonds in length, in which large Pt-endcapping groups were utilized.[10]

All the previous chapters, along with this one, focus on the use of sterically demanding endgroups in order to increase the stability of polyynes. Indeed, these endeavors have been successful when it comes to polyynes with ten triple bonds or less, but have failed to produce stable polyynes beyond this length. This chapter displays the synthetic achievements made toward the synthesis of polyynes well beyond ten triple bonds in length using an endgroup that is far superior in stabilizing long polyynes. The endgroup in question is a tris(3,5-di-*t*-butylphenyl)methyl moiety, which is referred to as the "supertrityl" endgroup within the Tykwinski group. This endgroup has not only been successful toward stabilizing symmetrical polyynes but has also allowed for the isolation of unsymmetrical TIPS-, Br- and even H-substituted polyynes, providing for their isolation and characterization. With few unsymmetrical polyynes being reported in the literature to date, most with only partial characterization, the

properties of these systems can now be probed for the first time in comparison to their symmetrical analogues.

## 5.2 Synthesis of Supertrityl Polyynes

The synthesis of a series of polyynes that utilize a tris(3,5-di-*tert*-butylphenyl)methyl (supertrityl = Tr*) endgroup (Figure 5-1, **5.1a-j**) has been achieved. The synthesis up to 40 sp-carbons long (20 triple bonds) was made possible due to the large size of the endgroup, which prevents decomposition through intermolecular reaction pathways (polymerization). The endgroup spans an impressive 14 Å in diameter, over three times the size of its *t*-butyl-endcapped cousin. The use of the supertrityl moiety, which places $sp^3$-carbons on the termini of the polyyne, minimizes perturbation of the polyyne π-system. This perturbation is enhanced when using π-conjugated,[20,21] as well as metal endcapping groups.[10] Minimization of this effect allows for a better representation of the electronic properties of carbyne; the all sp-carbon allotrope.

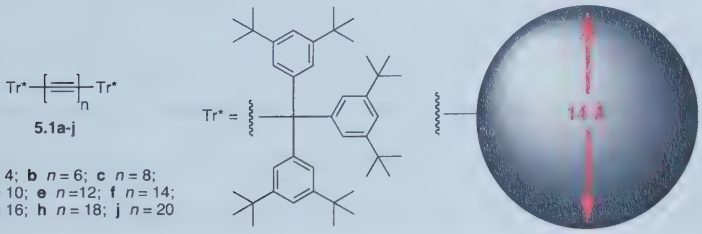


**Figure 5-1.** Supertrityl polyynes **5.1a-j**.

### 5.2.1 Synthesis of a Feedstock Starting Material Towards Supertrityl Polyynes

The supertrityl endgroup was synthesized in only a few steps using inexpensive, commercially available starting materials. A three fold Friedel-Craft alkylation of benzene with 2-chloro-2-methylpropane at low temperature gave 1,3,5-tri-*t*-butylbenzene (**5.2**) in 81% yield (Scheme 5-1).[22] Treatment with bromine in the presence of metallic iron at low temperature resulted in substitution of one *t*-butyl group with bromine yielding **5.3** in 83%.[23] Formation of the

Grignard, followed by addition to diethyl carbonate, led to the supertritylalcohol (**5.4**) in 92% yield. The supertrityl alcohol (**5.4**) was converted to the supertrityl chloride (**5-5**) using $SOCl_2$ in toluene at reflux and this was followed by addition of ethynylmagnesium bromide which gave supertritylacetylene (**5.6**) in 89% yield over the two steps.[24] The synthesis of supertritylacetylene (**5.6**) was scaled-up to produce bulk quantities up to 24 g of **5.6** in a single batch and used as feedstock for all supertrityl polyynes and precursors.

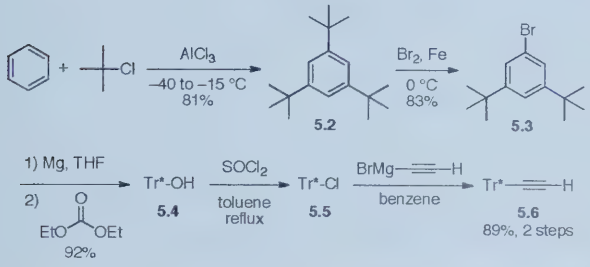


**Scheme 5-1.** Synthesis of supertritylacetylene **5.6**.

### 5.2.2 Synthesis of Supertrityldiyne

The next logical target in the synthesis of this polyyne series seemed to be that of the terminal supertrityl terminal diyne **5.7**. Typically, diynes are easily accessed via crosscoupling procedures in moderate to good yields. A number of different crosscoupling routes were attempted that gave desired results, albeit in modest yields (Table 5-1). Although the diyne could be made in appreciable quantities, the reactions generated unwanted side products and contained leftover starting materials that made purification quite difficult due to their similar solubilities and retention factors in chromatography. An interesting note about the Pd-catalyzed reactions between Tr*–C≡C–Br and H–C≡C–$SiMe_3$ is that the main recovered side product was supertritylacetylene **5.6** suggesting that there is considerable scrambling of H and Br in the reaction, which could be the main cause of the reactions not going to completion.

**Table 5-1.** Crosscoupling conditions toward the synthesis of diyne **5.7**.

| Entry | X | Y | R | Conditions | Product | Yield (%) |
|---|---|---|---|---|---|---|
| 1 | H | Br | | CuCl, $NH_2OH$•HCl *n*-butylamine MeOH/$H_2O$ (10:1) rt | | 0 |
| 2 | H | Br | | $PdCl_2(PPh_3)_2$, CuI THF diisopropylamine | | 55 |
| 3 | Br[b] | H | $SiMe_3$[c] | $PdCl_2(PPh_3)_2$, CuI THF diisopropylamine | 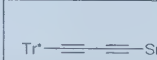 | 43[e] |
| 4 | Br[b] | H | $SiMe_3$[f] | $PdCl_2(PPh_3)_2$, CuI THF diisopropylamine | 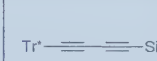 | 53[e] |

[a] See Chapter 7, compound **7.7**, for experimental details. [b] See Chapter 7, compound **7.6**, for experimental details. [c] 2 mole equiv. used. [d] See Chapter 7, compound **7.8**, for experimental details. [e] Approximate yield based on $^1H$ NMR analysis. [f] 20 mole equiv. used.

A cleaner, more efficient route towards the supertrityl diyne **5.7** starts with the supertrityl propargylic aldehyde (**5.8**) which was synthesized by deprotonation with BuLi, followed by addition to DMF. Acidic workup of the reaction gave **5.8** in 85% yield (Scheme 5-2). Dibromoolefination under conditions reported by Ramirez[25] led to **5.9** in 94% yield, and elimination using LDA produced supertrityldiyne **5.7** in quantitative yield.

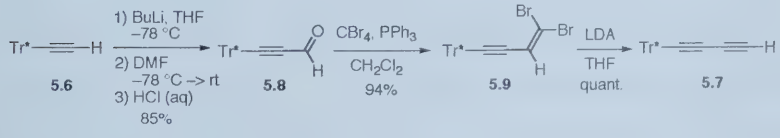


**Scheme 5-2.** Synthesis of supertrityldiyne 5.7.

### 5.2.3 Friedel-Craft Approach Towards Ketones as Polyyne Intermediates

Traditionally in the Tykwinski group, polyynes are synthesized through a step developed by Walton and coworkers that involves the Friedel-Crafts acylation of an acid chloride with a α,ω-

bis(TMS)polyyne to yield a ketone.[26] This route has been successfully applied to the synthesis of adamantyl, *t*-butyl,[19] phenyl,[20] perfluorophenyl,[21] trityl, and TIPS-endcapped polyynes.[16] This route was also applied to the synthesis of the supertrityl series.

The formation of supertrityl acid **5.10** was accomplished by lithiation of **5.6** with BuLi followed by addition of $CO_2$ (g) (Scheme 5-3). Upon acidic workup, acid **5.10** was obtained in a nearly quantitative yield. This reaction has the advantage that excess BuLi can be used, converting all of **5.6** to acid. Any valeric acid that is formed upon quenching BuLi with $CO_2$ can easily be removed by extraction with $Na_2CO_3$ (aq), while the supertrityl acid does not extract into the aqueous phase during this wash. This reproducibly gives very high yields of **5.10**.

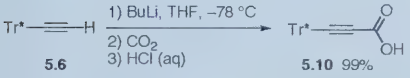

**5.6** **5.10** 99%

**Scheme 5-3.** Synthesis of acid **5.10**.

Acid **5.10** was converted to the acid chloride **5.11** quantitatively by reacting with $SOCl_2$. Reaction of the acid chloride with and α,ω-bis(trimethylsilyl)polyyne of appropriate length in the presence of $AlCl_3$ led to ketones **5.12**–**5.14** (Scheme 5-4). Yields of these reactions were reproducibly disappointing, leading only to trace amounts of desired products. It was found that upon addition of $AlCl_3$ to a solution of acid chloride in $CH_2Cl_2$ without any α,ω-bis(trimethylsilyl)polyyne, even at –78 °C, resulted in immediate decomposition as seen by the formation of a black solid. The milder Lewis acid $FeCl_3$ was tried, but this also led to decomposition. $BF_3$•$Et_2O$ was also employed as a catalyst but there was no reaction observed. Instead of isolating these products, they were typically carried on to the next step after a crude purification step by plugging through silica gel. However, it was clear through these experiments that a new route towards synthesizing these molecules would have to be developed.

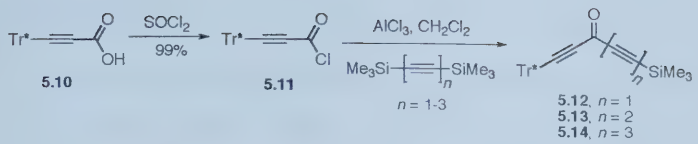


**Scheme 5-4.** Synthesis of ketones **5.12–5.14** via Friedel-Crafts acylation.

These ketones were carried on without isolation to the dibromoolefins[25,27] in a poor 10% yield for **5.15**, 12% for **5.16**, and finally 14% for **5.17** (yields calculated from the corresponding acid **5.10** or acid chloride **5.11**, see Scheme 5-5). FBW rearrangement[28-30] of **5.15** led to a 91% yield of triyne **5.18**. FBW rearrangement of **5.16** and **5.17** gave tetrayne **5.19** and pentayne **5.20**, respectively, which were not isolated, but carried directly to the next step. Tetra- and pentaynes **5.19** and **5.20** were homocoupled, albeit in moderate yield over two steps, under the conditions shown in Scheme 5-5 to generate the desired polyynes **5.1c** and **5.1d**, respectively. The homocoupling of triyne **5.18** was not pursued as the quantity of material originally produced was insufficient, and ultimately this route was abandoned. Although the reaction conditions led to the desired products, overall yields were devastatingly low and the limit of this route seems to end at 10 contiguous triple bonds.

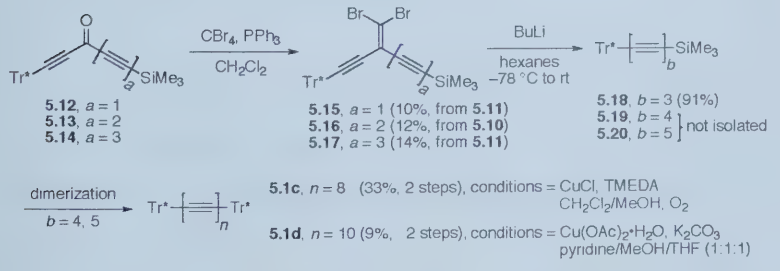


**Scheme 5-5.** Synthesis of hexa-, octa-, and decaynes (**5.1b-d**) via a dibromoolefination, FBW rearrangement, and finally a homocoupling reaction.

### 5.2.4 Alcohol Formation and Oxidation Towards Ketones as Polyyne Intermediates

Since Friedel-Crafts chemistry could not efficiently afford longer polyynes a new route was devised. The addition of lithiated **5.6** to triisopropylsilyl propargylic aldehyde gave alcohol **5.21** in a yield of 92%. Oxidation of alcohol **5.21** to ketone **5.22** using PCC proceeded in 97% yield. Dibromoolefination to give **5.23** (98%) followed by a FBW rearrangement (91%) led to unsymmetrical triyne **5.24**. An overall yield of 80% from **5.6** is far superior to original attempts using Friedel-Crafts chemistry, and with the use of TIPS groups, this resulted in much more robust products. The desilylation of **5.24** was carried out using TBAF to yield quantitatively the terminal triyne **5.25**.

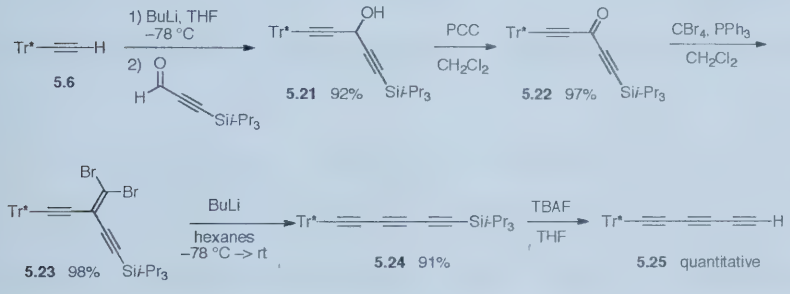


**Scheme 5-6.** Synthesis of supertrityl triyne **5-25**.

Now, with efficient routes to terminal di- (**5.7**) and triynes (**5.25**) in hand, a route towards longer polyyne analogues was sought. The deprotonation of **5.7** and **5.25** using BuLi followed by addition to TIPS propargylic aldehyde leads to alcohols **5.26** (91%) and **5.27** (35%), respectively. The oxidation of the alcohol **5.26** using PCC led to ketone **5.28** in excellent yield. The oxidation of **5.27** to ketone **5.29** was carried out using $MnO_2$ and was not isolated but carried directly to the next step as the ketone was assumed to be unstable since the alcohol showed slight decomposition when isolated. Dibromoolefination of **5.28** and **5.29** gave **5.30** and **5.31** in 94% and 51% yields (2 steps), respectively. An FBW rearrangement of **5.30** gave unsymmetrical tetrayne **5.32** in excellent yield. Deprotection of **5.32** under standard TBAF conditions to give the terminal tetrayne **5.34** proved to be a difficult task, leading only to decomposition. Alternative conditions were attempted

such as TBAF on silica or alumina, but decomposition was also seen in each case. The FBW rearrangement of **5.31** to give pentayne **5.33** was not attempted based on these results for the deprotection of the tetrayne **5.32**.

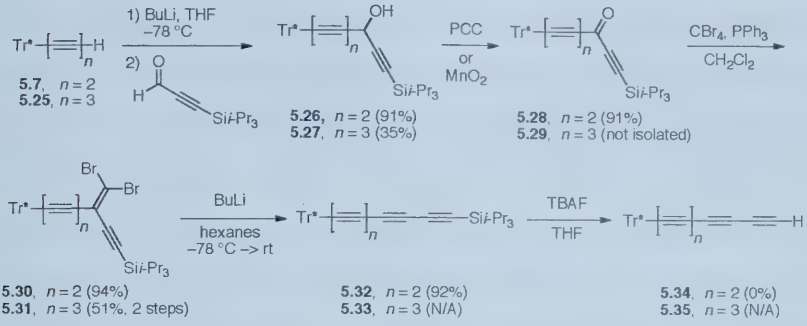


**5.7**, $n = 2$
**5.25**, $n = 3$

**5.26**, $n = 2$ (91%)
**5.27**, $n = 3$ (35%)

**5.28**, $n = 2$ (91%)
**5.29**, $n = 3$ (not isolated)

**5.30**, $n = 2$ (94%)
**5.31**, $n = 3$ (51%, 2 steps)

**5.32**, $n = 2$ (92%)
**5.33**, $n = 3$ (N/A)

**5.34**, $n = 2$ (0%)
**5.35**, $n = 3$ (N/A)

**Scheme 5-7.** Toward the synthesis of deprotected supertrityl tetrayne **5.34** and pentayne **5.35**.

At this stage, it seemed that five contiguous triple bonds would be the limit for making unsymmetrical polyynes in this fashion, since yields diminished rapidly at this point. Yet again, precursors that would only generate polyynes with up to 10 triple bonds in length were achievable. As well, a new problem was presented in the removal of the TIPS group, where using typical TBAF conditions results in complete decomposition of longer polyynes such as **5.34**. If mild conditions for the removal of the TIPS group from **5.32** could be found, an excellent route towards tetrayne **5.34** would be available. However, due to poor yields seen in the steps leading to pentayne **5.35**, and the limit of this chemistry towards making longer derivatives, a new procedure was sought that would provide pentayne **5.35** in better yield, fewer steps, and be applicable to longer derivatives.

### 5.2.5 Mild Removal of a TIPS Group

As mentioned, the removal of a TIPS group from an unsymmetrical supertrityl polyyne seemed to be limited to shorter derivatives ($n \leq 3$). There were only a handful of choices at this

stage, the most obvious of which included: 1) replacement of the TIPS group with a silyl group that is easier to remove under non-fluoride conditions, or 2) find a reagent that can mildly remove the TIPS group without harming the polyyne.

The problem associated with replacing the silyl group is that there are only a few logical choices. First is the TMS group, which only works well for shorter derivatives. In longer derivatives the TMS is less helpful in stabilizing the polyyne and is prone to "falling off" even under the most mild condtions.[16] Also, the TMS is introduced through a sequence that includes addition of the lithiated polyyne to a propargylic aldehyde. This generates an alkoxide intermediate that could pose problems such as promoting unwanted desilylation. The TES group would be the next logical choice and was considered since it is more stable to the conditions needed to make the alcohols. However, the TES group is more labile than the TIPS group and the ideal group should be larger in order to stabilize unsymmetrical polyynes, even up to the decayne. Perhaps the TBDMS group would suffice but working with this endgroup in the past has often been troublesome in terms of purification and yield. Also, fluoride is the reagent most relied upon to remove TBDMS groups, therefore, the same problems as the TIPS group would undoubtedly arise.

Since TIPS polyynes proved to be stable up to the decayne,[16] it seemed like the best protecting group would be the best for making stable polyynes, and, therefore, a mild TIPS desilylation protocol was sought. It was by a stroke of luck that the use of CsF was considered as a mild desilylating agent for the TIPS group: large quantities of the material had been graciously donated to the group by Raylo Chemicals (now Gilead Sciences, Edmonton).

To a solution of **5.32** in THF was added one equivalent of CsF and the resulting mixture monitored by TLC analysis. No desilylation was found, even after 24 h at rt and excess CsF was added. When a few drops of $H_2O$ was added to the reaction mixture, however, desilylation was observed, albeit slowly. After optimization of the conditions to that shown in Scheme 5-8, removal of the TIPS group from **5.32** occurred in only minutes, quantitatively, to generate terminal tetrayne **5.34**.

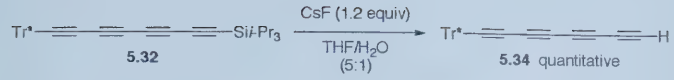


**Scheme 5-8.** Mild desilylation conditions developed to generate terminal tetrayne **5.34**.

### 5.2.6 Traditional Crosscoupling Methods as a Means to Longer Polyynes

Now, with a mild desilylation procedure for the TIPS group in hand, a more efficient route to pentayne **5.33**, and longer derivatives was pursued. A procedure that relied on crosscoupling seemed to be the most obvious choice with which to commence. Terminal supertrityl polyynes **5.36–5.39** were brominated in excellent yields (Scheme 5-9). The first, and most obvious, reaction to try was the Sonogashira crosscoupling.[31,32] Only modest yields of products **5.33**, as well as **5.40–5.43** were isolated with this approach. On the other hand, Negishi crosscoupling[33,34] between the Zn-acetylide, formed by treatment of 1-TIPS-6-TMS-triyne with methyllithium followed by $ZnCl_2$, and terminal bromide **5.36** appeared to be more promising with an 83% yield of **5.33** being obtained on the first attempt. However, these reaction conditions proved to be troublesome by way of incomplete reactions and irreproducible yields that suffered significantly as one progressed from pentayne **5.33** (80%) to nonayne **5.43** (product could not be isolated pure but UV-Vis analysis confirmed its formation) as a function of coupling partner length.[†] Despite the low yields, these very advanced intermediates could be synthesized, characterized and desilylated to obtain terminal polyynes **5.35** and **5.44–5.47** quantitatively.

---

[†] The first time this reaction was attempted for **5.33** the reaction contained significant amounts of unreacted starting materials after three days, as determined based on relative TLC and $^1$H NMR intensities. It also appeared from TLC and NMR analysis that the protonated TIPS-triyne was present in the reaction mixture. In order to promote formation for the Zn-acetylide in situ, diisopropylamine was added (see Sasaki, H.; Boyall, D.; Carreira, E. M. *Helv. Chim. Acta* **2001**, *84*, 964). Indeed, this appeared to lead to more product being formed, with starting materials disappearing from the reaction mixture, leading to an 83% isolated yield. However, in a second attempt at the reaction, the amine base was added at the beginning and low yield of product was isolated with the remainder going to an indeterminable mixture of products.

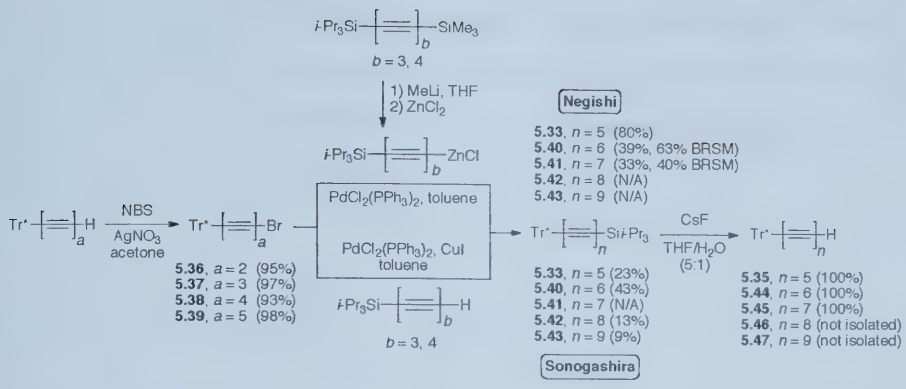


**Scheme 5-9.** Synthesis of longer unsymmetrical polyynes utilizing Sonogashira and Negishi crosscoupling conditions. BRSM - based on recovered starting material

A number of other routes involving crosscouplings of various other precursors were attempted in order to afford advanced intermediates towards the synthesis of dodecayne **5.1e**. This was before the discovery of the CsF protocol for the mild desilylation of a TIPS group. Since TBAF was still the main desilylating agent being used, dibromoolefins were sought after as precursors because removal of the TIPS group from dibromoolefin precursors such as **5.23** worked well (Scheme 5-10). The resulting dibromoolefin (**5.48**) could also be brominated efficiently using NBS in the presence of $AgNO_3$ to afford the terminal bromide **5.49**. As a result, these intermediates, or a mixture of polyyne and dibromoolefin precursors, could be homo- or crosscoupled to generate the corresponding di- or tetrabromoolefin and the desired polyyne achieved via a two- or four-fold FBW rearrangement in the final step (Table 5-2). A variety of conditions were screened towards the synthesis of dodecayne **5-1e** such as Cadiot-Chodkiewicz,[35] mixed Hay[10,36,37] and Sonogashira.[31,32] A handful of these reactions led to desired products (**5.50** and **5.51**), as well as interesting homocoupled side products (**5.52**), albeit in low to moderate yields. The unsymmetrical hexayne **5.40** was successfully synthesized from a two-fold FBW rearrangement of tetrabromoolefin **5.51**, albeit in a moderate yield of 43%. With unsatisfactory yields due to the formation of many side products and arduous purification to obtain desired

products, this route was beginning to look troublesome. Also, it was suspected that using this FBW rearrangement approach would prove problematic with longer derivatives since it has been reported that two-fold, and especially four-fold FBW rearrangements were unsuccessful to make long polyynes.[16] It is because of these problems that this crosscoupling/FBW rearrangement route towards making polyynes was abandoned.

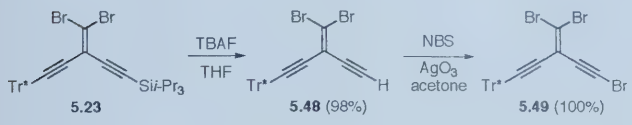


**5.23** **5.48** (98%) **5.49** (100%)

**Scheme 5-10.** Desilylation of **5.23** to give **5.48** followed by formation of terminal bromide **5.49**.

**Table 5-2.** Synthesis of $n = 12$ precursors by screening various crosscoupling conditions.

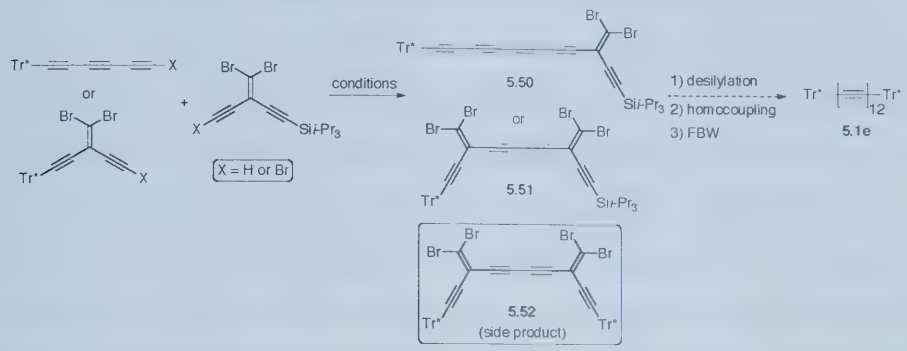


| Entry | Reactant 1[a] | Reactant 2 | Reactant 2 (mole equiv.) | Conditions | Product | Yield (%) |
|---|---|---|---|---|---|---|
| 1 | | 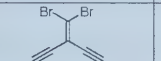 | 1.2 | CuCl,[b] $NH_2OH$•HCl *n*-butylamine MeOH/THF (1:1) | **5.51** | 3 |
| 2 | | 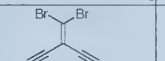 | 2.0 | CuCl,[b] $NH_2OH$•HCl *n*-butylamine MeOH/THF (1:1) | **5.51** | 24 |
| 3 | | 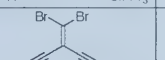 | 2.0 | CuCl,[c] TMEDA $CH_2Cl_2$, $O_2$ | **5.51** | 32 |
| 4 | | 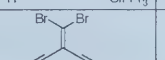 | 1.2 | CuCl,[b] $NH_2OH$•HCl *n*-butylamine MeOH/THF (1:1) | **5.50** | 7 |
| 5 | | 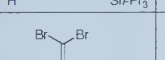 | 1.2 | CuCl,[b] $NH_2OH$•HCl *n*-butylamine THF 0 °C | **5.50** | 2 |
| 6 | | | 1.2 | CuCl,[b] $NH_2OH$•HCl *n*-butylamine THF/$H_2O$ (5:1) 0 °C | **5.50** | 3 |
| 7 | | 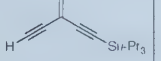 | 1.2 | CuI,[b] $NH_2OH$•HCl *n*-butylamine THF/$H_2O$ (10:1) | **5.50** | 6 |
| 8 | | 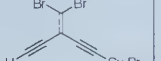 | 1.0 | CuI,[b] $NH_2OH$•HCl *n*-butylamine EtOH | **5.50** | 0 |
| 9 | | 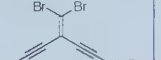 | 1.0 | $Pd(PPh_3)_4$, CuI[d] THF, DIPA 0 °C | **5.50** | 29 |
| 10 | | 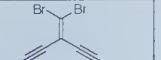 | 1.2 | $Pd(PPh_3)_4$, CuI[d] THF, DIPA, rt | **5.50** | 44 |

[a] Limiting reagent. [b] CuCl (0.2 mol equiv. used). [c] CuCl (2.0 mol equiv. used). [d] $Pd(PPh_3)_4$ and CuI (0.05 mol equiv. used of each).

### 5.2.7 Using a Modified Homocoupling Protocol to Generate Crosscoupled Products

The best and most reproducible yields of pentayne (**5.33**), hexa- to nonayne (**5.40** to **5.43**), and decayne (**5.53**) were obtained using a modified Glaser-Eglinton-Hay[36,38-41] coupling in which a mixture of appropriate deprotected supertritylpolyyne and α,ω-TMS-TIPS polyyne was crosscoupled (Table 5-3). The TMS group underwent protiodesilylation in situ, producing the necessary TIPS polyyne coupling partner. The high yields and good selectivity may be a result of the supertrityl polyyne preferring to crosscouple with the TIPS because of its smaller size, rather than homocoupling with itself. Of course, homocoupling of the supertrityl polyyne was observed, and it was formed in larger quantities as the length of the polyyne increased. The TIPS homocoupled product was also observed. Since the propensity of the TIPS precursor to homocouple appeared greater it was used in a five-fold excess. The products of this reaction were easily separable by column chromatography due to the difference in polarity between the supertrityl and the TIPS endgroups.

**Table 5-3.** Synthesis of supertrityl polyynes **5.33**, **5.40**–**5.43**, and **5.53** using a modified Glaser-Eglinton-Hay coupling protocol.

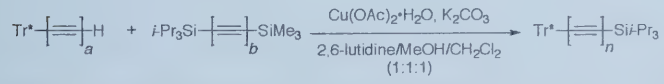


| *a* (substrate 1) | *b* (substrate 2) | *n* (product) | Yield (%) |
|---|---|---|---|
| 2 (**5.7**) | 3 | 5 (**5.33**) | 84 |
| 3 (**5.25**) | 3 | 6 (**5.40**) | 63 |
| 3 (**5.25**) | 4 | 7 (**5.41**) | 73 |
| 4 (**5.34**) | 4 | 8 (**5.42**) | 77 |
| 5 (**5.35**) | 4 | 9 (**5.43**) | 42 |
| 6 (**5.44**) | 4 | 10 (**5.53**) | 52 |

The dimerization of supertrityl terminal polyynes was carried out under traditional Hay conditions (Scheme 5-11).[36] This procedure proved to be very efficient for shorter polyynes **5.1a** (92%), **5.1b** (66%) and **5.1c** (97%). The low yield in the case of hexayne **5.1b** is most likely attributed to the fact that this polyyne is quite insoluble compared to the other analogues, making

isolation and purification more difficult. Although the Hay coupling protocol worked well for the $n$ = 4-8, for products that contained 10 or more triple bonds there was loss of acetylene(s) seen in the byproducts. For example, along with the production of decayne **5.1d**, there was a considerable amount of the nonayne ($n$ = 9) formed. In the case of the synthesis of dodecayne **5.1e** from **5.40**, undecayne ($n$ = 11), and decayne **5.1d** were formed as well. The products obtained from loss of acetylene ($n$ = 9, 10 and 11) are easily identifiable based on the characteristic UV-Vis absorption spectra of polyynes, and further support for the formation of these products was provided by high resolution mass spectral analysis. The nature of the acetylene loss under Hay conditions is still not understood but has been reported in a number of cases.[15,16,19] This side reaction remains a problem as well because purification of the mixture of polyynes is very difficult.

To avoid the problem of acetylene loss seen under standard Hay coupling conditions, the conditions reported by Eglinton were employed (Scheme 5-11).[40,41] Yields utilizing these conditions for decayne **5.1d** were modest, but no formation of nonayne was detected. For dodecayne **5.1e** these conditions also produced the desired product with no $n$ = 11 or 10 side products, however, there was considerable decomposition of product or starting materials (black baseline material seen by chromatography) leading to poor yields of desired product.

Due to the exposed nature of the polyyne core of the longer terminal supertrityl polyynes, it was possible that electrophilic and/or nucleophilic attack was an issue leading to undesired addition products. In this case, standard Eglinton coupling conditions could become a problem since nucleophilic pyridine was used as a base and a solvent. It therefore seemed wise to circumvent this problem by using a non-nucleophilic amine base such as 2,6-lutidine. Under these slightly modified conditions, yields of homocoupled polyyne products were much improved for decayne **5.1d** and dodecayne **5.1e** and remained good even up to eicosayne ($n$ = 20, **5.1j**), which was obtained in a 57% yield over two steps from unsymmetrical decayne **5.53** (Scheme 5-11). The terminally deprotected octa- (**5.46**), nona- (**5.47**), and decayne (**5.54**) generated from the desilylation of the TIPS protected precursors **5.42**, **5.43**, and **5.51** were predicted to be unstable to isolation, and they were therefore carried on directly to polyynes **5.1g**, **5.1h** and **5.1j** without isolation.

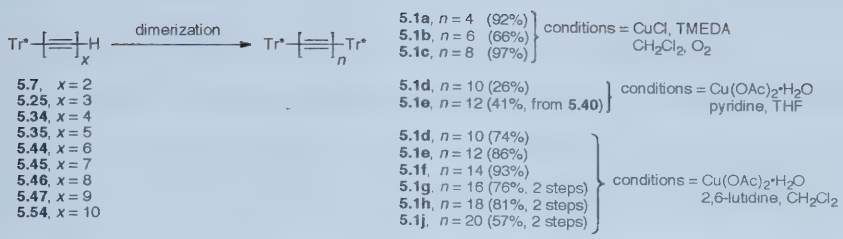
dimerization
5.7, x = 2
5.25, x = 3
5.34, x = 4
5.35, x = 5
5.44, x = 6
5.45, x = 7
5.46, x = 8
5.47, x = 9
5.54, x = 10
5.1a, n = 4 (92%)
5.1b, n = 6 (66%)
5.1c, n = 8 (97%)
conditions = CuCl, TMEDA
CH2Cl2, O2
5.1d, n = 10 (26%)
5.1e, n = 12 (41%, from 5.40)
conditions = Cu(OAc)2•H2O
pyridine, THF
5.1d, n = 10 (74%)
5.1e, n = 12 (86%)
5.1f, n = 14 (93%)
5.1g, n = 16 (76%, 2 steps)
5.1h, n = 18 (81%, 2 steps)
5.1j, n = 20 (57%, 2 steps)
conditions = Cu(OAc)2•H2O
2,6-lutidine, CH2Cl2

**Scheme 5-11.** Synthesis of polyynes **5.1a-c** using the Hay homocoupling protocol, **5.1d** and **5.1e** using the Eglinton homocoupling protocol, and **5.1d-j** using a modified Glaser-Eglinton-Hay homocoupling protocol.

From the list of products above one would most definitely be inclined to ask the question 'where is the diyne ($n$ = 2) generated from dimerization of the supertrityl acetylene **5.6**?' Indeed, homocoupling was attempted under the typical Hay conditions without success, even after stirring for 2 days. This in not uncommon as sterically hindered acetylenes are typically difficult or unable to couple.[17] In cases where Cu-catalysis alone is not successful, Pd-catalysis is often employed.[17,42] This was also unsuccessful even after stirring the reaction for 2 days at rt. This same reaction was heated to reflux for 24 hours resulting only in 100% recovery of starting material. It would be safe to say that steric repulsion plays a role here where the size of the endgroup prohibits dimerization.

## 5.3 Physical Properties of Supertritylpolyynes

### 5.3.1 UV-Vis Spectroscopic Analysis

The UV-Vis spectroscopic analysis of polyynes is a diagnostic tool in their characterization because these molecules display very distinct, signature spectra, with well resolved fine structure in the form of sharp absorbances. This fine structure arises from transitions of π-electrons from the ground state, lowest energy vibrational level ($\pi_{v=0}$), to various vibrational

levels in the excited state ($\pi^*_{\upsilon = 0, 1, 2...}$). Typically for polyynes the $\pi_{\upsilon = 0} \rightarrow \pi^*_{\upsilon = 0}$ transition (lowest energy transition) is the most probable resulting in the largest absorbance ($\lambda_{max}$).

The UV-Vis spectra of the supertrityl polyyne series (**5.1**) also shows the expected fine structure, and there is a bathochromic shift of the absorbances as a function of polyyne length (Figure 5-2). This bathochromic shift documents lowering of the HOMO → LUMO band gap energy as a function of polyyne length. The extinction coefficient for the longest wavelength band increases almost uniformly as a function of length. Something that is very interesting to note in the supertrityl series (**5.1**) is that at a polyyne length of $n$ = 16, the lowest energy wavelength band ($\pi_{\upsilon = 0} \rightarrow \pi^*_{\upsilon = 0}$ transition) is no longer the most intense absorption band (ε = 732000 $L \cdot mol^{-1} \cdot cm^{-1}$). Rather, the second lowest energy absorbance peak ($\pi_{\upsilon = 0} \rightarrow \pi^*_{\upsilon = 1}$) dominates with an extinction coefficient of 802000 $L \cdot mol^{-1} \cdot cm^{-1}$. This trend continues for the octadecayne **5.1h** ($n$ = 18) and the eicosayne **5.1j** ($n$ = 20). This observation is explained by the Franck-Condon principle which states that larger deformations along the nuclear coordinate of symmetry results in a higher probability of transitions to the higher energy vibronic states.[43] These deformations are to be expected as the polyynes become longer because there is increased flexibility in the molecule, as has been shown by X-ray crystallographic,[19,44,45] as well as Raman studies,[45] as described in previous chapters.

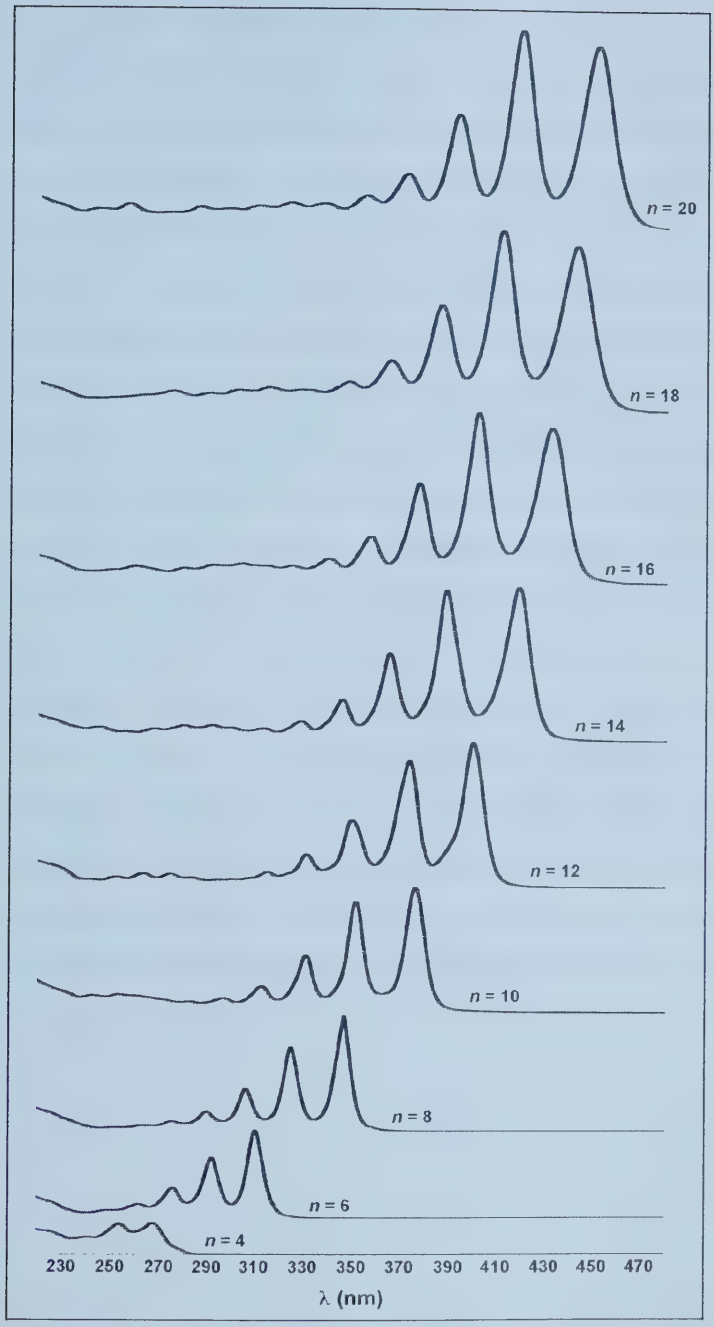


**Figure 5-2.** UV-Vis spectra of supertrityl polyyne series **5.1a-j** in hexanes.

The UV-Vis spectra of the supertrityl polyyne series were recorded in hexanes, $CH_2Cl_2$ and THF. In the least polar solvent, hexanes, the peaks are blue-shifted by 4-6 nm and the absorbance peaks are sharpened compared to that of $CH_2Cl_2$ and THF, as displayed by the overlaid spectra of **5.1j** (Figure 5-3). The red-shift of the absorbances in polar solvents is due to the ability of polar solvents to lower the energy levels of both the excited and unexcited states by attractive polarization forces between the solvent and the polyyne. The effect of lowering the ground state and excited state energies is more dramatic for the excited state, which in turn, lowers the $\pi \rightarrow \pi^*$ transition resulting in a bathochromic shift. Peaks in UV-Vis spectra usually display broadening when going from vapor phase (sharp peaks) to solution phase (broad peaks) and this broadening becomes more pronounced as the solvent used becomes more polar. As a result of the narrower peaks, the extinction coefficients are considerably higher for the hexanes solution as compared to the values obtained from solutions in $CH_2Cl_2$ and THF (Table 5-4). The spectra obtained of the supertrityl polyyne series from $CH_2Cl_2$ and THF are almost identical with respect to their absorbance wavelengths as well as their extinction coefficients. There was some decomposition of the longer polyynes in solutions of THF, possibly due to the formation of peroxides shortly after distillation, which resulted in lower extinction coefficients than expected. The extinction coefficient, as measured in hexanes, for the longest wavelength absorbance of eicosayne ($n$ = 20) is an astonishing 866000 $L \cdot mol^{-1} \cdot cm^{-1}$. What is more impressive is that empirically the second absorbance has an extinction coefficient that approaches nearly a million with a value of 936000 $L \cdot mol^{-1} \cdot cm^{-1}$ (Table 5-5).

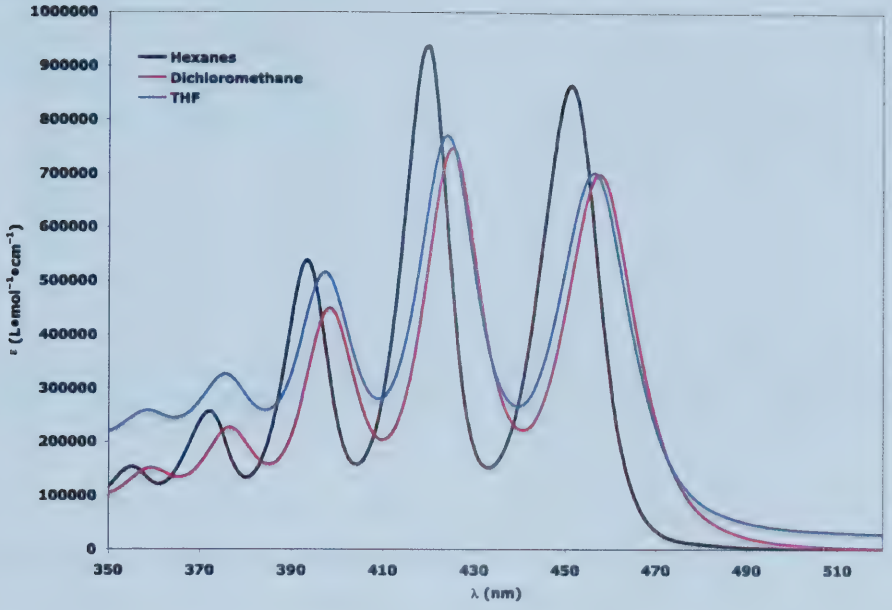


**Figure 5-3.** Overlaid UV-Vis spectra of **5.1j** ($n$ = 20) in hexanes (black), $CH_2Cl_2$ (red), and THF (blue) showing a blue-shift and sharper absorbances for the solution of **5.1j** in hexanes. The spectrum recorded in THF has been scaled to the approximate expected extinction coefficient for the longest absorbance wavelength.

**Table 5-4.** Data for the longest wavelength absorbance ($\lambda_{max}$).

| Compound | $n$ | hexanes | | $CH_2Cl_2$ | | THF | |
|---|---|---|---|---|---|---|---|
| | | $\lambda_{max}$ (nm) | $\varepsilon_{max}$ ($10^3$ $M^{-1}cm^{-1}$) | $\lambda_{max}$ (nm) | $\varepsilon_{max}$ ($10^3$ $M^{-1}cm^{-1}$) | $\lambda_{max}$ (nm) | $\varepsilon_{max}$ ($10^3$ $M^{-1}cm^{-1}$) |
| **5.1a** | 4 | 268 | 149 | 269 | 108 | 270 | 107 |
| **5.1b** | 6 | 310 | 412 | 315 | 247 | 315 | 257 |
| **5.1c** | 8 | 347 | 541 | 351 | 315 | 351 | 329 |
| **5.1d** | 10 | 376 | 595 | 381 | 363 | 381 | 390 |
| **5.1e** | 12 | 400 | 686 | 405 | 470 | 405 | 477 |
| **5.1f** | 14 | 419 | 726 | 423 | 521 | 423 | 527 |
| **5.1g** | 16 | 432 | 732 | 438 | 566 | 437 | 597 |
| **5.1h** | 18 | 443 | 805 | 449 | 633 | 447 | 607[a] |
| **5.1j** | 20 | 451 | 866 | 457 | 699 | 456 | N/A[b] |

[a] Sample solution started turning black over time. Possible decomposition due to peroxide formation in THF that resulted in a slightly lower extinction coefficient value than expected. [b] Severe decomposition occurred resulting in very low extinction coefficient values.

**Table 5-5.** Data for the second longest wavelength absorbance ($\lambda_{peak2}$).

| Compound | $n$ | hexanes | | $CH_2Cl_2$ | | THF | |
|---|---|---|---|---|---|---|---|
| | | $\lambda_{peak2}$ (nm) | $\varepsilon_{peak2}$ ($10^3$ $M^{-1}cm^{-1}$) | $\lambda_{peak2}$ (nm) | $\varepsilon_{peak2}$ ($10^3$ $M^{-1}cm^{-1}$) | $\lambda_{peak2}$ (nm) | $\varepsilon_{peak2}$ ($10^3$ $M^{-1}cm^{-1}$) |
| **5-1a** | 4 | 254 | 145 | 258 | 118 | 258 | 122 |
| **5-1b** | 6 | 292 | 286 | 295 | 193 | 296 | 198 |
| **5-1c** | 8 | 325 | 396 | 329 | 254 | 329 | 262 |
| **5-1d** | 10 | 352 | 527 | 356 | 325 | 356 | 345 |
| **5-1e** | 12 | 374 | 598 | 378 | 438 | 378 | 440 |
| **5-1f** | 14 | 389 | 709 | 393 | 511 | 393 | 508 |
| **5-1g** | 16 | 402 | 802 | 407 | 591 | 406 | 627 |
| **5-1h** | 18 | 412 | 875 | 417 | 676 | 416 | 654[a] |
| **5-1j** | 20 | 420 | 936 | 425 | 748 | 424 | N/A[b] |

[a] Sample solution started turning black over time. Possible decomposition due to peroxide formation in THF that resulted in a slightly lower extinction coefficient value than expected. [b] Severe decomposition occurred resulting in very low extinction coefficient values.

The effective conjugation length (ECL) is when redox, optical or other properties essentially cease to change as a function of length (i.e., for UV-Vis the ECL is achieved when $\Delta\lambda < 1$ nm) and take on the properties of the infinite-chain polymer. This property can be approximated by plotting the band gap or longest absorbance wavelength versus the number of repeat units in the oligomer. A plot of band gap energy ($E_g$) vs. $1/n$ (where $n$ is the number of triple bonds), at first glance, appears to be a linear trend for longer derivatives. This is a common extrapolation done in order to estimate the band gap for infinite polyyne.[10,15,16,46] A linear regression fit shows that when saturation occurs the band gap energy does not go to zero but arrives at a limiting value of 2.18 eV for the infinite polyyne, a phenomena known as Peierls distortion.[47] The band gap energy corresponds to a wavelength value of 569 nm and is very close or equal to previously reported values by Hirsch and coworkers (569 nm)[15] and Gladysz and coworkers (565 nm).[48] However, an expansion of the linear region in question reveals something very interesting (Figure 5-5). It would appear that the trend is actually non-linear in that the data points appear to be leveling off (red line), suggesting a much higher value for the band gap energy of carbyne, being 2.37 eV. This value corresponds to a smaller wavelength value of 523 nm for carbyne. It is believed that this is a more accurate picture of carbyne and data to support this claim will be presented in the sections to come.

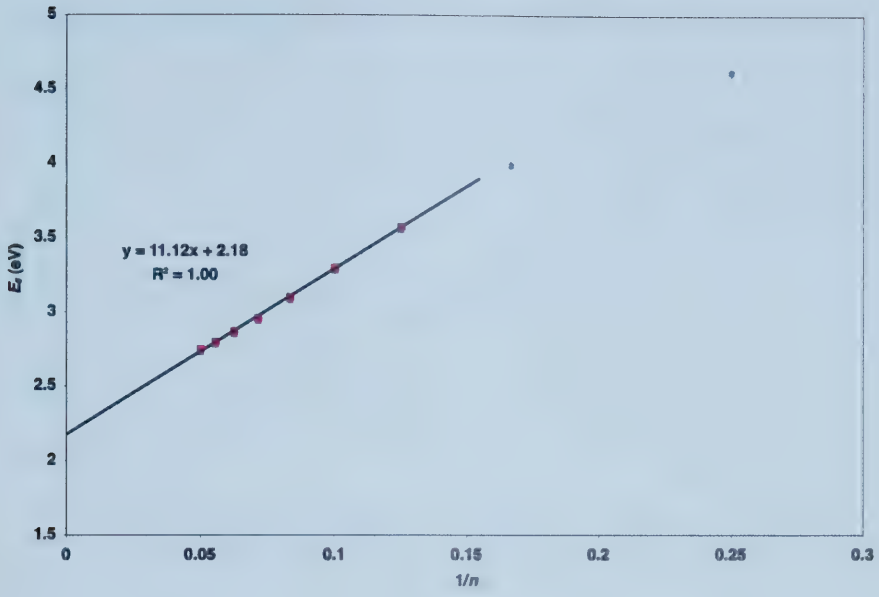


**Figure 5-4.** Plot of band gap energy ($E_g$) vs. $1/n$ (where $n$ is the number of triple bonds). Linear regression line fitted for $n$ = 8-20 (red squares) suggests a band gap energy for infinite polyyne (carbyne) of 2.18 eV ($\lambda$ = 569 nm).

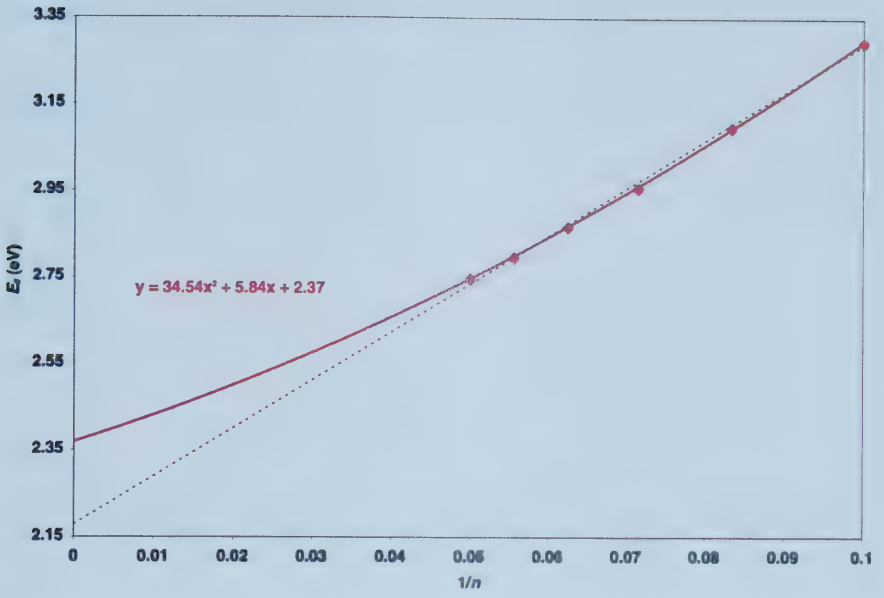


**Figure 5-5.** Expansion of the region $n$ = 10-20 with an extrapolation using a polynomial fit that results in an intercept of 2.37 eV, which corresponds to $\lambda$ = 523 nm for infinite polyyne (black dotted line inserted to show the linear regression line).

As far as individual $\lambda_{max}$ values, there is quite a large bathochromic shift ($\Delta\lambda$ = 42 nm) in going from $n$ = 4 to 6, but as the polyynes become longer this difference in wavelength gradually becomes less and less. The difference ($\Delta\lambda$) is considerable less in going from $n$ = 14 to 16 ($\Delta\lambda$ = 13 nm), from $n$ = 16 to 18 ($\Delta\lambda$ =11 nm), and from $n$ = 18 to 20 ($\Delta\lambda$ = 8 nm). This trend clearly shows that there is a rapid approach toward a uniform HOMO – LUMO gap versus length (i.e., for UV-Vis the ECL is achieved when $\Delta\lambda$ < 1 nm). This trend is also apparent when plotting $E_g$ versus $n$ (Figure 5-6). An approximate extrapolation (dashed line) would predict visually that the ECL of polyynes would fall somewhere around 30 triple bonds, which correlates nicely with previously reported data by Eisler et al.[16]

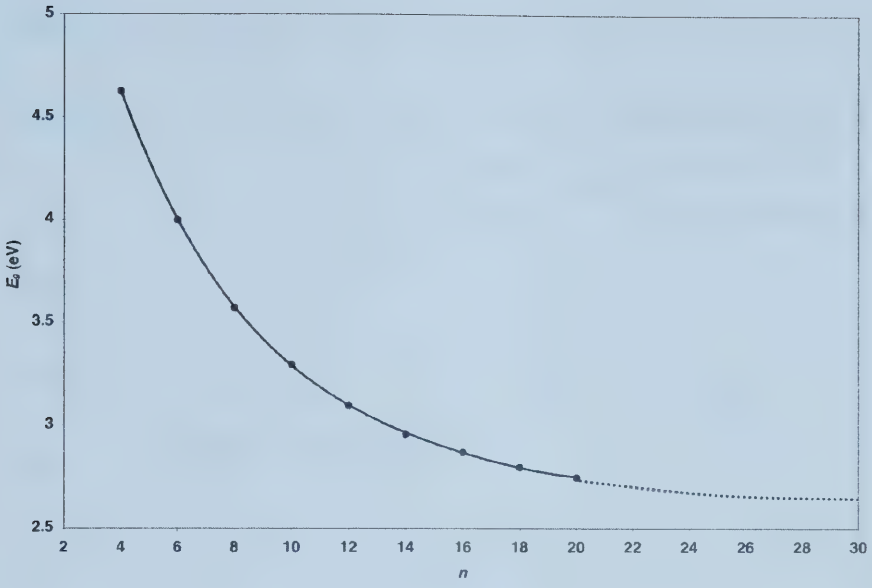


**Figure 5-6.** Plot of $E_g$ vs. number of triple bonds ($n$) showing the dramatic change in slope as a function of length. The dotted line is inserted as a guide to the eye to show that the ECL should occur at around 30 triple bonds in length.

A plot of the longest absorbance wavelength (blue) and the second longest absorbance wavelength (red) also clearly shows the rapid approach of the ECL (Figure 5-7). In the case of the longest wavelength ($\lambda_{max}$), the trend does not seem to approach saturation quite as rapidly as in the case of the second longest absorbance wavelength, and one can actually see the difference between the two absorbance wavelengths is increasing as a function of length. This trend is deceiving, however, because the difference in energy ($\Delta E(\nu^*_{0\text{-}1})$ = difference in energy between the first two excited state vibrational levels) is actually decreasing as a function of length (i.e., $\Delta E(\nu^*_{0\text{-}1})$ = 0.255 for $n$ = 4 eV and $\Delta E(\nu^*_{0\text{-}1})$ = 0.203 eV for $n$ = 20). It is unclear if this trend would continue as a function of length. In any case, however, this plot predicts the absorbance for carbyne would be much lower than 569 nm, as predicted by the linear regression plot in Figure 5-4, and even lower than the value predicted in Figure 5-5 (523 nm).

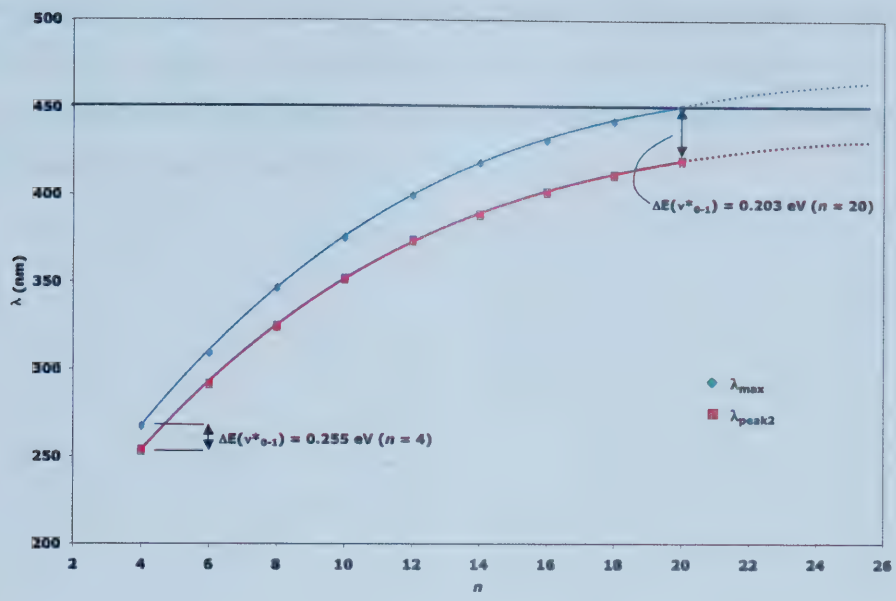


**Figure 5-7.** Plot of the longest wavelength ($\lambda_{max}$, blue line) and the second longest absorbance ($\lambda_{peak2}$, red line) wavelength. The dotted line is inserted as an approximate extrapolation to show that saturation is clearly occurring well before $\lambda = 569$ nm, as predicted in Figure 5-4. $\Delta E(v^*_{0\text{-}1})$ = difference in energy between the first and second excited state vibrational levels.

Lewis-Calvin plots for polyynes up to ten triple bonds typically result in a relatively good-fit linear regression line where $\lambda^2 = kn$ ($\lambda$ = longest absorbance wavelength of polyyne containing $n$ triple bonds).[2,16,37,49] The supertrityl polyyne series also displays a good-fit for the linear regression line up to 10 triple bonds with $R^2 = 0.999$ and a slope of $k = 11.65 \times 10^3$ nm$^2$ which is typical for polyynes (Figure 5-8, black triangles and black line). However, the supertrityl series displays a deviation from linearity starting at about $n = 10$ and beyond (Figure 5-8, red circles and red dashed line). There has been only a few cases in which polyynes beyond the length of 8 triple bonds have been synthesized and the corresponding Lewis-Calvin plot obtained.[37,49] This nonlinear trend has been previously reported by Armitage et *al.* in which they see a slight downward curvature for a Lewis-Calvin plot of dipheylpolyynes up to 10 triple bonds.[2] Walton

and coworkers also observed this deviation from linearity with the TES-endcapped polyyne series.[49] With an increased number of data points beyond $n$ = 10 for the supertrityl series we can now evaluate that saturation is indeed approaching, where the square of the longest absorbance wavelength is reaching a constant value.

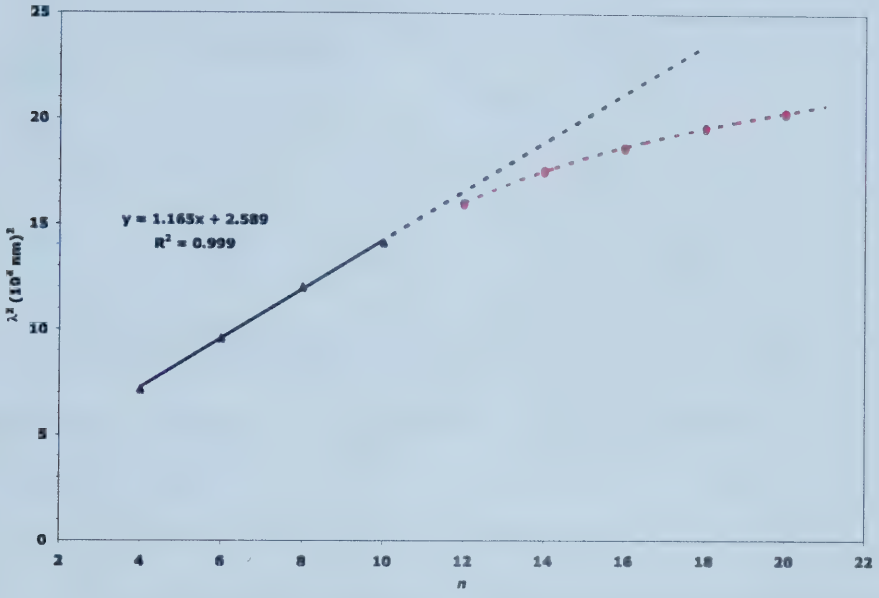


**Figure 5-8.** Lewis-Calvin plot ($\lambda^2 = kn$) of supertrityl polyyne series.

Considering electron correlation effects, the empirical power-law $E_g = 1/\lambda_{max} \sim n^{-x}$ can also be used to describe the relationship between $E_g$, $\lambda_{max}$ and $n$ (where $E_g$ is the energy of the HOMO → LUMO transition).[50-52] This analysis is similar to "Lewis-Calvin Law" of $E_g \sim n^{-0.5}$, which has been described in the previous section.[53] The power-law plot of $E_g$ vs. $n$ for the supertrityl series results in $E_g \sim n^{0.367}$ for the supertrityl series when plotted for $n$ = 4-12 (Figure 5-9). One can easily see that by $n$ = 14 there is a deviation from linearity, which means that $E_g$ is approaching a constant value and that saturation is starting to occur.

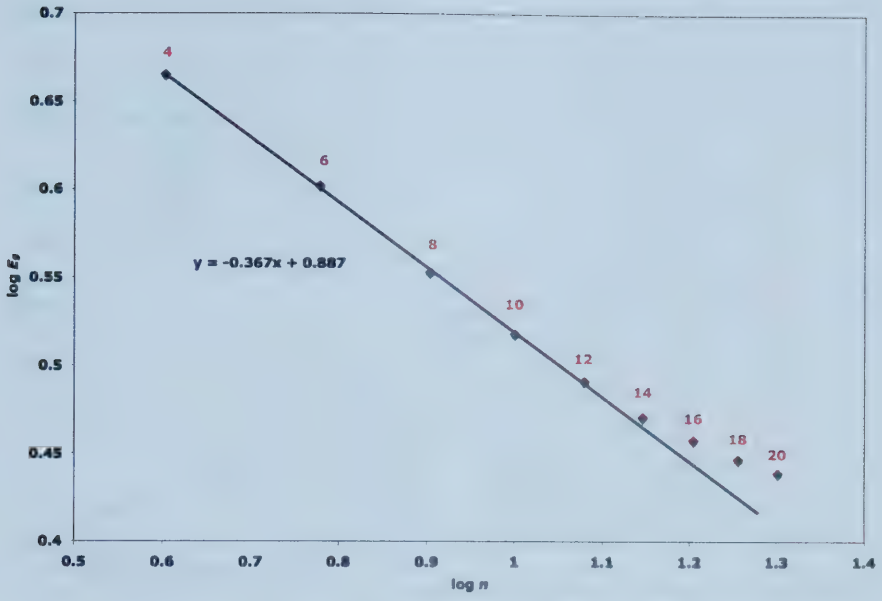


**Figure 5-9.** Power-law plot of $E_g$ vs. $n$ (inset in red) The solid line represents the line-of-best-fit for $n$ = 4-12.

With the ability to stabilize long polyynes using the supertrityl endgroup, the stability of the unsymmetrical polyyne precursors, such as the TIPS protected and H-terminated polyynes was also increased, allowing for their characterization by various methods. The UV-Vis spectra for the unsymmetrical Tr*-TIPS polyyne series from tetrayne **5.32** to decayne **5.53** were recorded as solutions in hexanes (Figure 5-10). The UV-Vis spectrum of tetrayne **5.32** (black line) has broad, overlapping absorbances with the longest absorbance wavelength ($\pi_{v=0} \rightarrow \pi^*_{v=0}$) at 264 nm and the most intense absorbance at 256 nm. As the polyynes become longer there is a sharpening of the absorbance, as well as a bathochromic shift, i.e., a lowering of the HOMO-LUMO band gap energy. It is interesting to note that the lowest energy transition ($\pi_{v=0} \rightarrow \pi^*_{v=0}$), marked by an asterisk for each polyyne, appears to change drastically in intensity as a function of polyyne length. For the penta- (**5.33**) and hexayne (**5.40**) it is the most intense absorbance but this absorbance seems to diminish to almost nothing by the length of the decayne (**5.53**).

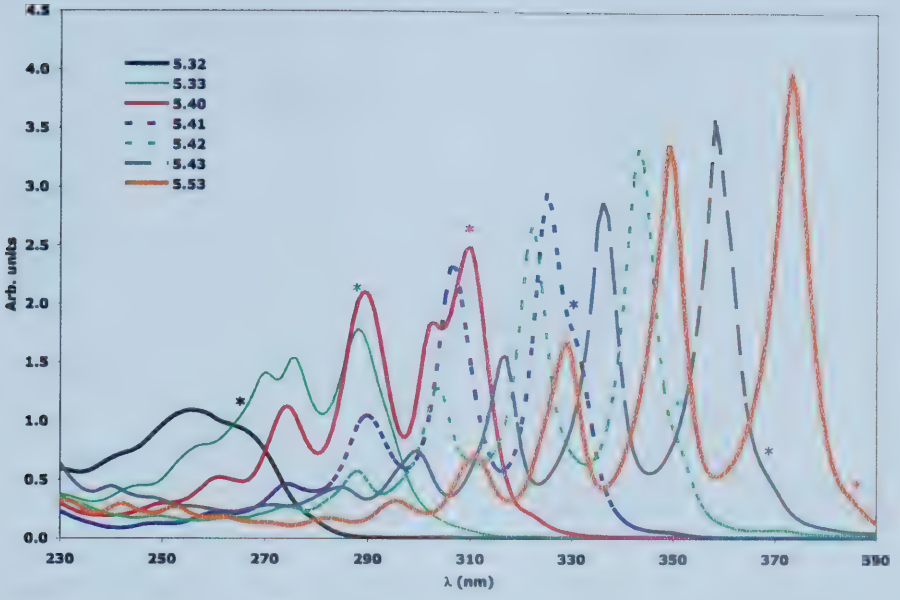


**Figure 5-10.** UV-Vis spectra of unsymmetrical Tr*-TIPS polyynes from tetrayne **5.32** to decayne **5.53** in hexanes. The y-axis represents arbitrary absorbance units.

The maximum absorbance wavelength ($\lambda_{max}$) of unsymmetrical TIPS-protected hexayne **5.40** in hexanes (310 nm) falls at the same wavelength as the symmetrical hexayne **5.1b** (310 nm) (Figure 5-11). However, there is an interesting change in the extinction coefficient where **5.40** (232000 L•mol$^{-1}$•cm $^{1}$) is nearly half that of **5.1b** (412000 L•mol $^{1}$•cm $^{1}$). There is also a dramatic difference in the shape of the spectrum of **5.40**, including broader peaks and a second, higher energy absorption that appears at 303 nm. Another interesting observation is that when one calculates the approximate area under the curve for symmetrical hexayne **5.1b** (ca. 383000) and compares it to the sum of the two low energy peaks (310 and 303 nm) in unsymmetrical hexayne **5.40** (ca. 329000), the values are quite similar. Finally, the sum of the extinction coefficients for the two lowest energy absorbances in **5.40** ($\varepsilon_{310} + \varepsilon_{310}$ = 403000 L•mol $^{-1}$•cm $^{1}$) is similar to that of **5.1b** (412000 L•mol$^{-1}$•cm$^{-1}$).

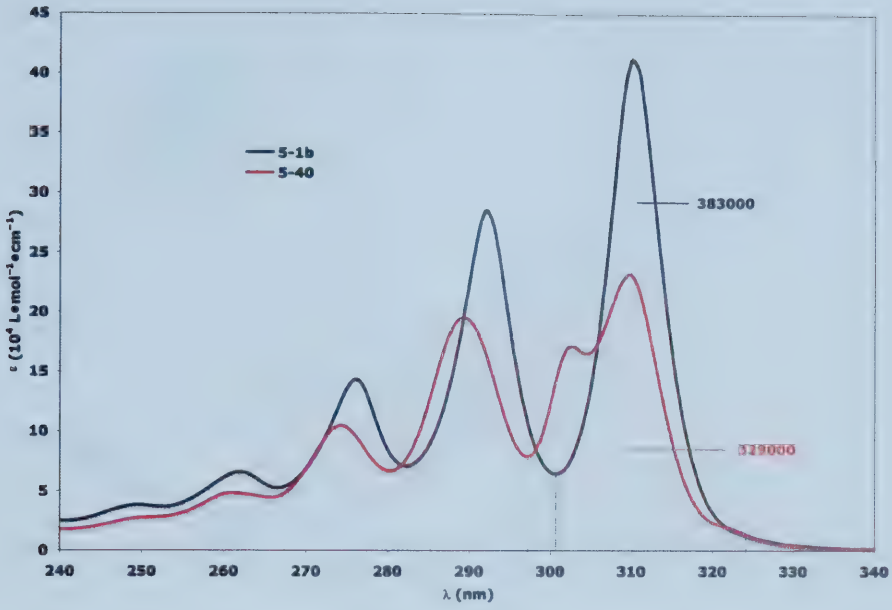


**Figure 5-11.** Overlay plot of hexaynes **5.1j** and **5.40** in hexanes showing the extinction coefficient and change in the absorbance spectrum for the unsymmetrical TIPS-protected hexayne **5.40**. The area under the curve was approximated in Excel using the equation 'SUMPRODUCT(A2:A30–A1:A29,(B2:B30+B1:B29)/2)', where the x-values are in cells A1 to A30, and y-values are in cells B1 to B30. This is an approximate method for finding the area under the curve by summing the area of the trapezoids generated from points on the y-axis (B1:B30) and point on the x-axis (A1:A30).

As was mentioned, with the increased stability of polyynes due to the supertrityl endgroup, came the ability to acquire UV-Vis absorption spectra for the supertrityl terminal polyyne series, generated from the removal of the TIPS group (Figure 5-12). There is also additional fine structure in the spectra of these molecules as well as red-shifted absorprions as a function of polyyne length. As with the Tr*-TIPS series, there is a diminishing intensity of both the longest and second longest wavelength, as a function of polyyne length.

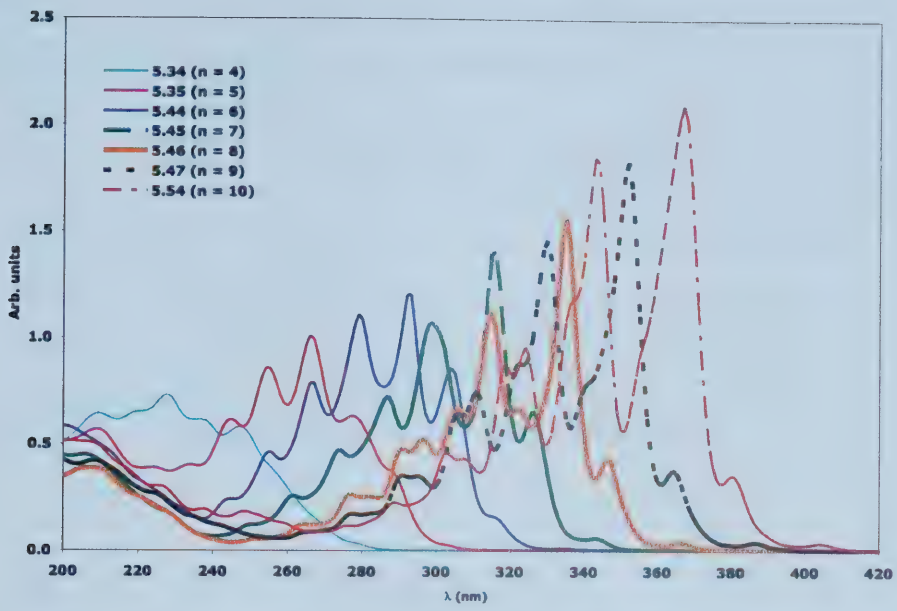


**Figure 5-12.** Overlay of UV-Vis spectra of supertrityl terminal polyynes from tetrayne **5.34** to decayne **5.54** in hexanes. The y-axis represents arbitrary absorbance units.

### 5.3.2 NMR Spectroscopic Analysis

The characterization of the supertrityl polyyne series by $^{13}C$ NMR spectroscopy was conducted. The series displays little change in the chemical shift of the terminal alkyne carbon resonances, which appear at ca. 69 and 57 ppm (Table 5-6). The remaining carbon signals resonate between a narrow range of 61.94-64.50 ppm. As one can see for $n = 20$ (**5.1j**) there is an amazing 20 carbon signals between as short range of 62.03 to 64.50 ppm. Coincidental overlap of only two carbon signals occurs in **5.1j** but this is easily distinguishable based on its two-fold increase in intensity. Astonishingly, all other signals are still resolved at 125 MHz. Broadening of the signals does begin to occur with so many peaks within a narrow range (Figure 5-13).

**Table 5-6.** Alkyne carbon signals for polyynes **5.1a-j**.

| Compound | *n* | Alkyne carbon chemical shifts in $CDCl_3$ (ppm) |
|---|---|---|
| **5.1a** | 4 | 69.06, 63.00, 62.36, 57.19 |
| **5.1b** | 6 | 68.78, 62.96, 62.90, 62.75, 62.42, 57.29 |
| **5.1c** | 8 | 68.65, 63.55, 63.49, 62.97, 62.60, 62.50, 62.19, 57.33 |
| **5.1d** | 10 | 68.60, 63.96, 63.78, 63.49, 63.11, 62.69, 62.54, 62.28, 62.06, 57.36 |
| **5.1e** | 12 | 68.57, 64.17, 63.92, 63.77, 63.49, 63.18, 62.86, 62.52, 62.50, 62.17, 61.99, 57.36 |
| **5.1f** | 14 | 68.57, 64.28, 64.00, 63.93, 63.69, 63.45, 63.24, 63.01, 62.74, 62.48, 62.44, 62.12, 61.96, 57.37 |
| **5.1g** | 16 | 68.56, 64.34, 64.05, 64.01, 63.81, 63.61, 63.45, 63.29, 63.12, 62.93, 62.69, 62.48, 62.41, 62.10, 61.95, 57.37 |
| **5.1h** | 18 | 68.55, 64.36, 64.06, 64.04, 63.85, 63.68, 63.55, 63.42, 63.31, 63.19, 63.05, 62.87, 62.65, 62.47, 62.39, 62.08, 61.94, 57.37 |
| **5.1j** | 20 | 68.63, 64.50, 64.19, 64.19, 64.03, 63.88, 63.77, 63.67, 63.58, 63.51, 63.43, 63.33, 63.20, 63.03, 62.81, 62.54, 62.54, 62.20, 62.03, 57.39 |

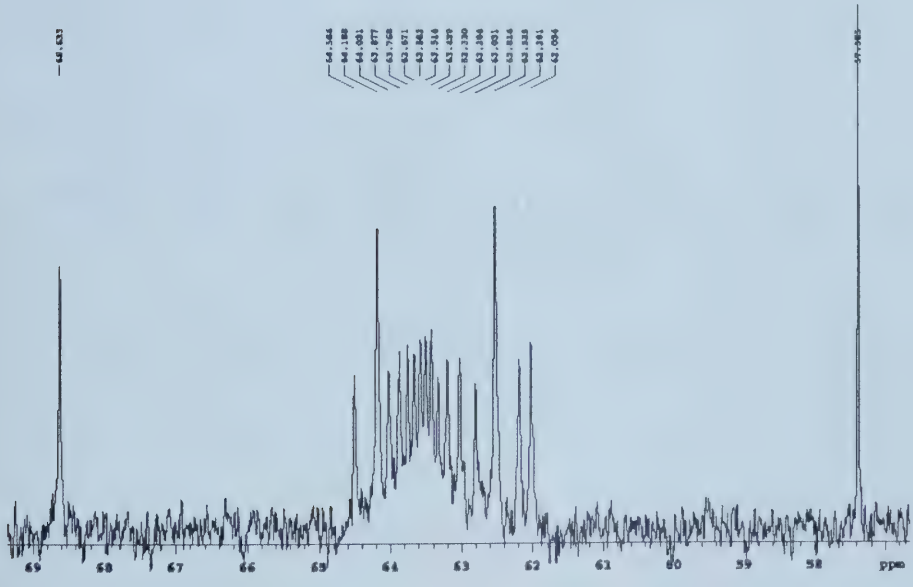


**Figure 5-13.** Expanded $^{13}C$ NMR spectra showing the alkyne resonances for **5.1j**.

A plot of the $^{13}C$ NMR shifts for the alkyne region versus polyyne length reveals the effect of the endgroups (Figure 5-14). One can see three distinct regions of polyyne signals. The most downfield signal, arising from the carbon presumably attached to the endgroup, falls into a narrow region of 68.55-69.06 ppm. The most upfield signal, attributed to the next carbon in the

chain, falls in an even narrower range of 57.19-57.39 ppm. The terminal carbons are thus affected by both endgroups in the shorter analogues, but as the polyynes become longer, this effect disappears (Figures 5-15 and 5-16).

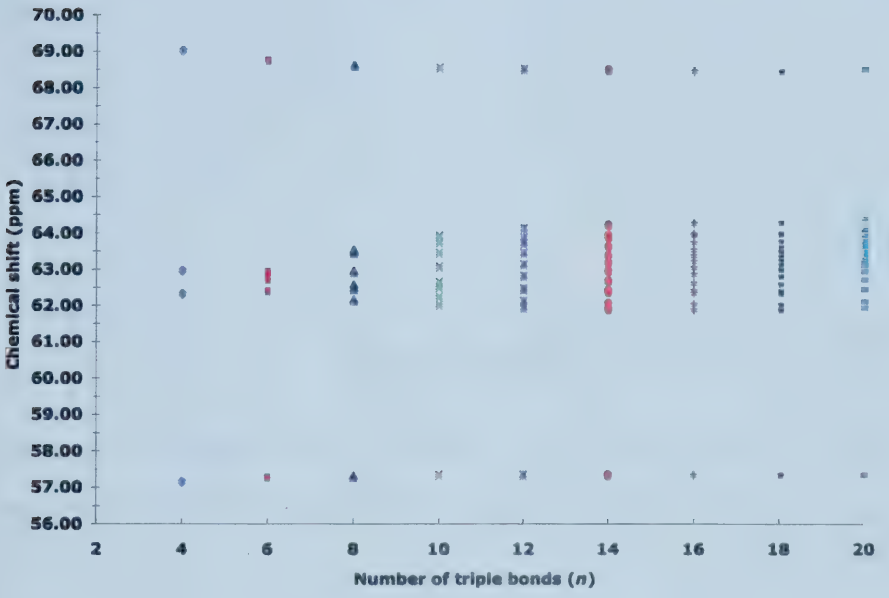


**Figure 5-14.** Plot of alkyne chemical shift versus the number of triple bonds (*n*).

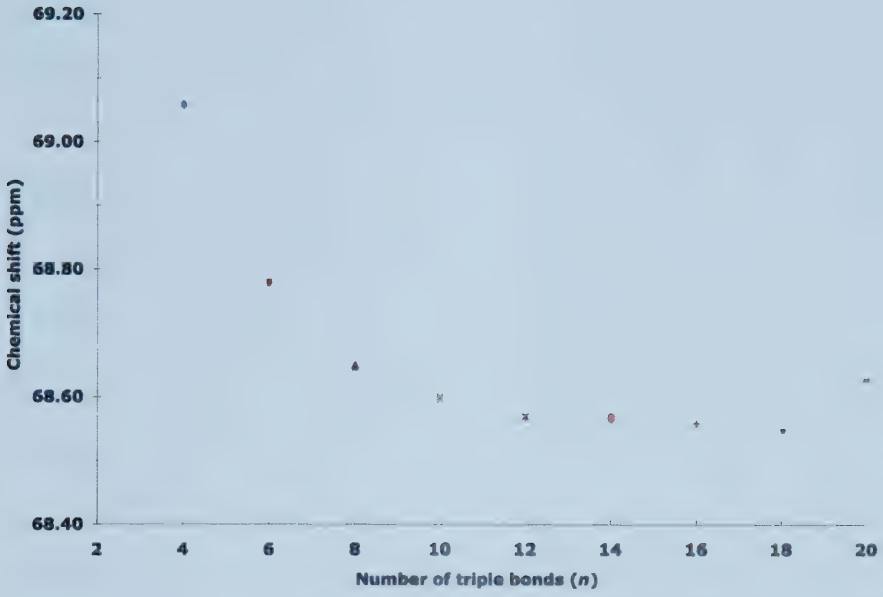


**Figure 5-15.** Plot of most downfield $^{13}C$ NMR carbon signal as a function of polyyne length ($n$) showing that the second endgroups influence on the chemical shift is nonexistent by $n \approx 10$.

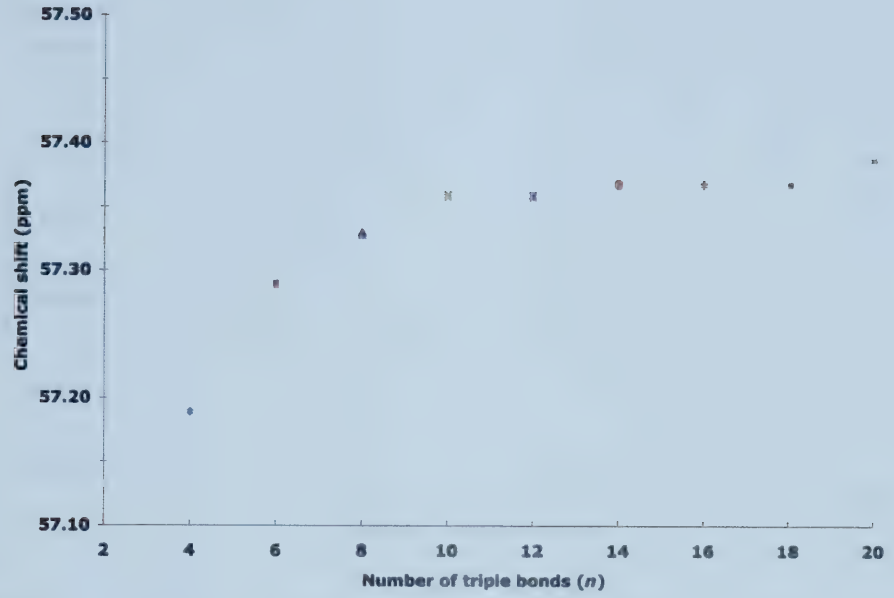


**Figure 5-16.** Plot of the most upfield alkyne $^{13}C$ NMR carbon signals as a function of polyyne length ($n$) showing that the second endgroups influence on the chemical shift is nonexistent by $n \approx 10$.

As might be expected, the internal carbons of the tetrayne **5.1a** are also affected by both endgroups more strongly than the longer derivatives and this is clearly seen in Figure 5-17. As the polyynes become longer, a more defined trend is seen in which the outer most carbon signals gradually shift to a constant range of about 61.94-64.50 ppm. As one might expect, this trend would continue, where more and more signals presenting themselves within this range leading towards a broad peak with its apex at ca. 63.4 ppm. This chemical shift would represent the lone carbon signal of carbyne.

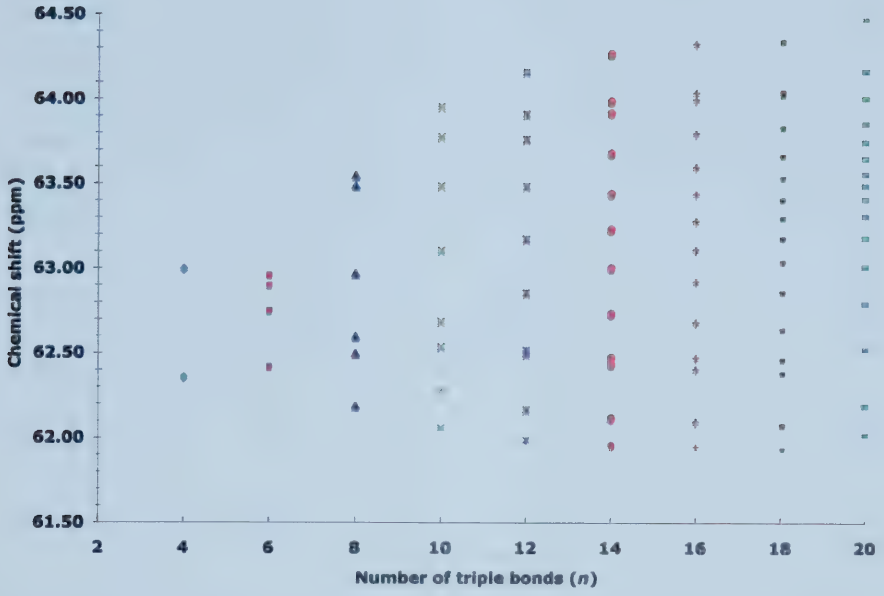


**Figure 5-17.** Plot of the $^{13}C$ NMR carbon signals of the internal alkynes of the polyyne as a function of polyyne length ($n$).

Looking into the $^{1}H$ NMR data for the terminal polyynes ($n$ = 1-7), an obvious trend appears for the chemical shift of the terminal acetylenic hydrogen as a function of length (Figure 5-18). For monoyne **5.6** the terminal hydrogen signal is found at the most downfield position (2.59 ppm), likely due to inductive effects resulting from the electron withdrawing supertrityl endgroup. This resonance shifts upfield for diyne **5.7** (2.10 ppm) and by the triyne (**5.25**) the trend in upfield shift seems to stop. This would indicate the endgroup effect has diminished by the triyne. At the length of the tetrayne (**5.34**) a reversal of the trend appears and there is a steady downfield shift as a function of length. This is most likely due to the increasing electron withdrawing effect of the polyyne backbone itself, which is additive based on each additional acetylene unit. This would also suggest an increase in acidity of the terminal hydrogen as a function of length, a premise supported by the mechanistic investigations done by Bohlmann and coworkers.[54]

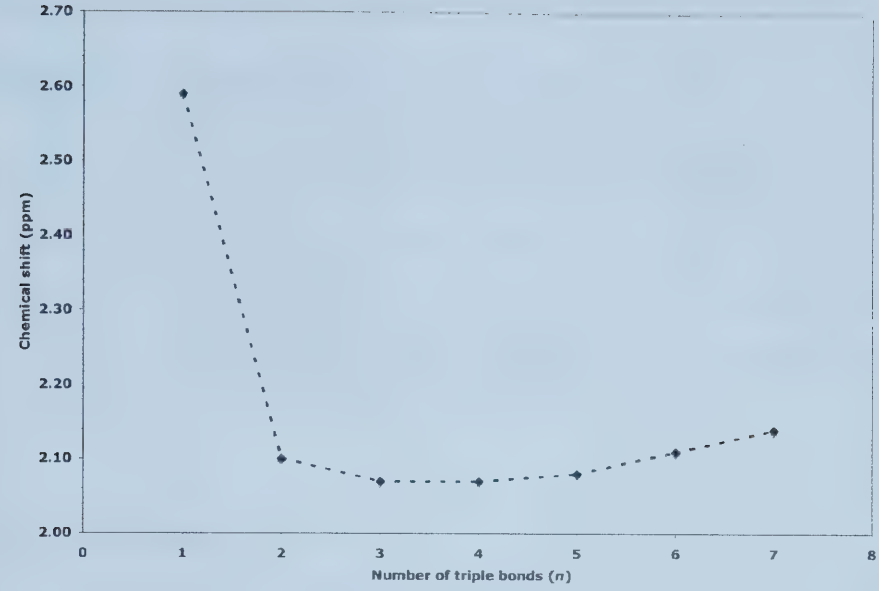


**Figure 5-18.** Plot of $^{1}$H NMR chemical shift of the terminal acetylene hydrogen as a function of polyyne length ($n$).

The $^{13}$C NMR data for $n$ = 1-7 have also been successfully collected (Table 5-7). The most useful trends seen in this data arise from the large upfield shift seen for the quaternary endgroup carbon (shown in red) in going from the monoyne (**5.6**) to the diyne (**5.7**). This observation was also seen for the terminal hydrogen chemical shifts of these compounds, where there was a considerable upfield shift when going from mono- (**5.6**) to diyne (**5.7**). Aside from this anomaly, the trend seen in going from $n$ = 2 (**5.7**) to $n$ = 7 (**5.45**) is that of a slight downfield shift as a function of polyyne length. Perhaps the amount of S-character for the terminal carbon is increasing as a function of polyyne length, causing an increase in electronegativity, which would explain the observation of hydrogen and carbon downfield shifts.

**Table 5-7.** $^{13}C$ NMR chemical shift data for the terminal polyyne series.

| Compound | *n* | $^{13}C$ NMR Chemical Shifts in $CDCl_3$ (ppm) |
|---|---|---|
| **5.6** | 1 | 149.7, 144.8, 123.8, 119.8, 90.7, 72.0, 56.1, 34.8, 31.4 |
| **5.7** | 2 | 149.9, 143.9, 123.8, 120.1, 83.5, 68.8, 68.1, 66.6, 56.7, 34.8, 31.4 |
| **5.25** | 3 | 150.1, 143.6, 123.7, 120.3, 84.8, 68.9, 68.5, 66.6, 61.6, 61.3, 57.0, 34.8, 31.4 |
| **5.34** | 4 | 150.1, 143.4, 123.7, 120.4, 85.7, 68.61, 68.58, 67.1, 62.24, 62.20, 61.6, 61.3, 57.2, 34.8, 31.4 |
| **5.35** | 5 | 150.2, 143.3, 123.7, 120.4, 86.2, 68.6, 68.5, 67.5, 62.8, 62.5, 62.4, 61.8, 61.5, 61.3, 57.3, 34.9, 31.4 |
| **5.44** | 6 | 150.2, 143.2, 123.7, 120.5, 86.6, 68.6, 68.4, 67.8, 63.22, 63.09, 62.48, 62.22, 62.00, 61.96, 61.85, 61.20, 57.3, 34.9, 31.4 |
| **5.45** | 7 | 150.2, 143.2, 123.7, 120.5, 86.9, 68.6, 68.3, 68.1, 63.53, 63.52, 62.82, 62.48, 62.31, 62.12, 62.12, 62.08, 61.98, 61.1, 57.3, 34.8, 31.3 |

### 5.3.3 DSC Analysis

One of the easiest and efficient methods for determining thermal stability is differential scanning calorimetry. The supertrityl polyyne series **5.1a-j** have been analyzed and most show a sharp exotherm ($T_{max}$), characteristic of a decomposition pathway via a topochemical polymerization.[1,55] A comparison of values as a function of length shows an expected decrease in stability as the polyynes become longer (Table 5-8). The hexadecayne **5.1g** seems to be more stable than the shorter tetradecayne **5.1f** (i.e., a slightly higher $T_{max}$). This is possibly due to changes in morphology and/or packing in the solid-state, but the overall trend shows an expected decrease in stability as a function of length. The exothermic maximum ($T_{max}$) values are extremely high compared to other polyyne derivatives of the same length demonstrating that these polyynes are stable by more than 100 °C in some cases. This increased stability can be attributed to the large size of the endgroups, which prevent decomposition pathways via intermolecular polymerizations by blocking the approach of neighboring molecules.

**Table 5-8.** Comparison of thermal decomposition points of known polyynes by DSC analysis.

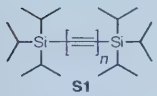

S1

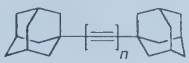

3.1

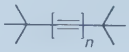

4.1

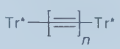

5.1

| Polyyne length (*n*) | Compound | Endgroup | $T_{max}$ |
|---|---|---|---|
| 4 | **S1c** | TIPS | 204[a] |
| | **3.1c** | adamantyl | 230[b] |
| | **4.1c** | *tert*-butyl | 221[c] |
| | **5.1a** | Supertrityl | **319** |
| 6 | **S1e** | TIPS | 177[a] |
| | **3.1e** | adamantyl | 205[b] |
| | **4.1e** | *tert*-butyl | 156[c] |
| | **5.1b** | Supertrityl | **323** |
| 8 | **S1f** | TIPS | 132[b] |
| | **3.1f** | adamantyl | 110 |
| | **4.1f** | *tert*-butyl | 139[a] |
| | **5.1c** | Supertrityl | **275** |
| 10 | **S1h** | TIPS | 123[b] |
| | **3.1h** | adamantyl | 90 |
| | **4.1h** | *tert*-butyl | 107[a] |
| | **5.1d** | Supertrityl | **220** |
| 12 | **5.1e** | Supertrityl | **168** |
| 14 | **5.1f** | Supertrityl | **151** |
| 16 | **5.1g** | Supertrityl | **159** |
| 18 | **5.1h** | Supertrityl | **137** |
| 20 | **5.1j** | Supertrityl | **116** |

[a] See reference 16. [b] See Chapter 3. [c] See Chapter 4.

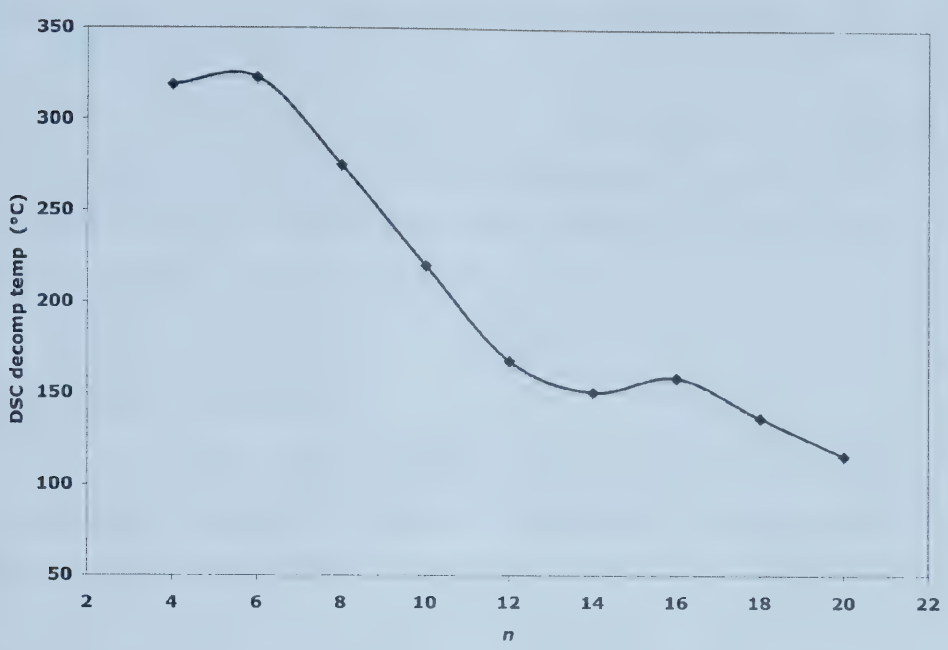


**Figure 5-19.** Plot of thermal decomposition ($T_{max}$) as a function of polyyne length.

The unsymmetrical Tr*-TIPS polyynes ($n$ = 3-9) have also analyzed by DSC and show considerable stability, albeit less so than the symmetrical bis(supertrityl) series (**5.1**). The DSC trace of triyne (**5.24**) shows two, intense, sharp endotherms with the first occurring at 174 °C and the second at 201 °C, which corresponds well to the melting point of the solid (194-198 °C). The third peak (exothermic) represents decomposition of the polyyne at an impressively high temperature of 341 °C. Tetrayne **5.32** displays an endotherm at 217 °C for the melting point and an exotherm ($T_{max}$) at 264 °C. Similar to the tetrayne **5.32**, pentayne **5.33** displayed an endotherm at 218 °C for the melting point. The exotherm ($T_{max}$), however, was slightly lower, showing up at 232 °C. The hexa- (**5.40**), hepta- (**5.41**), octa- (**5.42**), and nonayne (**5.43**) no longer displayed endothermic peaks as a result of melting, but showed exothermic decompositions ($T_{max}$) at 206 °C, 177 °C, 144 °C, and 135 °C, respectively. The continuous decrease in thermal stability as a

function of length is very clear, but it should be noted that the nonayne **5.43** is still stable at >100 °C.

With enhanced stabilities of the supertrityl terminal polyynes, obtaining DSC analysis was feasible up to tetrayne **5.34**. Diyne (**5.7**) displays an endotherm at 208 °C while triyne (**5.25**) had a slightly higher $T_{max}$, decomposing at an impressively high temperature of 217 °C. The stability of the tetrayne (**5.34**) dropped considerably with $T_{max}$ = 135 °C.

### 5.3.4 X-Ray Crystallographic Data

The main reason attributed to the stability of the supertrityl polyyne series is the extremely large size of the endgroup in comparison to previous derivatives. The supertrityl group spans a diameter of approximately 14 Å, which is about double that of the triisopropylsilyl endgroup (~7 Å in diameter). This size difference can clearly be seen in a comparison of the space-filling models for the bis(phenyl)tetrayne,[20] bis(*t*-butyl)tetrayne,[19] bis(adamantyl)tetrayne,[45] bis(TIPS)tetrayne,[16] and the bis(Tr*)tetrayne (Figure 5-20). Another contributing factor towards the stability is the ability of the supertrityl groups to partly shield the endmost acetylene carbons by projecting itself over the polyyne chain (shown by the line drawn between C(1)-C(2) and C(7)-C(8) bonds).

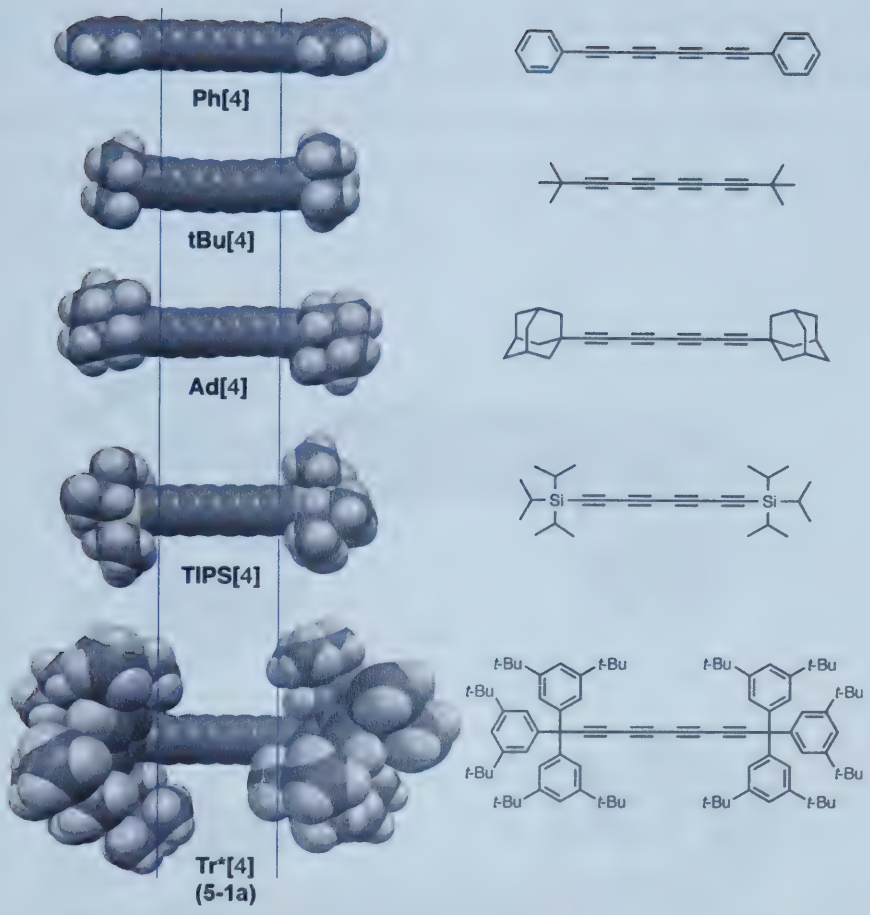


**Figure 5-20.** Comparison of various tetrayne endgroup sizes based on X-ray crystallographic data. The blue line is drawn along the C(1)-C(2) and C(7)-C(8) bonds to show how much the supertrityl endgroups overlap the polyyne core.

Crystals suitable for X-ray crystallography were also obtained for the unsymmetrical TIPS protected hexayne **5.40** (Figure 5-21a). The space-filling structure for **5.40** nicely displays the size contrast of the two endgroups. Another impressive attribute of solid-state structure of **5.40** is the degree of bending in the polyyne backbone, with bond angles ranging from 179.2(3)° to 173.8(3)°. It would seem, with such a bow in the molecule of **5.40**, that is would be quite a reactive species in the solid-state. As a result of the bulky endgroups, however, compound **5.40** is

quite stable with thermal decomposition occurring at 206 °C ($T_{max}$), as determined by DSC analysis. The X-ray crystal structure bis(supertrityl)hexayne **5.1b** ($T_{max}$ = 323 °C) helps to illustrate why this hexayne is so much more stable than the TIPS-substituted analogue **5.40** (Figure 5-21b). The endgroups project over the polyyne chain, partially shielding the first two to three alkyne carbons at either end (shown in red).

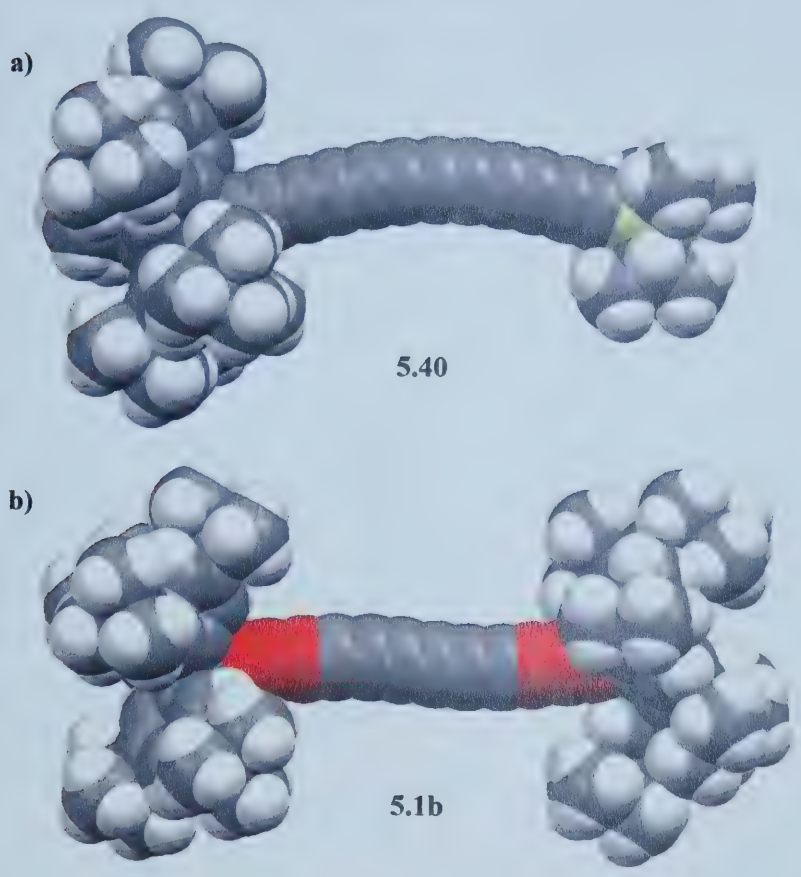


**Figure 5-21.** Space-filling model of hexaynes **5.40** and **5.1b** based on X-ray crystallographic data.

The solid-state packing of **5.1b** gives insight into the stability of the molecule as well as, perhaps, the lack of solubility in many common organic solvents. The packing, as viewed along the *a*-axis (Figure 5-22a), shows the molecules aligned in a stacked manner with each row being staggered, having the endgroups of one row positioned directly in the cavity created along the

polyyne chain between the two endgroups of the adjacent row. The interatomic distance between polyynes in adjacent rows is approximately 8 Å, double the distance required for interatomic crosslinking reactions to occur (polymerization). The packing, as viewed along the crystallographic *b*-axis, occurs in almost the same fashion as previously discussed, with interatomic distances between polyyne rows being approximately 7 Å (Figure 5-22b). As one can see, the solid-state packing is highly efficient, and may explain the low solubility of this particular polyyne. A cartoon depiction of the solid-state packing of **5.1b** is used for clarification (Figure 5-22c).

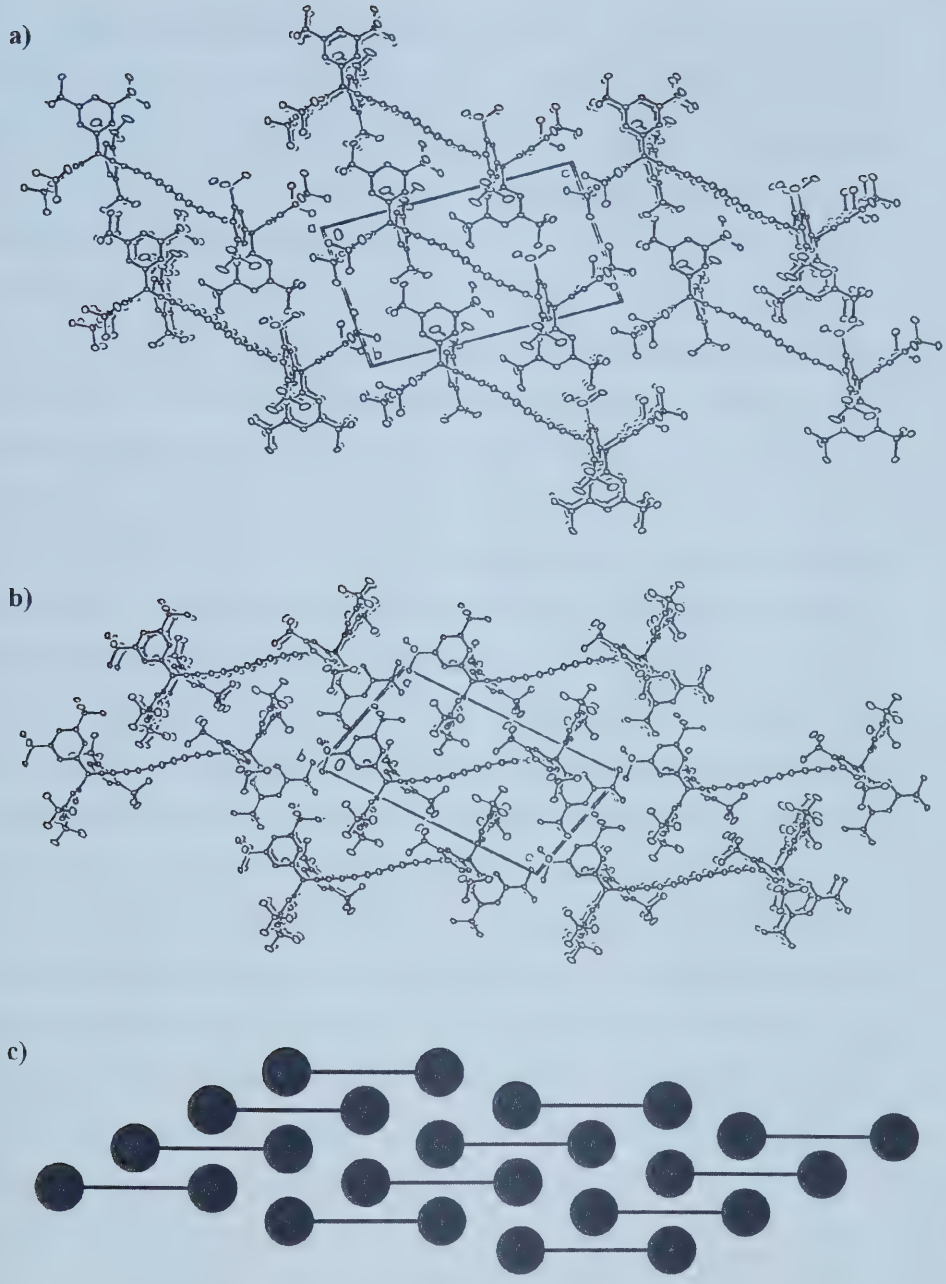


**Figure 5-22.** Crystal packing of hexayne **5.1b**, as viewed along the a) crystallographic *a*-axis and b) crystallographic *b*-axis (hydrogens removed for clarity, 20% probability level). c) Cartoon representation of the solid-state packing of **5.1b**.

What is even more impressive, in terms of unprecedented stability in polyynes, is that of terminal polyynes **5.6**, **5.7** and **5.25**. It is well known that acetylene, a monoyne with hydrogens at both termini, is a gas under ambient conditions and is highly flammable. In comparison, the replacement of a hydrogen with a TIPS group results in a flammable liquid but if a hydrogen is replaced with a supertrityl group (**5.6**), the resulting compound is now a stable solid with a melting point range of 193-194 °C. Diynes are typically less stable species unless a bulky endgroup is placed on one of the termini. Even then these compounds are typically only stable at low temperatures or in the solid state. The supertrityl diyne (**5.7**), however, is a stable solid with a melting point range of 192-194 °C and decomposes at 208 °C ($T_{max}$), as shown by DSC analysis. Terminal triynes are much less stable yet and have been known to explode even in the absence of air at low temperatures.[2] Recent work done by Bryce and coworkers has shown that terminal diynes, triynes and even tetraynes can be stabilized by the use of large endgroups, allowing for their characterization.[11-13] Supertrityl triyne **5.25** was isolated as a stable solid that could be stored indefinitely under ambient conditions. This triyne displayed thermal decomposition at an astonishing 206 °C, as determined by capillary thermolysis, and a $T_{max}$ of 217 °C as determined by DSC analysis. It is interesting to note that the mono-, di- and triyne all show decomposition around the same temperature. This might suggest that the endgroup has approximately the same amount of shielding of the polyyne in each case, as was discussed previously. This shielding can be seen in the space-filling models of each of these molecules (Figure 5-23). It should be noted that although X-ray data was not obtained, supertrityl terminal polyynes containing up to seven contiguous triple bonds have been isolated as solids and fully characterized spectroscopically. Partial characterization, which includes IR, UV-Vis, and mass spectrometries, has even been obtained on the terminal octa- (**5.46**), nona- (**5.47**), and decayne (**5.54**).

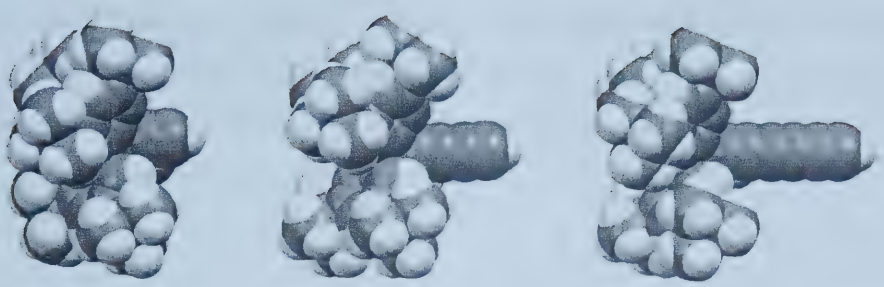

5.6 5.7 5.25

**Figure 5-23.** Space-filling models of monoyne **5.6**, diyne **5.7** and triyne **5.25** based on the X-ray crystallographic data (20% probability level).

## 5.4 Conclusions

A new, and far more stable, series of polyynes has been synthesized that utilize a very bulky endgroup (supertrityl). The ability to synthesize such stable molecules stems from the fact that the large endgroup, which spans a diameter of 14 Å, partially shields and prevents reactions from occurring on the reactive polyyne core. The shorter polyynes (up to $n$ = 10) have been successfully synthesized by a number of different routes, in which the key steps include: 1) Friedel-Craft acylation, dibromoolefination and FBW rearrangement, or 2) alcohol oxidation, dibromoolefination, and FBW rearrangement, and finally 3) a new Glaser-Eglinton-Hay coupling protocol. The combination of routes 2 and 3 successfully led to the formation of unsymmetrical polyynes up to 10 triple bonds in length where one end of the polyyne was capped with a supertrityl group and the other a TIPS group. Desilylation of the TIPS group by means of a mild desilylation using CsF protocol enabled the formation of terminal polyynes that were sufficiently stable for partial to full characterization by standard means. These polyynes were ultimately homocoupled to produce the desired symmetrical polyynes using a new, mild, homocoupling condition that resulted in good yields with little to no decomposition or formation of undesired side products via the loss of acetylene units.

The successful synthesis of stable polyynes provides for a more accurate picture of trends in the physical properties in terms of saturation. This ultimately gives a better description of the

properties of the sp-carbon allotrope carbyne. Indeed this series of polyynes shows evidence of saturation of properties for UV-Vis absorption and NMR spectroscopies. Based on these extrapolations, carbyne should have a UV-Vis absorption of approximately $\lambda_{max}$ = 523 nm and a carbon chemical shift of 63.4 ppm.

## 5.5 References


[1] Szafert, S.; Gladysz, J. A. *Chem. Rev.* **2006**, *106*, PR1.

[2] Armitage, J. B.; Entwistle, N.; Jones, E. R. H.; Whiting, M. C. *J. Chem. Soc.* **1954**, 147.

[3] Stahl, J.; Mohr, W.; de Quadras, L.; Peters, T. B.; Bohling, J. C.; Martín-Alvarez, J. M.; Owen, G. R.; Hampel, F.; Gladysz, J. A. *J. Am. Chem. Soc.* **2007**, *129*, 8282.

[4] Klinger, C.; Vostrowsky, O.; Hirsch, A. *Eur. J. Org. Chem.* **2006**, 1508.

[5] de Quadras, L.; Bauer, E. B.; Mohr, W.; Bohling, J. C.; Peters, T. B.; Martín-Alvarez, J. M.; Hampel, F.; Gladysz, J. A. *J. Am. Chem. Soc.* **2007**, *129*, 8296.

[6] Shir, I. B.; Sasmal, S.; Mejuch, T.; Sinha, M. K.; Kapon, M.; Keinan, E. *J. Org. Chem.* **2008**, *73*, 8772.

[7] Bernà, J. é.; Crowley, J. D.; Goldup, S. M.; Hänni, K. D.; Lee, A.-L.; Leigh, D. A. *Angew. Chem. Int. Ed.* **2007**, *46*, 5709.

[8] Sato, Y.; Yamasaki, R.; Saito, S. *Angew. Chem. Int. Ed.* **2009**, *48*, 504.

[9] Sugiyama, J.; Tomita, I. *Eur. J. Org. Chem.* **2007**, 4651.

[10] Zheng, Q.; Bohling, J. C.; Peters, T. B.; Frisch, A. C.; Hampel, F.; Gladysz, J. A. *Chem. Eur. J.* **2006**, *12*, 6486.

[11] West, K.; Wang, C.; Batsanov, A. S.; Bryce, M. R. *Org. Biomol. Chem.* **2008**, *6*, 1934.

[12] West, K.; Wang, C.; Batsanov, A. S.; Bryce, M. R. *J. Org. Chem.* **2006**, *71*, 8541.

[13] Wang, C.; Batsanov, A. S.; West, K.; Bryce, M. R. *Org. Lett.* **2008**, *10*, 3069.

[14] Mohr, W.; Stahl, J.; Hampel, F.; Gladysz, J. A. *Chem. Eur. J.* **2003**, *9*, 3324.

[15] Gibtner, T.; Hampel, F.; Gisselbrecht, J.-P.; Hirsch, A. *Chem. Eur. J.* **2002**, *8*, 408.

[16] Eisler, S.; Slepkov, A. D.; Elliott, E.; Luu, T.; McDonald, R.; Hegmann, F. A.; Tykwinski, R. R. *J. Am. Chem. Soc.* **2005**, *127*, 2666.

[17] Chalifoux, W. A.; Ferguson, M. J.; Tykwinski, R. R. *Eur. J. Org. Chem.* **2007**, 1101.

[18] Chalifoux, W. A.; Tykwinski, R. R. *C. R. Chimie* **2009**, *12*, 341.

[19] Chalifoux, W. A.; McDonald, R.; Ferguson, M. J.; Tykwinski, R. R. *Angew. Chem. Int. Ed.* **2009**, *48*, 7915.

[20] Luu, T.; Elliott, E.; Slepkov, A. D.; Eisler, S.; McDonald, R.; Hegmann, F. A.; Tykwinski, R. R. *Org. Lett.* **2005**, *7*, 51.

[21] Kendall, J.; McDonald, R.; Ferguson, M. J.; Tykwinski, R. R. *Org. Lett.* **2008**, *10*, 2163.

[22] Ditto, S. R.; Card, R. J.; Davis, P. D.; Neckers, D. C. *J. Org. Chem.* **1979**, *44*, 894.

[23] Bartlett, P. D.; Roha, M.; Stiles, R. M. *J. Am. Chem. Soc.* **1954**, *76*, 2349.

[24] Khuong, T.-A. V.; Zepeda, G.; Ruiz, R.; Khan, S. I.; Garcia-Garibay, M. A. *Cryst. Growth Des.* **2004**, *4*, 15.

[25] Ramirez, F.; Desai, N. B.; McKelvie, N. *J. Am. Chem. Soc.* **1962**, *84*, 1745.

[26] Walton, D. R. M.; Waugh, F. *J. Organomet. Chem.* **1972**, *37*, 45.

[27] Corey, E. J.; Fuchs, P. L. *Tetrahedron Lett.* **1972**, *13*, 3769.

[28] Wiechell, H. *Liebigs Ann. Chem.* **1894**, *279*, 337.

[29] Fritsch, P. *Liebigs Ann. Chem.* **1894**, *279*, 319.

[30] Buttenberg, W. P. *Liebigs Ann. Chem.* **1894**, *279*, 324.

[31] Sonogashira, K. In *Handbook of Organopalladium Chemistry for Organic Synthesis*; Negishi, E.-i., Ed; Wiley: New York, 2002; pp 493.

[32] Sonogashira, K. *J. Organomet. Chem.* **2002**, *653*, 46.

[33] Métay, E.; Hu, Q.; Negishi, E.-i. *Org. Lett.* **2006**, *8*, 5773.

[34] Hoheisel, T. N.; Frauenrath, H. *Org. Lett.* **2008**, *10*, 4525.

[35] Cadiot, P.; Chodkiewicz, W. In *Chemistry of Acetylenes*; Viehe, H. G., Ed; Dekker: New York, 1969; pp 597.

[36] Hay, A. S. *J. Org. Chem.* **1962**, *27*, 3320.

[37] Johnson, T. R.; Walton, D. R. M. *Tetrahedron* **1972**, *28*, 5221.

[38] Glaser, C. *Ann. Chem.* **1870**, *154*, 137.

[39] Glaser, C. *Ber. Dtsch. Chem. Ges.* **1869**, *2*, 422.

[40] Eglinton, G.; Galbraith, A. R. *Chem. Ind. (London)* **1956**, 737.

[41] Siemsen, P.; Livingston, R. C.; Diederich, F. *Angew. Chem. Int. Ed.* **2000**, *39*, 2632.

[42] Lei, A.; Srivastava, M.; Zhang, X. *J. Org. Chem.* **2002**, *67*, 1969.

[43] Atkins, P. W.; Friedman, R. S. *Molecular Quantum Mechanics*; 3 ed.; Oxford University Press: New York, 1997.

[44] Mohr, W.; Stahl, J.; Hampel, F.; Gladysz, J. A. *Inorg. Chem.* **2001**, *40*, 3263.

[45] Lucotti, A.; Tommasini, M.; Fazzi, D.; Del Zoppo, M.; Chalifoux, W. A.; Ferguson, M. J.; Zerbi, G.; Tykwinski, R. R. *J. Am. Chem. Soc.* **2009**, *131*, 4239.

[46] Zhuravlev, F.; Gladysz, J. A. *Chem. Eur. J.* **2004**, *10*, 6510.

[47] Hoffmann, R. *Angew. Chem. Int. Ed. Engl.* **1987**, *26*, 846.

[48] Dembinski, R.; Bartik, T.; Bartik, B.; Jaeger, M.; Gladysz, J. A. *J. Am. Chem. Soc.* **2000**, *122*, 810.

[49] Eastmond, R.; Johnson, T. R.; Walton, D. R. M. *Tetrahedron* **1972**, *28*, 4601.

[50] Bubeck, C. In *Electronic Materials – the Oligomer Approach*; Müllen, K.; Wegner, G., Eds; Wiley-VCH: Weinheim, 1998; Chapter 8.

[51] Luo, Y.; Norman, P.; Ruud, K.; Agren, H. *Chem. Phys. Lett.* **1998**, *285*, 160.

[52] Mathy, A.; Ueberhofen, K.; Schenk, R.; Gregorius, H.; Garay, R.; Müllen, K.; Bubeck, C. *Phys. Rev. B* **1996**, *53*, 4367.

[53] Lewis, G. N.; Calvin, M. *Chem. Rev.* **1939**, *25*, 273.

[54] Bohlmann, F.; Schönowsky, H.; Inhoffen, E.; Grau, G. *Chem. Ber.* **1964**, *97*, 794.

[55] Enkelmann, V. *Chem. Mater.* **1994**, *6*, 1337.

# Chapter 6 General Discussion and Conclusions

This thesis has summarized polyyne synthesis, old and new, as well as describing some of the properties that these molecules possess. It has been revealed that, although saturation of the spectroscopic properties (UV-Vis, NMR, Raman, etc.) is being approached, it has not been achieved. Therefore, the challenge of synthesizing even longer derivatives still remains in order to provide a complete understanding of the properties of the material known as carbyne.

Since the synthesis of stable polyynes up to 20 triple bonds has been accomplished using the supertrityl endgroup, it seems reasonable that longer derivatives should also be achievable. The route towards these molecules can be extended beyond what has been done in this thesis, and, therefore, this project remains unfinished. The synthesis of polyynes up to 30 triple bonds in length, the predicted saturation length, should allow for the defendable claim that a synthetic sp-carbon allotrope of carbon has been achieved (Scheme 6-1).

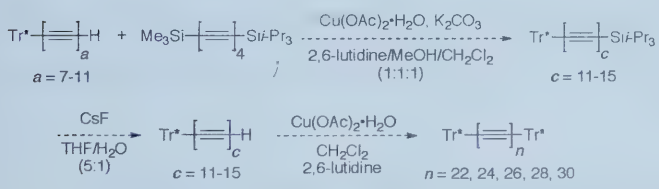


**Scheme 6-1.** Proposed synthesis of even longer supertrityl polyynes.

With the synthesis of the supertrityl polyyne series accomplished it is now possible to study polyynes beyond 10 triple bonds by Raman spectroscopic analysis. This would provide for better insight into the violation of mutual exclusion in the longer derivatives (static or dyamic symmetry breaking), as well as the dispersion of the frequency to lower energy. This trend towards lower energy was continuous in the adamantyl polyyne series with no indication of saturation by the length of the decayne. This analysis will provide insight into whether the stretching frequency resembles that of a cumulenic structure or saturates before, as seen in the X-ray crystallographic analysis of the *t*-butyl polyyne series.

A study that would undoubtedly support the violation of the mutual exclusion seen in the adamantyl polyyne series would involve the synthesis of polyynes that are statically bent. This has been achieved where a series of cyclic tetraynes, in which the termini are tethered by an alkyl chain linker, were synthesized (**1a-e**, Figure 6-1a).[1] Raman spectroscopic analyses have been done on these molecules and the preliminary results conclude that there is a Raman band seen in the IR for the noncentrosymmetric structure. This corresponds closely to that seen in the linear adamantyl polyynes, supporting that the violation of mutual exclusion is due to a bending of the polyyne. Further analysis of longer bent polyynes (**2**), such as that shown in Figure 6-1b, would provide further evidence as there should be a shift to lower frequency for the Raman signal.

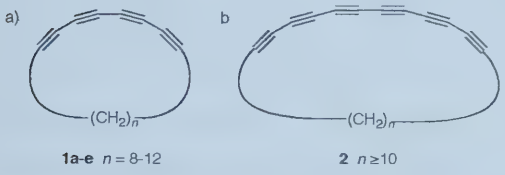


**Figure 6-1.** Structures of a) previously synthesized bent tetraynes (**1**) and b) proposed hexayne targets (**2**) using various lengths of alkyl linker.

Over the past few decades, the development of new procedures has allowed for the now rather routine synthesis of polyynes up to 10 triple bonds.[2] There are, however, only a few examples of polyynes synthesized beyond 10 triple bonds,[3-8] which seems to be a common limit when using currently reported procedures. The next challenge is to develop new procedures, or optimize old ones, in order to obtain polyynes beyond 10 triple bonds efficiently. Although the modified Eglinton-Glaser-Hay[9-13] approach shown in Chapter 5 works well and produces the desired products in decent yields, an excess of the TIPS polyyne coupling partner is required. One of the major drawbacks to this method is that the homocoupling pathway is just as competitive, leading to unwanted symmetrical polyyne products and making purification difficult in some cases. A more efficient crosscoupling protocol could alleviate this problem. Perhaps optimization of either the Negishi[14,15] or the Sonogashira[16,17] conditions shown in Chapter 5, through rigorous

catalyst screening, could provide for the desired unsymmetrical polyynes (up to $n$ = 15) more efficiently (Equation 1).

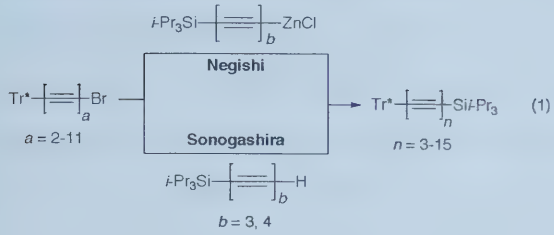


(1)

The synthesis of symmetrical odd numbered polyynes (i.e., $n$ = 3, 5, 7, etc.) is a field that has yet to be explored sufficiently, with only a handful of heptaynes[7,8,18-20] and only two intended syntheses of a nonayne.[7] The ability to make triynes, and even pentaynes, is a fairly well developed area, where the FBW rearrangement,[21-24] as well as crosscoupling methods,[14,25] are applicable. These routes are not feasible, as of yet anyway, towards the synthesis of odd numbered polyynes beyond the pentayne. If a practical route towards these molecules were developed, the physical properties of these molecules could be compared to their symmetrical cousins. If the Negishi or Sonogashira crosscoupling chemistry described above can be developed into a viable route towards unsymmetrical polyynes, then this should also be exploited in order to access symmetrical odd numbered polyynes ($n$ = 7, 9, 11, etc.) as shown in equation 2.

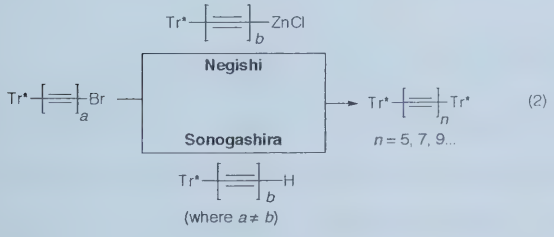


(2)

A somewhat obvious avenue that could be explored with respect to polyynes is the altering of the electronics. The most obvious way to do this is to incorporate aryl groups

substituted with electron donating (EDG) or electron withdrawing groups (EWG) at the termini of the polyyne chain, resulting in "push-pull" systems. This would lead to "molecular wires" that might demonstrate charge transfer characteristics; potentially useful in optoelectronic devices. Phenyl-endcapped derivatives up to decaynes have been synthesized, however, poor stability has been reported for the longer derivatives.[6,26] In order to make this idea feasible, stability needs to be engineered into the system or the polyyne core needs to be protected. Two ways to protect the polyyne core are to bulk up the endgroup[27] or through encapsulation.[19,28-30] The formation of rotaxanes is an obvious way to encapsulate the polyyne core (Figure 6-2). There have been reports of the formation of polyynes within macrocycles, resulting in polyyne rotaxanes.[31,32] The macrocycle sheath would act to protect the reactive polyyne core while the endgroup functionality would tune the electronics of the polyyne.

**Figure 6-2.** Generic encapsulation of an aryl-endcapped polyyne functionalized with electron donating groups (EDG) and electron withdrawing groups (EWG) as well as bulky groups to keep rotaxane from slipping off.

As a final thought, what if polyynes were not sought solely as a final target, but as an advanced intermediate towards other highly conjugated materials? The chemistry of alkynes has been studied thoroughly, but polyynes, on the other hand, remain a relatively untouched area. A question still remains: where does the electron density reside in a polyyne, at the central triple bond or somewhere else? Preliminary studies have been done where a [4+2] cycloaddition reaction have been carried out on bis(adamantyl)pentayne with tetraphenylcyclopentadieneone to probe the regiochemistry of this Diels-Alder reaction (Equation 3). The results suggest that the central triple bond (blue) may in fact be less reactive than the other triple bonds, where a 1:3 ratio

of products **A**:**B** was formed. Interestingly, a small amount of product **C** was also observed, which would result from a second [4+2] addition on compound **B**. Further studies are required, such as varying the lengths of the polyynes, as well as the stoichiometry of reagents, in order to gain further insight into these results.

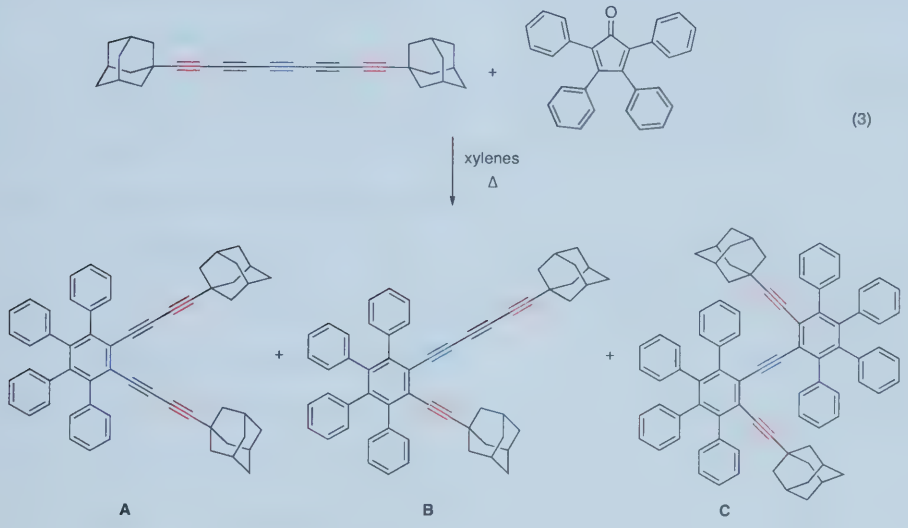


(3)

As one can clearly see, the synthesis of polyynes does not only need be treated as a final objective. Probing the reactivity of polyynes may allow for the formation of highly conjugated materials, such as compounds **A**-**C**, and lead to the discovery of new and interesting materials.

## 6.1 References


[1] Spantulescu, A.; Luu, T.; Zhao, Y.; McDonald, R.; Tykwinski, R. R. *Org. Lett.* **2008**, *10*, 609.

[2] Chalifoux, W. A.; Tykwinski, R. R. *C. R. Chimie* **2009**, *12*, 341.

[3] Zheng, Q.; Bohling, J. C.; Peters, T. B.; Frisch, A. C.; Hampel, F.; Gladysz, J. A. *Chem. Eur. J.* **2006**, *12*, 6486.

[4] Simpkins, S. M. E.; Weller, M. D.; Cox, L. R. *Chem. Comm.* **2007**, 4035.

[5] Mohr, W.; Stahl, J.; Hampel, F.; Gladysz, J. A. *Chem. Eur. J.* **2003**, *9*, 3324.

[6] Johnson, T. R.; Walton, D. R. M. *Tetrahedron* **1972**, *28*, 5221.

[7] Eastmond, R.; Johnson, T. R.; Walton, D. R. M. *Tetrahedron* **1972**, *28*, 4601.

[8] Bruce, M. I.; Zaitseva, N. N.; Nicholson, B. K.; Skelton, B. W.; White, A. H. *J. Organomet. Chem.* **2008**, *693*, 2887.

[9] Hay, A. S. *J. Org. Chem.* **1962**, *27*, 3320.

[10] Glaser, C. *Ann. Chem.* **1870**, *154*, 137.

[11] Glaser, C. *Ber. Dtsch. Chem. Ges.* **1869**, *2*, 422.

[12] Eglinton, G.; Galbraith, A. R. *Chem. Ind. (London)* **1956**, 737.

[13] Siemsen, P.; Livingston, R. C.; Diederich, F. *Angew. Chem. Int. Ed.* **2000**, *39*, 2632.

[14] Métay, E.; Hu, Q.; Negishi, E.-i. *Org. Lett.* **2006**, *8*, 5773.

[15] Hoheisel, T. N.; Frauenrath, H. *Org. Lett.* **2008**, *10*, 4525.

[16] Sonogashira, K. In *Handbook of Organopalladium Chemistry for Organic Synthesis*; Negishi, E.-i., Ed; Wiley: New York, 2002; pp 493.

[17] Sonogashira, K. *J. Organomet. Chem.* **2002**, *653*, 46.

[18] Bohlmann, F. *Chem. Ber.* **1953**, *86*, 657.

[19] Klinger, C.; Vostrowsky, O.; Hirsch, A. *Eur. J. Org. Chem.* **2006**, 1508.

[20] Antonova, A. B.; Bruce, M. I.; Ellis, B. G.; Gaudio, M.; Humphrey, P. A.; Jevric, M.; Melino, G.; Nicholson, B. K.; Perkins, G. J.; Skelton, B. W.; Stapleton, B.; White, A. H.; Zaitseva, N. N. *Chem. Comm.* **2004**, 960.

[21] Lucotti, A.; Tommasini, M.; Fazzi, D.; Del Zoppo, M.; Chalifoux, W. A.; Ferguson, M. J.; Zerbi, G.; Tykwinski, R. R. *J. Am. Chem. Soc.* **2009**, *131*, 4239.

[22] Eisler, S.; Slepkov, A. D.; Elliott, E.; Luu, T.; McDonald, R.; Hegmann, F. A.; Tykwinski, R. R. *J. Am. Chem. Soc.* **2005**, *127*, 2666.

[23] Eisler, S.; Chahal, N.; McDonald, R.; Tykwinski, R. R. *Chem. Eur. J.* **2003**, *9*, 2542.

[24] Chalifoux, W. A.; McDonald, R.; Ferguson, M. J.; Tykwinski, R. R. *Angew. Chem. Int. Ed.* **2009**, *48*, 7915.

[25] Dembinski, R.; Bartik, T.; Bartik, B.; Jaeger, M.; Gladysz, J. A. *J. Am. Chem. Soc.* **2000**, *122*, 810.

[26] Luu, T.; Elliott, E.; Slepkov, A. D.; Eisler, S.; McDonald, R.; Hegmann, F. A.; Tykwinski, R. R. *Org. Lett.* **2005**, *7*, 51.

[27] Gibtner, T.; Hampel, F.; Gisselbrecht, J.-P.; Hirsch, A. *Chem. Eur. J.* **2002**, *8*, 408.

[28] Sugiyama, J.; Tomita, I. *Eur. J. Org. Chem.* **2007**, 4651.

[29] Stahl, J.; Mohr, W.; de Quadras, L.; Peters, T. B.; Bohling, J. C.; Martín-Alvarez, J. M.; Owen, G. R.; Hampel, F.; Gladysz, J. A. *J. Am. Chem. Soc.* **2007**, *129*, 8282.

[30] de Quadras, L.; Bauer, E. B.; Mohr, W.; Bohling, J. C.; Peters, T. B.; Martín-Alvarez, J. M.; Hampel, F.; Gladysz, J. A. *J. Am. Chem. Soc.* **2007**, *129*, 8296.

[31] Sato, Y.; Yamasaki, R.; Saito, S. *Angew. Chem. Int. Ed.* **2009**, *48*, 504.

[32] Berná, J. é.; Goldup, S. M.; Lee, A.-L.; Leigh, D. A.; Symes, M. D.; Teobaldi, G.; Zerbetto, F. *Angew. Chem. Int. Ed.* **2008**, *47*, 4392.

# Chapter 7 Experimental Section

**General procedures and methods:** Reagents were purchased reagent grade from commercial suppliers and used without further purification. THF, benzene, toluene and $Et_2O$ were distilled from sodium/benzophenone. Hexanes and $CH_2Cl_2$ were distilled from $CaH_2$. Evaporation and concentration in vacuo was done at $H_2O$-aspirator pressure. Where appropriate, reactions were performed in standard, dry glassware under an inert atmosphere of $N_2$. Column chromatography: Silica gel 60 (230–400 mesh) from Rose Scientific Ltd. Thin-layer chromatography (TLC): aluminum sheets covered with silica gel 60 $F_{254}$ from Macherey-Nagel; visualization by UV light, $KMnO_4$ stain, or phosphomolybdic acid (PMA) stain. Mp: Gallenkamp apparatus; uncorrected. IR spectra ($cm^{-1}$): Nicolet Magna 750 FTIR (neat liquids and cast films) or Nic-Plan FTIR Microscope (neat liquids, solids and cast films). $^1H$ and $^{13}C$ NMR: Varian Inova 300, 400 and 500, Varian Mercury 400, or Varian Unity 500 at rt in $CDCl_3$; solvent peaks (7.24 ppm for $^1H$ and 77.0 ppm for $^{13}C$, respectively) as reference. EI MS: Kratos MS50 instrument. MALDI MS: Voyager Elite MALDI or Bruker 9.4T Apex-Qe FTICR; matrix employed was trans-2-[3-{4-*tert*-butylphenyl}-2-methyl-2-propenylidene]malononitrile (DCTB): APPI MS: Agilent 6220 Accurate-Mass TOF with APPI source. Elemental analyses were carried out by the Microanalytical Laboratory at the University of Alberta.

UV-visible spectra were acquired at ambient temperature; $\lambda$ in nm ($\varepsilon$ in $L \cdot mol^{-1} \cdot cm^{-1}$).

Differential scanning calorimetry (DSC) measurements were carried out under a flow of nitrogen with a heating rate of 10 °C/min using a *Perkin Elmer Pyris 1 Differential Scanning Calorimeter*. Melting points from DSC analysis are reported as the peak maxima, except in cases when the sample decomposed, in which case the onset temperature of the decomposition exothermic peak is reported, as well as the exothermic maxima corresponding to the decomposition.

Solution and solid-state Raman spectra were recorded with a Nicolet NXR9650 FT-Raman (resolution 4 $cm^{-1}$) equipped with a InGaAs detector and a Nd:$YVO_4$ laser providing a 1064 nm excitation line.

**X-ray Crystallography:** Unit cell parameters and intensity data were obtained on a Bruker PLATFORM/SMART 1000 CCD diffractometer or a Bruker D8/APEX II CCD using graphite-monochromated Mo K$\alpha$ radiation (0.71073 Å). Programs for diffractometer operation, data collection, data reduction and absorption correction were those supplied by Bruker. The structures were solved by direct methods using SHELXS-97[1] and SHELXS-86,[2] and refined by full-matrix least squares on $F^2$ using SHELXS-97[1] and SHELXL-93.[3] Crystallographic data for unpublished

compounds is available from the X-ray Crystallographic Laboratory, Department of Chemistry, University of Alberta. Data for published compounds can be obtained free of charge from The Cambridge Crystallographic Data Centre via www.ccdc.cam.ac.uk/data_request/cif by quoting the CCDC No. shown in the experimental write-up.

## 7.1 TBPS-Endcapped Polyynes (Chapter 2 data)

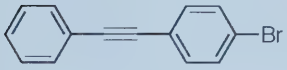


2.1

**Bromotolan (2.1) was synthesized as previously reported:**[4] Yield = 85%. Spectroscopic data is consistent with that reported.

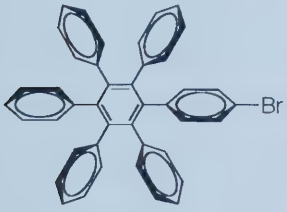


2.2

**Bromo-HPB (2.2) was synthesized as previously reported:**[4] Yield = 99%. Spectroscopic data is consistent with that reported.

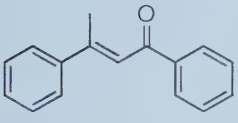


2.3

**Dypnone (2.3) was synthesized as previously reported.**[5] Yield = 36% (based on recovered starting material)

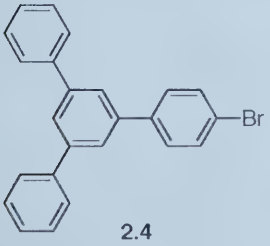


2.4

**Bromotriphenylbenzene (2.4) was synthesized as previously reported:**[6] Yield = 87%. Spectroscopic data is consistent with that reported.

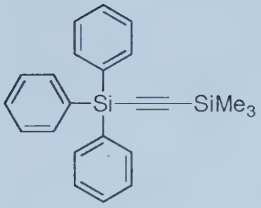


2.5

**2-(TMS)-1-(TPS)ethyne (2.5):**[7] To a solution of iodobenzene (5.34 g, 2.93 mL, 26.2 mmol) in $Et_2O$ (20 mL) cooled to –78 °C under a $N_2$ atmosphere was added BuLi (18 mL, 1.6M in hexanes, 29 mmol). The solution was warmed to 0 °C and added slowly, via cannula, to a solution of $SiCl_4$ (1.483 g, 1.000 mL, 8.729 mmol) in $Et_2O$ (10 mL) cooled to 0 °C under a $N_2$ atmosphere. The mixture was warmed to rt and stirred for 1.5 h. Lithiated trimethylsilylacetylene was then added (see below for details) and the resulting mixture stirred at rt under a $N_2$ atmosphere for 22 h. The reaction was cooled to 0 °C and quenched with saturated aqueous $NH_4Cl$ (20 mL). The mixture was warmed to rt and the resulting layers separated. The organic phase was washed with $H_2O$ (10 mL), brine (10 mL), and dried over $MgSO_4$. The solvent was removed in vacuo and the crude product purified by column chromatograpy (silica gel, hexanes) to yield **2.5** (2.318 g, 74%) as a pale yellow oil.

**Lithiated trimethylsilylacetylene:** To a solution of trimethylsilylacetylene (1.28 g, 1.85 mL, 13.1 mmol) in $Et_2O$ (15 mL) cooled to –78 °C under a $N_2$ atmosphere was added BuLi (8.2 mL, 2.5M in hexanes, 13 mmol), the mixture stirred for 10 min.

**Data for 2.5:** $R_f$ = 0.42 ($CH_2Cl_2$/hexanes 1:4); IR (microscope) 3069, 3050, 3023, 3000, 2959, 2899, 1589, 1429, 1251, 1114 $cm^{-1}$; $^1H$ NMR (400 MHz, $CDCl_3$): $\delta$ 7.80-7.76 (m, 6H), 7.54-7.45 (m, 9H), 0.38 (s, 9H); $^{13}C$ NMR (100 MHz, $CDCl_3$): $\delta$ 135.5, 133.4, 129.8, 127.9, 119.5, 108.0, 0.0; EI HRMS *m/z* calcd. for $C_{23}H_{24}Si_2$ ($M^+$) 356.1417, found 356.1412.

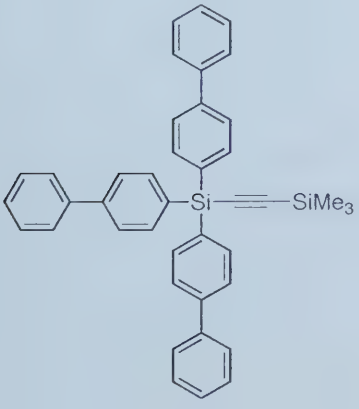


2.6

**1-(TBPS)-2-(TMS)ethyne (2.6):** To a solution of 4-iodobiphenyl (4.279 g, 15.27 mmol) in dry $Et_2O$ (50 mL) at –78 °C under a $N_2$ atmosphere was added dropwise BuLi (7.3 mL, 2.5M in hexanes, 18 mmol) and the solution was warmed to 0 °C. This solution was added to a solution of $SiCl_4$ (0.742 g, 0.500 mL, 4.37 mmol) in dry $Et_2O$ (10 mL) via cannula and the mixture was warmed to rt (solution A). Concurrently, to a solution of TMS acetylene (1.28 g, 1.84 mL, 13.1 mmol) in dry $Et_2O$ (10 mL) at –78 °C was added dropwise BuLi (5.2 mL, 2.5M in hexanes, 13 mmol) and the reaction mixture was warmed to 0 °C (solution B). Solution B was added to solution A via cannula and allowed to stir under a $N_2$ atmosphere at rt for 7 h. The reaction was quenched with saturated aqueous $NH_4Cl$ (5 mL) and $H_2O$ was then added to dissolve the inorganic salts. The organic layer was washed with brine and dried over $MgSO_4$. The crude product was purified by column chromatography (silica gel, $CH_2Cl_2$/hexanes 1:4) to yield **2.6** (1.95 g, 76%) as a white solid: Mp 142–144 °C; $R_f$ = 0.49 ($CH_2Cl_2$/hexanes 1:4); IR (microscope) 3024, 2955, 1597, 1386, 1248, 1116 $cm^{-1}$; $^1H$ NMR (500 MHz, $CDCl_3$): $\delta$ 7.81 (d, $^3J$ = 7.8 Hz, 6H), 7.66 (d, $^3J$ = 7.8 Hz, 6H), 7.64 (d, $^3J$ = 8.0 Hz, 6H), 7.46 (t, $^3J$ = 7.4 Hz, 6H), 7.37 (t, $^3J$ = 7.2 Hz, 3H), 0.31 (s, 9H); $^{13}C$ NMR (125 MHz, $CDCl_3$): $\delta$ 142.7, 140.9, 136.1, 132.1, 128.8, 127.5, 127.2, 126.8, 120.0, 107.8, –0.1; EI HRMS *m/z* calcd. for $C_{41}H_{36}Si_2$ ($M^+$) 584.2355, found 584.2346; Anal. calcd. for $C_{41}H_{36}Si_2$: C, 84.19; H, 6.20. Found: C, 84.22; H, 6.32.

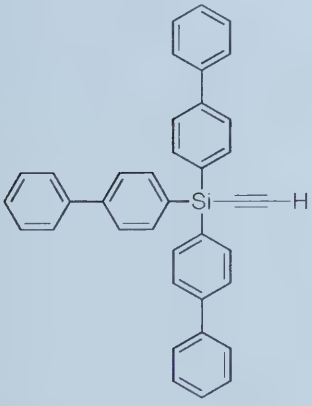


2.7

**TBPS acetylene (2.7):** A solution of **2.6** (2.143 g, 3.664 mmol) in a 1:1 mixture of THF (15 mL) and MeOH (15 mL) was cooled to 0 °C and $K_2CO_3$ (0.506 g, 3.66 mmol) was added. After stirring at 0 °C for 1 h, $H_2O$ (10 mL) was added and the mixture extracted with $Et_2O$ (100 mL). The organic layer was washed with brine and dried over $MgSO_4$. The crude product was purified by column chromatography (silica, $CH_2Cl_2$/hexanes 1:2) to yield **2.7** (1.601 g, 85%) as a white solid: Mp 172–175 °C; $R_f$ = 0.46 ($CH_2Cl_2$/hexanes 1:2); IR ($CH_2Cl_2$, cast film) 3267, 3024, 2035, 1596, 1117 $cm^{-1}$; $^1H$ NMR (400 MHz, $CDCl_3$): $\delta$ 7.79 (d, $^3J$ = 8.1 Hz, 6H), 7.64 (d, $^3J$ = 7.9 Hz, 6H), 7.60 (d, $^3J$ = 7.5 Hz, 6H), 7.44 (t, $^3J$ = 7.5 Hz, 6H), 7.35 (t, $^3J$ = 7.3 Hz, 3H), 2.85 (s, 1H); $^{13}C$

NMR (125 MHz, $CDCl_3$): $\delta$ 142.9, 140.8, 136.0, 131.4, 128.8, 127.6, 127.2, 126.9, 98.1, 85.3; EI HRMS *m/z* calcd. for $C_{38}H_{28}Si$ ($M^+$) 512.1960, found 512.1958; Anal. calcd. for $C_{38}H_{28}Si$: C, 89.02; H, 5.50. Found: C, 88.76; H, 5.74.

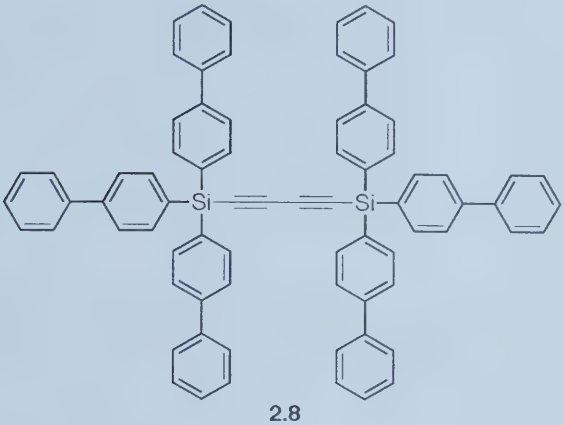


**2.8**

**1,4-Bis(TBPS)buta-1,3-diyne (2.8):** To a mixture of $PdCl_2(PPh_3)_2$ (10 mg, 0.016 mmol), CuI (3 mg, 0.02 mmol) and $Et_3N$ (95 mg, 0.13 mL, 0.94 mmol) was added **2.7** (200 mg, 0.390 mmol) in THF (5 mL). Ethyl bromoacetate (65 mg, 43 μL, 0.39 mmol) was added and the mixture stirred for 24 h at rt under a $N_2$ atmosphere. $H_2O$ (5 mL) was added and the resulting mixture extracted with $CH_2Cl_2$ (2 × 20 mL). The organic layers were combined, washed with brine and dried over $MgSO_4$. The resulting solution was concentrated under vacuum. $Et_2O$ was added to the crude product, which formed a precipitate. The mixture was filtered and the solid washed with $Et_2O$ to give **2.8** (0.156 g, 77%) as a white solid: Mp 296–298 °C; $R_f$ = 0.43 ($CH_2Cl_2$/hexanes 1:2); IR (microscope): 3024, 2068, 1595, 1385, 1115 $cm^{-1}$; $^1H$ NMR (400 MHz, $CDCl_3$): $\delta$ 7.78 (d, $^3J$ = 7.9 Hz, 12H), 7.65 (d, $^3J$ = 7.9 Hz, 12H), 7.60 (d, $^3J$ = 7.5 Hz, 12H), 7.43 (t, $^3J$ = 7.6 Hz, 12H), 7.34 (t, $^3J$ = 7.3 Hz, 6H); $^{13}C$ NMR (125 MHz, $CDCl_3$): $\delta$ 143.1, 140.8, 136.1, 130.9, 128.8, 127.7, 127.2, 127.0, 92.3, 82.4; MALDI MS (DCTB) *m/z* 1272.5 ([M + Matrix]$^+$, 100), 1022.4 ($M^+$, 30); DSC: Mp = 312 °C; decomposition, 340 °C (onset) and 389 °C (peak).

**X-ray Crystal Data for 2.8**: Single crystals of **2.8** suitable for X-ray crystallographic analysis were grown by slow evaporation of a solution of **2.8** in $CH_2Cl_2$/toluene (1:9). $C_{54}H_{36}Si_2$, $M_r$ = 1023.4; crystal dimensions: 0.54 × 0.34 × 0.28 $mm^3$; crystal system: monoclinic; space group $P2_1/c$ (No. 14), $a$ = 10.647 (2), $b$ = 22.251 (4), $c$ = 14.926 (3) Å; $\beta$ = 107.929 (3)°; $V$ = 3364.2 (11) Å$^3$, $Z$ = 2; $\rho_{calcd}$ = 1.192 g $cm^{-3}$; $\mu$ = 0.101 $mm^{-1}$; $\lambda$ = 0.71073 Å; T = –80 °C; 2$\theta$ max = 50.00°; total data collected = 22379; $R_1$ = 0.0645 for 3650 observed reflections with [$F_o^2 \geq 2\sigma(F_o^2)$]; $wR_2$ = 0.1701 for 352 variables and 5924 unique reflections with [$F_o^2 \geq -3\sigma(F_o^2)$]; residual electron density = 0.588 and –0.265 e Å$^{-3}$. CCDC 623034.

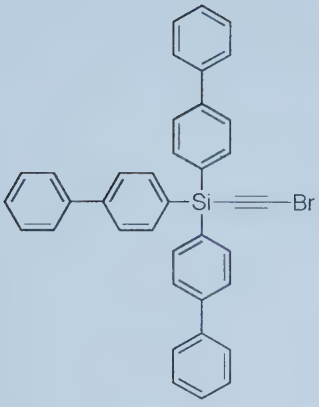


2.9

**1-Bromo-2-(TBPS)ethyne (2.9):** To a solution of **2.6** (163 mg, 0.279 mmol) and *N*-bromosuccinimide (58 mg, 0.33 mmol) in acetone (10 mL) was added $AgNO_3$ (5 mg, 0.03 mmol). The mixture was stirred for 30 min at rt under a $N_2$ atmosphere. $H_2O$ (5 mL) was added and the resulting mixture extracted with hexanes (2 × 20 mL). The organic layers were combined, washed with brine and dried over $MgSO_4$. The crude product was purified by column chromatography (silica, $CH_2Cl_2$/hexanes 1:2) to yield **2.9** (143 mg, 87%) as a white solid: Mp 166–168 °C; $R_f$ = 0.61 ($CH_2Cl_2$/hexanes 1:2); IR ($CH_2Cl_2$, cast film): 3060, 3025, 2122, 1596, 1386, 1117 $cm^{-1}$; $^1H$ NMR (500 MHz, $CDCl_3$): $\delta$ 7.78 (d, $^3J$ = 8.0 Hz, 6H), 7.65 (d, $^3J$ = 8.0 Hz, 6H), 7.62 (d, $^3J$ = 7.5 Hz, 6H), 7.45 (t, $^3J$ = 7.7 Hz, 6H), 7.36 (t, $^3J$ = 7.4 Hz, 3H); $^{13}C$ NMR (125 MHz, $CDCl_3$): $\delta$ 143.0, 140.8, 136.0, 131.4, 128.8, 127.6, 127.2, 126.9, 82.5, 67.2; EI HRMS *m/z* calcd. for $C_{38}H_{27}Si^{81}Br$ ($M^+$) 592.1045, found 592.1048; Anal. calcd. for $C_{38}H_{27}SiBr$: C, 77.15; H, 4.60. Found: C, 77.40; H, 4.67.

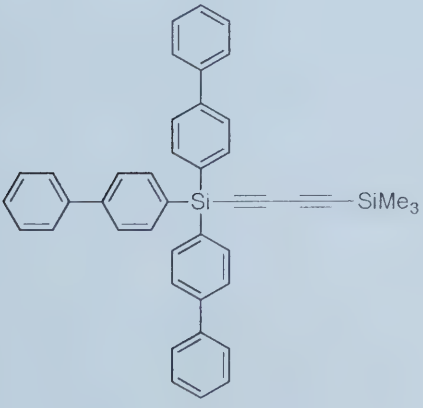


2.10

**1-(TBPS)-4-(TMS)-buta-1,3-diyne (2.10):** To a mixture of **2.9** (208 mg, 0.352 mmol) and TMS acetylene (70 mg, 0.10 mL, 0.71 mmol) in THF (5 mL) was added $PdCl_2(PPh_3)_2$ (12 mg, 0.018 mmol), CuI (3 mg, 0.02 mmol) and *i*-$Pr_2NH$ (0.18 g, 0.25 mL, 1.8 mmol) in that order. The mixture was stirred for 2 h at rt under a $N_2$ atmosphere. $H_2O$ (5 mL) was added and the resulting mixture was extracted with $Et_2O$ (2 × 20 mL). The organic layers were combined, washed with brine and dried over $MgSO_4$. The crude product was purified by column chromatography (silica gel, EtOAc/hexanes 1:10) to give **2.10** (96 mg, 45%) as a white solid: Mp 222–223 °C; $R_f$ = 0.55 ($CH_2Cl_2$/hexanes 1:2); IR (microscope): 3073, 3025, 2961, 2070, 1597, 1386, 1253, 1118 $cm^{-1}$; $^1H$ NMR (400 MHz, $CDCl_3$): $\delta$ 7.76 (d, $^3J$ = 8.1 Hz, 6H), 7.63 (d, $^3J$ = 8.1 Hz, 6H), 7.60 (d, $^3J$ = 7.4 Hz, 6H), 7.44 (t, $^3J$ = 7.6 Hz, 6H), 7.35 (t, $^3J$ = 7.3 Hz, 3H), 0.22 (s, 9H); $^{13}C$ NMR (125 MHz, $CDCl_3$): $\delta$ 143.0, 140.8, 136.1, 131.1, 128.8, 127.6, 127.2, 126.9, 92.4, 88.1, 87.8, 80.5, –0.5; EI HRMS *m/z* calcd. for $C_{43}H_{36}Si_2$ ($M^+$) 608.2355, found 608.2360.

**X-ray Crystal Data for 2.10**: Single crystals of **2.10** suitable for X-ray crystallographic analysis were grown by slow diffusion of MeOH into a solution of **2.10** in $CHCl_3$. $C_{43}H_{36}Si_2$, $M_r$ = 608.9; crystal dimensions: 0.46 × 0.29 × 0.14 $mm^3$; crystal system: monoclinic; space group *C*2/*c* (No. 15), *a* = 24.562 (3), *b* = 12.3329 (12), *c* = 24.149 (2) Å; $\beta$ = 95.7804 (16)°; *V* = 7278.0 (13) $Å^3$, *Z* = 8; $\rho$calcd = 1.220 g $cm^{-3}$; $\mu$ = 0.237 $mm^{-1}$; $\lambda$ = 0.71073 Å; T = –80 °C; 2$\theta$ max = 51.40°; total data collected = 25705; $R_1$ = 0.0503 for 5181 observed reflections with [$F_o^2 \geq 2\sigma(F_o^2)$]; $wR_2$ = 0.1356 for 442 variables and 6909 unique reflections with [$F_o^2 \geq -3\sigma(F_o^2)$]; residual electron density = 0.413 and –0.384 e $Å^{-3}$.

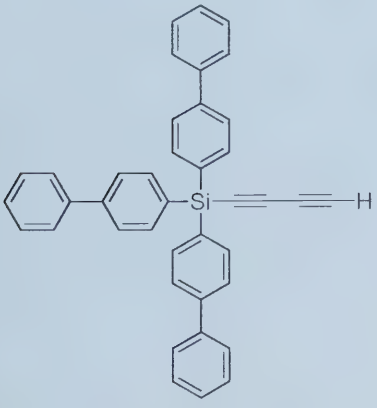


**2.13**

**1-(TBPS)-buta-1,3-diyne (2.13):** A solution of **2.10** (31 mg, 0.051 mmol) in a 1:1 mixture of THF (5 mL) and MeOH (5 mL) was cooled to 0 °C and $NaHCO_3$ (21 mg, 0.25 mmol) was added. After stirring at 0 °C for 28 h, $H_2O$ (10 mL) was added and the mixture extracted with hexanes (2 × 30 mL). The organic layer was washed with brine and dried over $MgSO_4$. The crude product

was purified by column chromatography (silica, $CH_2Cl_2$/hexanes 1:3) to yield **2.13** (25 mg, 93%) as a colorless oil: $R_f$ = 0.50 ($CH_2Cl_2$/hexanes 1:2); IR ($CH_2Cl_2$, cast film) 3272, 3024, 2188, 2035, 1596, 1116 $cm^{-1}$; $^1H$ NMR (500 MHz, $CDCl_3$): $\delta$ 7.78 (d, $^3J$ = 8.0 Hz, 6H), 7.66 (d, $^3J$ = 7.9 Hz, 6H), 7.62 (d, $^3J$ = 7.6 Hz, 6H), 7.45 (t, $^3J$ = 7.6 Hz, 6H), 7.37 (t, $^3J$ = 7.3 Hz, 3H), 2.25 (s, 1H); $^{13}C$ NMR (125 MHz, $CDCl_3$): $\delta$ 143.1, 140.8, 136.1, 130.8, 128.8, 127.7, 127.2, 126.9, 91.7, 79.6, 68.4, 68.2; EI HRMS *m/z* calcd. for $C_{40}H_{28}Si$ ($M^+$) 536.1960, found 536.1989.

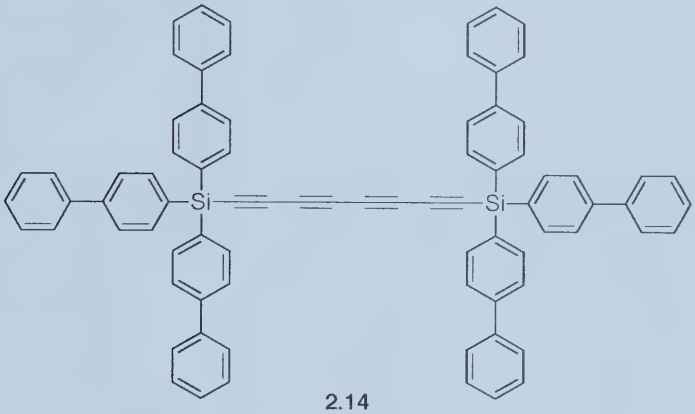


2.14

**1,8-Bis(TBPS)octa-1,3,5,7-tetrayne (2.14):** To a mixture of CuCl (4 mg, 0.05 mmol) in $CH_2Cl_2$ (5 mL) was added TMEDA (10 mg, 14 μL, 0.090 mmol). $O_2$ was bubbled through the solution for 5 min and a solution of **2.13** (24 mg, 0.045 mmol) in $CH_2Cl_2$ (1 mL) was added and stirred for 5 min. The reaction mixture was passed through a plug of silica gel with $CH_2Cl_2$ and then concentrated under vacuum to give **2.14** (20 mg, 83%) as a yellow solid: Mp 273–275 °C; $R_f$ = 0.43 ($CH_2Cl_2$/hexanes 1:2); IR (microscope): 3071, 3024, 2041, 1595, 1386, 1115 $cm^{-1}$; $^1H$ NMR (400 MHz, $CDCl_3$): $\delta$ 7.76 (d, $^3J$ = 8.0 Hz, 12H), 7.66 (d, $^3J$ = 8.0 Hz, 12H), 7.61 (d, $^3J$ = 7.5 Hz, 12H), 7.45 (t, $^3J$ = 7.6 Hz, 12H), 7.36 (t, $^3J$ = 7.3 Hz, 6H); $^{13}C$ NMR (100 MHz, $CDCl_3$): $\delta$ 143.3, 140.7, 136.1, 130.4, 128.8, 127.7, 127.2, 127.0, 91.8, 83.3, 63.5, 62.9; MALDI MS (DCTB) *m/z* 1321.6 ($[M + Matrix + H]^+$, 100).

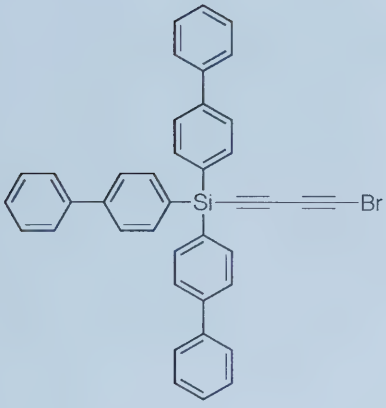


2.15

**1-Bromo-4-(TBPS)-buta-1,3-diyne (2.15):** A solution of **2.10** (28 mg, 0.046 mmol) and *N*-bromosuccinimide (18 mg, 0.10 mmol) in acetone (5 mL) was cooled to 0 °C and $AgNO_3$ (5 mg, 0.03 mmol) was added. The mixture was stirred for 24 h at 0 °C under a $N_2$ atmosphere. $H_2O$ (10 mL) was added and the resulting mixture extracted with hexanes (2 × 20 mL). The organic layers were combined, washed with brine and dried over $MgSO_4$. The crude product was purified by column chromatography (silica, EtOAc/hexanes 1:10) to yield **2.15** (27 mg, 96%) as a pale yellow oil: $R_f$ = 0.49 ($CH_2Cl_2$/hexanes 1:2); IR ($CH_2Cl_2$, cast film): 3057, 3024, 2247, 2179, 2093, 1596, 1117 $cm^{-1}$; $^1H$ NMR (400 MHz, $CDCl_3$): $\delta$ 7.77 (d, $^3J$ = 7.9 Hz, 6H), 7.65 (d, $^3J$ = 8.0 Hz, 6H), 7.62 (d, $^3J$ = 7.5 Hz, 6H), 7.45 (t, $^3J$ = 7.5 Hz, 6H), 7.36 (t, $^3J$ = 7.3 Hz, 3H); $^{13}C$ NMR (100 MHz, $CDCl_3$): $\delta$ 143.1, 140.8, 136.1, 130.9, 128.8, 127.7, 127.2, 126.9, 92.4, 78.3, 66.1, 42.4; EI HRMS *m/z* 487.2 ($[M - C_4Br]^+$, 100).

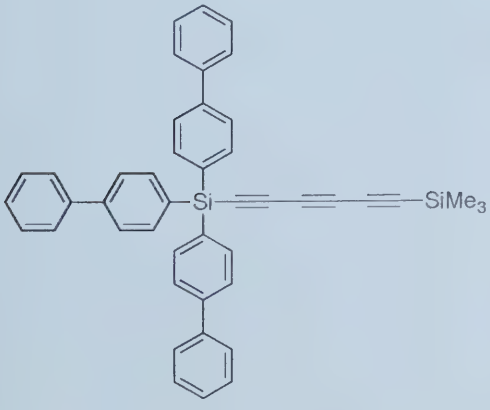


2.16

**1-(TBPS)-6-(TMS)hexa-1,3,5-triyne (2.16):** To a mixture of **2.15** (141 mg, 0.229 mmol) and TMS acetylene (112 mg, 161 µL, 1.14 mmol) in THF (25 mL) was added $PdCl_2(PPh_3)_2$ (8 mg,

0.01 mmol), CuI (2 mg, 0.01 mmol) and *i*-$Pr_2NH$ (116 mg, 161 μL, 1.15 mmol) in that order. The mixture was stirred for 18 h at rt under a $N_2$ atmosphere. The reaction mixture was concentrated to ~ 5 mL then co-evaporated with $CH_2Cl_2$ (2 × 30 mL). The crude product was purified by column chromatography (silica gel, $CH_2Cl_2$/hexanes 1:4) to give **2.16** (58 mg, 40%) as a yellow solid: Mp 142–144 °C; $R_f$ = 0.34 ($CH_2Cl_2$/hexanes 1:4); IR (microscope): 3060, 3025, 2960, 2160, 2068, 1597, 1386, 1245, 1114 $cm^{-1}$; $^1H$ NMR (500 MHz, $CDCl_3$): $\delta$ 7.78 (d, $^3J$ = 8.0 Hz, 6H), 7.65 (d, $^3J$ = 8.2 Hz, 6H), 7.61 (d, $^3J$ = 7.3 Hz, 6H), 7.45 (t, $^3J$ = 7.6 Hz, 6H), 7.36 (t, $^3J$ = 7.4 Hz, 3H), 0.21 (s, 9H); $^{13}C$ NMR (125 MHz, $CDCl_3$): $\delta$ 143.2, 140.7, 136.1, 130.7, 128.8, 127.7, 127.2, 127.0, 92.2, 88.7, 87.7, 82.1, 63.5, 61.9, –0.6; EI HRMS *m/z* calcd. for $C_{45}H_{36}Si_2$ ($M^+$) 632.2355, found 632.2348.

## 7.2 Adamantyl-Endcapped Polyynes (Chapter 3 data)

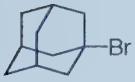


3.4

**1-Bromoadamantane (3.4) was synthesized as previously reported[8] (Yield = 76%), or purchased from Aldrich.** CAS: 768-90-1

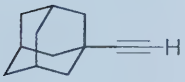


3.2

**1-Ethynyladamantane (3.2) was synthesized as previously reported:**[9] Yield = 82%. Spectroscopic data is consistent with that reported.[10] CAS: 40430-66-8

**Alternate procedure used for the synthesis of 3.2:**

**Part A:** A mixture of 1-bromoadamantane **3.4** (46.5 g, 0.216 mol) and vinyl bromide (90 mL, 1.30 mol) was cooled to –78 °C under a $N_2$ atmosphere (Note: flask was pre-cooled as vinyl bromide is very volatile). $AlCl_3$ (7.20 g, 0.0540 mol) was added in small portions. The mixture was stirred for 2 h at –78 °C, warmed to –40 °C, stirred for 30 min and finally warmed to –10 °C and stirred for 15 min (Note: **VERY EXOTHERMIC**). The reaction was cooled to –40 °C and $Et_2O$ (100 mL) was added. The reaction was quenched with the very slow addition of $H_2O$ (50 mL) at –40 °C. The mixture was slowly warmed to rt and more $Et_2O$ (150 mL) and $H_2O$ (50 mL) was added. The layers were separated and the organic layer was washed with brine (50 mL), and dried over $Na_2SO_4$. The solvent was removed in vacuo to obtain the crude intermediate.

This procedure (**Part A**) was repeated a second time to make more intermediate using the following: 1-bromoadamantane (**3.4**) = 54.0 g (0.251 mol); vinyl bromide = 105 mL (1.51 mol); $AlCl_3$ = 8.37 g (0.0628 mol): **Note:** This reaction was done in two smaller batches to minimize danger from this potentially exothermic reaction.

**Part B:** The intermediate from the two batches in **Part A** were combined, dissolved in DMSO (500 mL) and KOH (105 g, 1.87 mol) was added. The reaction was stirred with a mechanical stirring device while heating to 100 °C for 8 h using a reflux apparatus. The reaction was cooled to rt and stirred an additional 16 h. The reaction was poured into $H_2O$ (400 mL) while rinsing forward with $Et_2O$ (100 mL) and $H_2O$ (100 mL). The mixture was extracted with ether (2 × 400 mL). The organic layers were combined, washed with $H_2O$ (2 × 200 mL), brine (200 mL), and dried over $Na_2SO_4$. The solvent was removed in vacuo and the crude product purified by

distillation/sublimation under reduced pressure (~90 °C, ~1 torr) into a cooled flask to give **3.2** (58.3 g, 78%) as a white solid. Spectroscopic data consistent with that reported.[10]

**3.3**

**3-Adamantyl-2-propynoic acid (3.3):**[9,11] To a solution of **3.2** (5.214 g, 32.53 mmol) in $Et_2O$ (50 mL) at –78 °C under a $N_2$ atmosphere was added BuLi (13.0 mL, 2.5M in hexanes, 33.5 mmol). This solution was stirred for 10 min and $CO_2$ was bubbled through the solution for 20 min at –78 °C. The reaction was allowed to warm to 0 °C and bubbling of $CO_2$ was stopped. The reaction was allowed to warm to rt and then the reaction was quenched with 10% HCl (aq). The organic layer was washed with brine and dried over $MgSO_4$. The solvent was removed in vacuo to yield **3.3** (quantitative) as a white solid: $^1$H NMR (400 MHz, $CDCl_3$): $\delta$ 9.73 (br s, 1H), 1.94-1.99 (m, 3H), 1.88-1.92 (m, 6H), 1.63-1.73 (m, 6H);[11] $^{13}$C NMR (100 MHz, $CDCl_3$): $\delta$ 158.7, 99.1, 71.5, 41.3, 36.0, 29.7, 27.5.

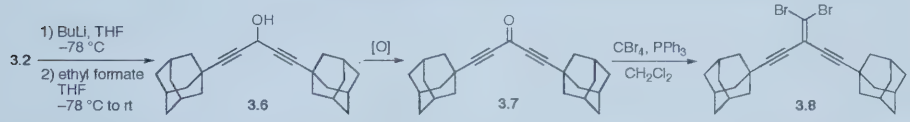


**3.8:** To a solution of **3.2** (1.925 g, 12.01 mmol) in THF (50 mL) was added BuLi (4.80 mL, 2.5M in hexanes, 12.0 mmol) dropwise at 0 °C. The mixture was stirred for 20 min at 0 °C and then a solution of ethyl formate (404 mg, 5.46 mmol) in THF (2 mL) was added dropwise over 10 min at 0 °C. The mixture was warmed to rt and stirred for 3 h. The reaction was quenched with saturated $NH_4Cl$ (25 mL) and extracted with $Et_2O$ (100 mL). The organic layer was washed with $H_2O$ (20 mL), brine (20 mL), and dried over $Na_2SO_4$. The solvent was removed in vacuo and the crude alcohol **3.6** dissolved in $CH_2Cl_2$ (100 mL). To this solution was added celite (6 g), molecular sieves (6 g) and PCC (1.775 g, 8.234 mmol) and the reaction stirred at rt under a $N_2$ atmosphere for 3h. The mixture was filtered through a silica plug with $CH_2Cl_2$ and the volume reduced in vacuo to ca. 20 mL and held for further use (ketone **3.7** solution). Concurrently, to a solution of $CBr_4$ (3.622 g, 10.92 mmol) in $CH_2Cl_2$ (100 mL) was added $PPh_3$ (6.475 g, 24.69 mmol) and the mixture stirred for 1 h at rt under a $N_2$ atmosphere. The ketone **3.7** solution was added slowly over 10 min and allowed to stir at rt under a $N_2$ atmosphere for 30 min. Hexanes were added to precipitate the phosphine salts and the solution was filtered through a pad of celite. The oily residue left in the flask was taken up in minimal $CH_2Cl_2$ and subjected to hexanes followed by filtration through celite. This process was carried out three times. The filtrate was filtered through celite until the filtrate remained a clear solution. The solvent was removed in vacuo and the crude product passed through a plug of silica gel with hexanes and the solvent removed in vacuo. The

resulting solid was stirred in hot hexanes (5 mL) for 5 min, cooled to rt, and filtered to yield **3.8** as an off-white solid. A second crop was obtained by concentrating the filtrate, stirring the resulting solid in hot hexanes (2 mL) for 5 min, cooling to rt and filtering to give **3.8**, which was combined with the first crop (total yield = 1.494 g, 54%): Mp 242-245 °C (Note: before melting decomposition was observed >180 °C); $R_f$ = 0.37 (hexanes); IR (cast film, $CDCl_3$) 2903, 2851, 2210, 1450 $cm^{-1}$; $^1H$ NMR (400 MHz, $CDCl_3$): $\delta$ 1.92-1.98 (m, 6H), 1.88-1.92 (m, 12H), 1.64-1.72 (m, 12H); $^{13}C$ NMR (100 MHz, $CDCl_3$): $\delta$ 114.7, 105.2, 104.6, 77.2, 42.1, 36.3, 30.5, 27.8; EI HRMS *m/z* calcd. for $C_{26}H_{30}{}^{79}Br^{81}Br$ ($M^+$) 502.0694, found 502.0690; Anal. calcd. for $C_{26}H_{30}Br_2$: C, 62.17; H, 6.02. Found: C, 62.16; H, 6.05.

**X-ray Crystal Data for 3.8:** Single crystals of **3.8** suitable for X-ray crystallographic analysis were grown by slow evaporation of a solution of **3.8** in $CHCl_3$. $C_{26}H_{30}Br_2$, $M_r$ = 502.32; crystal dimensions: 0.59 × 0.50 × 0.25 $mm^3$; crystal system: monoclinic; space group *I2/a* (an alternate setting of *C2/c* [No. 15]), $a$ = 11.9406 (9), $b$ = 12.4003 (10), $c$ = 15.7634 (12) Å; $\beta$ = 106.3440 (9)°; $V$ = 2239.7 (3) $Å^3$, $Z$ = 4; $\rho_{calcd}$ = 1.490 g $cm^{-3}$; $\mu$ = 3.629 $mm^{-1}$; $\lambda$ = 0.71073 Å; T = –100 °C; $2\theta$ max = 52.68°; total data collected = 8287; $R_1$ = 0.0275 for 2025 observed reflections with $[F_o^2 \geq 2\sigma(F_o^2)]$; $wR_2$ = 0.0681 for 129 variables and 2280 unique reflections with $[F_o^2 \geq -3\sigma(F_o^2)]$; residual electron density = 0.424 and –0.517 e $Å^{-3}$.

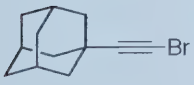


**3.9**

**3.9 was synthesized as previously reported:**[12] Yield = 98%. Mp 131-133 °C (lit. 130-133 °C). Spectroscopic data consistent with that reported.

**3.10**

**3.10 was synthesized as previously reported:**[12] Yield = 87%. Mp 146-148 °C (lit. 150-152 °C). Spectroscopic data consistent with that reported.

**3.11**

**3.11 was synthesized as previously reported:**[12] Yield = 79%. Mp 109-110 °C (decomposed after melting; lit. 104-108 °C). Spectroscopic data consistent with that reported.

**X-ray Crystal Data for 3.11:** Single crystals of **3.11** suitable for X-ray crystallographic analysis were grown by slow diffusion of MeOH into a solution of **3.11** in hexanes. $C_{14}H_{16}$, $M_r$ = 184.27; crystal dimensions: 0.45 × 0.43 × 0.20 $mm^3$; crystal system: monoclinic; space group $P2_1/n$ (an

alternate setting of $P2_1/c$ [No. 14]), $a$ = 15.002 (2), $b$ = 7.5389 (11), $c$ = 20.514 (3) Å; $\beta$ = 109.547 (2)°; $V$ = 2186.4 (5) Å$^3$, $Z$ = 8; $\rho$calcd = 1.120 g cm$^{-3}$; $\mu$ = 0.063 mm$^{-1}$; $\lambda$ = 0.71073 Å; T = –80 °C; 2$\theta$ max = 54.96°; total data collected = 17779; $R_1$ = 0.0640 for 3378 observed reflections with [$F_o^2 \geq 2\sigma(F_o^2)$]; $wR_2$ = 0.1957 for 334 variables and 4981 unique reflections with [$F_o^2 \geq -3\sigma(F_o^2)$]; residual electron density = 0.442 and –0.148 e Å$^{-3}$.

**3.15**

**3.15:** To a solution of **3.21** (3.470 g, 7.881 mmol) in hexanes (100 mL) at –78 °C was added BuLi (3.80 mL, 2.5M in hexanes, 9.50 mmol) dropwise under a $N_2$ atmosphere. The reaction mixture was stirred at –78 °C for 10 min, warmed to 0 °C over 10 min and allowed to stir at 0 °C for and additional 30 min. The reaction was warmed to rt, stirred for 1 h, and then cooled to 0 °C and quenched with saturated $NH_4Cl$ (20 mL). The resulting layers were separated and the organic layer was dried over $Na_2SO_4$. The solvent was removed in vacuo and the crude product was recrystallized from MeOH to yield **3.15** (2.193 g, 99%) as an orange crystalline solid: Mp 124-126 °C; $R_f$ = 0.48 (hexanes); IR (microscope) 2959, 2903, 2852, 2201, 2168, 2077, 1450 cm$^{-1}$; $^1$H NMR (400 MHz, $CDCl_3$): $\delta$ 1.92-1.97 (m, 3H), 1.84-1.86 (m, 6H), 1.61-1.70 (m, 6H), 0.17 (s, 9H); $^{13}$C NMR (125 MHz, $CDCl_3$): $\delta$ 88.4, 87.8, 85.8, 64.4, 62.5, 61.2, 41.9, 36.1, 30.3, 27.6, –0.5; EI HRMS *m/z* calcd. for $C_{19}H_{24}Si$ ($M^+$) 280.1647, found 280.1649; DSC: Mp 136 °C; decomposition, 242 °C (onset) and 261 (peak).

**X-ray Crystal Data for 3.15:** Single crystals of **3.15** suitable for X-ray crystallographic analysis were grown by slow diffusion of acetone into a solution of **3.15** in $CHCl_3$ followed by slow evaporation. $C_{19}H_{24}Si$, $M_r$ = 280.47; crystal dimensions: 0.54 × 0.27 × 0.12 mm$^3$; crystal system: monoclinic; space group $P2_1/c$ (No. 14), $a$ = 9.9015 (10), $b$ = 20.359 (2), $c$ = 8.5843 (8) Å; $\beta$ = 92.274 (2)°; $V$ = 1729.1 (3) Å$^3$, $Z$ = 4; $\rho$calcd = 1.077 g cm$^{-3}$; $\mu$ = 0.126 mm$^{-1}$; $\lambda$ = 0.71073 Å; T = –80 °C; 2$\theta$ max = 54.92°; total data collected = 14390; $R_1$ = 0.0656 for 3019 observed reflections with [$F_o^2 \geq 2\sigma(F_o^2)$]; $wR_2$ = 0.2006 for 208 variables and 3961 unique reflections with [$F_o^2 \geq -3\sigma(F_o^2)$]; residual electron density = 0.673 and –0.281 e Å$^{-3}$.

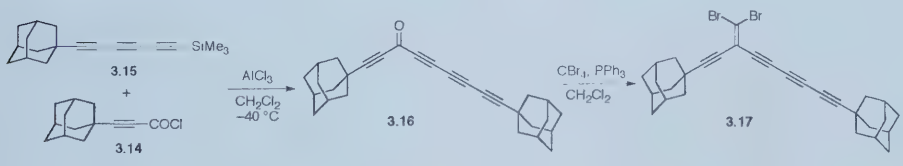


**3.17:** A solution of **3.3** (0.623 g, 3.05 mmol) in $SOCl_2$ (3 mL) was stirred at rt for 12 h covered with a $CaCl_2$ drying tube. The excess $SOCl_2$ was removed under reduced pressure to give acid

chloride **3.14**. To the acid chloride **3.14** was added **3.15** (0.712 g, 2.54 mmol) and the resulting mixture dissolved in $CH_2Cl_2$ (10 mL). This solution was added to a mixture of $AlCl_3$ (0.425 g, 3.19 mmol) in $CH_2Cl_2$ (40 mL) dropwise at –40 °C. The reaction was allowed to stir at –40 °C for 1.5 h under a $N_2$ atmosphere. The reaction mixture was quenched slowly with $H_2O$ (20 mL) at –40 °C, warmed to rt and the layers separated. The organic layer was washed with brine (20 mL) and dried over $MgSO_4$. The filtrate was concentrated in vacuo to ca. 5 mL, plugged through silica gel with $CH_2Cl_2$, and concentrated to ca 5 mL (ketone **3.16**). Concurrently, to a solution of $CBr_4$ (1.706 g, 5.144 mmol) in $CH_2Cl_2$ (40 mL) was added $PPh_3$ (3.005 g, 11.46 mmol) and stirred under a $N_2$ atmosphere for 1 h. The ketone (**3.16**) solution was added and the resulting mixture stirred under a $N_2$ atmosphere until deemed complete by TLC analysis; ca. 10 min. Hexanes were added to precipitate the phosphine salts as a white solid along with an oily residue. The supernatant was decanted and filtered through a pad of celite. The oily residue left in the flask was dissolved in minimal $CH_2Cl_2$ and hexanes were added; the heterogeneous mixture was then decanted and the supernatant filtered through celite (this procedure was repeated three times). The solvent was removed and the crude product was purified by column chromatography (silica gel, hexanes) to yield **3.17** (0.553 g, 40%) as a yellow solid: $R_f$ = 0.45 (hexanes); IR (microscope) 2904, 2851, 2213, 2181, 2103 (w), 1451 $cm^{-1}$; $^1H$ NMR (400 MHz, $CDCl_3$): $\delta$ 1.92-1.98 (m, 6H), 1.88-1.90 (m, 6H), 1.85-1.87 (m, 6H), 1.61-1.72 (m, 12H); $^{13}C$ NMR (100 MHz, $CDCl_3$): $\delta$ 113.5, 110.3, 106.4, 91.3, 80.2, 76.0, 72.0, 70.7, 64.6, 60.4, 42.0, 41.8, 36.2, 36.1, 30.6, 30.5, 27.8, 27.6; EIMS *m/z* 550.1 ($M^+$, 79), 390.2 ($[M - 2\times Br]^+$, 31), 135.1 ($[C_{10}H_{15}]^+$, 100); EI HRMS *m/z* calcd. for $C_{30}H_{30}{}^{79}Br^{81}Br$ ($M^+$) 550.0694, found 550.0695.

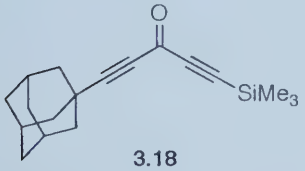


**3.18**

**3.18:** A solution of **3.3** (0.660 g, 3.23 mmol) in $SOCl_2$ (3 mL) was stirred at rt for 12 h covered with a $CaCl_2$ drying tube. The excess $SOCl_2$ was removed under reduced pressure. Bis(trimethylsilyl)acetylene (0.631 g, 3.70 mmol) was added to the residue and the resulting mixture was dissolved in $CH_2Cl_2$ (5 mL). This solution was added to a mixture of $AlCl_3$ (0.475 g, 3.56 mmol) in $CH_2Cl_2$ (10 mL) dropwise at 0 °C. The reaction was allowed to stir at 0 °C for 3 h. The reaction mixture was quenched slowly with $H_2O$ (10 mL) at 0 °C. The organic layer was washed with saturated $NH_4Cl$ (15 mL) and dried over $MgSO_4$. The solvent was removed in vacuo and the crude product was purified by column chromatography (silica gel, $CH_2Cl_2$/hexanes 1:3) to yield **3.18** (0.489 g, 53%) as an orange solid: Mp 71–73 °C; $R_f$ = 0.63 ($CH_2Cl_2$/hexanes 1:1); IR (microscope) 2910, 2854, 2206, 2147, 1630, 1452, 1229, 1117 $cm^{-1}$; $^1H$ NMR (400 MHz, $CDCl_3$): $\delta$ 1.94-1.99 (m, 3H), 1.90-1.92 (m, 6H), 1.70-1.67 (m, 6H), 0.23 (s, 9H); $^{13}C$ NMR (125 MHz,

$CDCl_3$): $\delta$ 161.0, 102.8, 102.0, 97.5, 81.1, 41.3, 36.0, 29.9, 27.4, –1.0; EIMS *m/z* 284.2 ($M^+$, 59), 269.1 ([M – Me]$^+$, 55), 241.1 ([M – Me – CO]$^+$, 100); EI HRMS *m/z* calcd. for $C_{18}H_{24}OSi$ ($M^+$) 284.1596, found 284.1601; Anal. calcd. for $C_{18}H_{24}OSi$: C, 76.00; H, 8.50. Found: C, 75.92; H, 8.42.

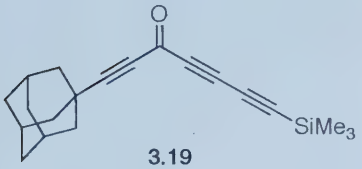


**3.19**

**3.19:** A solution of **3.3** (0.652 g, 3.19 mmol) in $SOCl_2$ (3 mL) was stirred at rt for 20 h covered with a $CaCl_2$ drying tube. The excess $SOCl_2$ was removed in vacuo, 1,4-bis(trimethylsilyl)-1,3-butadiyne (0.685 g, 3.51 mmol) added to the residue and the resulting mixture dissolved in $CH_2Cl_2$ (5 mL). This solution was added to a mixture of $AlCl_3$ (0.469 g, 3.51 mmol) in $CH_2Cl_2$ (10 mL) dropwise at –23 °C under a $N_2$ atmosphere. The reaction was allowed to stir at –23 °C for 2 h. The reaction mixture was quenched slowly with $H_2O$ (10 mL) at –23 °C and allowed to warm to rt. The organic layer was washed with saturated $NH_4Cl$ (15 mL) and dried over $MgSO_4$. The solvent was removed and the crude product was purified by column chromatography (silica gel, $CH_2Cl_2$/hexanes 1:3) to yield **3.19** (0.410 g, 42%) as an brown oil: $R_f$ = 0.59 ($CH_2Cl_2$/hexanes 1:1); IR (microscope) 2909, 2854, 2199, 2099, 1628, 1452, 1254, 1038 $cm^{-1}$; $^1H$ NMR (500 MHz, $CDCl_3$): $\delta$ 1.95-1.99 (m, 3H), 1.89-1.91 (m, 6H), 1.64-1.73 (m, 6H), 0.21 (s, 9H); $^{13}C$ NMR (125 MHz, $CDCl_3$): $\delta$ 159.9, 103.3, 98.4, 85.9, 81.1, 74.5, 74.2, 41.3, 36.0, 30.0, 27.4, –0.8; EIMS *m/z* 308.2 ($M^+$, 34), 293.1 ([M – Me]$^+$, 52), 280.2 ([M – CO]$^+$, 44), 265.1 ([M – Me – CO]$^+$, 100); EI HRMS *m/z* calcd. for $C_{20}H_{24}OSi$ ($M^+$) 308.1596, found 308.1600.

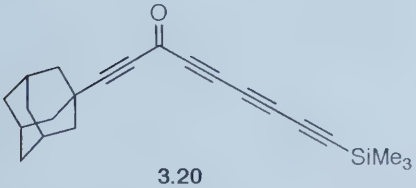


**3.20**

**3.20:** A solution of **3.3** (78 mg, 0.38 mmol) in $SOCl_2$ (1 mL) was stirred at rt for 17 h. The $SOCl_2$ was removed in vacuo, 1,6-bis(trimethylsilyl)hexa-1,3,5-triyne[13] (55 mg, 0.25 mmol) added and the mixture dissolved in $CH_2Cl_2$ (3 mL). This solution was added to a mixture of $AlCl_3$ (65 mg, 0.49 mmol) in $CH_2Cl_2$ (5 mL) dropwise at –20 °C and stirred for 30 min at –20 °C under a $N_2$ atmosphere. The reaction was quenched with $H_2O$ (5 mL) and the layers separated. The aqueous layer was extracted with $CH_2Cl_2$ (5 mL). The organic layers were combined, washed with brine (5 mL) and dried over $MgSO_4$. The volume was reduced to 1 mL in vacuo and the crude product

purified by column chromatography (silica gel, $CH_2Cl_2$/hexanes 1:3) to yield **3.20** (36 mg, 43%) as a dark brown oil (**Note: This compound is extremely unstable to isolation and resulted in partial decomposition, resulting in spectra of an impure sample and only partial characterization**): $R_f$ = 0.61 ($CH_2Cl_2$/hexanes 1:1); IR (cast film, $CHCl_3$) 2906, 2852, 2204, 2184, 1626 $cm^{-1}$; $^1H$ NMR (500 MHz, $CDCl_3$): $\delta$ 1.94-2.02 (m, 3H), 1.89-1.92 (m, 6H), 1.64-1.74 (m, 6H), 0.21 (s, 9H); $^{13}C$ NMR (125 MHz, $CDCl_3$): $\delta$ 159.5, 104.0, 93.3, 87.0, 81.1, 74.6, 73.8, 72.0, 59.5, 41.3, 36.0, 30.2, 27.4, –0.8.

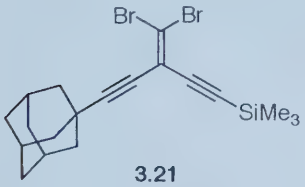


**3.21**

**3.21:** To a solution of $CBr_4$ (0.833 g, 2.51 mmol) in $CH_2Cl_2$ (10 mL) was added $PPh_3$ (1.367 g, 5.21 mmol) and stirred at rt for 30 min under and atmosphere of $N_2$. A solution of **3.18** (0.593 g, 2.09 mmol) in $CH_2Cl_2$ (5 mL) was added dropwise then the resulting mixture stirred at rt for 1 h. Hexanes were added to precipitate the phosphine salts as a white solid along with an oily residue. The supernatant was decanted and filtered through a pad of celite. The oily residue left in the flask was dissolved in minimal $CH_2Cl_2$ and hexanes were added; the heterogeneous mixture was then decanted and the supernatant filtered through celite (this procedure was repeated three times). The solvent was removed and the crude product was purified by column chromatography (silica gel, hexanes) to yield **3.21** (0.745 g, 81%) as a yellow solid: Mp 80-82 °C; $R_f$ = 0.49 (hexanes); IR (microscope) 2906, 2852, 2208, 2152, 1451, 1251 $cm^{-1}$; $^1H$ NMR (500 MHz, $CDCl_3$): $\delta$ 1.93-1.97 (m, 3H), 1.89-1.92 (m, 6H), 1.67-1.69 (m, 6H), 0.20 (s, 9H); $^{13}C$ NMR (125 MHz, $CDCl_3$): $\delta$ 114.5, 107.8, 105.4, 101.6, 100.8, 76.6, 42.1, 36.3, 30.6, 27.8, –0.4; EI HRMS *m/z* calcd. for $C_{19}H_{24}{}^{79}Br^{81}BrSi$ ($M^+$) 439.9946, found 439.9994; Anal. calcd. for $C_{19}H_{24}Br_2Si$: C, 51.83; H, 5.49. Found: C, 51.99; H, 5.54.

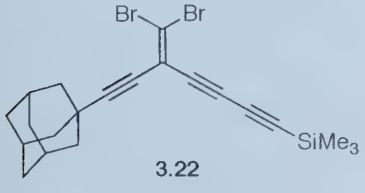


**3.22**

**3.22:** To a solution of $CBr_4$ (0.344 g, 1.04 mmol) in $CH_2Cl_2$ (10 mL) was added $PPh_3$ (0.614 g, 2.34 mmol) and stirred at rt for 30 min under a $N_2$ atmosphere. A solution of **3.19** (0.288 g, 0.934 mmol) in $CH_2Cl_2$ (5 mL) was added dropwise and the resulting mixture stirred at rt for 30 min. Hexanes were added to precipitate the phosphine salts as a white solid along with an oily residue.

The supernatant was decanted and filtered through a pad of celite. The oily residue left in the flask was dissolved in minimal $CH_2Cl_2$ and hexanes were added; the heterogeneous mixture was then decanted and the supernatant filtered through celite (this procedure was repeated three times). The solvent was removed and the crude product was purified by column chromatography (silica gel, hexanes) to yield **3.22** (0.320 g, 74%) as a brown solid: Mp 114-116 °C; $R_f$ = 0.56 (hexanes); IR (microscope) 2960, 2901, 2852, 2215, 2101, 1449, 1250 $cm^{-1}$; $^1H$ NMR (500 MHz, $CDCl_3$): $\delta$ 1.93-1.97 (m, 3H), 1.87-1.90 (m, 6H), 1.64-1.72 (m, 6H), 0.20 (s, 9H); $^{13}C$ NMR (125 MHz, $CDCl_3$): $\delta$ 113.5, 109.8, 106.3, 94.6, 87.3, 79.5, 76.1, 72.8, 42.0, 36.2, 30.6, 27.8, –0.6; EI HRMS *m/z* calcd. for $C_{21}H_{24}{}^{79}Br^{81}BrSi$ ($M^+$) 463.9994, found 463.9983; Anal. calcd. for $C_{21}H_{24}Br_2Si$: C, 54.32; H, 5.21. Found: C, 54.19; H, 5.30.

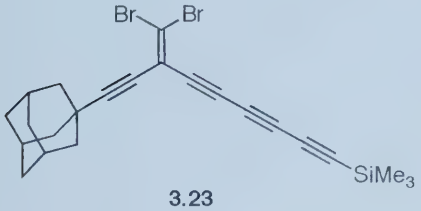


**3.23**

**3.23 (synthesis from 3.3):** To a solution of **3.3** (0.711 g, 3.48 mmol) in $CH_2Cl_2$ (100 mL) was added $SOCl_2$ (2.45 g, 1.50 mL, 20.6 mmol) and stirred at rt under a $N_2$ atmosphere for 24 h. The solvent was removed in vacuo, 1,6-bis(trimethylsilyl)hexa-1,3,5-triyne[13] (0.531 g, 2.43 mmol) added and the mixture dissolved in $CH_2Cl_2$ (10 mL). This solution was added dropwise to a mixture of $AlCl_3$ (0.356 g, 2.68 mmol) and $CH_2Cl_2$ (50 mL) at –20 °C then stirred at –20 °C for 1.5 h under a $N_2$ atmosphere. The reaction was quenched with $H_2O$ (20 mL), washed with brine (20 mL), and dried over $MgSO_4$. The solution was concentrated in vacuo to a volume of ~10 mL and held for later use (ketone **3.20**). Concurrently, to a solution of $CBr_4$ (1.388 g, 4.19 mmol) in $CH_2Cl_2$ (50 mL) was added $PPh_3$ (2.302 g, 8.78 mmol) and the mixture stirred for 1 h under a $N_2$ atmosphere. The ketone solution (**3.20**) was added dropwise and the mixture stirred at rt for 18 h under a $N_2$ atmosphere. The reaction mixture was concentrated in vacuo to ~20 mL and then hexanes were added to precipitate the phosphine salts as a white solid along with an oily residue. The supernatant was decanted and filtered through a pad of celite. The oily residue left in the flask was dissolved in minimal $CH_2Cl_2$ and hexanes were added; the heterogeneous mixture was then decanted and the supernatant filtered through celite (this procedure was repeated five times). The solvent was removed in vacuo and the crude product purified by column chromatography (silica gel, hexanes) to yield **3.23** (0.427 g, 36%) as an amber oil: $R_f$ = 0.56 (hexanes); IR (microscope) 2959, 2930, 2907, 2851, 2228, 2175, 2075, 1451 $cm^{-1}$; $^1H$ NMR (300 MHz, $CDCl_3$): $\delta$ 1.92-1.99 (m, 3H), 1.87-1.91 (m, 6H), 1.62-1.75 (m, 6H), 0.20 (s, 9H); $^{13}C$ NMR (125 MHz, $CDCl_3$): $\delta$ 113.3, 111.2, 106.8, 91.2, 87.8, 79.6, 75.8, 72.9, 70.0, 61.0, 42.0, 36.2, 30.7, 27.7, –0.6; EI HRMS

*m/z* calcd. for $C_{23}H_{24}{}^{79}Br^{81}BrSi$ ($M^+$) 487.9994, found 487.9960. Note: NMR spectra show bis(TMS)triyne.

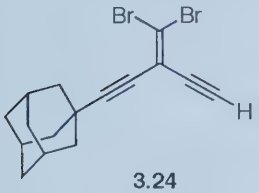


**3.24**

**3.24:** To a solution of **3.21** (0.662 g, 1.50 mmol) in THF (5 mL) and MeOH (5 mL) was added $K_2CO_3$ (0.208 g, 1.50 mmol). After stirring for 1 h, the solvent was removed in vacuo and the crude product was purified by passing through a short plug of silica gel with hexanes to yield **3.24** (0.527 g, 95%) as an off-white solid: Mp 101 °C (decomp); $R_f$ = 0.45 (hexanes); IR (microscope) 3295, 2901, 2852, 2228, 2197, 1450, 1101 $cm^{-1}$; $^1H$ NMR (500 MHz, $CDCl_3$): $\delta$ 3.41 (s, 1H), 1.94-1.98 (m, 3H), 1.89-1.92 (m, 6H), 1.66-1.72 (m, 6H); $^{13}C$ NMR (125 MHz, $CDCl_3$): $\delta$ 113.6, 108.2, 105.9, 83.1, 80.2, 76.7, 42.1, 36.2, 30.6, 27.8; EIMS *m/z* 368.0 ($M^+$, 100), 289 ($[M - Br]^+$, 16); Anal. calcd. for $C_{16}H_{16}Br_2$: C, 52.21; H, 4.38. Found: C, 52.59; H, 4.46.

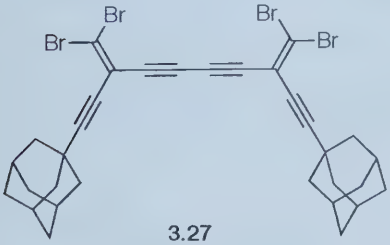


**3.27**

**3.27:** To a mixture of CuCl (171 mg, 1.73 mmol) in $CH_2Cl_2$ (30 mL) was added TMEDA (420 mg, 0.600 mL, 3.61 mmol). $O_2$ was bubbled through the solution for 20 min and a solution of **3.24** (628 mg, 1.71 mmol) in $CH_2Cl_2$ (10 mL) was added and stirred for 20 min. The reaction mixture was quenched with $H_2O$ (20 mL) and the resulting layers separated. The organic layer was washed with $H_2O$ (10 mL), saturated $NH_4Cl$ (20 mL), and dried over $MgSO_4$. The solvent was removed in vacuo and the crude product was purified by passing through a short plug of silica gel ($CH_2Cl_2$/hexanes 1:4) to yield **3.27** (0.600 g, 96%) as a pale yellow solid: $R_f$ = 0.64 ($CH_2Cl_2$/hexanes 1:4); IR (microscope) 2899, 2847, 2223, 2143, 1449, 1100 $cm^{-1}$; $^1H$ NMR (400 MHz, $CDCl_3$): $\delta$ 1.95-2.00 (m, 6H), 1.90-1.93 (m, 12H), 1.66-1.74 (m, 12H); $^{13}C$ NMR (125 MHz, $CDCl_3$): $\delta$ 113.6, 110.3, 106.6, 80.7, 78.9, 75.9, 42.0, 36.2, 30.7, 27.8; EI HRMS *m/z* calcd. for $C_{32}H_{30}{}^{71}Br_2{}^{81}Br_2$ ($M^+$) 733.9040, found 733.9079; Anal. calcd. for $C_{32}H_{30}Br_4$: C, 52.35; H, 4.12. Found: C, 52.13; H, 4.29.

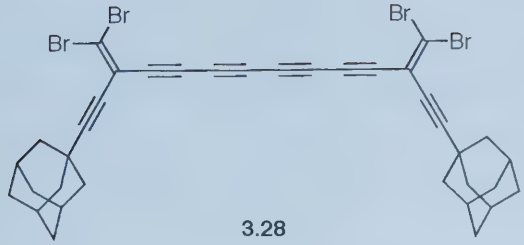

3.28

**3.28:** To a solution of **3.22** (1.618 g, 3.485 mmol) in THF (20 mL) and MeOH (20 mL) was added $K_2CO_3$ (0.522 g, 3.78 mmol). After stirring for 1 h the reaction was quenched with $H_2O$ (50 mL), extracted with $Et_2O$ (2 × 100 mL), the organic phases combined, and dried over $Na_2SO_4$. The volume was reduced in vacuo to ca. 5 mL and $CH_2Cl_2$ (20 mL) was added. This solution was added to the Hay catalyst, which was prepared by mixing CuCl (0.345 g, 3.49 mmol) in $CH_2Cl_2$ (100 mL), adding TMEDA (1.386 g, 1.800 mL, 11.93 mmol) and then bubbling $O_2$ through the solution for 20 min. The reaction was stirred at rt for 30 min and quenched with $H_2O$ (50 mL). The layers were separated and the organic layer was washed with $H_2O$ (50 mL), brine (50 mL), and dried over $MgSO_4$. The solvent was removed in vacuo and the crude product was purified by column chromatography (silica gel, hexanes) to yield **3.28** (1.001 g, 73%) as a yellow solid: $R_f$ = 0.52 (hexanes); IR (microscope) 2904, 2849, 2217, 2203, 1495, 1450, 1099 $cm^{-1}$; $^1H$ NMR (500 MHz, $CDCl_3$): $\delta$ 1.94-1.98 (m, 6H), 1.86-1.93 (m, 12H), 1.65-1.72 (m, 12H); $^{13}C$ NMR (125 MHz, $CDCl_3$): $\delta$ 113.1, 112.2, 107.2, 79.4, 75.6, 74.4, 70.1, 64.7, 42.0, 36.2, 30.7, 27.7; EIMS *m/z* 781.9 ($M^+$, 31), 93.1 ($[C_7H_9]^+$, 100), 79.9 ($[Br]^+$, 82).

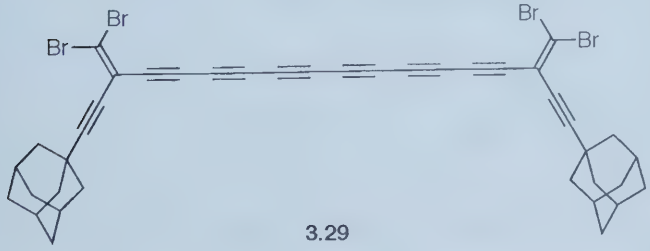

3.29

**3.29:** To a solution of **3.23** (103 mg, 0.211 mmol) in THF (2 mL) and MeOH (2 mL) was added $K_2CO_3$ (29 mg, 0.211 mmol). The reaction was stirred at rt for 30 min, quenched with $H_2O$ (5 mL) and extracted with $Et_2O$ (2 × 15 mL). The organic layers were combined, washed with brine (15 mL), and dried over $MgSO_4$. The volume was reduced to ca. 5 mL, $CH_2Cl_2$ (20 mL) added, and the volume reduced again to ca. 5 mL. This was repeated one more time and then the solution was held for later use. To a mixture of CuCl (21 mg, 0.211 mmol) in $CH_2Cl_2$ (10 mL) was added TMEDA (154 mg, 200 µL, 1.33 mmol). $O_2$ was bubbled through the solution for 20 min and the crude intermediate solution was added and the reaction stirred at rt for 20 min. The reaction mixture was quenched with $H_2O$ (15 mL) and the resulting layers separated. The organic layer was

washed with $H_2O$ (5 mL), brine (15 mL), and dried over $Na_2SO_4$. The solvent was removed in vacuo and the crude product was purified by column chromatography (silica gel, hexanes) to yield **3.29** (53 mg, 60%) as an orange solid: $R_f$ = 0.76 (hexanes); IR (cast film, $CHCl_3$) 2903, 2850, 2215, 2154, 1450 $cm^{-1}$; $^1H$ NMR (300 MHz, $CDCl_3$): $\delta$ 1.92-2.00 (m, 6H), 1.87-1.91 (m, 12H), 1.62-1.74 (m, 12H); $^{13}C$ NMR (125 MHz, $CDCl_3$): $\delta$ 113.0, 112.9, 107.4, 79.3, 75.5, 73.5, 70.3, 66.0, 64.2, 62.4, 42.0, 36.2, 30.7, 27.7.

**3.30**

**3.30:** To a solution of **3.22** (267 mg, 0.575 mmol) in hexanes (30 mL) at –78 °C was added BuLi (0.30 mL, 2.5M in hexanes, 0.75 mmol) dropwise under a $N_2$ atmosphere. The reaction mixture was stirred at –78 °C for 10 min, warmed to 0 °C over 15 min and quenched with saturated $NH_4Cl$ (10 mL). The resulting layers were separated and the organic layer washed with $H_2O$ (10 mL), brine (10 mL) and dried over $MgSO_4$. The solvent was removed in vacuo and the crude product purified by column chromatography (silica gel, hexanes) to yield **3.30** (146 mg, 83%) as a white solid that rapidly turned brownish-black: $R_f$ = 0.62 (hexanes).

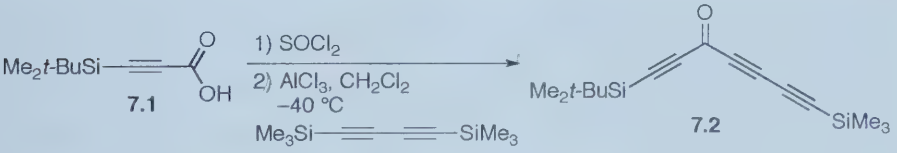


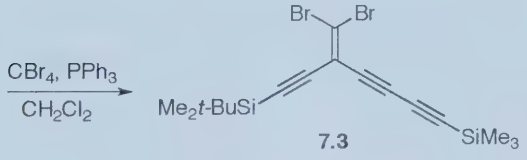


**7.3:** A solution of **7.1** (2.925 g, 15.87 mmol) in $SOCl_2$ (12 mL) was stirred at rt for 16 h covered with a $CaCl_2$ drying tube. The excess $SOCl_2$ was removed in vacuo, 1,4-bis(trimethylsilyl)-1,3-butadiyne (2.774 g, 14.27 mmol) added to the residue and the resulting mixture dissolved in $CH_2Cl_2$ (20 mL). This solution was added to a mixture of $AlCl_3$ (2.330 g, 17.47 mmol) in $CH_2Cl_2$ (100 mL) dropwise at 0 °C under a $N_2$ atmosphere and then stirred at 0 °C for 2 h. The reaction was quenched slowly with $H_2O$ (50 mL) at 0 °C and allowed to warm to rt. The organic layer was washed with brine (2 × 50 mL) and dried over $MgSO_4$. The mixture was filtered, concentrated to ca. 10 mL, passed through a plug of silica gel, and then concentrated to ca. 15 mL (ketone **7.2**). Concurrently, to a solution of $CBr_4$ (7.900 g, 23.82 mmol) in $CH_2Cl_2$ (150 mL) was added $PPh_3$ (13.32 g, 50.78 mmol) and the mixture stirred for 1 h under a $N_2$ atmosphere. The ketone solution

(**7.2**) was added dropwise and the mixture stirred at rt for 24 h under a $N_2$ atmosphere. The reaction mixture was concentrated in vacuo to ca. 20 mL and then hexanes were added to precipitate the phosphine salts as a white solid along with an oily residue. The supernatant was decanted and filtered through a pad of celite. The oily residue left in the flask was dissolved in minimal $CH_2Cl_2$ and hexanes were added; the heterogeneous mixture was then decanted and the supernatant filtered through celite (this procedure was repeated three times). The solvent was removed in vacuo and the crude product purified by column chromatography (silica gel, hexanes) to yield **7.3** (4.745 g, 75%) as an orange oil: $R_f$ = 0.39 (hexanes); IR (neat) 2955, 2929, 2897, 2858, 2206, 2155, 2106 $cm^{-1}$; $^1H$ NMR (400 MHz, $CDCl_3$): $\delta$ 0.97 (s, 9H), 0.23 (s, 9H), 0.16 (s, 6H); $^{13}C$ NMR (100 MHz, $CDCl_3$): $\delta$ 113.4, 112.4, 102.3, 99.8, 95.0, 87.2, 80.3, 72.2, 26.1, 16.7, –0.6, –5.0; EIMS *m/z* 444.0 ($M^+$, 30), 386.9 ([M – *t*Bu]$^+$, 87), ([M – Si*t*BuMe$_2$ – Br$_2$]$^+$, 100); EI HRMS *m/z* calcd. for $C_{17}H_{24}Si_2{}^{79}Br^{81}Br$ ($M^+$) 443.9763, found 443.9735; Anal. calcd. for $C_{17}H_{24}Si_2Br_2$: C, 45.95; H, 5.44. Found: C, 45.53; H, 5.45.

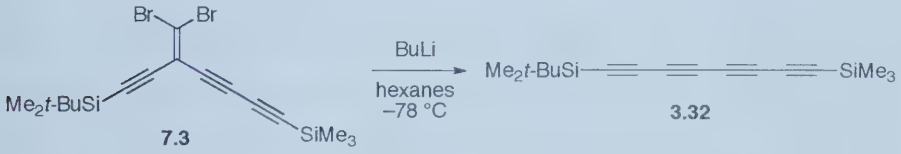


**7.3** **3.32**

**3.32:** To a solution of **7.3** (1.166 g, 2.624 mmol) in hexanes (70 mL) was added BuLi (1.26 mL, 2.5M in hexanes, 3.2 mmol) dropwise under a $N_2$ atmosphere. The reaction mixture was stirred at –78 °C for 10 min, warmed to rt over 20 min and quenched with saturated $NH_4Cl$ (20 mL). The resulting layers were separated and the organic layer dried over $Na_2SO_4$. The solvent was removed in vacuo and the crude product purified by column chromatography (silica gel, hexanes) to yield **3.32** (0.602 g, 81%) as a yellow oil (Note: compound **3.32** decomposes slowly as a neat oil, even at –20 °C. It can be repurified by passing through a plug of silica): $R_f$ = 0.58 (hexanes); IR (cast film, $CHCl_3$) 2955, 2929, 2898, 2858, 2177, 2044 $cm^{-1}$; $^1H$ NMR (400 MHz, $CDCl_3$): $\delta$ 0.93 (s, 9H), 0.19 (s, 9H), 0.12 (s, 6H); $^{13}C$ NMR (100 MHz, $CDCl_3$): $\delta$ 88.5, 87.90, 87.86, 87.0, 62.3, 62.2, 62.0, 61.8, 26.0, 16.9, –0.6, –5.0; EIMS *m/z* 284.1 ($M^+$, 35), 227.1 ([M – *t*Bu]$^+$, 100); EI HRMS *m/z* calcd. for $C_{17}H_{24}Si_2$ ($M^+$) 284.1417, found 284.1414; Anal. calcd. for $C_{17}H_{24}Si_2$: C, 71.76; H, 8.50. Found: C, 71.05; H, 8.52.

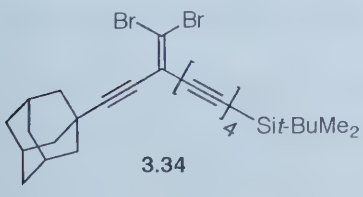


**3.34**

**3.34:** A solution of **3.3** (262 mg, 1.28 mmol) in $SOCl_2$ (2 mL) was stirred at rt for 20 h. The $SOCl_2$ was removed in vacuo, the residue dissolved in $CH_2Cl_2$ (3 mL), and this solution added to a mixture of $AlCl_3$ (190 mg, 1.42 mmol) in $CH_2Cl_2$ (30 mL) dropwise at –40 °C under a $N_2$ atmosphere. A solution of 1-TBS-8-TMS-octa-1,3,5,7-tetrayne **3.32** (219 mg, 0.770 mmol) in $CH_2Cl_2$ (3 mL) was then added dropwise and the resulting mixture stirred for 2 h at –40 °C under a $N_2$ atmosphere. The reaction was quenched with $H_2O$ (20 mL), the mixture warmed to rt, and the layers separated. The organic layer was washed with brine (20 mL) and dried over $MgSO_4$. The solution was concentrated to ca. 10 mL and held for later use (ketone **3.33**). Concurrently, to a solution of $CBr_4$ (1.078 g, 3.250 mmol) in $CH_2Cl_2$ (60 mL) was added $PPh_3$ (1.784 g, 6.802 mmol) and the mixture stirred for 1 h under a $N_2$ atmosphere. The ketone solution (**3.33**) was added dropwise and the mixture stirred at rt for 16 h under a $N_2$ atmosphere. The reaction mixture was concentrated in vacuo to ~20 mL and then hexanes were added to precipitate the phosphine salts as a white solid along with an oily residue. The supernatant was decanted and filtered through a pad of celite. The oily residue left in the flask was dissolved in minimal $CH_2Cl_2$ and hexanes were added; the heterogeneous mixture was then decanted and the supernatant filtered through celite (this procedure was repeated five times). The solvent was removed in vacuo and the crude product purified by column chromatography (silica gel, hexanes) to yield **3.34** (59 mg, 14%) as a brown oil: $R_f$ = 0.51 (hexanes); IR (cast film, $CHCl_3$) 2907, 2855, 2218, 2141, 2056 $cm^{-1}$; $^1H$ NMR (300 MHz, $CDCl_3$): $\delta$ 1.92-2.00 (m, 3H), 1.87-1.91 (m, 6H), 1.62-1.74 (m, 6H), 0.93 (s, 9H), 0.14 (s, 6H); $^{13}C$ NMR (125 MHz, $CDCl_3$): $\delta$ 113.1, 112.0, 107.0, 89.0, 88.4, 79.5, 75.7, 72.6, 70.4, 65.8, 61.5, 61.1, 42.0, 36.2, 30.7, 27.7, 26.0, 16.9, –5.0; EIMS *m/z* 554.1 ($M^+$, 88), 497.0 ($[M - t\text{Bu}]^+$, 100); EI HRMS *m/z* calcd. for $C_{28}H_{30}Si^{79}Br^{81}Br$ ($M^+$) 556.0443, found 556.0461.

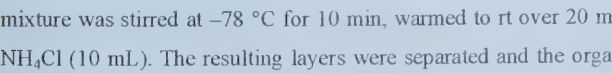


**3.35**

**3.35 (FBW rearrangement):** To a solution of **3.34** (59 mg, 0.11 mmol) in hexanes (25 mL) was added BuLi (53 μL, 2.5M in hexanes, 0.13 mmol) dropwise under a $N_2$ atmosphere. The reaction mixture was stirred at –78 °C for 10 min, warmed to rt over 20 min and quenched with saturated $NH_4Cl$ (10 mL). The resulting layers were separated and the organic layer washed with $H_2O$ (10 mL), brine (10 mL) and dried over $Na_2SO_4$. The solvent was removed in vacuo and the crude product purified by column chromatography (silica gel, hexanes) to yield **3.35** (12 mg, 29%) as a yellow solid.

**3.35 (mixed Hay coupling):** To a solution of CuCl (64 mg, 0.65 mmol) in THF (5 mL), MeOH (5 mL) and TMEDA (0.20 mL) was bubbled $O_2$ for 10 min. To this was added a solution of **3.15** (181 mg, 0.645 mmol) and **3.36** (168 mg, 0.645 mmol) in THF (3 mL) and MeOH (3 mL) and the resulting mixture stirred for 1 h. The reaction was quenched with $H_2O$ (15 mL) and the resulting

mixture extracted with hexanes (2 × 30 mL). The organic phase were combined and washed with $H_2O$ (15 mL), brine (15 mL), and dried over $Na_2SO_4$. The solvent was removed in vacuo and the crude product purified by column chromatography (silica gel, hexanes) to yield **3.35** (45 mg, 18%) as a yellow solid.

**Data for 3.35:** $R_f$ = 0.56 (hexanes); IR (cast film, $CCl_4$) 2930, 2855, 2203, 2170, 2072, 1452 $cm^{-1}$; $^1H$ NMR (400 MHz, $CDCl_3$): $\delta$ 1.93-1.97 (m, 3H), 1.84-1.87 (m, 6H), 1.61-1.71 (m, 6H), 0.93 (s, 9H), 0.13 (s, 6H); $^{13}C$ NMR (100 MHz, $CDCl_3$): $\delta$ 88.6, 88.4, 87.7, 64.6, 63.2, 63.1, 62.8, 62.2, 62.1, 61.9, 61.7, 61.6, 41.7, 36.0, 30.4, 27.5, 26.0, 16.9, –5.0; EIMS *m/z* 394.2 ($M^+$, 52), 337.1 ([M – *t*Bu]$^+$, 100); EI HRMS calcd. for $C_{28}H_{30}Si$ ($M^+$) 394.2117, found 394.2113.

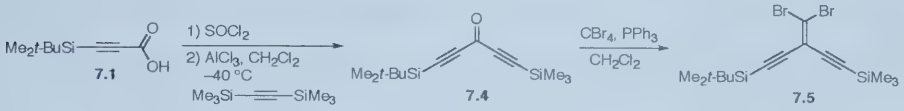


**7.5:** A solution of **7.1** (2.404 mg, 13.04 mmol) in $SOCl_2$ (5 mL) was stirred at rt for 20 h. The $SOCl_2$ was removed in vacuo, 1,2-bis(trimethylsilyl)acetylene (2.441 g, 14.33 mmol) added to the residue, and the resulting mixture dissolved in $CH_2Cl_2$ (15 mL). This solution was added dropwise to a mixture of $AlCl_3$ (1.930 g, 14.47 mmol) in $CH_2Cl_2$ (100 mL) at 0 °C under a $N_2$ atmosphere and then stirred at 0 °C for 3 h. The reaction was quenched slowly with $H_2O$ (50 mL) at 0 °C and allowed to warm to rt. The organic layer was washed with brine (2 × 50 mL) and dried over $MgSO_4$. The solvent was removed in vacuo, the crude product passed through a plug of silica gel with $CH_2Cl_2$, and the solvent removed in vacuo to yield crude ketone **7.4**. Concurrently, to a solution of $CBr_4$ (6.490 g, 19.57 mmol) in $CH_2Cl_2$ (200 mL) was added $PPh_3$ (10.96 g, 41.79 mmol) and the mixture stirred for 1 h under a $N_2$ atmosphere. The crude ketone (**7.4**) was dissolved in $CH_2Cl_2$ (50 mL), added dropwise, and the mixture stirred at rt for 2 h under a $N_2$ atmosphere. The reaction mixture was concentrated in vacuo to ca. 50 mL and then hexanes were added to precipitate the phosphine salts as a white solid along with an oily residue. The supernatant was decanted and filtered through a pad of celite. The oily residue left in the flask was dissolved in minimal $CH_2Cl_2$ and hexanes were added; the heterogeneous mixture was then decanted and the supernatant filtered through celite (this procedure was repeated three times). The solvent was removed in vacuo and the crude product purified by column chromatography (silica gel, hexanes) to yield **7.5** (1.988 mg, 36%) as a brown oil.

**Data for 7.4:** $R_f$ = 0.59 ($CH_2Cl_2$/hexanes 1:1); IR (microscope) 2956, 2932, 2899, 2860, 2161, 1632 $cm^{-1}$; $^1H$ NMR (400 MHz, $CDCl_3$): $\delta$ 0.96 (s, 9H), 0.24 (s, 9H), 0.18 (s, 6H); $^{13}C$ NMR (100 MHz, $CDCl_3$): $\delta$ 160.1, 103.4, 102.6, 99.4, 98.7, 25.9, 16.8, –0.9, –5.4; EIMS *m/z* 264.1 ($M^+$, 7), 497.0 ([M – $C_4H_8$]$^+$, 100); EI HRMS *m/z* calcd. for $C_{14}H_{24}OSi_2$ ($M^+$) 264.1366, found 264.1363.

**Data for 7.5:** $R_f$ = 0.52 (hexanes); IR (microscope) 2955, 2929, 2898, 2858, 2156, 2133 $cm^{-1}$; $^1H$ NMR (400 MHz, $CDCl_3$): $\delta$ 0.95 (s, 9H), 0.21 (s, 9H), 0.15 (s, 6H); $^{13}C$ NMR (100 MHz, $CDCl_3$):

$\delta$ 114.4, 110.1, 102.6, 101.3, 100.6, 100.2, 26.1, 16.8, –0.5, –5.0; EIMS *m/z* 420.0 ($M^+$, 14), 362.9 ($[M - t\text{Bu}]^+$, 66), 145.0 ($[M - Br_2 - Si t\text{BuMe}_2]^+$, 100); EI HRMS *m/z* calcd. for $C_{15}H_{24}Si_2{}^{79}Br^{81}Br$ ($M^+$) 419.9763, found 419.9762.

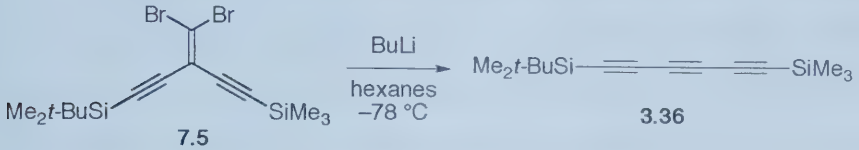


**7.5** **3.36**

**3.36:** To a solution of **7.5** (2.000 g, 4.758 mmol) in hexanes (150 mL) was added BuLi (2.3 mL, 2.5M in hexanes, 5.7 mmol) dropwise under a $N_2$ atmosphere. The reaction mixture was stirred at –78 °C for 10 min, warmed to rt over 30 min and stirred for 1 h. The reaction was cooled to –78 °C and quenched with saturated $NH_4Cl$ (50 mL). The resulting layers were separated and the organic layer washed with $H_2O$ (50 mL), brine (50 mL), and dried over $Na_2SO_4$. The solvent was removed in vacuo and the crude product purified by column chromatography (silica gel, hexanes) to yield **3.36** (0.636 g, 51%) as an amber oil: $R_f$ = 0.60 (hexanes); IR (microscope) 2955, 2930, 2898, 2858, 2159, 1471 $cm^{-1}$; $^1H$ NMR (400 MHz, $CDCl_3$): $\delta$ 0.92 (s, 9H), 0.18 (s, 9H), 0.12 (s, 6H); $^{13}C$ NMR (100 MHz, $CDCl_3$): $\delta$ 88.5, 88.0, 87.3, 86.3, 62.1, 61.5, 26.0, 16.8, –0.6, –5.0; EIMS *m/z* 260.1 ($M^+$, 14), 203.1 ($[M - t\text{Bu}]^+$, 100); EI HRMS *m/z* calcd. for $C_{15}H_{24}Si_2$ ($M^+$) 260.1417, found 260.1414.

**3.1a**

**3.1a was synthesized by adaptation of a known procedure:**[14] To a solution of **3.2** (226 mg, 1.41 mmol) in THF (40 mL) was added $PdCl_2(PPh_3)_2$ (49 mg, 0.071 mmol), CuI (14 mg, 0.071 mmol), ethyl bromoacetate (200 µL, 1.80 mmol) and $Et_3N$ (400 µL, 2.87 mmol) in that order. The reaction mixture was stirred at rt for 18 h under a $N_2$ atmosphere. The reaction was quenched with $H_2O$ (20 mL) and then extracted with $Et_2O$ (3 × 20 mL). The organic layers were combined, washed with brine (20 mL), and then dried over $MgSO_4$. The solvent was removed in vacuo and the crude product was passed through a short silica gel plug with $CH_2Cl_2$. The filtrate was treated with activated charcoal, filtered through a celite pad, and concentrated to dryness. The crude product was recrystallized from dioxane to yield **3.1a** (186 mg, 59%) as an off-white solid: Mp 338-341 °C (lit. 348-350 °C);[9] $R_f$ = 0.36 (hexanes); IR (microscope) 2899, 2848, 2164, 2137, 1449, 1098 $cm^{-1}$; $^1H$ NMR (300 MHz, $CDCl_3$): $\delta$ 1.92-1.98 (m, 6H), 1.82-1.88 (m, 12H), 1.60-1.70 (m, 12H); $^{13}C$ NMR (100 MHz, $CDCl_3$): $\delta$ 86.0, 64.0, 42.4, 36.2, 30.1, 27.8; EI HRMS calcd. for $C_{24}H_{30}$ ($M^+$) 318.2347, found 318.2352.

3.1b

**3.1b**: To a solution of **3.8** (0.269 g, 0.536 mmol) in hexanes (60 mL) at –78 °C was added BuLi (260 μL, 2.5M in hexanes, 0.65 mmol) dropwise under a $N_2$ atmosphere. The reaction mixture was stirred at –78 °C for 10 min and then warmed to rt over 20 min. The reaction was cooled to –78 °C and quenched by the addition of saturated $NH_4Cl$ (10 mL). The mixture was warmed to rt, the layers separated and the organic layer dried over $Na_2SO_4$. The solvent was removed in vacuo and the crude product was purified by column chromatography (silica gel, hexanes) to yield **3.1b** (0.149 g, 81%) as a white solid: Mp 242-244 °C (lit. 237-241 °C);[15] $R_f$ = 0.37 (hexanes); IR (cast film, $CH_2Cl_2$) 2914, 2901, 2850, 2211, 1448 $cm^{-1}$; $^1H$ NMR (400 MHz, $CDCl_3$): $\delta$ 1.90-1.96 (m, 6H), 1.82-1.86 (m, 12H), 1.60-1.70 (m, 12H); $^{13}C$ NMR (100 MHz, $CDCl_3$): $\delta$ 86.6, 64.7, 61.6, 42.1, 36.1, 30.2, 27.7; EI HRMS calcd. for $C_{26}H_{30}$ ($M^+$) 342.2347, found 342.2343.

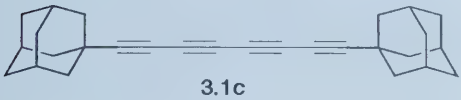

3.1c

**3.1c**: To a solution of CuCl (114 mg, 1.15 mmol) in $CH_2Cl_2$ (20 mL) was added TMEDA (300 μL, 1.99 mmol), and $O_2$ was bubbled through the solution for 20 min. A solution of **3.11** (212 mg, 1.15 mmol) in $CH_2Cl_2$ (5 mL) was added to the catalyst mixture and allowed to stir at rt for 1 h. The reaction was quenched with $H_2O$ (10 mL) and the organic layer washed with saturated $NH_4Cl$ (20 mL) and dried over $MgSO_4$. The solvent was removed in vacuo and the crude product was purified by column chromatography (silica gel, hexanes) to yield **3.1c** (210 mg, quantitative) as a white solid: Mp 215-217 °C (lit. 217-219 °C);[15] $R_f$ = 0.44 (hexanes); IR (microscope) 2921, 2852, 2217, 1450 $cm^{-1}$; UV-Vis (hexanes) $\lambda_{max}$ ($\varepsilon$) 247 (273000), 235 (200000), 224 (81000), 214 (23000) nm; UV-Vis (THF) $\lambda_{max}$ ($\varepsilon$) 250 (229000), 238 (168000), 226 (71000) nm; $^1H$ NMR (500 MHz, $CDCl_3$): $\delta$ 1.90-1.98 (m, 6H), 1.82-1.88 (m, 12H), 1.60-1.70 (m, 12H); $^{13}C$ NMR (125 MHz, $CDCl_3$): $\delta$ 87.2, 64.8, 61.9, 61.6, 41.9, 36.1, 30.3, 27.6; EI HRMS calcd. for $C_{28}H_{30}$ ($M^+$) 366.2347, found 366.2348; DSC: decomposition, 224 °C (onset) and 230 °C (peak).

**X-ray Crystal Data for 3.1c**: Single crystals of **3.1c** suitable for X-ray crystallographic analysis were grown by slow evaporation of a solution of **3.1c** in THF at rt. $C_{28}H_{30}$, $M_r$ = 366.54; crystal dimensions: 0.58 × 0.35 × 0.34 $mm^3$; crystal system: monoclinic; space group *C*2/*c* (No. 15), $a$ = 17.0112 (15), $b$ = 12.7895 (12), $c$ = 11.8476 (11) Å; $\beta$ = 97.3220 (10)°; $V$ = 2556.6 (4) $Å^3$, $Z$ = 4; $\rho$calcd = 1.140 g $cm^{-3}$; $\mu$ = 0.066 $mm^{-1}$; $\lambda$ = 0.71073 Å; T = –80 °C; 2$\theta$ max = 52.80°; total data collected = 9416; $R_1$ = 0.0658 for 1912 observed reflections with $[F_o^2 \geq 2\sigma(F_o^2)]$; $wR_2$ = 0.2112 for 253 variables and 2618 unique reflections with $[F_o^2 \geq -3\sigma(F_o^2)]$; residual electron density = 0.269 and –0.144 e $Å^{-3}$. CCDC-660940.

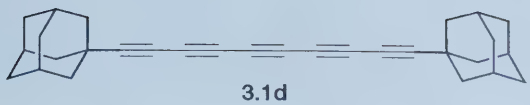

**3.1d**

**3.1d:** To a solution of **3.17** (0.553 g, 1.00 mmol) in hexanes (100 mL) at –78 °C was added BuLi (480 μL, 2.5M in hexanes, 1.20 mmol) dropwise under a $N_2$ atmosphere. The reaction mixture was stirred at –78 °C for 10 min, and then warmed to 0 °C over 10 min. The reaction was quenched at 0 °C with saturated $NH_4Cl$ (20 mL). The mixture was warmed to rt, extracted with a mixture of $CH_2Cl_2$ (20 mL) and hexanes (100 mL), and the organic layer was dried over $Na_2SO_4$. The solvent was removed in vacuo, the crude product was stirred in hot hexanes, cooled to 0 °C and filtered to yield **3.1d** (0.274 g, 70%) as a pale yellow solid: $R_f$ = 0.52 (hexanes); IR (cast film, $CH_2Cl_2$) 2929, 2911, 2851, 2206, 1449 $cm^{-1}$; UV-Vis (hexanes) $\lambda_{max}$ (ε) 272 (405000), 258 (278000), 245 (114000), 233 (35000), 223 (12000); UV-Vis (THF) $\lambda_{max}$ (ε) 276 (332000), 261 (228000), 248 (96000), 234 (35000) nm; $^1H$ NMR (400 MHz, $CDCl_3$): δ 1.92-1.97 (m, 6H), 1.83-1.87 (m, 12H), 1.61-1.71 (m, 12H); $^{13}C$ NMR (100 MHz, $CDCl_3$): δ 87.9, 64.7, 62.2, 62.1, 61.8, 41.8, 36.0, 30.3, 27.5; EI HRMS calcd. for $C_{30}H_{30}$ ($M^+$) 390.2347, found 390.2343; DSC: decomposition, 215 °C (onset) and 225 °C (peak).

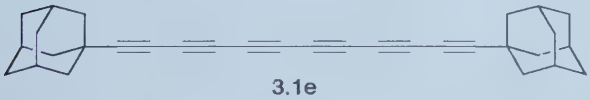

**3.1e**

**3.1e:** To a solution of **3.27** (0.829 g, 1.13 mmol) in hexanes (175 mL) at –78 °C was added BuLi (1.10 mL, 2.5M in hexanes, 2.71 mmol) dropwise. The reaction mixture was stirred at –78 °C for 10 min, warmed to 0 °C over 10 min and allowed to stir at 0 °C for 1 h. The reaction was quenched at 0 °C with saturated $NH_4Cl$ (50 mL). The mixture was warmed to rt, $CH_2Cl_2$ (100 mL) was added to dissolve the precipitate and the layers separated. The organic layer was dried over $MgSO_4$. The solvent was removed in vacuo, the crude product was dissolved in minimal hot toluene and passed through a short plug of silica gel with hexanes. The product was then recrystallized from toluene to yield **3.1e** (0.348 g, 74%) as a yellow solid: $R_f$ = 0.48 (hexanes); IR (microscope) 2912, 2852, 2191, 2171, 1450, 1320 $cm^{-1}$; UV-Vis (hexanes) $\lambda_{max}$ (ε) 295 (480000), 279 (343000), 264 (151000), 251 (50000), 240 (17000); UV-Vis (THF) $\lambda_{max}$ (ε) 300 (361000), 283 (262000), 268 (109000), 254 (34000) nm; $^1H$ NMR (500 MHz, $CDCl_3$): δ 1.92-1.97 (m, 6H), 1.81-1.90 (m, 12H), 1.61-1.70 (m, 12H); $^{13}C$ NMR (125 MHz, $CDCl_3$): δ 88.3, 64.7, 62.7, 62.6, 62.0, 61.7, 41.7, 36.0, 30.4, 27.5; EI HRMS calcd. for $C_{32}H_{30}$ ($M^+$) 414.2347, found 414.2344; DSC: decomposition, 189 °C (onset), 205 °C (peak).

**X-ray Crystal Data for 3.1f**: Single crystals of **3.1e** suitable for X-ray crystallographic analysis were grown by slow diffusion of MeOH into a solution of **3.1e** in toluene at rt. $C_{32}H_{30}$, $M_r$ =

414.58; crystal dimensions: 0.53 × 0.28 × 0.07 $mm^3$; crystal system: monoclinic; space group $P\bar{1}$ (No. 2), $a$ = 9.819 (2), $b$ = 10.829 (2), $c$ = 11.772 (3) Å; $\alpha$ = 90.172 (4)°; $\beta$ = 105.664 (3)°; $\gamma$ = 102.286 (3)°; $V$ = 1175.2 (4) $Å^3$, $Z$ = 2; $\rho$calcd = 1.172 g $cm^{-3}$; $\mu$ = 0.066 $mm^{-1}$; $\lambda$ = 0.71073 Å; T = –80 °C; 2$\theta$ max = 50.00°; total data collected = 7101; $R_1$ = 0.0544 for 2870 observed reflections with [$F_o^2 \geq 2\sigma(F_o^2)$]; $wR_2$ = 0.1551 for 289 variables and 4112 unique reflections with [$F_o^2 \geq -3\sigma(F_o^2)$]; residual electron density = 0.221 and –0.162 e $Å^{-3}$. CCDC-660941.

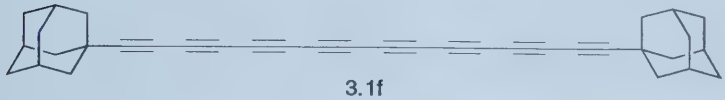

**3.1f**

**3.1f (Hay coupling):** To a mixture of CuCl (95 mg, 0.958 mmol) in THF (5 mL) and MeOH (5 mL) was added TMEDA (0.230 mg, 0.300 mL, 1.92 mmol). $O_2$ was bubbled through the solution for 20 min, a solution of **3.30**[16] (146 mg, 0.479 mmol) in THF (5 mL) was added and the mixture was stirred for 30 min at rt. The reaction was quenched with $H_2O$ (15 mL) and extracted with $Et_2O$ (2 × 30 mL). The organic layer was washed with brine and then dried over $MgSO_4$. The solvent was removed in vacuo and the crude product was immediately purified by passing through a short plug of silica gel with $CH_2Cl_2$. The solvent was removed in vacuo and the resulting solid was washed with ether to yield **3.1f**[17] (83 mg, 75%) as a yellow solid.

**3.1f (two-fold FBW rearrangement):** To a solution of **3.28** (85 mg, 0.11 mmol) in hexanes (150 mL) at –78 °C was added BuLi (0.13 mL, 2.5M in hexanes, 0.33 mmol) dropwise. The reaction mixture was stirred at –78 °C for 1.5 h under a $N_2$ atmosphere, warmed to –20 °C over 10 min and stirred for and additional 10 min. The reaction was quenched at –20 °C with saturated $NH_4Cl$ (50 mL). The mixture was warmed to rt, the layers separated and the organic layer dried over $Na_2SO_4$. The solvent was removed in vacuo and the crude product was purified by column chromatography (silica gel, hexanes) to yield **3.1f**[17] (19 mg, 38%) as a yellow solid.

**Data for 3.1f:** $R_f$ = 0.56 (hexanes); IR (microscope) 2902, 2850, 2203, 2126, 2021(w), 1449 $cm^{-1}$; UV-Vis (hexanes) $\lambda_{max}$ ($\varepsilon$) 335 (617000), 314 (497000), 297 (225000), 282 (79000), 268 (29000) nm; UV-Vis (THF) $\lambda_{max}$ ($\varepsilon$) 340 (428000), 319 (338000), 301 (153000), 286 (61000), 273 (29000) nm; $^1$H NMR (500 MHz, $CDCl_3$): $\delta$ 1.92-1.98 (m, 6H), 1.83-1.88 (m, 12H), 1.60-1.72 (m, 12H); $^{13}$C NMR (125 MHz, $CDCl_3$): $\delta$ 88.8, 64.6, 63.4, 63.3, 62.9, 62.3, 61.7, 61.5, 41.7, 36.0, 30.4, 27.5; MALDI MS (DCTB) $m/z$ 462.6 ($M^+$, 100); MALDI HRMS $m/z$ calcd. for $C_{36}H_{30}$ ($M^+$) 462.2342, found 462.2342; DSC: decomposition, 105 °C (onset), 110 °C (peak).

**3.1h**

**3.1h:** To a solution of **3.23** (0.295 g, 0.604 mmol) in hexanes (30 mL) at –78 °C under a $N_2$ atmosphere was added BuLi (290 μL, 2.5M in hexanes, 0.725 mmol) dropwise. The mixture was stirred for 10 min at –78 °C and then allowed to warm to rt over 30 min. The reaction was cooled to –78 °C and then quenched with saturated $NH_4Cl$ (10 mL). The mixture was warmed to rt, the layers separated, and the organic layer dried over $Na_2SO_4$. The volume was reduced in vacuo to ca. 10 mL and then held for later use (**3.31**).[18] To a solution of $Cu(OAc)_2 \cdot H_2O$ (1.21 g, 6.04 mmol) in pyridine (20 mL) and MeOH (20 mL) was added $K_2CO_3$ (0.835 g, 6.04 mmol) and then the **3.31** solution. The reaction was stirred at rt for 1.5 h, quenched with $H_2O$ (100 mL) and then extracted with $CHCl_3$ (150 mL). The aqueous phase was extracted again with $CHCl_3$ (50 mL), the organic layers combined, washed with $H_2O$ (50 mL), saturated aqueous $NH_4Cl$ (50 mL), and dried over $MgSO_4$. The solvent was removed in vacuo and the crude product was passed through a short plug of silica gel with $CHCl_3$. The volume was reduced in vacuo until a precipitate formed, cooled to 0 °C, and filtered to yield **3.1h**[17] (45 mg, 29%) as an orange solid: $R_f$ = 0.62 (hexanes); IR (microscope) 2902, 2851, 2193, 2078, 1449 $cm^{-1}$; UV-Vis (hexanes) $\lambda_{max}$ 367, 344, 324, 306, 291, 278, 266, 258, 249, 239, 229, 220 nm; UV-Vis (THF) $\lambda_{max}$ 373, 349, 328, 310, 294, 280 nm; $^1H$ NMR (500 MHz, $CDCl_3$): $\delta$ 1.93-1.98 (m, 6H), 1.84-1.88 (m, 12H), 1.62-1.71 (m, 12H); $^{13}C$ NMR (125 MHz, $CDCl_3$): $\delta$ 89.1, 64.6, 63.9, 63.7, 63.5, 63.0, 62.6, 62.1, 61.6, 61.4, 41.7, 36.0, 30.4, 27.5; MALDI MS (DCTB) *m/z* 510.3 ($M^+$, 100, $C_{40}H_{30}$); MALDI HRMS (DCTB) *m/z* calcd. for $C_{40}H_{30}$ ($M^+$) 510.2342, found 510.2339; DSC: decomposition, 83 °C (onset) and 90 °C (peak).

**3.1k**

**3.1k:** To a solution of **3.35** (45 mg, 0.11 mmol) in THF (10 mL) and $H_2O$ (2 mL) was added KF (33 mg, 0.57 mmol) and the resulting mixture stirred for 30 min. The reaction was quenched with $H_2O$ (10 mL) and the resulting mixture extracted with $Et_2O$ (30 mL). The layers were separated and the organic phase washed with $H_2O$ (10 mL), brine (10 mL), and dried over $Na_2SO_4$. The filtrated was concentrated to ca. 10 mL and added to a solution of $PdCl_2(PPh_3)_2$ (4 mg, 0.006 mmol), CuI (1 mg, 0.005), $Et_3N$ (31 μL, ) in THF (20 mL) and the reaction stirred at rt under a $N_2$ atmosphere for 1 h. The solvent was removed in vacuo and the crude product purified by column chromatography (silica gel, $CHCl_3$) to yield **3.1k**[19] (Note: compound **3.1k** was not isolated due to extreme instability in the solid-state. Also, the $n$ = 11 (**3.1j**) side product also formed, however, enough pure **3.1k** was isolated to obtain a pure UV-Vis spectrum): $R_f$ = 0.63 (hexanes); UV-Vis (THF) $\lambda_{max}$ 398, 371, 348, 330, 314, 284, 274, 263, 252, 241 nm.

## 7.3 *t*-Butyl-Endcapped Polyynes (Chapter 4 data)

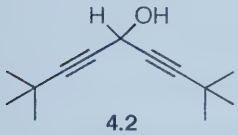


**4.2**

**4.2:**[20] A solution of 3,3-dimethylbutyne (1.077 g, 13.11 mmol) in THF (50 mL) was cooled to 0 °C under a $N_2$ atmosphere and HexLi (5.7 mL, 2.3M in hexanes, 13 mmol) was added dropwise. The mixture was stirred for 20 min at 0 °C and ethyl formate (0.441 g, 5.96 mmol) was added dropwise over 10 min at 0 °C. The mixture was warmed to rt and stirred for 2 h. The reaction was quenched by the addition of saturated aqueous $NH_4Cl$ (20 mL) and extracted with $Et_2O$ (2 × 50 mL). The organic layer was washed with brine (20 mL) and dried over $MgSO_4$. The solvent was removed in vacuo and the crude product purified by column chromatography (silica gel, EtOAc/hexanes 1:4) to yield **4.2** (1.100 g, 96%) as a white solid: Mp 75-76 °C (lit. Mp = 75-77 °C);[20] $R_f$ = 0.43 (EtOAc/hexanes, 1:4); IR (microscope) 3348, 2969, 2929, 2900, 2867, 2242, 1458 $cm^{-1}$; $^1H$ NMR (400 MHz, $CDCl_3$): $\delta$ 5.06 (d, $J$ = 7.2 Hz, 1H), 2.02 (d, $J$ = 7.2 Hz, 1H), 1.20 (s, 18H); $^{13}C$ NMR (100 MHz, $CDCl_3$): $\delta$ 92.8, 76.8, 52.6, 30.7, 27.3; EI HRMS *m/z* calcd. for $C_{13}H_{19}O$ ($[M - H]^+$) 191.1436, found 191.1433. CAS: 50428-39-2.

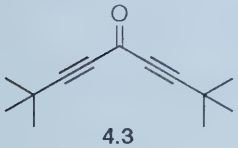


**4.3**

**4.3:** To a solution of **4.2** (1.079 g, 5.611 mmol) in $CH_2Cl_2$ (50 mL) was added celite (5 g), molecular sieves (5 g) and PCC (2.113 g, 9.802 mmol) in that order and the reaction stirred at rt under a $N_2$ atmosphere for 24 h. The mixture was filtered through a silica plug with $CH_2Cl_2$ and the solvent removed in vacuo to yield **4.3** (0.946 g, 89%) as a yellow solid: Mp 61-62°C (lit. Mp = 66.5 °C);[21] $R_f$ = 0.60 (EtOAc/hexanes, 1:4); IR (microscope) 2974, 2933, 2904, 2871, 2255, 2207, 1631, 1458, 1273 $cm^{-1}$; $^1H$ NMR (400 MHz, $CDCl_3$): $\delta$ 1.27 (s); $^{13}C$ NMR (100 MHz, $CDCl_3$): $\delta$ 161.9, 101.3, 80.9, 29.9, 27.8; EIMS m/z 190.1 ($M^+$, 34), 175.1 ($[M - CH_3]^+$, 36), 162.1 ($[M - CO]^+$, 18), 147.1 ($[M - CH_3 - CO]^+$, 49); EI HRMS *m/z* calcd. for $C_{13}H_{18}O$ ($M^+$) 190.1358, found 190.1357. CAS: 35845-67-1.

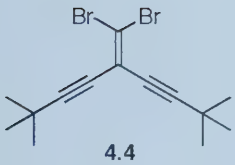


**4.4**

**4.4:** To a solution of $CBr_4$ (2.345 g, 7.071 mmol) in $CH_2Cl_2$ (60 mL) was added $PPh_3$ (3.978 g, 15.17 mmol) and the mixture stirred for 1 h at rt under a $N_2$ atmosphere. A solution of **4.3** (0.897 g, 4.714 mmol) in $CH_2Cl_2$ (10 mL) was added slowly over 10 min and the reaction mixture stirred at rt under a $N_2$ atmosphere for 20 h. Hexanes were added to precipitate the phosphine salts as a white solid along with an oily residue. The supernatant was decanted and filtered through a pad of celite. The oily residue left in the flask was dissolved in minimal $CH_2Cl_2$ and hexanes were added; the heterogeneous mixture was then decanted and the supernatant filtered through celite (this procedure was repeated three times). The solvent was removed in vacuo and the crude product passed through a plug of silica gel with hexanes, the solvent removed in vacuo and the crude product purified by column chromatography (silica gel, hexanes) to yield **4.4** (1.535 g, 94%) as a yellow oil: $R_f$ = 0.41 (hexanes); IR (microscope) 2971, 2929, 2899, 2868, 2219, 1455 $cm^{-1}$; $^1H$ NMR (500 MHz, $CDCl_3$): $\delta$ 1.26 (s); $^{13}C$ NMR (125 MHz, $CDCl_3$): $\delta$ 114.6, 105.2, 104.9, 76.8, 30.4, 28.4; EI HRMS *m/z* calcd. for $C_{14}H_{18}{}^{79}Br^{81}Br$ ($M^+$) 345.9755, found 345.9758.

**4.5**

**4.5:**[22] To a solution of 3,3-dimethylbutyne (4.17 g, 50.8 mmol) in MeOH (270 mL) and $H_2O$ (30 mL) was added CuCl (0.752 g, 7.60 mmol), $NH_2OH$•HCl (1.056 g, 15.20 mmol) and *n*-butylamine (15 mL). A solution of 1-bromo-3-methyl-1-butyn-3-ol (12.44 g, 76.31 mmol) in MeOH (30 mL) was added slowly over 30 min and the reaction was stirred at rt for 18 h. The volume of the reaction was reduced in vacuo to ca. 50 mL and $Et_2O$ was added (200 mL). The mixture was washed with saturated aqueous $NH_4Cl$ (5 × 50 mL), brine (50 mL), and dried over $Na_2SO_4$. The solvent was removed in vacuo and the crude product purified by column chromatography (silica gel, EtOAc/hexanes 1:3) to yield **4.5** (6.35 g, 76%) as a pale yellow solid. The product was recrystallized from petroleum ether to yield **4.5** (5.11 g, 61%) as a white solid: Mp 96-97°C (lit. Mp = 99-100 °C)[22]; $R_f$ = 0.40 (EtOAc/hexanes, 1:3); IR (microscope) 3341, 2972, 2932, 2867, 2259, 1363 $cm^{-1}$; $^1H$ NMR (300 MHz, $CDCl_3$): $\delta$ 1.94 (s, 1H), 1.50 (s, 6H), 1.22 (s, 9H); $^{13}C$ NMR (125 MHz, $CDCl_3$): $\delta$ 89.4, 81.1, 67.2, 65.6, 63.0, 31.2, 30.4, 28.0; EIMS *m/z* 164.1 ($M^+$, 13), 149.1 ($[M - CH_3]^+$, 100); EI HRMS *m/z* calcd. for $C_{11}H_{16}O$ ($M^+$) 164.1201, found 164.1204; Anal. calcd. for $C_{11}H_{16}O$: C, 80.44; H, 9.82. Found: C, 80.43; H, 9.83. CAS: 56391-23-2.

**4.6**

**4.6**[23]: To a solution of **4.13** (1.512 g, 4.175 mmol) in hexanes (100 mL) at –78 °C was added BuLi (2.0 mL, 2.5M in hexanes, 5.0 mmol) dropwise under a $N_2$ atmosphere. The reaction mixture was stirred at –78 °C for 10 min, warmed to 0 °C over 20 min and the reaction was quenched by the addition of saturated aqueous $NH_4Cl$ (25 mL). The layers were separated and the organic layer dried over $Na_2SO_4$. The solvent was removed in vacuo and the crude product was purified by column chromatography (silica gel, hexanes) to yield **4.6** (0.724 g, 86%) as a pale yellow solid. Mp 36-38 °C; $R_f$ = 0.45 (hexanes); IR (microscope) 2971, 2932, 2901, 2868, 2203, 2170, 2076, 1456 $cm^{-1}$; $^1H$ NMR (500 MHz, $CDCl_3$): $\delta$ 1.23 (s, 9H), 0.17 (s, 9H); $^{13}C$ NMR (125 MHz, $CDCl_3$): $\delta$ 88.3, 88.2, 85.8, 64.2, 62.3, 61.2, 30.3, 28.2, –0.5; EIMS *m/z* 202.1 ($M^+$, 43), 187.1 ($[M - CH_3]^+$, 100); EI HRMS *m/z* calcd. for $C_{13}H_{18}Si$ ($M^+$) 202.1178, found 202.1178.

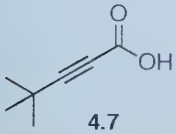

**4.7**

**4,4-Dimethyl-2-pentynoic acid (4.7):** A solution of 3,3-dimethylbutyne (1.154 g, 14.05 mmol) in THF (50 mL) was cooled to –78 °C under a $N_2$ atmosphere and BuLi (5.6 mL, 2.5 M in hexanes, 14 mmol) was added dropwise. The mixture was stirred at –78 °C for 30 min and $CO_2$ (g) (passed through a drying tube filled with drierite) was bubbled through the reaction mixture for 20 min. The mixture was warmed to rt, the flow of $CO_2$ was stopped, the reaction quenched by the addition of $H_2O$ (10 mL), acidified with 10% aqueous HCl, and then extracted with $Et_2O$ (100 mL). The organic layer was extracted with 5% aqueous $Na_2CO_3$ (2 × 50 mL). The aqueous layers were combined, acidified with 10% aqueous HCl and extracted with $Et_2O$ (100 mL). The organic layer was washed with brine then dried over $MgSO_4$. The solvent was removed in vacuo to yield 4,4-dimethyl-2-pentynoic acid **4.7** (1.404 g, 79%) as a colorless oil: (lit. Mp = 47-48 °C);[24] IR (cast film, $CH_2Cl_2$) 2975, 2872, 2219, 1686, 1410, 1277 $cm^{-1}$;[25] $^1H$ NMR (300 MHz, $CDCl_3$): $\delta$ 11.58 (br s, 1H), 1.26 (s, 9H);[26] $^{13}C$ NMR (125 MHz, $CDCl_3$): $\delta$ 158.9, 99.6, 71.3, 29.8, 27.6; EIMS *m/z* 125.1 ($[M - H]^+$, 10), 111.0 ($[M - Me]^+$, 72), 83.0 ($[M - CH_3 - CO]^+$, 100); EI HRMS *m/z* calcd. for $C_7H_9O$ $[M - H]^+$ 125.0603, found 125.0602.

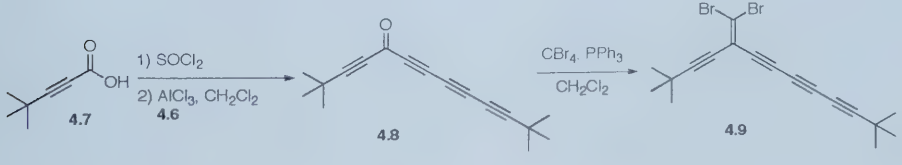


**4.7** **4.6** **4.8** **4.9**

**4.9:** A solution of **4.7** (0.618 g, 4.90 mmol) in $CHCl_3$[27] (25 mL) and $SOCl_2$ (4 mL) was stirred at reflux for 24 h covered with a $CaCl_2$ drying tube. The solvent was removed in vacuo and **4.6** (0.185 g, 0.914 mmol) was added to the residue and the resulting mixture was dissolved in $CH_2Cl_2$ (10 mL). This solution was added dropwise to a mixture of $AlCl_3$ (0.667 g, 5.00 mmol) in $CH_2Cl_2$ (20 mL) at –40 °C. The reaction was allowed to stir at –40 °C for 1 h. The reaction mixture was quenched slowly by the addition of $H_2O$ (10 mL) at –40 °C and allowed to warm to rt. The organic layer was washed with brine (10 mL) and then dried over $MgSO_4$. The solvent was removed in vacuo. The crude intermediate (**4.8**) was passed through a plug of silica gel with $CH_2Cl_2$, and the filtrate concentrated to ca. 10 mL and held for later. To a solution of $CBr_4$ (0.663 g, 2.00 mmol) in $CH_2Cl_2$ (20 mL) was added $PPh_3$ (1.075 g, 4.099 mmol) and stirred at rt for 1 h under a $N_2$ atmosphere. The solution of **4.8** was added dropwise and the reaction mixture was stirred at rt until judged complete by TLC analysis (ca. 0.5 hrs). Hexanes were added to precipitate the phosphine salts as a white solid along with an oily residue. The supernatant was decanted and filtered through a pad of celite. The oily residue left in the flask was dissolved in minimal $CH_2Cl_2$ and hexanes were added; the heterogeneous mixture was then decanted and the supernatant filtered through celite (this procedure was repeated three times). The filtrate was filtered through celite until the filtrate remained a clear solution. The solvent was removed and the crude product was purified by column chromatography (silica gel, hexanes) to yield **4.9** (0.162 g, 45%) as an amber oil: $R_f$ = 0.43 (hexanes); IR (microscope) 2971, 2930, 2899, 2867, 2213, 2185, 1455 $cm^{-1}$; $^1H$ NMR (400 MHz, $CDCl_3$): $\delta$ 1.25 (s, 9H), 1.24 (s, 9H); $^{13}C$ NMR (100 MHz, $CDCl_3$): $\delta$ 113.4, 110.5, 106.7, 91.8, 80.1, 75.6, 72.0, 70.5, 64.4, 60.4, 30.3, 30.2, 28.5, 28.4; EI HRMS *m/z* calcd. for $C_{18}H_{18}{}^{79}Br^{81}Br$ ($M^+$) 393.9755, found 393.9743.

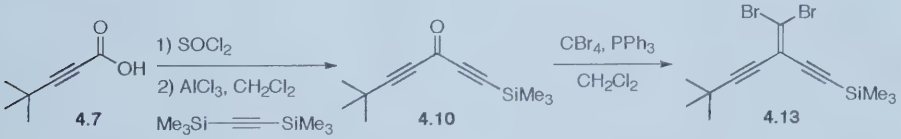


**4.13:** A solution of **4.7** (0.719 g, 5.70 mmol) in $SOCl_2$ (3 mL) was stirred at rt for 20 h covered with a $CaCl_2$ drying tube. The excess $SOCl_2$ was removed in vacuo. Bis(trimethylsilyl)acetylene (1.068 g, 6.27 mmol) was added to the residue and the resulting mixture was dissolved in $CH_2Cl_2$ (10 mL). This solution was added to a mixture of $AlCl_3$ (0.847 g, 6.35 mmol) in $CH_2Cl_2$ (60 mL) dropwise at –40 °C. The reaction was allowed to stir at –40 °C for 1 h. The solution was warmed to rt, stirred for 3 h, cooled to 0 °C, quenched slowly by the addition of $H_2O$ (25 mL); **caution, exothermic**. The organic layer was allowed to warm to rt and washed with brine (25 mL) and dried over $MgSO_4$. The solvent was removed in vacuo and the crude product (**4.10**) was passed through a plug of silica gel with $CH_2Cl_2$, concentrated to ca. 10 mL and held for later. To a solution of $CBr_4$ (3.805 g, 11.47 mmol) in $CH_2Cl_2$ (100 mL) was added $PPh_3$ (6.720 g, 25.62 mmol) and stirred at rt for 30 min under a $N_2$ atmosphere. The solution of **4.10** was added

dropwise and the reaction mixture was stirred at rt for 16 h. Hexanes were added to precipitate the phosphine salts as a white solid along with an oily residue. The supernatant was decanted and filtered through a pad of celite. The oily residue left in the flask was dissolved in minimal $CH_2Cl_2$ and hexanes were added; the heterogeneous mixture was then decanted and the supernatant filtered through celite (this procedure was repeated three times). The filtrate was filtered through celite until the filtrate remained a clear solution. The solvent was removed and the crude product was purified by column chromatography (silica gel, hexanes) to yield **4.13** (1.654 g, 80%) as an amber oil: $R_f$ = 0.48 (hexanes); IR (microscope) 2970, 2900, 2214, 2149, 1251 $cm^{-1}$; $^1H$ NMR (300 MHz, $CDCl_3$): $\delta$ 1.26 (s, 9H), 0.21 (s, 9H); $^{13}C$ NMR (100 MHz, $CDCl_3$): $\delta$ 114.4, 107.9, 105.8, 101.7, 100.7, 76.3, 30.4, 28.4, –0.4; EIMS *m/z* 362.0 ($M^+$, 75), 346.9 ([M – $CH_3$]$^+$, 35), 283.0 ([M – $^{81}Br$]$^+$, 100); EI HRMS *m/z* calcd. for $C_{13}H_{18}{}^{79}Br^{81}BrSi$ ($M^+$) 361.9524, found 361.9521.

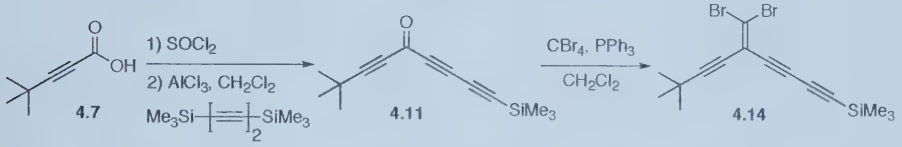


**4.14:** A solution of **4.7** (0.864 g, 6.85 mmol) in $SOCl_2$ (5 mL) was stirred at rt for 20 h covered with a $CaCl_2$ drying tube. The excess $SOCl_2$ was removed in vacuo. 1,4-Bis(trimethylsilyl)-1,3-butadiyne (1.11 g, 5.71 mmol) was added to the residue and the resulting mixture was dissolved in $CH_2Cl_2$ (15 mL). This solution was added to a mixture of $AlCl_3$ (0.852 g, 6.39 mmol) in $CH_2Cl_2$ (100 mL) dropwise at –40 °C. The reaction was allowed to stir at –40 °C for 1 h then warmed to rt and stirred for 30 min. The reaction mixture was quenched slowly by the addition of $H_2O$ (20 mL) at –40 °C and allowed to warm to rt. The organic layer was separated, washed with brine (20 mL), and dried over $MgSO_4$. The solvent was removed in vacuo and the crude product (**4.11**) was passed through a plug of silica gel with $CH_2Cl_2$ then concentrated to ca. 5 mL and held for later. To a solution of $CBr_4$ (2.85 g, 8.59 mmol) in $CH_2Cl_2$ (60 mL) was added $PPh_3$ (4.79 g, 18.3 mmol) and stirred at rt for 1 h under a $N_2$ atmosphere. The solution of **4.11** was added dropwise and the reaction mixture was stirred at rt for 16 h. Hexanes were added to precipitate the phosphine salts as a white solid along with an oily residue. The supernatant was decanted and filtered through a pad of celite. The oily residue left in the flask was dissolved in minimal $CH_2Cl_2$ and hexanes were added; the heterogeneous mixture was then decanted and the supernatant filtered through celite (this procedure was repeated three times). The filtrate was filtered through celite until the filtrate remained a clear solution. The solvent was removed and the crude product was purified by column chromatography (silica gel, hexanes) to yield **4.14** (0.976 g, 44%) as an amber oil: $R_f$ = 0.46 (hexanes); IR (microscope) 2970, 2929, 2900, 2868, 2220, 2096, 1251 $cm^{-1}$; $^1H$ NMR (500 MHz, $CDCl_3$): $\delta$ 1.25 (s, 9H), 0.20 (s, 9H); $^{13}C$ NMR (125 MHz, $CDCl_3$): $\delta$ 113.5, 109.9, 106.6, 94.6,

87.3, 79.6, 75.7, 72.7, 30.3, 28.4, -0.6; EI HRMS *m/z* calcd. for $C_{15}H_{18}{}^{79}Br^{81}BrSi$ ($M^+$) 385.9524, found 385.9525.

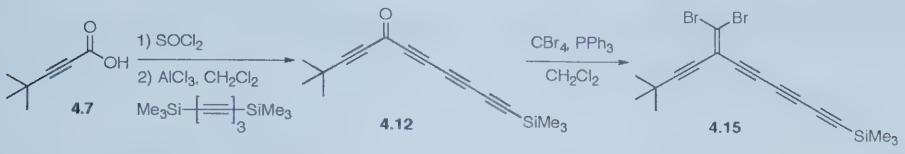


**4.15:** A solution of **4.7** (0.494 g, 3.92 mmol) in $SOCl_2$ (2 mL) was stirred at rt for 20 h covered with a $CaCl_2$ drying tube. The excess $SOCl_2$ was removed in vacuo. 1,6-Bis(trimethylsilyl)-1,3,5-hexatriyne[13] (0.711 g, 3.25 mmol) was added to the residue and the resulting mixture was dissolved in $CH_2Cl_2$ (10 mL). This solution was added to a mixture of $AlCl_3$ (0.530 g, 3.97 mmol) in $CH_2Cl_2$ (40 mL) dropwise at –40 °C. The reaction was allowed to stir at –40 °C for 2 h. The reaction mixture was quenched slowly by the addition of $H_2O$ (20 mL) at –40 °C and allowed to warm to rt. The organic layer was washed with brine (20 mL) and dried over $MgSO_4$. The solvent was removed in vacuo and the crude intermediate (**4.12**) was passed through a short column of silica gel eluting with hexanes, first to remove unreacted 1,6-bis(trimethylsilyl)-1,3,5-hexatriyne followed by $CH_2Cl_2$ to remove **4.12**. The fraction containing **4.12** was concentrated to ca. 5 mL and held for later. To a solution of $CBr_4$ (1.634 g, 4.927 mmol) in $CH_2Cl_2$ (30 mL) was added $PPh_3$ (2.754 g, 10.50 mmol) and stirred at rt for 1 h under a $N_2$ atmosphere. The solution of **4.12** was added dropwise and the reaction mixture was stirred at rt for 18 h. Hexanes were added to precipitate the phosphine salts as a white solid along with an oily residue. The supernatant was decanted and filtered through a pad of celite. The oily residue left in the flask was dissolved in minimal $CH_2Cl_2$ and hexanes were added; the heterogeneous mixture was then decanted and the supernatant filtered through celite (this procedure was repeated three times). The filtrate was filtered through celite until the filtrate remained a clear solution. The solvent was removed and the crude product was purified by column chromatography (silica gel, hexanes) to yield **4.15** (0.381 g, 29%) as an orange-brown oil: $R_f$ = 0.44 (hexanes); IR (microscope) 2969, 2211, 2075, 1355, 1252 $cm^{-1}$; $^1H$ NMR (400 MHz, $CDCl_3$): $\delta$ 1.26 (s, 9H), 0.20 (s, 9H); $^{13}C$ NMR (100 MHz, $CDCl_3$): $\delta$ 113.2, 111.3, 107.1, 91.2, 87.8, 79.6, 75.4, 72.8, 70.1, 61.0, 30.3, 28.5, -0.6; EI HRMS *m/z* calcd. for $C_{17}H_{18}{}^{79}Br^{81}BrSi$ ($M^+$) 409.9524, found 409.9523.

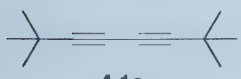

**4.1a**

**4.1a** was synthesized following literature procedure:[28] DSC: Mp = 135 °C.

**X-ray Crystal Data for 4.1a**: Single crystals of **4.1a** suitable for X-ray crystallographic analysis were grown by slow evaporation of a solution of **4.1a** in $Et_2O$/MeOH (4:1) at rt. $C_{12}H_{18}$, $M_r$ = 162.26; monoclinic crystal system; space group $P2_1/c$ (No. 14), $a$ = 10.883 (3), $b$ = 10.917 (4), $c$ =

11.255 (4) Å; $\beta$ = 118.191 (4)°; $V$ = 1178.6 (7) Å$^3$; $Z$ = 4; $\rho_{calcd}$ = 0.914 g cm$^{-3}$; $\mu$ = 0.051 mm$^{-1}$; $\lambda$ = 0.71073 Å; T = –80 °C; 2$\theta$ max = 50.58°; total data collected = 2143; $R_1$ = 0.0846 for 1581 observed reflections with [$F_o^2 \geq 2\sigma(F_o^2)$]; $wR_2$ = 0.2756 for 110 variables and 2143 unique reflections with [$F_o^2 \geq -3\sigma(F_o^2)$]; residual electron density = 0.478 and –0.249 e Å$^{-3}$. CCDC-729156.

**4.1b**

**4.1b:** To a solution of **4.4** (1.497 g, 4.325 mmol) in hexanes (50 mL) at –78 °C was added HexLi (2.26 mL, 2.3M in hexanes, 5.19 mmol) dropwise under a $N_2$ atmosphere. The reaction mixture was stirred at –78 °C for 10 min, warmed to rt over 20 min, and quenched by the addition of saturated aqueous $NH_4Cl$ (20 mL). The layers were separated and the organic layer dried over $MgSO_4$. The solvent was removed in vacuo and the crude product was passed through a plug of silica gel with hexanes. The solvent was removed in vacuo to yield **4.1b** (crude yield of 0.857 g, > 95% pure by $^1$H NMR) as an off-white solid. Greater purity was achieved by recrystallization from pet. ether to yield **4.1b** (0.342 g, 42%) as a white solid. Mp 73-74 °C (lit.[29] 70 °C); $R_f$ = 0.49 (hexanes); UV-Vis (hexanes) $\lambda_{max}$ ($\varepsilon$) 213 (178000), 204 (125000), 195 (59000) nm; IR (microscope) 2969, 2930, 2902, 2867, 2212, 1453 cm$^{-1}$; $^1$H NMR (400 MHz, $CDCl_3$): $\delta$ 1.22 (s); $^{13}$C NMR (100 MHz, $CDCl_3$): $\delta$ 87.0, 64.4, 61.4, 30.4, 28.1; EI HRMS *m/z* calcd. for $C_{14}H_{18}$ ($M^+$) 186.1409, found 186.1407; Anal. calcd. for $C_{14}H_{18}$: C, 90.26; H, 9.74. Found: C, 89.84; H, 9.77; DSC: Mp = 78 °C.

**X-ray Crystal Data for 4.1b**: Single crystals of **4.1b** suitable for X-ray crystallographic analysis were grown by slow diffusion of MeOH into a solution of **4.1b** in $Et_2O$ at rt followed by slow evaporation. $C_{14}H_{18}$, $M_r$ = 186.28; orthorhombic crystal system; space group *Cmca* (No. 64), $a$ = 8.7174 (13), $b$ = 17.826 (3), $c$ = 8.4901 (13) Å; $V$ = 1319.3 (3) Å$^3$; $Z$ = 4; $\rho_{calcd}$ = 0.938 g cm$^{-3}$; $\mu$ = 0.052 mm$^{-1}$; $\lambda$ = 0.71073 Å; T = –80 °C; 2$\theta$ max = 51.34°; total data collected = 4517; $R_1$ = 0.0787 for 560 observed reflections with [$F_o^2 \geq 2\sigma(F_o^2)$]; $wR_2$ = 0.2573 for 40 variables and 672 unique reflections with [$F_o^2 \geq -3\sigma(F_o^2)$]; residual electron density = 0.413 and –0.169 e Å$^{-3}$. CCDC-729157.

**4.1c**

**4.1c:** To a solution of **4.5** (1.556 g, 9.474 mmol) in benzene (300 mL) was added freshly ground KOH (1.067 g, 19.02 mmol). The reaction mixture was heated to reflux until judged complete by TLC analysis (ca. 2 hrs). The reaction was cooled to rt and filtered through a plug of silica. Hay catalyst was prepared by dissolving CuCl (1.027 g, 10.37 mmol) and TMEDA (2.90 mL, 19.2

mmol) in benzene (50 mL) and bubbling $O_2$ through the solution for 20 min. The Hay catalyst was filtered and added to the intermediate solution and the resultant mixture was stirred for 16 h at rt. The reaction was quenched by the addition of $H_2O$ (100 mL) and the layers separated. The organic layer was washed with water (100 mL), brine (2 × 50 mL) and dried over $Na_2SO_4$. The solvent was removed in vacuo and the crude product was purified by column chromatography (silica gel, hexanes) to yield **4.1c** (0.783 g, 79%) as a white solid: Mp 98-99 °C (lit.[29] 99-100 °C); $R_f$ = 0.53 (hexanes); UV-Vis (hexanes) $\lambda_{max}$ ($\varepsilon$) 240 (277000), 229 (195000), 218 (83000), 209 (25000) nm; UV-Vis (THF) $\lambda_{max}$ ($\varepsilon$) 243 (274000), 231 (187000), 220 (75000) nm; IR (cast film, $CH_2Cl_2$) 2972, 2930, 2900, 2867, 2221, 1455 $cm^{-1}$; $^1H$ NMR (500 MHz, $CDCl_3$): $\delta$ 1.23 (s); $^{13}C$ NMR (125 MHz, $CDCl_3$): $\delta$ 87.7, 64.5, 61.8, 61.5, 30.3, 28.2; EI HRMS *m/z* calcd. for $C_{16}H_{18}$ ($M^+$) 210.1409, found 210.1406. Anal. calcd. for $C_{16}H_{18}$: C, 91.37; H, 8.63. Found: C, 90.99; H, 8.77; DSC: Mp = 106 °C; decomposition, 180 °C (onset) and 221°C (peak).

**X-ray Crystal Data for 4.1c**:[30] Single crystals of **4.1c** suitable for X-ray crystallographic analysis were grown by slow evaporation of a solution of **4.1c** in pet. ether/MeOH (4:1) at rt. $C_{16}H_{18}$, $M_r$ = 210.30; orthorhombic crystal system; space group *Pbcn* (No. 60), $a$ = 11.0520 (12), $b$ = 11.6678 (13), $c$ = 22.507 (3) Å; $V$ = 2902.4 (6) $Å^3$; $Z$ = 8; $\rho_{calcd}$ = 0.963 g $cm^{-3}$; $\mu$ = 0.054 $mm^{-1}$; $\lambda$ = 0.71073 Å; T = –80 °C; $2\theta$ max = 52.80°; total data collected = 21568; $R_1$ = 0.0516 for 2275 observed reflections with $[F_o^2 \geq -2\sigma(F_o^2)]$; $wR_2$ = 0.1549 for 145 variables and 2975 unique reflections with $[F_o^2 \geq -3\sigma(F_o^2)]$; residual electron density = 0.189 and –0.152 e $Å^{-3}$. CCDC-729158.

**4.1d**

**4.1d:** To a solution of **4.9** (110 mg, 0.279 mmol) in hexanes (20 mL) at –78 °C was added dropwise HexLi (0.150 mL, 2.3M in hexanes, 0.335 mmol). The reaction mixture was stirred at –78 °C for 10 min under a $N_2$ atmosphere, warmed to rt over 20 min, and stirred for 10 min. The reaction was quenched by the addition of saturated aqueous $NH_4Cl$ (10 mL), the layers separated and the organic layer was dried over $MgSO_4$. The solvent was removed in vacuo and the crude product was purified by column chromatography (silica gel, hexanes) to yield **4.1d** as a pale yellow solid (49 mg, 75%). Mp 115-116 °C; $R_f$ = 0.50 (hexanes); UV-vis (hexanes) $\lambda_{max}$ 266, 252, 240, 228, 218 nm; IR (microscope) 2979, 2929, 2898, 2866, 2206, 2119, 1453 $cm^{-1}$; $^1H$ NMR (500 MHz, $CDCl_3$): $\delta$ 1.23 (s); $^{13}C$ NMR (125 MHz, $CDCl_3$): $\delta$ 88.4, 64.4, 62.1, 62.0, 61.7, 30.2, 28.3;[31,32] EI HRMS *m/z* calcd. for $C_{18}H_{18}$ ($M^+$) 234.1409, found 234.1409.

**4.1e**

**4.1e**: To a mixture of CuCl (120 mg, 1.21 mmol) in THF (5 mL) and MeOH (5 mL) was added TMEDA (281 mg, 365 µL, 2.42 mmol). $O_2$ was bubbled through the solution for 10 min and a solution of **4.6** (244 mg, 1.21 mmol) in MeOH (5 mL) and THF (5 mL) was added. The mixture was stirred for 1 hr at rt, quenched by the addition of $H_2O$ (25 mL), and then extracted with hexanes (2 × 50 mL). The organic layers were combined, washed with brine and dried over $MgSO_4$. The solvent was removed in vacuo and the crude product was purified by column chromatography (silica gel, hexanes) to yield **4.1e** (147 mg, 94%) as a yellow solid: $R_f$ = 0.46 (hexanes); UV-Vis (hexanes) $\lambda_{max}$ (ε) 289 (478000), 273 (347000), 259 (146000), 247 (47000), 236 (14000) nm; UV-Vis (THF) $\lambda_{max}$ (ε) 293 (401000), 276 (281000), 262 (116000), 250 (38000) nm; IR (microscope) 2972, 2929, 2898, 2864, 2195, 2076, 1454, 1303, 1197 $cm^{-1}$; $^1H$ NMR (500 MHz, $CDCl_3$): $\delta$ 1.24 (s); $^{13}C$ NMR (100 MHz, $CDCl_3$): $\delta$ 88.8, 64.4, 62.52, 62.51, 61.9, 61.6, 30.2, 28.3; EI HRMS *m/z* calcd. for $C_{20}H_{18}$ ($M^+$) 258.1408, found 258.1406; Anal. calcd. for $C_{20}H_{18}$: C, 92.98; H, 7.02. Found: C, 92.74; H, 7.17; DSC: decomposition, 145 °C (onset) and 156 °C (peak).

**4.1f**

**4.1f**: To a solution of **4.14** (0.900 g, 2.33 mmol) in hexanes (100 mL) at –78 °C was added HexLi (1.2 mL, 2.3M in hexanes, 2.8 mmol) dropwise. The reaction mixture was stirred at –78 °C for 10 min under a $N_2$ atmosphere, warmed to rt over 20 min, and stirred for 10 min. The reaction was quenched by the addition of saturated aqueous $NH_4Cl$ (20 mL), the layers separated, and the organic layer was dried over $Na_2SO_4$. The solvent was reduced in vacuo to ca. 10 mL. THF (20 mL) was added and the volume was reduced in vacuo to ca. 10 mL (**4.16**) and held for later. Concurrently, to a mixture of CuCl (0.236 mg, 2.38 mmol) in THF (20 mL) and MeOH (20 mL) was added TMEDA (0.54 g, 0.70 mL, 4.7 mmol). $O_2$ was bubbled through the solution for 20 min and the solution of **4.16** was added. The mixture was stirred for 1 h at rt, quenched by the addition of $H_2O$ (25 mL), and extracted with hexanes (100 mL). The aqueous layer was extracted again with hexanes (2 × 20 mL) and the organic layers combined. The organic phase was washed with saturated aqueous $NH_4Cl$ then dried over $Na_2SO_4$. The solvent was removed in vacuo and the

crude product was purified by column chromatography (silica gel, hexanes). The product fractions were combined, the solvent was removed in vacuo and the resulting solid was recrystallized from pet. ether to yield **4.1f** (0.217 mg, 61%) as a yellowish-orange solid: $R_f$ = 0.52 (hexanes); UV-Vis (hexanes) $\lambda_{max}$ ($\varepsilon$) 330 (643000), 310 (518000), 293 (236000), 278 (86000), 264 (31000), 227 (18000), 220 (22000), 212 (30000), 204 (28000) nm; UV-Vis (THF) $\lambda_{max}$ ($\varepsilon$) 335 (519000), 314 (385000), 297 (170000), 281 (65000), 269 (28000) nm; IR (microscope) 2972, 2930, 2898, 2867, 2208, 2127, 2020, 1237 $cm^{-1}$; $^1H$ NMR (500 MHz, $CDCl_3$): $\delta$ 1.24 (s); $^{13}C$ NMR (125 MHz, $CDCl_3$): $\delta$ 89.4, 64.4, 63.4, 63.2, 62.9, 62.3, 61.7, 61.4, 30.1, 28.4; EI HRMS *m/z* calcd. for $C_{24}H_{18}$ ($M^+$) 306.1408, found 306.1407; DSC: decomposition, 117 °C (onset), 127 °C and 139 °C (peaks).

**X-ray Crystal Data for 4.1f**: Single crystals of **4.1f** suitable for X-ray crystallographic analysis were grown by slow evaporation of a solution of **4.1f** in $CH_2Cl_2$ at 4 °C. $C_{24}H_{18}$, $M_r$ = 306.38; orthorhombic crystal system; space group *Pnma* (No. 62), $a$ = 16.4819 (10), $b$ = 6.8028 (4), $c$ = 17.4876 (10) Å; $V$ = 1960.8 (2) $Å^3$; $Z$ = 4; $\rho_{calcd}$ = 1.038 g $cm^{-3}$; $\mu$ = 0.059 $mm^{-1}$; $\lambda$ = 0.71073 Å; T = –100 °C; $2\theta$ max = 51.44°; total data collected = 14185; $R_1$ = 0.0412 for 1407 observed reflections with $[F_o^2 \geq 2\sigma(F_o^2)]$; $wR_2$ = 0.1330 for 139 variables and 2043 unique reflections with $[F_o^2 \geq -3\sigma(F_o^2)]$; residual electron density = 0.353 and –0.111 e $Å^{-3}$. CCDC-729159.

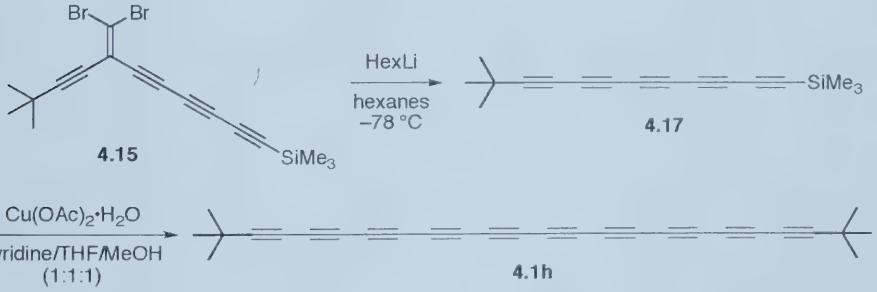


**4.1h:** To a solution of **4.15** (120 mg, 0.293 mmol) in hexanes (15 mL) at –78 °C was added dropwise HexLi (0.15 mL, 2.3M in hexanes, 0.35 mmol). The reaction mixture was stirred at –78 °C for 10 min under a $N_2$ atmosphere then warmed to rt over 20 min and stirred for 10 min. The reaction was quenched by the addition of saturated aqueous $NH_4Cl$ (5 mL), the layers separated and the organic layer was dried over $Na_2SO_4$. The solvent was reduced in vacuo to *ca.* 10 mL. THF (20 mL) was added, the volume reduced in vacuo to ca. 5 mL and passed though a plug of silica gel with hexanes. THF (20 mL) was added to the filtrate and the volume was reduced in vacuo to ca. 5 mL (**4.17**). This solution was added to solution of $Cu(OAc)_2•H_2O$ (117 mg, 0.586 mmol) in THF (2 mL), MeOH (2 mL) and pyridine (2 mL) and then stirred at rt for 2 h. Hexanes (25 mL) were added to the solution and the resulting mixture was washed with $H_2O$ (2 × 10 mL). The organic layer was washed with saturated aqueous $NH_4Cl$ then dried over $Na_2SO_4$. This

mixture was filtered through a plug of silica gel with hexanes and the solvent was removed in vacuo to yield **4.1h** (28 mg, 54%) as an orange solid: $R_f$ = 0.51 (hexanes); UV-Vis (hexanes) $\lambda_{max}$ ($\varepsilon$) 362 (736000), 339 (619000), 320 (309000), 303 (124000), 288 (45000), 275 (18000), 255 (28000), 247 (38000), 237 (47000), 227 (38000), 219 (26000) nm; UV-Vis (THF) $\lambda_{max}$ ($\varepsilon$) 368 (530000), 345 (449000), 324 (223000), 307 (94000), 291 (40000), 279 (20000) nm; IR (microscope) 2970, 2926, 2866, 2204, 2115, 2080, 2009, 1456 $cm^{-1}$; $^1H$ NMR (500 MHz, $CDCl_3$): $\delta$ 1.24 (s); $^{13}C$ NMR (125 MHz, $CDCl_3$): $\delta$ 89.6, 64.3, 63.8, 63.5 (2), 63.0, 62.6, 62.1, 61.6, 61.4, 30.1, 28.4; MALDI MS (DCTB) *m/z* 354.2 ($M^+$, 100); MALDI HRMS *m/z* calcd. for $C_{28}H_{18}$ ($M^+$) 354.1403, found 354.1404; DSC: decomposition, 100°C (onset), 107 °C (peak).

**X-ray Crystal Data for 4.1h**: Single crystals of **4.1h** suitable for X-ray crystallographic analysis were grown by slow evaporation of a $CH_2Cl_2$ solution at 4 °C. $C_{28}H_{18}$, $M_r$ = 354.42; monoclinic crystal system; space group $P2_1/n$ (an alternate setting of $P2_1/c$ [No. 14]), $a$ = 5.3923 (17), $b$ = 18.777 (6), $c$ = 31.598 (10) Å; $\beta$ = 94.474 (4)°; $V$ = 3189.6 (17) $Å^3$; $Z$ = 6; $\rho_{calcd}$ = 1.107 g $cm^{-3}$; $\mu$ = 0.063 $mm^{-1}$; $\lambda$ = 0.71073 Å; T = –100 °C; $2\theta$ max = 50.70°; total data collected = 22855; $R_1$ = 0.0896 for 4076 observed reflections with [$F_o^2 \geq 2\sigma(F_o^2)$]; $wR_2$ = 0.2304 for 389 variables and 5938 unique reflections with [$F_o^2 \geq -3\sigma(F_o^2)$]; residual electron density = 0.964 and –0.235 e $Å^{-3}$. CCDC-729160.

## 7.4 Supertrityl-Endcapped Polyynes (Chapter 5 data)

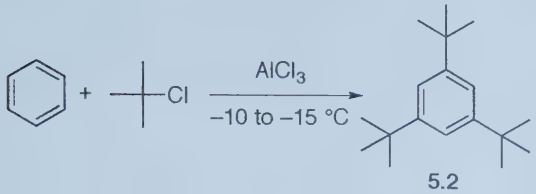


5.2

**5.2 was synthesized as previously reported:**[33] Mp 72-73 °C (lit. 72.5-73 °C); $^1$H NMR (400 MHz, $CDCl_3$): $\delta$ 7.28 (s, 3H), 1.36 (s, 27H); $^{13}$C NMR (100 MHz, $CDCl_3$): $\delta$ 149.9, 119.4, 34.9, 31.6. CAS 1460-02-2.

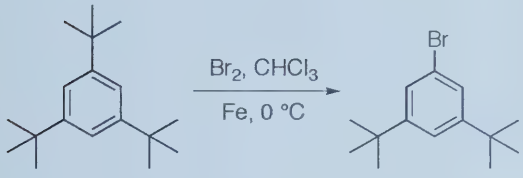


5.2 5.3

**5.3 was synthesized following a procedure analogous to that reported by Bartlett et al.:**[33] Mp 52-56 °C (lit. 63-64 °C); $^1$H NMR (500 MHz, $CDCl_3$): $\delta$ 7.31 (s, 3H), 1.29 (s, 18H); $^{13}$C NMR (125 MHz, $CDCl_3$): $\delta$ 153.0, 125.7, 122.2, 121.1, 35.0, 31.3. CAS 22385-77-9.

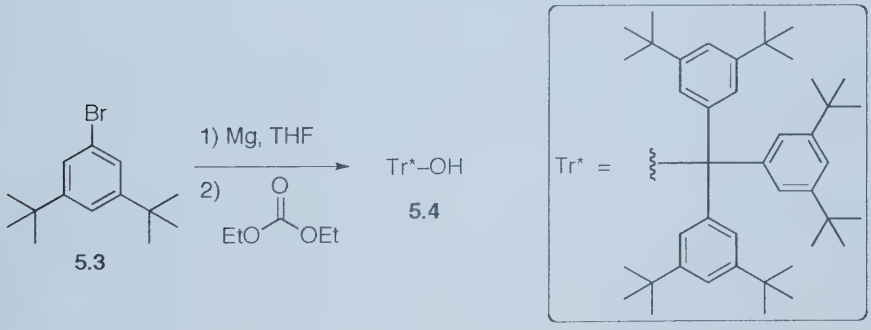


5.3 5.4

**5.4 was synthesized by adaptation of a known procedure:**[34] To a mixture of freshly ground Mg (0.952 g, 39.2 mmol) in THF (20 mL) under a $N_2$ atmosphere was slowly added a solution of **5.3** (9.184 g, 34.11 mmol) in THF (20 mL). A small crystal of $I_2$ was added to promote Grignard formation. The reaction was maintained at a gentle reflux while slowly diluting with THF (40 mL). The reaction was cooled to rt and a solution of diethyl carbonate (1.15 g, 1.18 mL, 9.75 mmol) in THF (10 mL) was slowly added and reaction was stirred at rt for 44 h. The reaction was cooled to 0 °C, quenched with saturated $NH_4Cl$ (50 mL) and extracted with $Et_2O$ (150 mL). The

layers were separated, the organic phase washed with $H_2O$ (50 mL), brine (50 mL), and dried over $Na_2SO_4$. The solvent was removed in vacuo and the crude product purified by column chromatography (silica gel, gradient of hexanes –> EtOAc/hexanes 1:20) to yield **5.4** (5.328 g, 92%) as a pale yellow solid: $^1$H NMR (400 MHz, $CDCl_3$): $\delta$ 7.30 (t, $J$ = 2 Hz, 3H), 7.06 (d, $J$ = 2 Hz, 6H), 2.78 (s, 1H), 1.24 (s, 54H); $^{13}$C NMR (100 MHz, $CDCl_3$): $\delta$ 149.6, 146.7, 122.6, 120.3, 83.4, 34.8, 31.5.

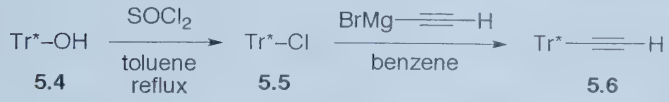


**5.4** **5.5** **5.6**

**5.6:** To a solution of **5.4** (26.36 g, 44.16 mmol) in toluene (700 mL) was added $SOCl_2$ (16.12 mL, 220.8 mmol) and the solution refluxed for 20 h with the condenser covered with a $CaCl_2$ drying tube. The solvent was removed in vacuo and the resulting residue (**5.5**) dissolved in benzene (1.5 L). Ethynylmagnesium bromide (265 mL, 0.5 M in THF, 133 mmol) was added and the resulting mixture stirred for 6 days at rt under a $N_2$ atmosphere. The reaction was cooled to 0 °C, quenched with saturated $NH_4Cl$ (200 mL) and the layers separated. The aqueous layer was extracted with hexanes (200 mL) then the layers separated. The organic phases were combined and dried over $MgSO_4$. The solvent was removed in vacuo and the resulting crude product recrystallized from hexanes to yield **5.6** as a tan solid (19.65 g, 74%). The filtrate was concentrated in vacuo and the remaining crude product purified by column chromatography (silica gel, hexanes) to yield **5.6** (4.03 g, total yield = 23.68 g, 89%) as a tan solid: Mp 193-194 °C (lit. 199-200 °C);[34] $R_f$ = 0.42 (hexanes); IR (microscope) 3306, 3070 (w), 2961, 2904, 2865, 2124 (vw), 2095 (vw), 1591 cm$^{-1}$; $^1$H NMR (400 MHz, $CDCl_3$): $\delta$ 7.23 (t, $J$ = 2 Hz, 3H), 6.98 (d, $J$ = 2 Hz, 6H), 2.59 (s, 1H), 1.18 (s, 54H); $^{13}$C NMR (125 MHz, $CDCl_3$): $\delta$ 149.7, 144.8, 123.8, 119.8, 90.7, 72.0, 56.1, 34.8, 31.4; EIMS m/z 604.5 ($M^+$, 95), 547.4 ([M – $t$Bu]$^+$, 100); EI HRMS $m/z$ calcd. for $C_{45}H_{64}$ ($M^+$) 604.5008, found 604.5009; Anal. calcd. for $C_{45}H_{64}$: C, 89.34; H, 10.66. Found: C, 89.36; H, 10.73; DSC: Mp = 196 °C.

**X-ray Crystal Data for 5.6:** Single crystals of **5.6** suitable for X-ray crystallographic analysis were grown by slow evaporation of a $CH_2Cl_2$ solution at rt. $C_{45}H_{64}$, $M_r$ = 605.0; monoclinic crystal system; space group $P2_1/n$ (an alternate setting of $P2_1/c$ [No. 14]), $a$ = 10.4280 (10), $b$ = 10.2685 (10), $c$ = 40.794 (4) Å; $\beta$ = 90.6188 (15)°; $V$ = 4368.0 (7) Å$^3$; $Z$ = 4; $\rho_{calcd}$ = 1.017 g cm$^{-3}$; $\mu$ = 0.145 mm$^{-1}$; $\lambda$ = 0.71073 Å; T = –80 °C; 2$\theta$ max = 50.50°; total data collected = 30178; $R_1$ = 0.0656 for 5937 observed reflections with [$F_o^2 \geq 2\sigma(F_o^2)$]; $wR_2$ = 0.1782 for 455 variables and 7925 unique reflections with [$F_o^2 \geq -3\sigma(F_o^2)$]; residual electron density = 0.388 and –0.304 e Å$^{-3}$.

**7.6**

**7.6:** To a solution of **5.6** (1.090 g, 1.802 mmol) in acetone (150 mL) was added *N*-bromosuccinimide (0.355 g, 1.99 mmol) and $AgNO_3$ (62 mg, 0.36 mmol) and the reaction mixture stirred at rt for 15 h. The reaction was quenched with $H_2O$ (100 mL) and the resulting mixture extracted with hexanes (2 × 100 mL). The organic layers were combined and washed with $H_2O$ (50 mL), brine (50 mL), and dried over $Na_2SO_4$. The solvent was removed in vacuo and the crude product purified by column chromatography (silica gel, $CH_2Cl_2$/hexanes 1:10) to yield **6.6** (1.219 g, 99%) as a white solid: $R_f$ = 0.50 ($CH_2Cl_2$/hexanes 1:10); IR (microscope) 3073 (w), 2963, 2905, 2867, 1593 $cm^{-1}$; $^1H$ NMR (500 MHz, $CDCl_3$): $\delta$ 7.26 (t, $J$ = 2 Hz, 3H), 6.95 (d, $J$ = 2 Hz, 6H), 1.21 (s, 54H); $^{13}C$ NMR (125 MHz, $CDCl_3$): $\delta$ 149.8, 144.6, 123.8, 120.0, 86.8, 57.3, 42.2, 34.8, 31.4; MALDI MS *m/z* 683.3 ($M^+$, 15), 626.4 ([M – *t*Bu]$^+$, 50), 603.6 ([M – Br]$^+$, 100); EIMS *m/z* 625.3 ([M – *t*Bu]$^+$, 60), 604.5 ([M – Br + H]$^+$, 100); MALDI HRMS *m/z* calcd. for $C_{45}H_{63}$ [M – Br]$^+$ 603.4924, found 603.4922.

**X-ray Crystal Data for 7.6:** Single crystals of **7.6** suitable for X-ray crystallographic analysis were grown by slow evaporation of a $CDCl_3$ solution at rt. $C_{45}H_{63}Br$, $M_r$ = 683.86; triclinic crystal system; space group $P\bar{1}$ (No. 2), $a$ = 10.3734 (7), $b$ = 10.4700 (7), $c$ = 19.2635 (13) Å; $\alpha$ = 88.7349 (10)°; $\beta$ = 77.9313 (9)°; $\gamma$ = 88.6899 (10)°; $V$ = 2045.1 (2) Å$^3$; $Z$ = 2; $\rho_{calcd}$ = 1.111 g cm$^{-3}$; $\mu$ = 1.032 mm$^{-1}$; $\lambda$ = 0.71073 Å; T = –80 °C; 2$\theta$ max = 55.10°; total data collected = 17869; $R_1$ = 0.0423 for 7375 observed reflections with [$F_o^2 \geq 2\sigma(F_o^2)$]; $wR_2$ = 0.1147 for 442 variables and 9308 unique reflections with [$F_o^2 \geq -3\sigma(F_o^2)$]; residual electron density = 0.759 and –0.592 e Å$^{-3}$.

**7.7**

**7.7:** To a deoxygenated solution of **5.6** (174 mg, 0.288 mmol) and 1-bromo-3-methyl-1-butyn-3-ol (70 mg, 0.431 mmol) in THF (10 mL) and diisopropylamine (146 mg, 204 µL, 1.44 mmol) was added $PdCl_2(PPh_3)_2$ (10 mg, 0.014 mmol) and CuI (3 mg, 0.01 mmol). The reaction was stirred at rt under a $N_2$ atmosphere for 20 h. The solvent was removed in vacuo and the residue purified by column chromatography (silica gel, gradient elution with EtOAc/hexanes 1:10 → 1:4) to yield **7.7** (108 mg, 55%) as a yellow solid: $R_f$ = 0.41 (EtOAc/hexanes 1:4); IR (microscope) 3364 (br), 3071 (w), 2964, 2905, 2868, 2245, 1592 $cm^{-1}$; $^1H$ NMR (400 MHz, $CDCl_3$): $\delta$ 7.24 (t, $J$ = 2 Hz, 3H), 6.91 (d, $J$ = 2 Hz, 6H), 1.93 (s, 1H), 1.53 (s, 6H), 1.19 (s, 54H); $^{13}C$ NMR (125 MHz, $CDCl_3$): $\delta$ 149.9, 144.2, 123.8, 120.1, 87.1, 81.9, 67.9, 67.8, 65.7, 56.9, 34.8, 31.4, 31.2; EIMS *m/z* 686.5 ($M^+$, 7), 629.5 ([M – *t*Bu]$^+$, 29), 57.1 ([*t*Bu]$^+$, 100); EI HRMS *m/z* calcd. for $C_{50}H_{70}O$ ($M^+$) 686.5427, found 686.5422.

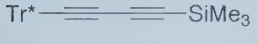


**7.8**

**7.8:** To a deoxygenated solution of **7.6** (140 mg, 0.205 mmol) and trimethylsilylacetylene (401 mg, 4.09 mmol) in THF (10 mL) and diisopropylamine (1.04 g, 1.50 mL, 10.3 mmol) was added $PdCl_2(PPh_3)_2$ (14 mg, 0.021 mmol) and CuI (4 mg, 0.02 mmol). The reaction was stirred at rt under a $N_2$ atmosphere for 18 h. The solvent was removed in vacuo and the residue passed through a plug of silica gel with $CH_2Cl_2$/hexanes (1:10) to yield crude **6.8** (ca. 53% yield based on $^1H$ NMR). Note: Only a small amount was purified for characterization purposes since this route was abandoned: Mp 222-223 °C; $R_f$ = 0.52 ($CH_2Cl_2$/hexanes 1:10); IR (microscope) 3071 (w), 2963, 2905, 2868, 2223, 2101, 1592 $cm^{-1}$; $^1H$ NMR (500 MHz, $CDCl_3$): $\delta$ 7.23 (t, $J$ = 2 Hz, 3H), 6.91 (d, $J$ = 2 Hz, 6H), 1.18 (s, 54H). 0.17 (s, 9H); $^{13}C$ NMR (125 MHz, $CDCl_3$): $\delta$ 149.8, 144.1 123.8, 120.1, 88.8, 85.23, 85.17, 69.0, 56.9, 39.0, 34.8, 31.4, –0.3; EI MS $m/z$ 700.6 ($M^+$, 92), 643.3 ([M – $t$Bu]$^+$, 100).

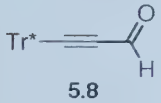


**5.8**

**5.8:** A solution of **5.6** (2.853 g, 4.716 mmol) in THF (150 mL) was cooled to –78 °C under a $N_2$ atmosphere, BuLi (1.886 mL, 2.5 M in hexanes, 4.716 mmol) was added, and the mixture stirred at –78 °C for 10 min. DMF (0.474 mL, 6.13 mmol) was added slowly over 5 min, the mixture stirred for 10 min and then warmed to rt and stirred another 30 min. The reaction was quenched by pouring into a mixture of ice (200 g) and conc. HCl (0.94 mL, 9.43 mmol). The mixture was warmed to rt, the pH adjusted to ~7 with saturated $NaHCO_3$, extracted with hexanes (200 mL), and the resulting layers separated. The organic phase was washed with $H_2O$ (50 mL), brine (50 mL) and dried over $MgSO_4$. The solvent was removed in vacuo and the crude product purified by column chromatography (silica gel) by first eluting with $CH_2Cl_2$/hexanes (1:20) to remove unreacted **5.6** then with $CH_2Cl_2$/hexanes (1:2) to yield **5.8** (2.532 g, 85%) as a white solid: Mp 195-196 °C; $R_f$ = 0.55 ($CH_2Cl_2$/hexanes1:1); IR (microscope) 3071 (w), 2964, 2905, 2868, 2198, 1670, 1592 $cm^{-1}$; $^1H$ NMR (500 MHz, $CDCl_3$): $\delta$ 9.36 (s, 1H), 7.28 (t, $J$ = 2 Hz, 3H), 6.93 (d, $J$ = 2 Hz, 6H), 1.19 (s, 54H); $^{13}C$ NMR (125 MHz, $CDCl_3$): $\delta$ 177.0, 150.2, 143.1, 123.7, 120.5, 104.2, 84.2, 56.8, 34.9, 31.3; EIMS m/z 632.5 ($M^+$, 16), 603.5 ([M – CHO]$^+$, 10), 575.4 ([M – $t$Bu]$^+$, 17), 548.4 ([M – $t$-Bu – CHO + H]$^+$, 16); EI HRMS $m/z$ calcd. for $C_{46}H_{64}O$ ($M^+$) 632.4957, found 632.4950.

**X-ray Crystal Data for 5.8:** Single crystals of **5.8** suitable for X-ray crystallographic analysis were grown by slow evaporation of a hexanes solution at rt. $C_{46}H_{64}O$, $M_r$ = 632.97; triclinic crystal system; space group $P\bar{1}$ (No. 2), $a$ = 10.3538 (6), $b$ = 10.4701 (6), $c$ = 19.2148 (11) Å; $\alpha$ = 88.8202 (7)°; $\beta$ = 78.0275 (7)°; $\gamma$ = 88.6992 (7)°; $V$ = 2036.9 (2) Å$^3$; $Z$ = 2; $\rho_{calcd}$ = 1.1032 g cm$^{-3}$; $\mu$ = 1.032 mm$^{-1}$; $\lambda$ = 0.71073 Å; T = –100 °C; 2$\theta$ max = 52.80°; total data collected = 16422; $R_1$ =

0.0458 for 6513 observed reflections with [$F_o^2 \geq 2\sigma(F_o^2)$]; $wR_2$ = 0.1322 for 496 variables and 8324 unique reflections with [$F_o^2 \geq -3\sigma(F_o^2)$]; residual electron density = 0.377 and –0.248 e Å$^{-3}$.

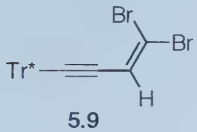


**5.9**

**5.9:** To a solution of $CBr_4$ (3.128 g, 9.432 mmol) in $CH_2Cl_2$ (150 mL) was added $PPh_3$ (5.195 g, 19.81 mmol) and the resulting mixture stirred at rt under a $N_2$ atmosphere for 1 h. A solution of **5.8** (2.532 g, 4.000 mmol) in $CH_2Cl_2$ (20 mL) was added and the reaction stirred for 10 min. The reaction mixture was concentrated to ca. 20 mL and hexanes were added to precipitate the phosphine salts as a white solid along with an oily residue. The supernatant was decanted and filtered through a pad of celite. The oily residue left in the flask was dissolved in minimal $CH_2Cl_2$ and hexanes were added; the heterogeneous mixture was then decanted and the supernatant filtered through celite (this procedure was repeated three times). The filtrate was filtered through celite until the filtrate remained a clear solution. The solvent was removed in vacuo and the crude product was purified by column chromatography (silica gel, hexanes) to yield **5.9** (2.970 g, 94%) as a white solid: Mp 158-159 °C; $R_f$ = 0.31 (hexanes); IR (microscope) 3069 (w), 2958, 2904, 2868, 2213, 1592 cm$^{-1}$; $^1$H NMR (500 MHz, $CDCl_3$): $\delta$ 7.25 (t, $J$ = 2 Hz, 3H), 6.98 (d, $J$ = 2 Hz, 6H), 6.71 (s, 1H), 1.20 (s, 54H); $^{13}$C NMR (125 MHz, $CDCl_3$): $\delta$ 149.8, 144.4, 123.9, 120.4, 120.0, 105.2, 100.2, 81.0, 57.3, 34.9, 31.4; $^{13}$C NMR (APT, 125 MHz, $CDCl_3$): $\delta$ 149.8 (C), 144.4 (C), 123.9 (CH), 120.4 (CH), 120.0 (CH), 105.2 (C), 100.2 (C), 81.0 (C), 57.3 (C), 34.9 (C), 31.4 ($CH_3$); EIMS *m/z* 773.7 ([M – $CH_3$]$^+$, 5), 731.0 ([M – *t*Bu]$^+$, 89), 595.0 ([M – 2 × *t*Bu – Br]$^+$, 22), 57.0 (*t*Bu$^+$, 100); Anal. calcd. for $C_{47}H_{64}Br_2$: C, 71.56; H, 8.18. Found: C, 71.69; H, 8.25.

**5.7**

**5.7:** To a solution of diisopropylamine (2.39 g, 3.33 mL, 23.6 mmol) in THF (100 mL) cooled to –78 °C under a $N_2$ atmosphere was added BuLi (9.43 mL, 2.5 M in hexanes, 23.6 mmol). The mixture was stirred at –78 °C for 10 min and a solution of **5.9** (2.970 g, 3.765 mmol) in THF (25 mL) was then added slowly over 5 min. The reaction was warmed to rt, stirred for 10 min, cooled to 0 °C, and quenched with saturated $NH_4Cl$ (50 mL). The mixture was extracted with hexanes (200 mL) and the layers separated. The organic phase was washed with $H_2O$ (50 mL), brine (50 mL), and dried over $MgSO_4$. The solvent was removed in vacuo and the crude product purified by column chromatography (silica gel, $CH_2Cl_2$/hexanes 1:10) to yield **5.7** (2.349 g, 99%) as a white solid: Mp 192-194 °C; $R_f$ = 0.29 (hexanes); IR (microscope) 3315, 3067 (w), 2953, 2903, 2865, 2224, 1589 cm$^{-1}$; $^1$H NMR (400 MHz, $CDCl_3$): $\delta$ 7.25 (t, $J$ = 2 Hz, 3H), 6.93 (d, $J$ = 2 Hz, 6H),

2.10 (s, 1H), 1.20 (s, 54H); $^{13}$C NMR (100 MHz, $CDCl_3$): $\delta$ 149.9, 143.9, 123.8, 120.1, 83.5, 68.8, 68.1, 66.6, 56.7, 34.8, 31.4; EIMS *m/z* 628.5 ($M^+$, 4), 571.4 ([M – *t*Bu]$^+$, 11), 57.1 ([*t*Bu]$^+$, 100); EI HRMS *m/z* calcd. for $C_{47}H_{64}$ ($M^+$) 628.5008, found 628.5002; Anal. calcd. for $C_{47}H_{64}$: C, 89.74; H, 10.26. Found: C, 89.50; H, 10.40; DSC: decomposition, 205 °C (onset) and 208 °C (peak).

**X-ray Crystal Data for 5.7:** Single crystals of **5.7** suitable for X-ray crystallographic analysis were grown by slow evaporation of a $CDCl_3$ solution at rt. $C_{47}H_{64}$, $M_r$ = 628.98; triclinic crystal system; space group $P\bar{1}$ (No. 2), $a$ = 10.3367 (13), $b$ = 10.4631 (13), $c$ = 19.275 (2) Å; $\alpha$ = 88.5549 (18)°; $\beta$ = 78.0127 (18)°; $\gamma$ = 88.5903 (19)°; $V$ = 2038.2 (4) Å$^3$; $Z$ = 2; $\rho_{calcd}$ = 1.025 g cm$^{-3}$; $\mu$ = 0.057 mm$^{-1}$; $\lambda$ = 0.71073 Å; T = –80 °C; 2$\theta$ max = 54.96°; total data collected = 17675; $R_1$ = 0.0555 for 7021 observed reflections with [$F_o^2 \geq 2\sigma(F_o^2)$]; $wR_2$ = 0.1599 for 451 variables and 9200 unique reflections with [$F_o^2 \geq -3\sigma(F_o^2)$]; residual electron density = 0.334 and –0.209 e Å$^{-3}$.

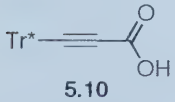


**5.10**

**5.10:** To a solution of **5.6** (0.889 g, 1.47 mmol) in THF (70 mL) cooled to –78 °C under a $N_2$ atmosphere was added BuLi (1.76 mL, 2.5M in hexanes, 4.41 mmol) dropwise. The mixture was stirred at –78 °C for 30 min and $CO_2$ (g) (passed through a drying tube filled with drierite) was bubbled through the reaction mixture for 30 min. The mixture was warmed to rt, the flow of $CO_2$ was stopped and the reaction stirred for 1 h. The reaction was cooled to 0 °C and quenched by the addition of $H_2O$ (20 mL), acidified with 10% aqueous HCl, and then extracted with $Et_2O$ (100 mL). The organic layer was washed with 5% aqueous $Na_2CO_3$ (2 × 25 mL, **Note:** this wash removes only the valeric acid formed from the excess BuLi used), 10% HCl (25 mL), brine (25 mL), and dried over $Na_2SO_4$. The solvent was removed in vacuo to yield **5.10** (0.943 g, 99%) as an off-white solid: Mp 180-181 °C; IR (microscope) 3500-2500 (br), 2963, 2869, 2237, 1688, 1593 cm$^{-1}$; $^1$H NMR (500 MHz, $CDCl_3$): $\delta$ ~8.2 (br s, 1H), 7.27 (t, $J$ = 2 Hz, 3H), 6.93 (d, $J$ = 2 Hz, 6H), 1.19 (s, 54H); $^{13}$C NMR (100 MHz, $CDCl_3$): $\delta$ 157.3, 150.1, 143.0, 123.8, 120.4, 97.4, 75.5, 56.5, 34.8, 31.3; EIMS m/z 647.5 ([M – H]$^+$, 28), 604.5 ([M – $CO_2$]$^+$, 62), 547.4 ([M – *t*Bu – $CO_2$]$^+$, 100); EI HRMS *m/z* calcd. for $C_{46}H_{63}O_2$ [M – H]$^+$ 647.4828, found 647.4829; Anal. calcd. for $C_{46}H_{64}O_2$•THF (1:1 complex): C, 83.28; H, 10.06. Found: C, 83.58; H, 9.84.

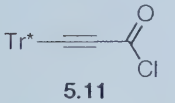


**5.11**

**5.11:** A solution of **5.10** (0.896 g, 1.38 mmol) in $SOCl_2$ (1.150 g, 0.705 mL, 9.66 mmol) and $CHCl_3$ (50 mL) was stirred at reflux for 20 h with a drying tube on the condenser. The solvent was removed in vacuo to obtain **5.11** (0.908 g, 99%) as a tan solid: Mp 197-201°C; IR (microscope)

3076 (w), 2962, 2904, 2868, 2205, 1749, 1589 $cm^{-1}$; $^1H$ NMR (500 MHz, $CDCl_3$): $\delta$ 7.31 (t, $J$ = 2 Hz, 3H), 6.92 (d, $J$ = 2 Hz, 6H), 1.21 (s, 54H); $^{13}C$ NMR (125 MHz, $CDCl_3$): $\delta$ 150.4, 149.4, 142.3, 123.7, 120.7, 104.0, 79.6, 56.9, 34.9, 31.3; $^{13}C$ – $^1H$ HMQC (500 MHz, $CDCl_3$), selected correlations: $\delta$ 7.31 ↔ 120.7, 6.92 ↔ 123.7, 1.21 ↔ 31.3; EIMS $m/z$ 666.5 ($M^+$, 1), 574.4 ([M – $t$Bu - Cl]$^+$, 17), 57.1 ([$t$Bu]$^+$, 100); EI HRMS $m/z$ calcd. for $C_{46}H_{63}O^{35}Cl$ ($M^+$) 666.4567, found 666.4575.

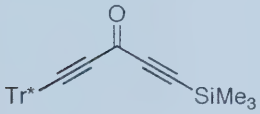


**5.12**

**5.12:** To a mixture of $AlCl_3$ (130 mg, 0.960 mmol) in $CH_2Cl_2$ (15 mL) under a $N_2$ atmosphere was added a solution of **5.11** (256 mg, 0.384 mmol) and 1,2-bis(trimethylsilyl)acetylene (98 mg, 0.575 mmol) in $CH_2Cl_2$ (5 mL). The reaction was stirred at rt for 4 h. The reaction was quenched with 5% aqueous $NaHCO_3$ (10 mL). The organic phase was washed with 5% aqueous $NaHCO_3$ (10 mL), $H_2O$ (10 mL), brine (10 mL), and dried over $Na_2SO_4$. The solvent was removed in vacuo and the crude product purified by column chromatography (silica gel, gradient of hexanes to $CH_2Cl_2$/hexanes 1:2). The fractions containing **5.12** were concentrated and redissolved in $CH_2Cl_2$ to be carried directly to **5.15** (Note: a small amount was used for characterization): Mp 156-159 °C; $R_f$ = 0.55 ($CH_2Cl_2$/hexanes 1:1); IR (microscope) 3078 (w), 2960, 2905, 2868, 2205, 2152, 1623, 1592 $cm^{-1}$; $^1H$ NMR (300 MHz, CDCl3): $\delta$ 7.27 (t, $J$ = 2 Hz, 3H), 6.93 (d, $J$ = 2 Hz, 6H), 1.19 (s, 54H), 0.22 (s, 9H); $^{13}C$ NMR (100 MHz, $CDCl_3$): $\delta$ 160.8, 150.2, 143.1, 123.8, 120.4, 103.0, 100.4, 97.5, 84.6, 56.8, 34.9, 31.4, –0.8; EIMS $m/z$ 728.5 ($M^+$, 14), 672.5 ([M – $t$Bu + H]$^+$, 45), 603.5 ([M – $Me_3SiC{\equiv}CC{=}O$]$^+$, 42), 57.1 ([$t$Bu]$^+$, 100); EI HRMS $m/z$ calcd. for $C_{51}H_{72}OSi$ ($M^+$) 728.5352, found 728.5353.

**X-ray Crystal Data for 5.12:** Single crystals of **5.12** suitable for X-ray crystallographic analysis were grown by slow evaporation of a $Et_2O$/MeOH (4:1) solution at 4 °C. $C_{51}H_{72}OSi$, $M_r$ = 729.18; orthorhombic crystal system; space group $P2_12_12_1$ (No. 19), $a$ = 10.9631 (14), $b$ = 19.692 (3), $c$ = 22.208 (3) Å; $V$ = 4794.4 (11) $Å^3$; $Z$ = 4; $\rho_{calcd}$ = 1.010 g $cm^{-3}$; $\mu$ = 0.081 $mm^{-1}$; $\lambda$ = 0.71073 Å; T = –80 °C; $2\theta$ max = 52.80°; total data collected = 38176; $R_1$ = 0.0490 for 7904 observed reflections with [$F_o^2 \geq 2\sigma(F_o^2)$]; $wR_2$ = 0.1106 for 545 variables and 9822 unique reflections with [$F_o^2 \geq -3\sigma(F_o^2)$]; residual electron density = 0.230 and –0.160 e $Å^{-3}$.

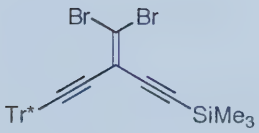


**5.15**

**5.15:** To a solution of $CBr_4$ (191 mg, 0.576 mmol) in $CH_2Cl_2$ (10 mL) was added $PPh_3$ (322 mg, 1.23 mmol) and the mixture stirred at rt under a $N_2$ atmosphere for 1 h. A solution of **5.12** (theoretically 0.384 mmol of **5.12** generated from 256 mg of acid choride **5.11**; see synthesis of **5.12**) in $CH_2Cl_2$ (5 mL) was added and the resulting mixture stirred under a $N_2$ atmosphere for 1 h. Hexanes were added to precipitate the phosphine salts as a white solid along with an oily residue. The supernatant was decanted and filtered through a pad of celite. The oily residue left in the flask was dissolved in minimal $CH_2Cl_2$ and hexanes were added; the heterogeneous mixture was then decanted and the supernatant filtered through celite (this procedure was repeated three times). The filtrate was filtered through celite until the filtrate remained a clear solution. The solvent was removed in vacuo and the crude product was purified by column chromatography (silica gel, hexanes) to yield **5.15** (33 mg, 10%) as a white solid: IR (microscope) 3072 (w), 2957, 2905, 2868, 2229, 2149, 1592 $cm^{-1}$; $^1H$ NMR (500 MHz, $CDCl_3$): $\delta$ 7.24 (t, $J$ = 2 Hz, 3H), 6.98 (d, $J$ = 2 Hz, 6H), 1.20 (s, 54H), 0.20 (s, 9H); $^{13}C$ NMR (100 MHz, $CDCl_3$): $\delta$ 149.8, 144.2, 123.9, 119.9, 114.8, 108.0, 103.7, 101.7, 100.7, 80.6, 57.2, 34.8, 31.4, –0.4; EIMS $m/z$ 884.7 ($M^+$, 87), 827.4 ($[M - t\text{Bu}]^+$, 100).

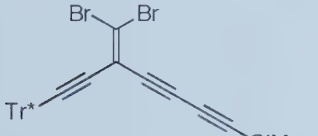


**5.16**

**5.16:** A solution of **5.10** (217 mg, 0.334 mmol) in $SOCl_2$ (1 mL) was stirred for 17 h covered with a drying tube ($CaCl_2$). The excess $SOCl_2$ was removed in vacuo to obtain acid chloride **5.11**, 1,4-bis(trimethylsilyl)butadiyne (65 mg, 0.33 mmol) was added, and the mixture dissolved in $CH_2Cl_2$ (5 mL). This solution was added dropwise to a mixture of $AlCl_3$ (49 mg, 0.37 mmol) in $CH_2Cl_2$ cooled to –40 °C under a $N_2$ atmosphere, and the resulting mixture was stirred at –40 °C for 2 h. The reaction was quenched with $H_2O$ (10 mL), warmed to rt, and the layers separated. The aqueous phase was extracted with $CH_2Cl_2$ (10 mL), the organic phases combined, washed with brine (10 mL), and dried over $MgSO_4$. The solvent was removed in vacuo and the crude ketone purified by column chromatography (silica gel, eluted with hexanes first to remove unreacted diyne followed by $CH_2Cl_2$ to remove ketone **5.13**). The ketone fractions were combined and concentrated to ca. 5 mL and held for later use (ketone **5.13**). To solution of $CBr_4$ (444 mg, 1.34 mmol) in $CH_2Cl_2$ (25 mL) under a $N_2$ atmosphere was added $PPh_3$ (788 mg, 3.00 mmol) and the

resulting mixture stirred for 1 h. The ketone (**5.13**) solution was added slowly and the reaction stirred for 20 min. The solvent was removed in vacuo and the crude product was purified by column chromatography (silica gel, hexanes) to yield **5.16** (36 mg, 12%) as a yellow oil: $R_f$ = 0.44 ($CH_2Cl_2$/hexanes 1:10); IR (microscope) 3071 (w), 2963, 2904, 2868, 2221, 2099, 1592 $cm^{-1}$; $^1H$ NMR (500 MHz, $CDCl_3$): $\delta$ 7.25 (t, $J$ = 2 Hz, 3H), 6.96 (d, $J$ = 2 Hz, 6H), 1.20 (s, 54H), 0.20 (s, 9H); $^{13}C$ NMR (125 MHz, $CDCl_3$): $\delta$ 149.9, 144.1, 123.8, 120.0, 114.0, 109.0, 104.9, 94.5, 87.4, 80.2, 79.9, 72.9, 57.3, 34.9, 31.4, –0.6; EIMS $m/z$ 908.2 ($M^+$, 24), 851.3 ([M – $t$Bu]$^+$, 60).

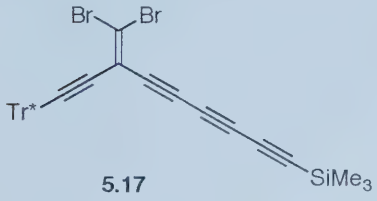


**5.17**

**5.17:** To a mixture of $AlCl_3$ (97 mg, 0.73 mmol) in $CH_2Cl_2$ (25 mL) cooled to 0 °C under a $N_2$ atmosphere was added dropwise a solution of **5.11** (244 mg, 0.366 mmol) and 1,6-bis(trimethylsilyl)hexa-1,3,5-triyne[13] (159 mg, 0.731) in $CH_2Cl_2$ (5 mL). The reaction was stirred at 0 °C for 3 h, the reaction quenched with $H_2O$ (15 mL), warmed to rt and the resulting mixture extracted with $Et_2O$ (75 mL). The organic phase was washed with brine (15 mL) and dried over $MgSO_4$. The solvent was removed in vacuo and the crude ketone (**5.14**) purified by column chromatography (silica gel, eluted with hexanes to remove unreacted triyne followed by $CH_2Cl_2$ to remove ketone). The ketone fractions were combined and concentrated to ca. 5 mL and held for later use (**5.14**). To solution of $CBr_4$ (243 mg, 0.733 mmol) in $CH_2Cl_2$ (20 mL) under a $N_2$ atmosphere was added $PPh_3$ (434 mg, 1.65 mmol) and the resulting mixture stirred for 1 h. The ketone (**5.14**) solution was added slowly and the reaction stirred for 16 h. Hexanes were added to precipitate the phosphine salts as a white solid along with an oily residue. The supernatant was decanted and filtered through a pad of celite. The oily residue left in the flask was dissolved in minimal $CH_2Cl_2$ and hexanes were added; the heterogeneous mixture was then decanted and the supernatant filtered through celite (this procedure was repeated three times). The filtrate was filtered through celite until the filtrate remained a clear solution. The solvent was removed in vacuo and the crude product was purified by column chromatography (silica gel, hexanes) to yield **5.17** (48 mg, 14%) as a yellow oil: $R_f$ = 0.47 ($CH_2Cl_2$/hexanes 1:10); IR (microscope) 3070 (w), 2963, 2905, 2867, 2220, 2180 (w), 2076, 1592 $cm^{-1}$; $^1H$ NMR (500 MHz, $CDCl_3$): $\delta$ 7.25 (t, $J$ = 2 Hz, 3H), 6.95 (d, $J$ = 2 Hz, 6H), 1.19 (s, 54H), 0.21 (s, 9H); $^{13}C$ NMR (125 MHz, $CDCl_3$): $\delta$ 149.9, 144.0, 123.8, 120.0, 113.7, 110.8, 105.4, 91.0, 87.9, 79.9, 79.8, 73.0, 70.0, 61.0, 57.3, 34.9, 31.4, –0.6; EIMS $m/z$ 932.2 ($M^+$, 50), 875.0 ([M – $t$Bu]$^+$, 100).

**Data for ketone 5.14:** $R_f$ = 0.33 ($CH_2Cl_2$/hexanes 1:10); $^1H$ NMR (500 MHz, $CDCl_3$): $\delta$ 7.29 (t, $J$ = 2 Hz, 3H), 6.93 (d, $J$ = 2 Hz, 6H), 1.21 (s, 54H), 0.23 (s, 9H).

**5.18**

**5.18:** To a solution of **5.15** (33 mg, 0.037 mmol) in hexnaes (5 mL) cooled to –78 °C under a $N_2$ atmosphere was added BuLi (18 μL, 2.5M in hexanes, 0.045 mmol) dropwise. The reaction was stirred for 10 min at –78 °C and then the reaction was warmed to rt over 30 min. The reaction was quenched with saturated aqueous $NH_4Cl$ (5 mL), the layers separated, and the organic phase dried over $Na_2SO_4$. The solvent was removed in vacuo and the crude product purified by column chromatography (silica gel, hexanes) to yield **5.18** (22 mg, 81%) as a white solid: $R_f$ = 0.53 ($CH_2Cl_2$/hexanes 1:10); IR (microscope) 3068 (w), 2963, 2905, 2868, 2212, 2173, 2075, 1592 $cm^{-1}$; $^1H$ NMR (500 MHz, $CDCl_3$): $\delta$ 7.26 (t, $J$ = 2 Hz, 3H), 6.91 (d, $J$ = 2 Hz, 6H), 1.19 (s, 54H), 0.19 (s, 9H); $^{13}C$ NMR (125 MHz, $CDCl_3$): $\delta$ 150.0, 143.7, 123.7, 120.2, 88.6, 86.0, 85.5, 68.7, 62.7, 62.0, 57.1, 34.8, 31.4, –0.5; EIMS *m/z* 725.0 ($M^+$, 50), 611.4 ($[M - (2 \times t\text{Bu})]^+$, 40), 57.1 ($[t\text{Bu}]^+$, 100); MALDI MS *m/z* 725.6 ($M^+$, 100), 667.5 ($[M - t\text{Bu}]^+$, 70); MALDI HRMS *m/z* calcd. for $C_{52}H_{72}Si$ ($M^+$) 724.5398, found 724.5394.

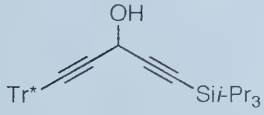


**5.21**

**5.21:** A solution of **5.6** (3.189 g, 5.271 mmol) in THF (200 mL) was cooled to –78 °C under a $N_2$ atmosphere BuLi (2.1 mL, 2.5 M in hexanes, 5.3 mmol) was added. A solution of 3-TIPS-propargylic aldehyde (1.056 g, 5.020 mmol) in THF (10 mL) was added over 5 min, the resulting mixture warmed to rt and stirred for 1 h. The reaction was cooled to 0 °C, quenched with saturated $NH_4Cl$ (100 mL), and the resulting mixture extracted with $Et_2O$ (200 mL). The organic phase was washed with saturated $NH_4Cl$ (100 mL), $H_2O$ (100 mL), brine (100 mL), and dried over $Na_2SO_4$. The solvent was removed in vacuo and the crude product purified by column chromatography (silica gel, $CH_2Cl_2$/hexanes 1:3) to yield **5.21** (3.760 g, 92%) as a pale yellow oil that solidified upon standing: Mp 54-57 °C; $R_f$ = 0.47 ($CH_2Cl_2$/hexanes 1:1); IR (microscope) 3460 (w), 3071 (w), 2963, 2904, 2867, 2232 (w), 2176 (w), 1593 $cm^{-1}$; $^1H$ NMR (500 MHz, $CDCl_3$): $\delta$ 7.23 (t, $J$ = 2 Hz, 3H), 6.95 (d, $J$ = 2 Hz, 6H), 5.31 (d, $J$ = 8 Hz), 2.10 (d, $J$ = 8 Hz), 1.19 (s, 54H), 1.07-1.02 (m, 21H); $^{13}C$ NMR (125 MHz, $CDCl_3$): $\delta$ 149.7, 144.7, 123.8, 119.8, 104.5, 91.8, 85.3, 80.8, 56.2, 53.3, 34.8, 31.4, 18.6, 11.1; EIMS *m.z* 814.7 ($M^+$, 3), 757.8 ($[M - t\text{Bu}]^+$, 40), 603.5 ($[M - i\text{-}Pr_3Si\text{-}C{\equiv}C\text{-}CHOH]^+$, 51), 547.3 ($[M - t\text{-}Bu - i\text{-}Pr_3Si\text{-}C{\equiv}C\text{-}CHO]^+$, 30).

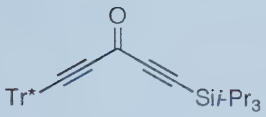


**5.22**

**5.22**: To a solution of **5.21** (3.862 g, 4.736 mmol) in $CH_2Cl_2$ (200 mL) was added celite (4 g), molecular sieves (4 g) and PCC (2.053 g, 9.524 mmol) in that order and the reaction stirred at rt under a $N_2$ atmosphere for 24 h. The mixture was filtered through a silica plug with $CH_2Cl_2$ and the solvent removed in vacuo to yield **5.22** (3.736 g, 97%) as a white solid: Mp 115-118 °C; $R_f$ = 0.47 ($CH_2Cl_2$/hexanes 1:2); IR (microscope) 3070 (w), 2963, 2905, 2868, 2207, 2153, 1630, 1593, $cm^{-1}$; $^1H$ NMR (500 MHz, $CDCl_3$): $\delta$ 7.27 (t, $J$ = 2 Hz, 3H), 6.94 (d, $J$ = 2 Hz, 6H), 1.19 (s, 54H), 1.12-1.04 (m, 21H); $^{13}C$ NMR (125 MHz, $CDCl_3$): $\delta$ 160.6, 150.1, 143.2, 123.8, 120.4, 105.3, 99.9, 95.5, 85.1, 56.8, 34.8, 31.4, 18.5, 11.1; EIMS *m/z* 812.5 ($M^+$, 20), 756.4 ([M – *t*Bu + H]$^+$, 100), 603.5 ([M – *i*Pr$_3$SiC≡CCO]$^+$, 88); MALDI HRMS *m/z* calcd. for $C_{57}H_{84}OSi$ ($M^+$) 812.6286, found 812.6283.

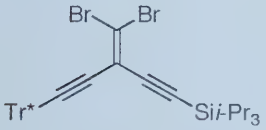


**5.23**

**5.23**: To a solution of $CBr_4$ (3.105 g, 9.362 mmol) in $CH_2Cl_2$ (200 mL) was added $PPh_3$ (5.135 g, 19.58 mmol) and the resulting mixture stirred at rt under a $N_2$ atmosphere for 1 h. A solution of **5.22** (3.736 g, 4.593 mmol) in $CH_2Cl_2$ (50 mL) was added and the reaction stirred for 21 h. The reaction mixture was concentrated to ca. 50 mL and hexanes were added to precipitate the phosphine salts as a white solid along with an oily residue. The supernatant was decanted and filtered through a pad of celite. The oily residue left in the flask was dissolved in minimal $CH_2Cl_2$ and hexanes were added; the heterogeneous mixture was then decanted and the supernatant filtered through celite (this procedure was repeated three times). The filtrate was filtered through celite until the filtrate remained a clear solution. The solvent was removed in vacuo and the crude product was purified by column chromatography (silica gel, $CH_2Cl_2$/hexanes 1:10) to yield **5.23** (4.345 g, 98%) as a white solid: Mp 135-136 °C; $R_f$ = 0.58 ($CH_2Cl_2$/hexanes 1:10); IR (microscope) 3073 (w), 2962, 2867, 2226, 2145 (w), 1592 $cm^{-1}$; $^1H$ NMR (400 MHz, $CDCl_3$): $\delta$ 7.23 (t, $J$ = 2 Hz, 3H), 6.99 (d, $J$ = 2 Hz, 6H), 1.19 (s, 54H), 1.09-1.05 (m, 21H); $^{13}C$ NMR (100 MHz, $CDCl_3$): $\delta$ 149.7, 144.3, 123.9, 119.9, 115.0, 108.0, 103.5, 102.3, 98.8, 81.0, 57.3, 34.8, 31.4, 18.6, 11.2; EIMS *m/z* 968.6 ($M^+$, 18), 911.9 ([M – *t*Bu]$^+$, 32), 57 ([*t*Bu]$^+$, 100); MALDI HRMS *m/z* calcd. for $C_{58}H_{84}{}^{79}Br_2Si$ ($M^+$) 966.4704, found 966.4709.

**5.24**

**5.24**: To a solution of **5.23** (4.436 g, 4.577 mmol) in hexanes (200 mL) at –78 °C was added BuLi (2.2 mL, 2.5M in hexanes, 5.5 mmol) dropwise under a $N_2$ atmosphere. The reaction mixture was stirred at –78 °C for 10 min, warmed to rt over 30 min and the reaction was quenched by the addition of saturated aqueous $NH_4Cl$ (50 mL). The layers were separated and the organic layer dried over $Na_2SO_4$. The solvent was removed in vacuo and the crude product was purified by column chromatography (silica gel, hexanes) to yield **5.24** (3.357 g, 91%) as a white solid: Mp 194-198 °C; $R_f$ = 0.67 ($CH_2Cl_2$/hexanes 1:10); IR (microscope) 3070 (w), 2963, 2905, 2867, 2211, 2172, 2072, 1592 $cm^{-1}$; $^1H$ NMR (400 MHz, $CDCl_3$): $\delta$ 7.25 (t, $J$ = 2 Hz, 3H), 6.91 (d, $J$ = 2 Hz, 6H), 1.19 (s, 54H), 1.09-1.06 (m, 21H); $^{13}C$ NMR (100 MHz, $CDCl_3$): $\delta$ 150.0, 143.8, 123.7, 120.2, 90.2, 85.0, 83.6, 69.0, 62.5, 61.6, 57.1, 34.8, 31.4, 18.5, 11.3; MALDI MS *m/z* 808.3 ($M^+$, 100), 751.1 ([M – *t*Bu]$^+$, 41); MALDI HRMS *m/z* calcd. for $C_{58}H_{84}Si$ ($M^+$) 808.6337, found 808.6330; DSC: Endotherm = 174 °C;[35] Mp = 201 °C; decomposition, 323 °C (onset) and 341 (peak).

**X-ray Crystal Data for 5.24:** Single crystals of **5.24** suitable for X-ray crystallographic analysis were grown by slow evaporation of a $CH_2Cl_2$ solution containing a few drops of MeOH at rt. $C_{58}H_{84}Si$, $M_r$ = 809.34; triclinic crystal system; space group $P\bar{1}$ (No. 2), $a$ = 10.297 (3), $b$ = 10.367 (3), $c$ = 25.911 (7) Å; $\alpha$ = 96.060 (3)°; $\beta$ = 99.065 (3)°; $\gamma$ = 92.404 (3)°; $V$ = 2711.2 (12) Å$^3$; $Z$ = 2; $\rho_{calcd}$ = 0.991 g $cm^{-3}$; $\mu$ = 0.076 $mm^{-1}$; $\lambda$ = 0.71073 Å; T = –100 °C; 2$\theta$ max = 52.80°; total data collected = 21818; $R_1$ = 0.0493 for 8586 observed reflections with [$F_o^2 \geq 2\sigma(F_o^2)$]; $wR_2$ = 0.1445 for 562 variables and 11074 unique reflections with [$F_o^2 \geq -3\sigma(F_o^2)$]; residual electron density = 0.404 and –0.301 e Å$^{-3}$.

**5.25**

**5.25:** To a solution of **5.24** (2.218 g, 2.740 mmol) in wet THF (100 mL THF and 5 drops $H_2O$) was added TBAF (3.0 mL, 1.0M in THF, 3.0 mmol). The solution was stirred at rt for 15 min. The reaction was quenched with saturated $NH_4Cl$ (50 mL) and extracted with hexanes (100 mL). The organic phase was washed with saturated aqueous $NH_4Cl$ (50 mL), $H_2O$ (50 mL), brine (50 mL), and dried over $Na_2SO_4$. The solvent was removed in vacuo and the crude product purified by slurry washing with $Et_2O$ to yield **5.25** (1.632 g, 91%) as a white solid: Mp 206 °C (decomp); $R_f$ = 0.46 ($CH_2Cl_2$/hexanes 1:10); IR (microscope) 3282, 3075 (w), 2964, 2906, 2868, 2218, 1590 $cm^{-1}$; $^1H$ NMR (500 MHz, $CDCl_3$): $\delta$ 7.26 (t, $J$ = 2 Hz, 3H), 6.90 (d, $J$ = 2 Hz, 6H), 2.07 (s, 1H), 1.19 (s, 54H); $^1H$ NMR (500 MHz, $CD_2Cl_2$): $\delta$ 7.32 (t, $J$ = 2 Hz, 3H), 6.96 (d, $J$ = 2 Hz, 6H), 2.21 (s, 1H), 1.22 (s, 54H); $^{13}C$ NMR (125 MHz, $CDCl_3$): $\delta$ 150.1, 143.6, 123.7, 120.3, 84.8, 68.9, 68.5, 66.6,

61.6, 61.3, 57.0, 34.8, 31.4; $^{13}$C NMR (125 MHz, $CD_2Cl_2$): $\delta$ 150.7, 143.9, 124.0, 120.9, 85.0, 69.0, 68.7, 67.4, 62.0, 61.2, 57.5, 35.1, 31.5; EI MS *m/z* 652.5 ($M^+$, 18), 595.4 ([M – *t*Bu]$^+$, 74), 57.1 ([*t*Bu]$^+$, 100); EI HRMS *m/z* calcd. for $C_{49}H_{64}$ ($M^+$) 652.5008, found 652.5001; Anal. calcd. for $C_{49}H_{64}$: C, 90.12; H, 9.88. Found: C, 89.89; H, 10.06; DSC: decomposition, 212 °C (onset) and 217 °C (peak).

**X-ray Crystal Data for 5.25:** Single crystals of **5.25** suitable for X-ray crystallographic analysis were grown by slow evaporation of a xylenes solution at rt. $C_{49}H_{64}$, $M_r$ = 653.00; trigonal crystal system; space group *P*31*c* (No. 159), $a$ = 14.154 (3), $c$ = 12.123 (2) Å; $V$ = 2103.4 (7) Å$^3$; $Z$ = 2; $\rho_{calcd}$ = 1.031 g cm$^{-3}$; $\mu$ = 0.057 mm$^{-1}$; $\lambda$ = 0.71073 Å; T = –100 °C; 2$\theta$ max = 50.96°; total data collected = 14896; $R_1$ = 0.0403 for 1952 observed reflections with [$F_o^2 \geq 2\sigma(F_o^2)$]; $wR_2$ = 0.0885 for 148 variables and 2618 unique reflections with [$F_o^2 \geq -3\sigma(F_o^2)$]; residual electron density = 0.128 and –0.179 e Å$^{-3}$.

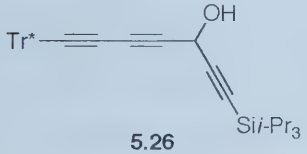


**5.26**

**5.26**: A solution of **5.7** (1.983 g, 3.153 mmol) in THF (100 mL) was cooled to –78 °C under a $N_2$ atmosphere, BuLi (1.26 mL, 2.5 M in hexanes, 3.15 mmol) was added and the mixture stirred for 10 min. A solution of 3-TIPS propargylic aldehyde (632 mg, 3.00 mmol) in THF (10 mL) was added dropwise over 5 min, the resulting mixture warmed to rt over 30 min and stirred for and additional 1 h. The reaction was quenched with saturated $NH_4Cl$ (50 mL) and the resulting mixture extracted with hexanes (200 mL). The organic phase was washed with $H_2O$ (50 mL), brine (50 mL), and dried over $MgSO_4$. The solvent was removed in vacuo and the crude product purified by column chromatography (silica gel, eluted with $CH_2Cl_2$/hexanes 1:10 until unreacted **5.7** starting was removed then a slow gradient to $CH_2Cl_2$/hexanes 1:1) to yield **5.26** (2.285 g, 91%) as a yellow oil that solidified upon standing: Mp 70-72 °C; $R_f$ = 0.28 ($CH_2Cl_2$/hexanes 1:2); IR (microscope) 3425 (br, w), 3072 (w), 2963, 2904, 2867, 2256 (w), 2176 (w), 1592 cm$^{-1}$; $^1$H NMR (400 MHz, $CDCl_3$): $\delta$ 7.26 (t, $J$ = 2 Hz, 3H), 6.93 (d, $J$ = 2 Hz, 6H), 5.18 (d, $J$ = 8 Hz, 1H), 2.18 (d, $J$ = 8 Hz, 1H), 1.20 (s, 54H), 1.12-1.03 (m, 21H); $^{13}$C NMR (100 MHz, $CDCl_3$): $\delta$ 149.9, 144.0, 123.8, 120.1, 103.0, 87.8, 86.7, 74.0, 69.7, 67.6, 57.0, 53.1, 34.8, 31.4, 18.5, 11.1; $^{13}$C NMR (APT, 100 MHz, $CDCl_3$): $\delta$ 149.9 (C), 144.0 (C), 123.8 (CH), 120.1 (CH), 103.0 (C), 87.8 (C), 86.7 (C), 74.0 (C), 69.7 (C), 67.6 (C), 57.0 (C), 53.1 (CH), 34.8 (C), 31.4 ($CH_3$), 18.5 ($CH_3$), 11.1 (CH); MALDI HRMS *m/z* calcd. for $C_{59}H_{86}OSi$ ($M^+$) 838.6443, found 838.6443.

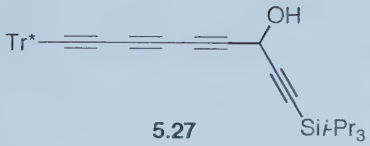


**5.27**

**5.27:** To a solution of **5.25** (240 mg, 0.368 mmol) in THF (60 mL) cooled to –78 °C under a $N_2$ atmosphere was added BuLi (0.15 mL, 2.5 in hexanes, 0.37 mmol) and the mixture stirred for 10 min. To this mixture was added a solution of 3-TIPS propargylic aldehyde (74 mg, 0.35 mmol) in THF (5 mL) and the reaction stirred at –78 °C for 1 h. The reaction was quenched with saturated aqueous $NH_4Cl$ (20 mL), the mixture warmed to rt and extracted with hexanes (100 mL). The organic phase was dried over $MgSO_4$. The solvent was removed in vacuo and the crude product purified by column chromatography (silica gel, gradient with hexanes → $CH_2Cl_2$/hexanes 1:1) to yield **5.27** (106 mg, 35%) as a brown oil: $R_f$ = 0.38 (EtOAc/hexanes 1:10); IR (microscope) 3419 (br), 3072 (w), 2963, 2905, 2867, 2216, 1592 $cm^{-1}$; $^1H$ NMR (400 MHz, $CDCl_3$): $\delta$ 7.27 (t, $J$ = 2 Hz, 3H), 6.92 (d, $J$ = 2 Hz, 6H), 5.17 (br s, 1H), 2.22 (br s, 1H), 1.20 (s, 54H), 1.12-1.02 (m, 21); $^{13}C$ NMR (100 MHz, $CDCl_3$): $\delta$ 150.1, 143.6, 123.7, 120.3, 102.3, 87.6, 86.6, 73.6, 69.8, 68.5, 65.5, 60.9, 57.1, 53.1, 34.8, 31.4, 18.5, 11.1; MALDI MS *m/z* 1725.1 ([2 × M]$^+$, 55), 862.0 (overlapping [M]$^+$ and [2 × M]$^{2+}$, 100).

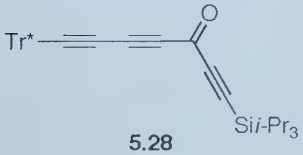


**5.28**

**5.28**: To a solution of **5.26** (361 mg, 0.430 mmol) in $CH_2Cl_2$ (25 mL) was added celite (0.5 g), molecular sieves (0.5 g), and PCC (185 mg, 0.860 mmol) in that order and the reaction stirred at rt under a $N_2$ atmosphere for 5 h. The mixture was filtered through a plug of silica with $CH_2Cl_2$ and the solvent removed in vacuo to yield **5.28** (329 mg, 91%) as an orange solid: Mp 58-60 °C; $R_f$ = 0.55 ($CH_2Cl_2$/hexanes 1:2); IR (microscope) 3068 (w), 2963, 2905, 2868, 2221, 2149, 1628, 1592 $cm^{-1}$; $^1H$ NMR (500 MHz, $CDCl_3$): $\delta$ 7.27 (t, $J$ = 2 Hz, 3H), 6.90 (d, $J$ = 2 Hz, 6H), 1.89 (s, 54H), 1.16-1.05 (m, 21H); $^{13}C$ NMR (125 MHz, $CDCl_3$): $\delta$ 159.5, 150.2, 143.1, 123.7, 120.5, 104.8, 98.1, 97.2, 77.2, 75.6, 67.1, 57.5, 34.8, 31.3, 18.5, 11.0; MALDI HRMS *m/z* calcd. for $C_{59}H_{84}OSi$ ($M^+$) 836.6286, found 836.6289.

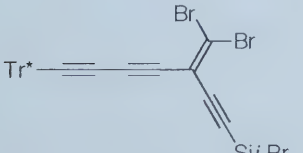


**5.30**

**5.30**: To a solution of $CBr_4$ (285 mg, 0.860 mmol) in $CH_2Cl_2$ (50 mL) was added $PPh_3$ (474 mg, 1.81 mmol) and the resulting mixture stirred at rt under a $N_2$ atmosphere for 1 h. A solution of **5.28** (329 mg, 0.393 mmol) in $CH_2Cl_2$ (10 mL) was added and the reaction stirred for 30 min. The reaction mixture was concentrated to ca. 20 mL and hexanes were added to precipitate the phosphine salts as a white solid along with an oily residue. The supernatant was decanted and filtered through a pad of celite. The oily residue left in the flask was dissolved in minimal $CH_2Cl_2$ and hexanes were added; the heterogeneous mixture was then decanted and the supernatant filtered through celite (this procedure was repeated three times). The filtrate was filtered through celite until the filtrate remained a clear solution. The solvent was removed in vacuo and the crude product was purified by column chromatography (silica gel, hexanes) to yield **5.30** (305 mg, 78%) as a pale yellow solid: Mp 210-211 °C; $R_f$ = 0.57 ($CH_2Cl_2$/hexanes 1:10); IR (microscope) 3069 (w), 2962, 2905, 2866, 2227, 2154, 1591 $cm^{-1}$; $^1H$ NMR (300 MHz, $CDCl_3$): $\delta$ 7.26 (t, $J$ = 2 Hz, 3H), 6.94 (d, $J$ = 2 Hz, 6H), 1.19 (s, 54H), 1.11-1.07 (m, 21H); $^{13}C$ NMR (125 MHz, $CDCl_3$): $\delta$ 150.0, 143.8, 123.8, 120.2, 114.1, 110.6, 101.5, 100.0, 93.9, 81.0, 73.0, 68.3, 57.3, 34.8, 31.4, 18.6, 11.1; MALDI HRMS m/z calcd. for $C_{60}H_{84}{}^{79}Br_2Si$ ($M^+$) 990.4704, found 990.4703; Anal. calcd. for $C_{60}H_{84}Br_2Si$: C, 72.56; H, 8.52. Found: C, 72.27; H, 8.44.

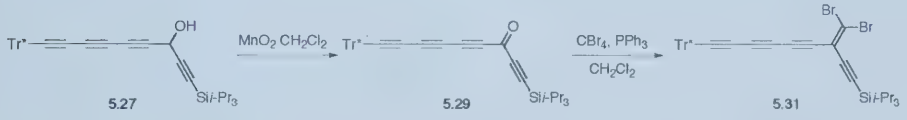


**5.31:** To a solution of **5.27** (106 mg, 0.123 mmol) in $CH_2Cl_2$ (20 mL) was added $MnO_2$ (107 mg, 1.23 mmol) and the reaction stirred at rt for 2 h. The reaction was sonicated for 5 min, filtered through a pad of celite and the filtrate concentrated to ca. 5 mL (**5.29**). Concurrently, to a solution of $CBr_4$ (92 mg, 0.28 mmol) in $CH_2Cl_2$ (20 mL) under a $N_2$ atmosphere was added $PPh_3$ (148 mg, 0.56 mmol) and the resulting mixture stirred for 1 h. To this was added the ketone solution (**5.29**) and the reaction stirred for 5 min. The mixture was concentrated to ca. 5 mL and hexanes were added to precipitate the phosphine salts as a white solid along with an oily residue. The supernatant was decanted and filtered through a pad of celite. The oily residue left in the flask was dissolved in minimal $CH_2Cl_2$ and hexanes were added; the heterogeneous mixture was then decanted and the supernatant filtered through celite (this procedure was repeated three times). The filtrate was filtered through celite until the filtrate remained a clear solution. The solvent was removed in vacuo and the crude product was purified by column chromatography (silica gel, hexanes) to yield **5.31** (64 mg, 51%) as a colorless oil: $R_f$ = 0.28 (hexanes); IR (microscope) 3068 (w), 2963, 2905, 2867, 2208, 2184, 1592 $cm^{-1}$; $^1H$ NMR (400 MHz, $CDCl_3$): $\delta$ 7.26 (t, $J$ = 2 Hz, 3H), 6.91 (d, $J$ = 2 Hz, 6H), 1.19 (s, 54H), 1.12-1.06 (m, 21H); $^{13}C$ NMR (100 MHz, $CDCl_3$): $\delta$ 150.1, 143.5, 123.7, 120.3, 113.6, 112.6, 101.0, 100.9, 89.4, 80.8, 71.9, 71.2, 68.9, 61.3, 57.4, 34.8, 31.4, 18.6, 11.1; EIMS $m/z$ 1016.8 ($M^+$, 49), 959.7 ([M – $t$Bu]$^+$, 100); MALDI HRMS $m/z$

calcd. for $C_{62}H_{84}{}^{79}Br_2Si$ ($M^+$) 1014.4704, found 1014.4701.

**5.32**

**5.32**: To a solution of **5.30** (1.856 g, 1.869 mmol) in hexanes (200 mL) at –78 °C was added BuLi (0.90 mL, 2.5M in hexanes, 2.2 mmol) dropwise under a $N_2$ atmosphere. The reaction mixture was stirred at –78 °C for 10 min, warmed to rt over 30 min, and quenched by the addition of saturated aqueous $NH_4Cl$ (50 mL). The layers were separated and the organic layer dried over $MgSO_4$. The solvent was removed in vacuo and the crude product was purified by recrystallization from $Et_2O$/MeOH to yield **5.32** (1.425 g, 92%) as a yellow solid: Mp 204-206 °C; $R_f$ = 0.32 (hexanes); IR (microscope) 3069 (w), 2963, 2905, 2868, 2207, 2141, 2057, 1592 $cm^{-1}$; UV-Vis (hexanes) λ 264 (sh), 256, 241 (sh), 209 nm; $^1H$ NMR (500 MHz, $CDCl_3$): δ 7.25 (t, $J$ = 2 Hz, 3H), 6.89 (d, $J$ = 2 Hz, 6H), 1.18 (s, 54H), 1.07-1.05 (m, 21H); $^{13}C$ NMR (100 MHz, $CDCl_3$): δ 150.1, 143.5, 123.7, 120.3, 89.8, 85.7, 85.1, 68.8, 62.61, 62.59, 62.1, 61.8, 57.2, 34.8, 31.4, 18.5, 11.3; MALDI HRMS *m/z* calcd. for $C_{60}H_{84}Si$ ($M^+$) 832.6337, found 832.6339; Anal. calcd. for $C_{60}H_{84}Si$: C, 86.47; H, 10.16. Found: C, 85.88; H, 10.12; DSC: Mp = 217 °C; decomposition, 218 °C (onset) and 264 °C (peak).

**5.33**

**5.33 (modified Glaser-Eglinton-Hay coupling)**:[30-40] To a solution of **5.7** (187 mg, 0.297 mmol) and 1-TIPS-6-TMS-hexa-1,3,5-triyne[13] (450 mg, 1.49 mmol) in $CH_2Cl_2$ (10 mL), MeOH (10 mL) and 2,6-lutidine (10 mL) was added $K_2CO_3$ (205 mg, 1.49 mmol) and the mixture stirred for 10 min at rt. To the mixture was added $Cu(OAc)_2 \cdot H_2O$ (593 mg, 2.97 mmol) and the reaction stirred at rt until it was deemed complete by TLC; ca. 17 h. The reaction was quenched with saturated $NH_4Cl$ (25 mL) and the resulting mixture extracted with hexanes (100 mL). The organic phase was washed with saturated $NH_4Cl$ (25 mL), $H_2O$ (2 × 25 mL), brine (25 mL), and dried over $MgSO_4$. The solution was filtered through a plug of silica, the solvent removed in vacuo and the crude product purified by column chromatography (silica, hexanes) to yield **5.33** (213 mg, 84%) as a yellow solid.

**5.33 (Negishi protocol)**:[41,42] To a solution of 1-TIPS-6-TMS-hexa-1,3,5-triyne[13] (195 mg, 0.644 mmol) in THF (10 mL) cooled to –78 °C under a $N_2$ atmosphere was added methyllithium (0.40 mL, 1.6M in $Et_2O$, 0.64 mmol) and the mixture stirred for 5 min. The reaction was warmed to 0 °C, ZnCl (0.80 mL, 1.0M in $Et_2O$, 0.80 mmol) was added, the mixture warmed to rt, and stirred for 30 min. This solution was added via cannula to a deoxygenated solution of **5.36** (228 mg, 0.322 mmol) and $PdCl_2(PPh_3)_2$ (22 mg, 0.032 mmol) in toluene (10 mL) and the mixture stirred at

rt under a $N_2$ atmosphere for 24 h. Diisopropylamine (0.5 mL) was added and the reaction stirred for another 24 h at rt under a $N_2$ atmosphere. The reaction was quenched with $H_2O$ (10 mL) and the resulting mixture extracted with hexanes (50 mL). The organic phase was washed with $H_2O$ (10 mL), brine (10 mL), and dried over $MgSO_4$. The solvent was removed in vacuo and the crude product purified by column chromatography (silica gel, hexanes) to yield **5.33** (227 mg, 80%) as a yellow solid.

**5.33 (Sonogashira protocol):**[43,44] To a solution of 1-TIPS-6-TMS-hexa-1,3,5-triyne[13] (445 mg, 1.47 mmol) in THF (20 mL) and MeOH (20 mL) was added $K_2CO_3$ (203 mg, 1.47 mmol) and the resulting mixture stirred for 30 min. Saturated aqueous $NH_4Cl$ (20 mL) was added and the resulting mixture extracted with hexanes (2 × 50 mL). The organic phases were combined, washed with $H_2O$ (20 mL), brine (20 mL), and dried over $MgSO_4$. The filtrate was concentrated to ca. 5 mL and held for later use (TIPS-triyne solution). Concurrently, to a deoxygenated solution of **5.36** (520 mg, 0.735 mmol) in toluene (50 mL) at 0 °C was added $PdCl_2(PPh_3)_2$ (26 mg, 0.037 mmol), CuI (7 mg, 0.037 mmol), diisopropylamine (0.22 g, 0.31 mL, 2.2 mmol), and the TIPS-triyne solution, in that order. The reaction was stirred at 0 °C under a $N_2$ atmosphere for 7 h, quenched by the addition of $H_2O$ (20 mL), and extracted with hexanes (50 mL). The organic phase was washed with saturated $NH_4Cl$ (20 mL), $H_2O$ (10 mL), brine (10 mL), and dried over $MgSO_4$. The solvent was removed in vacuo and the crude product purified by column chromatography (silica gel, hexanes) to yield **5.33** (145 mg, 23%) as a yellow solid.

**Data for 5.33:** Mp 180-183 °C; $R_f$ = 0.35 (hexanes); IR (microscope) 3069 (w), 2963, 2904, 2867, 2200, 2105, 2046 (w), 1592 $cm^{-1}$; UV-Vis (hexanes) $\lambda_{max}$ 288, 276, 270, 258 (sh) nm; $^1H$ NMR (400 MHz, $CDCl_3$): $\delta$ 7.26 (t, $J$ = 2 Hz, 3H), 6.89 (d, $J$ = 2 Hz, 6H), 1.19 (s, 54H), 1.09-1.05 (m, 21H); $^{13}C$ NMR (125 MHz, $CDCl_3$): $\delta$ 150.1, 143.4, 123.7, 120.4, 89.6, 86.1, 86.0, 68.7, 62.86, 62.84, 62.68, 62.22, 62.21, 61.6, 57.3, 34.8, 31.4, 18.5, 11.3; APPI HRMS *m/z* calcd. for $C_{62}H_{85}Si$ ($[M + H]^+$) 857.6415, found 857.6407; Anal. calcd. for $C_{62}H_{84}Si$: C, 86.85; H, 9.87. Found: C, 86.13; H, 9.58; DSC: Mp = 218 °C; decomposition, 199 °C (onset) and 232 °C (peak); Note: During DSC analysis an endotherm occurred slightly after the exotherm started. This was seen also during capillary Mp determination where the sample turned brown, melted, and then went black.

**5.34**

**5.34:** To a solution of **5.32** (1.073 g, 1.288 mmol) in THF (100 mL) and $H_2O$ (20 mL) was added CsF (0.235 g, 1.54 mmol). The reaction was stirred at rt until deemed complete by TLC analysis: ca. 60 min. The reaction was quenched with saturated $NH_4Cl$ (50 mL) then extracted with hexanes (100 mL). The organic layer was washed with $H_2O$ (50 mL), brine (50 mL), and dried over $MgSO_4$. The solvent was removed in vacuo and the crude product purified by passing through a

plug of silica gel with $CH_2Cl_2$/hexanes (1:5). The collected solution was treated with activated charcoal, filtered through celite, and the solvent removed in vacuo to yield **5.34** (0.884 g, quantitative) as a yellow solid: $R_f$ = 0.29 (hexanes); IR (microscope) 3264, 3072 (w), 2963, 2905, 2867, 2208, 2159, 1592 $cm^{-1}$; UV-Vis (hexanes) λ 247, 236, 228, 220, 209 nm; $^1H$ NMR (400 MHz, $CDCl_3$): $\delta$ 7.27 (t, $J$ = 2 Hz, 3H), 6.91 (d, $J$ = 2 Hz, 6H), 2.07 (s, 1H), 1.20 (s, 54H); $^{13}C$ NMR (100 MHz, $CDCl_3$): $\delta$ 150.1, 143.4, 123.7, 120.4, 85.7, 68.61, 68.58, 67.1, 62.24, 62.20, 61.6, 61.3, 57.2, 34.8, 31.4; APPI HRMS *m/z* calcd. for $C_{51}H_{65}$ ($[M + H]^+$) 677.5081, found 677.5080; Anal. calcd. for $C_{51}H_{64}$: C, 90.47; H, 9.53. Found: C, 90.38; H, 9.55; DSC: decomposition, 120 °C (onset) and 135 °C (peak).

**5.35**

**5.35:** To a solution of **5.33** (327 mg, 0.381 mmol) in THF (30 mL) and $H_2O$ (6 mL) was added CsF (70 mg, 0.46 mmol). The reaction was stirred at rt until deemed complete by TLC analysis: ca 30 min. The reaction was quenched with saturated $NH_4Cl$ (15 mL) and extracted with hexanes (50 mL). The organic layer was washed with $H_2O$ (15 mL), brine (15 mL), and dried over $MgSO_4$. The solvent was removed in vacuo and the crude product purified by passing through a plug of silica gel with $CH_2Cl_2$/hexanes (1:5) to yield **5.35** (263 mg, 99%) as a yellow solid: $R_f$ = 0.29 (hexanes); IR (microscope) 3277, 3067 (w), 2964, 2905, 2867, 2206, 2183 (w), 2116, 1590 $cm^{-1}$; UV-Vis (hexanes) $\lambda_{max}$ 288 (sh), 278, 266, 255, 245, 209 nm; $^1H$ NMR (500 MHz, $CDCl_3$): $\delta$ 7.27 (t, $J$ = 2 Hz, 3H), 6.90 (d, $J$ = 2 Hz, 6H), 2.08 (s, 1H), 1.20 (s, 54H); $^1H$ NMR (400 MHz, $CD_2Cl_2$): $\delta$ 7.32 (t, $J$ = 2 Hz, 3H), 6.94 (d, $J$ = 2 Hz, 6H), 2.26 (s, 1H), 1.21 (s, 54H); $^{13}C$ NMR (125 MHz, $CDCl_3$): $\delta$ 150.2, 143.3, 123.7, 120.4, 86.2, 68.6, 68.50, 67.49, 62.8, 62.5, 62.4, 61.8, 61.5, 61.3, 57.3, 34.9, 31.4; $^{13}C$ NMR (100 MHz, $CD_2Cl_2$): $\delta$ 150.9, 143.6, 124.0, 121.1, 86.5, 69.2, 68.33, 68.28, 62.8, 62.7, 62.5, 62.1, 61.9, 61.2, 57.7, 35.1, 31.5; APPI HRMS *m/z* calcd. for $C_{53}H_{65}$ ($[M + H]^+$) 701.5081, found 701.5069.

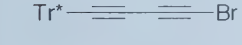


**5.36**

**5.36:** To a mixture of **5.7** (485 mg, 0.771 mmol) in acetone (100 mL) was added *N*-bromosuccinimide (165 mg, 0.925 mmol) and $AgNO_3$ (39 mg, 0.23 mmol). The reaction was stirred at rt until deemed complete by TLC; ca. 4 h. The reaction was quenched with $H_2O$ (50 mL) and extracted with a $CH_2Cl_2$/hexanes (1:4) solution. The layers were separated and the organic phase washed with $H_2O$ (50 mL), brine (50 mL), and dried over $MgSO_4$. The solvent was removed in vacuo and the crude product purified by passing through a plug of silica gel using $CH_2Cl_2$/hexanes (1:10) to yield **5.36** (520 mg, 95%) as a white solid: Mp 185-188 °C; $R_f$ = 0.20 (hexanes); IR (microscope) 3076 (w), 2966, 2906, 2869, 2130, 1588 $cm^{-1}$; $^1H$ NMR (300 MHz,

$CDCl_3$): $\delta$ 7.24 (t, $J$ = 2 Hz, 3H), 6.91 (d, $J$ = 2 Hz, 6H), 1.19 (s, 54H); $^{13}C$ NMR (125 MHz, $CDCl_3$): $\delta$ 149.9, 144.0, 123.7, 120.1, 82.3, 68.8, 66.0, 56.8, 39.0, 34.8, 31.4; MALDI HRMS *m/z* calcd. for $C_{47}H_{63}{}^{79}Br$ ($M^+$) 706.4108, found 706.4107.

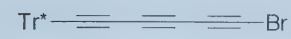

**5.37**

**5.37:** To a mixture of **5.25** (1.128 g, 1.727 mmol) in acetone (200 mL) was added *N*-bromosuccinimide (370 mg, 2.07 mmol) and $AgNO_3$ (59 mg, 0.35 mmol). The reaction was stirred at rt until deemed complete by TLC; ca. 20 h. The reaction was quenched with $H_2O$ (100 mL) and then extracted with a $CH_2Cl_2$ (2 × 250 mL). The organic layers were combined, washed with brine (50 mL), and dried over $MgSO_4$. The solvent was removed in vacuo and the crude product purified by passing through a plug of silica gel using $CH_2Cl_2$/hexanes (1:5) to yield **5.37** (1.226 g, 97%) as a yellow solid: Mp 130 °C (decomp); $R_f$ = 0.38 (hexanes); IR (microscope) 3070 (w), 2964, 2905, 2867, 2217, 2097 (w), 1592 $cm^{-1}$; $^1H$ NMR (500 MHz, $CDCl_3$): $\delta$ 7.26 (t, $J$ = 2 Hz, 3H), 6.91 (d, $J$ = 2 Hz, 6H), 1.19 (s, 54H); $^{13}C$ NMR (125 MHz, $CDCl_3$): $\delta$ 150.1, 143.6, 123.7, 120.3, 84.5, 68.5, 66.4, 62.4, 60.0, 57.1, 40.0, 34.8, 31.4; MALDI MS *m/z* 730.3 ($M^+$, 100), 673.2 ([M – *t*Bu]$^+$, 70); MALDI HRMS *m/z* calcd. for $C_{49}H_{63}{}^{79}Br$ ($M^+$) 730.4108, found 730.4109; Anal. calcd. for $C_{49}H_{63}Br$: C, 80.41; H, 8.68. Found: C, 80.37; H, 8.60.

**5.38**

**5.38:** To a mixture of **5.34** (87 mg, 0.13 mmol) in acetone (10 mL) was added *N*-bromosuccinimide (27 mg, 0.15 mmol) and $AgNO_3$ (7 mg, 0.04 mmol). The reaction was stirred in the dark at rt until deemed complete by TLC; ca. 16 h. The reaction was quenched with $H_2O$ (20 mL) and extracted with hexanes (50 mL). The layers were separated and the organic phase washed with $H_2O$ (10 mL), brine (10 mL), and dried over $MgSO_4$. The solvent was removed in vacuo and the crude product purified by passing through a plug of silica gel using $CH_2Cl_2$/hexanes (1:5) to yield **5.38** (90 mg, 93%) as a yellow solid: Mp 180 °C (decomp); $R_f$ = 0.32 (hexanes); IR (microscope) 2962, 2904, 2867, 2209, 2151, 1591 $cm^{-1}$; $^1H$ NMR (500 MHz, $CDCl_3$): $\delta$ 7.27 (t, $J$ = 2 Hz, 3H), 6.91 (d, $J$ = 2 Hz, 6H), 1.20 (s, 54H); $^{13}C$ NMR (125 MHz, $CDCl_3$): $\delta$ 150.1, 143.4, 123.7, 120.4, 85.5, 68.7, 66.3, 62.4, 62.0, 61.9, 60.3, 57.2, 41.0, 34.8, 31.4; APPI HRMS *m/z* calcd. for $C_{51}H_{64}{}^{79}Br$ ([M + H]$^+$) 755.4186, found 755.4173.

**5.39**

**5.39:** To a mixture of **5.35** (143 mg, 0.204 mmol) in acetone (50 mL) was added *N*-

bromosuccinimide (42 mg, 0.23 mmol) and $AgNO_3$ (13 mg, 0.078 mmol). The reaction was stirred in the dark at rt until deemed complete by TLC; ca. 21 h. The reaction was quenched with $H_2O$ (25 mL) and extracted with a $CH_2Cl_2$ (100 mL). The aqueous layer was extracted again with $CH_2Cl_2$ (25 mL), the organic layers combined, washed with brine (25 mL), and dried over $MgSO_4$. The solvent was removed in vacuo and the crude product purified by passing through a plug of silica gel using $CH_2Cl_2$/hexanes (1:5) to yield **5.39** (149 mg, 94%) as a yellow solid: $R_f$ = 0.58 ($CH_2Cl_2$/hexanes 1:10); IR (microscope) 3069 (w), 2962, 2903, 2867, 2202, 2128 (w), 2112 (w), 1590 $cm^{-1}$; $^1H$ NMR (500 MHz, $CDCl_3$): $\delta$ 7.26 (t, $J$ = 2 Hz, 3H), 6.89 (d, $J$ = 2 Hz, 6H), 1.19 (s, 54H); $^{13}C$ NMR (125 MHz, $CDCl_3$): $\delta$ 150.2, 143.3, 123.7, 120.4, 86.1, 68.7, 66.2, 62.60, 62.55, 62.23, 62.16, 62.02, 60.0, 57.3, 41.8, 34.8, 31.4; APPI HRMS $m/z$ calcd. for $C_{53}H_{64}{}^{79}Br$ ($[M + H]^+$) 779.4186, found 779.4172.

**5.40**

**5.40 (modified Glaser-Eglinton-Hay coupling):**[36-40] To a solution of **5.25** (100 mg, 0.153 mmol) and 1-TIPS-6-TMS-hexa-1,3,5-triyne[13] (232 mg, 0.766 mmol) in $CH_2Cl_2$ (5 mL), MeOH (5 mL) and 2,6-lutidine (5 mL) was added $K_2CO_3$ (106 mg, 0.766 mmol) and the mixture stirred for 10 min at rt. To the mixture was added $Cu(OAc)_2 \cdot H_2O$ (305 mg, 1.53 mmol) and reaction stirred at rt until the reaction was deemed complete by TLC and UV-Vis analyses; ca. 6 h. The reaction was quenched with saturated $NH_4Cl$ (15 mL) and the resulting mixture extracted with hexanes (50 mL). The organic phase was washed with $H_2O$ (2 × 10 mL), brine (10 mL), and dried over $MgSO_4$. The solvent removed in vacuo and the crude product purified by column chromatography (silica, hexanes) to yield **5.40** (85 mg, 63%) as a yellow solid.

**5.40 (via a FBW rearrangement):**[45-47] To a solution of **5.50** (260 mg, 0.216 mmol) in hexanes (30 mL) cooled to –78 °C under a $N_2$ atmospohere was added BuLi (0.22 mL, 2.5M in hexanes, 0.54 mmol) and the reaction stirred at –78 °C for 10 min. The reaction warmed to rt over 30 min, quenched with saturated aqueous $NH_4Cl$ (10 mL) and the organic layer dried over $MgSO_4$. The solvent was removed in vacuo and the crude product purified by column chromatography (silica gel, hexanes) to yield **5.40** (81 mg, 43%) as a yellow solid.

**5.40 (Negishi protocol):**[41,42] To a solution of 1-TIPS-6-TMS-hexa-1,3,5-triyne[13] (96 mg, 0.32 mmol) in THF (10 mL) cooled to –78 °C under a $N_2$ atmosphere was added methyllithium (0.20 mL, 1.6M in $Et_2O$, 0.32 mmol)[48] and the mixture stirred for 10 min. The reaction was warmed to 0 °C, ZnCl (0.32 mL, 1.0M in $Et_2O$, 0.32 mmol) was added, the mixture warmed to rt, and stirred for 30 min. This solution was added via cannula to a deoxygenated solution of **5.37** (116 mg, 0.159 mmol) and $PdCl_2(PPh_3)_2$ (11 mg, 0.016 mmol) in toluene (10 mL) and the mixture stirred at 0 °C under a $N_2$ atmosphere for 45 h. The reaction was quenched with $H_2O$ (20 mL) and the resulting mixture extracted with hexanes (20 mL). The organic phase was washed with $H_2O$ (20

mL), brine (20 mL), and dried over $MgSO_4$. The solvent was removed in vacuo and the crude product purified by column chromatography (silica gel, hexanes) to yield **5.40** (55 mg, 39%) as a yellow solid (**Note:** yield = 63% based on 44 mg of recovered **5.37**).

**5.40 (Sonogashira protocol):**[43,44] To a solution of 1-TIPS-6-TMS-hexa-1,3,5-triyne[13] (50 mg, 0.16 mmol) in THF (5 mL) and MeOH (5 mL) was added $K_2CO_3$ (23 mg, 0.16 mmol) and the resulting mixture stirred for 30 min. Saturated aqueous $NH_4Cl$ (10 mL) was added and the resulting mixture extracted with hexanes (2 × 25 mL). The organic phases were combined, washed with $H_2O$ (5 mL), brine (5 mL), and dried over $Na_2SO_4$. The filtrate was concentrated to ca. 2 mL and held for later use (TIPS-triyne solution). Concurrently, to a deoxygenated solution of **5.37** (60 mg, 0.082 mmol) in toluene (15 mL) at 0 °C was added $PdCl_2(PPh_3)_2$ (3 mg, 0.004 mmol), CuI (1 mg, 0.005 mmol), diisopropylamine (25 mg, 35 μL, 0.25 mmol), and the TIPS-triyne solution, in that order. The reaction was stirred at 0 °C under a $N_2$ atmosphere for 26 h, quenched by the addition of $H_2O$ (10 mL), and extracted with hexanes (25 mL). The organic phase was washed with $H_2O$ (10 mL), brine (10 mL), and dried over $MgSO_4$. The solvent was removed in vacuo and the crude product purified by column chromatography (silica gel, hexanes) to yield **5.40** (31 mg, 43%) as a yellow solid.

**Data for 5.40**: Mp 145 °C (decomp); $R_f$ = 0.44 (hexanes); IR (microscope) 2962, 2867, 2206, 2167, 2070, 2038 (w), 1592 $cm^{-1}$; UV-Vis (hexanes) $\lambda_{max}$ (ε) 310 (232000), 303 (171000), 289 (195000), 274 (105000), 261 (49000) nm; $^1H$ NMR (400 MHz, $CDCl_3$): $\delta$ 7.26 (t, $J$ = 2 Hz, 3H), 6.88 (d, $J$ = 2 Hz, 6H), 1.18 (s, 54H), 1.06 (s, 21H); $^{13}C$ NMR (100 MHz, $CDCl_3$): $\delta$ 150.2, 143.3, 123.7, 120.4, 89.5, 86.7, 86.5, 68.7, 63.15, 63.11, 62.60, 62.58, 62.51, 62.42, 62.22, 61.4, 57.3, 34.8, 31.3, 18.5, 11.3; MALDI HRMS *m/z* calcd. for $C_{64}H_{84}Si$ ($M^+$) 880.6337, found 880.6328; DSC: decomposition, 182 °C (onset) and 206 °C (peak).

**X-ray Crystal Data for 5.40:** Single crystals of **5.40** suitable for X-ray crystallographic analysis were grown by slow evaporation of a $CDCl_3$/hexanes (1:1) solution at rt. $C_{64}H_{84}Si$, $M_r$ = 881.4; triclinic crystal system; space group $P\bar{1}$ (No. 2), $a$ = 10.2575 (7), $b$ = 14.6634 (11), $c$ = 21.9595 (16) Å; $\alpha$ = 76.520 (1)°; $\beta$ = 89.555 (1)°; $\gamma$ = 86.272 (1)°; $V$ = 3205.0 (4) $Å^3$; $Z$ = 2; $\rho_{calcd}$ = 1.003 g $cm^{-3}$; $\mu$ = 0.073 $mm^{-1}$; $\lambda$ = 0.71073 Å; T = –100 °C; $2\theta$ max = 50.50°; total data collected = 22875; $R_1$ = 0.0635 for 6600 observed reflections with $[F_o^2 \geq 2\sigma(F_o^2)]$; $wR_2$ = 0.1884 for 586 variables and 11578 unique reflections with $[F_o^2 \geq -3\sigma(F_o^2)]$; residual electron density = 0.407 and –0.258 e $Å^{-3}$.

**5.41**

**5.41 (modified Glaser-Eglinton-Hay coupling):**[30-40] To a solution of **5.25** (131 mg, 0.201 mmol) and 1-TIPS-8-TMS-octa-1,3,5,7-tetrayne[49] (328 mg, 1.00 mmol) in $CH_2Cl_2$ (10 mL), MeOH (10

mL) and 2,6-lutidine (10 mL) was added $K_2CO_3$ (139 mg, 1.00 mmol) and the mixture stirred for 10 min at rt. To the mixture was added $Cu(OAc)_2 \cdot H_2O$ (401 mg, 2.01 mmol) and the reaction stirred at rt until it was deemed complete by TLC; ca. 7 h. The reaction was quenched with saturated $NH_4Cl$ (25 mL) and the resulting mixture extracted with hexanes (100 mL). The organic phase was washed with saturated $NH_4Cl$ (25 mL), $H_2O$ (2 × 25 mL), brine (25 mL), and dried over $MgSO_4$. The solution was filtered through a plug of silica, the solvent removed in vacuo and the crude product purified by column chromatography (silica, hexanes) to yield **5.41** (133 mg, 73%) as a yellow solid.

**5.41 (Negishi protocol):**[41,42] To a solution of 1-TIPS-8-TMS-octa-1,3,5,7-tetrayne[49] (424 mg, 1.30 mmol) in THF (50 mL) cooled to –78 °C under a $N_2$ atmosphere was added methyllithium (0.81 mL, 1.6M in $Et_2O$, 1.3 mmol) and the mixture stirred for 10 min. The reaction was warmed to 0 °C, ZnCl (1.4 mL, 1.0M in $Et_2O$, 1.4 mmol) was added, the mixture warmed to rt, and stirred for 30 min. This solution was added via cannula to a deoxygenated solution of **5.37** (475 mg, 0.649 mmol) and $PdCl_2(PPh_3)_2$ (46 mg, 0.065 mmol) in toluene (50 mL) and the mixture stirred at rt under a $N_2$ atmosphere for 72 h. The reaction was quenched with $H_2O$ (50 mL) and the resulting mixture extracted with hexanes (100 mL). The organic phase was washed with $H_2O$ (50 mL), brine (50 mL), and dried over $MgSO_4$. The solvent was removed in vacuo and the crude product purified by column chromatography (silica gel, hexanes) to yield **5.41** (192 mg, 33%) as a yellow solid (**Note:** yield = 40% based on 85 mg of recovered **5.37**). Greater purity was achieved by recrystallization of **5.41** from $Et_2O$/MeOH (123 mg, 21%).

**Data for 5.41:** Mp 130 °C (decomp); $R_f$ = 0.40 (hexanes); IR (microscope) 3065 (w), 2963, 2904, 2867, 2202, 2146, 2039, 1592 $cm^{-1}$; UV-Vis (hexanes) $\lambda_{max}$ 325, 306, 290, 274, 261 nm; $^1H$ NMR (500 MHz, $CDCl_3$): $\delta$ 7.26 (t, $J$ = 2 Hz, 3H), 6.88 (d, $J$ = 2 Hz, 6H), 1.18 (s, 54H), 1.16-1.04 (m, 21H); $^{13}C$ NMR (125 MHz, $CDCl_3$): $\delta$ 150.2, 143.2, 123.7, 120.5, 89.4, 87.2, 86.7, 68.6, 63.45, 63.42, 62.84, 62.78 (2 coincidental peaks), 62.58, 62.44, 62.42, 62.14, 61.3, 57.3, 34.8, 31.3, 18.5, 11.3; APPI HRMS *m/z* calcd. for $C_{66}H_{85}Si$ ($[M + H]^+$) 905.6415, found 905.6415; Anal. calcd. for $C_{66}H_{84}Si$: C, 87.55; H, 9.35. Found: C, 87.30; H, 9.48; DSC: decomposition, 158 °C (onset) and 177 °C (peak).

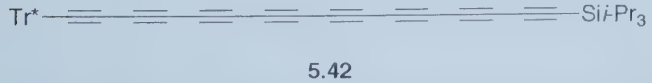


5.42

**5.42 (modified Glaser-Eglinton-Hay coupling):**[30-10] To a solution of **5.34** (103 mg, 0.152 mmol) and 1-TIPS-8-TMS-octa-1,3,5,7-tetrayne[49] (248 mg, 0.761 mmol) in $CH_2Cl_2$ (5 mL), MeOH (5 mL) and 2,6-lutidine (5 mL) was added $K_2CO_3$ (105 mg, 0.761 mmol) and the mixture stirred for 10 min at rt. To the mixture was added $Cu(OAc)_2 \cdot H_2O$ (303 mg, 1.52 mmol) and the reaction stirred at rt until it was deemed complete by TLC; ca. 7 h. The reaction was quenched with saturated $NH_4Cl$ (15 mL) and the resulting mixture extracted with hexanes (50 mL). The organic

phase was washed with saturated $NH_4Cl$ (15 mL), 1M HCl (2 × 15 mL), brine (15 mL), and dried over $MgSO_4$. The solution was filtered through a plug of silica, the solvent removed in vacuo and the crude product purified by column chromatography (silica, hexanes) to yield **5.42** (109 mg, 77%) as a yellow solid.

**5.42 (Negishi protocol):**[41,42] To a solution of 1-TIPS-8-TMS-octa-1,3,5,7-tetrayne[49] (205 mg, 0.628 mmol) in THF (10 mL) and MeOH (10 mL) was added $K_2CO_3$ (87 mg, 0.63 mmol) and the reaction stirred at rt for 10 min. Hexanes (25 mL) were added to the reaction and the mixture was washed with saturated aqueous $NH_4Cl$ (10 mL), $H_2O$ (2 × 10 mL), brine (10 mL), and dried over $MgSO_4$. The mixture was filtered, concentrated to ca. 5 mL, and passed through a plug of silica gel with hexanes. This solution was concentrated to ca. 5 mL, diluted with THF (10 mL), cooled to –78 °C under a $N_2$ atmosphere, and BuLi (0.23 mL, 2.5M in hexanes, 0.57 mmol) was added. The mixture was stirred for 10 min, ZnCl (0.63 mL, 1.0M in $Et_2O$, 0.63 mmol) added, and the reaction warmed to rt. This solution was added via cannula to a deoxygenated solution of **5.38** (237 mg, 0.314 mmol) and $PdCl_2(PPh_3)_2$ (22 mg, 0.0631mmol) in toluene (20 mL) and the mixture stirred at 0 °C under a $N_2$ atmosphere for 19 h. The reaction was quenched with saturated aqueous $NH_4Cl$ (20 mL) and the resulting mixture extracted with hexanes (100 mL). The organic phase was washed with $H_2O$ (50 mL), brine (50 mL), and dried over $MgSO_4$. Only starting materials were observed by TLC analysis with desired product formation detected.

**5.42 (Sonogashira protocol):**[43,44] To a solution of 1-TIPS-6-TMS-hexa-1,3,5-triyne[50] (205 mg, 0.628 mmol) in THF (10 mL) and MeOH (10 mL) was added $K_2CO_3$ (87 mg, 0.63 mmol) and the resulting mixture stirred for 30 min. Saturated aqueous $NH_4Cl$ (10 mL) was added and the resulting mixture extracted with hexanes (25 mL). The organic phases were combined, washed with $H_2O$ (2 × 10 mL), brine (10 mL), and dried over $MgSO_4$. The filtrate was concentrated to ca. 2 mL and held for later use (TIPS-triyne solution). Concurrently, to a deoxygenated solution of **5.38** (237 mg, 0.314 mmol) in toluene (20 mL) at 0 °C was added $PdCl_2(PPh_3)_2$ (10 mg, 0.014 mmol), CuI (2 mg, 0.01 mmol), diisopropylamine (0.72 g, 1.0 mL, 7.1 mmol), and the TIPS-triyne solution, in that order. The reaction was stirred at 0 °C under a $N_2$ atmosphere for 6 h, quenched by the addition of $H_2O$ (10 mL), and extracted with hexanes (25 mL). The organic phase was washed with $H_2O$ (10 mL), brine (10 mL), and dried over $MgSO_4$. The solvent was removed in vacuo and the crude product purified by column chromatography (silica gel, hexanes) to yield **5.42** (38 mg, 13%) as a yellow solid.

**Data for 5.42:** $R_f$ = 0.44 (hexanes); IR (microscope) 3067 (w), 2962, 2867, 2201, 2119, 2017, 1592 $cm^{-1}$; UV-Vis (hexanes) $\lambda_{max}$ 343, 322, 304, 288, 274, 208 nm; $^1H$ NMR (500 MHz, $CDCl_3$): $\delta$ 7.27 (t, $J$ = 2 Hz, 3H), 6.88 (d, $J$ = 2 Hz, 6H), 1.19 (s, 54H), 1.11-1.03 (m, 21H); $^{13}C$ NMR (125 MHz, $CDCl_3$): $\delta$ 150.2, 143.2, 123.7, 120.5, 89.3, 87.5, 86.9, 68.6, 63.7, 63.6, 63.2, 63.2 63.0, 62.8, 62.7, 62.5, 62.31 (2 coincidental peaks), 62.1, 61.2, 57.3, 34.8, 31.3, 18.5, 11.3; MALDI MS *m/z* 928.7 ($M^+$, 100), 872.5 ($[M - t\text{Bu}]^+$, 85); APPI HRMS *m/z* calcd. for $C_{68}H_{85}Si$ ($[M + H]^+$)

929.6415, found 929.6410; Anal. calcd. for $C_{68}H_{84}Si$: C, 87.87; H, 9.11. Found: C, 87.74; H, 9.19; DSC: decomposition, 138 °C (onset) and 144 °C (peak).

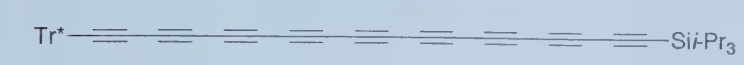


**5.43**

**5.43 (modified Glaser-Eglinton-Hay coupling):**[36-40] To a solution of **5.35** (255 mg, 0.364 mmol) and 1-TIPS-8-TMS-octa-1,3,5,7-tetrayne[49] (594 mg, 1.82 mmol) in $CH_2Cl_2$ (15 mL), MeOH (15 mL) and 2,6-lutidine (15 mL) was added $K_2CO_3$ (251 mg, 1.82 mmol), and the mixture stirred for 10 min at rt. To the mixture was added $Cu(OAc)_2 \cdot H_2O$ (727 mg, 3.64 mmol) and reaction stirred at rt until the reaction was deemed complete by TLC; ca. 6 h. The reaction was quenched with saturated $NH_4Cl$ (25 mL) and the resulting mixture extracted with hexanes (100 mL). The organic phase was washed with saturated $NH_4Cl$ (25 mL), 1M HCl (2 × 50 mL), brine (25 mL), and dried over $MgSO_4$. The mixture was filtered through a plug of silica with $CH_2Cl_2$/hexanes (1:10), the solvent removed in vacuo and the crude product purified by column chromatography (silica, hexanes) to yield **5.43** (146 mg, 42%) as a yellowish-orange solid.

**5.43 (Negishi protocol):**[41,42] To a solution of 1-TIPS-8-TMS-octa-1,3,5,7-tetrayne[49] (24 mg, 0.072 mmol) in THF (5 mL) cooled to –78 °C under a $N_2$ atmosphere was added methyllithium (45 µL, 1.6M in $Et_2O$, 0.072 mmol) and the mixture stirred for 10 min. The reaction was warmed to 0 °C, ZnCl (79 µL, 1.0M in $Et_2O$, 0.079 mmol) was added, the mixture warmed to rt, and stirred for 30 min. This solution was added via cannula to a deoxygenated solution of **5.39** (28 mg, 0.036 mmol) and $PdCl_2(PPh_3)_2$ (3 mg, 0.004 mmol) in toluene (5 mL) and the mixture stirred at rt under a $N_2$ atmosphere for 48 h. The reaction was quenched with saturated $NH_4Cl$ (10 mL) and the resulting mixture extracted with hexanes (50 mL). The organic phase was washed with $H_2O$ (10 mL), brine (10 mL), and dried over $MgSO_4$. The solvent was removed in vacuo and the crude product purified by column chromatography (silica gel, hexanes) to yield impure **5.43** (19 mg). This was purified again by column chromatography (silica gel, hexanes) to yield 11 mg of a yellow solid that again, was not pure **5.43** and the isolation of it pure was thus abandoned.

**5.43 (Sonogashira protocol):**[43,44] To a solution of 1-TIPS-6-TMS-hexa-1,3,5-triyne[50] (258 mg, 0.790 mmol) in THF (10 mL) and MeOH (10 mL) was added $K_2CO_3$ (109 mg, 0.790 mmol) and the resulting mixture stirred for 30 min. Saturated aqueous $NH_4Cl$ (20 mL) was added and the resulting mixture extracted with hexanes (50 mL). The organic phases were combined, washed with $H_2O$ (2 × 20 mL), brine (20 mL), and dried over $MgSO_4$. The filtrate was concentrated to ca. 5 mL, plugged through silica gel, and the resulting solution concentrated to ca. 10 mL and held for later use (TIPS-triyne solution). Concurrently, to a deoxygenated solution of **5.39** (149 mg, 0.191 mmol) in THF (20 mL) at rt was added $PdCl_2(PPh_3)_2$ (7 mg, 0.01 mmol), CuI (2 mg, 0.01 mmol), diisopropylamine (58 mg, 81 µL, 0.57 mmol), and the TIPS-triyne solution, in that order. The

reaction was stirred at rt under a $N_2$ atmosphere for 2 h, quenched by the addition of saturated aqueous $NH_4Cl$ (15 mL), and extracted with hexanes (50 mL). The organic phase was washed with $H_2O$ (2 × 15 mL), brine (15 mL), and dried over $MgSO_4$. The solvent was removed in vacuo and the crude product purified by column chromatography (silica gel, hexanes) to yield **5.43** (16 mg, 9%) as a yellow solid.

**Data for 5.43:** $R_f$ = 0.43 (hexanes); IR (microscope) 3069 (w), 2963, 2904, 2867, 2201, 2159 (w), 2097, 2023 (w), 1996, 1592 $cm^{-1}$; UV-Vis (hexanes) $\lambda_{max}$ 359, 336, 317, 300, 285 nm; $^1H$ NMR (400 MHz, $CDCl_3$): $\delta$ 7.26 (t, $J$ = 2 Hz, 3H), 6.88 (d, $J$ = 2 Hz, 6H), 1.18 (s, 54H), 1.14-1.00 (m, 21H); $^{13}C$ NMR (100 MHz, $CDCl_3$): $\delta$ 150.2, 143.2, 123.7, 120.5, 89.3, 87.7, 87.1, 68.6, 63.9, 63.8, 63.4, 63.3, 63.2, 63.05, 63.02, 62.65, 62.57, 62.53, 62.3, 62.2, 62.1, 61.2, 57.4, 34.9, 31.3, 18.5, 11.3; APPI HRMS *m/z* calcd. for $C_{70}H_{85}Si$ ($[M + H]^+$) 953.6415, found 953.6412; DSC: decomposition, 123 °C (onset), 135 °C (peak).

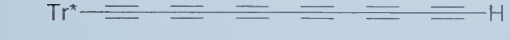


**5.44**

**5.44**: To a solution of **5.40** (162 mg, 0.184 mmol) in THF (50 mL) and $H_2O$ (10 mL) was added CsF (34 mg, 0.22 mmol). The reaction was stirred at rt until deemed complete by TLC analysis: ca. 15 min. The reaction was quenched with saturated $NH_4Cl$ (20 mL) and extracted with hexanes (100 mL). The organic layer was washed with $H_2O$ (20 mL), brine (20 mL), and dried over $MgSO_4$. The solvent was removed in vacuo and the crude product purified by passing through a plug of silica gel with $CH_2Cl_2$/hexanes (1:10) to yield **5.44** (124 mg, 93%) as a yellow solid: $R_f$ = 0.32 (hexanes); IR (microscope) 3279, 3068 (w), 2963, 2905, 2867, 2200, 2172, 2074, 1591 $cm^{-1}$; UV-Vis (hexanes) $\lambda_{max}$ 316 (sh), 304, 293, 279, 267, 255, 244 (sh) nm; $^1H$ NMR (500 MHz, $CDCl_3$): $\delta$ 7.27 (t, $J$ = 2 Hz, 3H), 6.89 (d, $J$ = 2 Hz, 6H), 2.11 (s, 1H), 1.19 (s, 54H); $^{13}C$ NMR (125 MHz, $CDCl_3$): $\delta$ 150.2, 143.2, 123.7, 120.5, 86.6, 68.6, 68.4, 67.8, 63.2, 63.1, 62.5, 62.2, 62.00, 61.96, 61.85, 61.2, 57.3, 34.9, 31.4; MALDI MS *m/z* 624.5 ($M^+$), 667.4 ($[M - t\text{Bu}]^+$); MALDI HRMS *m/z* calcd. for $C_{55}H_{64}$ ($M^+$) 724.5003, found 724.5004.

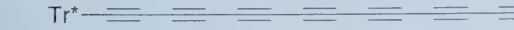


**5.45**

**5.45:** To a solution of **5.41** (34 mg, 0.038 mmol) in THF (15 mL) and $H_2O$ (3 mL) was added CsF (7 mg, 0.05 mmol). The reaction was stirred at rt until deemed complete by TLC analysis: ca. 20 min. The reaction was quenched with saturated aqueous $NH_4Cl$ (15 mL) and extracted with hexanes (50 mL). The organic layer was washed with $H_2O$ (15 mL), brine (15 mL), and dried over $MgSO_4$. The mixture was filtered, concentrated to ca. 5 mL and the crude product purified by passing through a plug of silica gel with $CH_2Cl_2$/hexanes (1:10). The product (**5.45**) was isolated

as a yellow solid that rapidly started turning brown. Thus, the solid was redissolved immediately in $CDCl_3$ for NMR analysis and therefore no yield was recorded: $R_f$ = 0.30 (hexanes); IR (microscope) 3273, 2962, 2904, 2867, 2205, 2154, 2051, 1591 $cm^{-1}$; UV-Vis (hexanes) $\lambda_{max}$ 343, 326, 316, 298, 287, 274, 261, 250, 206 nm; $^1H$ NMR (400 MHz, $CDCl_3$): $\delta$ 7.26 (t, $J$ = 2 Hz, 3H), 6.87 (d, $J$ = 2 Hz, 6H), 2.14 (s, 1H), 1.18 (s, 54H); $^1H$ NMR (400 MHz, $CD_2Cl_2$): $\delta$ 7.31 (t, $J$ = 2 Hz, 3H), 6.93 (d, $J$ = 2 Hz, 6H), 2.23 (s, 1H), 1.20 (s, 54H); $^{13}C$ NMR (100 MHz, $CDCl_3$): $\delta$ 150.2, 143.2, 123.7, 120.5, 86.9, 68.6, 68.3, 68.1, 63.53, 63.52, 62.82, 62.48, 62.31, 62.12 (2 coincidental peaks), 62.08, 61.98, 61.1, 57.3, 34.8, 31.3; $^{13}C$ NMR (125 MHz, $CD_2Cl_2$): $\delta$ 150.9, 143.6, 124.0, 121.1, 87.1, 69.19, 68.9, 68.2, 63.62, 63.60, 62.9, 62.8, 62.6, 62.5, 62.4, 62.3, 62.14, 61.06, 57.8, 35.2, 31.5; APPI HRMS $m/z$ calcd. for $C_{57}H_{65}$ ($[M + H]^+$) 749.5081, found 749.5070.

5.46

**5.46 was formed in situ (for experimental procedure see 5.1f) and assumed to be too unstable to isolate as a neat solid. Therefore, 5.46 was partially characterized in solution before carrying out homocoupling to give 5.1g:** $R_f$ = 0.35 (hexanes); IR (hexanes) 3303 (w), 3271, 3070 (w), 2962, 2905, 2866, 2200, 2129, 2024, 1592 $cm^{-1}$; UV-Vis (hexanes) $\lambda_{max}$ 366 (weak), 346, 335, 322, 315, 306, 296, 291, 282, 277, 264, 207 nm; HRMS $m/z$ calcd. for $C_{59}H_{65}$ $[M + H]^+$ 773.5081, found 773.5086.

5.47

**5.47 was formed in situ (for experimental procedure see 5.1h) and was assumed to be too unstable to isolate as a neat solid. Therefore, 5.47 was partially characterized in solution before carrying out homocoupling to give 5.1h:** $R_f$ = 0.40 (hexanes); IR (hexanes) 3304, 3256, 3066 (w), 2963, 2926, 2862, 2201, 2164 (w), 2104, 2001, 1592 $cm^{-1}$; UV-Vis (hexanes) $\lambda_{max}$ 386 (weak), 364, 352, 341, 330, 322, 311, 306, 295, 291, 277, 208 nm; MALDI HRMS $m/z$ calcd. for $C_{61}H_{64}$ ($M^+$) 796.5003, found 796.5002.

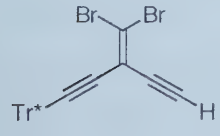


5.48

**5.48:** To a solution of **5.23** (1.010 g, 1.042 mmol) in wet THF (50 mL) was added TBAF (1.04 mL, 1.0M in THF, 1.04 mmol) and the reaction was stirred at rt for 10 min. The reaction was quenched with saturated aqueous $NH_4Cl$ (20 mL) and the mixture extracted with $Et_2O$ (2 × 50

mL). The organic phases were combined, washed with $H_2O$ (25 mL), brine (25 mL), and dried over $Na_2SO_4$. The solvent was removed in vacuo and the crude product purified by column chromatography (silica gel, $CH_2Cl_2$/hexanes 1:10) to yield **5.48** (0.834 g, 98%) as a white solid: Mp 140-143 °C; $R_f$ = 0.47 ($CH_2Cl_2$/hexanes 1:10); IR (microscope) 3307, 3268, 3072 (w), 2962, 2905, 2868, 2226, 2103 (w), 1592 $cm^{-1}$; $^1H$ NMR (500 MHz, $CDCl_3$): $\delta$ 7.25 (t, $J$ = 2 Hz, 3H), 6.97 (d, $J$ = 2 Hz, 6H), 3.40 (s, 1H), 1.19 (s, 54H); $^{13}C$ NMR (125 MHz, $CDCl_3$): $\delta$ 149.8, 144.2, 123.9, 120.0, 114.1, 107.9, 104.4, 83.3, 80.7, 80.3, 57.2, 34.8, 31.4; EIMS *m/z* 812.3 ($M^+$, 48), 755.1 ($[M - t\text{Bu}]^+$, 78), 57.1 ($[t\text{Bu}]^+$, 100).

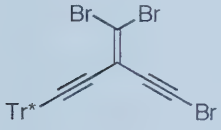


**5.49**

**5.49:** To a mixture of **5.48** (725 mg, 0.892 mmol) in acetone (70 mL) was added *N*-bromosuccinimide (193 mg, 1.08 mmol) and $AgNO_3$ (30 mg, 0.18 mmol) and the reaction stirred at rt for 14 h. The reaction was quenched with $H_2O$ (50 mL) then extracted with hexanes (150 mL). The organic layer was washed with brine (50 mL) and dried over $Na_2SO_4$. The solvent was removed in vacuo and the crude product purified by passing through a plug of silica gel using $CH_2Cl_2$/hexanes (1:10) to yield **5.49** (794 mg, 100%) as a white solid: Mp 88 °C (decomp); $R_f$ = 0.52 ($CH_2Cl_2$/hexanes 1:10); IR (microscope) 3073 (w), 2963, 2904, 2867, 2231, 2184, 1592 $cm^{-1}$; $^1H$ NMR (500 MHz, $CDCl_3$): $\delta$ 7.24 (t, $J$ = 2 Hz, 3H), 6.96 (d, $J$ = 2 Hz, 6H), 1.19 (s, 54H); $^{13}C$ NMR (125 MHz, $CDCl_3$): $\delta$ 149.9, 144.1, 123.9, 120.0, 114.5, 107.5, 104.4, 80.5, 77.3, 57.3, 57.2, 34.9, 31.4; EI MS *m/z* 890.0 ($M^+$, 31), 833.3 ($[M - t\text{Bu}]^+$, 100).

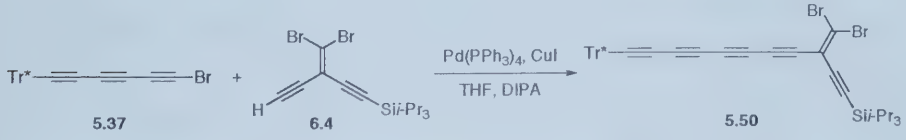


**5.37** **6.4** **5.50**

**5.50:** To a deoxygenated solution of $Pd(PPh_3)_4$ (10 mg, 0.0087 mmol) and CuI (2 mg, 0.011mmol) in THF (25 mL) and diisopropylamine (73 µL, 0.52 mmol) was added a deoxygenated solution of **5.37** (127 mg, 0.173 mmol) and **6.4**[51] (81 mg, 0.208) in THF (5 mL). The resulting mixture was stirred for 15 h at rt under a $N_2$ atmosphere. The reaction was quenched with saturated aqueous $NH_4Cl$ (20 mL) and the resulting mixture extracted with hexanes (50 mL). The organic phase was washed with $H_2O$ (20 mL), brine (20 mL), and dried over $MgSO_4$. The solvent was removed in vacuo and the crude product purified by column chromatography (silica gel, hexanes) to yield **5.50** (80 mg, 44%) as a yellow solid: $R_f$ = 0.28 (hexanes); IR (microscope) 3069 (w), 2962, 2905, 2866, 2215, 2137, 1592 $cm^{-1}$; $^1H$ NMR (500 MHz, $CDCl_3$): $\delta$ 7.27 (t, $J$ = 2 Hz, 3H), 6.90 (d, $J$ = 2 Hz,

6H), 1.19 (s, 54H), 1.11-1.07 (m, 21H); $^{13}$C NMR (125 MHz, $CDCl_3$): $\delta$ 150.2, 143.4, 123.7, 120.4, 113.7, 113.3, 101.4, 100.6, 87.9, 80.4, 71.9, 71.3, 68.8, 66.7, 62.3, 60.6, 57.3, 34.8, 31.4, 18.6, 11.1; EIMS *m/z* 1040.9 ($M^+$, 22), 983.9 ([M – *t*Bu]$^+$, 100); MALDI HRMS *m/z* calcd. for $C_{64}H_{84}{}^{79}Br_2Si$ $(M)^+$ 1038.4704, found 1038.4700.

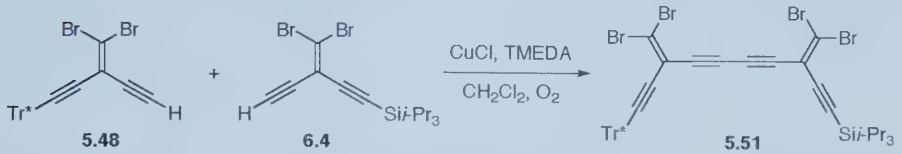


**5.51:** To a mixture of CuCl (24 mg, 0.24 mmol) in $CH_2Cl_2$ (10 mL) was added TMEDA (73 µL, 0.48 mmol) and then $O_2$ bubbled through the solution for ca. 10 min. A solution of **5.48** (98 mg, 0.121) and **6.4**[51] (212 mg, 0.543 mmol) in $CH_2Cl_2$ (5 mL) was added and the resulting mixture stirred at rt for 18 h. The reaction was quenched with $H_2O$ (5 mL) and the resulting layers separated. The organic phase was washed with $H_2O$ (5 mL), brine (5 mL), and dried over $MgSO_4$. The solvent was removed in vacuo and the crude product purified by column chromatography (silica gel, gradient elution hexanes → $CH_2Cl_2$/hexanes 1:10) to yield **5.51** (46 mg, 32%) as a yellow solid (48 mg of homocoupled **5.52** was also isolated): $R_f$ = 0.52 ($CH_2Cl_2$/hexanes 1:10); IR (microscope) 3069 (w), 2963, 2904, 2866, 2218, 2142 (w), 1592 cm$^{-1}$; $^1$H NMR (400 MHz, $CDCl_3$): $\delta$ 7.25 (t, $J$ = 2 Hz, 3H), 6.96 (d, $J$ = 2 Hz, 6H), 1.19 (s, 54H), 1.14-1.07 (m, 21H); $^{13}$C NMR (125 MHz, $CDCl_3$): $\delta$ 149.9, 144.0, 123.8, 120.0, 114.0, 113.7, 112.5, 110.0, 105.3, 101.1, 100.7, 80.9, 80.2, 79.9, 79.4, 79.0, 57.3, 34.9, 31.4, 18.6, 11.1; MALDI HRMS *m/z* calcd. for $C_{64}H_{84}{}^{79}Br_4Si$ $(M)^+$ 1196.3070, found 1196.3069.

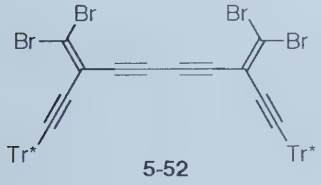


5-52

**5.52 (homocoupled side product from the synthesis of 5.51):** $R_f$ = 0.38 ($CH_2Cl_2$/hexanes 1:10); IR (microscope) 3072 (w), 2960, 2905, 2868, 2223, 2141 (w), 1592 cm$^{-1}$; $^1$H NMR (400 MHz, $CDCl_3$): $\delta$ 7.24 (t, $J$ = 2 Hz, 6H), 6.96 (d, $J$ = 2 Hz, 12H), 1.18 (s, 108H); $^{13}$C NMR (100 MHz, $CDCl_3$): $\delta$ 149.9, 144.1, 123.8, 120.0, 114.1, 109.9, 105.2, 80.7, 79.8, 79.1, 57.3, 34.9, 31.4; MALDI HRMS *m/z* calcd. for $C_{98}H_{126}{}^{79}Br_4$ $(M)^+$ 1618.6588, found 1618.6559.

5.54

**5.54 was formed in situ (for experimental procedure see 5.1j) and was assumed to be too unstable to isolate as a neat solid. Therefore, 5.54 was partially characterized in solution before carrying out homocoupling to give 5.1j**: $R_f$ = 0.42 (hexanes); IR (microscope) 3302, 3281, 3069 (w), 2963, 2904, 2867, 2200, 2180 (w), 2147, 2084, 1987, 1592 $cm^{-1}$; UV-Vis (hexanes) $\lambda_{max}$ 404 (weak), 380, 367, 343, 324, 319, 303, 289 nm; MALDI HRMS *m/z* calcd. for $C_{63}H_{64}$ ($M^+$) 820.5003, found 820.5000.

**5.1a**

**5.1a:** To a mixture of CuCl (19 mg, 0.19 mmol) in $CH_2Cl_2$ (10 mL) was added TMEDA (60 mg, 78 µL, 0.52 mmol). $O_2$ was bubbled through the solution for 5 min and a solution of **5.7** (109 mg, 0.173 mmol) in $CH_2Cl_2$ (5 mL) was added and the mixture stirred for 30 min. The reaction was quenched through the addition of saturated aqueous $NH_4Cl$ (10 mL) and the layers separated. The organic phase was washed with $H_2O$ (10 mL), brine (10 mL), and then dried over $MgSO_4$. The solvent was removed in vacuo and the crude product purified by column chromatography (silica gel, $CH_2Cl_2$/hexanes 1:20) to yield **5.1a** (100 mg, 92%) as a white solid: Mp 295-297 °C; $R_f$ = 0.28 (hexanes); IR (microscope) 3068 (w), 2963, 2905, 2868, 2216, 1592 $cm^{-1}$; UV-Vis (hexanes) $\lambda_{max}$ (ε) 268 (149000), 254 (145000), 241 (84000), 208 (169000) nm; UV-Vis ($CH_2Cl_2$) $\lambda_{max}$ (ε) 269 (108000), 258 (118000) nm; UV-Vis (THF) $\lambda_{max}$ (ε) 270 (107000), 258 (122000) nm; $^1H$ NMR (500 MHz, $CDCl_3$): $\delta$ 7.25 (t, $J$ = 2 Hz, 6H), 6.91 (d, $J$ = 2 Hz, 12H), 1.19 (s, 108H); $^{13}C$ NMR (125 MHz, $CDCl_3$): $\delta$ 150.0, 143.7, 123.7, 120.3, 85.26, 69.06, 63.00, 62.36, 57.19, 34.8, 31.4; MALDI HRMS *m/z* calcd. for $C_{94}H_{126}$ ($M^+$) 1254.9854, found 1254.9848; Anal. calcd. for $C_{94}H_{126}$: C, 89.89; H, 10.11. Found: C, 89.38; H, 10.29; DSC: decomposition, 315 °C (onset) and 319 °C (peak).

**X-ray Crystal Data for 5.1a:** Single crystals of **5.1a** suitable for X-ray crystallographic analysis were grown by slow evaporation of a $Et_2O$/MeOH (5:1) solution at rt. $C_{94}H_{126}$, $M_r$ = 1256.0; monoclinic crystal system; space group $P2_1/n$ (an alternate setting of $P2_1/c$ [No. 14]), $a$ = 28.705 (9), $b$ = 10.621 (3), $c$ = 29.280 (9) Å; $\beta$ = 92.763 (4)°; $V$ = 8916 (5) $Å^3$; $Z$ = 4; $\rho_{calcd}$ = 0.963 g $cm^{-3}$; $\mu$ = 0.054 $mm^{-1}$; $\lambda$ = 0.71073 Å; T = –100 °C; 2$\theta$ max = 50.50°; total data collected = 61984; $R_1$ = 0.0584 for 10594 observed reflections with $[F_o^2 \geq 2\sigma(F_o^2)]$; $wR_2$ = 0.1699 for 962 variables and 16159 unique reflections with $[F_o^2 \geq -3\sigma(F_o^2)]$; residual electron density = 0.376 and –0.297 e $Å^{-3}$.

**5.1b**

**5.1b:** To a mixture of CuCl (13 mg, 0.13 mmol) in $CH_2Cl_2$ (20 mL) was added TMEDA (46 mg, 59 µL, 0.40 mmol). $O_2$ was bubbled through the solution for 5 min, a solution of **5.25** (86 mg, 0.13

mmol) in $CH_2Cl_2$ (5 mL) was then added and the reaction mixture stirred for 20 min. The reaction was plugged through silica gel with $CH_2Cl_2$ and the solvent removed in vacuo to yield **5.1b** (57 mg, 66%) as a yellow solid: Mp 270 °C (decomp); $R_f$ = 0.25 (hexanes); IR (microscope) 3069 (w), 2960, 2903, 2866, 2201, 2178, 1592 $cm^{-1}$; UV-Vis (hexanes) $\lambda_{max}$ ($\varepsilon$) 310 (412000), 292 (286000), 276 (144000), 262 (66000), 250 (38000), 208 (153000) nm; UV-Vis ($CH_2Cl_2$) $\lambda_{max}$ ($\varepsilon$) 315 (247000), 295 (193000), 279 (110000) nm; UV-Vis (THF) $\lambda_{max}$ ($\varepsilon$) 315 (257000), 296 (198000) nm; $^1H$ NMR (500 MHz, $CDCl_3$): $\delta$ 7.25 (t, $J$ = 2 Hz, 6H), 6.88 (d, $J$ = 2 Hz, 12H), 1.18 (s, 108H); $^{13}C$ NMR (100 MHz, $CDCl_3$): $\delta$ 150.2, 143.3, 123.7, 120.4, 86.27, 68.78, 62.96, 62.90, 62.75, 62.42, 57.29, 34.8, 31.4; MALDI HRMS *m/z* calcd. for $C_{98}H_{126}$ ($M^+$) 1302.9854, found 1302.9843; Anal. calcd. for $C_{98}H_{126}$: C, 90.26; H, 9.74. Found: C, 89.98; H, 9.79; DSC: decomposition, 300 °C (onset), 323 °C (peak) and 347 (peak).

**X-ray Crystal Data for 5.1b:** Single crystals of **5.1b** suitable for X-ray crystallographic analysis were grown by slow evaporation of a xylenes solution at rt. $C_{98}H_{126}$, $M_r$ = 1303.99; triclinic crystal system; space group $P\bar{1}$ (No. 2), $a$ = 10.5799 (10), $b$ = 10.7732 (10), $c$ = 19.6616 (18) Å; $\alpha$ = 84.7319 (14)°; $\beta$ = 75.3405 (14)°; $\gamma$ = 87.4321 (14)°; $V$ = 2158.4 (3) $Å^3$; $Z$ = 1; $\rho_{calcd}$ = 1.003 g $cm^{-3}$; $\mu$ = 0.056 $mm^{-1}$; $\lambda$ = 0.71073 Å; T = –100 °C; 2$\theta$ max = 50.76°; total data collected = 15603; $R_1$ = 0.0538 for 4479 observed reflections with $[F_o^2 \geq 2\sigma(F_o^2)]$; $wR_2$ = 0.1535 for 486 variables and 7893 unique reflections with $[F_o^2 \geq -3\sigma(F_o^2)]$; residual electron density = 0.408 and –0.195 e $Å^{-3}$.

**5.1c**

**5.1c:** To a mixture of CuCl (6 mg, 0.06 mmol) in $CH_2Cl_2$ (10 mL) was added TMEDA (16 mg, 21 µL, 0.14 mmol). $O_2$ was bubbled through the solution for 5 min, **5.34** (38 mg, 0.056 mmol) was added, and the reaction mixture stirred for 20 min. The reaction was plugged through silica gel with $CH_2Cl_2$ and the solvent removed in vacuo to yield **5.1c** (37 mg, 97%) as a yellow solid: $R_f$ = 0.26 (hexanes); IR (microscope) 3070 (w), 2963, 2905, 2868, 2206, 2124, 2018 (w), 1592 $cm^{-1}$; UV-Vis (hexanes) $\lambda_{max}$ ($\varepsilon$) 347 (541000), 325 (396000), 306 (200000), 290 (91000), 276 (47000), 207 (168000) nm; UV-Vis ($CH_2Cl_2$) $\lambda_{max}$ ($\varepsilon$) 351 (315000), 329 (254000), 310 (139000), 293 (73000), 279 (41000) nm; UV-Vis (THF) $\lambda_{max}$ ($\varepsilon$) 351 (329000), 329 (262000), 310 (144000), 293 (77000) nm; $^1H$ NMR (300 MHz, $CDCl_3$): $\delta$ 7.26 (t, $J$ = 2 Hz, 6H), 6.88 (d, $J$ = 2 Hz, 12H), 1.18 (s, 108H); $^{13}C$ NMR (100 MHz, $CDCl_3$): $\delta$ 150.2, 143.2, 123.7, 120.5, 86.78, 68.65, 63.55, 63.49, 62.97, 62.60, 62.50, 62.19, 57.33, 34.8, 31.3; MALDI MS *m/z* 1351.2 ($M^+$); MALDI HRMS *m/z* calcd. for $C_{102}H_{126}$ ($M^+$) 1350.9854, found 1350.9840; Anal. calcd. for $C_{102}H_{126}$: C, 90.61; H, 9.39. Found: C, 90.46; H, 9.47; DSC: decomposition, 260 °C (onset) and 275 °C (peak).

**5.1d**

**5.1d:** To a solution of **5.35** (80 mg, 0.11 mmol) in $CH_2Cl_2$ (20 mL) was added $Cu(OAc)_2 \cdot H_2O$ (46 mg, 0.23 mmol) and 2,6-lutidine (50 mg, 54 μL, 0.47 mmol). The reaction was monitored by TLC and UV-Vis analysis until deemed complete; ca. 14 h. The solvent was removed in vacuo and the residue purified by column chromatography (silica gel, $CH_2Cl_2$/hexanes 1:5) to yield **5.1d** (59 mg, 74%) as a yellowish-orange solid: $R_f$ = 0.28 (hexanes); IR (microscope) 2963, 2905, 2866, 2201, 2080, 1981 (w), 1592 $cm^{-1}$; UV-Vis (hexanes) $\lambda_{max}$ (ε) 376 (595000), 352 (527000), 331 (276000), 313 (130000), 297 (74000), 283 (58000), 209 (237000) nm; UV-Vis ($CH_2Cl_2$) $\lambda_{max}$ (ε) 381 (363000), 356 (325000), 334 (176000), 316 (85000), 300 (45000) nm; UV-Vis (THF) $\lambda_{max}$ (ε) 381 (390000), 356 (345000), 334 (187000), 316 (90000), 300 (49000) nm; $^1H$ NMR (500 MHz, $CDCl_3$): $\delta$ 7.26 (t, $J$ = 2 Hz, 6H), 6.88 (d, $J$ = 2 Hz, 12H), 1.18 (s, 108H); $^{13}C$ NMR (100 MHz, $CDCl_3$): $\delta$ 150.2, 143.2, 123.7, 120.5, 87.04, 68.60, 63.96, 63.78, 63.49, 63.11, 62.69, 62.54, 62.28, 62.06, 57.36, 34.9, 31.3; MALDI MS *m/z* 1399.3 ($M^+$, 35), 1342.1 ([M – *t*Bu]$^+$, 100); MALDI HRMS *m/z* calcd. for $C_{106}H_{126}$ ($M^+$) 1398.9854, found 1398.9874; Anal. calcd. for $C_{106}H_{126}$: C, 90.93; H, 9.07. Found: C, 90.62; H, 9.24; DSC: decomposition, 204 °C (onset) and 220 °C (peak).

**5.1e**

**5.1e:** To a solution of **5.40** (252 mg, 0.286 mmol) in THF (50 mL) and $H_2O$ (10 mL) was added CsF (52 mg, 0.34 mmol) and the reaction monitored by TLC for completion, ca. 10 min. The reaction was quenched with saturated $NH_4Cl$ (25 mL) and the resulting mixture extracted with hexanes (150 mL). The organic layer was washed with $H_2O$ (25 mL), brine (25 mL), and dried over $MgSO_4$. The solvent was removed in vacuo and the crude intermediate (**5.44**) passed through a plug of silica gel with $CH_2Cl_2$/hexanes (1:10). To the filtrate (ca. 200 mL) was added $Cu(OAc)_2 \cdot H_2O$ (285 mg, 1.43 mmol) and 2,6-lutidine (1.2 mL, 10 mmol) and the reaction was stirred at rt for 3 days. The reaction was concentrated to ca. 10 mL, passed through a plug of silica gel with $CH_2Cl_2$/hexanes (1:10) and the solvent removed in vacuo to yield **5.1e** (179 mg, 86%) as an orange solid: $R_f$ = 0.34 (hexanes); IR (microscope) 3069 (w), 2963, 2906, 2867, 2201, 2156, 2112 (w), 2042, 1956 (w), 1592 $cm^{-1}$; UV-Vis (hexanes) $\lambda_{max}$ (ε) 400 (686000), 374 (598000), 350 (318000), 331 (157000), 315 (73000), 274 (64000), 263 (65000), 252 (49000), 208 (166000) nm; UV-Vis ($CH_2Cl_2$) $\lambda_{max}$ (ε) 405 (470000), 378 (438000), 355 (240000), 335 (118000), 319 (61000), 286 (45000), 277 (55000), 265 (55000), 254 (43000) nm; UV-Vis (THF) $\lambda_{max}$ (ε) 405 (477000), 378 (440000), 354 (240000), 335 (121000), 319 (64000) nm; $^1H$ NMR (400 MHz, $CDCl_3$): $\delta$ 7.26 (t, $J$ = 2 Hz, 6H), 6.87 (d, $J$ = 2 Hz, 12H), 1.18 (s, 108H); $^{13}C$ NMR (125 MHz, $CDCl_3$): $\delta$ 150.2,

143.1, 123.7, 120.5, 87.16, 68.57, 64.17, 63.92, 63.77, 63.49, 63.18, 62.86, 62.52, 62.50, 62.17, 61.99, 57.36, 34.8, 31.3; MALDI MS *m/z* 1448.0 ([M + H]$^+$, 65), 1389.9 ([M – *t*Bu]$^+$, 100); MALDI HRMS *m/z* calcd. for $C_{110}H_{126}$ ($M^+$) 1446.9854, found 1446.9849; Anal. calcd. for $C_{110}H_{126}$: C, 91.23; H, 8.77. Found: C, 91.13; H, 8.86; DSC: decomposition, 148 °C (onset) and 168 °C (peak).

**5.1f**

**5.1f:** To a solution of **5.41** (129 mg, 0.142 mmol) in THF (25 mL) and $H_2O$ (5 mL) was added CsF (26 mg, 0.171 mmol) and the reaction monitored by TLC for completion, ca. 20 min. The reaction was quenched with saturated $NH_4Cl$ (15 mL) and the resulting mixture extracted with hexanes (50 mL). The organic layer was washed with $H_2O$ (15 mL), brine (15 mL), and dried over $MgSO_4$. The mixture was filtered, the resulting solution concentrated in vacuo to ca. 5 mL and the crude intermediate (**5.45**) passed through a plug of silica gel with $CH_2Cl_2$/hexanes (1:5). The filtrate was concentrated to ca. 25 mL and diluted with $CH_2Cl_2$ (25 mL). To this solution was added $Cu(OAc)_2$•$H_2O$ (142 mg, 0.710 mmol), 2,6-lutidine (1 mL), and the reaction stirred at rt for 24 h. The reaction was concentrated to ca. 5 mL, passed through a plug of silica gel with $CH_2Cl_2$/hexanes (1:10) and the solvent removed in vacuo to yield **5.1f** (96 mg, 90%) as a yellowish-orange solid: $R_f$ = 0.21 (hexanes); IR (microscope) 2960, 2926, 2866, 2201, 2128, 2015, 1939 (w), 1897 (w), 1592 cm$^{-1}$; UV-Vis (hexanes) $\lambda_{max}$ (ε) 419 (726000), 389 (709000), 365 (414000), 346 (194000), 329 (93000), 313 (58000), 299 (62000), 292 (72000), 280 (71000), 268 (55000), 245 (62000), 208 (172000) nm; UV-Vis ($CH_2Cl_2$) $\lambda_{max}$ (ε) 423 (521000), 393 (511000), 369 (296000), 349 (146000), 331 (78000), 315 (57000), 295 (66000), 283 (64000), 270 (50000), 248 (62000) nm; UV-Vis (THF) $\lambda_{max}$ (ε) 423 (527000), 393 (508000), 368 (297000), 348 (150000), 331 (80000), 314 (59000) nm; $^1$H NMR (500 MHz, $CDCl_3$): $\delta$ 7.26 (t, $J$ = 2 Hz, 6H), 6.87 (d, $J$ = 2 Hz, 12H), 1.18 (s, 108H); $^{13}$C NMR (100 MHz, $CDCl_3$): $\delta$ 150.3, 143.1, 123.7, 120.5, 87.24, 68.57, 64.28, 64.00, 63.93, 63.69, 63.45, 63.24, 63.01, 62.74, 62.48, 62.44, 62.12, 61.96, 57.37, 34.9, 31.3;‡ MALDI HRMS *m/z* calcd. for $C_{114}H_{126}$ ($M^+$) 1494.9854, found 1494.9860; Anal. calcd. for $C_{114}H_{126}$: C, 91.51; H, 8.49. Found: C, 91.33; H, 8.59; DSC: decomposition, 132 °C (onset) and 151 °C (peak).

**5.1g**

**5.1g:** To a solution of **5.42** (108 mg, 0.116 mmol) in THF (25 mL) and $H_2O$ (5 mL) was added

‡ During the initial NMR analysis a pin diode malfunctioned resulting in partial $^1$H–$^{13}$C coupling. This can be seen in the NMR spectrum of **5.1f** (included below). All quaternary carbons were uneffected and thus these chemical shifts are reported. After the instrument was repaired the same sample was rerun to obtain the chemical shifts of the remaining signals.

CsF (21 mg, 0.14 mmol) and the reaction monitored by TLC for completion, ca. 20 min. The reaction was quenched with saturated $NH_4Cl$ (10 mL) and the resulting mixture extracted with hexanes (50 mL). The organic layer was washed with $H_2O$ (10 mL), brine (10 mL), and dried over $MgSO_4$. The solution was concentrated to ca. 5 mL and the crude intermediate (**5.46**) passed through a plug of silica gel with $CH_2Cl_2$/hexanes (1:5). The filtrate was concentrated to ca. 25 mL and diluted with $CH_2Cl_2$ (25 mL). To the resulting solution was added $Cu(OAc)_2 \cdot H_2O$ (116 mg, 0.580 mmol) and 2,6-lutidine (1.0 mL) and the reaction stirred at rt for 24 h. The reaction was concentrated to ca. 5 mL, the crude product purified by passing through a plug of silica gel with $CH_2Cl_2$/hexanes (1:10) and the solvent removed in vacuo to yield **5.1g** (68 mg, 76%) as an orange solid: $R_f$ = 0.36 (hexanes); IR (microscope) 3068 (w), 2963, 2905, 2867, 2201, 2166 (w), 2106, 2055 (w), 1991, 1925 (w), 1592 $cm^{-1}$; UV-Vis (hexanes) $\lambda_{max}$ ($\varepsilon$) 432 (732000), 402 (802000), 378 (462000), 357 (215000), 340 (110000), 325 (77000), 304 (87000), 292 (80000), 280 (65000), 259 (73000), 207 (178000) nm; UV-Vis ($CH_2Cl_2$) $\lambda_{max}$ ($\varepsilon$) 438 (566000), 407 (591000), 381 (356000), 361 (177000), 343 (99000), 327 (79000), 265 (72000) nm; UV-Vis (THF) $\lambda_{max}$ ($\varepsilon$) 437 (597000), 406 (629000), 380 (383000), 360 (196000), 343 (114000), 327 (92000) nm; $^1H$ NMR (500 MHz, $CDCl_3$): $\delta$ 7.26 (t, $J$ = 2 Hz, 6H), 6.88 (d, $J$ = 2 Hz, 12H), 1.18 (s, 108H); $^{13}C$ NMR (100 MHz, $CDCl_3$): $\delta$ 150.3, 143.1, 123.7, 120.5, 87.27, 68.56, 64.34, 64.05, 64.01, 63.81, 63.61, 63.45, 63.29, 63.12, 62.93, 62.69, 62.48, 62.41, 62.10, 61.95, 57.37, 34.9, 31.3; MALDI MS *m/z* 1542.9 ($M^+$), 1485.9 ([M – *t*Bu]$^+$); MALDI HRMS *m/z* calcd. for $C_{118}H_{126}$ ($M^+$) 1542.9854, found 1542.9860; DSC: decomposition, 137 °C (onset) and 159 °C (peak).

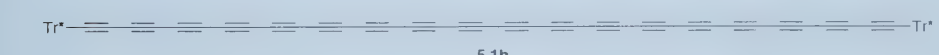


**5.1h**

**5.1h:** To a solution of **5.43** (97 mg, 0.10 mmol) in THF (25 mL) and $H_2O$ (5 mL) was added CsF (19 mg, 0.12 mmol) and the reaction monitored by TLC for completion, ca. 20 min. The reaction was quenched with saturated $NH_4Cl$ (15 mL) and the resulting mixture extracted with hexanes (50 mL). The organic layer was washed with $H_2O$ (15 mL), brine (15 mL), and dried over $MgSO_4$. The solution was concentrated to ca. 5 mL and the crude intermediate (**5.47**) passed through a plug of silica gel with $CH_2Cl_2$/hexanes (1:5). The filtrate was concentrated to ca. 25 mL and diluted with $CH_2Cl_2$ (25 mL). $Cu(OAc)_2 \cdot H_2O$ (102 mg, 0.510 mmol) and 2,6-lutidine (1.0 mL) were added and the reaction stirred at rt for 24 h. The reaction was concentrated to ca. 5 mL, the crude product purified by passing through a plug of silica gel with $CH_2Cl_2$/hexanes (1:10), and the solvent removed in vacuo to yield **5.1h** (66 mg, 81%) as an orange solid: $R_f$ = 0.36 (hexanes); IR (microscope) 3068 (w), 2962, 2866, 2201, 2151, 2082, 2053 (w), 2033 (w), 1974, 1917 (w), 1592 $cm^{-1}$; UV-Vis (hexanes) $\lambda_{max}$ ($\varepsilon$) 443 (805000), 412 (875000), 387 (498000), 365 (238000), 348 (138000), 315 (109000), 302 (97000), 290 (81000), 275 (91000), 207 (189000) nm; UV-Vis ($CH_2Cl_2$) $\lambda_{max}$ ($\varepsilon$) 449 (633000), 417 (676000), 391 (407000), 370 (202000), 351 (122000), 334

(95000), 319 (95000), 305 (84000), 279 (86000) nm; UV-Vis (THF) $\lambda_{max}$ ($\varepsilon$) 447 (607000), 416 (654000), 390 (404000), 369 (210000), 351 (136000), 333 (108000), 319 (107000), 305 (97000) nm; $^1$H NMR (400 MHz, $CDCl_3$): $\delta$ 7.26 (t, $J$ = 2 Hz, 6H), 6.87 (d, $J$ = 2 Hz, 12H), 1.18 (s, 108H); $^{13}$C NMR (100 MHz, $CDCl_3$): $\delta$ 150.3, 143.1, 123.7, 120.5, 87.28, 68.55, 64.36, 64.06, 64.04, 63.85, 63.68, 63.55, 63.42, 63.31, 63.19, 63.05, 62.87, 62.65, 62.47, 62.39, 62.08, 61.94, 57.37, 34.9, 31.3; MALDI MS *m/z* 1592.0 ($M^+$, 20), 1533.9 ([M – *t*Bu]$^+$, 100); MALDI HRMS *m/z* calcd. for $C_{122}H_{126}$ ($M^+$) 1590.9854, found 1590.9849; DSC: decomposition, 124 °C (onset) and 137 °C (peak).

5.1j

**5.1j:** To a solution of **5.53** (86 mg, 0.088 mmol) in THF (25 mL) and $H_2O$ (5 mL) was added CsF (16 mg, 0.11 mmol) and the reaction monitored by TLC for completion, ca. 10 min. The reaction was quenched with saturated $NH_4Cl$ (20 mL) and the resulting mixture extracted with hexanes (50 mL). The organic layer was washed with $H_2O$ (20 mL), brine (20 mL), and dried over $MgSO_4$. The solution was concentrated to ca. 5 mL and the crude intermediate (**5.54**) passed through a plug of silica gel with $CH_2Cl_2$/hexanes (1:10). The filtrate was concentrated to ca. 5 mL then diluted with $CH_2Cl_2$ (25 mL). To this solution was added 2,6-lutidine (2 mL) and $Cu(OAc)_2$•$H_2O$ (88 mg, 0.44 mmol) and the reaction was monitored by TLC and UV-Vis analysis until deemed complete; ca. 3 h. The reaction was concentrated to ca. 5 mL, hexanes were added (20 mL) and the solution concentrated again to ca. 5 mL. The crude mixture was passed through a plug of silica gel with hexanes and the solvent was removed in vacuo to yield **5.1j** (41 mg, 57%) as an orange-red solid: $R_f$ = 0.38 (hexanes); IR (microscope) 3071 (w), 2963, 2905, 2867, 2200, 2134, 2101 (w), 2061, 2013 (w), 1956, 1905 (w), 1592 cm$^{-1}$; UV-Vis (hexanes) $\lambda_{max}$ ($\varepsilon$) 451 (866000), 420 (936000), 393 (539000), 372 (258000), 355 (155000), 337 (117000), 324 (120000), 311 (105000), 299 (90000), 286 (98000), 257 (111000), 207 (197000) nm; UV-Vis ($CH_2Cl_2$) $\lambda_{max}$ ($\varepsilon$) 457 (699000), 425 (748000), 398 (449000), 376 (227000), 359 (152000), 342 (117000), 328 (110000), 314 (98000) nm; UV-Vis (THF) $\lambda_{max}$ ($\varepsilon$) 456, 424, 397, 376, 358, 341 nm; $^1$H NMR (500 MHz, $CDCl_3$): $\delta$ 7.27 (t, $J$ = 2 Hz, 6H), 6.88 (d, $J$ = 2 Hz, 12H), 1.19 (s, 108H); $^{13}$C NMR (125 MHz, $CDCl_3$): $\delta$ 150.2, 143.1, 123.7, 120.5, 87.33, 68.63, 64.50, 64.19 (2 coincidental peaks), 64.03, 63.88, 63.77, 63.67, 63.58, 63.51, 63.43, 63.33, 63.20, 63.03, 62.82, 62.54 (2 coincidental peaks), 62.20, 62.04, 57.39, 34.8, 31.3; MALDI MS *m/z* 1639.0 ($M^+$, 14), 1581.9 ([M – *t*Bu]$^+$, 100); MALDI HRMS *m/z* calcd. for $C_{126}H_{126}$ ($M^+$) 1638.9854, found 1638.9850; Anal. calcd. for $C_{126}H_{126}$: C, 92.26; H, 7.74. Found: C, 92.07; H, 7.90; DSC: decomposition, 105 °C (onset) and 116 °C (peak).

## 7.5 References


[1] Sheldrick, G. M. SHELXL-97. Program for crystal structure determination. University of Göttingen, Germany, 1997.

[2] Sheldrick, G. M. *Acta Crystallogr., Sect. A: Found. Crystallogr.* **1990**, *A46*, 467.

[3] Sheldrick, G. M. SHELXL-93. Program for crystal structure determination. University of Göttingen, Germany, 1993.

[4] Kübel, C.; Chen, S.-L.; Müllen, K. *Macromolecules* **1998**, *31*, 6014.

[5] Wayne, W.; Adkins, H. *Org. Synth.* **1955**, *21*, 39.

[6] Elmorsy, S. S.; Khalil, A. G. M.; Girges, M. M.; Salama, T. A. *Tetrahedron Lett.* **1997**, *38*, 1071.

[7] Ishizaki, M.; Hoshino, O. *Tetrahedron* **2000**, *56*, 8813.

[8] Stetter, H. *Chem. Ber.* **1959**, *92*, 1629.

[9] Stetter, H.; Goebel, P. *Chem. Ber.* **1962**, *95*, 1039.

[10] Broxterman, Q. B.; Hogeveen, H.; Kingma, R. F. *Tetrahedron Lett.* **1986**, *27*, 1055.

[11] Zhang, B.; Breslow, R. *J. Am. Chem. Soc.* **1997**, *119*, 1676.

[12] Jiang, M. X.-W.; Rawat, M.; Wulff, W. D. *J. Am. Chem. Soc.* **2004**, *126*, 5970.

[13] Eisler, S.; Chahal, N.; McDonald, R.; Tykwinski, R. R. *Chem. Eur. J.* **2003**, *9*, 2542.

[14] Lei, A.; Srivastava, M.; Zhang, X. *J. Org. Chem.* **2002**, *67*, 1969.

[15] Müller, T.; Hullinger, J.; Seichter, W.; Weber, E.; Weber, T.; Wübbenhorst, M. *Chem. Eur. J.* **2000**, *6*, 54.

[16] Compound **3.30** decomposes rapidly (over a couple of minutes) as a neat solid and it was therefore prepared and used immediately in the oxidative homocoupling step.

[17] Compounds **3.1f** and **3.1h** decompose rapidly (over a few minutes) as a neat solids but are relatively stable when stored in solution at temperatures below –20 °C.

[18] Compound **3.31** decomposes rapidly (in seconds) as a neat solid and is therefore important to keep this intermediate in solution.

[19] Compound **3.1k** decomposes rapidly as a neat solid (seconds) and when stored in solution (a few days) at temperatures below –20 °C.

[20] Hauptmann, H. *Tetrahedron Lett.* **1974**, *15*, 3593.

[21] Ivitzky, P. *Bull. Soc. Chim. Fr.* **1924**, *35*, 357.

[22] Rösner, M.; Köbrich, G. *Angew. Chem. Int. Ed. Engl.* **1975**, *14*, 708.

[23] Ladika, M.; Stang, P. J. *J. Chem. Soc., Chem. Comm.* **1981**, 459.

[24] Moureu, C.; Delange, R. *Bull. Soc. Chim. Fr.* **1903**, 648.

[25] Mansfield, G. H.; Whiting, M. C. *J. Chem. Soc.* **1956**, 4761.

[26] Knorr, R.; Pires, C.; Behringer, C.; Menke, T.; Freudenreich, J.; Rossmann, E. C.; Böhrer, P. *J. Am. Chem. Soc.* **2006**, *128*, 14845.

[27] Armarego, W. L. F.; Chai, C. L. L. *Purification of Laboratory Chemicals*; 5 ed.; Butterworth-Heinemann: Amsterdam, 2003.

[28] Li, J.-H.; Liang, Y.; Xie, Y.-X. *J. Org. Chem.* **2005**, *70*, 4393.

[29] Bohlmann, F. *Chem. Ber.* **1953**, *86*, 657.

[30] The crystallographic analysis of tetrayne **4.1c** has previously been reported but no coordinates were made available to the CCDC; see Lagow, R. J.; Kampa, J. J.; Wei, H.-C.; Battle, S. L.; Genge, J. W.; Laude, D. A.; Harper, C. J.; Bau, R.; Stevens, R. C.; Haw, J. F.; Munson, E. *Science* **1995**, *267*, 362.

[31] Zeisberg, R.; Bohlmann, F. *Chem. Ber.* **1974**, *107*, 3800.

[32] Bohlmann, F.; Brehm, M. *Org. Magn. Resonance* **1979**, *12*, 535.

[33] Bartlett, P. D.; Roha, M.; Stiles, R. M. *J. Am. Chem. Soc.* **1954**, *76*, 2349.

[34] Khuong, T.-A. V.; Zepeda, G.; Ruiz, R.; Khan, S. I.; Garcia-Garibay, M. A. *Cryst. Growth Des.* **2004**, *4*, 15.

[35] Origin of endotherm unknown, however, it is consistent with a melting - recrystallization process; see Alamo, R.; Mandelkern, L. *J. Polym. Sci., Part B* **1986**, *24*, 2087-2105.

[36] Hay, A. S. *J. Org. Chem.* **1962**, *27*, 3320.

[37] Glaser, C. *Ann. Chem.* **1870**, *154*, 137.

[38] Glaser, C. *Ber. Dtsch. Chem. Ges.* **1869**, *2*, 422.

[39] Eglinton, G.; Galbraith, A. R. *Chem. Ind. (London)* **1956**, 737.

[40] Siemsen, P.; Livingston, R. C.; Diederich, F. *Angew. Chem. Int. Ed.* **2000**, *39*, 2632.

[41] Métay, E.; Hu, Q.; Negishi, E.-i. *Org. Lett.* **2006**, *8*, 5773.

[42] Hoheisel, T. N.; Frauenrath, H. *Org. Lett.* **2008**, *10*, 4525.

[43] Sonogashira, K. In *Handbook of Organopalladium Chemistry for Organic Synthesis*; Negishi, E.-i., Ed; Wiley: New York, 2002; pp 493.

[44] Sonogashira, K. *J. Organomet. Chem.* **2002**, *653*, 46.

[45] Wiechell, H. *Liebigs Ann. Chem.* **1894**, *279*, 337.

[46] Fritsch, P. *Liebigs Ann. Chem.* **1894**, *279*, 319.

[47] Buttenberg, W. P. *Liebigs Ann. Chem.* **1894**, *279*, 324.

[48] The use of MeLi•LiBr complex (1.5M in $Et_2O$) was also attempted but there was no appreciable difference in the reaction rate or yield compared to using MeLi (1.6M in $Et_2O$).

[49] Luu, T.; McDonald, R.; Tykwinski, R. R. *Org. Lett.* **2006**, *8*, 6035.

[50] Eisler, S.; Tykwinski, R R. *J. Am. Chem. Soc.* **2000**, *122*, 10736.

[51] Eisler, S.; Slepkov, A. D.; Elliott, E.; Luu, T.; McDonald, R.; Hegmann, F. A.; Tykwinski, R. R. *J. Am. Chem. Soc.* **2005**, *127*, 2666.

# Appendix A Synthesis of Trityl-Endcapped Polyynes

One of the main aspects towards polyyne synthesis is finding ways to impart stability into the molecules. One way to do this is to place bulky endgroups on the termini of the polyyne chain, which prevents the polyynes from closely approaching one another and undergoing intermolecular reactions (polymerization). This approach has been the driving force of research within the Tykwinski group and thus stable polyyne analogues were achieved up to ten triples bonds in length. Unfortunately, this seems to be a recurring synthetic limit of polyyne length with longer derivatives being difficult to synthesize and isolate as stable materials. In the case of TBPS endgroups (chapter 2), the size was over three times larger than the adamantyl and *t*-butyl, showing promise as a good stabilizing group for polyynes. This endgroup, however, proved to be too labile and thus prevented the synthesis of longer derivatives. The lability of the endgroup stems from the weaker Si–C bond, which is polarized and more prone to cleavage as a function of length. Replacement of silicon at the terminus with a carbon atom results in a triphenylmethyl (trityl) endgroup and was believed to circumvent the problem of endgroup cleavage.

The tritylchloride was available on the shelf and therefore was used as a model endgroup in order to test that the reaction conditions typically employed in the Tykwinski group for making polyynes would be compatible. The first step was the synthesis of the trityl (Tr) acetylene (**A1**, Figure A-1), which was easily achieved using a previously reported procedure.[1] The

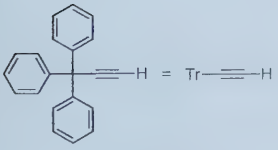


**A1**

**Figure A-1.** Trityl (Tr) acetylene **A1**.

tritylacetylene was deprotonated with hexyllithium, added to $CO_2$ and upon acidic workup provided acid **A2** in quantitative yield (Scheme A-1). The acid **A2** was converted to acid chloride **A3** quantitatively by treating with $SOCl_2$ in $CHCl_3$.

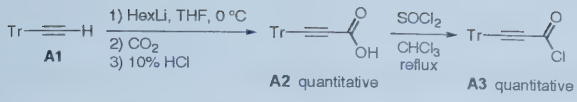


**Scheme A-1.** Synthesis of acid **A2** and acid chloride **A3**.

The Friedel-Craft reaction acylation of **A3** proved difficult in all cases towards making ketones **A4-A6** (Scheme A-2). Ketone **A4** was only formed in trace amount and when it was taken forward to dibromoolefin **A7** under conditions reported by Ramirez,[2] no desired product was isolable. It is believed that the ketone decomposed as a result of poor stability when isolated as a neat compound. In the case of ketones **A5** and **A6**, isolation was omitted and they were carried forward directly to **A8** and **A9** in 40% and 41% yields, respectively. Dibromoolefin **A8** was subjected to a FBW rearrangement to yield unsymmetrical tetrayne **A10**, which was not isolated but immediately carried forward under a modified Eglinton[3,4] homocoupling protocol reported by Haley and coworkers[5] to give octayne **A11** in 27% yield from **A8**.

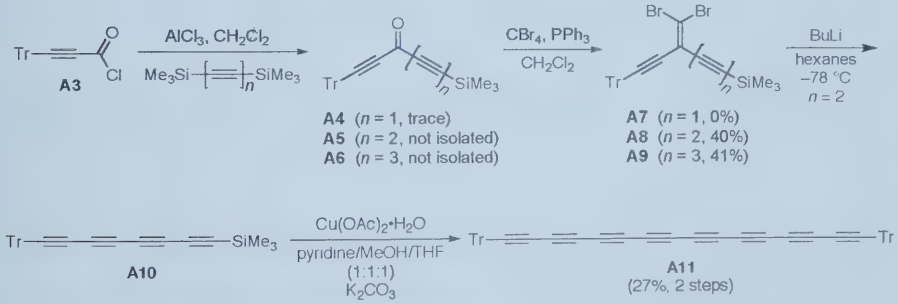


**Scheme A-2.** Synthesis of dibromoolefins **A7-A9** via a Friedel-Crafts reaction followed by dibromoolefination. Compound **A8** was subjected to a FBW rearrangement followed by dimerization under modified Eglinton conditions to give octayne **A11**.

The successful synthesis of octayne **A11** allowed for its stability to be probed and compared to other octayne derivatives. The DSC analysis of **A11** resulted in decomposition

occurring at 155 °C ($T_{max}$). This shows improved stability over analogues such as the adamantyl (**3.1f**, $T_{max}$ = 110 °C), TIPS (**S1f**, $T_{max}$ = 132 °C), and *t*-butyl (**4.1f**, $T_{max}$ = 139 °C).

Although the synthesis of octayne **A11** was successful using the chemistry above there seemed to be a problem with stability regarding the ketone intermediates, as demonstrated by **A4**, which completely decomposed upon attempted isolation. The incorporation of the larger, more stable TIPS group in place of the TMS was believed to alleviate this problem. The same synthetic steps shown above were employed, which included the Friedel-Crafts reaction between the acid chloride **A3**, formed from acid **A2**, and 1-TIPS-2-TMS acetylene to form ketone **A12** (Scheme A-3). The ketone was taken on directly without isolation to give dibromoolefin **A13** in a modest 19% yield over 3 steps from **A2**. The FBW rearrangement of **A13** to triyne **A14** proceeded in 62% yield.

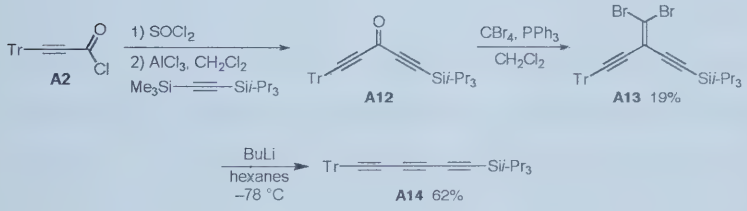


**Scheme A-3.** Synthesis of triyne **A14** via a FBW rearrangement.

Because the yields obtained for dibromoolefins **A7**-**A9** were poor and the incorporation of the TIPS didn't seem to improve this, a simple stability test was done. Based on past experience, the dibromoolefination step was not considered to be the problem as yields were typically good and a wide range of functional groups were tolerable. Therefore, it was believed that the Friedel-Crafts step was the problematic step since a large amount of black material is removed from the reaction when plugged through silica gel. It was found that the addition of a substoichiometric amount $AlCl_3$ to a solution of triyne **A14** in $CH_2Cl_2$ at room temperature led to immediate decomposition of **A14**, resulting in the formation of insoluble black material. At –78 °C the decomposition was much slower but when warmed to –40 °C immediate decomposition

occurred. Decomposition was also seen when $FeCl_3$ was added to a solution of **A14** in $CH_2Cl_2$ at –40 °C but was much slower than $AlCl_3$, and when warmed to 0 °C, decomposition occurred. The treatment of 1,6-bis(TMS)hexatriyne under the same reaction conditions does not lead to decomposition. These results suggest that it may be the trityl endgroup itself that is sensitive to strong Lewis acids and that this would also pose a problem with other substrates such as the acid chloride **A3** and the ketone intermediates. This would explain the low yields and large amounts of insoluble black material formed during the Friedel-Crafts reaction.

## A.1 Conclusions

The synthesis of trityl endcapped polyynes can be successfully done using the Friedel-Crafts protocol, followed by dibromoolefination and FBW rearrangement. There is, however, a problem using strong Lewis acids, such as $AlCl_3$ and $FeCl_3$, which seem to react with the trityl endgroup, causing decomposition of starting materials, intermediates and products. The TIPS group can be used in place of the smaller, more labile TMS group, possibly leading to more stable intermediates, however, this does not improve yields from the Friedel-Crafts reaction. Therefore, it seemed clear that, although this procedure can produce desired products in moderate yields, a cleaner, more efficient procedure is needed when using trityl endgroups (see chapter 5).

## A.2 Experimental Section

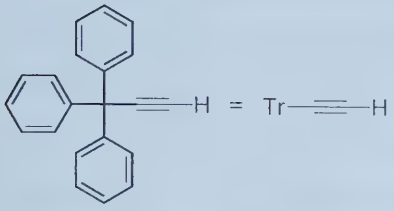


**A1**

**A1** was synthesized as previously reported.[1] Yield = 74%. Spectroscopic data consistent with that reported.

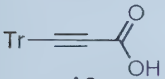


**A2**

**A2** (acid): To a solution of **A1** (1.453 g, 5.415 mmol) in THF (150 mL) cooled to 0 °C under a $N_2$ atmosphere was added hexyllithium (2.35 mL, 2.3M in hexanes, 5.4 mmol). The reaction was stirred for 30 min and $CO_2$ (g) (passed through a drying tube filled with drierite) was bubbled through the solution for 30 min. The $CO_2$ (g) was stopped and the mixture stirred for another 30 min. The reaction was acidified to pH ~ 1 with 10% HCl (aq), saturated aqueous $NH_4Cl$ (50 mL) added and the resulting mixture extracted with $Et_2O$ (2 × 150 mL). The organic phases were combined, washed with brine (50 mL), and dried over $MgSO_4$. The solvent was removed in vacuo to yield **A2** (1.746 g, quantitative) as a pale yellow solid: Mp 181-183 °C; IR (microscope) 3059, 3025 (br), 2234, 1687 $cm^{-1}$; $^1H$ NMR (500 MHz, $CDCl_3$): $\delta$ 9.42 (br s, 1H); 7.24-7.33 (m, 9H), 7.18-7.22 (m, 6H); $^{13}C$ NMR (125 MHz, $CDCl_3$): $\delta$ 157.3, 143.0, 129.1, 128.3, 127.4, 95.7, 76.4, 55.9; EIMS *m/z* 312.1 ($M^+$, 9), 268.1 ($[M - CO_2]^+$, 100); EI HRMS *m/z* calcd. for $C_{22}H_{16}O_2$ ($M^+$) 312.1150. found 312.1158.

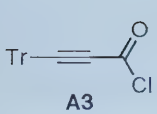


A3

**A3**: To a solution of **A2** (1.143 g, 3.662 mmol) in purified $CHCl_3$[6] (100 mL) was added $SOCl_2$ (3.05 g, 1.87 mL, 25.6 mmol) and the reaction stirred at reflux under a $N_2$ atmosphere for 17 h. The solvent was removed in vacuo to yield **A3** (1.219 g, quantitative) as a green solid: Mp 184-188 °C; IR (microscope) 3085, 3066, 3028, 2315, 2262, 2203, 2169, 1741 $cm^{-1}$; $^1H$ NMR (500 MHz, $CDCl_3$): $\delta$ 7.27-7.35 (m, 9H), 7.15-7.19 (m, 6H); $^{13}C$ NMR (125 MHz, $CDCl_3$): $\delta$ 149.6, 142.4, 129.0, 128.5, 127.7, 101.6, 80.3, 56.2; EIMS *m/z* 330.1 ($M^+$, 3), 295.1 ($[M - Cl]^+$, 77), 267.1 ($[M - CO - Cl]^+$, 100); EI HRMS *m/z* calcd. for $C_{22}H_{15}O^{35}Cl$ ($M^+$) 330.0812, found 330.0818.

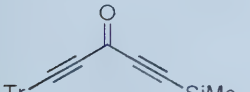


A4

**A4:** To a solution of acid chloride **A3** (334 mg, 1.01 mmol) and 1,2-bis(TMS)acetylene (258 mg, 1.51 mmol) in $CH_2Cl_2$ (40 mL) at rt was added $AlCl_3$ (337 mg, 2.53 mmol) and the reaction stirred under a $N_2$ atmosphere for 1 h. The reaction mixture was filtered through a silica plug and the solvent removed in vacuo to yield crude **A4** as a brownish-black oil that was carried on directly to **A7**: $R_f$ = 0.31 ($CH_2Cl_2$/hexanes 1:1); IR (microscope) 3061, 3031, 2962, 2204, 2154, 1633, 1598 $cm^{-1}$.

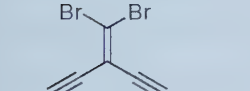


A7

**A7:** To a solution of $CBr_4$ (0.683 g, 2.06 mmol) in $CH_2Cl_2$ (30 mL) was added $PPh_3$ (1.122 g, 4.278 mmol) and the reaction stirred for 1 h under a $N_2$ atmosphere. Crude ketone **A4** (theoretically 1.01 mmol, see **A4** synthesis) was dissolved in $CH_2Cl_2$ (5 mL), added to the ylide

and stirred under a $N_2$ atmosphere for 16 h. The reaction was concentrated in vacuo to ca. 20 mL and hexanes were added to precipitate the phosphine salts as a white solid along with an oily residue. The supernatant was decanted and filtered through a pad of celite. The oily residue left in the flask was dissolved in minimal $CH_2Cl_2$ and hexanes were added; the heterogeneous mixture was then decanted and the supernatant filtered through celite (this procedure was repeated three times). The filtrate was filtered through celite until the filtrate remained a clear solution. The solvent was removed in vacuo and the crude product purified by column chromatography (silica gel, hexanes) to yield only trace amounts of **A9**, not suitable for characterization.

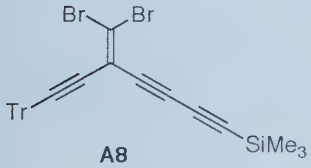


**A8**

**A8:** A solution of acid **A2** (312 mg, 0.999 mmol) in $SOCl_2$ (5 mL) was stirred at rt for 16 h covered with a $CaCl_2$ drying tube. The $SOCl_2$ was removed in vacuo, 1,4-bis(trimethylsilyl)buta-1,3-diyne (194 mg, 0.999 mmol) added and the mixture dissolved in $CH_2Cl_2$ (5 mL). This solution was added dropwise to a mixture of $AlCl_3$ (150 mg, 1.10 mmol) in $CH_2Cl_2$ (30 mL) cooled to 0 °C under a $N_2$ atmosphere. The reaction was stirred for 3 h at 0 °C under a $N_2$ atmosphere. The reaction was quenched with saturated aqueous $NH_4Cl$ (20 mL), the layers separated and the organic phase dried over $MgSO_4$. The solvent was removed in vacuo and the crude ketone **A5** purified by column chromatography (silica gel, eluted with hexanes first to remove unreacted 1,4-bis(trimethylsilyl)buta-1,3-diyne followed by $CH_2Cl_2$ to remove **A5**). The ketone fractions were combined, concentrated in vacuo to ca. 5 mL and held for further use. Concurrently, to a solution of $CBr_4$ (503 mg, 1.52 mmol) in $CH_2Cl_2$ (30 mL) was added $PPh_3$ (838 mg, 3.20 mmol) and the reaction stirred for 1 h under a $N_2$ atmosphere. The solution of **A5** was added dropwise and the reaction stirred for 22 h. The reaction was concentrated in vacuo and the crude product purified by column chromatography (silica gel, $CH_2Cl_2$/hexanes 1:4) to yield **A8** (228 mg, 40%) as a yellow oil: $R_f$ = 0.61 ($CH_2Cl_2$/hexanes 1:2); IR (microscope) 3059, 3031, 2962, 2219, 2092, 1597 $cm^{-1}$;

$^1$H NMR (500 MHz, $CDCl_3$): $\delta$ 7.32-7.21 (m, 15H), 0.22 (s, 9H); $^{13}$C NMR (125 MHz, $CDCl_3$): $\delta$ 144.1, 129.2, 128.1, 127.1, 113.3, 111.1, 103.0, 95.0, 87.2, 81.0, 80.1, 72.4, 56.6, –0.6; EIMS *m/z* 572.0 ($M^+$, 3), 557.0 ($[M - CH_3]^+$, 5), 493.1 ($[M - Br]^+$, 11), 412.2 ($[M - Br_2]^+$, 100); EI HRMS *m/z* calcd. for $C_{30}H_{24}Si^{79}Br^{81}Br$ ($M^+$) 571.9993, found 571.9979.

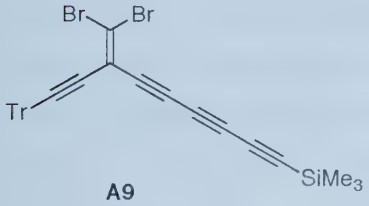


**A9**

**A9:** To a mixture of $AlCl_3$ (110 mg, 0.825 mmol) in $CH_2Cl_2$ (20 mL) cooled to 0 °C under a $N_2$ atmosphere was added a solution of **A3** (105 mg, 0.317 mmol) and 1,6-bis(trimethylsilyl)hexa-1,3,5-triyne (83 mg, 0.38 mmol) in $CH_2Cl_2$ (5 mL). The reaction was stirred for 3 h at 0 °C under a $N_2$ atmosphere then filtered through a plug of alumina to yield a solution of **A6**. Concurrently, to a solution of $CBr_4$ (267 mg, 0.805 mmol) in $CH_2Cl_2$ (10 mL) was added $PPh_3$ (461 mg, 1.76 mmol) and the reaction stirred for 1 h under a $N_2$ atmosphere. This solution was added to the solution of **A6** and the reaction stirred for 10 min. The reaction was concentrated in vacuo to ca. 20 mL and hexanes were added to precipitate the phosphine salts as a white solid along with an oily residue. The supernatant was decanted and filtered through a pad of celite. The oily residue left in the flask was dissolved in minimal $CH_2Cl_2$ and hexanes were added; the heterogeneous mixture was then decanted and the supernatant filtered through celite (this procedure was repeated three times). The filtrate was filtered through celite until the filtrate remained a clear solution. The solvent was removed in vacuo and the crude product purified by column chromatography (silica gel, hexanes) to yield **A9** (78 mg, 41%) as a yellow solid: $R_f$ = 0.44 ($CH_2Cl_2$/hexanes 1:4); IR (microscope) 3059, 3030, 2960, 2218, 2178, 2074, 1597 cm$^{-1}$; $^1$H NMR (500 MHz, $CDCl_3$): $\delta$ 7.31-7.20 (m, 15H), 0.21 (s, 9H); $^{13}$C NMR (125 MHz, $CDCl_3$): $\delta$ 144.0, 129.2, 128.1, 127.1, 113.1, 112.4, 103.5, 91.5, 87.8, 80.8, 80.2, 72.5, 70.3, 61.0, 56.6, –0.6; EIMS *m/z* 596.0 ($M^+$, 1), 583.0 ($[M - CH_3]^+$, 1), 515.1 ($[M - Br]^+$, 8), 436.2 ($[M - Br_2]^+$, 100); EI HRMS *m/z* calcd. for $C_{32}H_{24}Si^{79}Br^{81}Br$ ($M^+$) 595.9993, found 595.9990.

A11

**A11:** To a solution of **A8** (223 mg, 0.390 mmol) in hexanes (30 mL) at –78 °C was added BuLi (0.19 mL, 2.5M in hexanes, 0.48 mmol) dropwise under a $N_2$ atmosphere. The reaction mixture was stirred at –78 °C for 10 min, warmed to 0 °C over 30 min, and quenched by the addition of saturated aqueous $NH_4Cl$ (10 mL). The layers were separated and the organic layer dried over $Na_2SO_4$. The volume was reduced in vacuo to ca. 5 mL, THF (5 mL) was added, the volume reduced again to ca. 5 mL and held for later use (**A10**). To a solution of $Cu(OAc)_2 \cdot H_2O$ (156 mg, 0.780 mmol) in MeOH (10 mL), THF (10 mL) and pyridine (10 mL) was added $K_2CO_3$ (54 mg, 0.390 mmol) and the solution of **A10**. The reaction was stirred at rt until deemed complete by UV-Vis spectroscopic analysis; ca. 2 h. The reaction was diluted with hexanes (60 mL) and the mixture washed with $H_2O$ (2 × 15 mL), brine (15 mL), and dried over $Na_2SO_4$. The solvent was removed in vacuo and the crude product purified by column chromatography (silica gel, $CH_2Cl_2$/hexanes 1:4) to yield **A11** (35 mg, 27%) as a yellowish-orange solid: $R_f$ = 0.43 ($CH_2Cl_2$/hexanes 1:5); UV-Vis (THF) $\lambda_{max}$ 345, 324, 305, 289, 275, 263 nm; IR (microscope) 3061, 3023, 2205, 2124, 2018, 1598 $cm^{-1}$; $^1H$ NMR (400 MHz, $CDCl_3$): $\delta$ 7.25-7.31 (m, 9H), 7.14-7.18 (m, 6H); $^{13}C$ NMR (125 MHz, $CDCl_3$): $\delta$ 143.3, 129.0, 128.3, 127.4, 85.2, 69.8, 63.5, 63.2, 63.0, 62.9, 62.7, 62.7, 56.7; MALDI MS *m/z* ($M^+$) 678.4; DSC: decomposition, 76 °C (onset), 155 °C (peak).

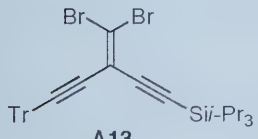


A13

**A13:** A solution of **A2** (1.125 g, 3.602 mol) in $SOCl_2$ (5 mL) was stirred at rt covered with a $CaCl_2$ drying tube for 18 h. The solvent was removed in vacuo, the resulting residue dissolved in $CH_2Cl_2$ (5 mL), and the solvent removed in vacuo to yield **A3**. To this residue was added 1-TIPS-2-TMS acetylene (1.097 g, 4.309 mmol) and the resulting mixture dissolved in $CH_2Cl_2$ (20 mL).

This solution was added dropwise to a mixture of $AlCl_3$ (0.532 g, 3.99 mmol) in $CH_2Cl_2$ (60 mL) at 0 °C and stirred for 4 h under a $N_2$ atmosphere. The reaction was quenched with saturated aqueous $NH_4Cl$ (20 mL), the resulting layer separated and the organic phase dried over $MgSO_4$. The solvent was removed in vacuo and the residue purified by passing through a short plug of silica gel. The filtrate was concentrated in vacuo to ca. 10 mL and held for later use (**A12**). Concurrently, to a solution of $CBr_4$ (2.389 g, 7.204 mmol) in $CH_2Cl_2$ (60 mL) was added $PPh_3$ (4.253 g, 16.21 mmol) and the reaction stirred for 1 h under a $N_2$ atmosphere. The ketone (**A12**) solution was added and the reaction stirred for 16 h. The reaction was concentrated in vacuo to ca. 20 mL and hexanes were added to precipitate the phosphine salts as a white solid along with an oily residue. The supernatant was decanted and filtered through a pad of celite. The oily residue left in the flask was dissolved in minimal $CH_2Cl_2$ and hexanes were added; the heterogeneous mixture was then decanted and the supernatant filtered through celite (this procedure was repeated three times). The filtrate was filtered through celite until the filtrate remained a clear solution. The solvent was removed in vacuo and the crude product purified by column chromatography (silica gel, hexanes) to yield **A13** (0.435 g, 19%) as a yellow solid: $R_f$ = 0.53 ($CH_2Cl_2$/hexanes 1:4); IR (microscope) 3085, 3060, 3030, 2943, 2890, 2865, 2227, 2141 (w), 1597 $cm^{-1}$; $^1H$ NMR (400 MHz, $CDCl_3$): $\delta$ 7.30-7.21 (m, 15H), 1.06-1.11 (m, 21H); $^{13}C$ NMR (100 MHz, $CDCl_3$): $\delta$ 144.3, 129.2, 128.0, 127.0, 114.7, 107.9, 102.3, 102.0, 99.4, 82.3, 56.5, 18.6, 11.1; EIMS *m/z* 632.1 ($M^+$, 21), 589.0 ([M – *i*-Pr]$^+$, 27), 472.3 ([M – $Br_2$]$^+$, 90), 315.1 ([M – $Br_2$ – *i*-Pr]$^+$, 100); EI HRMS *m/z* calcd. for $C_{34}H_{36}Si^{79}Br^{81}Br$ ($M^+$) 632.0933, found 632.0926.

**A14**

**A14: :** To a solution of **A13** (419 mg, 0.662 mmol) in hexanes (40 mL) at –78 °C was added BuLi (0.32 mL, 2.5M in hexanes, 0.80 mmol) dropwise under a $N_2$ atmosphere. The reaction mixture was stirred at –78 °C for 10 min, warmed to rt over 30 min, and quenched by the addition of saturated aqueous $NH_4Cl$ (15 mL). The layers were separated and the organic layer dried over $Na_2SO_4$. The solvent was removed in vacuo and the crude product purified by recrystallization

from $Et_2O$/MeOH to yield **A14** (194 mg, 62%) as a yellow solid: Mp 114-115 °C; $R_f$ = 0.58 ($CH_2Cl_2$/hexanes 1:4); IR (microscope) 3084, 3058, 3031, 2942, 2890, 2864, 2210, 2167, 2075, 1597 $cm^{-1}$; $^1H$ NMR (500 MHz, $CDCl_3$): $\delta$ 7.22-7.30 (m, 9H), 7.16-7.21 (m, 6H), 1.02-1.11 (m, 21H); $^{13}C$ NMR (125 MHz, $CDCl_3$): $\delta$ 143.8, 129.1, 128.2, 127.2, 89.8, 84.9, 83.8, 70.1, 63.7, 60.9, 56.4, 18.5, 11.3; EI HRMS *m/z* calcd. for $C_{34}H_{36}Si$ ($M^+$) 472.2586, found 472.2594; Anal. calcd. for $C_{34}H_{36}Si$: C, 86.38; H, 7.68. Found: C, 86.01; H, 7.77; DSC: Mp = 120 °C; decomposition, 275 °C (onset), 310 °C (peak).

## A.3 References


[1] Karlen, S. D.; Ortiz, R.; Chapman, O. L.; Garcia-Garibay, M. A. *J. Am. Chem. Soc.* **2005**, *127*, 6554.

[2] Ramirez, F.; Desai, N. B.; McKelvie, N. *J. Am. Chem. Soc.* **1962**, *84*, 1745.

[3] Siemsen, P.; Livingston, R. C.; Diederich, F. *Angew. Chem. Int. Ed.* **2000**, *39*, 2632.

[4] Eglinton, G.; Galbraith, A. R. *Chem. Ind. (London)* **1956**, 737.

[5] Haley, M. M.; Bell, M. L.; Brand, S. C.; Kimball, D. B.; Pak, J. J.; Wan, W. B. *Tetrahedron Lett.* **1997**, *38*, 7483.

[6] Armarego, W. L. F.; Chai, C. L. L. *Purification of Laboratory Chemicals*; 5th ed.; Butterworth-Heinemann: Amsterdam, 2003.

# Appendix B DFT Simulation Data

**Table B-1.** The full list of harmonic frequencies, IR and Raman intensities, irreproducible representations of the normal modes for bent H-(C≡C)$_5$-H (the $A_1$ Я–mode and $B_1$ IR mode are highlighted, see Figure B-1). Data from DFT calculations (PBEPBE/cc-pVQZ).

| | | | |
|---|---|---|---|
| | A1 | B2 | A2 |
| Frequencies -- | 37.0748 | 104.7298 | 105.6228 |
| Red. masses -- | 6.3607 | 6.1963 | 6.1744 |
| Frc consts -- | 0.0052 | 0.0400 | 0.0406 |
| IR Inten -- | 1.1678 | 0.2650 | 0.0000 |
| Raman Activ -- | 20.1676 | 2.7410 | 5.8357 |
| | A1 | B1 | B2 |
| Frequencies -- | 195.3283 | 196.5923 | 291.3922 |
| Red. masses -- | 6.4054 | 6.5264 | 7.7171 |
| Frc consts -- | 0.1440 | 0.1486 | 0.3861 |
| IR Inten -- | 2.8577 | 3.0687 | 0.2719 |
| Raman Activ -- | 0.5078 | 0.1439 | 1.9130 |
| | A2 | A1 | A1 |
| Frequencies -- | 291.9566 | 408.6436 | 420.0195 |
| Red. masses -- | 7.7336 | 8.9831 | 9.5309 |
| Frc consts -- | 0.3884 | 0.8838 | 0.9907 |
| IR Inten -- | 0.0000 | 0.4272 | 0.8164 |
| Raman Activ -- | 2.4382 | 7.8233 | 0.7835 |
| | B1 | B2 | A2 |
| Frequencies -- | 420.6720 | 473.2443 | 473.9628 |
| Red. masses -- | 9.5401 | 10.8860 | 10.9003 |
| Frc consts -- | 0.9947 | 1.4364 | 1.4427 |
| IR Inten -- | 1.0546 | 0.6121 | 0.0000 |
| Raman Activ -- | 0.1233 | 1.8760 | 4.2411 |
| | A1 | B1 | B2 |
| Frequencies -- | 501.8307 | 502.7315 | 508.2243 |
| Red. masses -- | 11.9842 | 11.9848 | 11.9466 |
| Frc consts -- | 1.7782 | 1.7846 | 1.8180 |
| IR Inten -- | 0.0006 | 0.0844 | 22.7056 |
| Raman Activ -- | 24.5398 | 0.6810 | 51.0085 |
| | A2 | B2 | A2 |
| Frequencies -- | 510.4177 | 582.2064 | 582.7941 |
| Red. masses -- | 11.9369 | 1.2340 | 1.2340 |
| Frc consts -- | 1.8323 | 0.2464 | 0.2469 |
| IR Inten -- | 0.0000 | 10.1244 | 0.0000 |
| Raman Activ -- | 53.3428 | 18.4995 | 25.4794 |
| | A1 | B1 | B2 |
| Frequencies -- | 582.8944 | 583.4059 | 770.0301 |
| Red. masses -- | 1.2339 | 1.2382 | 9.0716 |
| Frc consts -- | 0.2470 | 0.2483 | 3.1692 |
| IR Inten -- | 76.7740 | 87.3925 | 10.6309 |
| Raman Activ -- | 12.3369 | 0.6216 | 0.0007 |
| | A1 | B2 | A1 |
| Frequencies -- | 1118.5020 | 1428.9668 | 2007.6353 |
| Red. masses -- | 9.5260 | 10.4580 | 8.0553 |
| Frc consts -- | 7.0216 | 12.5817 | 19.1295 |
| IR Inten -- | 0.1445 | 3.2612 | 0.0137 |
| Raman Activ -- | 62.3799 | 2.1357 | 3423.0643 |
| | B2 | A1 | A1 |
| Frequencies -- | 2082.0934 | 2103.5759 | 2179.3398 |
| Red. masses -- | 6.9962 | 11.6847 | 9.1799 |
| Frc consts -- | 17.8695 | 30.4637 | 25.6885 |
| IR Inten -- | 16.9081 | 1.0196 | 0.1889 |
| Raman Activ -- | 132.5631 | 36432.1078 | 240.2585 |
| | B2 | B2 | A1 |
| Frequencies -- | 2210.2193 | 3394.5904 | 3395.1662 |
| Red. masses -- | 11.2105 | 1.1463 | 1.1463 |
| Frc consts -- | 32.2659 | 7.7824 | 7.7853 |
| IR Inten -- | 4.3222 | 422.7597 | 18.9659 |
| Raman Activ -- | 348.4529 | 13.8992 | 52.4905 |

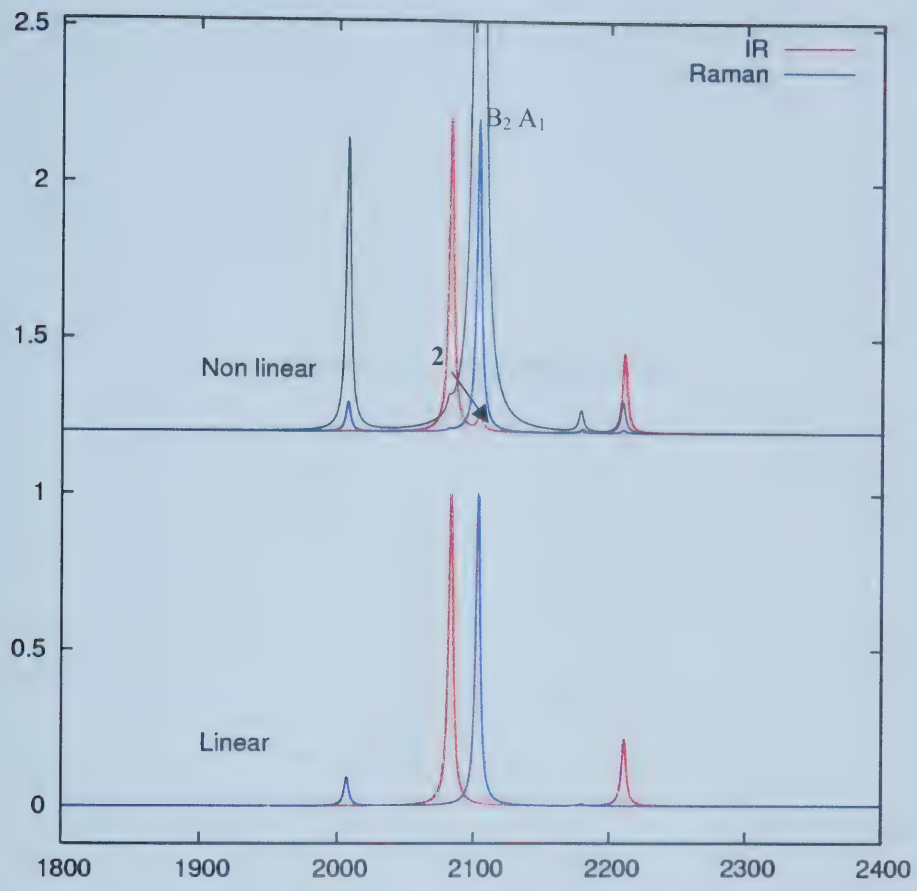


**Figure B-1.** Simulated Raman and IR spectra of the linear and bent conformations of H-(C≡C)$_{10}$-H (according to PBEPBE/cc-pVQZ). The thinner black curve is the Raman spectrum enhanced by a factor of 10. Activation of the strong IR line is observed as a shoulder of the strong Raman line (arrow 2). The activation in the IR of the strong Raman line is by converse more evident (arrow 1). Simulated peaks are Lorentzian functions with a FWHM = 4 cm$^{-1}$.

# Appendix C Selected Spectra

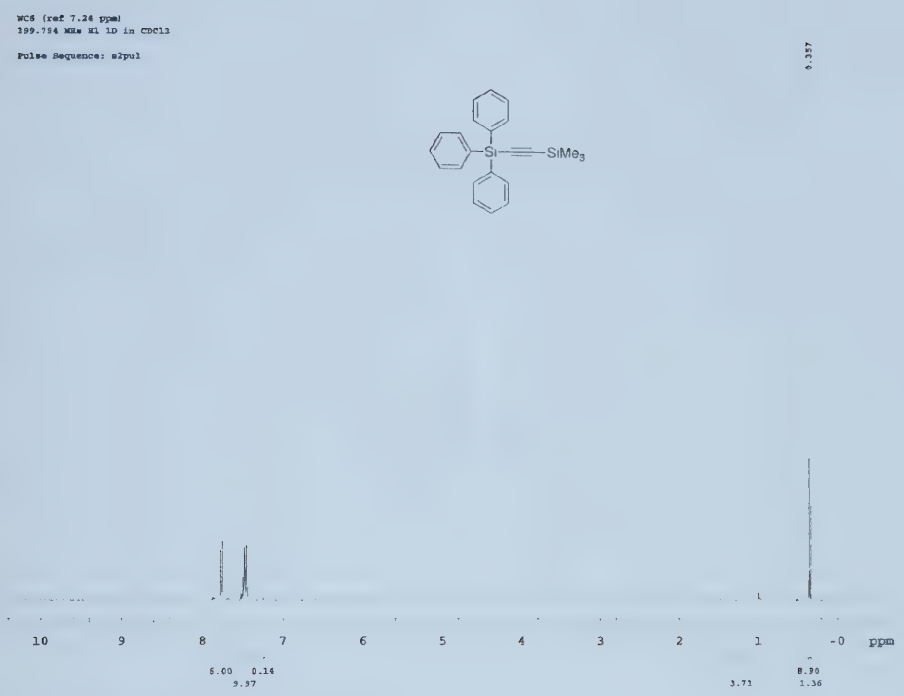


**Figure C-1.** $^{1}$H NMR spectrum of **2.5**.

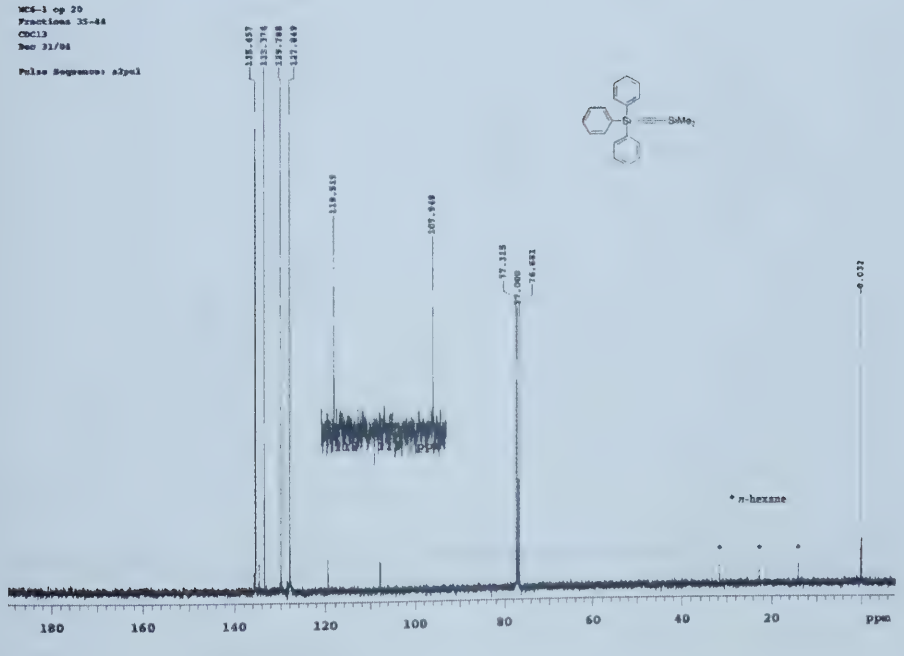


**Figure C-2.** $^{13}$C NMR spectrum of **2.5**.

**Figure C-3.** $^{1}$H NMR spectrum of **2.6**.

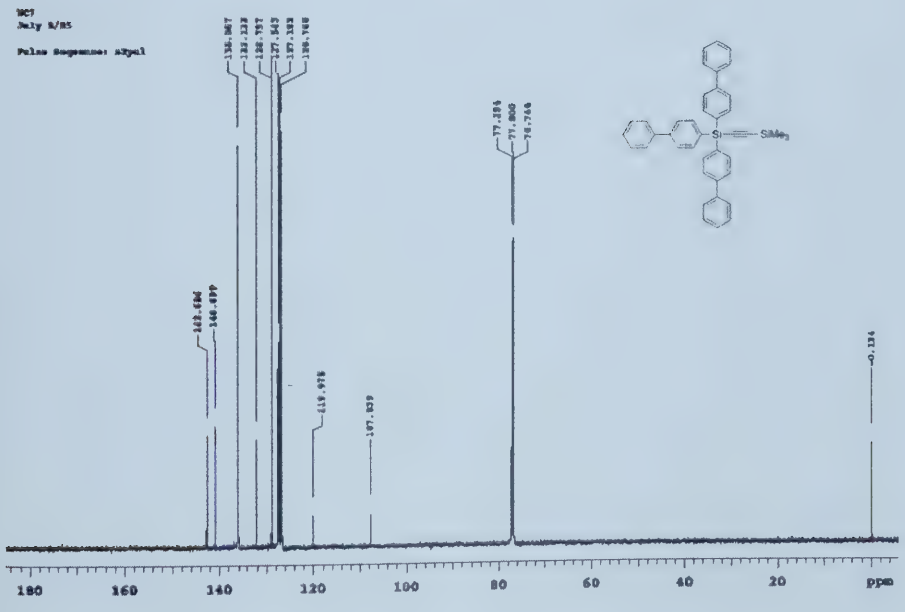


**Figure C-4.** $^{13}$C NMR spectrum of **2.6**.

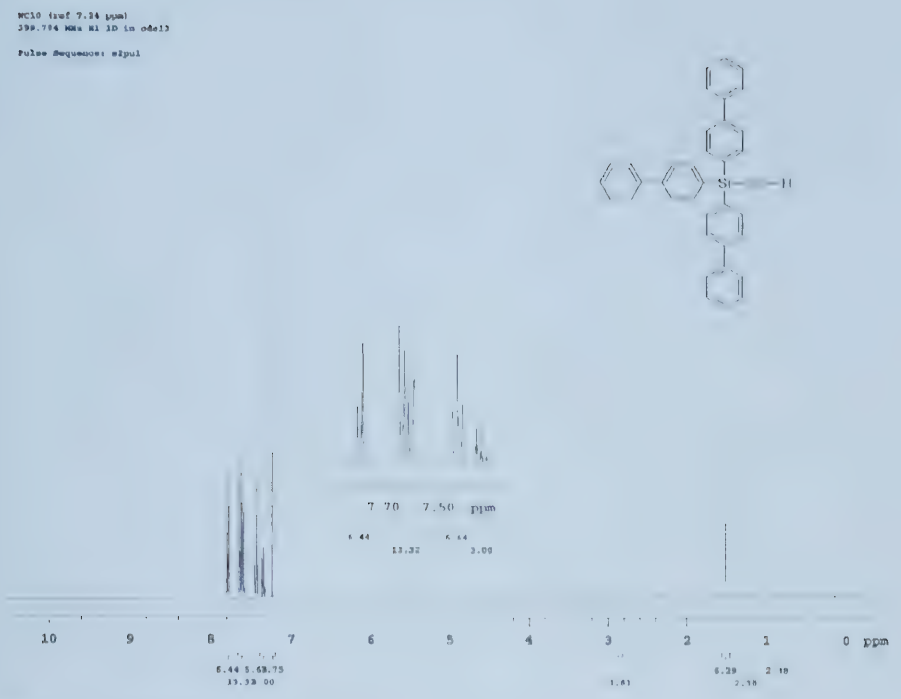


**Figure C-5.** $^{1}$H NMR spectrum of **2.7**.

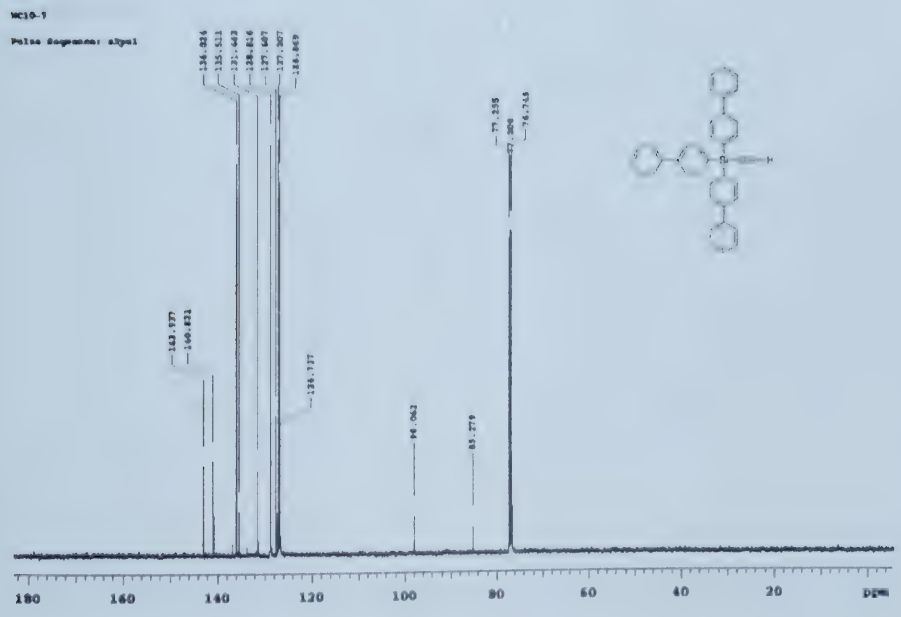


**Figure C-6.** $^{13}$C NMR spectrum of **2.7**.

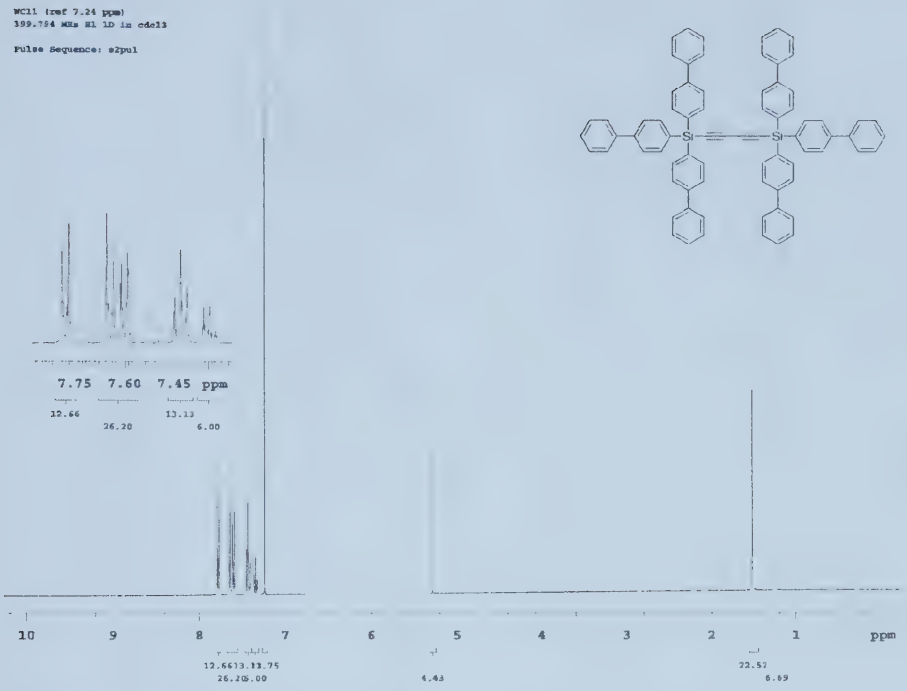


**Figure C-7.** $^{1}$H NMR spectrum of **2.8**.

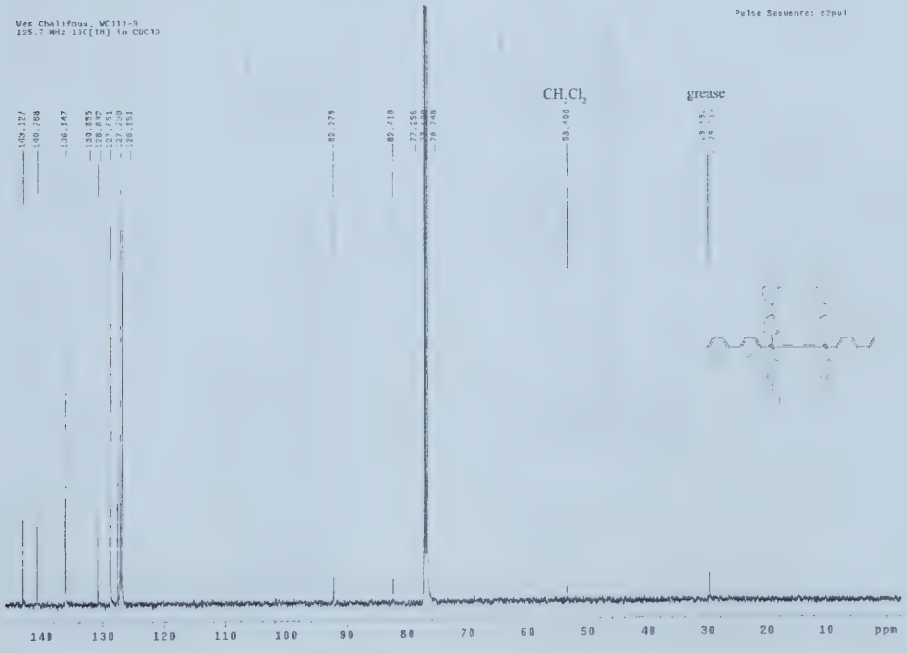


**Figure C-8.** $^{13}$C NMR spectrum of **2.8**.

**Figure C-9.** $^{1}$H NMR spectrum of **2.9**.

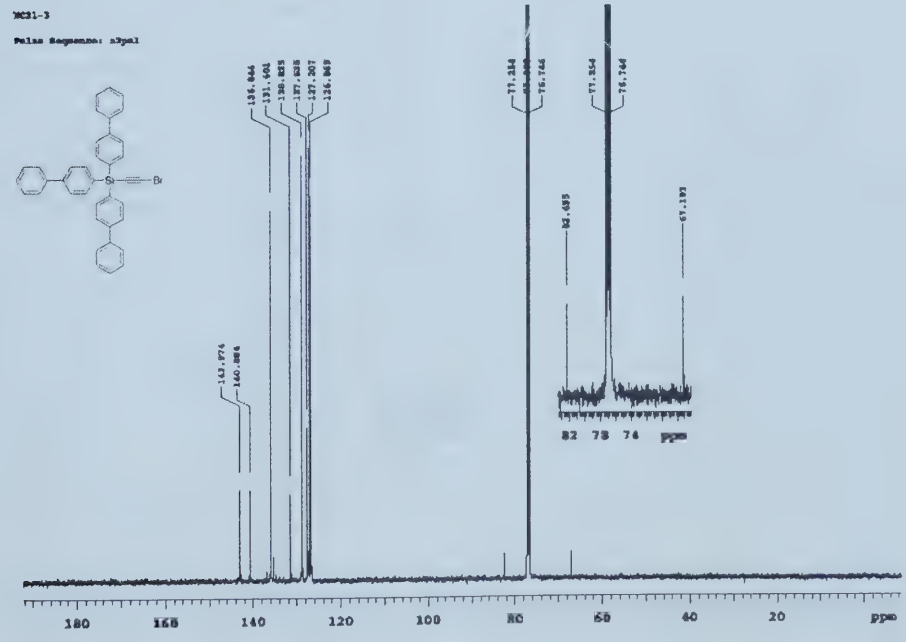


**Figure C-10.** $^{13}$C NMR spectrum of **2.9**.

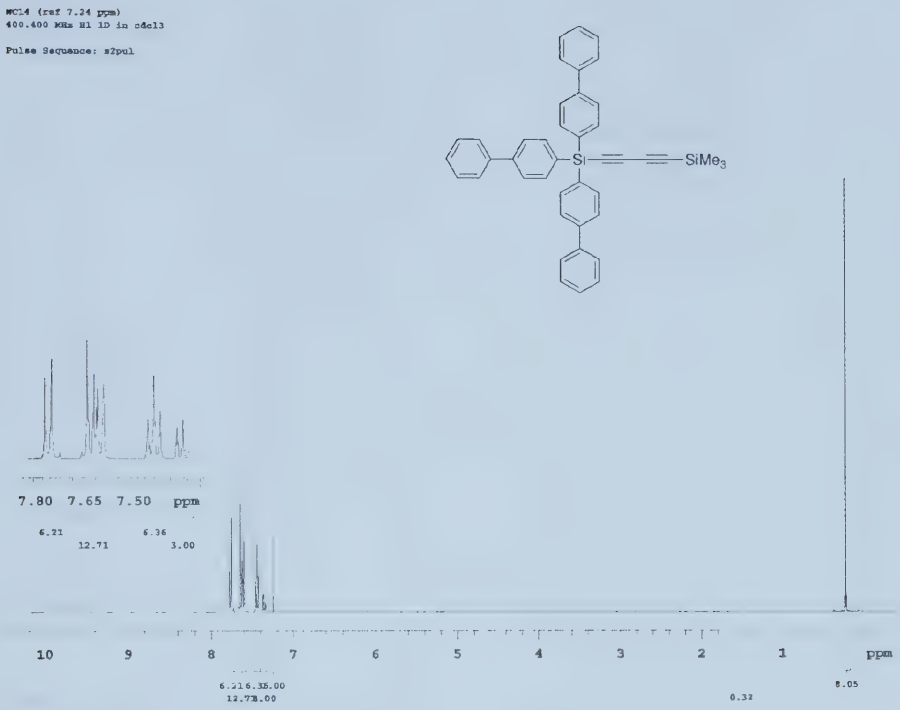


**Figure C-11.** $^{1}$H NMR spectrum of **2.10**.

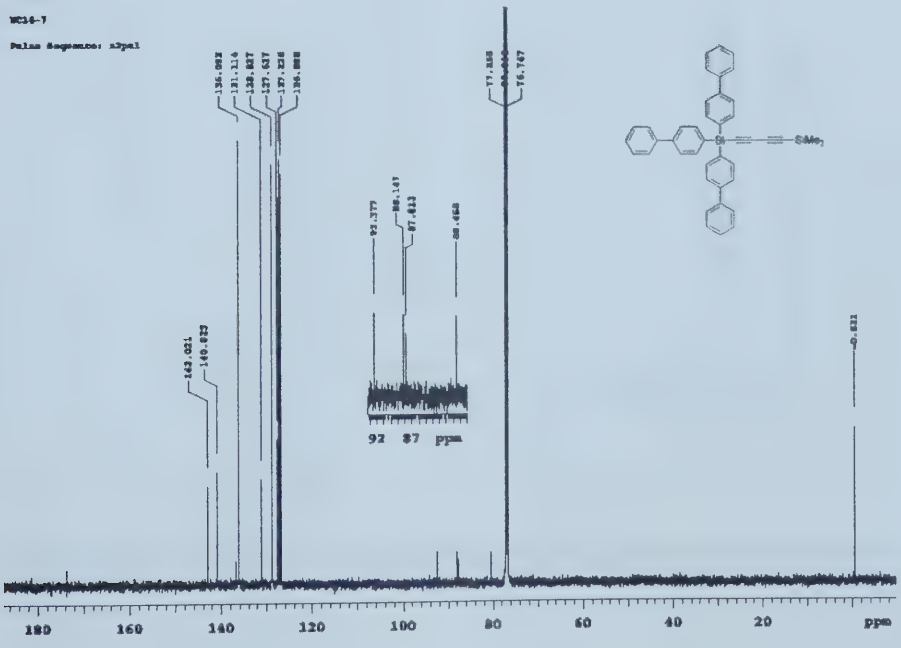


**Figure C-12.** $^{13}$C NMR spectrum of **2.10**.

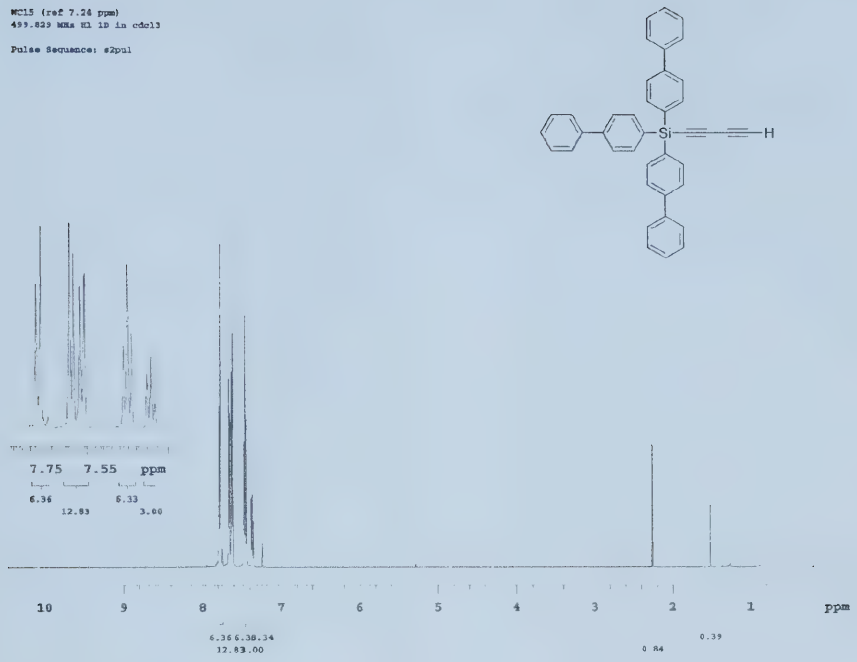


**Figure C-13.** $^{1}$H NMR spectrum of **2.13**.

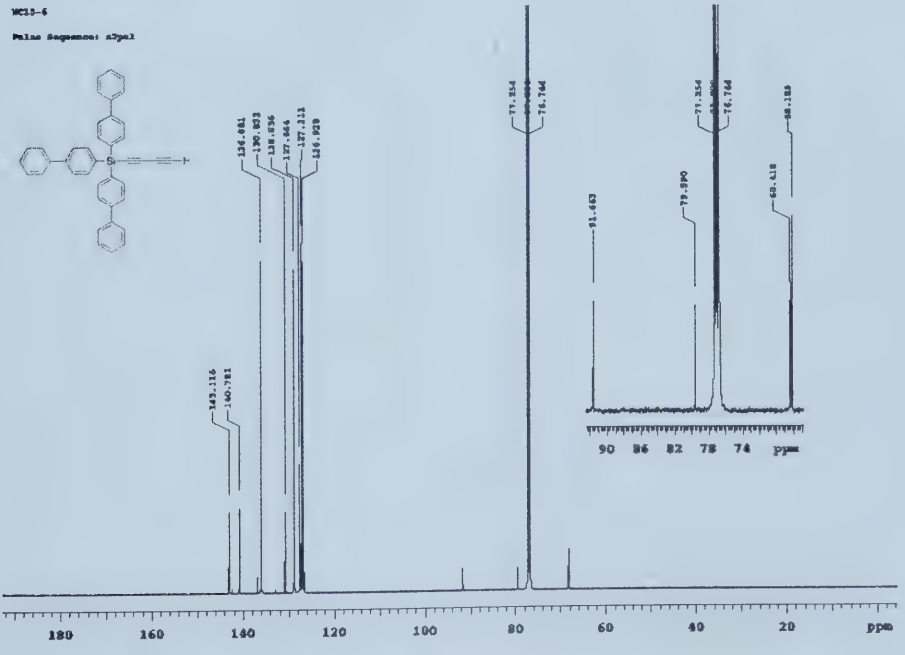


**Figure C-14.** $^{13}$C NMR spectrum of **2.13**.

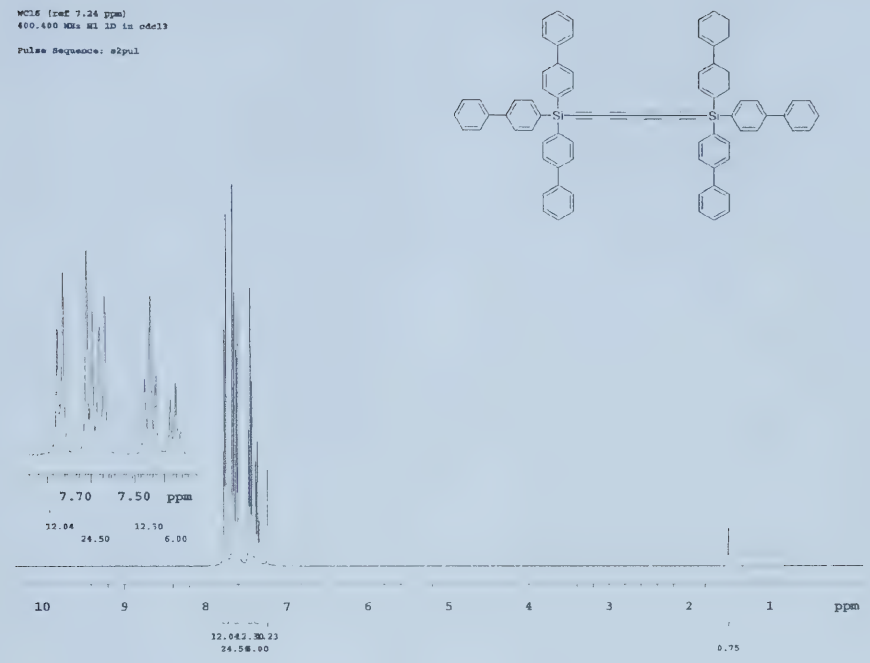


**Figure C-15.** $^{1}$H NMR spectrum of **2.14**.

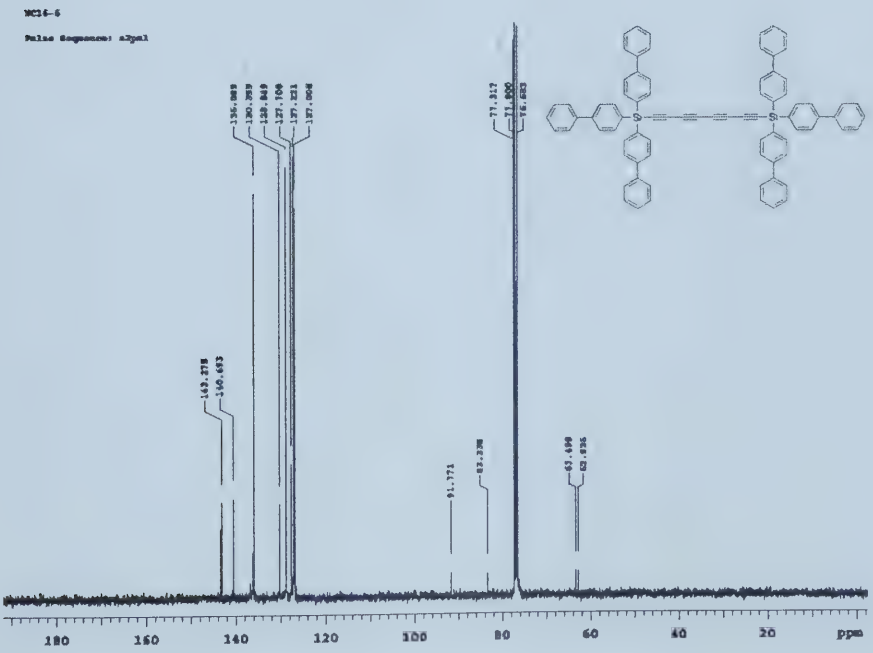


**Figure C-16.** $^{13}$C NMR spectrum of **2.14**.

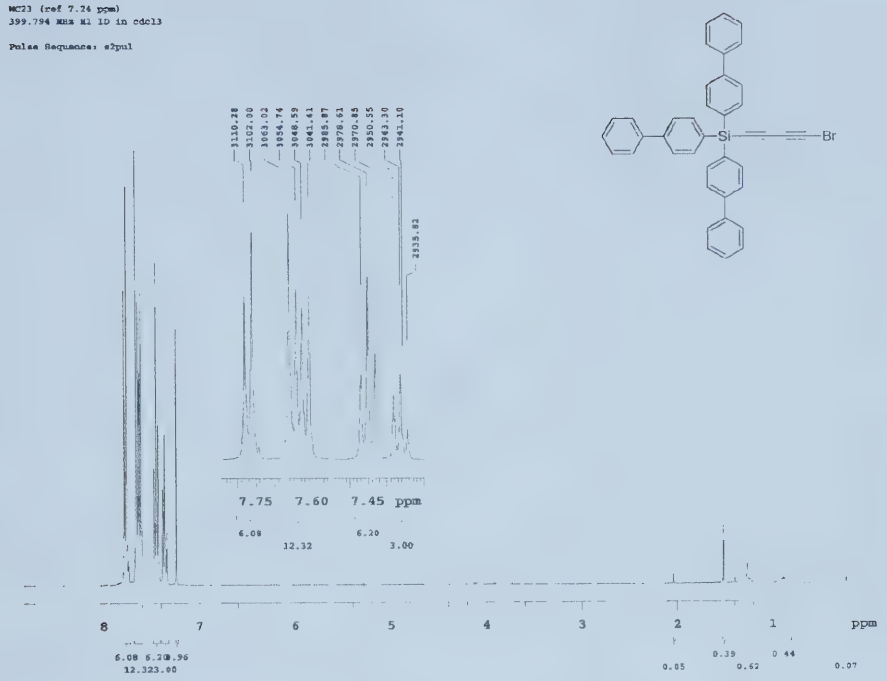


**Figure C-17.** $^{1}$H NMR spectrum of **2.15**.

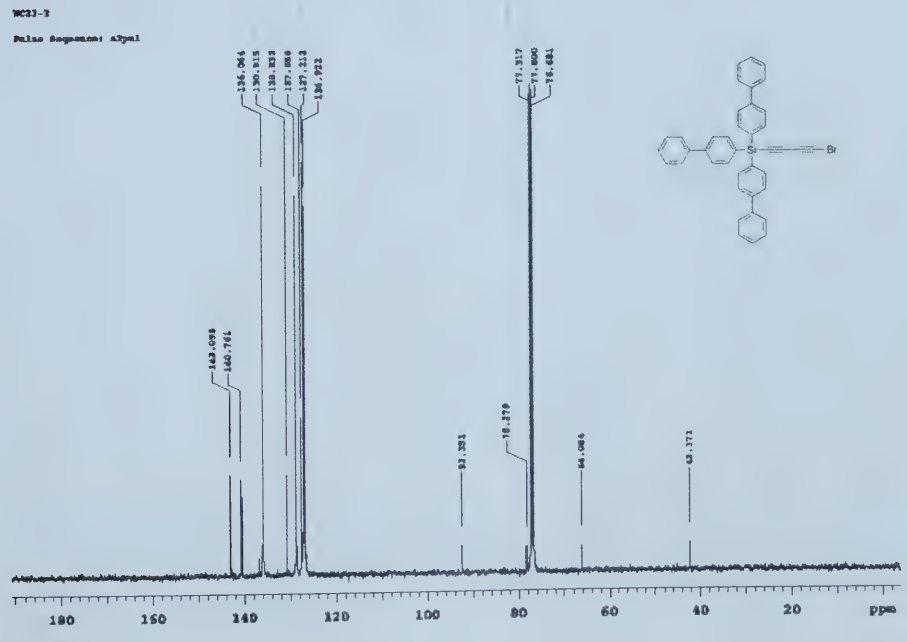


**Figure C-18.** $^{13}$C NMR spectrum of **2.15**.

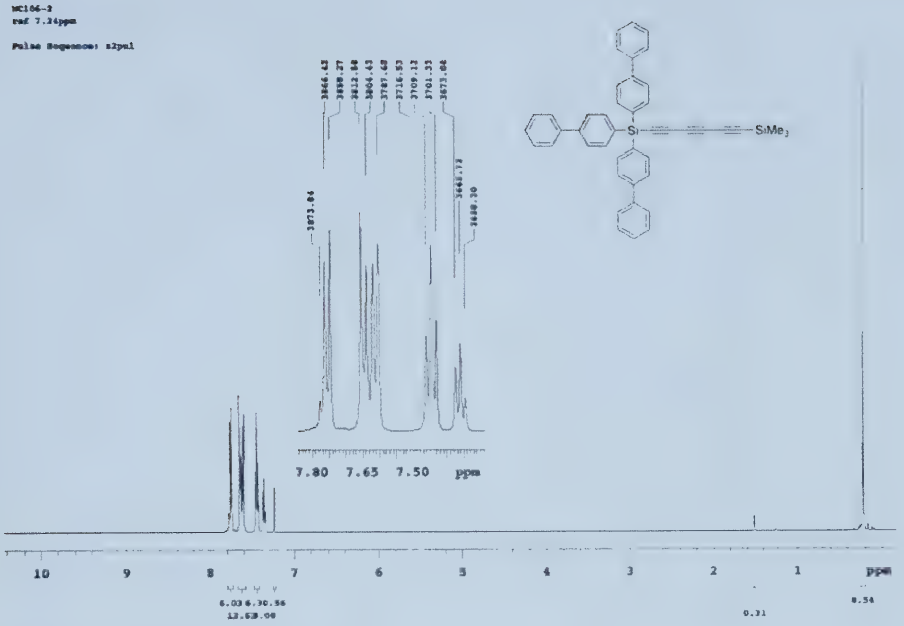


**Figure C-19.** $^{1}$H NMR spectrum of **2.16**.

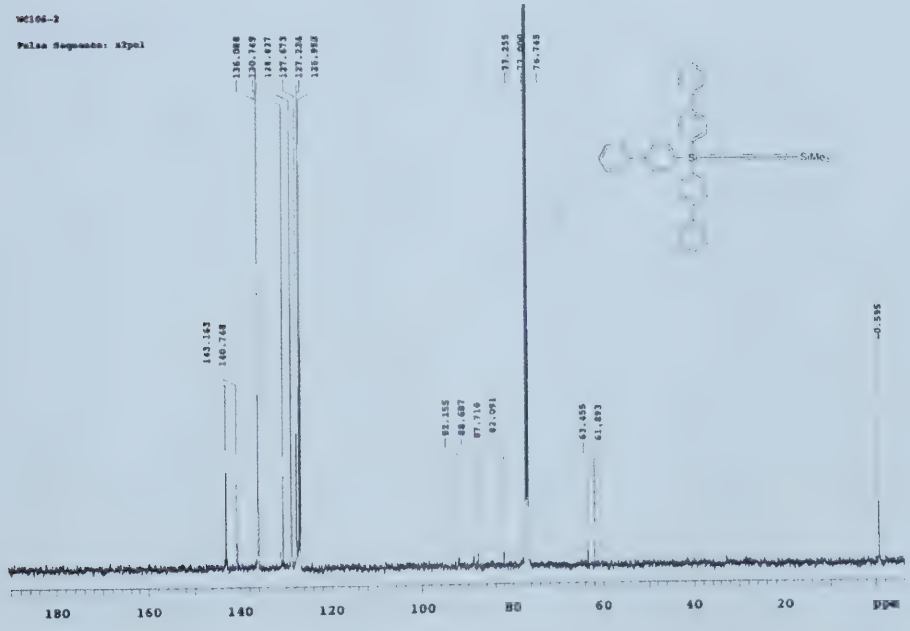


**Figure C-20.** $^{13}$C NMR spectrum of **2.16**.

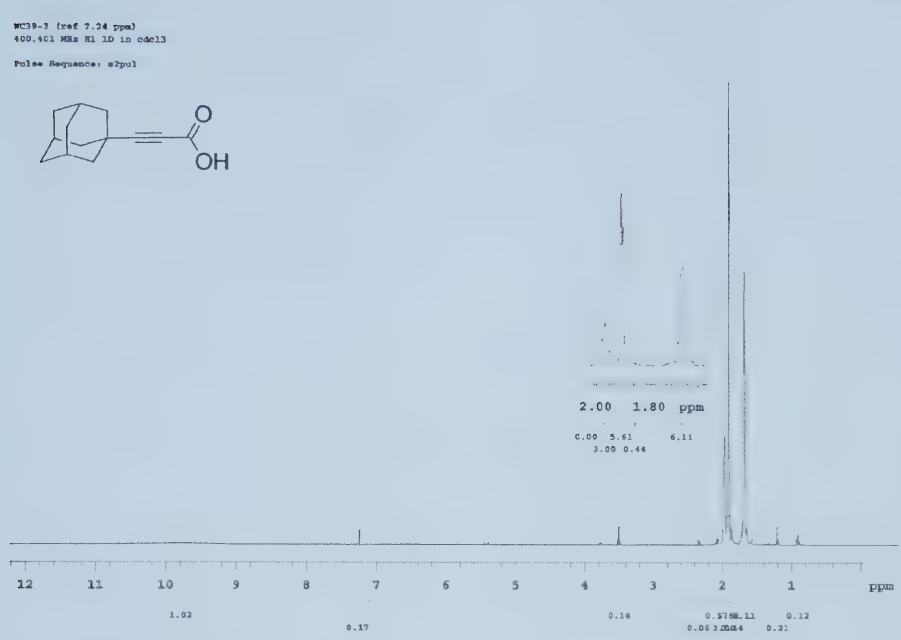


**Figure C-21.** $^{1}$H NMR spectrum of **3.3**.

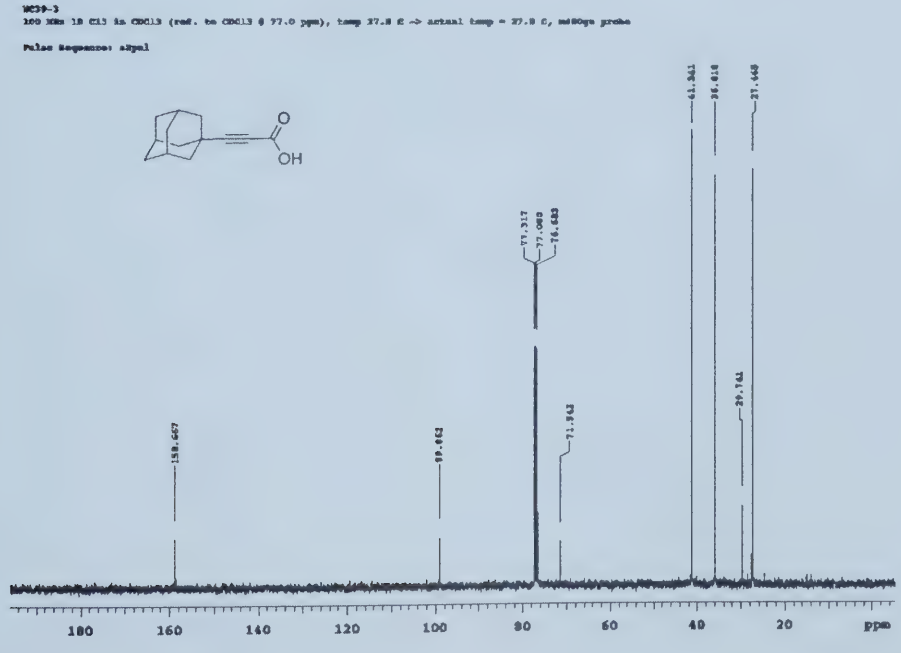


**Figure C-22.** $^{13}$C NMR spectrum of **3.3**.

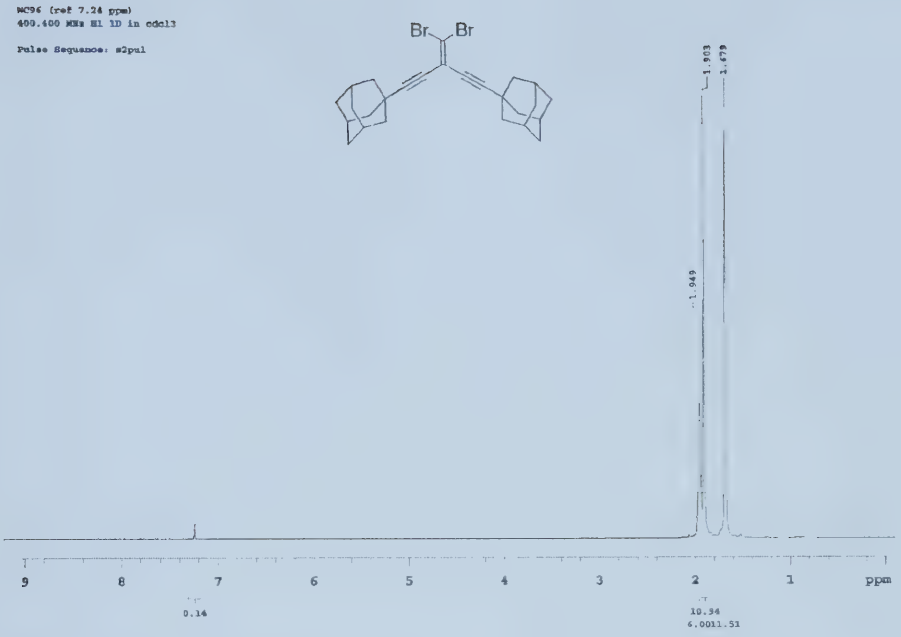


**Figure C-23.** $^{1}$H NMR spectrum of **3.8**.

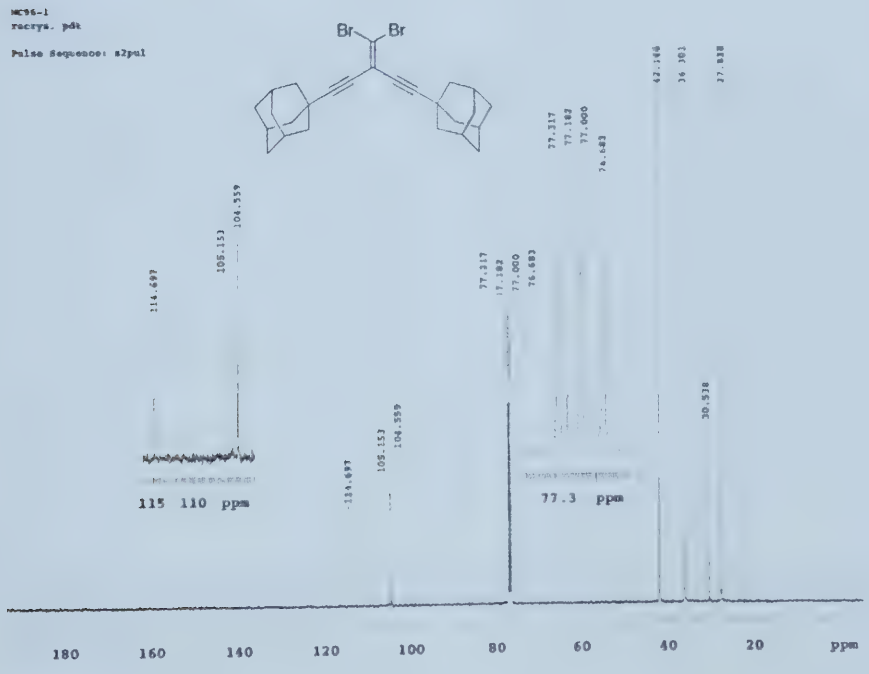


**Figure C-24.** $^{13}$C NMR spectrum or **3.8**.

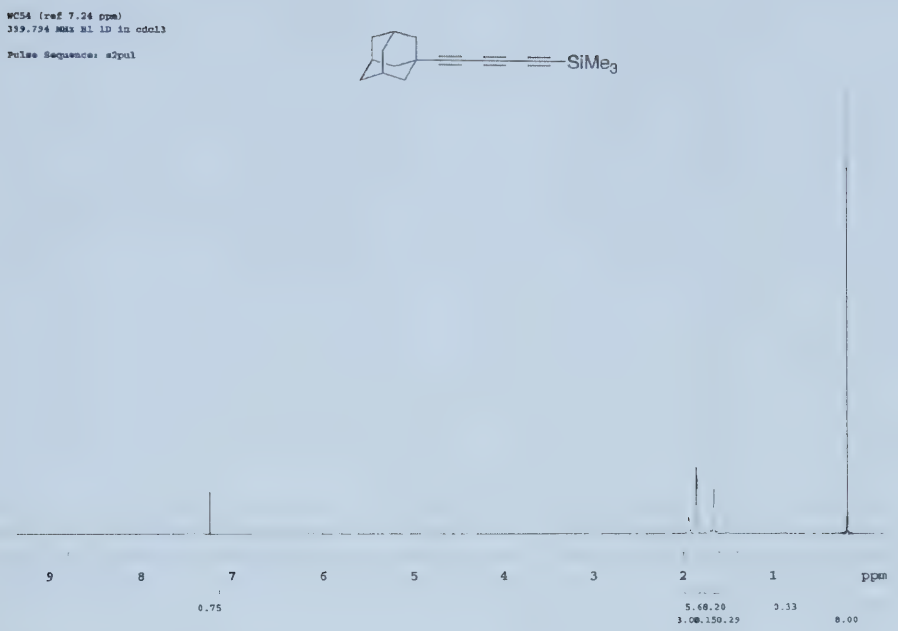


**Figure C-25.** $^{1}$H NMR spectrum of **3.15**.

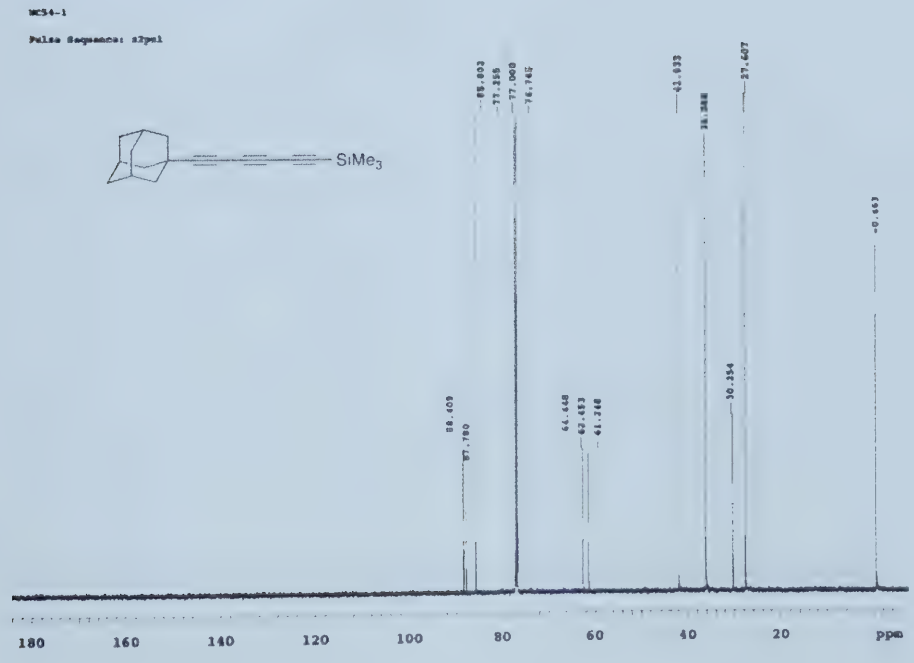


**Figure C-26.** $^{13}$C NMR spectrum of **3.15**.

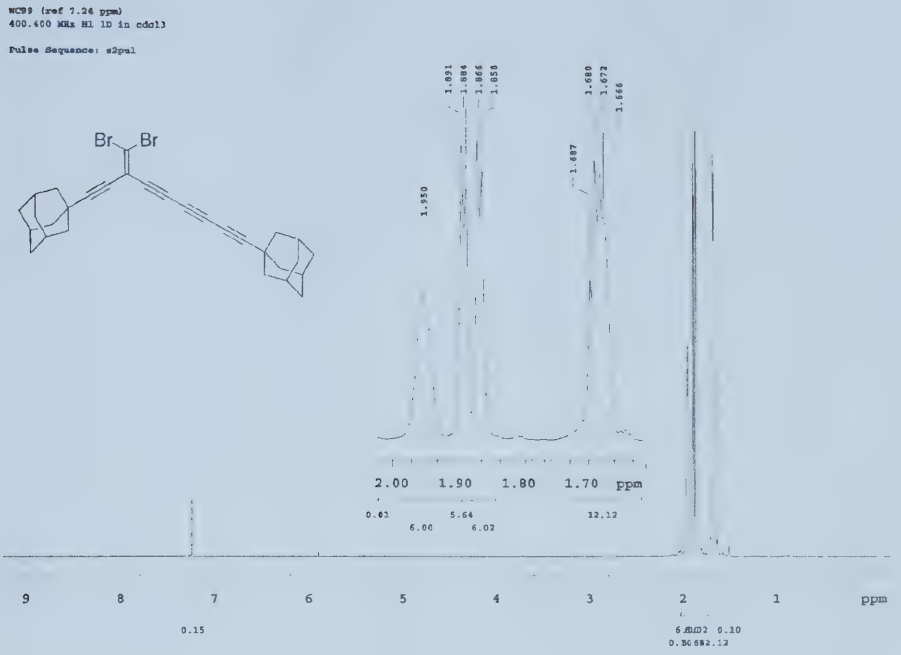


**Figure C-27.** $^{1}$H NMR spectrum of **3.17**.

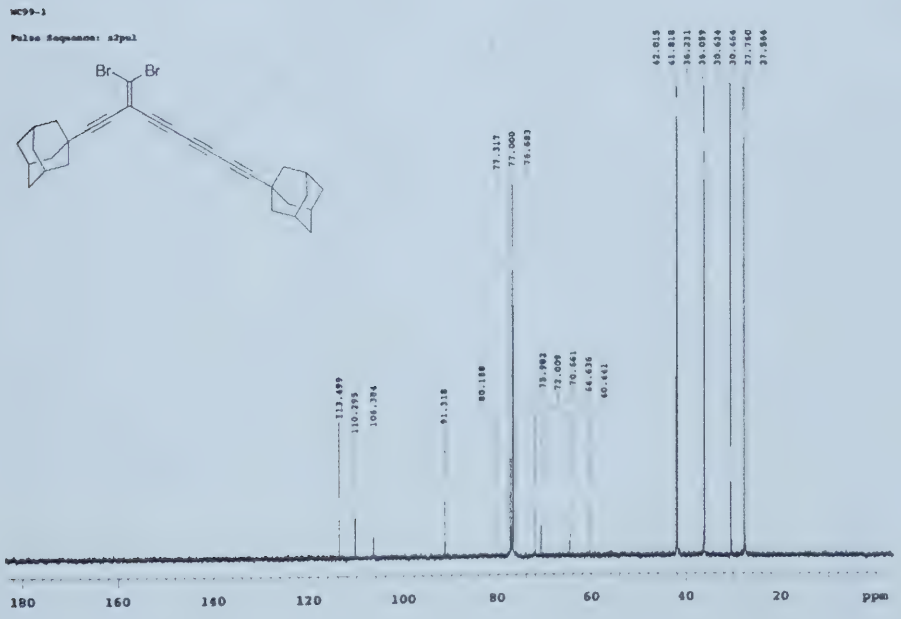


**Figure C-28.** $^{13}$C NMR spectrum of **3.17**.

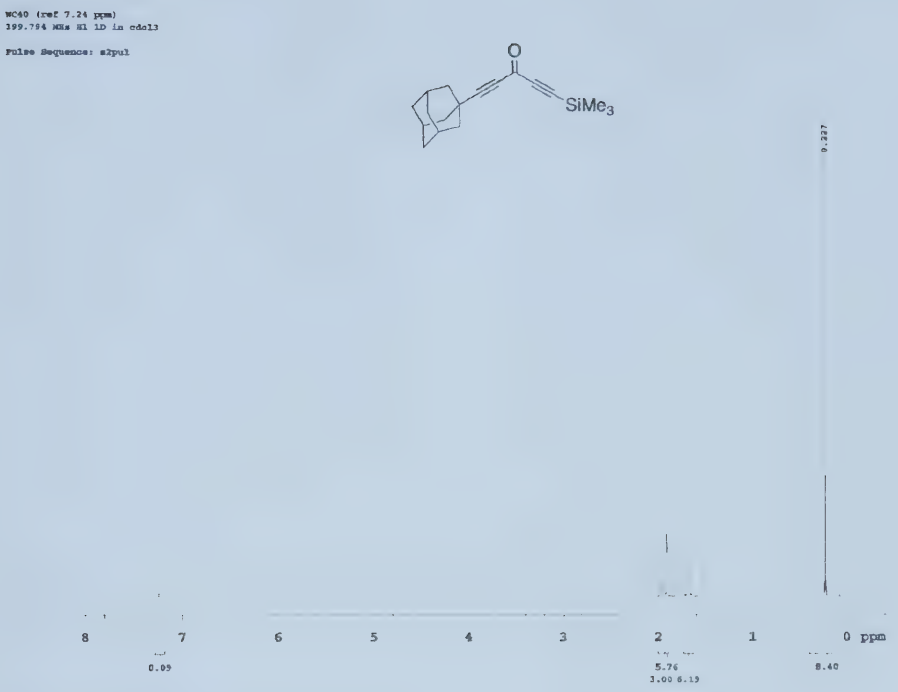


**Figure C-29.** $^{1}$H NMR spectrum of **3.18**.

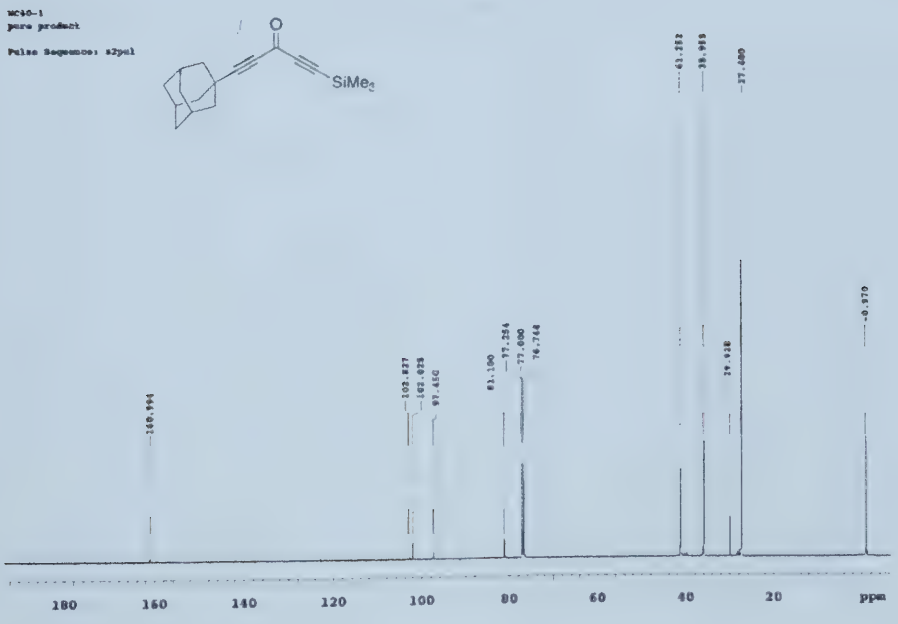


**Figure C-30.** $^{13}$C NMR spectrum of **3.18**.

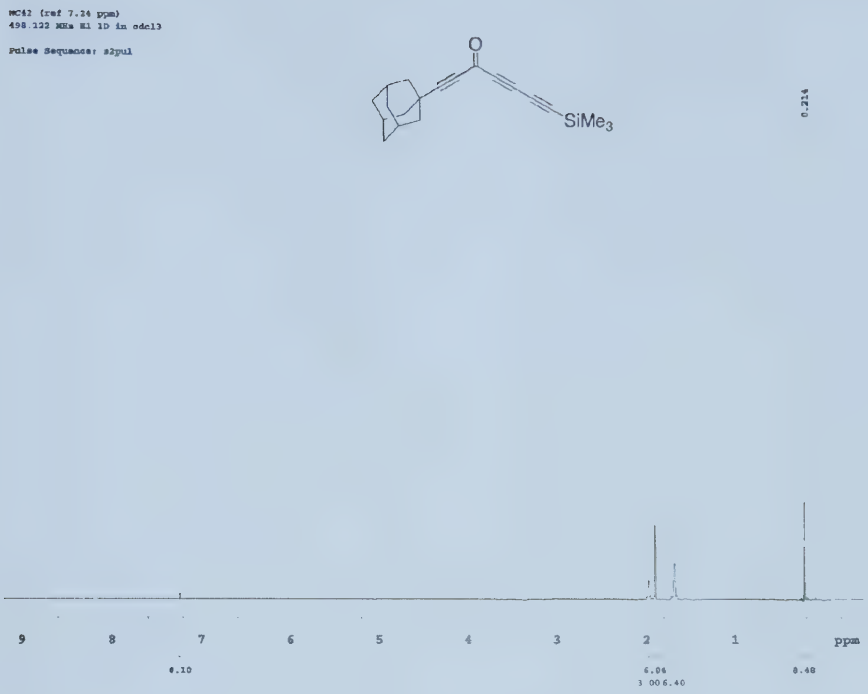


**Figure C-31.** $^{1}$H NMR spectrum of **3.19**.

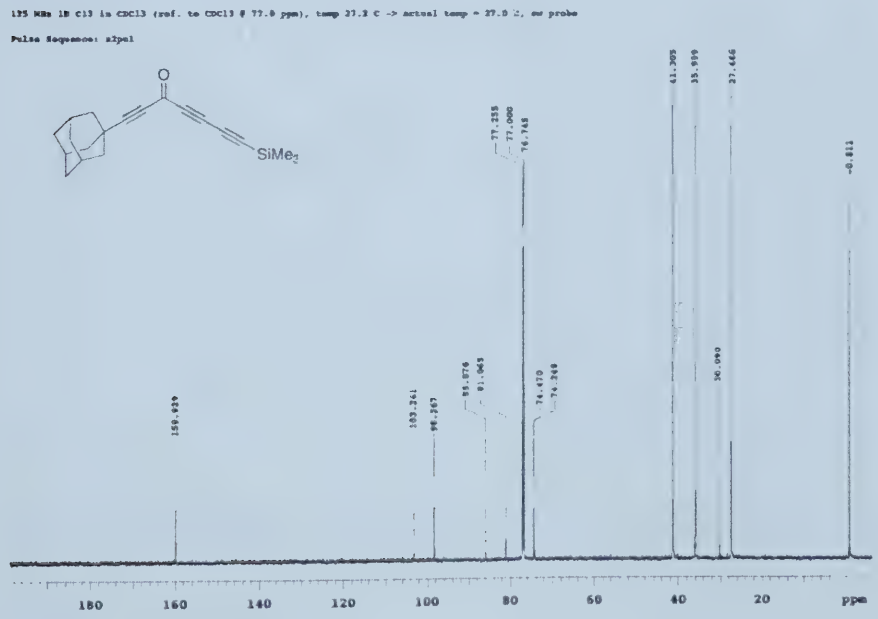


**Figure C-32.** $^{13}$C NMR spectrum of **3.19**.

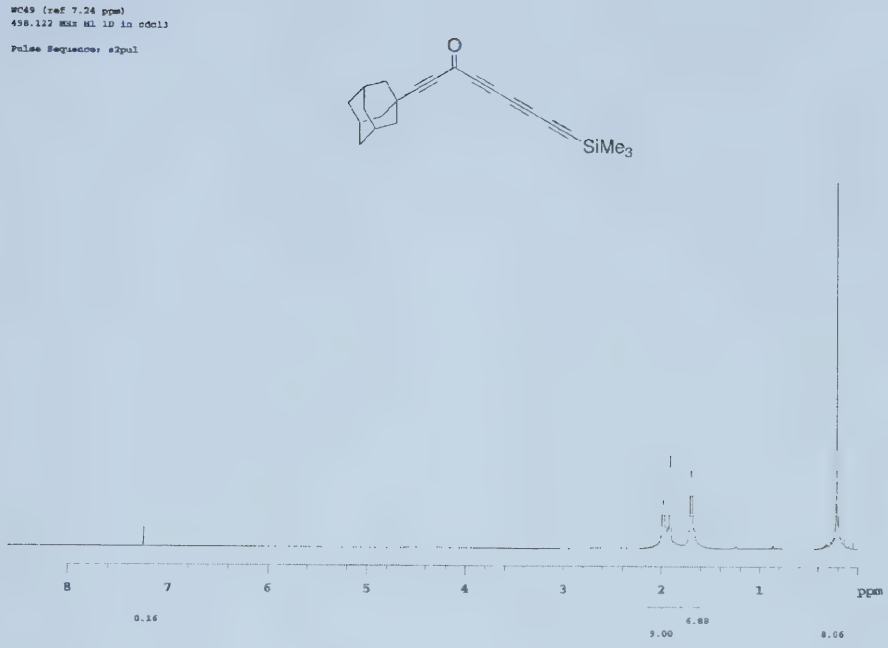


**Figure C-33.** $^{1}$H NMR spectrum of **3.20**.

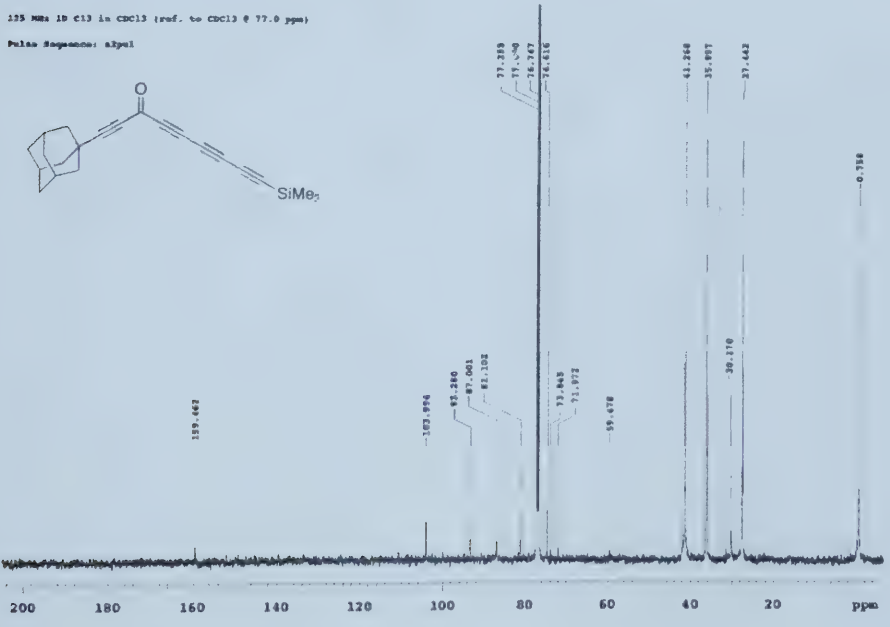


**Figure C-34.** $^{13}$C NMR spectrum of **3.20**.

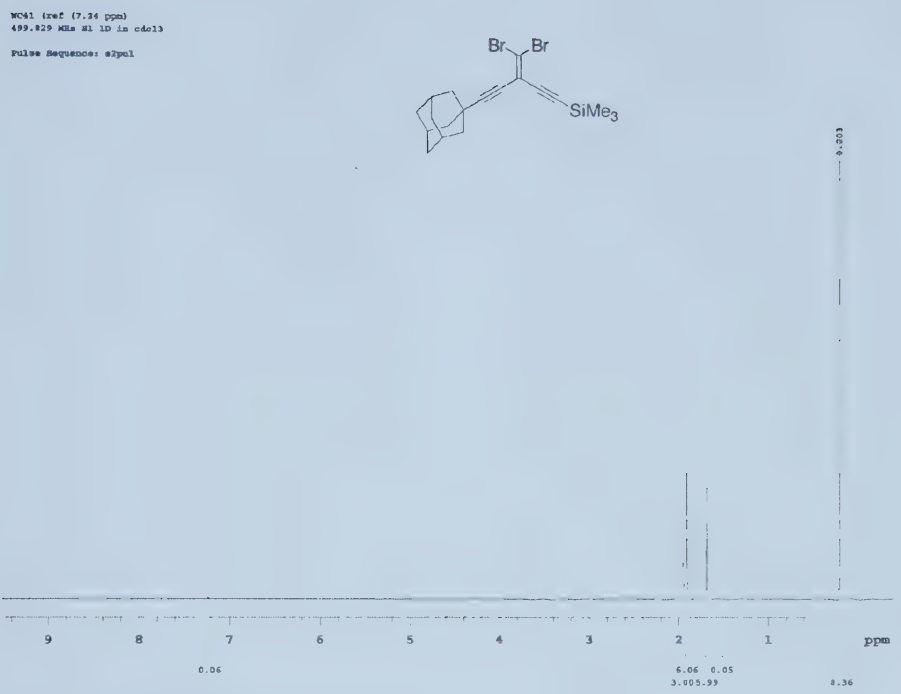


**Figure C-35.** $^{1}$H NMR spectrum of **3.21**.

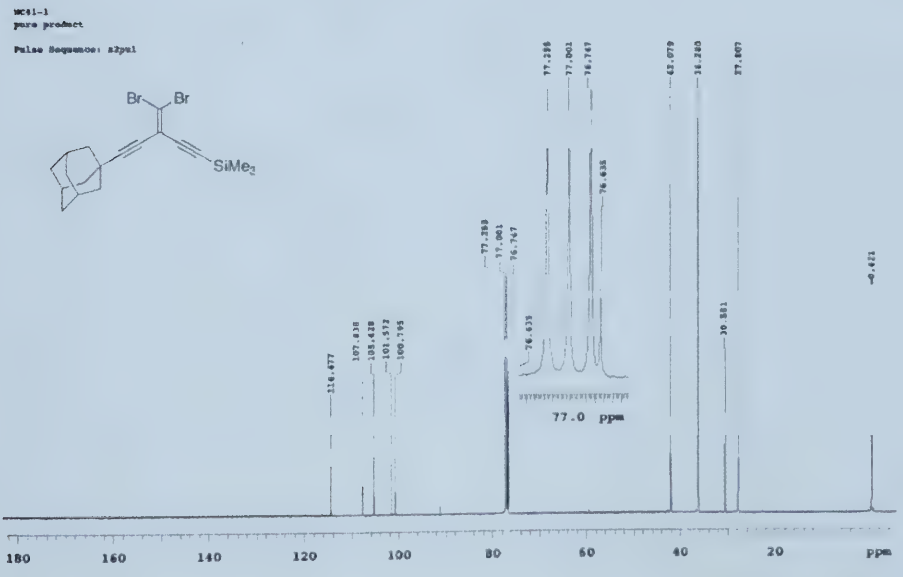


**Figure C-36.** $^{13}$C NMR spectrum of **3.21**.

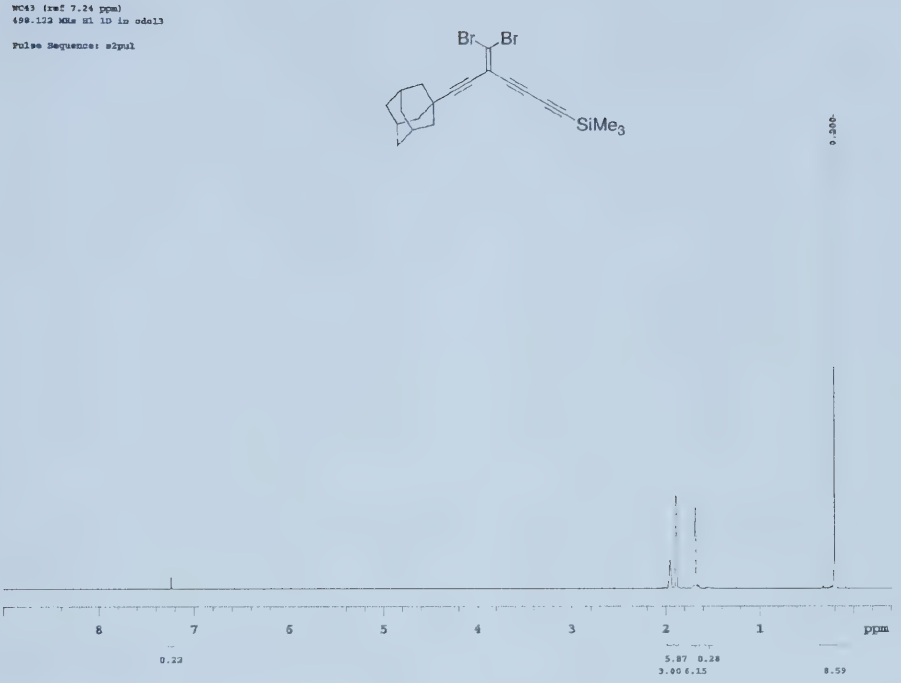


**Figure C-37.** $^{1}$H NMR spectrum of **3.22**.

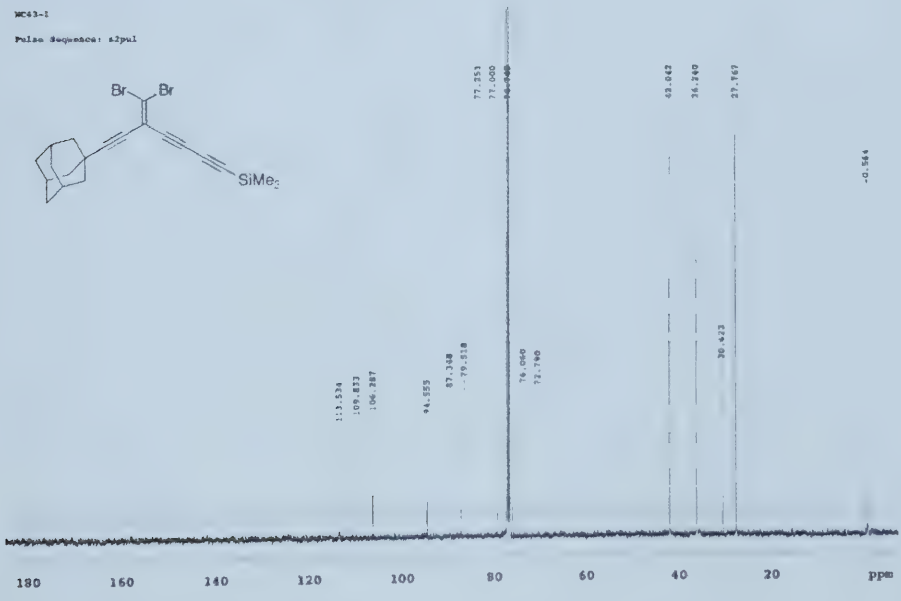


**Figure C-38.** $^{13}$C NMR spectrum of **3.22**.

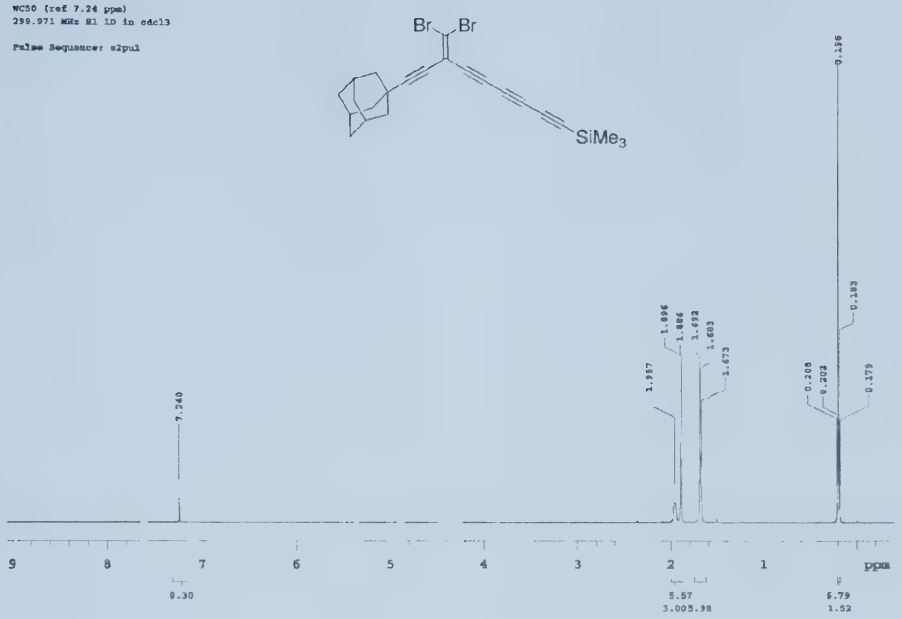


**Figure C-39.** $^{1}$H NMR spectrum of **3.23**.

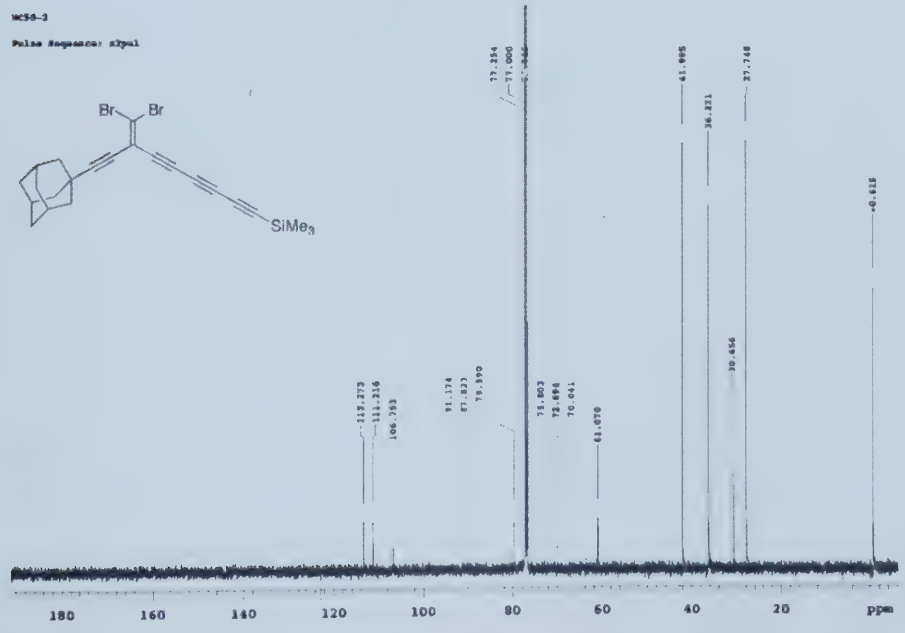


**Figure C-40.** $^{13}$C NMR spectrum of **3.23**.

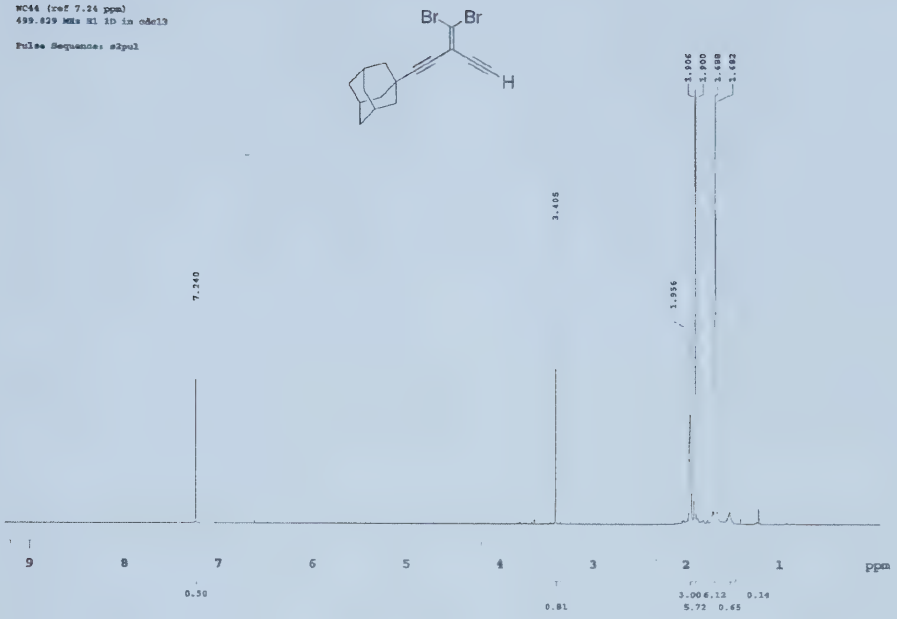


**Figure C-41.** $^{1}$H NMR spectrum of **3.24**.

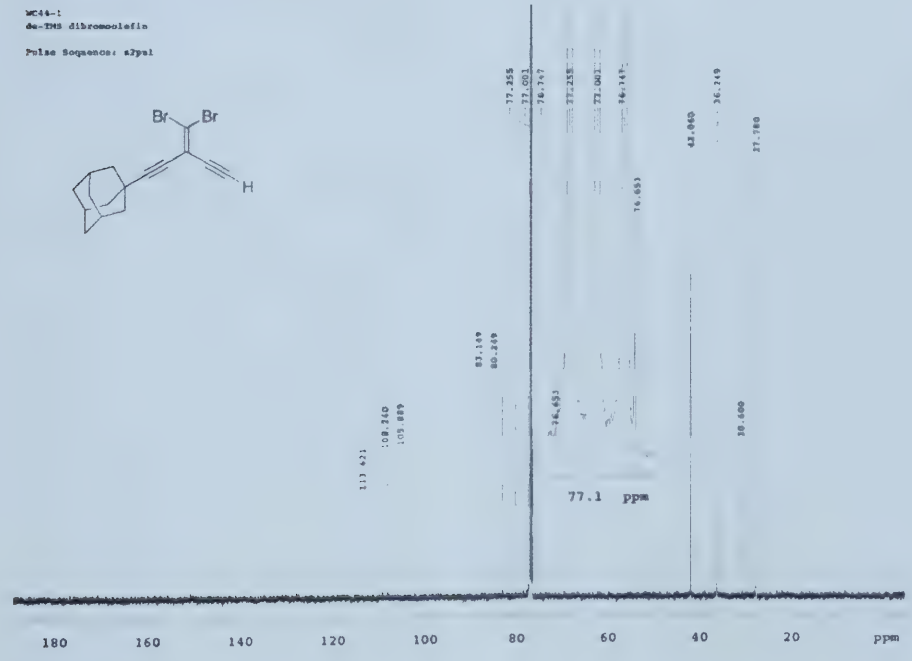


**Figure C-42.** $^{13}$C NMR spectrum of **3.24**.

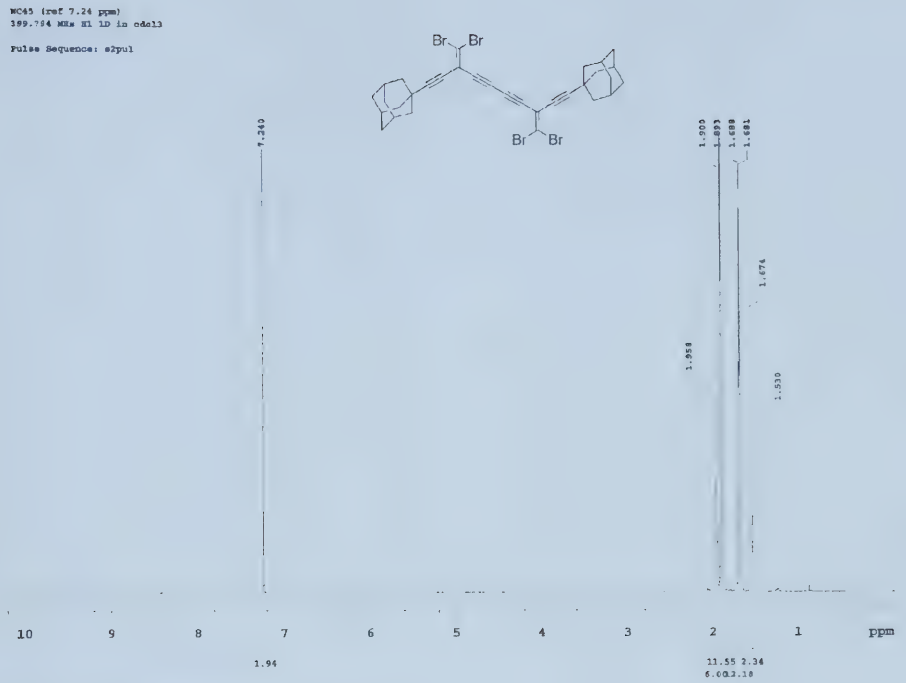


**Figure C-43.** $^{1}$H NMR spectrum of **3.27**.

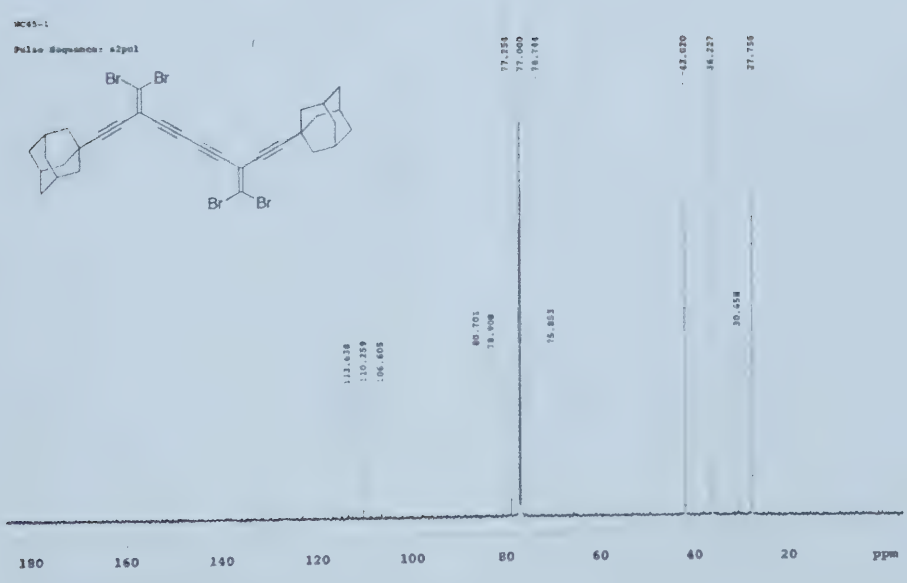


**Figure C-44.** $^{13}$C NMR spectrum of **3.27**.

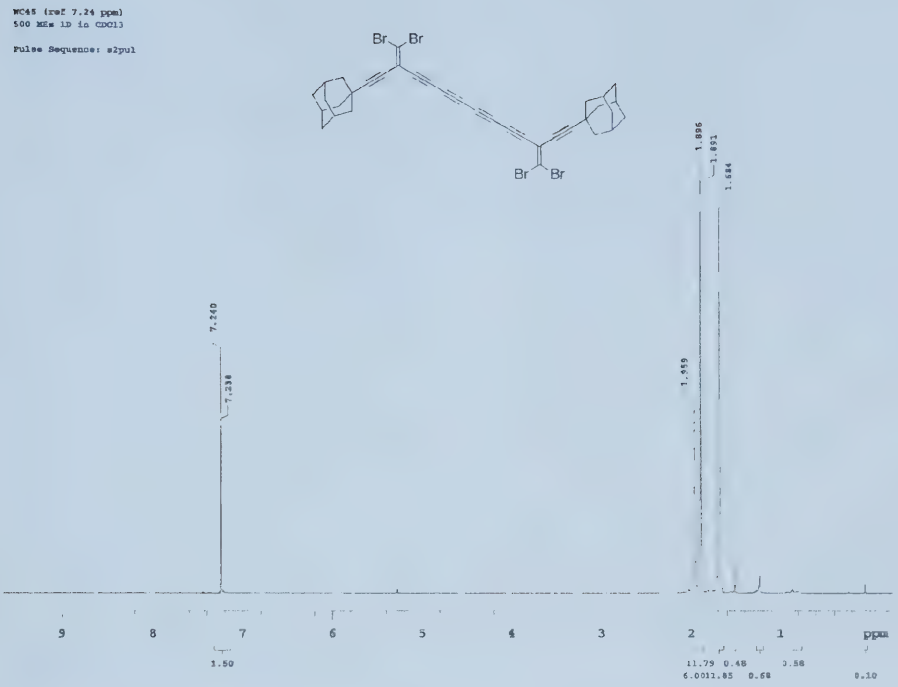


**Figure C-45.** $^{1}$H NMR spectrum of **3.28**.

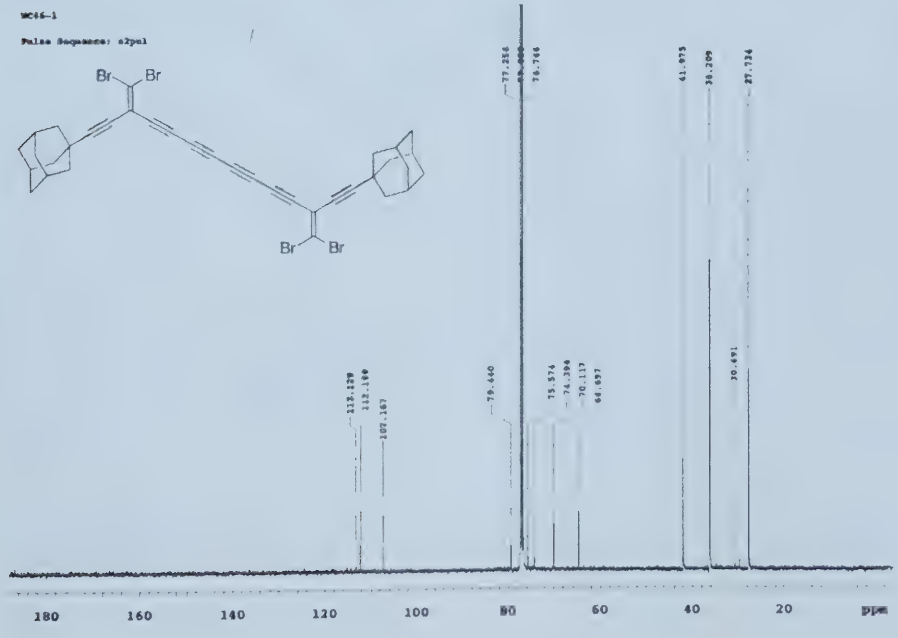


**Figure C-46.** $^{13}$C NMR spectrum of **3.28**.

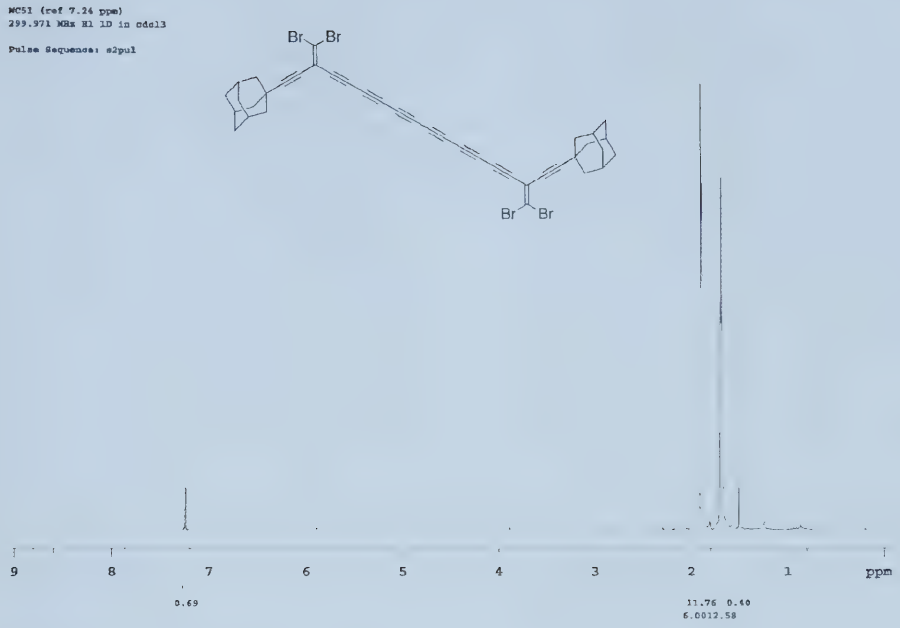


**Figure C-47.** $^{1}$H NMR spectrum of **3.29**.

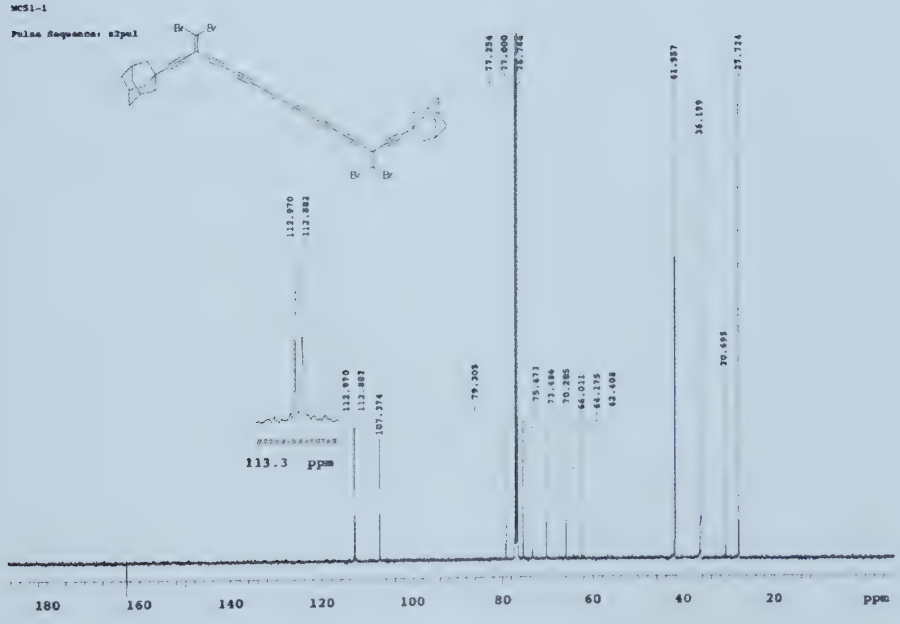


**Figure C-48.** $^{13}$C NMR spectrum of **3.29**.

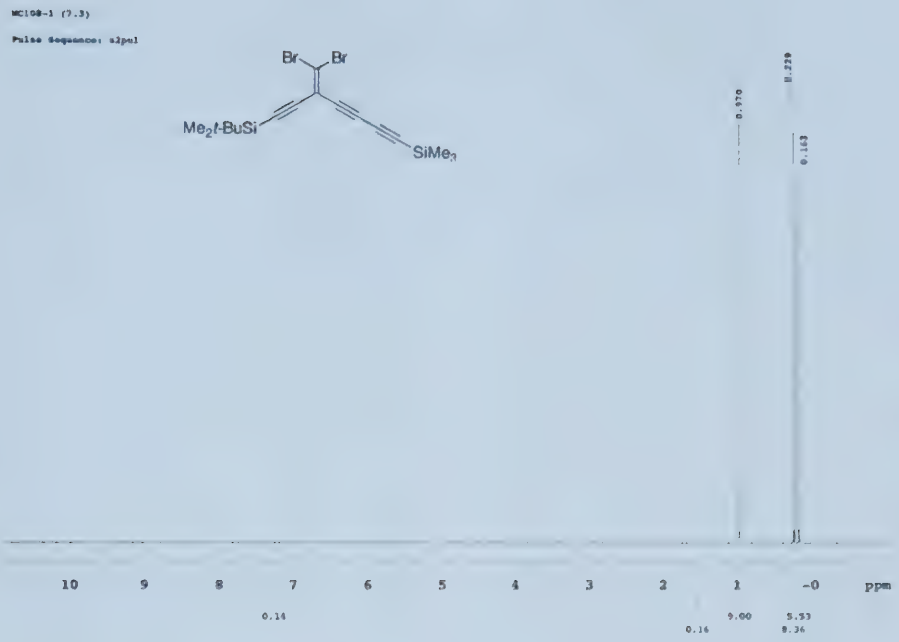


**Figure C-49.** $^{1}$H NMR spectrum of **7.3**.

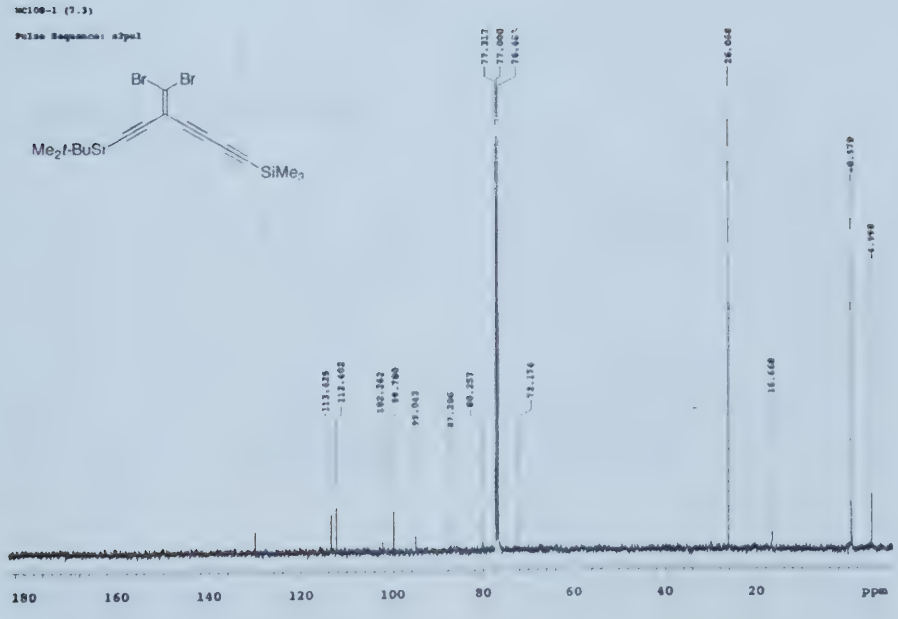


**Figure C-50.** $^{13}$C NMR spectrum of **7.3**.

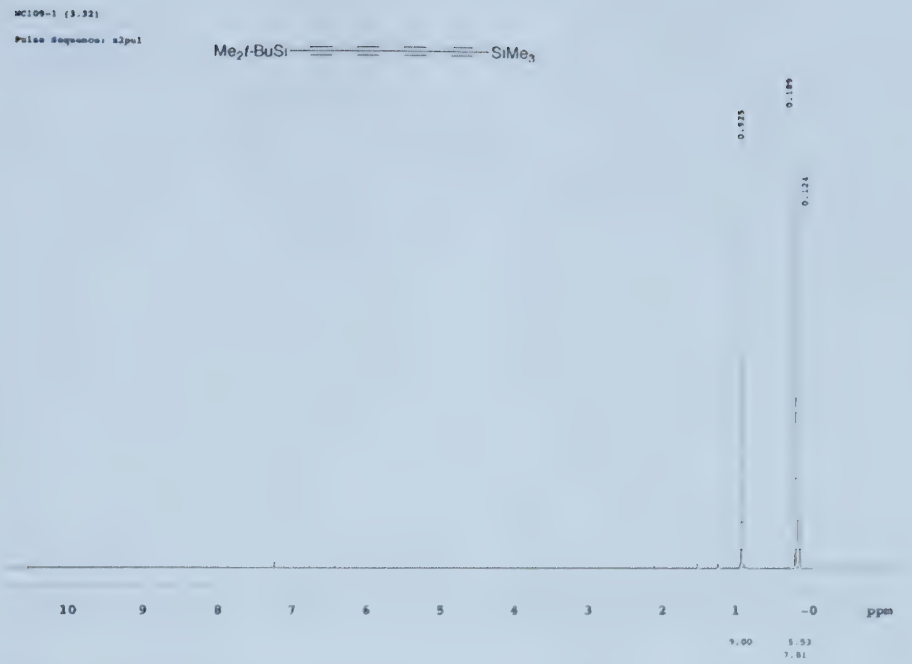


**Figure C-51.** $^{1}$H NMR spectrum of **3.32**.

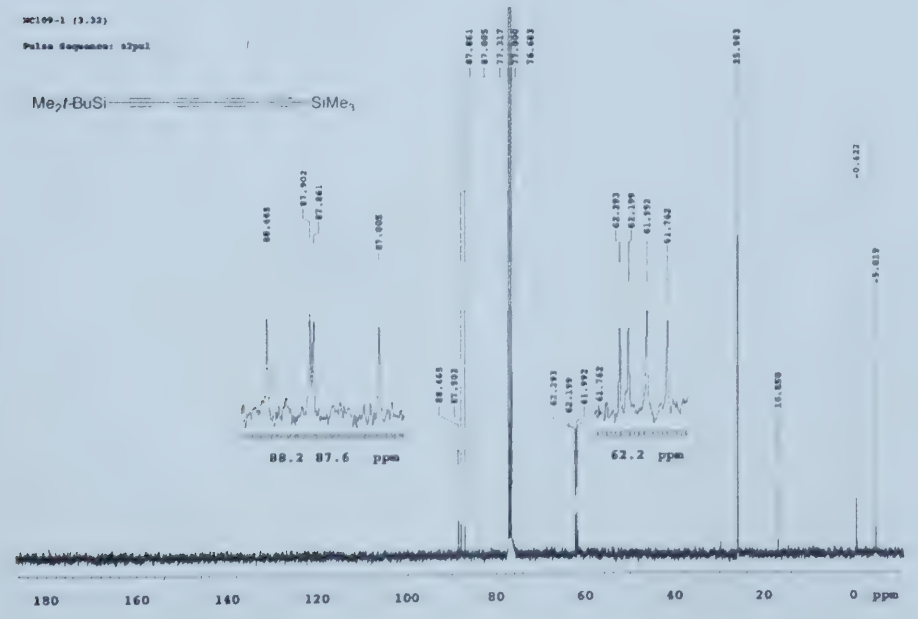


**Figure C-52.** $^{13}$C NMR spectrum of **3.32**.

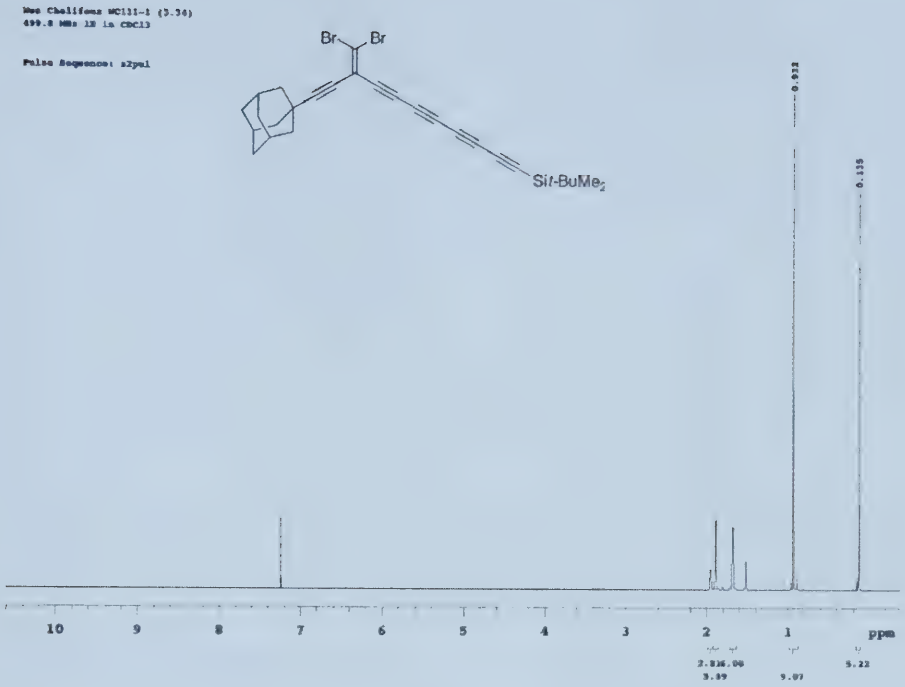


**Figure C-53.** $^{1}$H NMR spectrum of **3.34**.

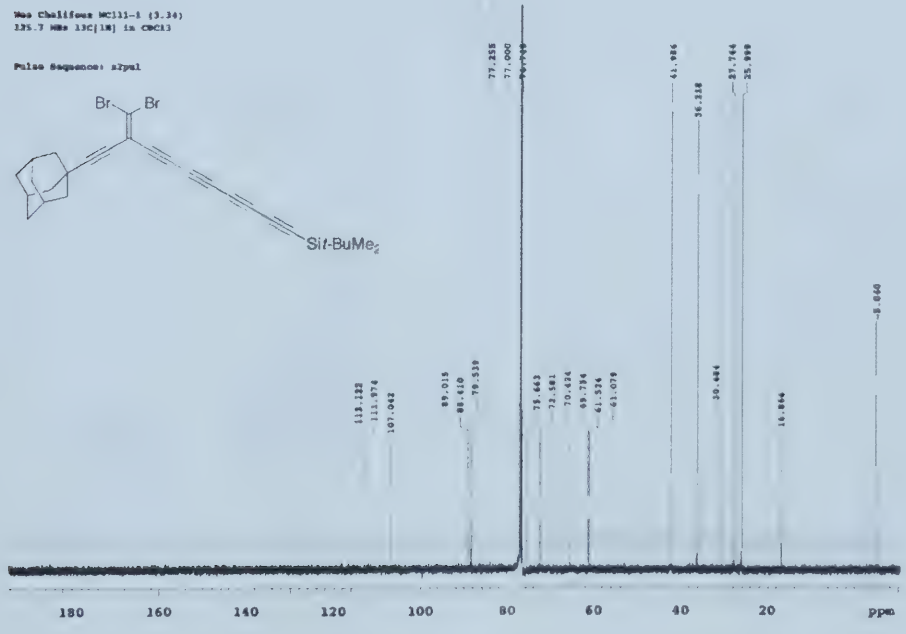


**Figure C-54.** $^{13}$C NMR spectrum of **3.34**.

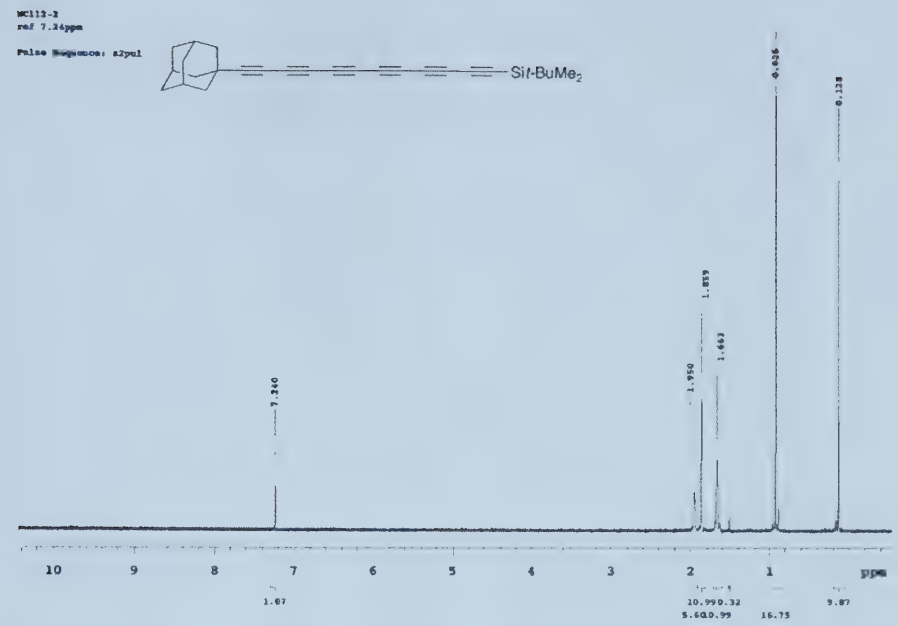


**Figure C-55.** $^{1}$H NMR spectrum of **3.35**.

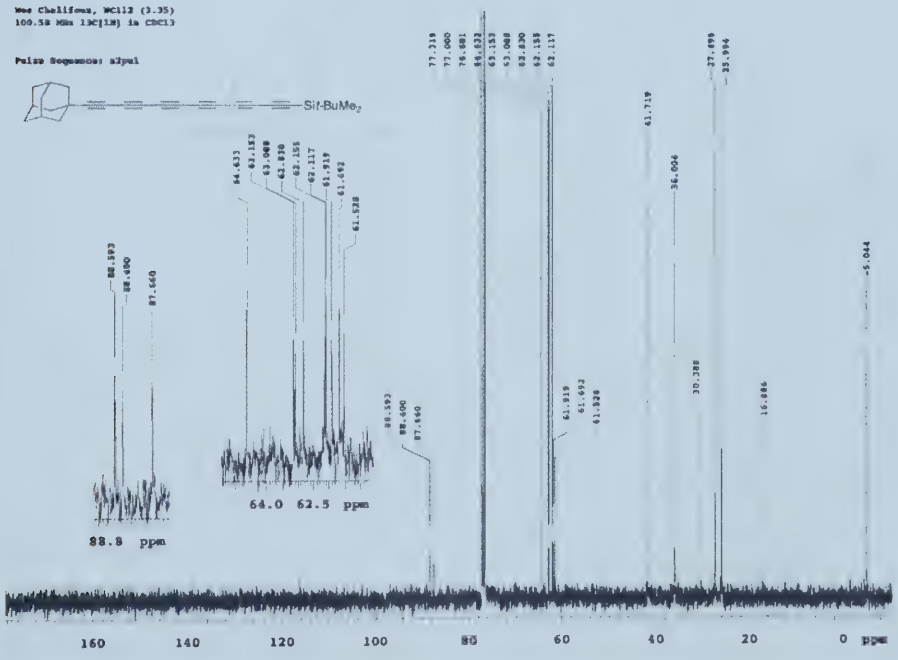


**Figure C-56.** $^{13}$C NMR spectrum of **3.35**.

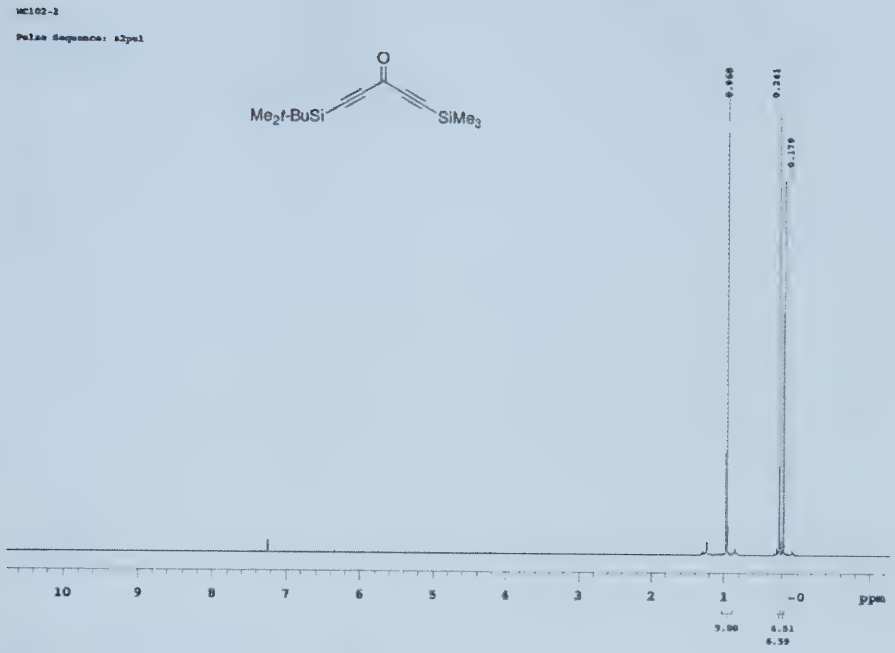


**Figure C-57.** $^{1}$H NMR spectrum of **7.4**.

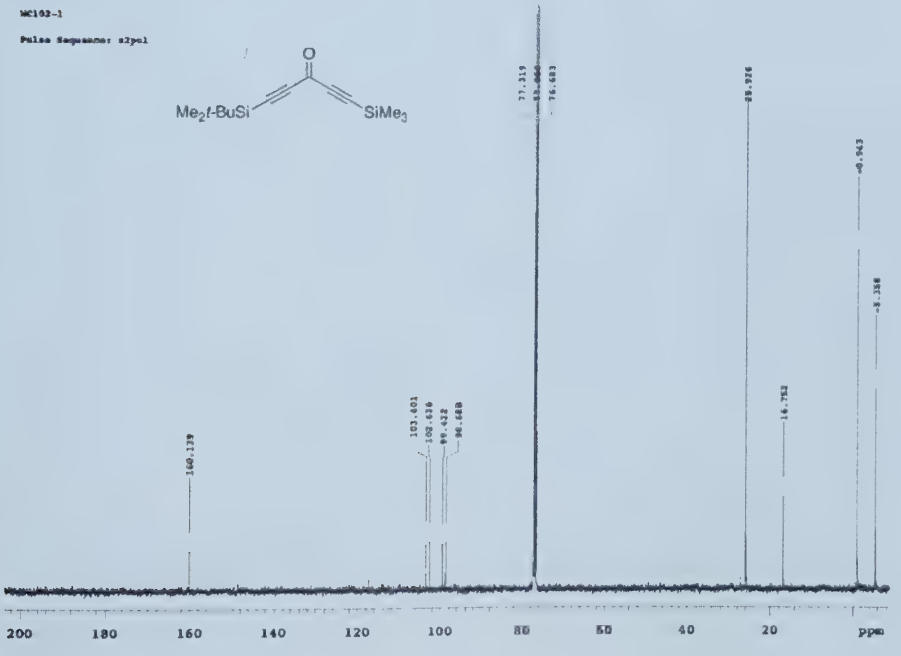


**Figure C-58.** $^{13}$C NMR spectrum of **7.4**.

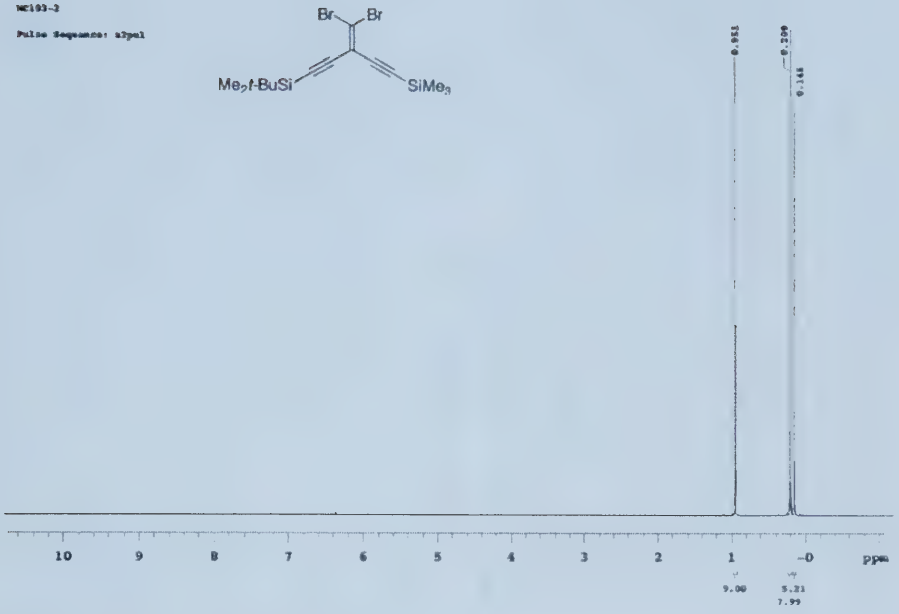


**Figure C-59.** $^{1}$H NMR spectrum of **7.5**.

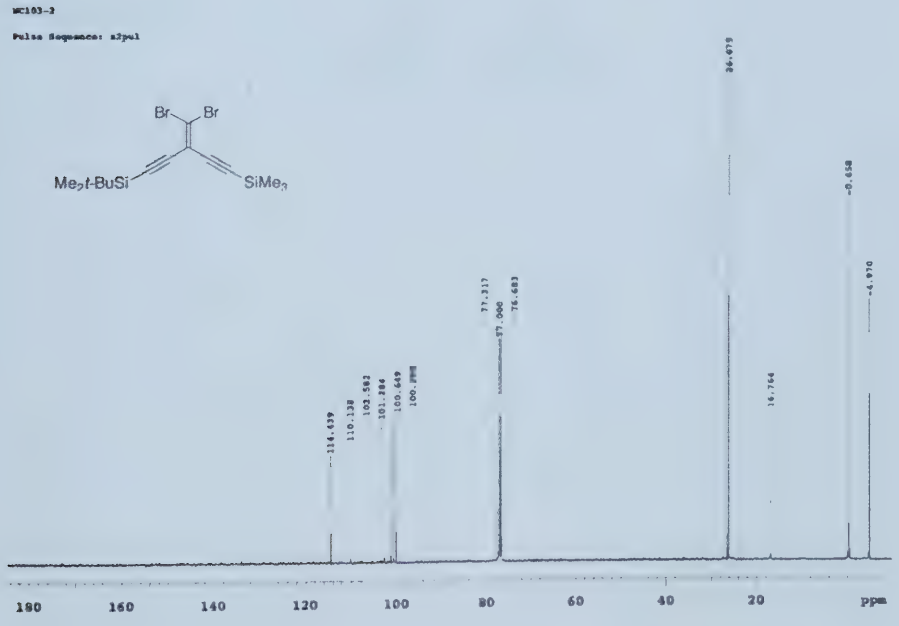


**Figure C-60.** $^{13}$C NMR spectrum of **7.5**.

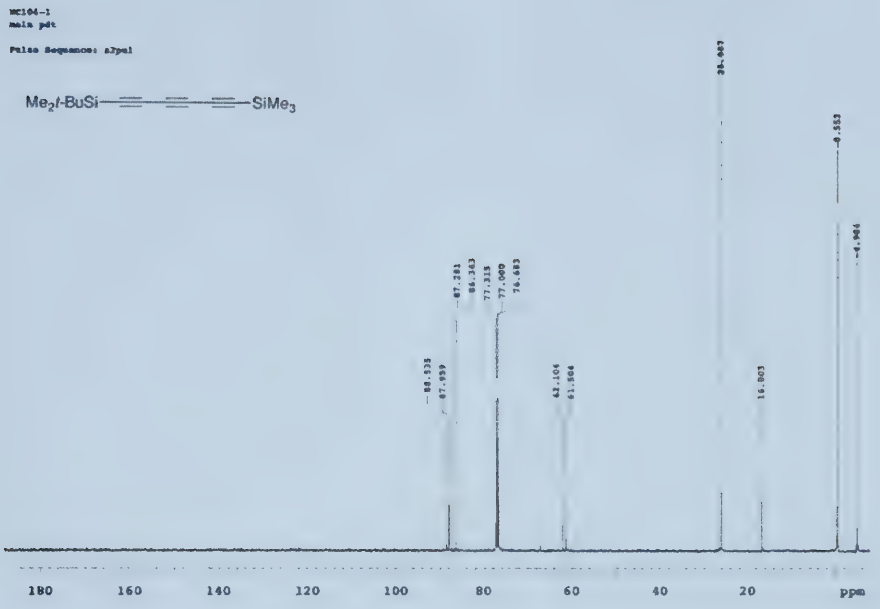


**Figure C-61.** $^{13}C$ NMR spectrum of **3.36**.

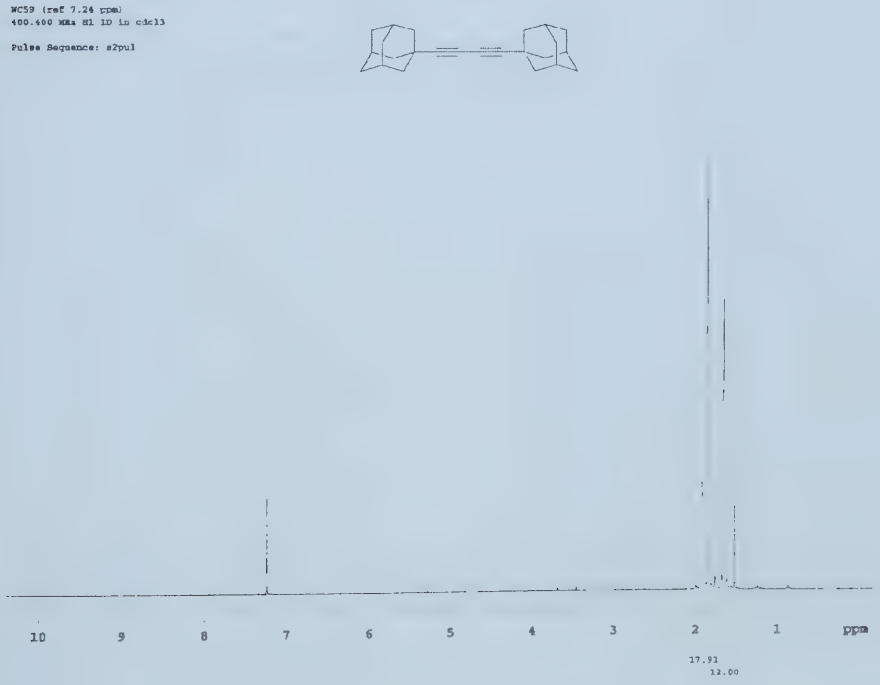


**Figure C-62.** $^{1}H$ NMR spectrum o **3.1a**.

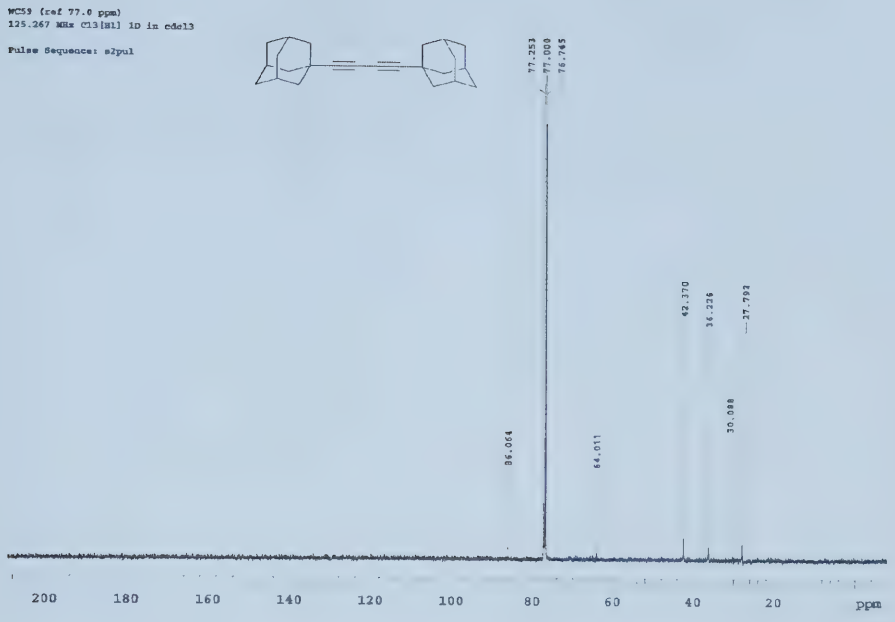


**Figure C-63.** $^{13}$C NMR spectrum of **3.1a**.

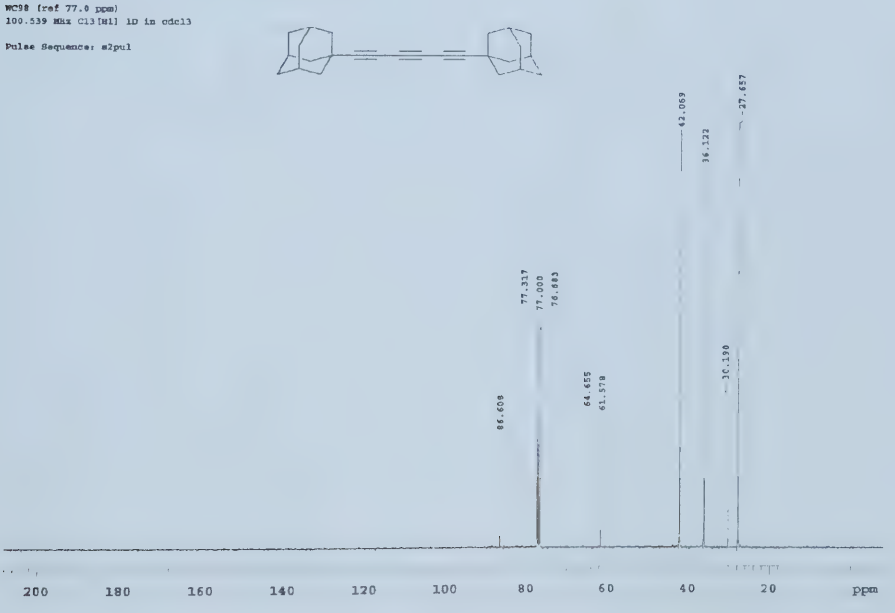


**Figure C-64.** $^{13}$C NMR spectrum of **3.1b**.

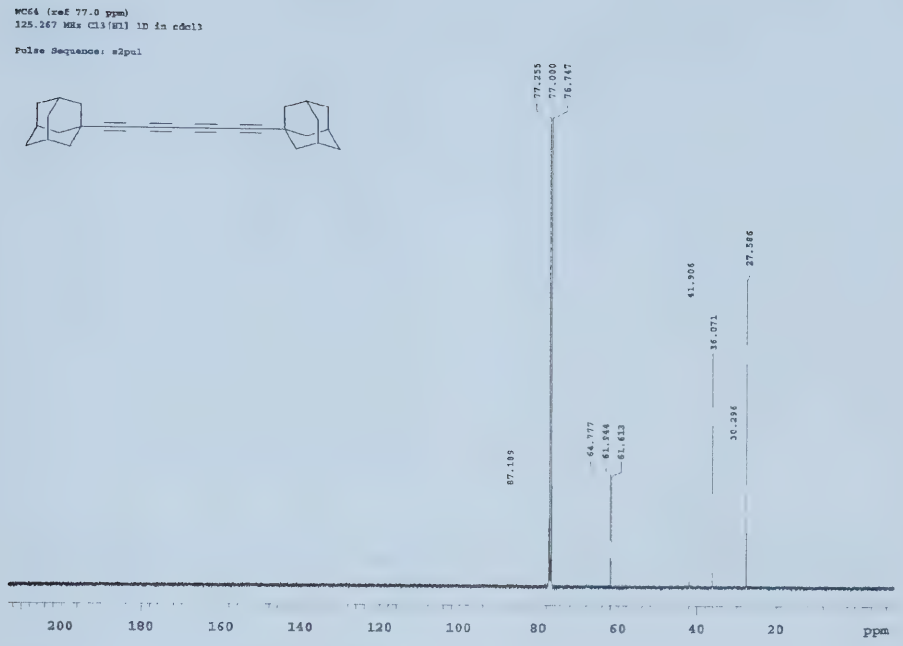


**Figure C-65.** $^{13}C$ NMR spectrum of **3.1c**.

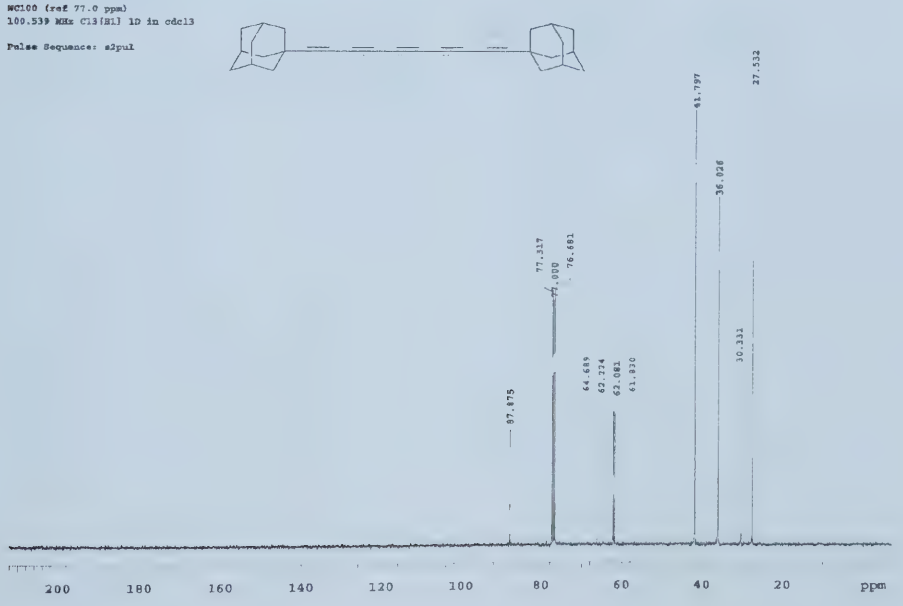


**Figure C-66.** $^{13}C$ NMR spectrum of **3.1d**.

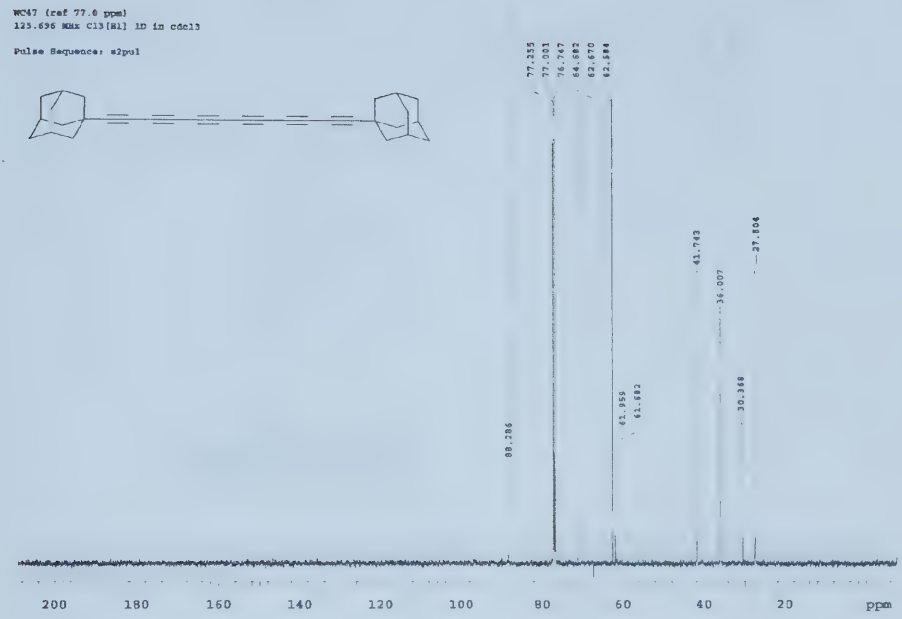


**Figure C-67.** $^{13}C$ NMR spectrum of **3.1e**.

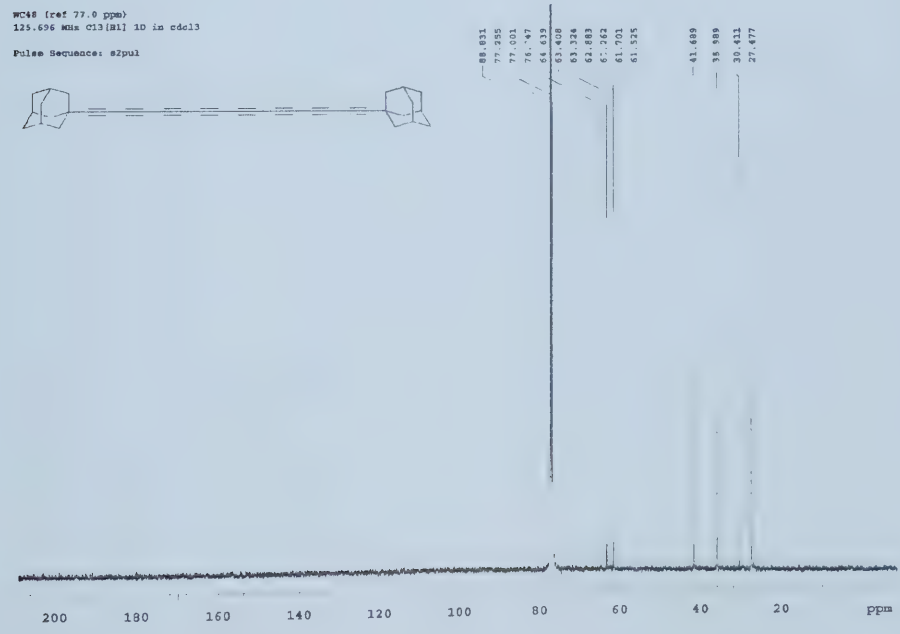


**Figure C-68.** $^{13}C$ NMR spectrum of **3.1f**.

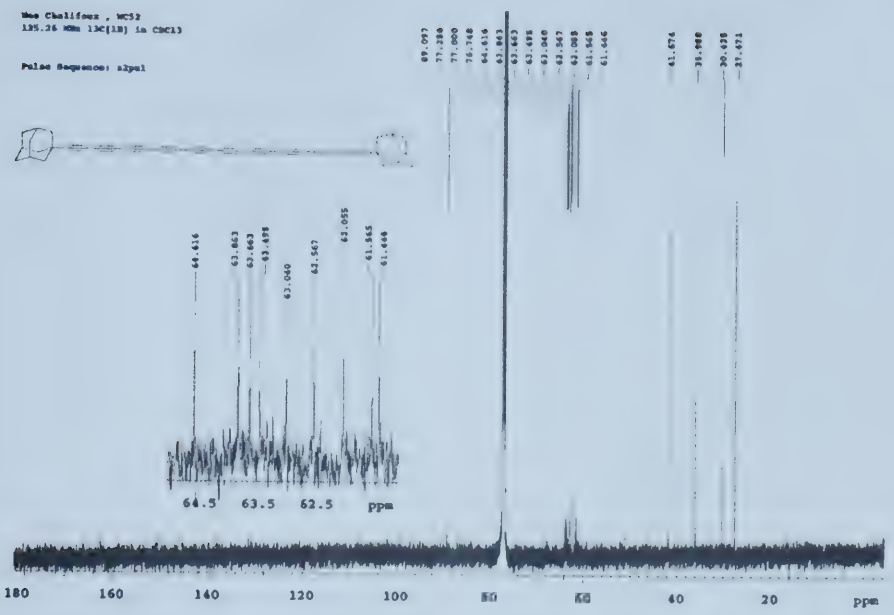


**Figure C-69**. $^{13}C$ NMR spectrum of **3.1h**.

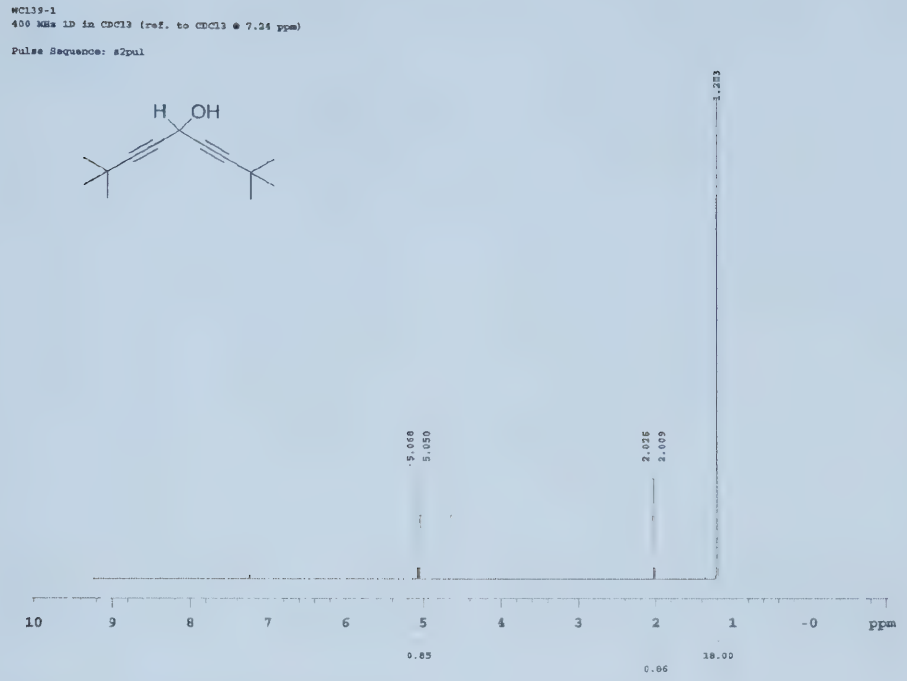


**Figure C-70.** $^{1}$H NMR spectrum of **4.2**.

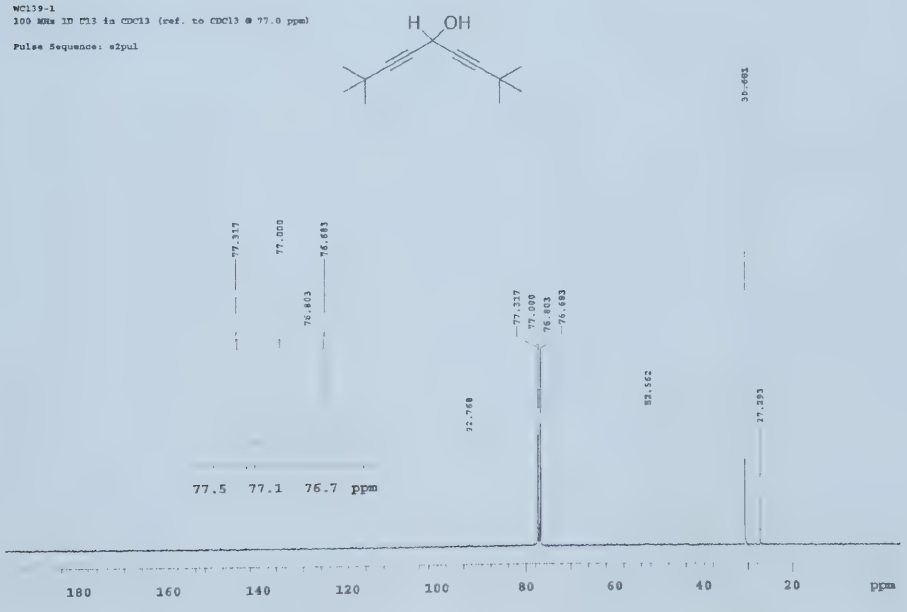


**Figure C-71.** $^{13}$C NMR spectrum of **4.2**.

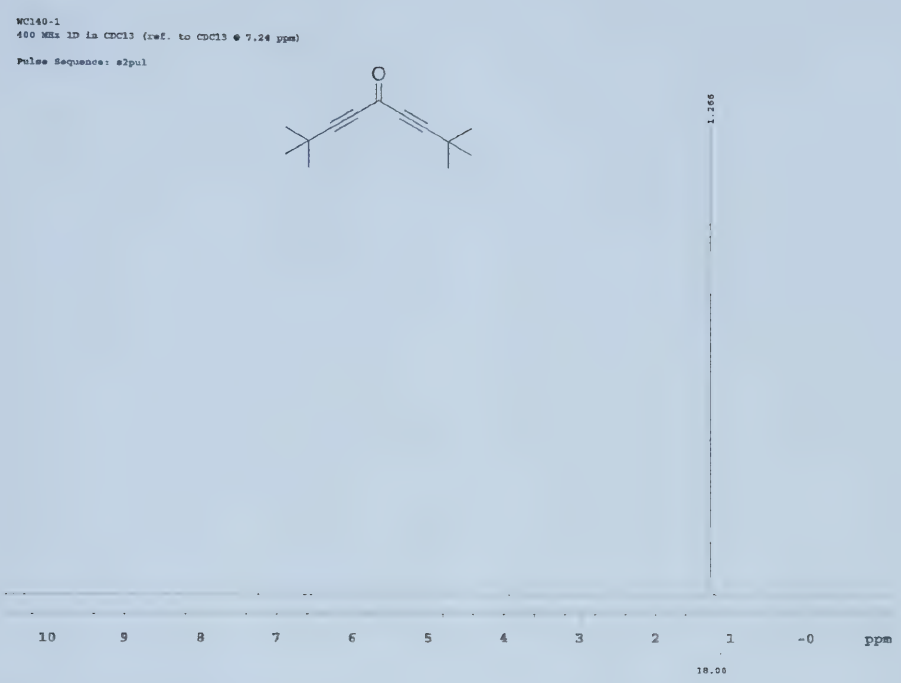


**Figure C-72.** $^{1}$H NMR spectrum of **4.3**.

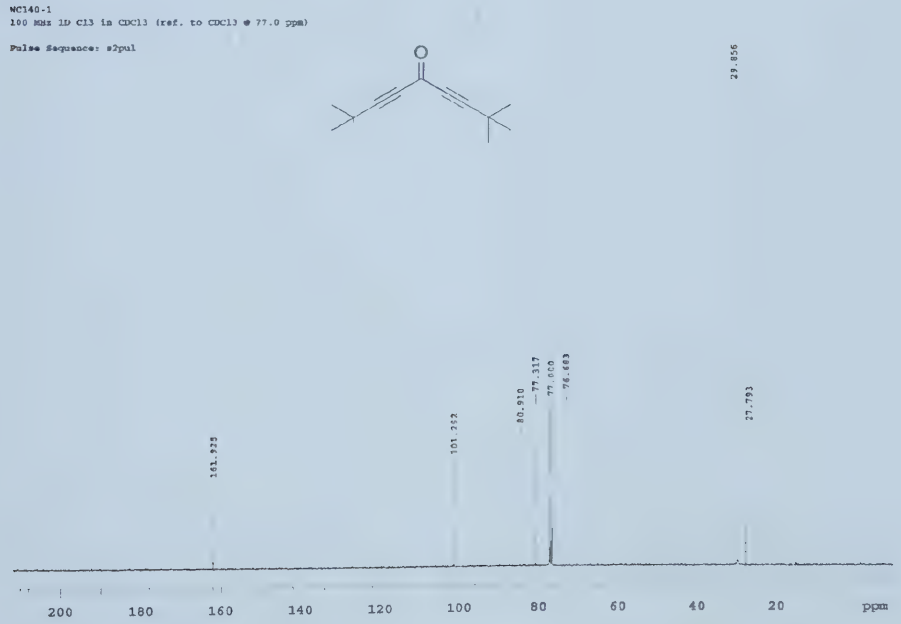


**Figure C-73.** $^{13}$C NMR spectrum for **4.3**.

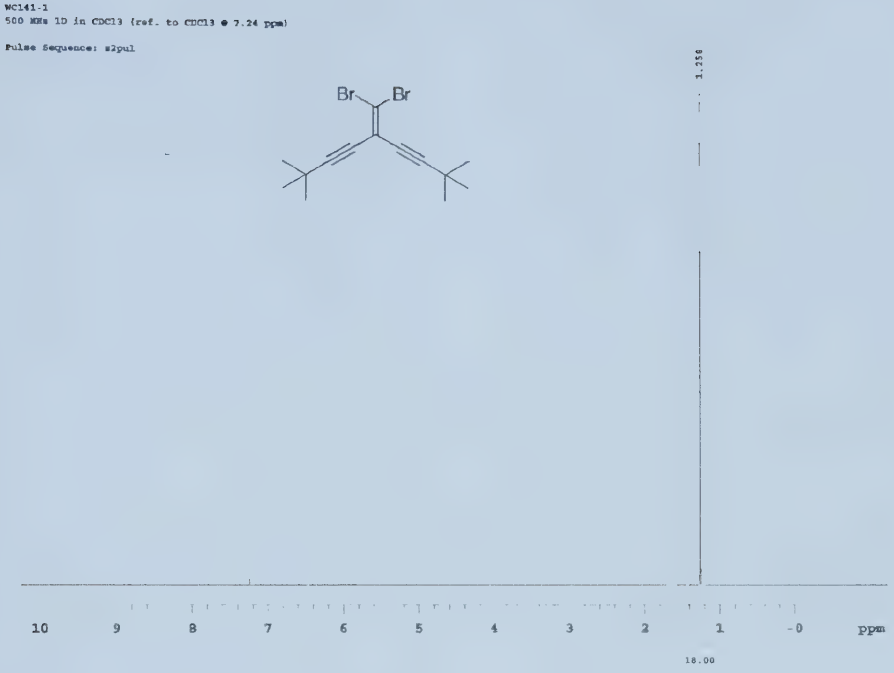


**Figure C-74.** $^{1}$H NMR spectrum of **4.4**.

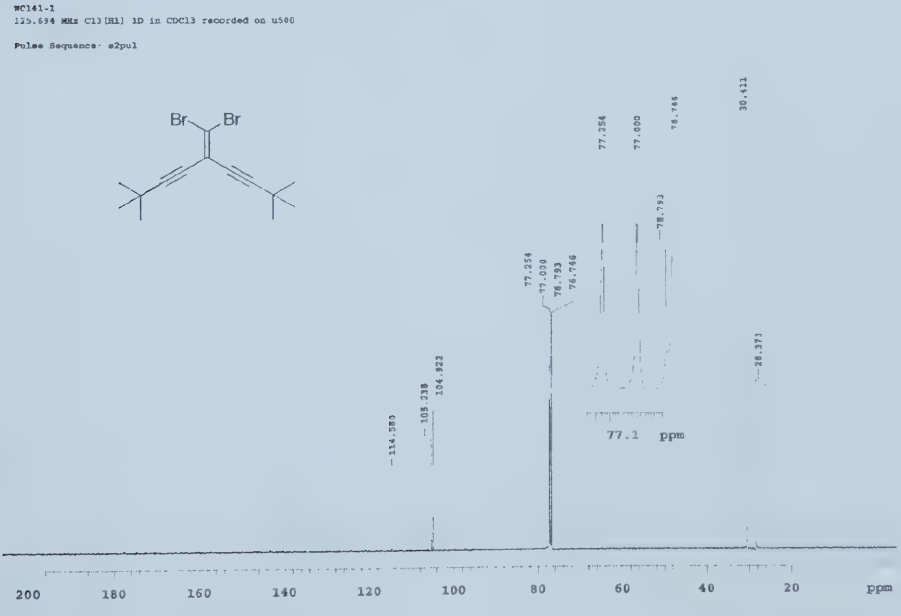


**Figure C-75.** $^{13}$C NMR spectrum of **4.4**.

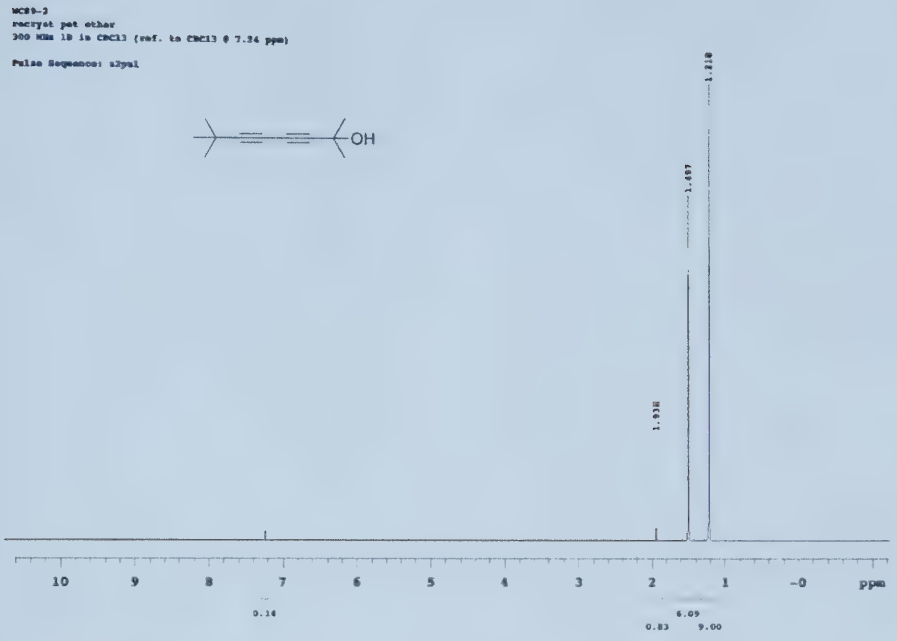


**Figure C-76.** $^{1}$H NMR spectrum of **4.5**.

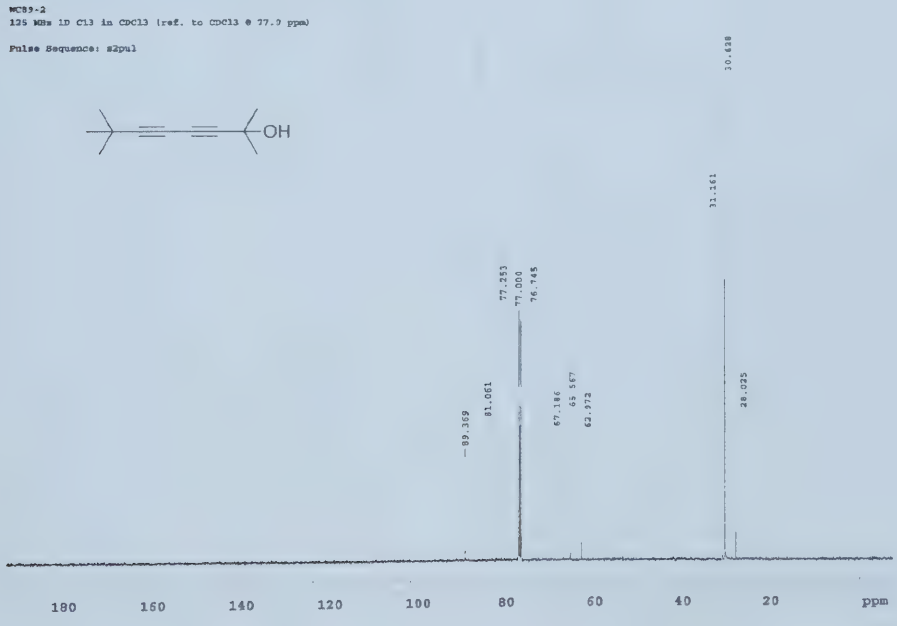


**Figure C-77.** $^{13}$C NMR spectrum of **4.5**.

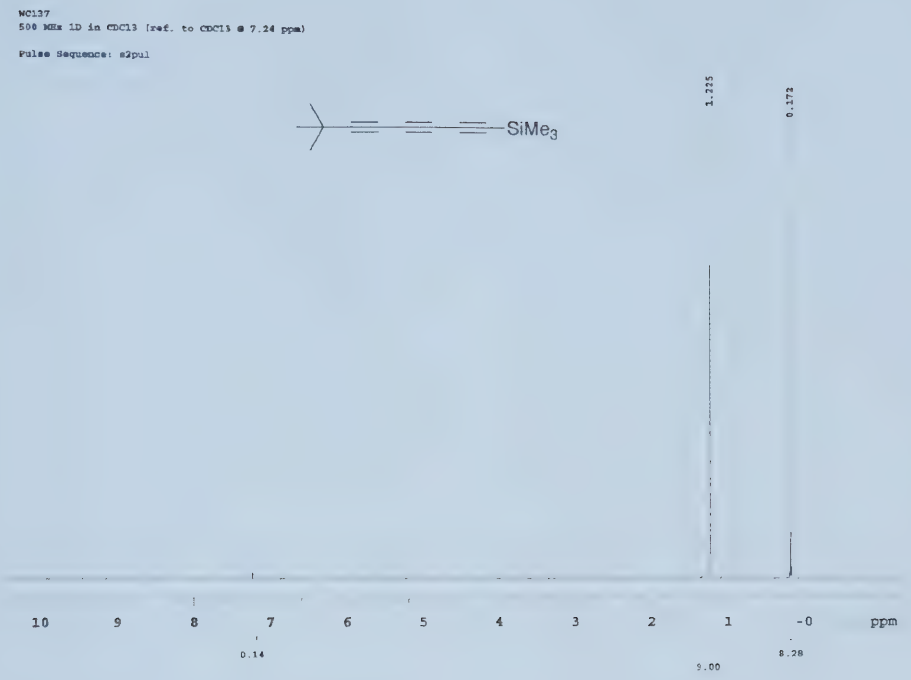


**Figure C-78.** $^{1}$H NMR spectrum of **4.6**.

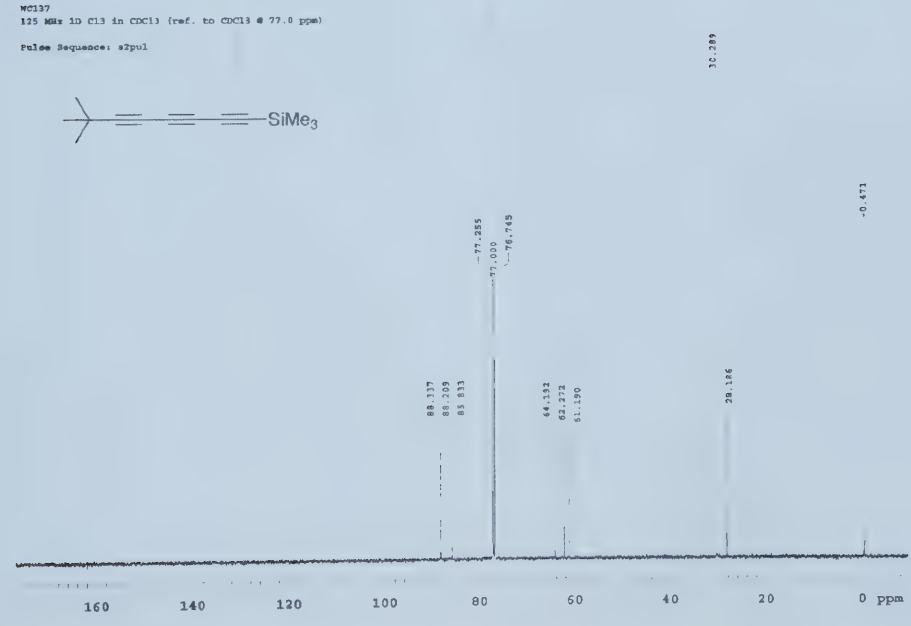


**Figure C-79.** $^{13}$C NMR spectrum of **4.6**.

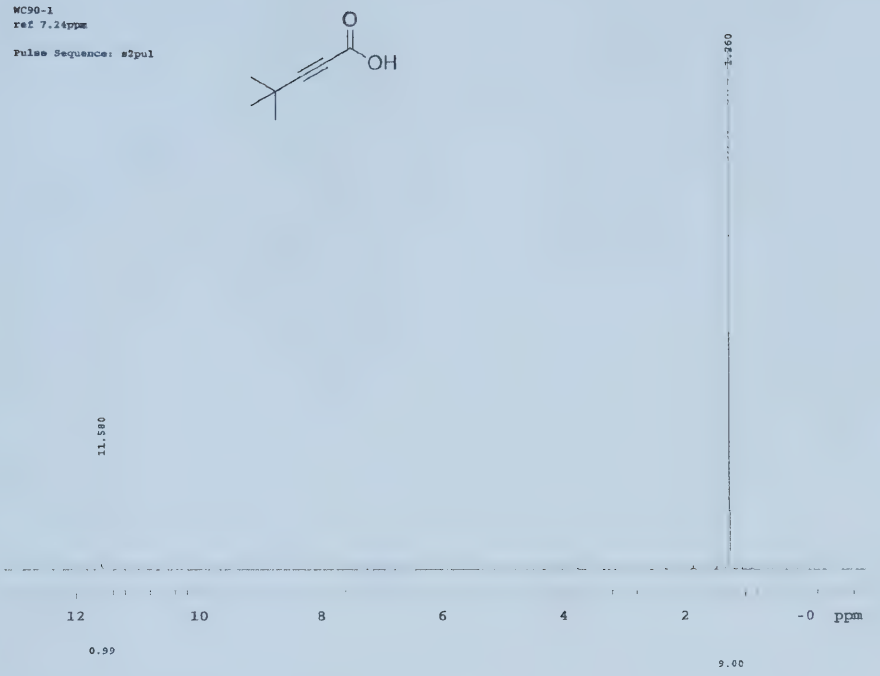


**Figure C-80.** $^{1}$H NMR spectrum of **4.7**.

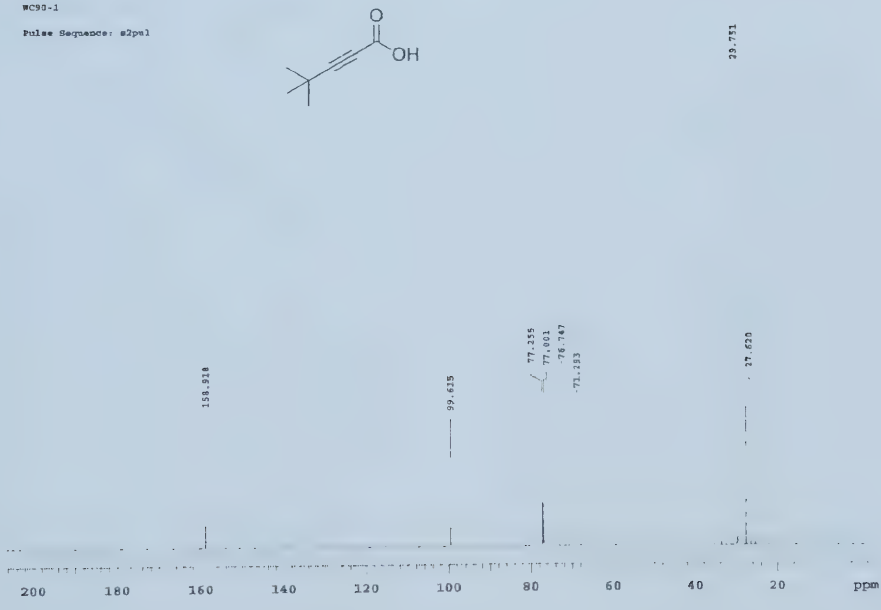


**Figure C-81.** $^{13}$C NMR spectrum of **4.7**.

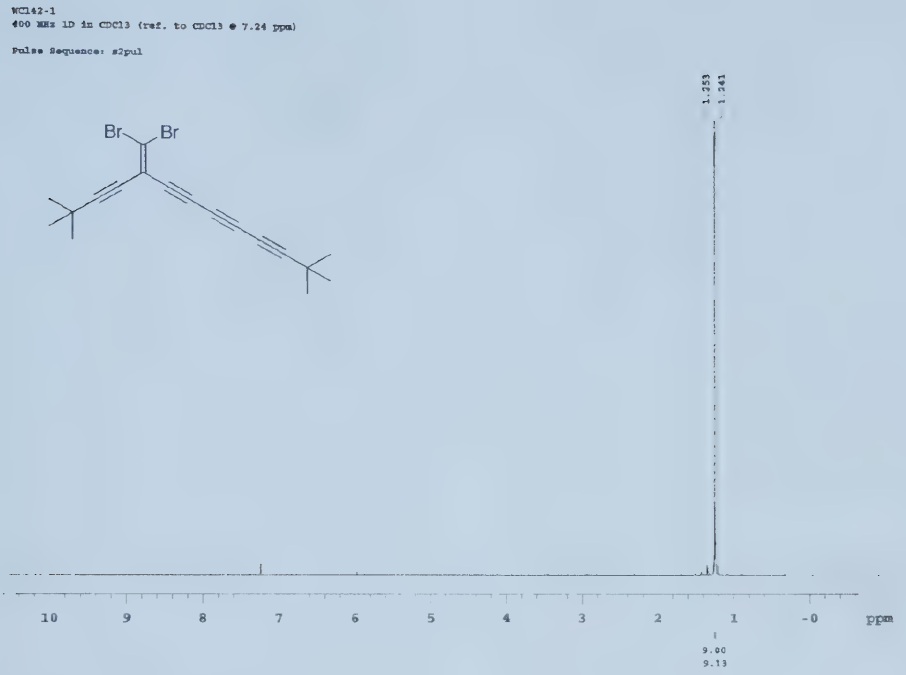


**Figure C-82.** $^{1}$H NMR spectrum of **4.9**.

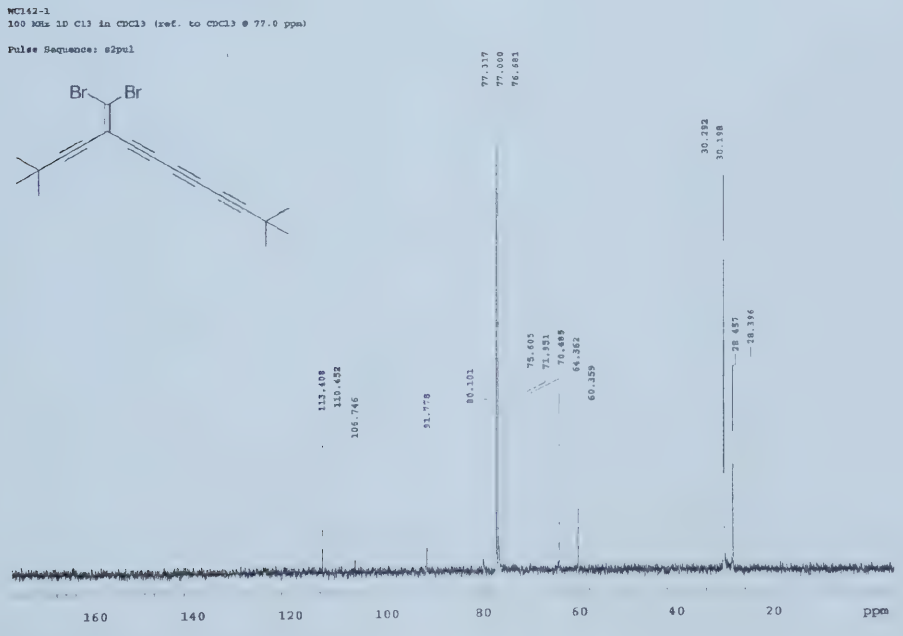


**Figure C-83.** $^{13}$C NMR spectrum of **4.9**.

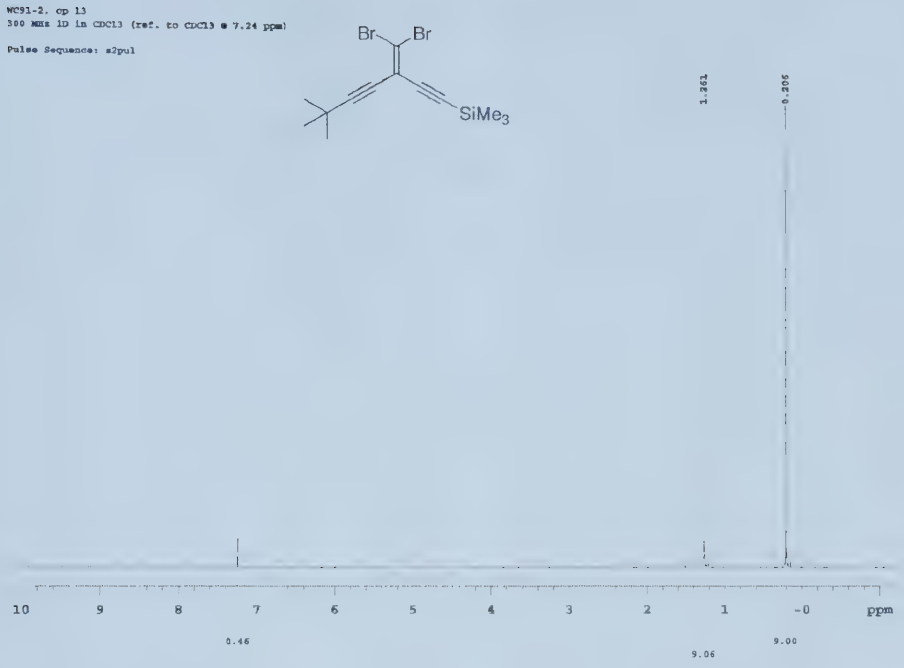


**Figure C-84.** $^{1}$H NMR spectrum of **4.13**.

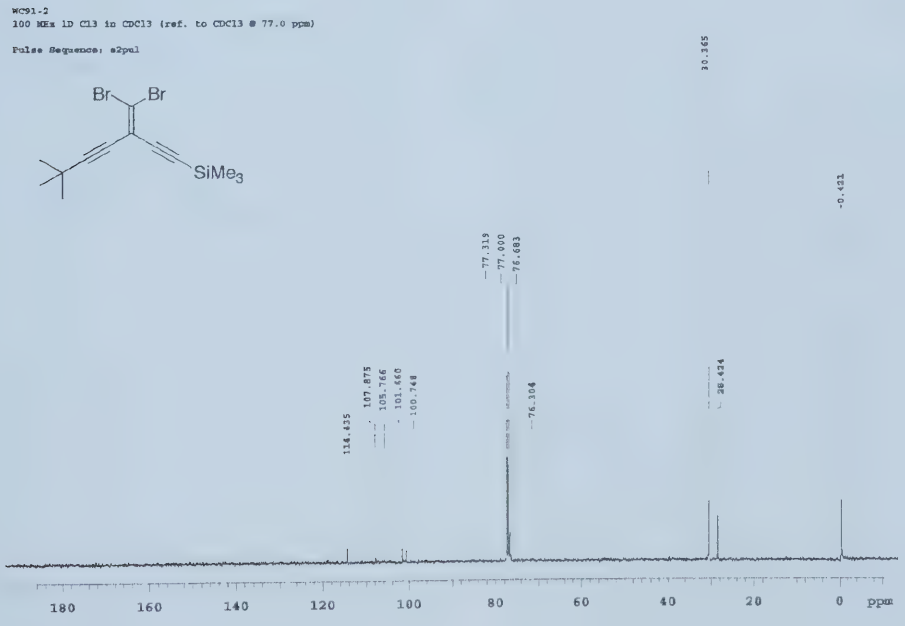


**Figure C-85.** $^{13}$C NMR spectrum of **4.13**.

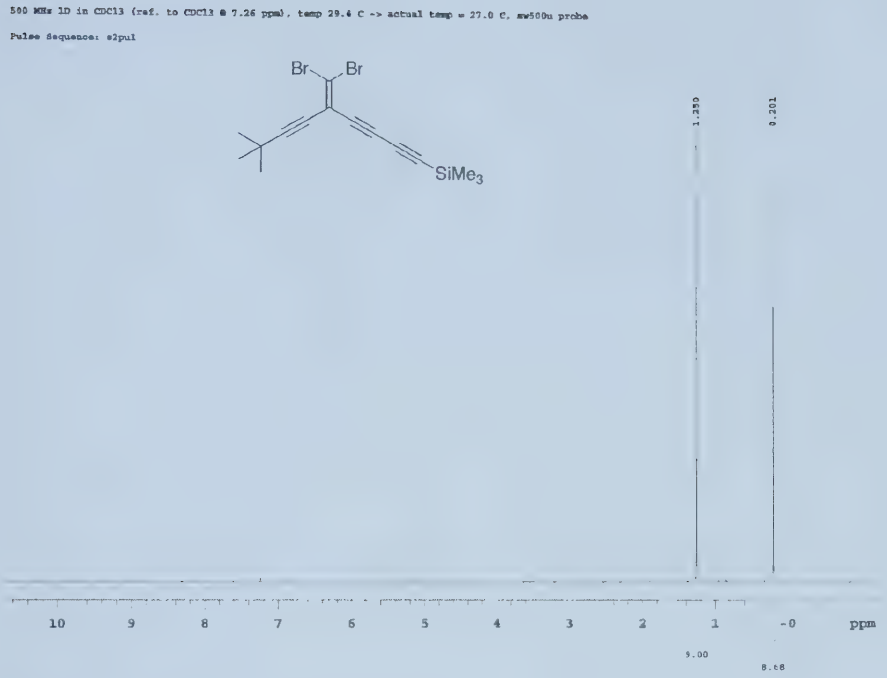


**Figure C-86.** $^{1}$H NMR spectrum of **4.14**.

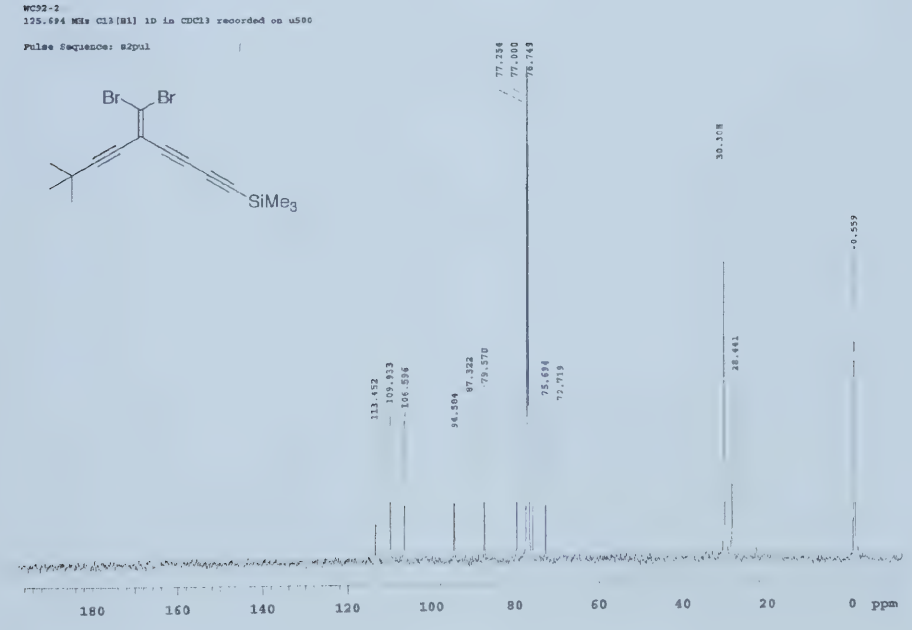


**Figure C-87.** $^{13}$C NMR spectrum of **4.14**.

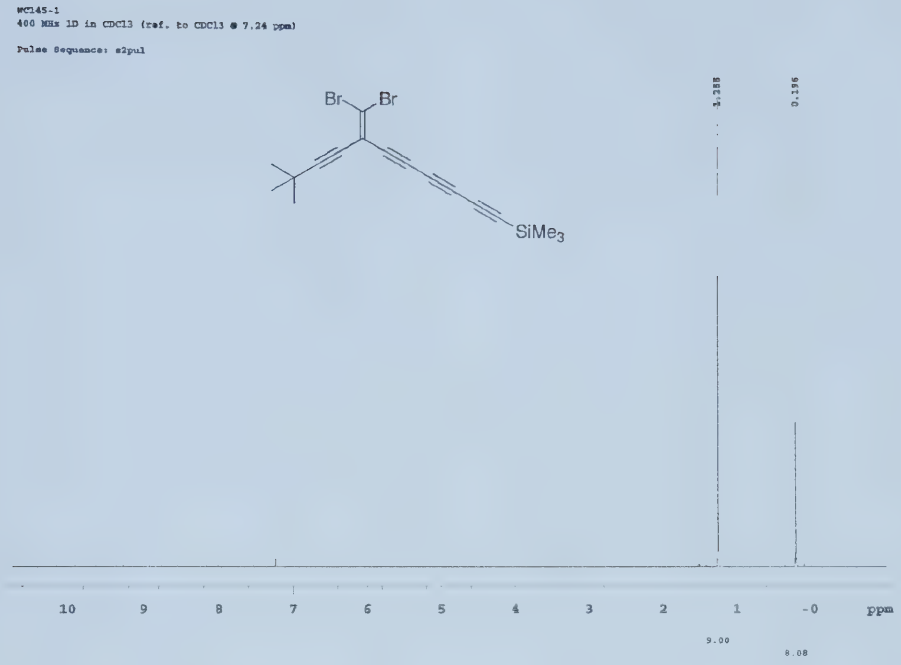


**Figure C-88.** $^{1}$H NMR spectrum of **4.15**.

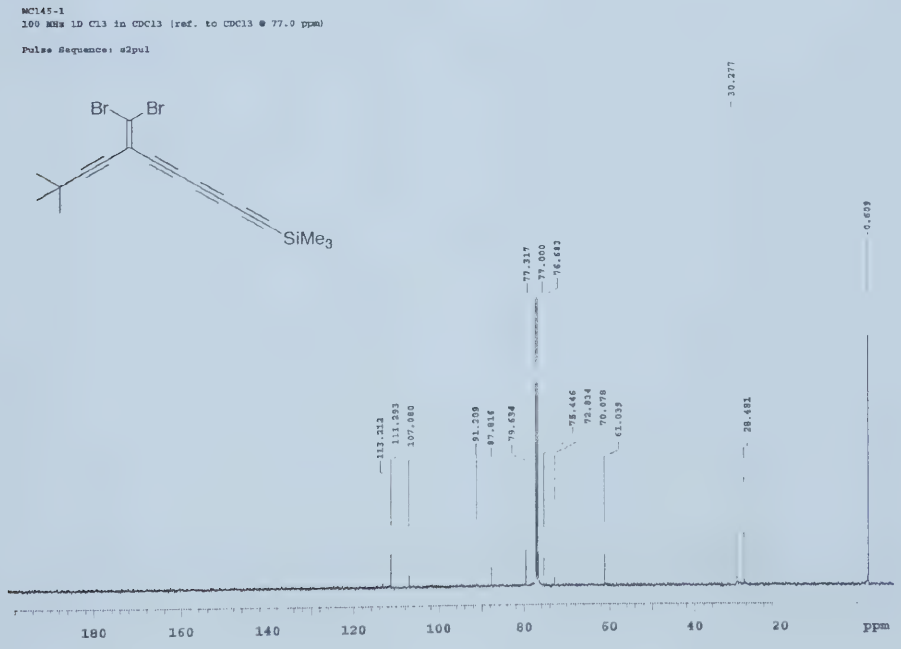


**Figure C-89.** $^{13}$C NMR spectrum of **4.15**.

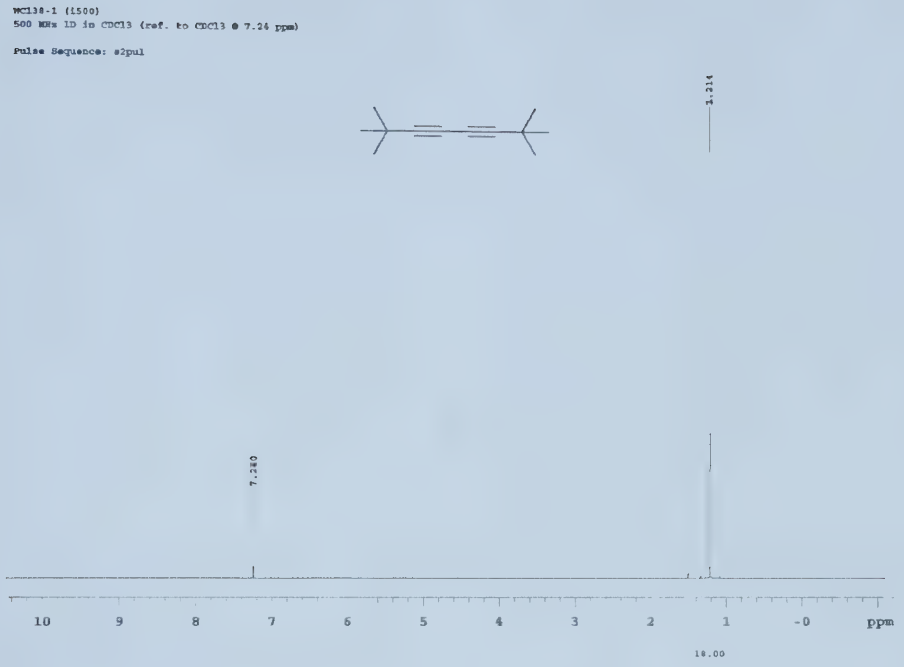


**Figure C-90.** $^{1}$H NMR spectrum of **4.1a**.

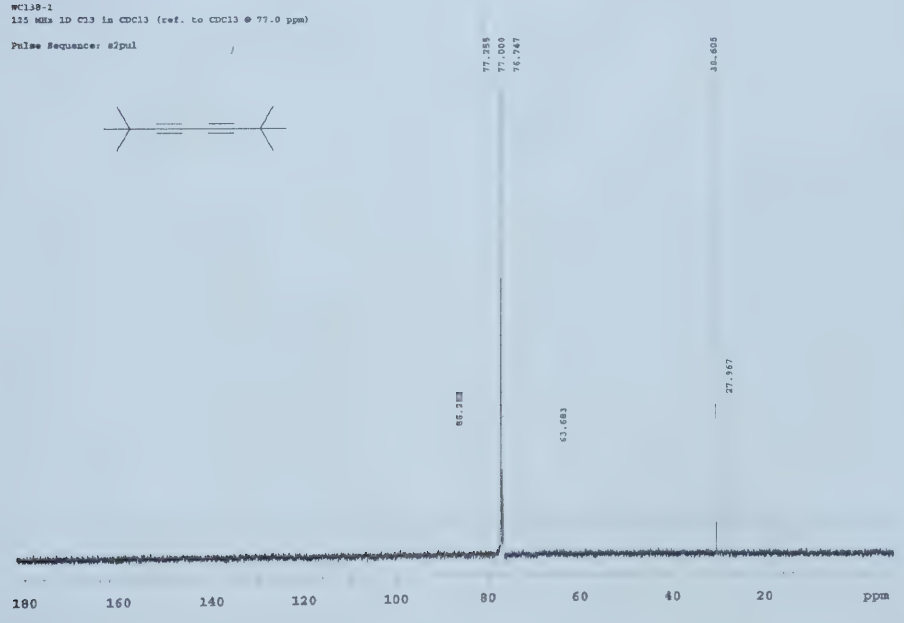


**Figure C-91.** $^{13}$C NMR spectrum of **4.1a**.

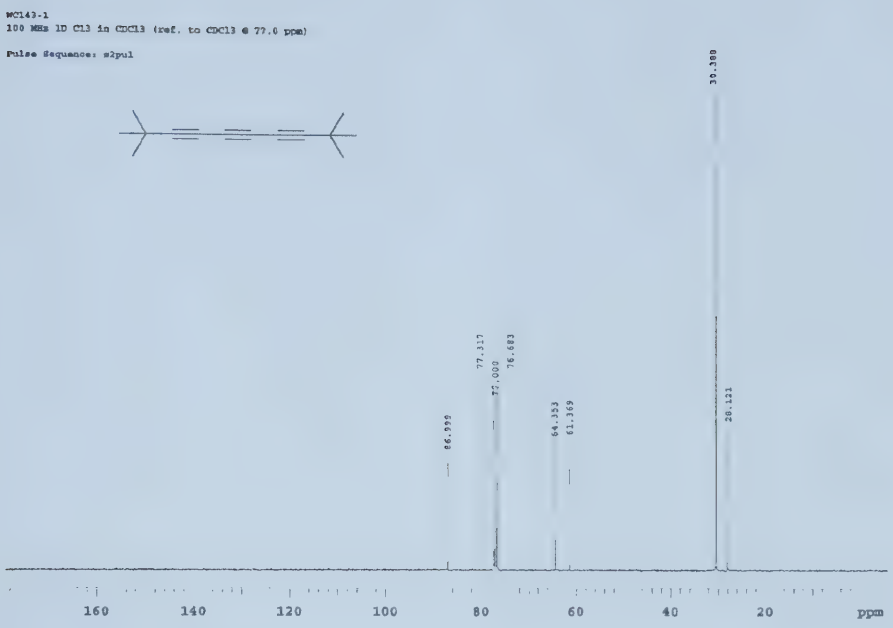


**Figure C-92.** $^{13}$C NMR spectrum of **4.1b**.

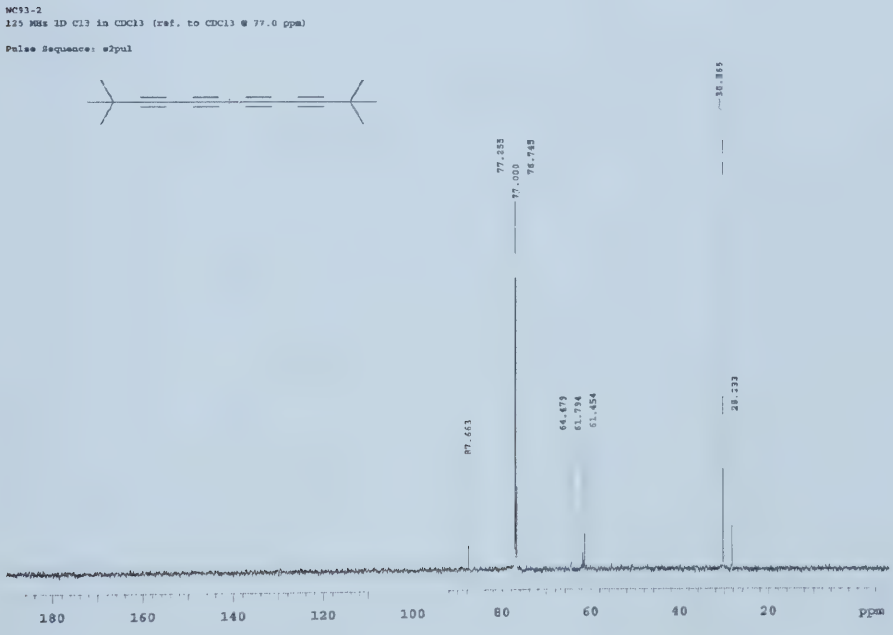


**Figure C-93.** $^{13}$C NMR spectrum of **4.1c**.

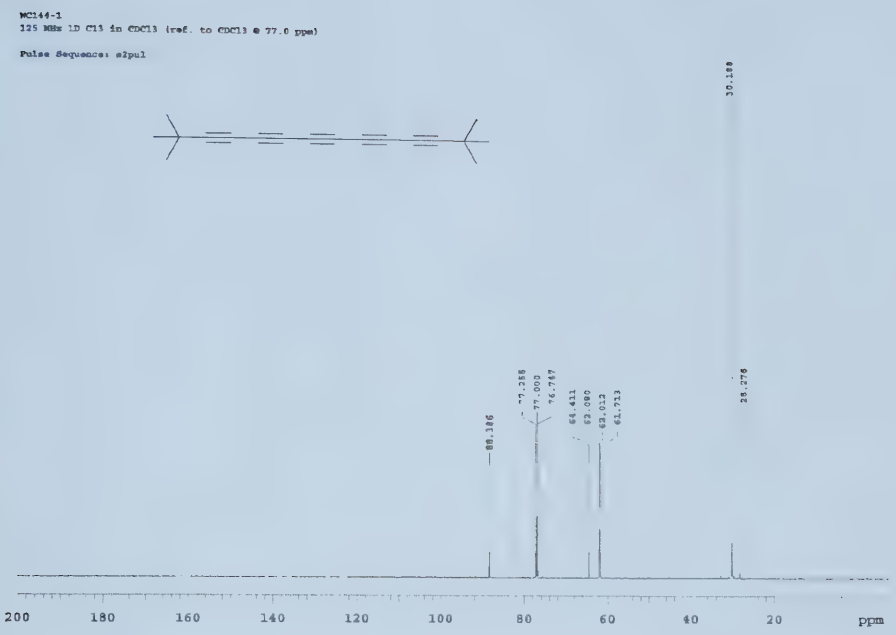


**Figure C-94.** $^{13}C$ NMR spectrum of **4.1d**.

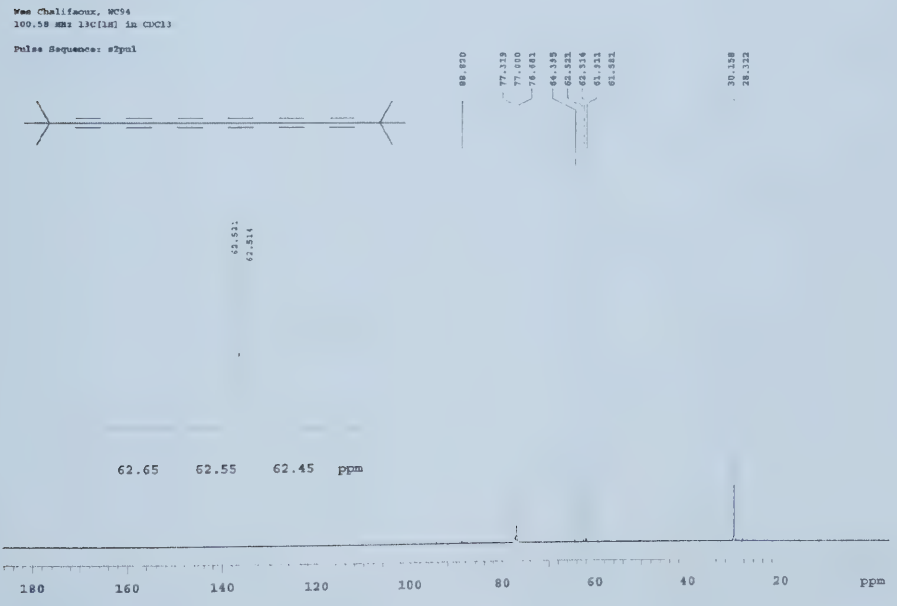


**Figure C-95.** $^{13}C$ NMR spectrum of **4.1e**.

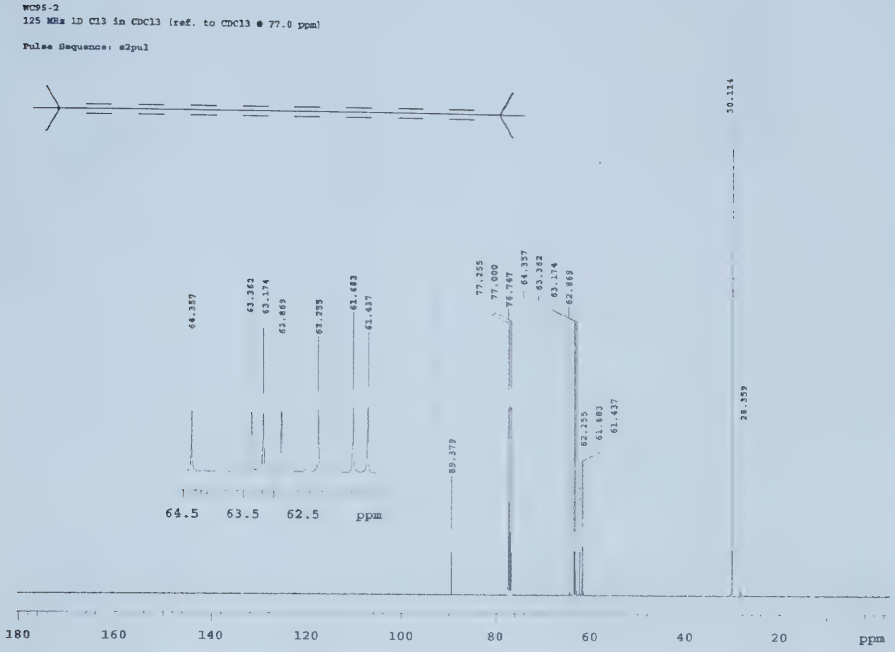


**Figure C-96.** $^{13}$C NMR spectrum of **4.1f**.

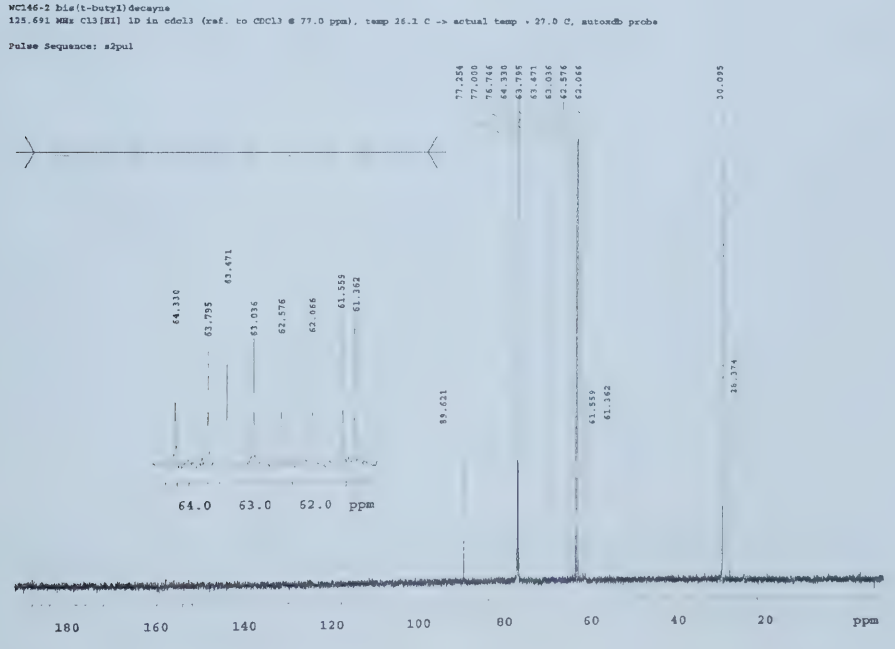


**Figure C-97.** $^{13}$C NMR spectrum of **4.1h**.

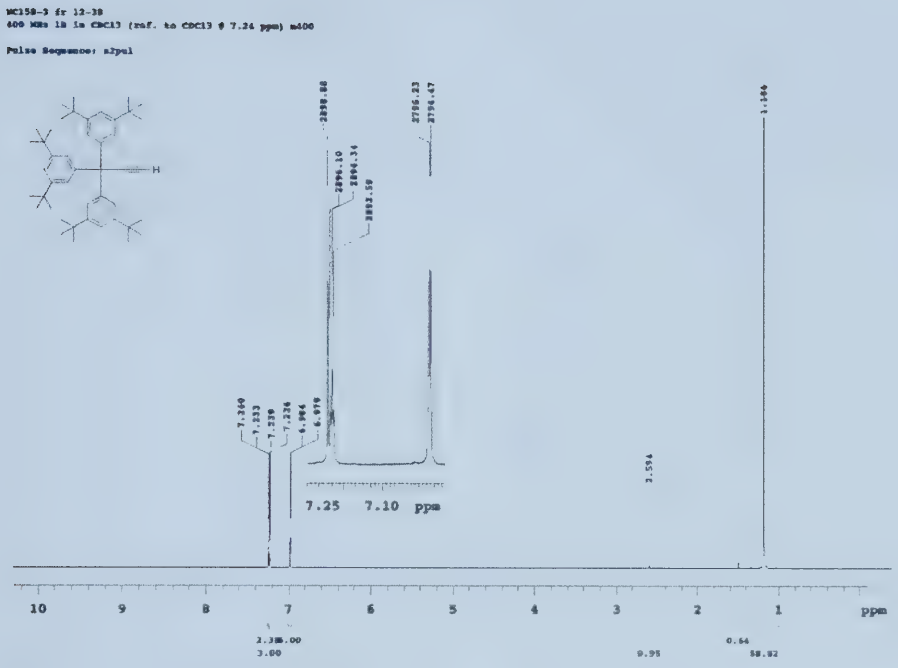


**Figure C-98.** $^{1}H$ NMR spectrum of **5.6**.

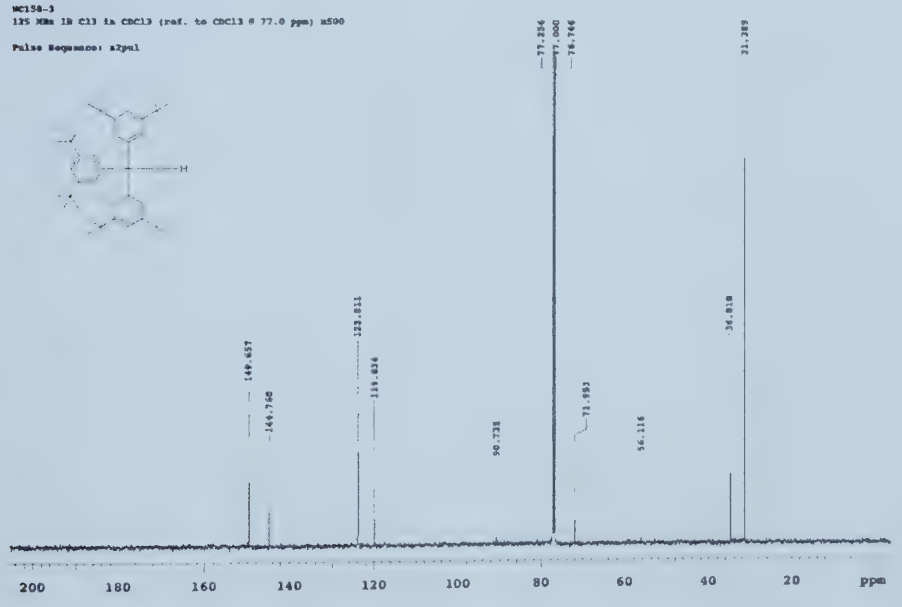


**Figure C-99.** $^{13}C$ NMR spectrum of **5.6**.

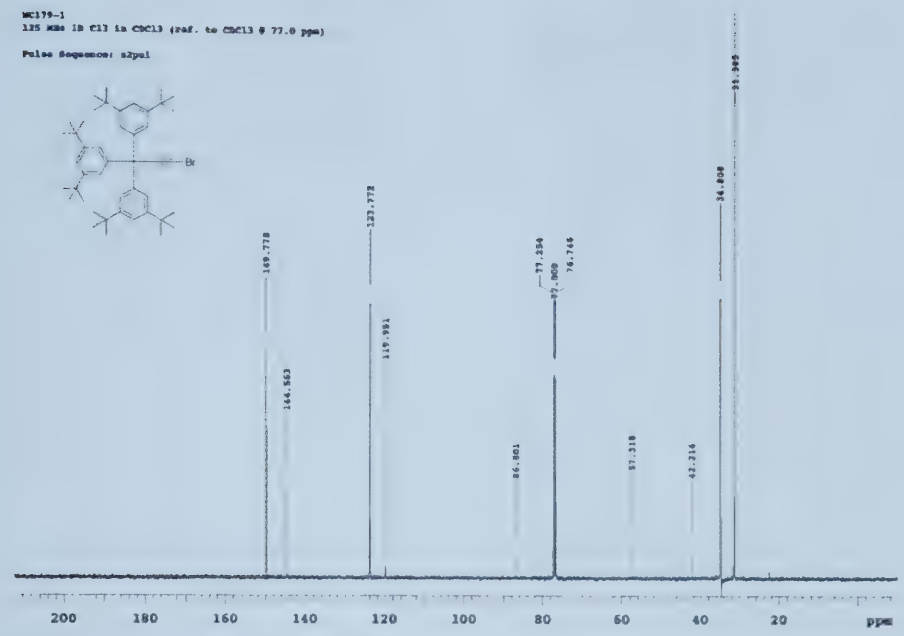


**Figure C-100.** $^{13}C$ NMR spectrum of **7.6**.

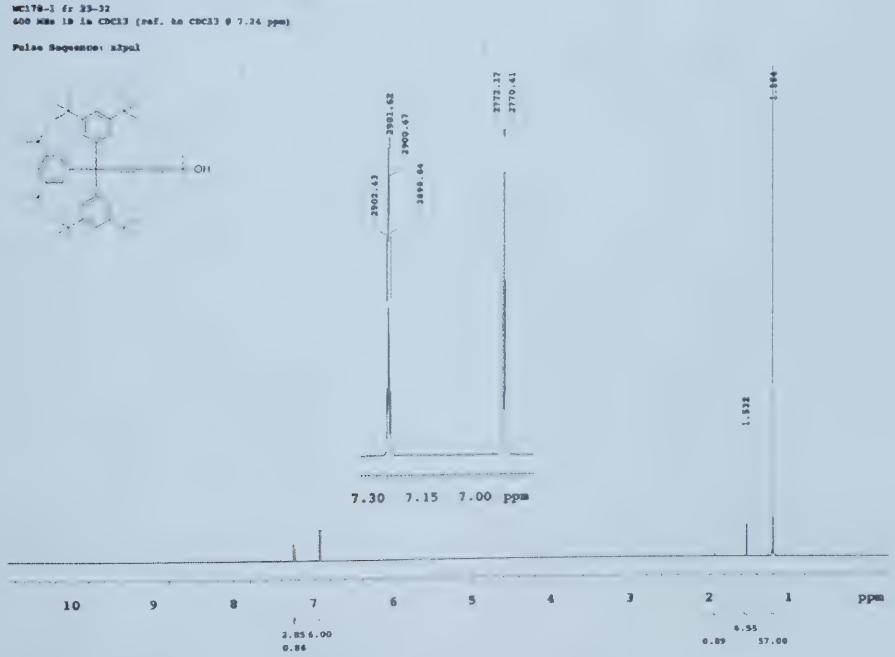


**Figure C-101.** $^{1}H$ NMR spectrum of **7.7**.

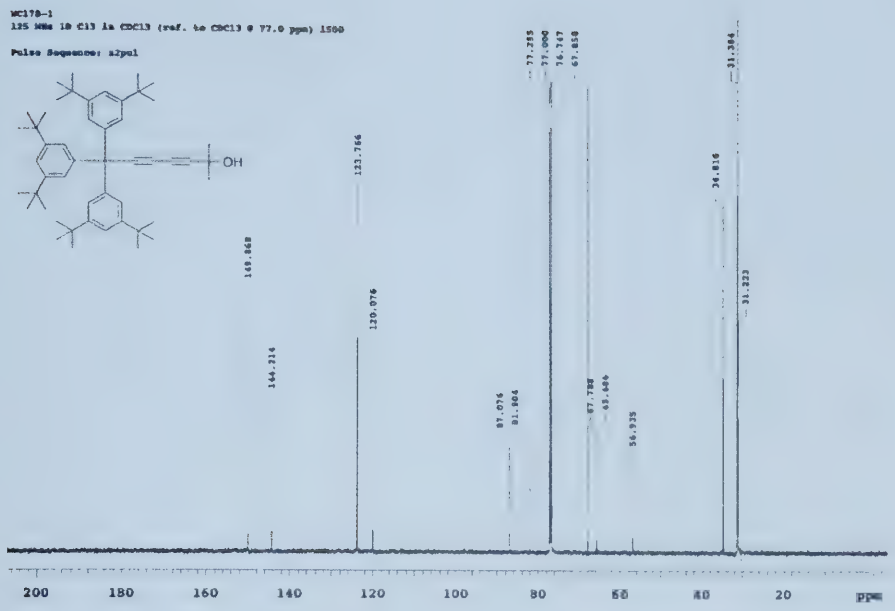


**Figure C-102.** $^{13}C$ NMR spectrum of **7.7**.

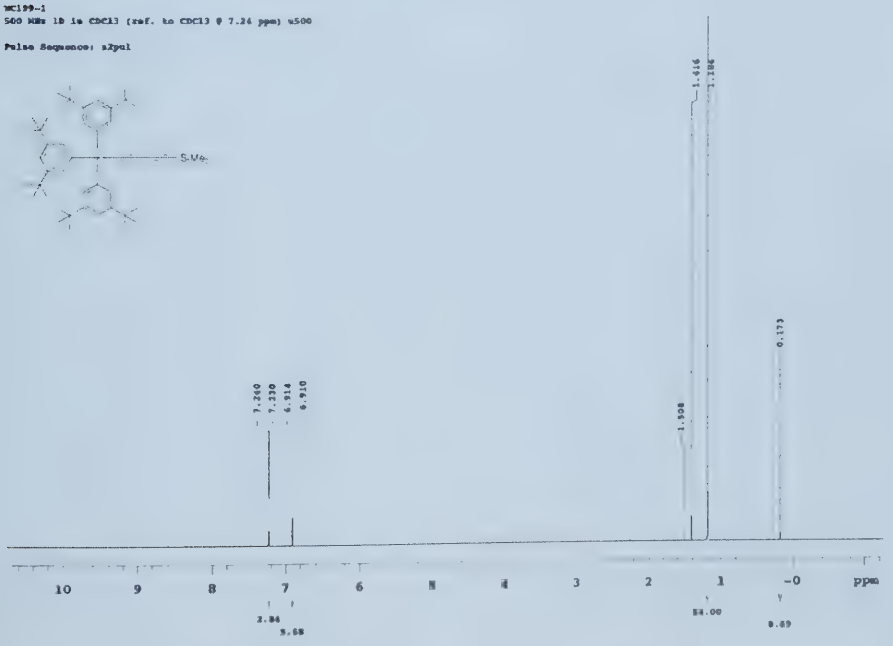


**Figure C-103.** $^{1}H$ NMR spectrum of **7.8**.

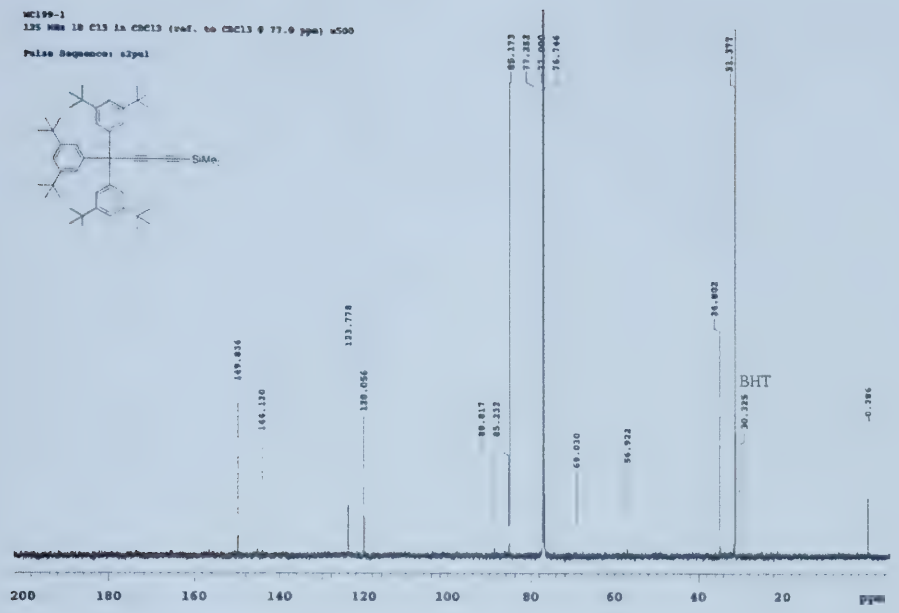


**Figure C-104.** $^{13}C$ NMR spectrum of **7.8**.

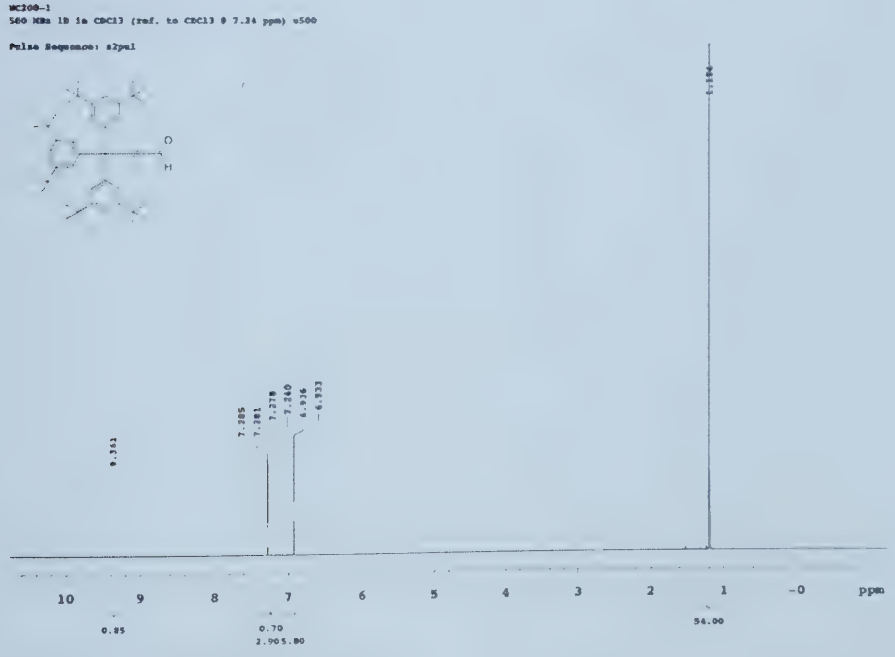


**Figure C-105.** $^{1}H$ NMR spectrum of **5.8**.

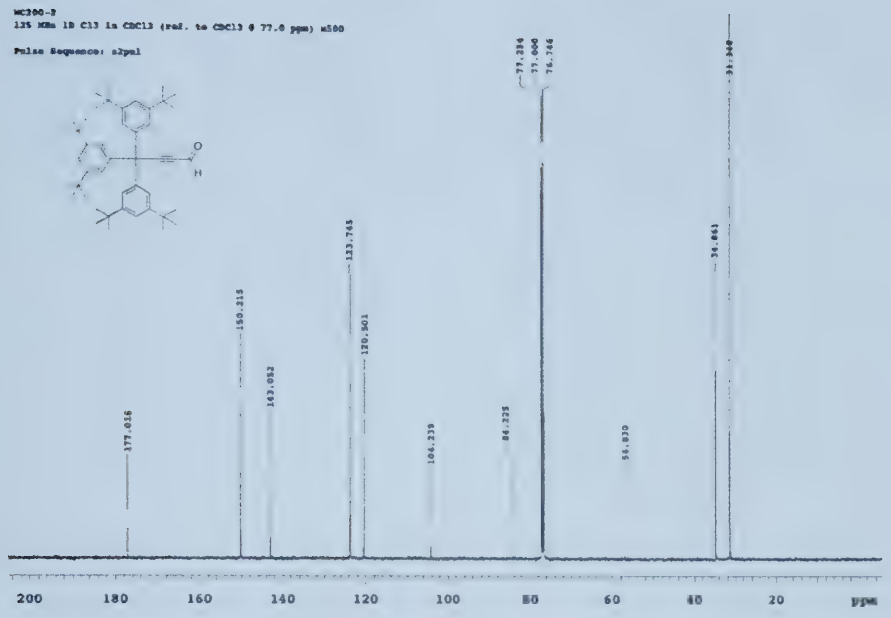


**Figure C-106.** $^{13}$C NMR spectrum of **5.8**.

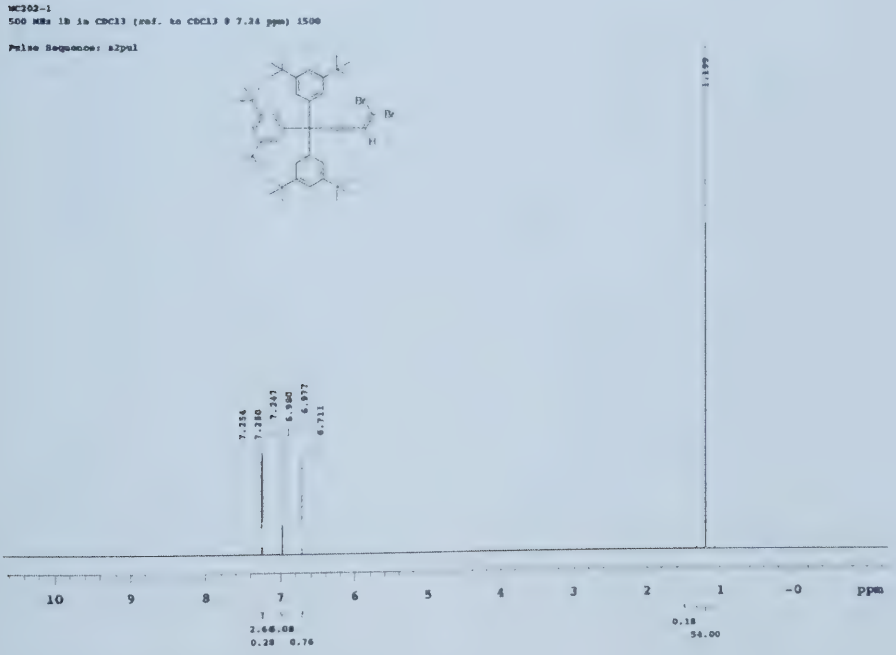


**Figure C-107.** $^{1}$H NMR spectrum of **5.9**.

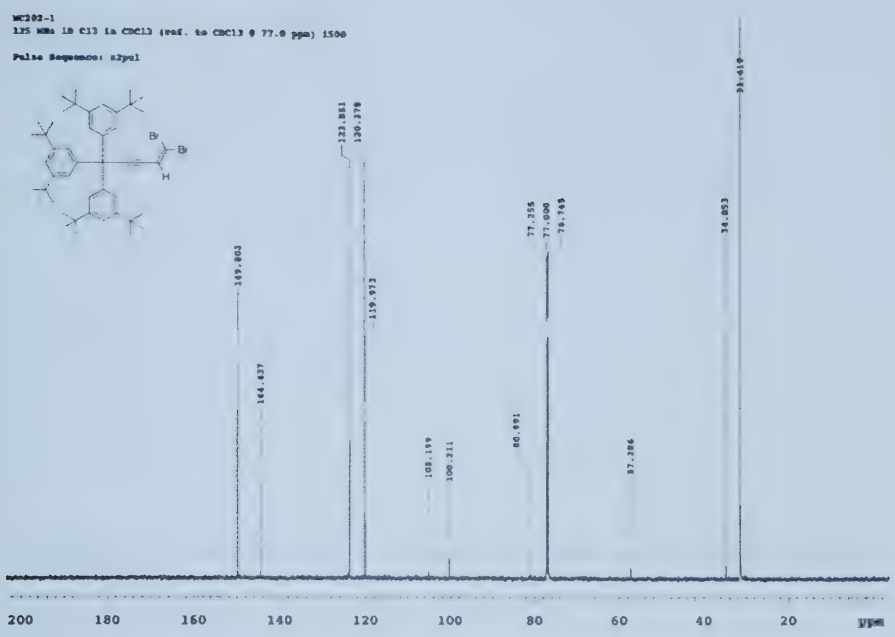


**Figure C-108.** $^{13}C$ NMR spectrum of **5.9**.

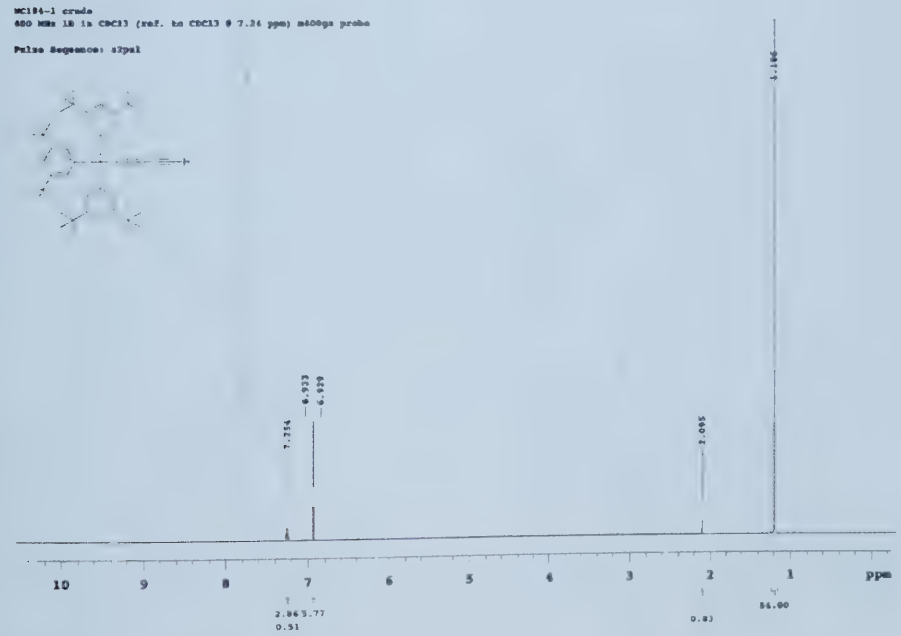


**Figure C-109.** $^{1}H$ NMR spectrum of **5.7**.

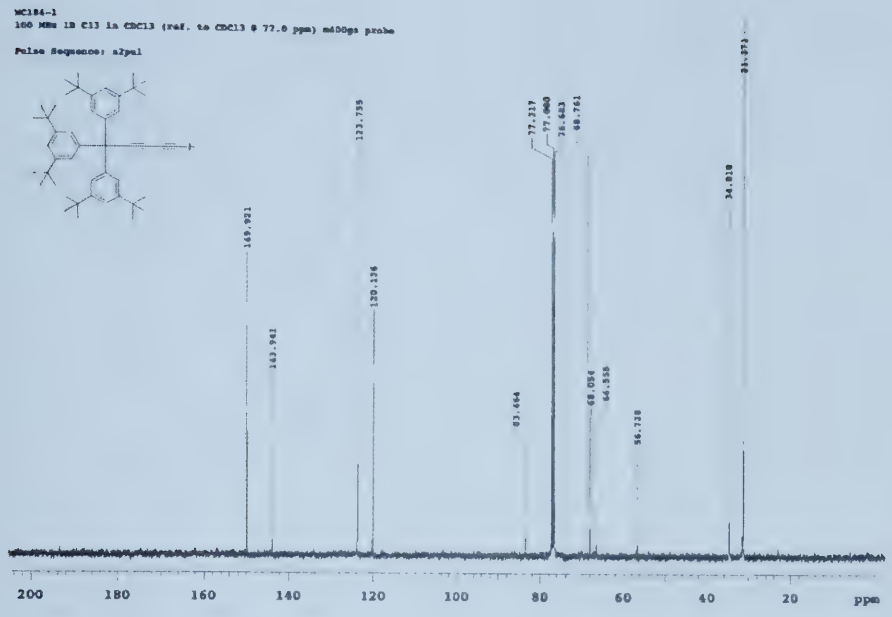


**Figure C-110.** $^{13}C$ NMR spectrum of **5.7**.

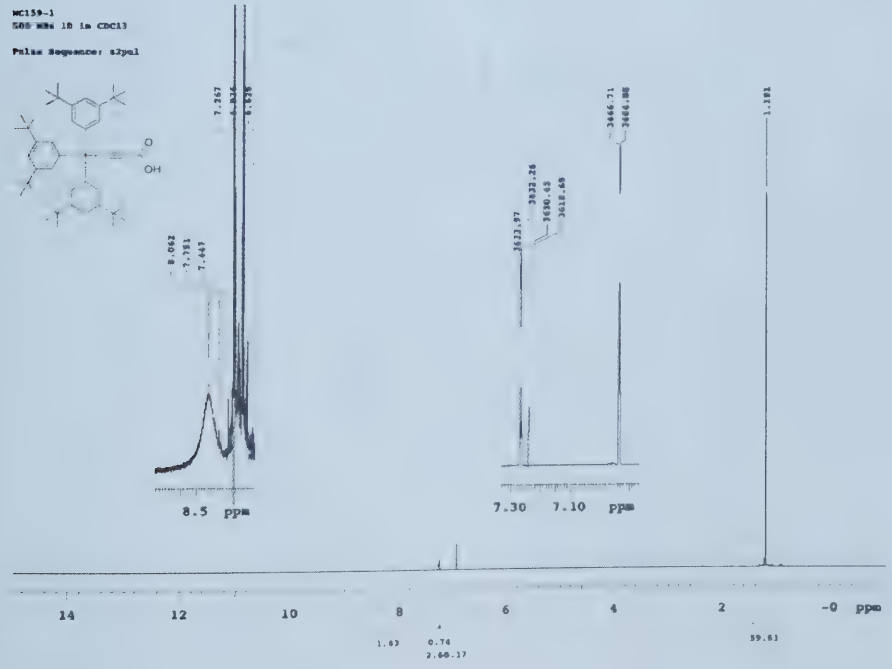


**Figure C-111.** $^{1}H$ NMR spectrum of **5.10**.

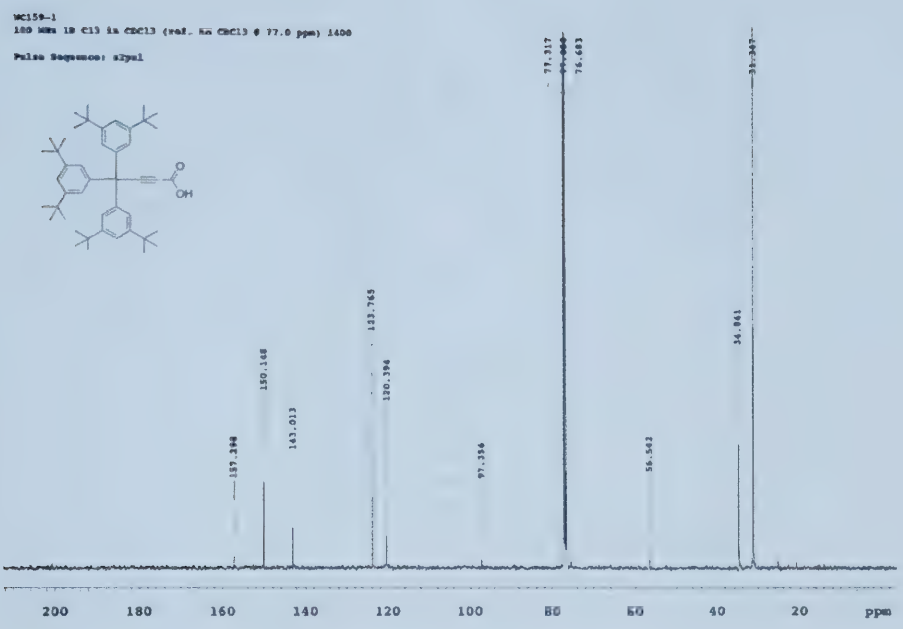


**Figure C-112.** $^{13}$C NMR spectrum of **5.10**.

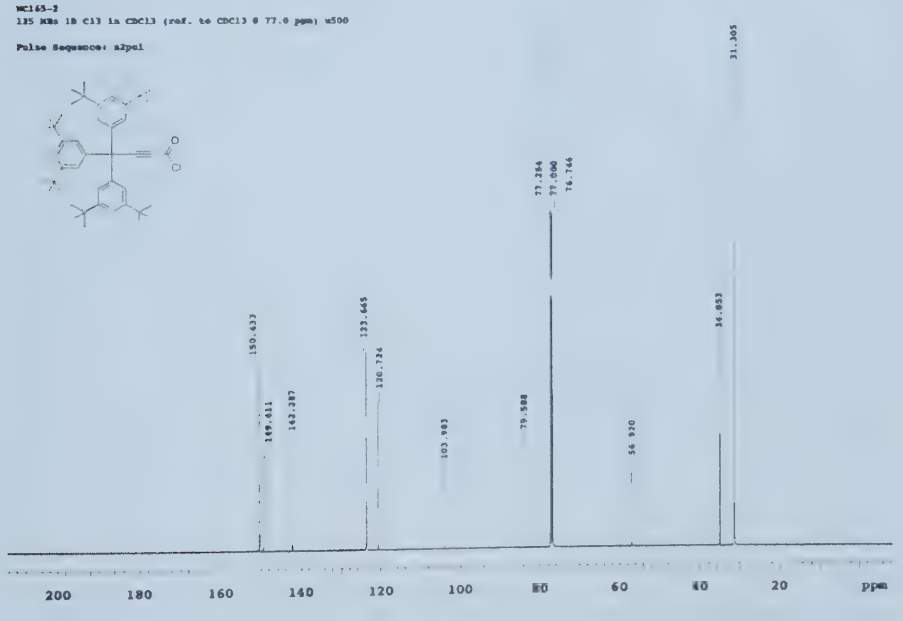


**Figure C-113.** $^{13}$C NMR spectrum of **5.11**.

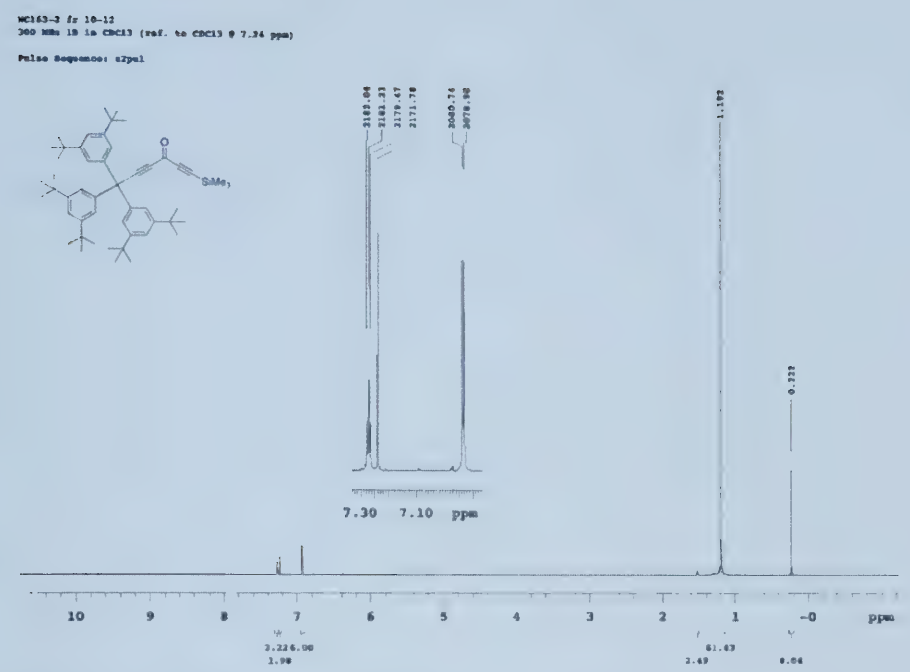


**Figure C-114.** $^{1}$H NMR spectrum of **5.12**.

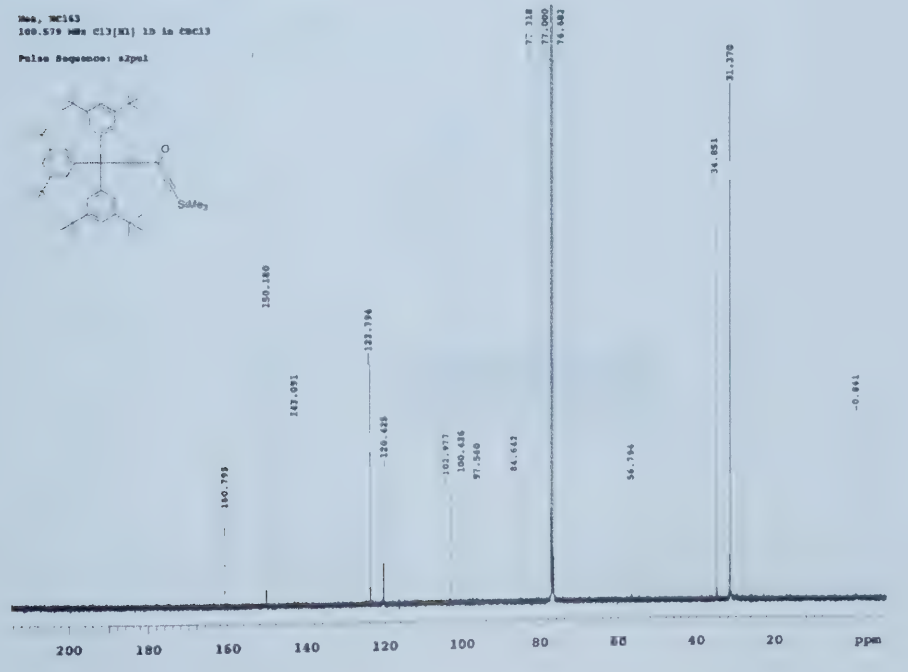


**Figure C-115.** $^{13}$C NMR spectrum of **5.12**.

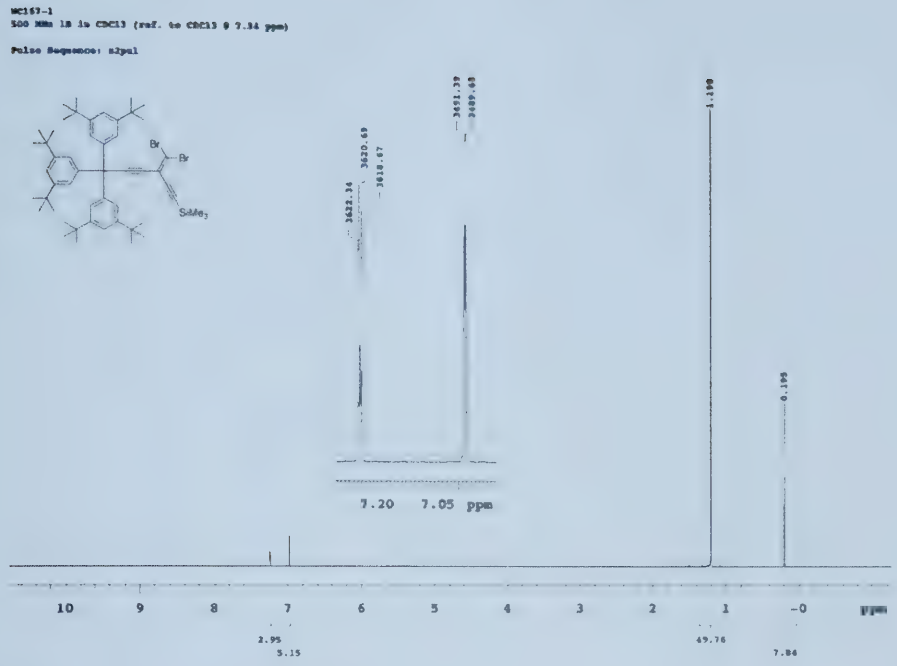


**Figure C-116.** $^{1}$H NMR spectrum of 5.15.

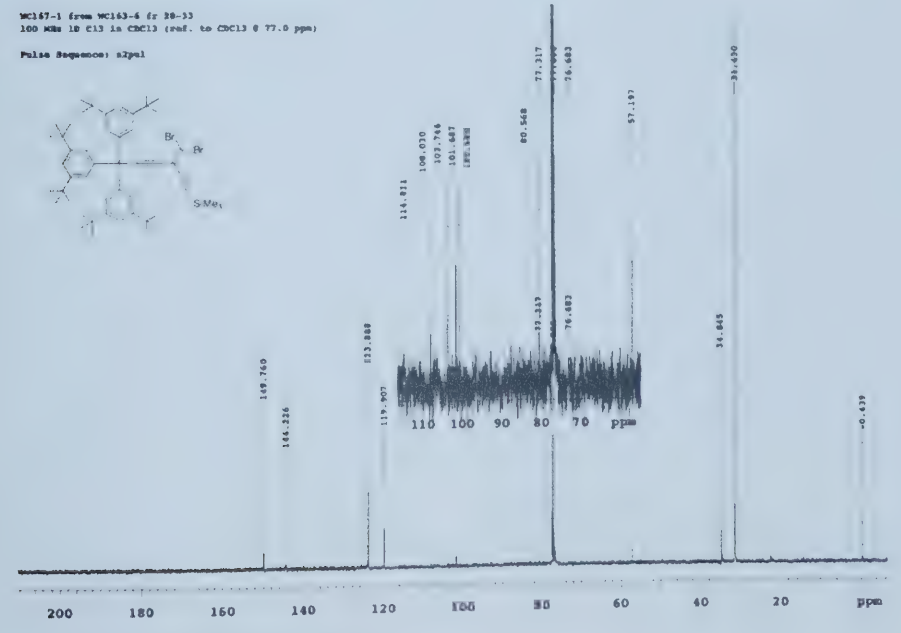


**Figure C-117.** $^{13}$C NMR spectrum of 5.15.

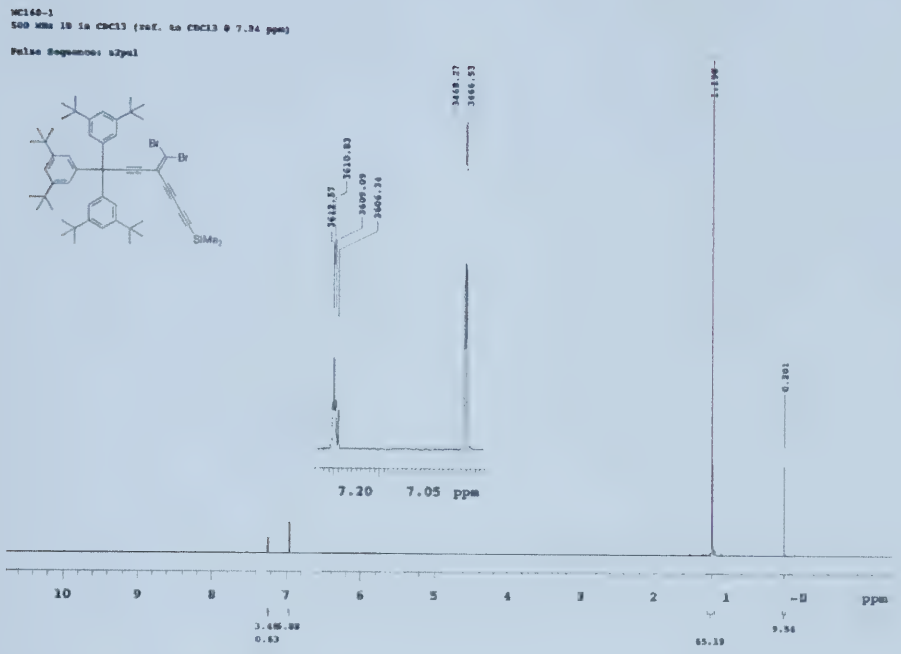


**Figure C-118.** $^{1}$H NMR spectrum of **5.16**.

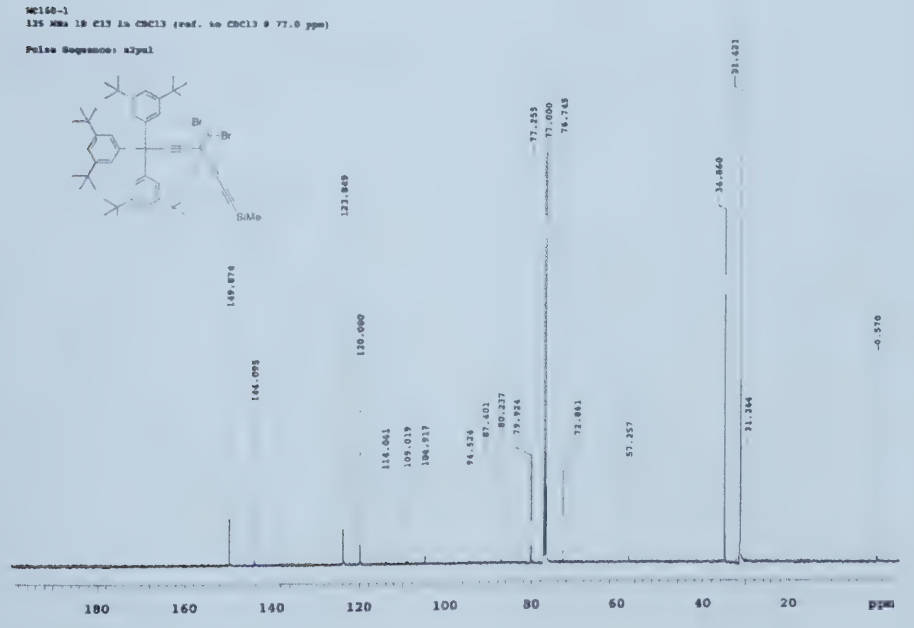


**Figure C-119.** $^{13}$C NMR spectrum of **5.16**.

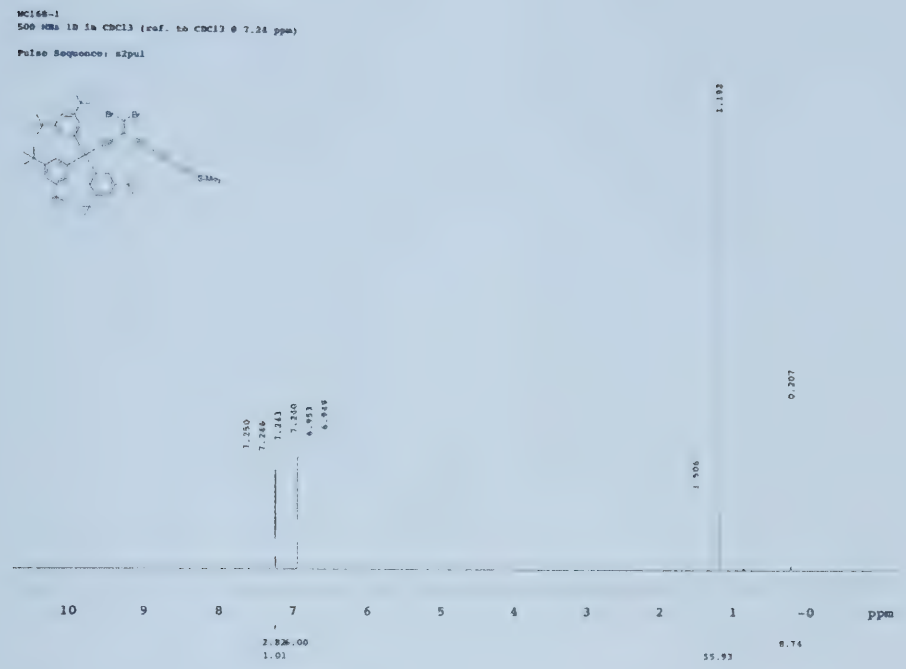


**Figure C-120.** $^{1}H$ NMR spectrum of **5.17**.

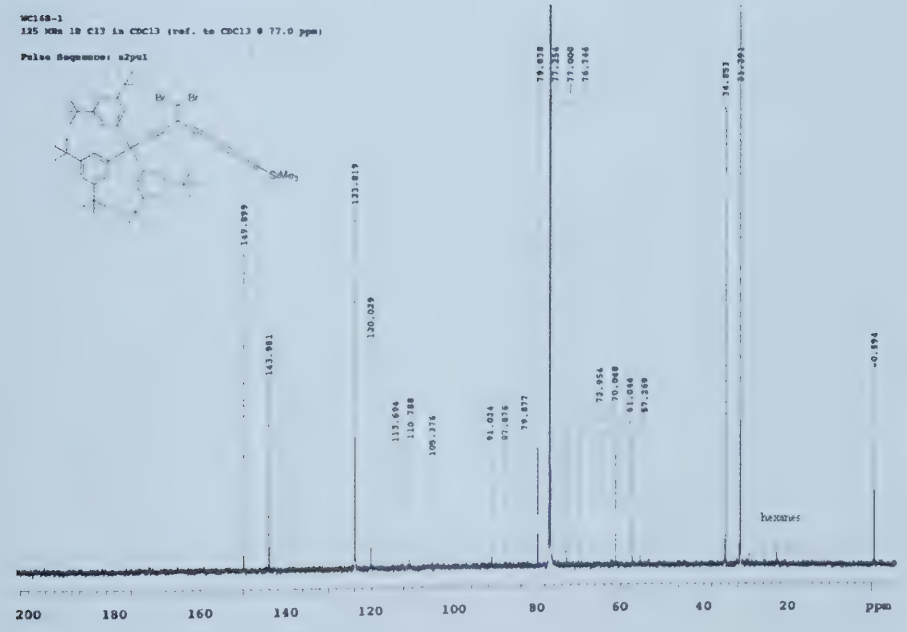


**Figure C-121.** $^{13}C$ NMR spectrum of **5.17**.

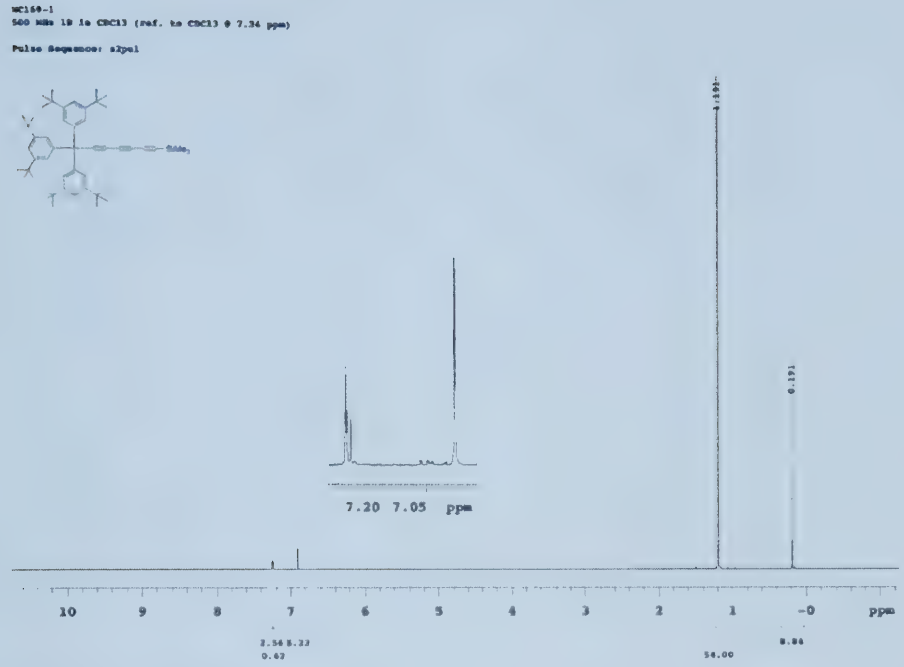


**Figure C-122.** $^{1}$H NMR spectrum of **5.18**.

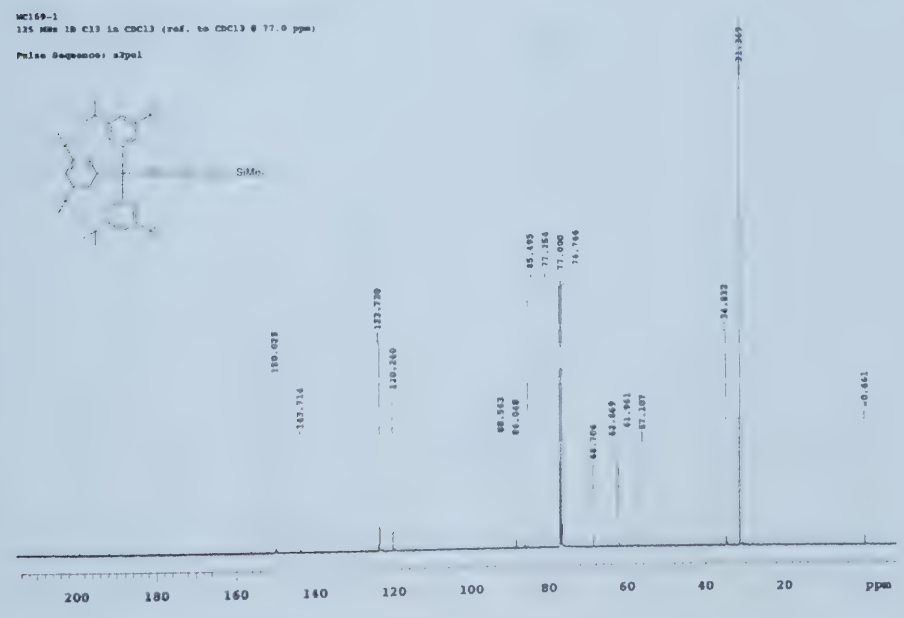


**Figure C-123.** $^{13}$C NMR spectrum of **5.18**.

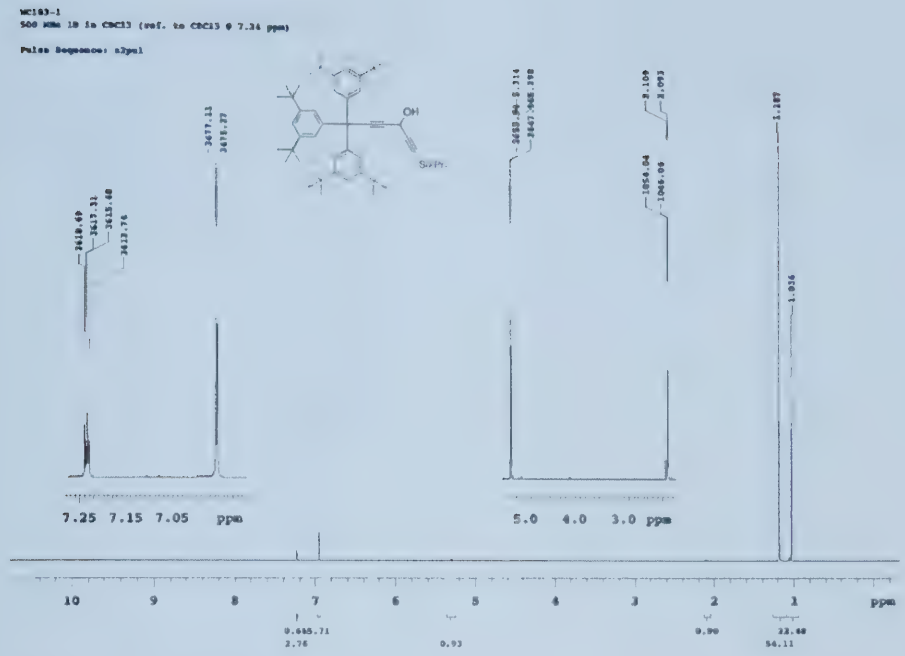


**Figure C-124.** $^{1}$H NMR spectrum of **5.21**.

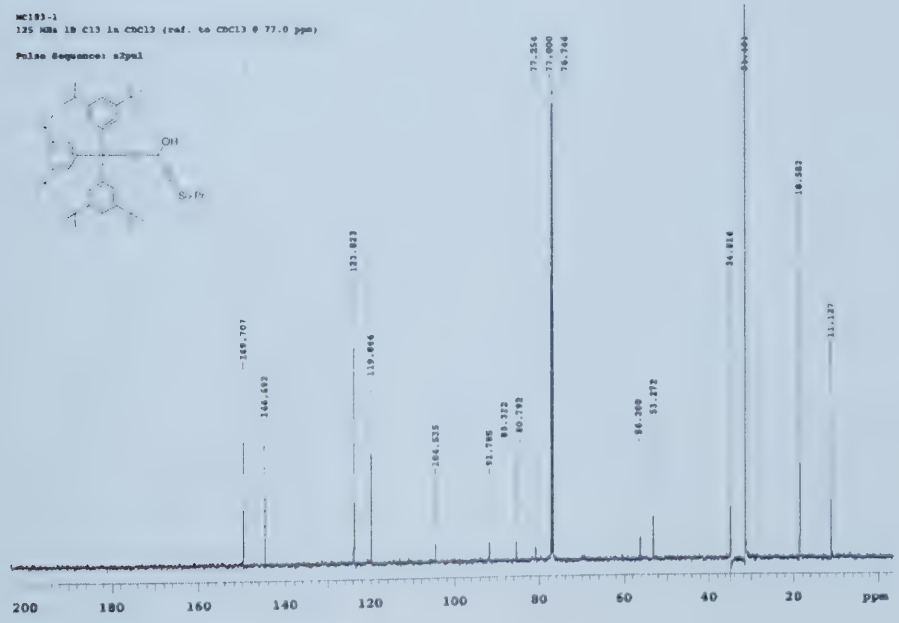


**Figure C-125.** $^{13}$C NMR spectrum of **5.21**.

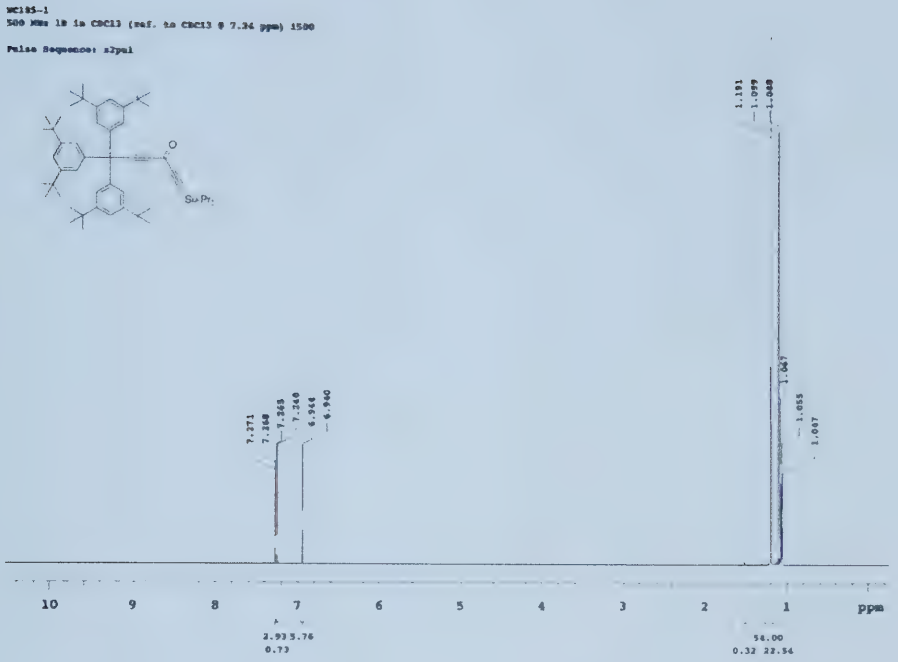


**Figure C-126.** $^{1}$H NMR spectrum of 5.22.

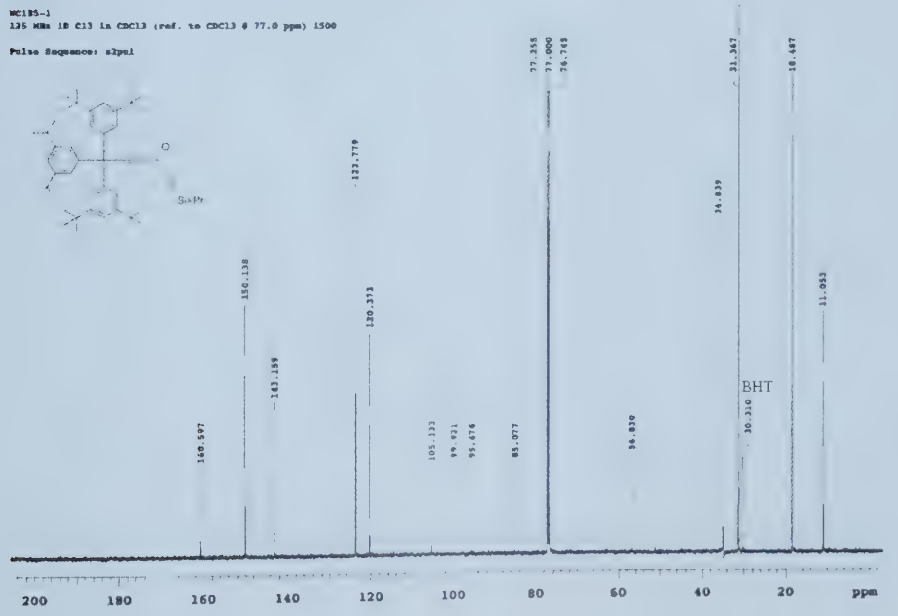


**Figure C-127.** $^{13}$C NMR spectrum of 5.22.

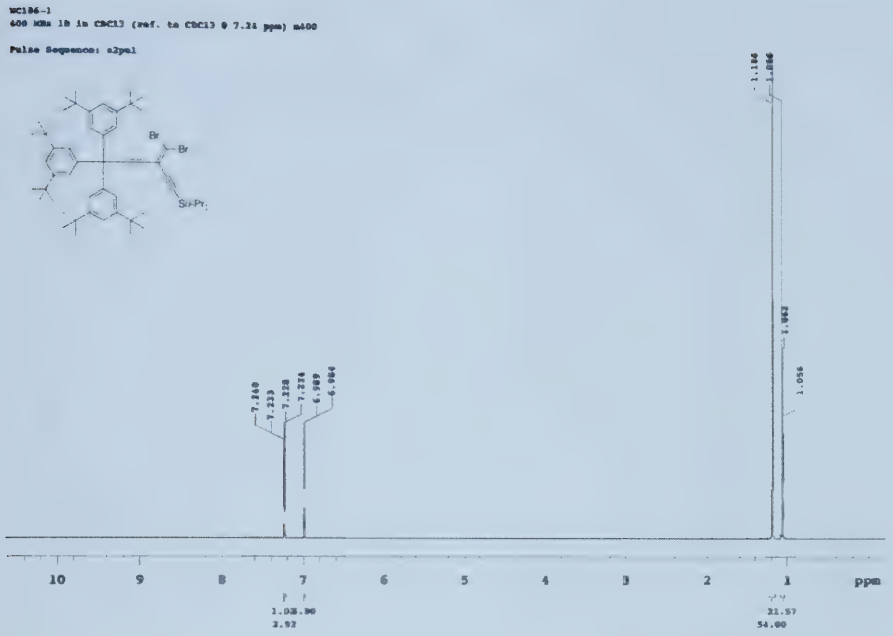


**Figure C-128.** $^{1}H$ NMR spectrum of **5.23**.

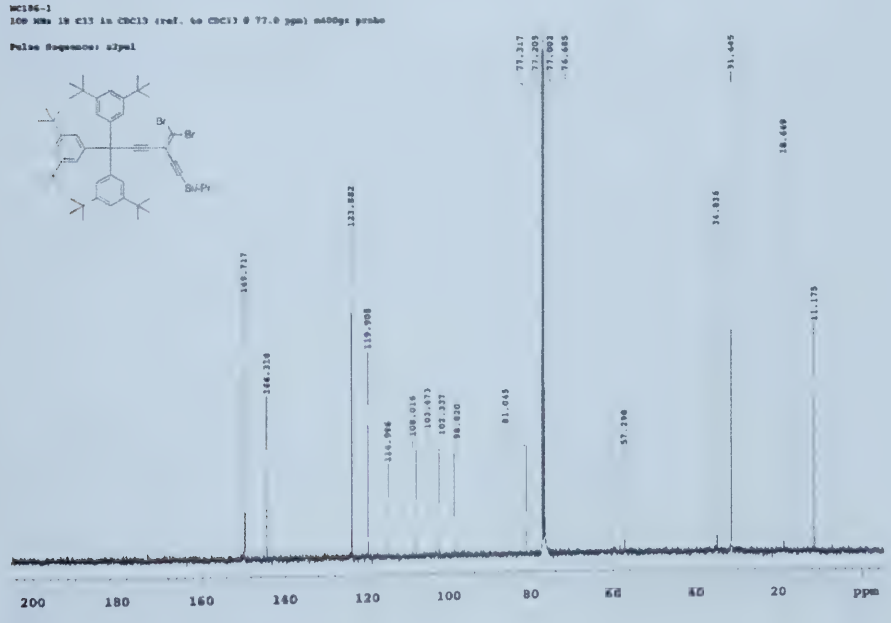


**Figure C-129.** $^{13}C$ NMR spectrum of **5.23**.

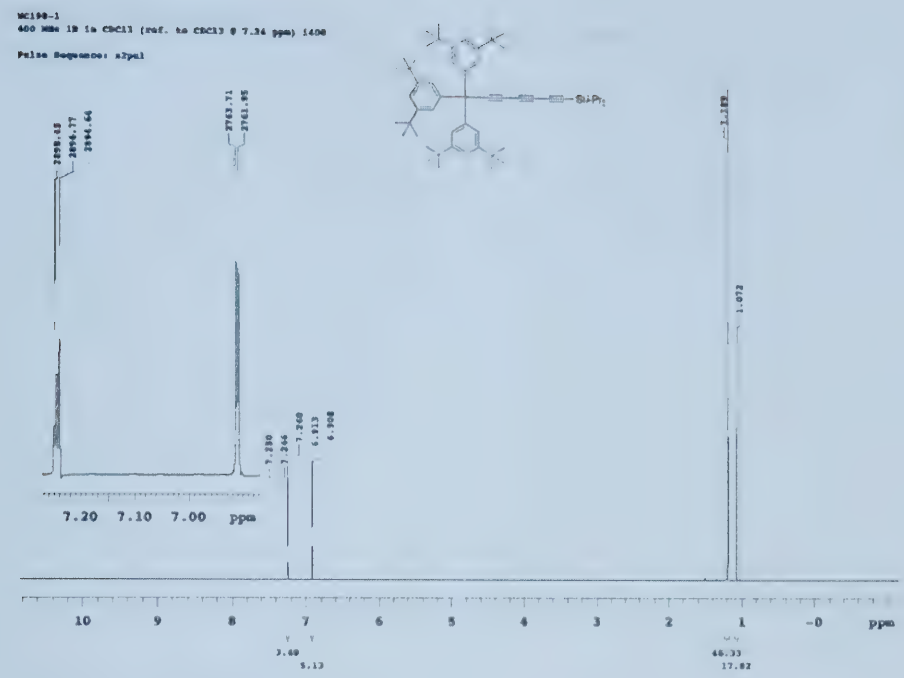

**Figure C-130.** $^{1}$H NMR spectrum of 5.24.

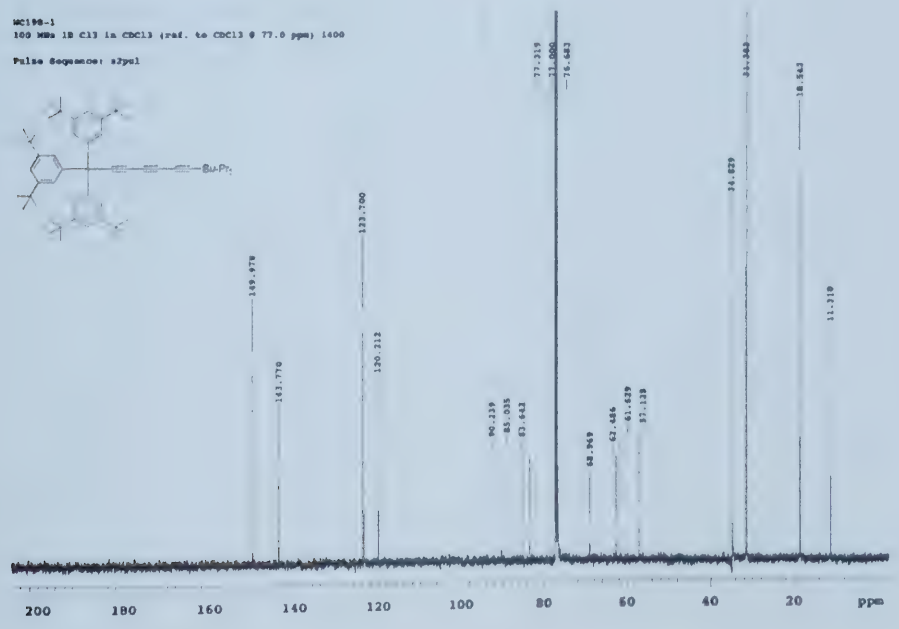

**Figure C-131.** $^{13}$C NMR spectrum of 5.24.

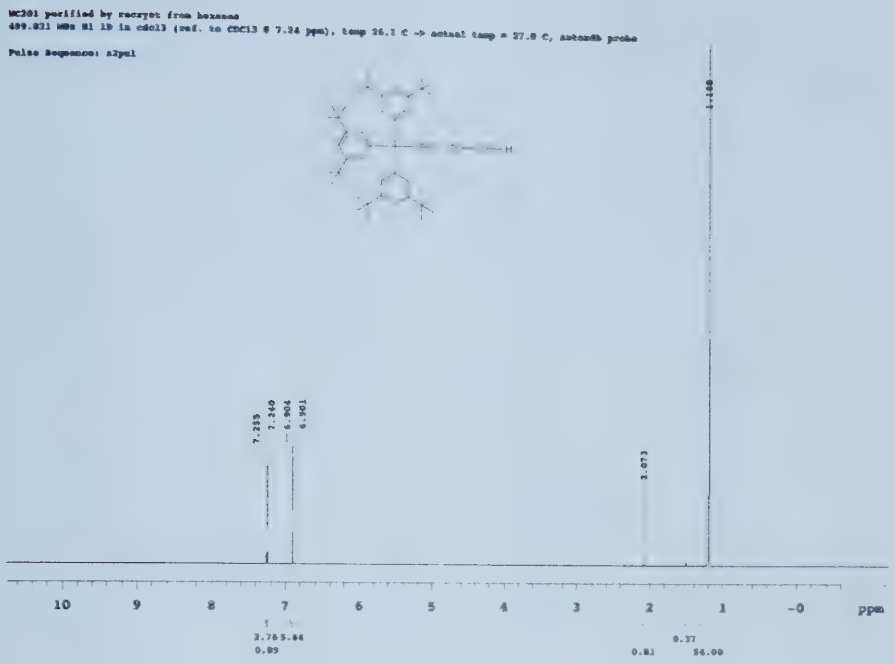


**Figure C-132.** $^{1}$H NMR spectrum of 5.25.

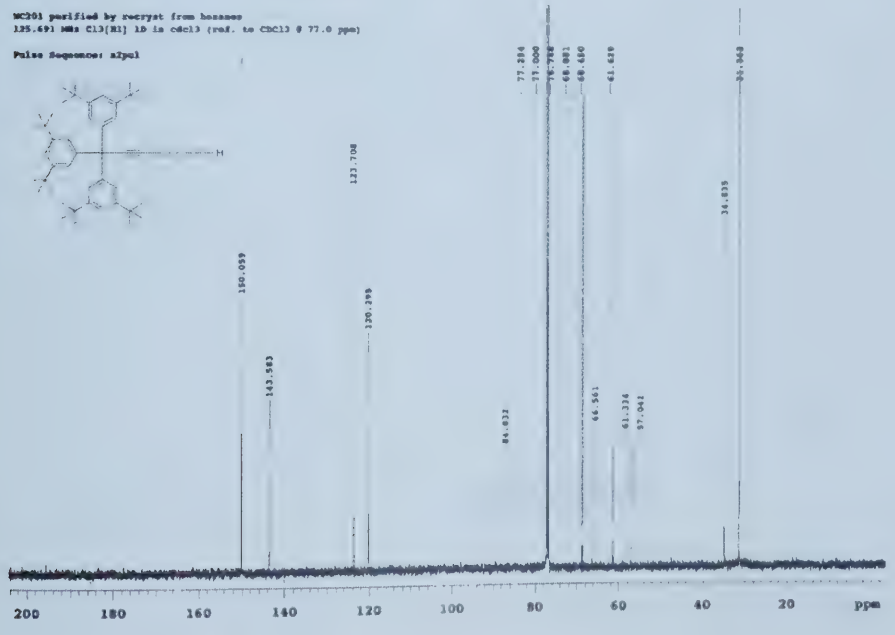


**Figure C-133.** $^{13}$C NMR spectrum of 5.25.

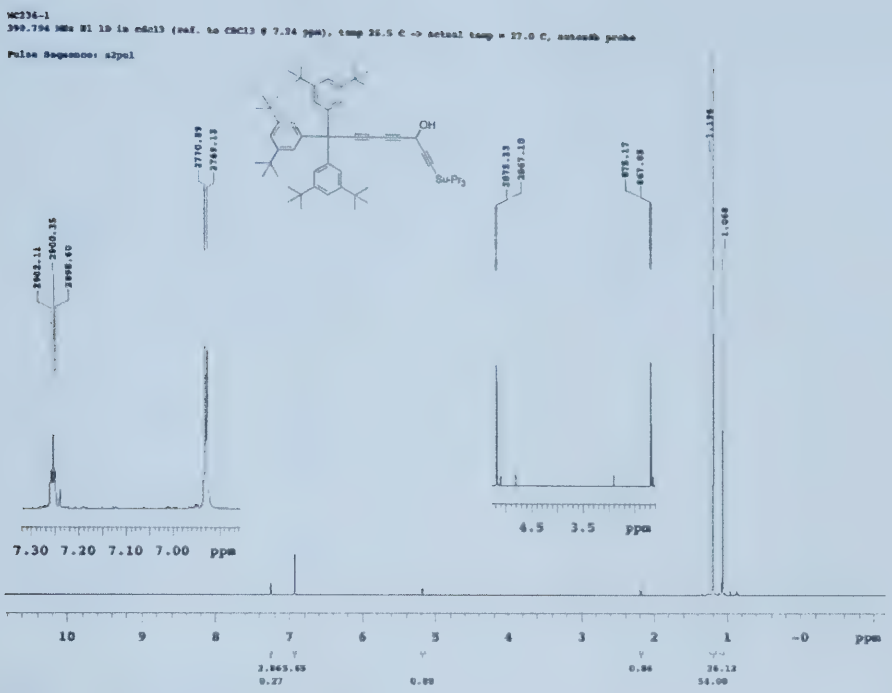


**Figure C-134.** $^{1}$H NMR spectrum of 5.26.

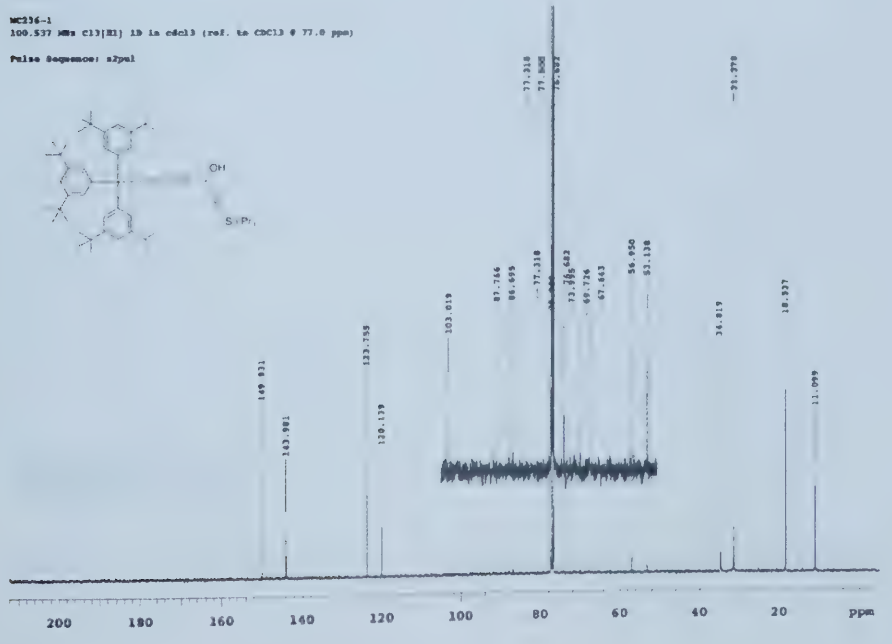


**Figure C-135.** $^{13}$C NMR spectrum of 5.26.

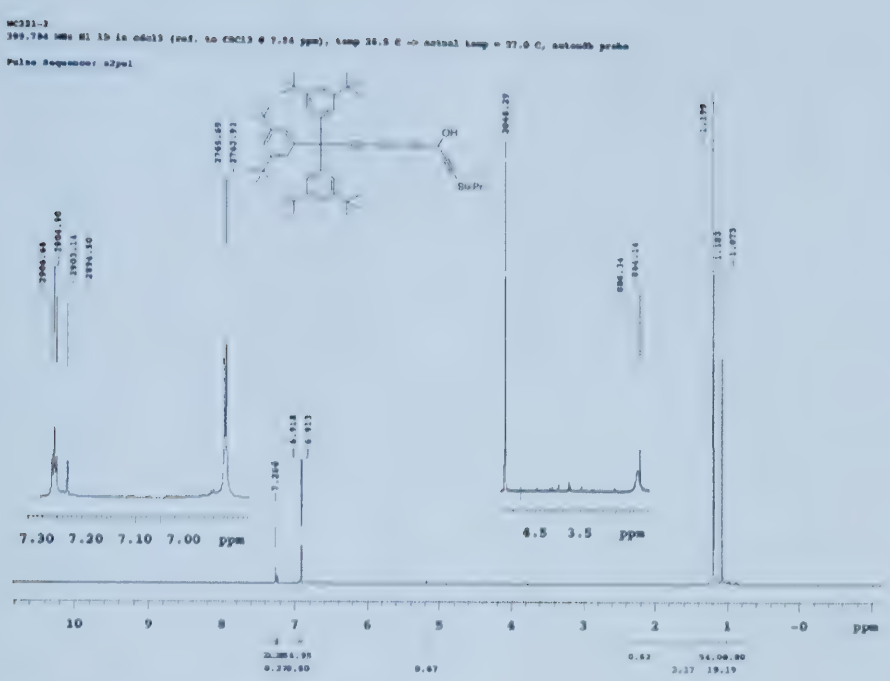

Figure C-136. $^{1}$H NMR spectrum of 5.27.

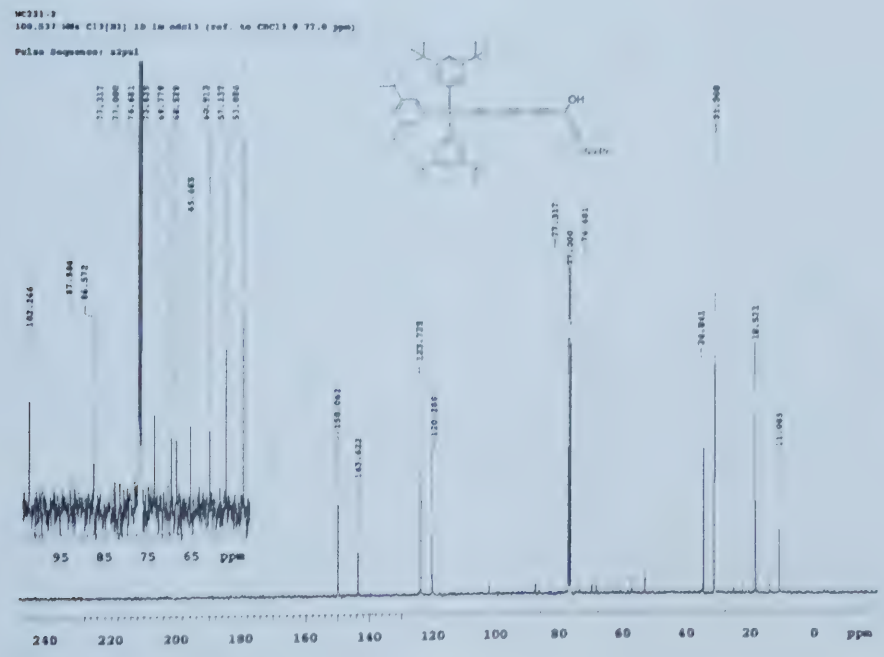

Figure C-137. $^{13}$C NMR spectrum of 5.27.

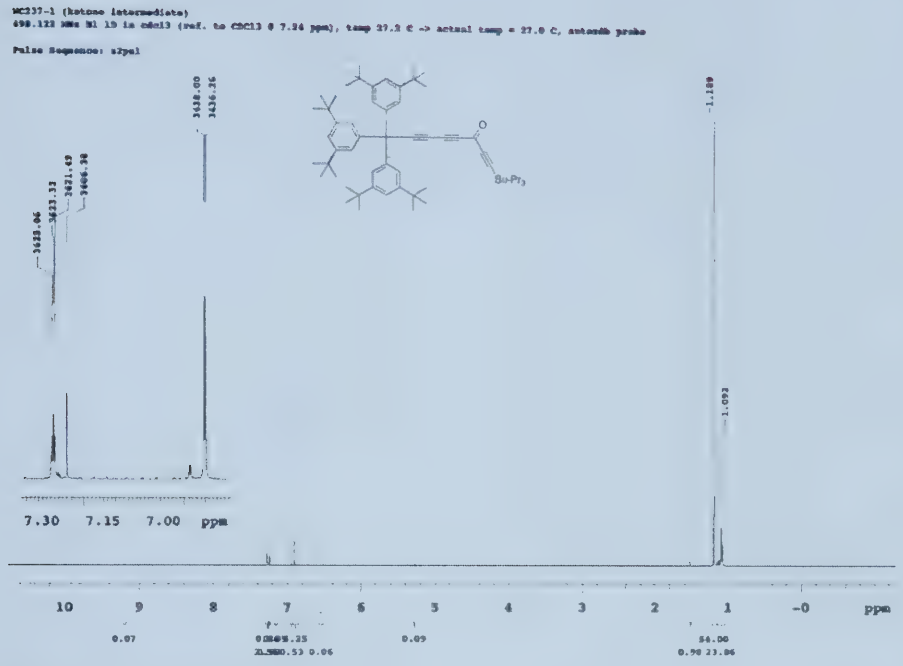


**Figure C-138.** $^{1}$H NMR spectrum of 5.28.

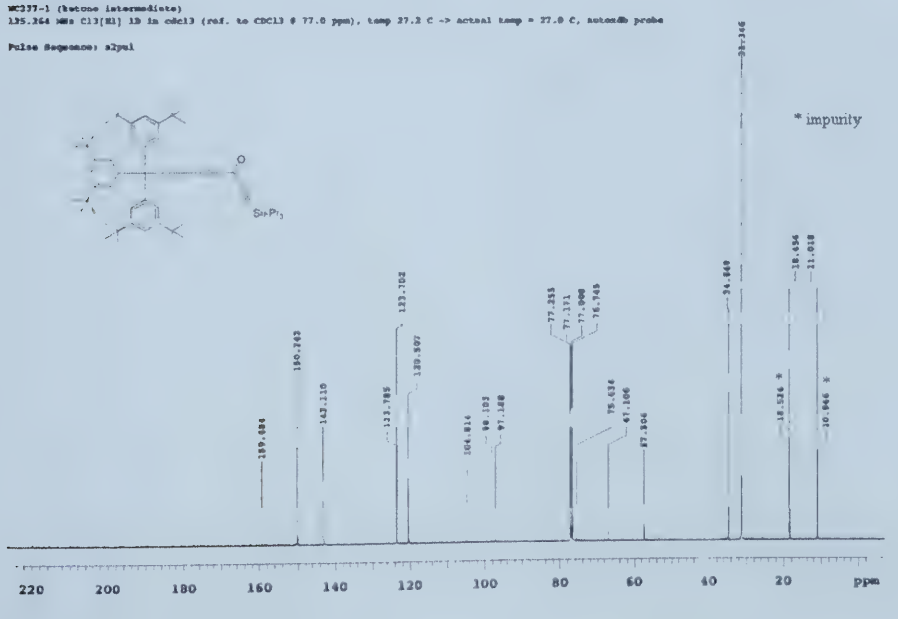


**Figure C-139.** $^{13}$C NMR spectrum of 5.28.

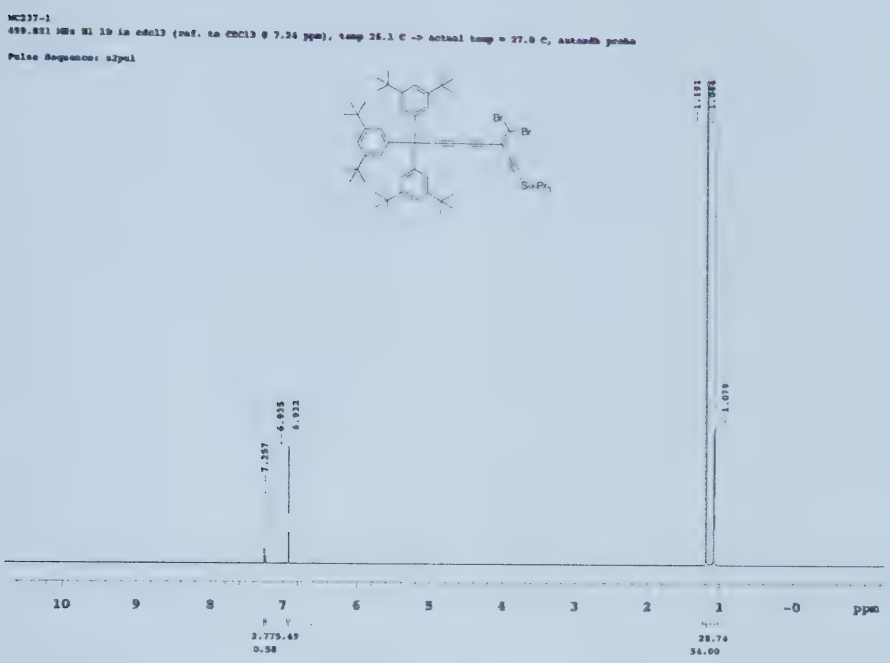


**Figure C-140.** $^{1}$H NMR spectrum of **5.30**.

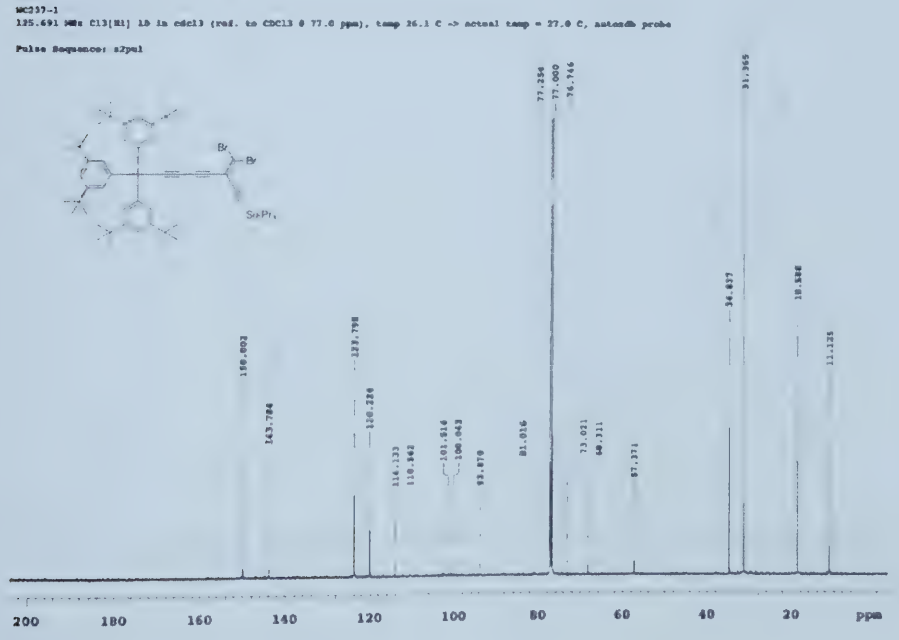


**Figure C-141.** $^{13}$C NMR spectrum of **5.30**.

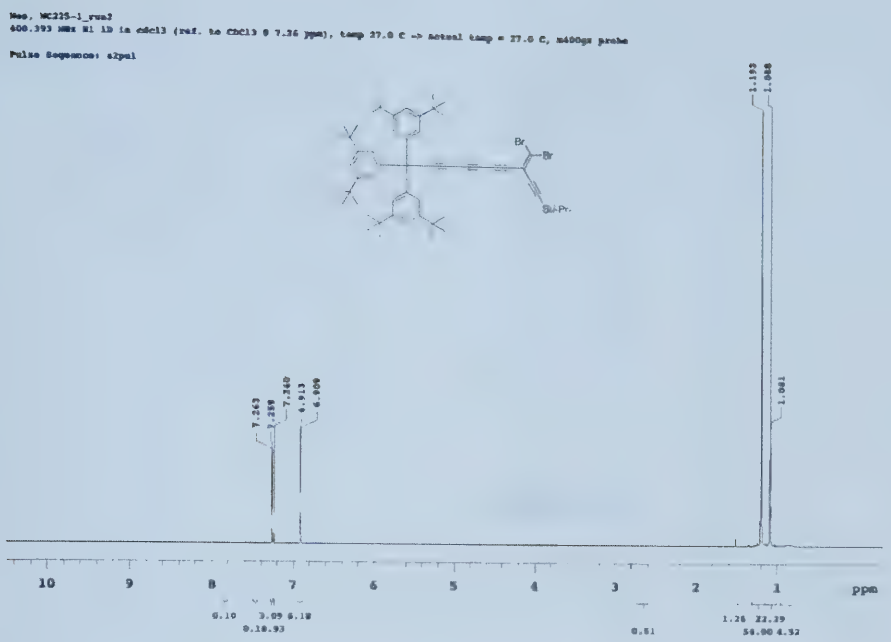


**Figure C-142.** $^{1}$H NMR spectrum of **5.31**.

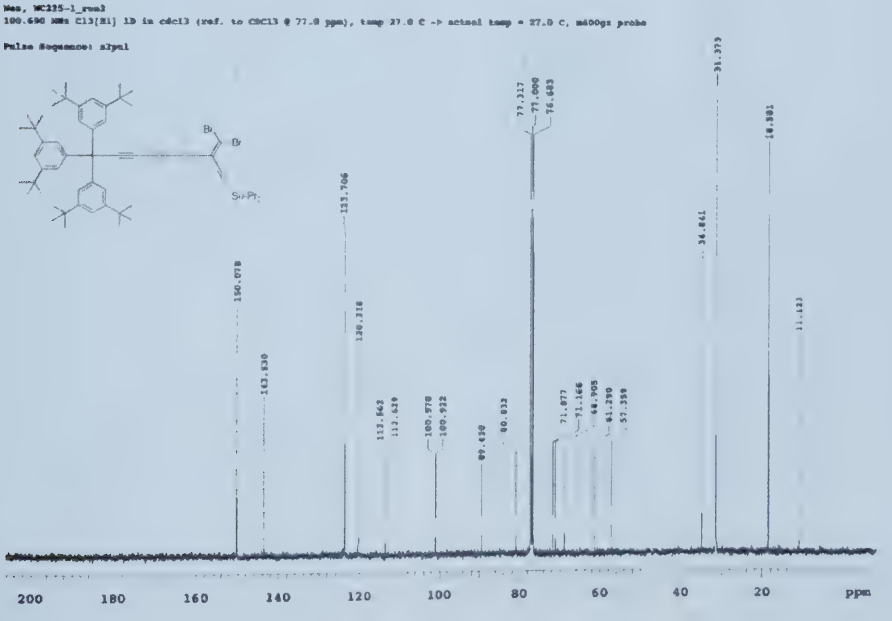


**Figure C-143.** $^{13}$C NMR spectrum of **5.31**.

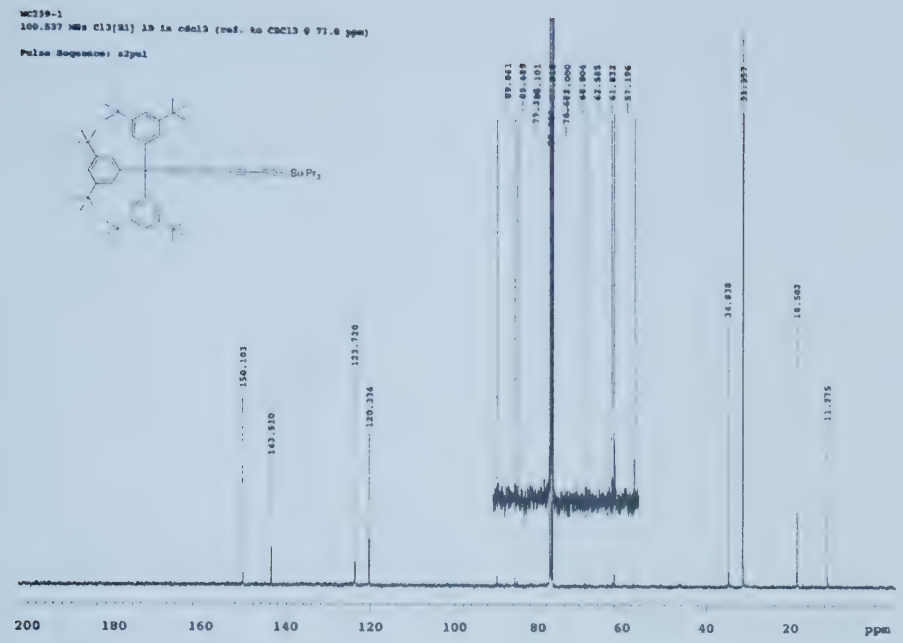


**Figure C-144.** $^{13}C$ NMR spectrum of 5.32.

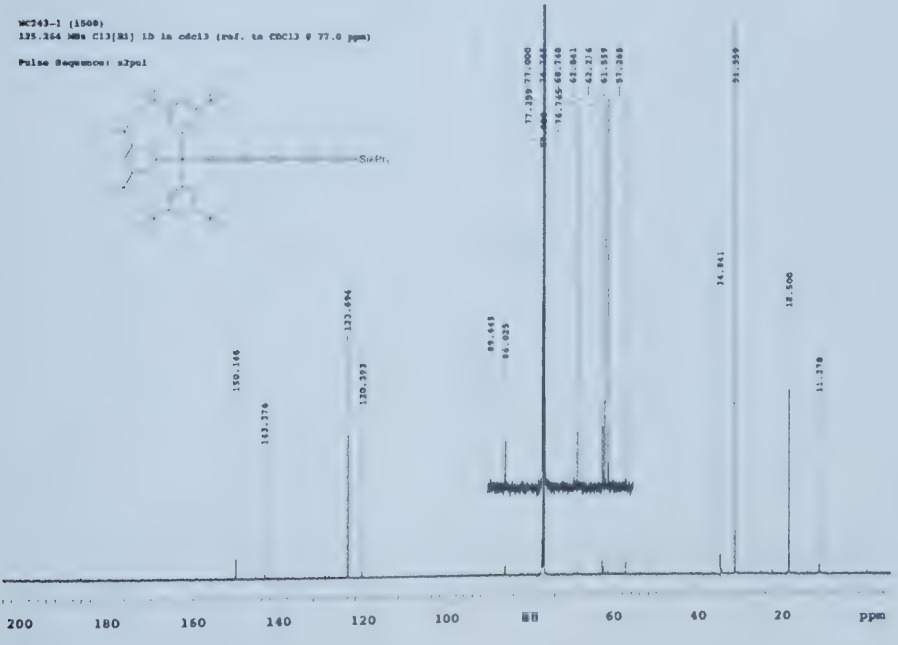


**Figure C-145.** $^{13}C$ NMR spectrum of 5.33.

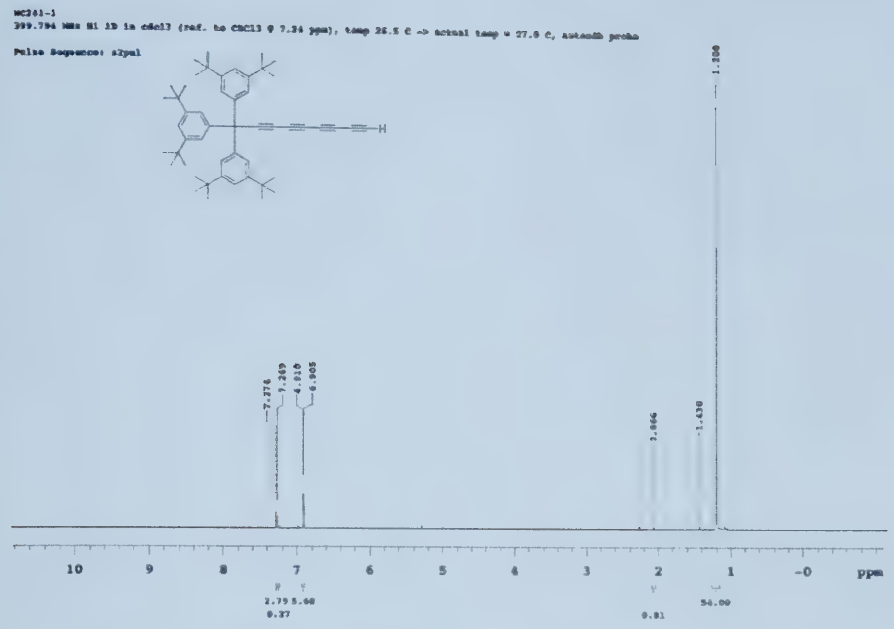


**Figure C-146.** $^{1}$H NMR spectrum of **5.34**.

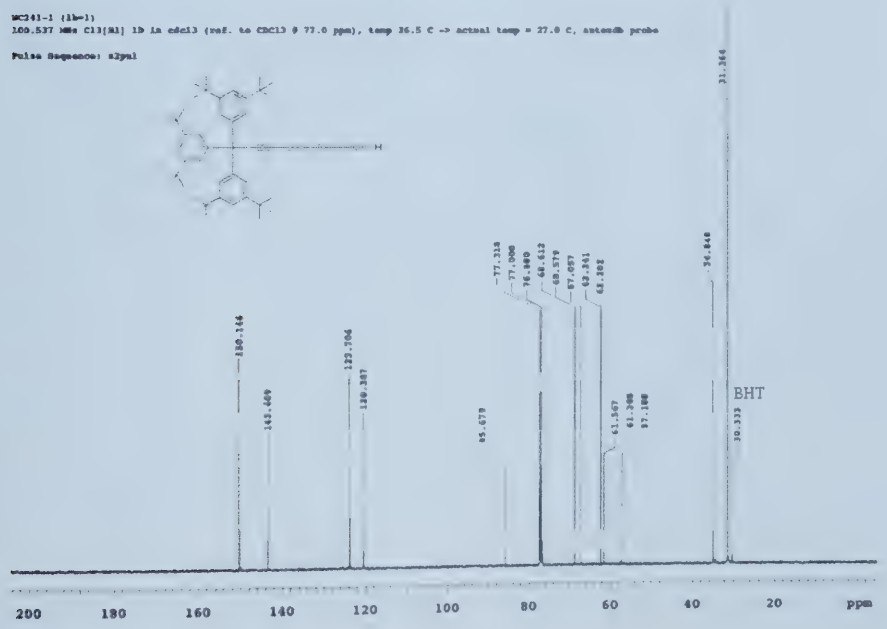


**Figure C-147.** $^{13}$C NMR spectrum of **5.34**.

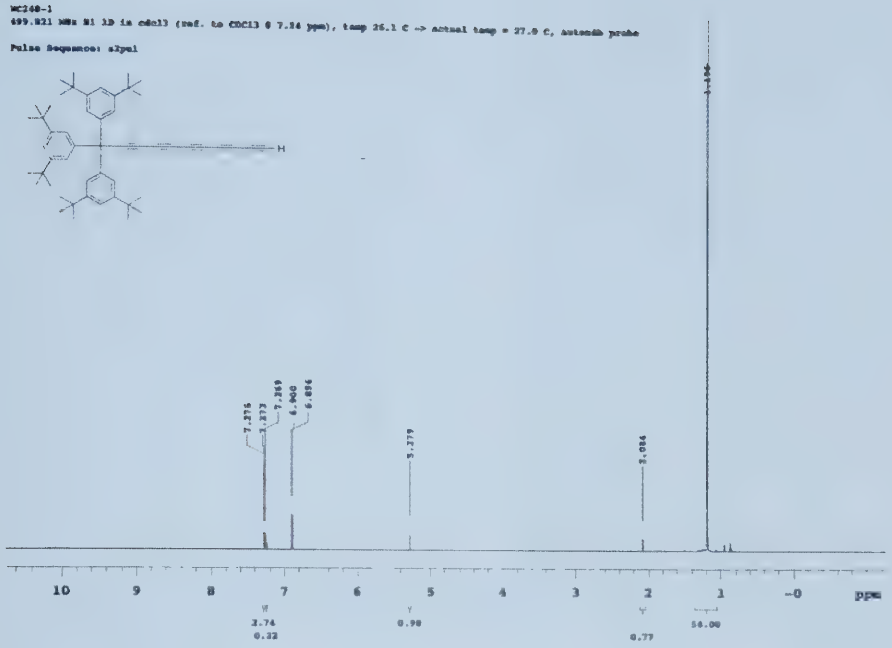


**Figure C-148.** $^{1}$H NMR spectrum of 5.35.

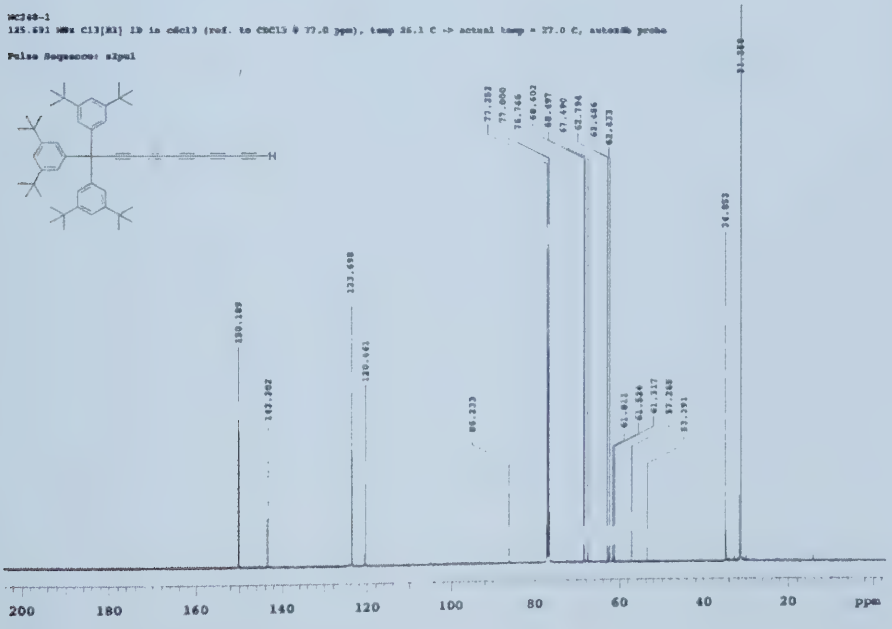


**Figure C-149.** $^{13}$C NMR spectrum of 5.35.

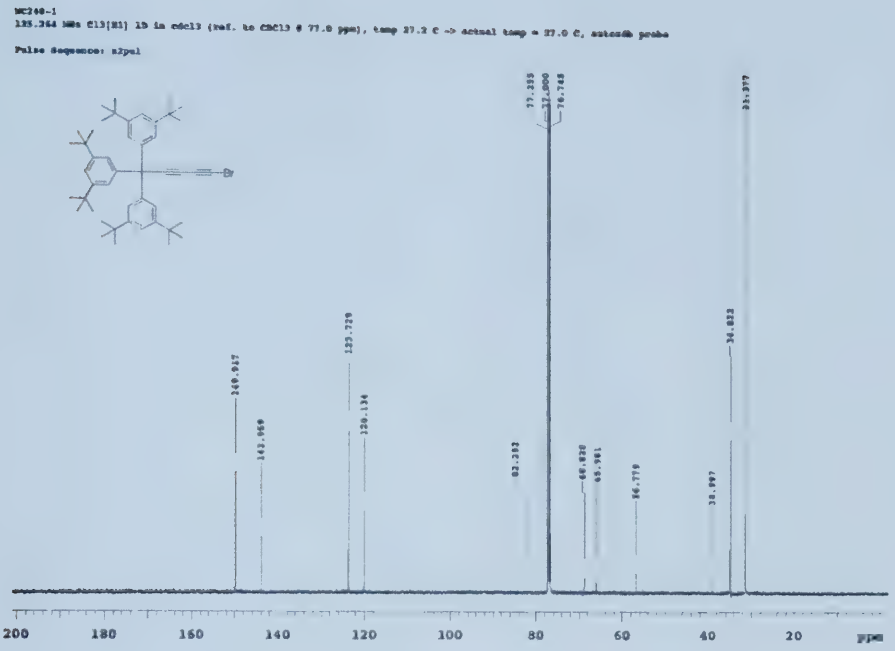


**Figure C-150.** $^{13}$C NMR spectrum of **5.36**.

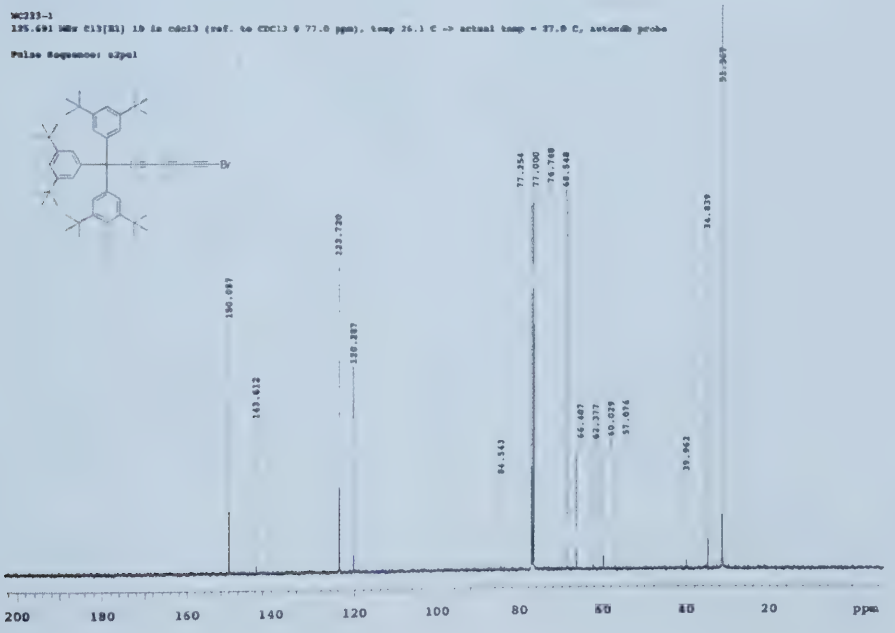


**Figure C-151.** $^{13}$C NMR spectrum of **5.37**.

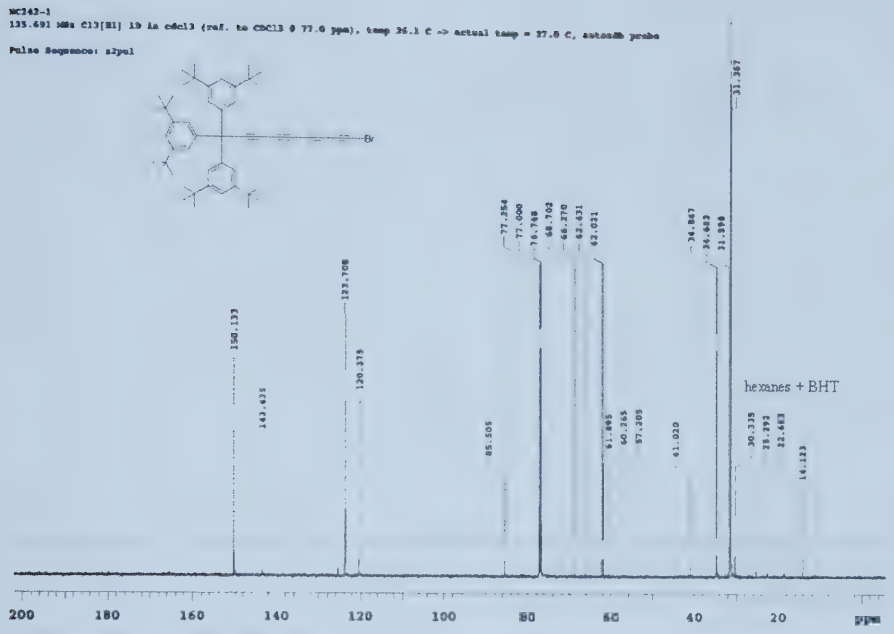


**Figure C-152.** $^{13}$C NMR spectrum of **5.38**.

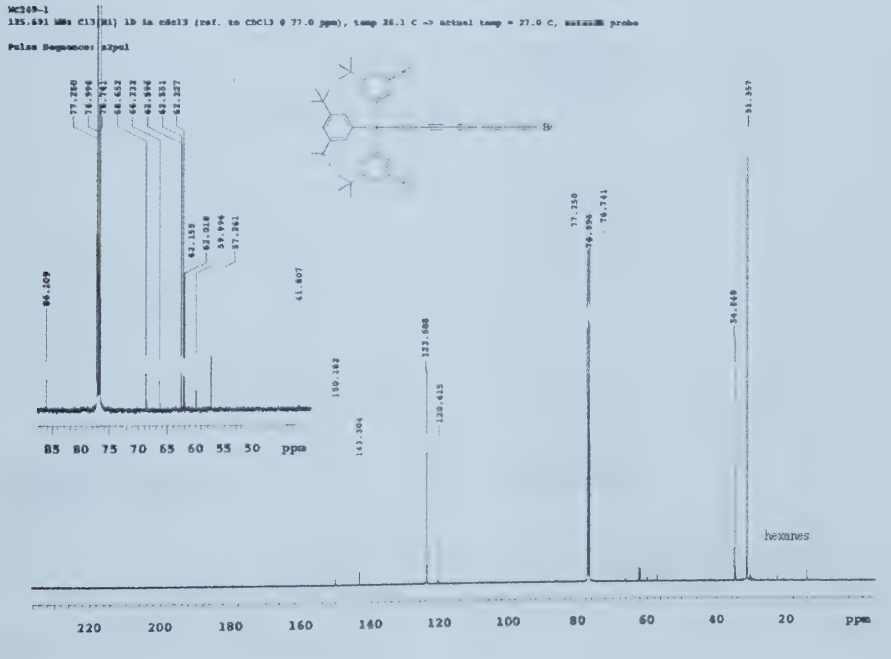


**Figure C-153.** $^{13}$C NMR spectrum of **5.39**.

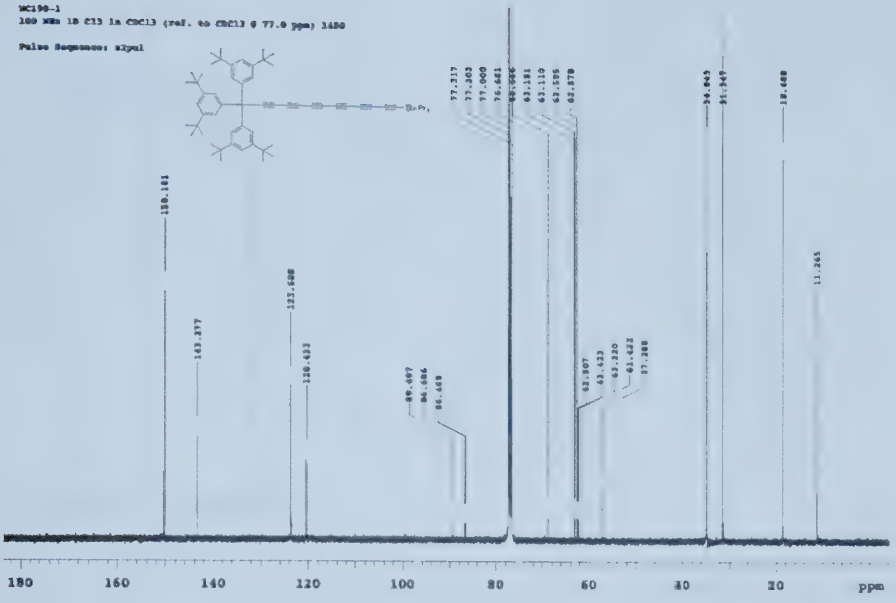


**Figure C-154.** $^{13}C$ NMR spectrum of **5.40**.

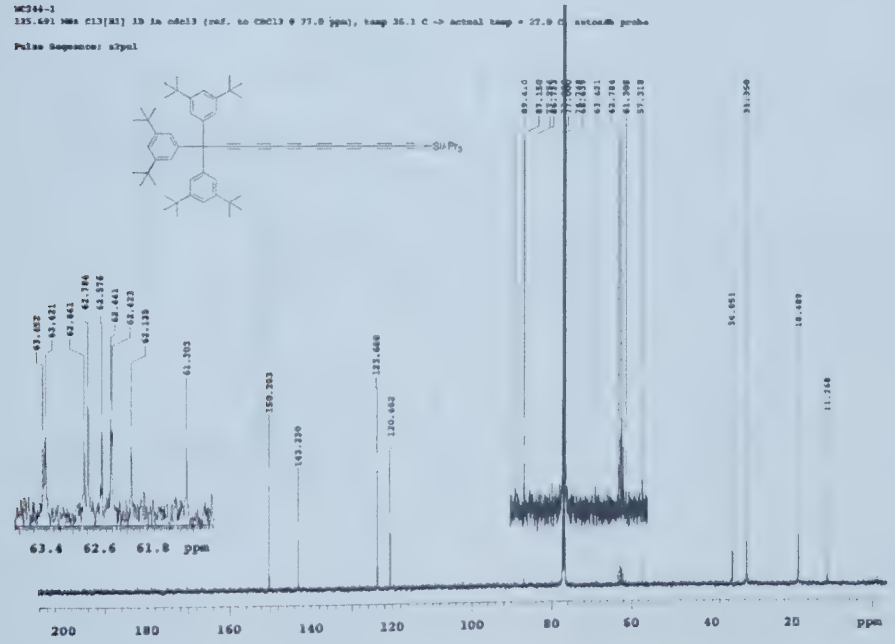


**Figure C-155.** $^{13}C$ NMR spectrum of **5.41**.

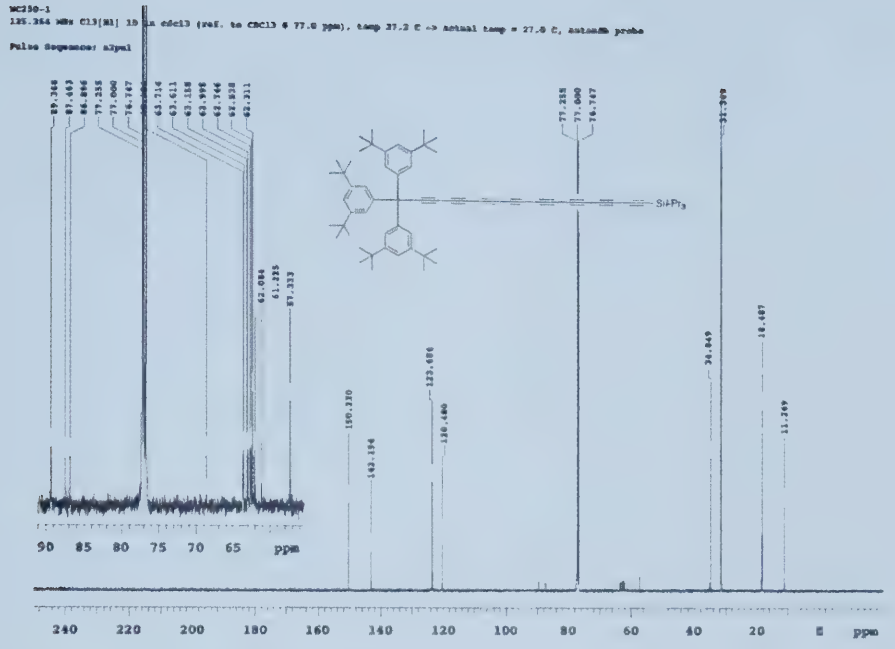

**Figure C-156.** $^{13}C$ NMR spectrum of **5.42**.

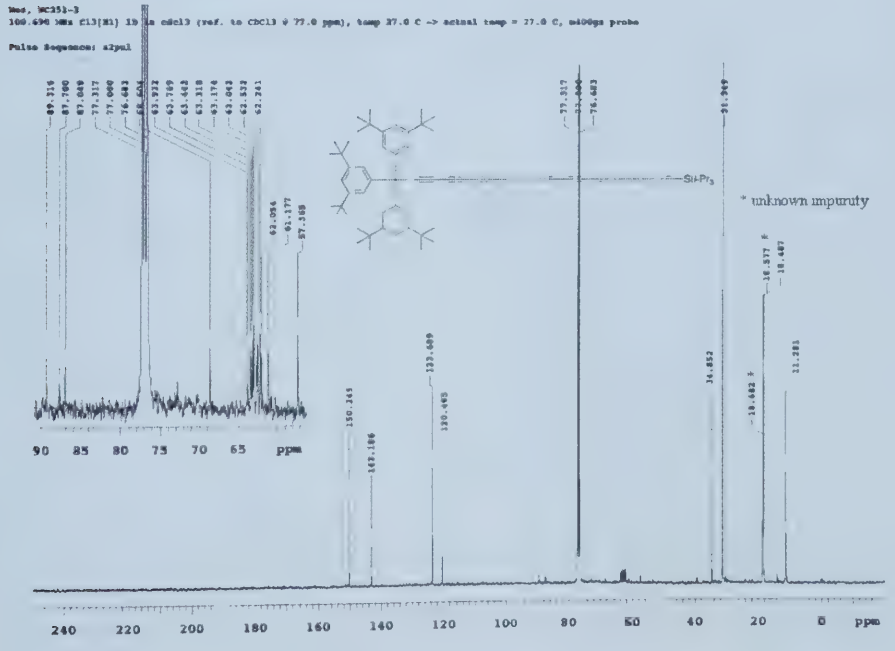


**Figure C-157.** $^{13}C$ NMR spectrum of **5.43**.

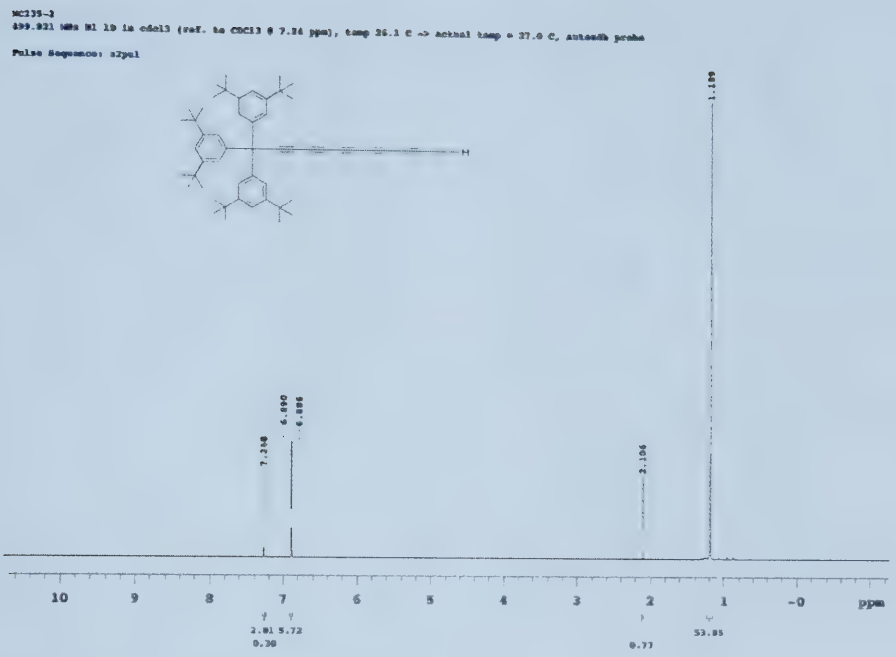


**Figure C-158.** $^{1}$H NMR spectrum of **5.44**.

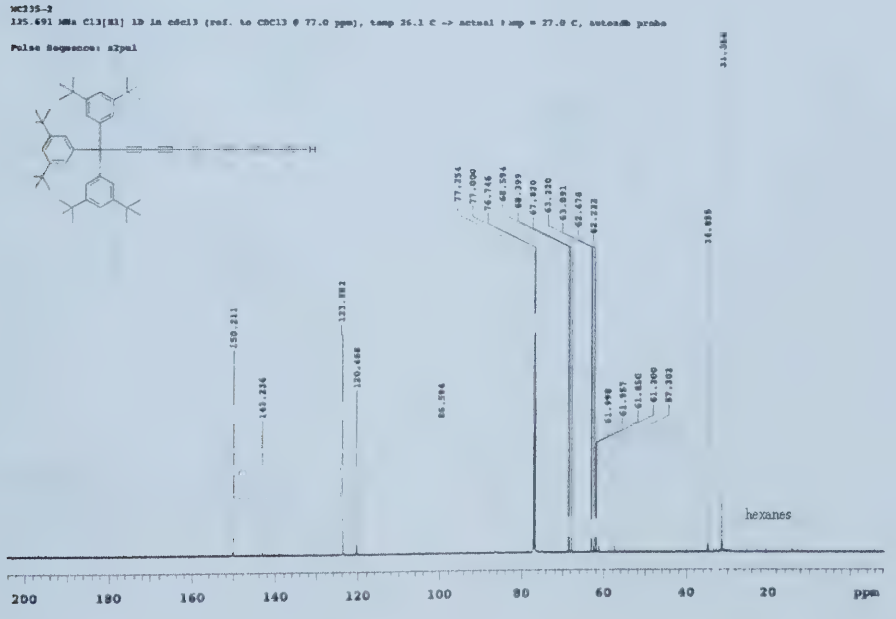


**Figure C-159.** $^{13}$C NMR spectrum of **5.44**.

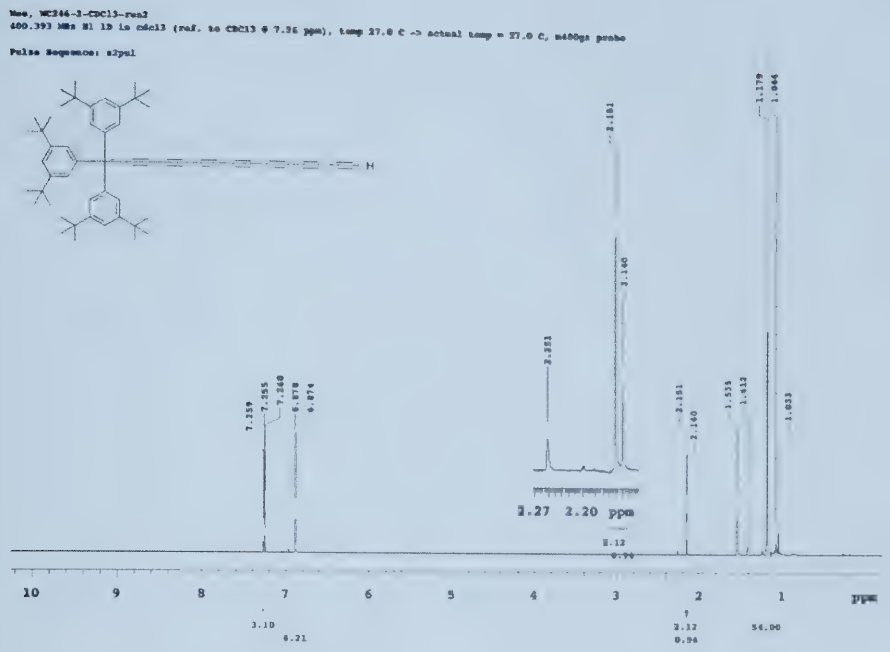


**Figure C-160.** $^{1}H$ NMR spectrum of **5.45**.

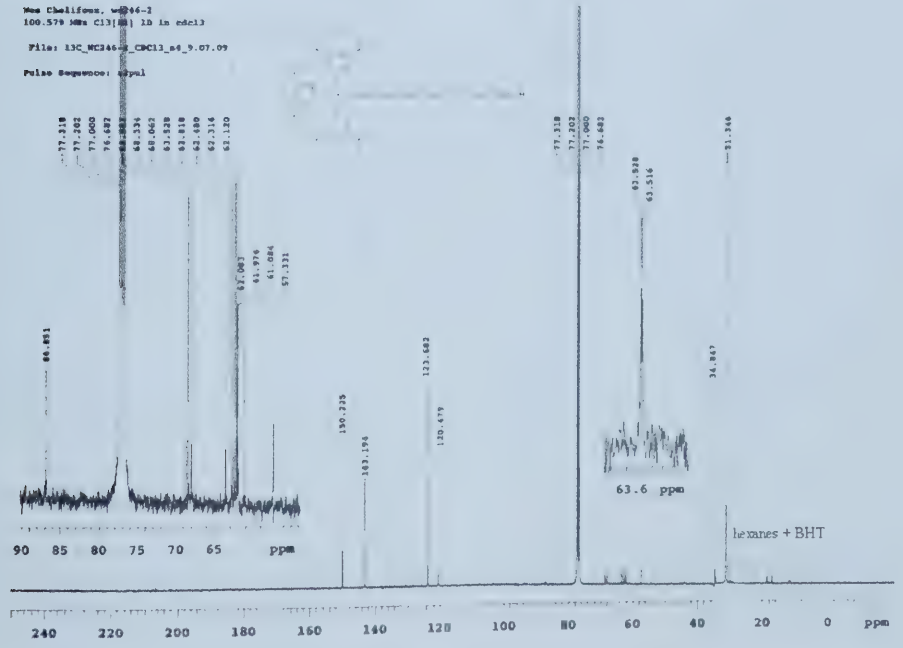


**Figure C-161.** $^{13}C$ NMR spectrum of **5.45**.

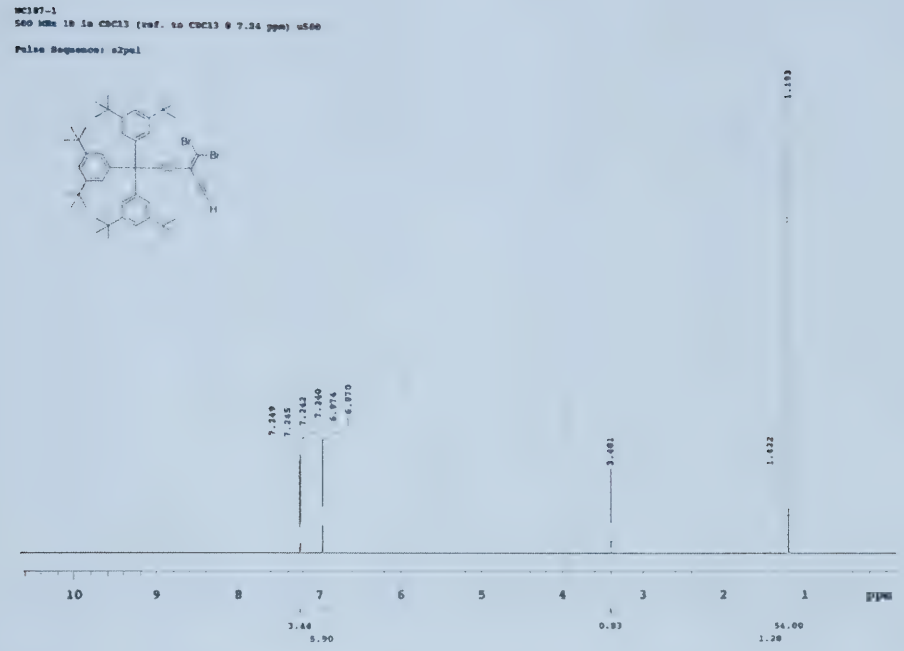


**Figure C-162.** $^{1}$H NMR spectrum of **5.48**.

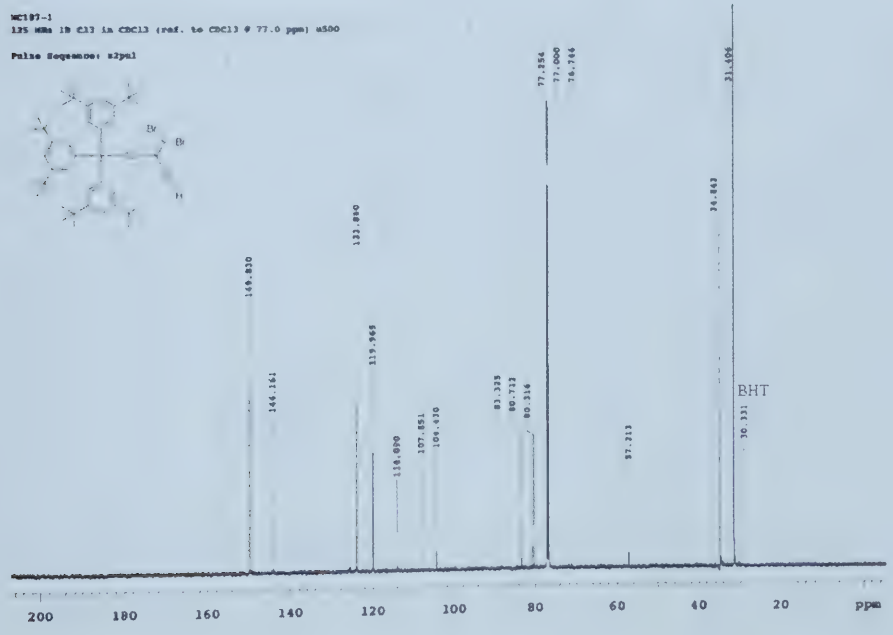


**Figure C-163.** $^{13}$C NMR spectrum of **5.48**.

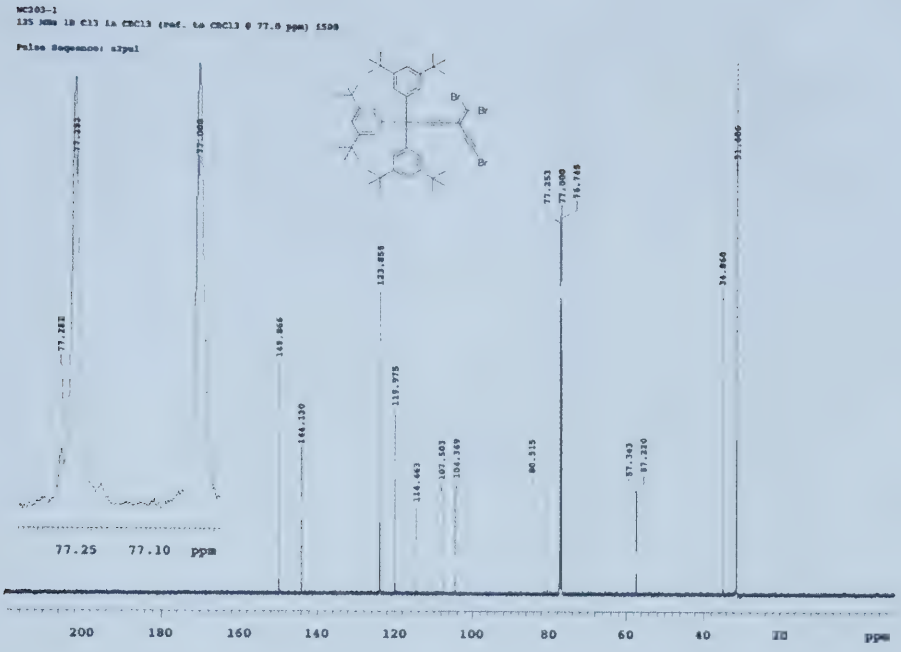

**Figure C-164.** $^{13}C$ NMR spectrum of **5.49**.

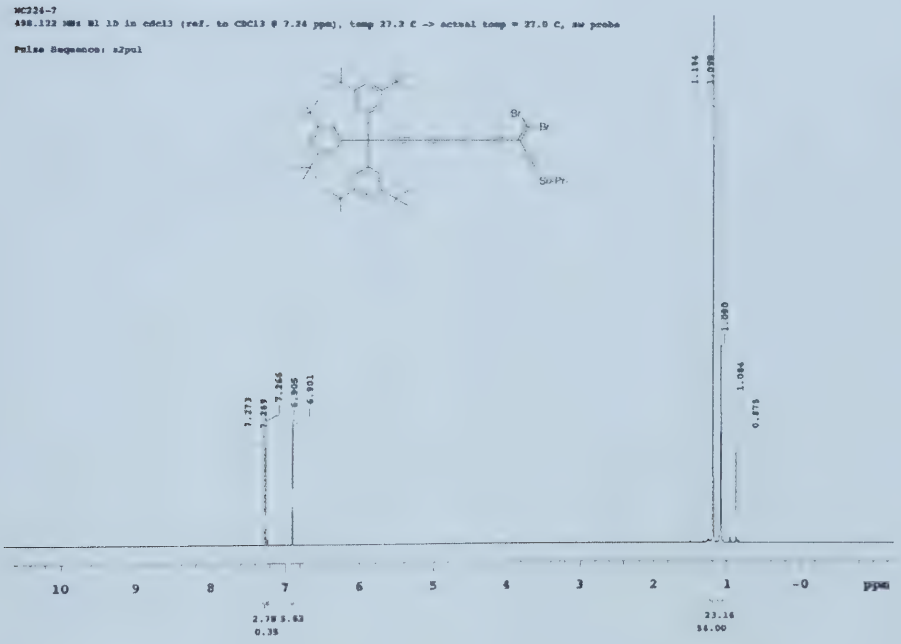

**Figure C-165.** $^{1}H$ NMR spectrum of **5.50**.

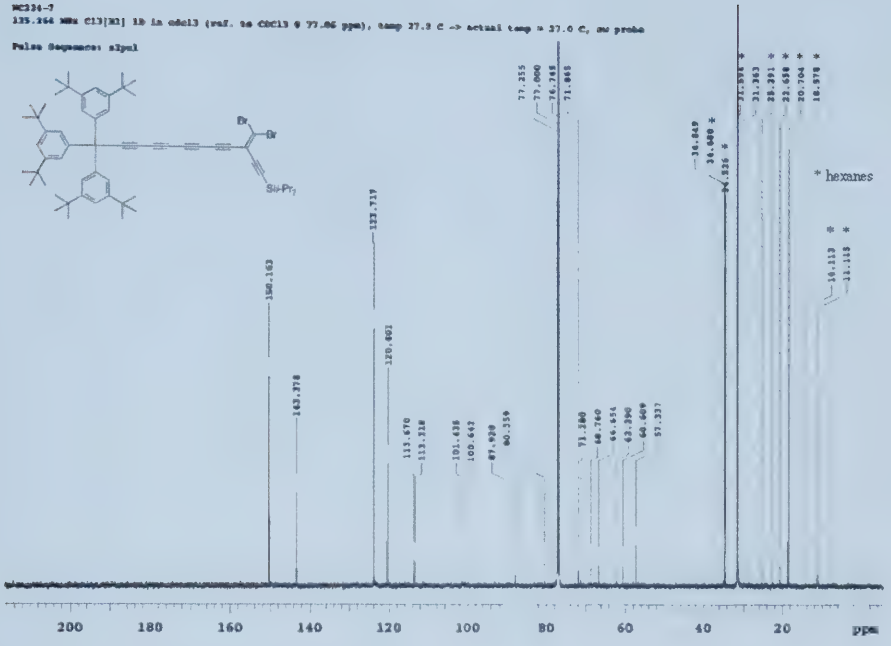


**Figure C-166.** $^{13}C$ NMR spectrum of **5.50**.

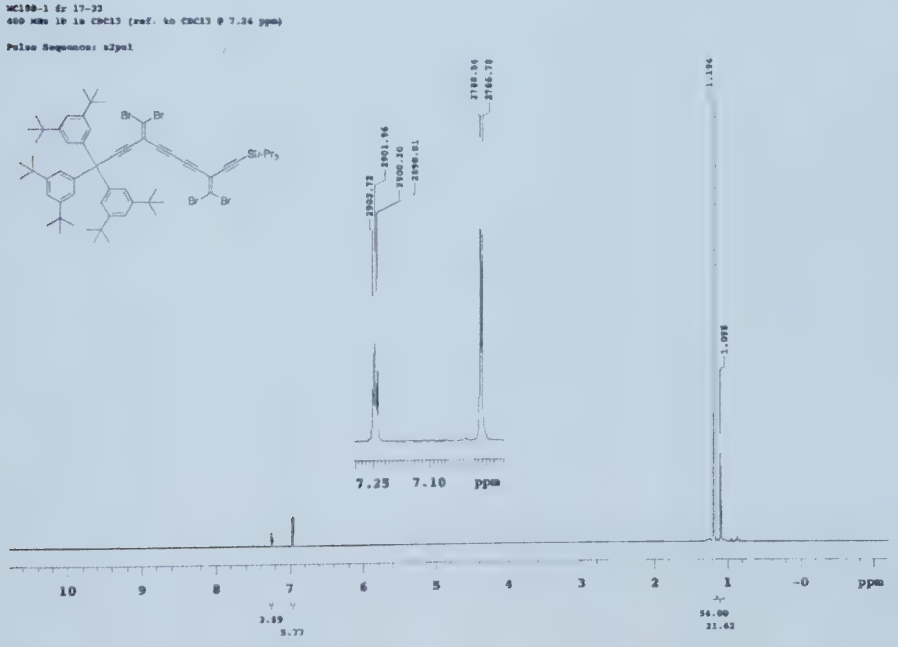


**Figure C-167.** $^{1}H$ NMR spectrum of **5.51**.

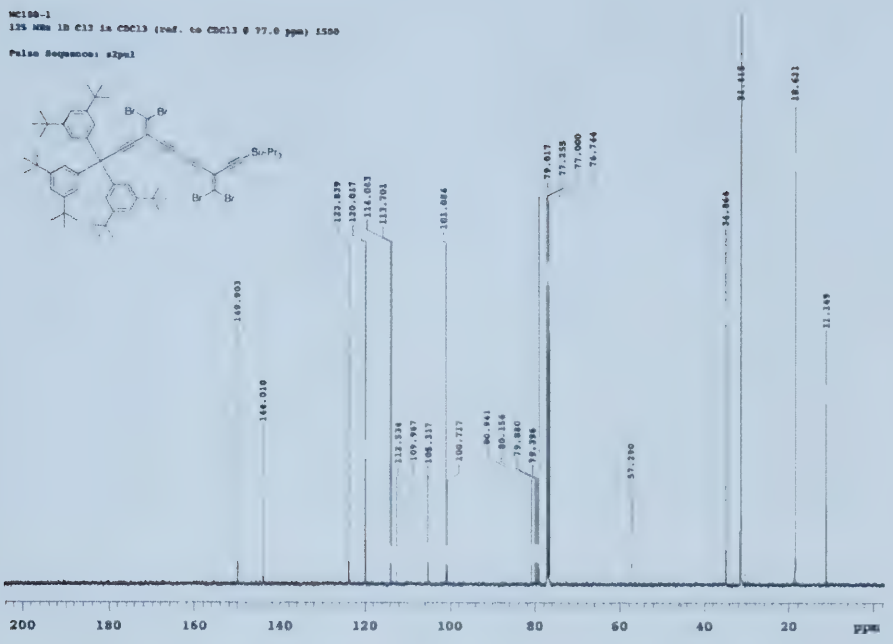


**Figure C-168.** $^{13}C$ NMR spectrum of **5.51**.

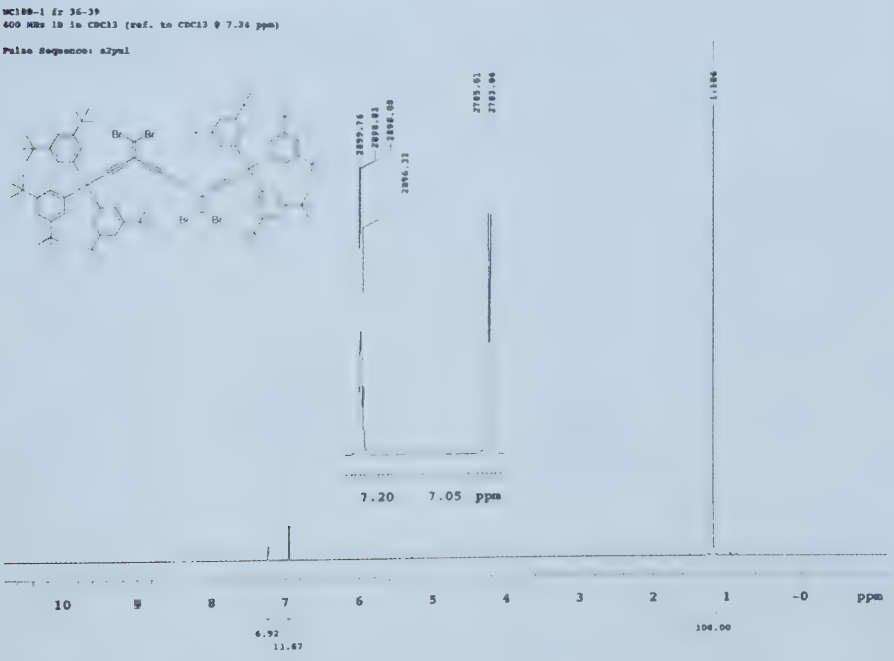


**Figure C-169.** $^{1}H$ NMR spectrum of **5.52**.

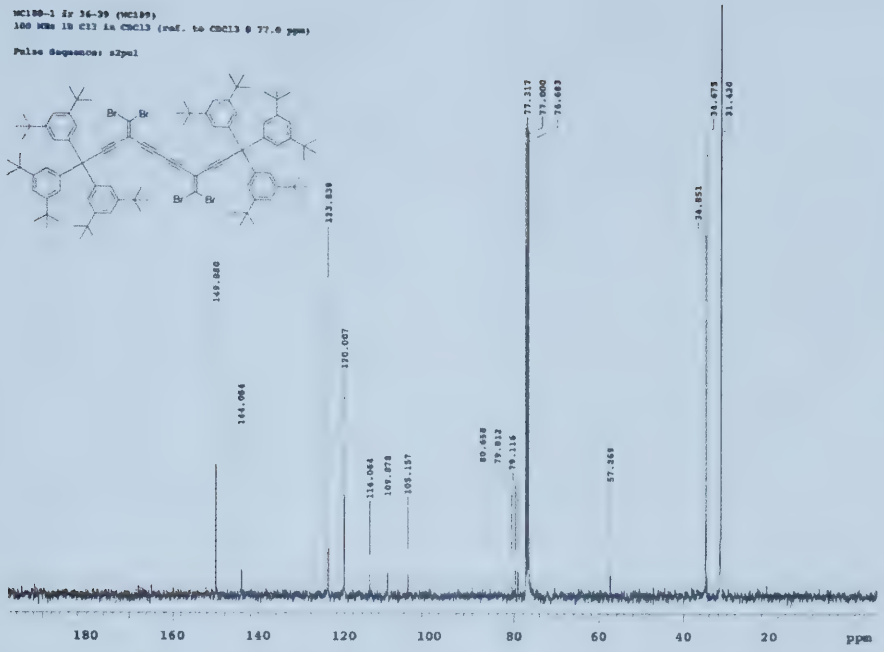


**Figure C-170.** $^{13}$C NMR spectrum of **5.52**.

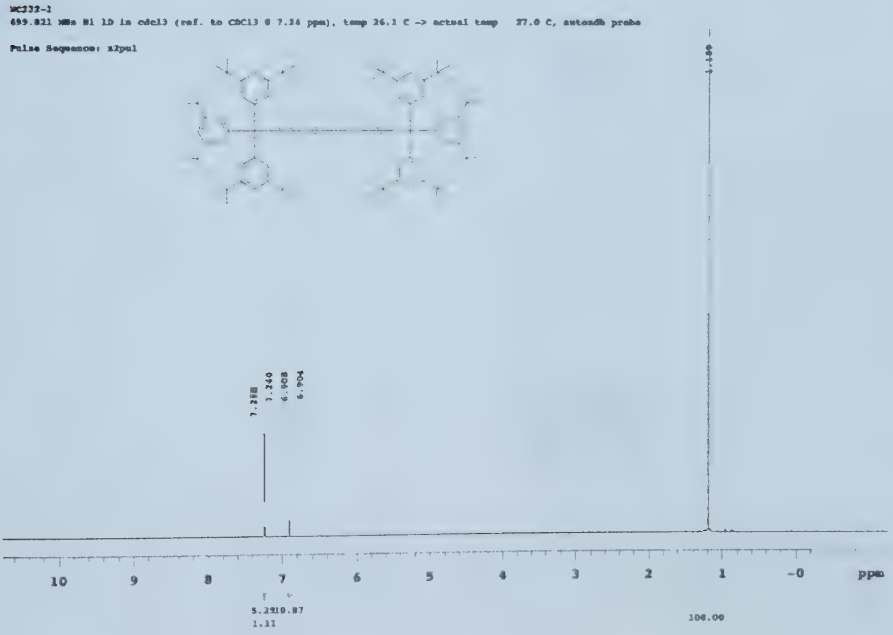


**Figure C-171.** $^{1}$H NMR spectrum of **5.1a**.

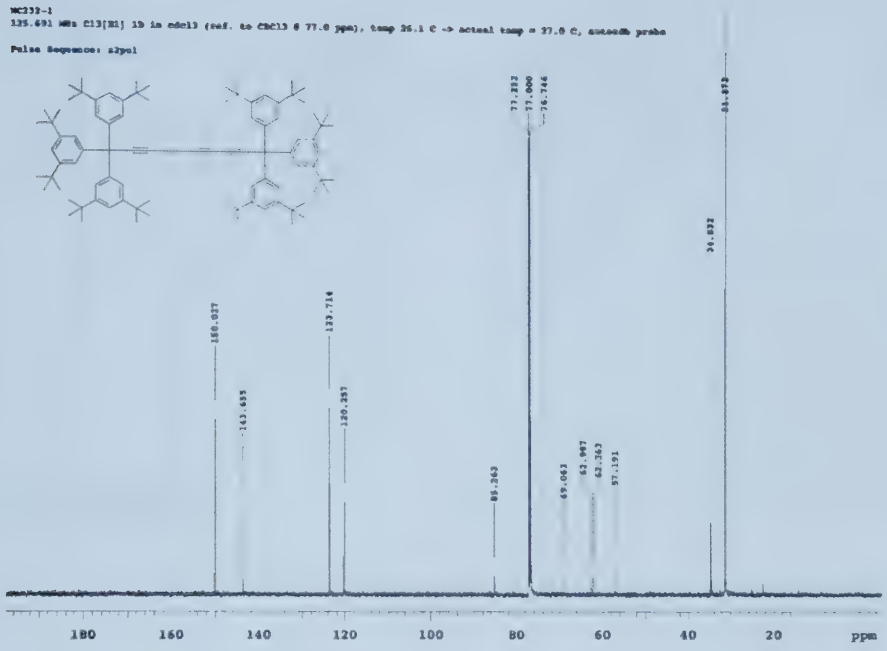


**Figure C-172.** $^{13}C$ NMR spectrum of **5.1a**.

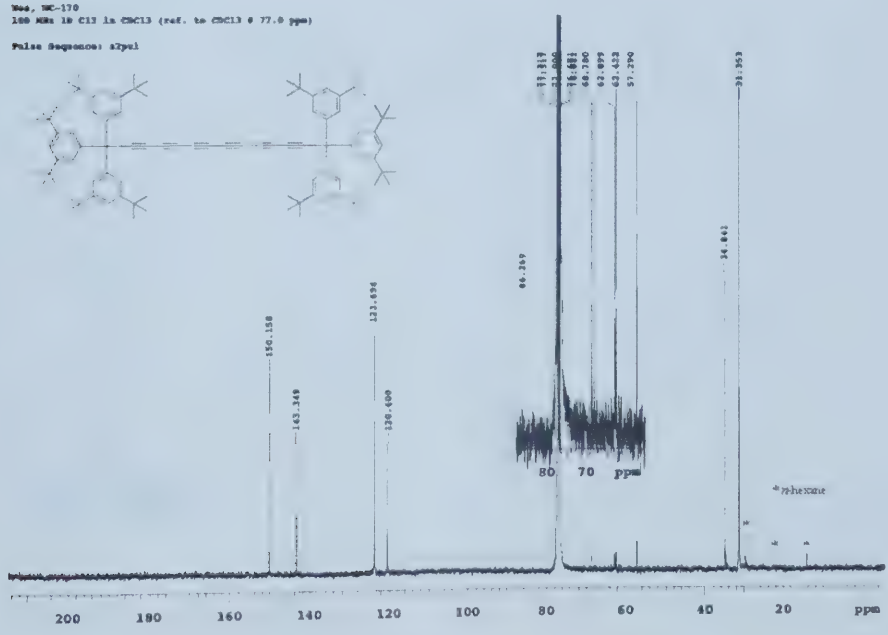


**Figure C-173.** $^{13}C$ NMR spectrum of **5.1b**.

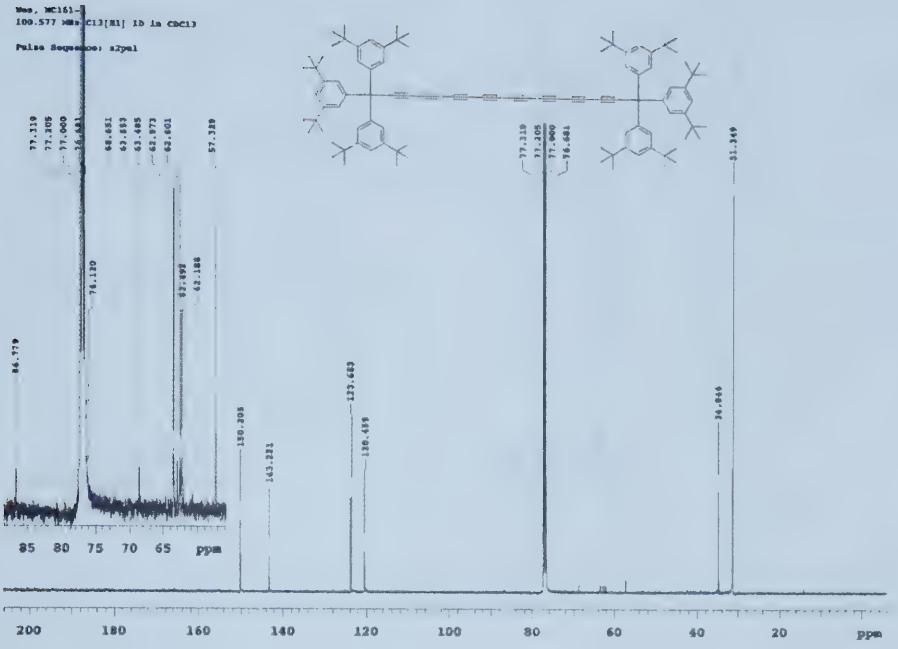

**Figure C-174.** $^{13}$C NMR spectrum of **5.1c**.

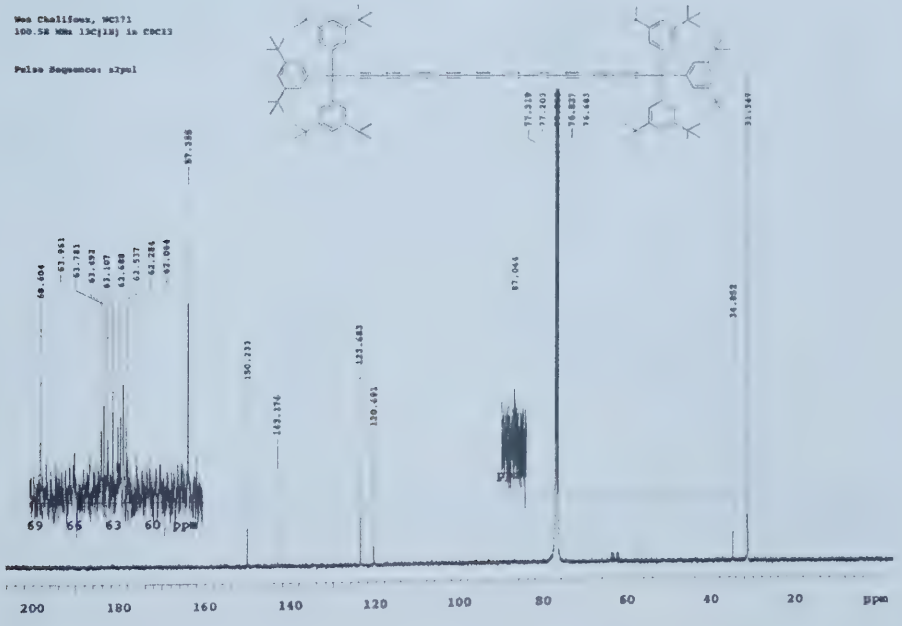

**Figure C-175.** $^{13}$C NMR spectrum of **5.1d**.

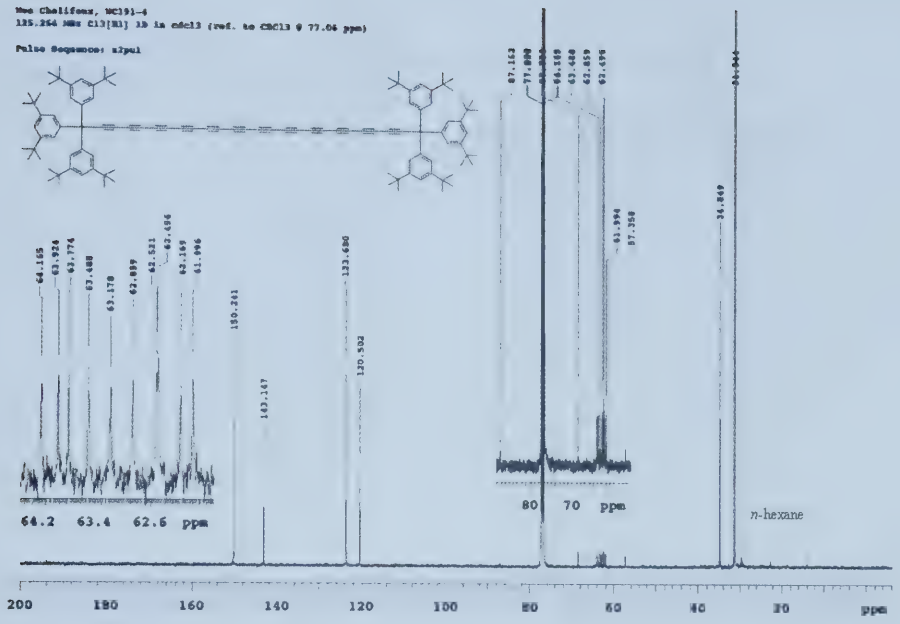


**Figure C-176.** $^{13}C$ NMR spectrum of **5.1e**.

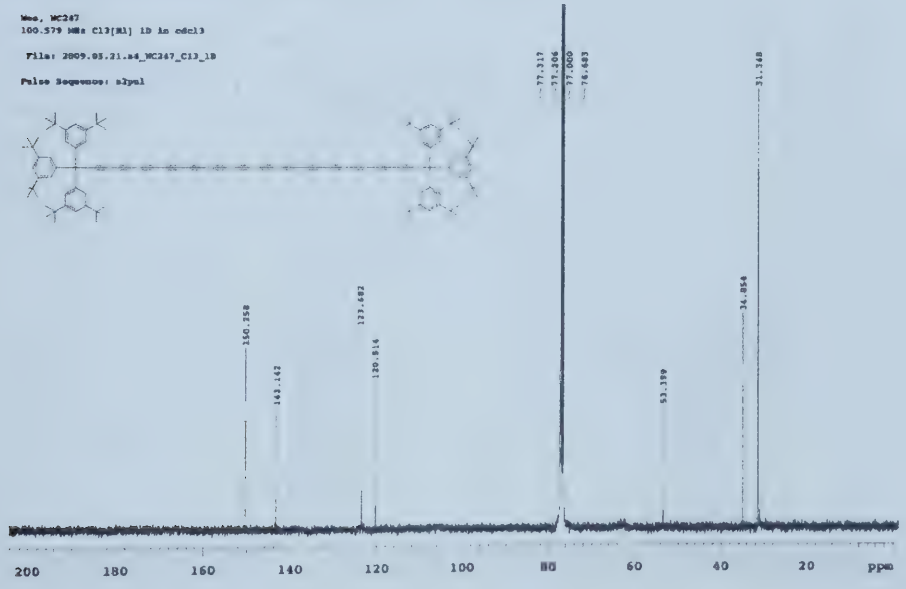


**Figure C-177.** $^{13}C$ NMR spectrum of **5.1f** (fully decoupled).

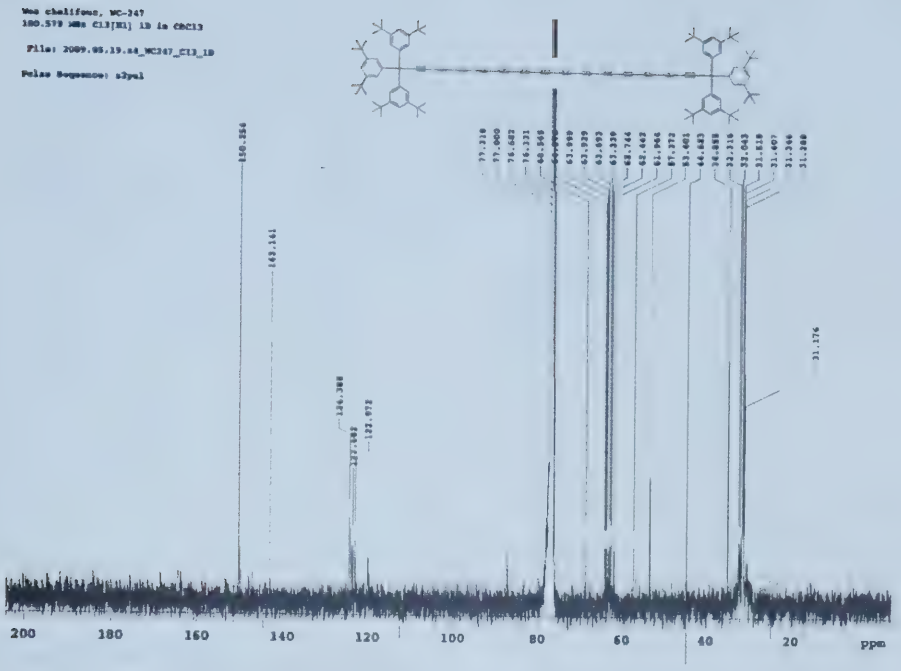


**Figure C-178.** $^{13}C$ NMR spectrum of **5.1f** ($^{1}H$–$^{13}C$ coupling observed).

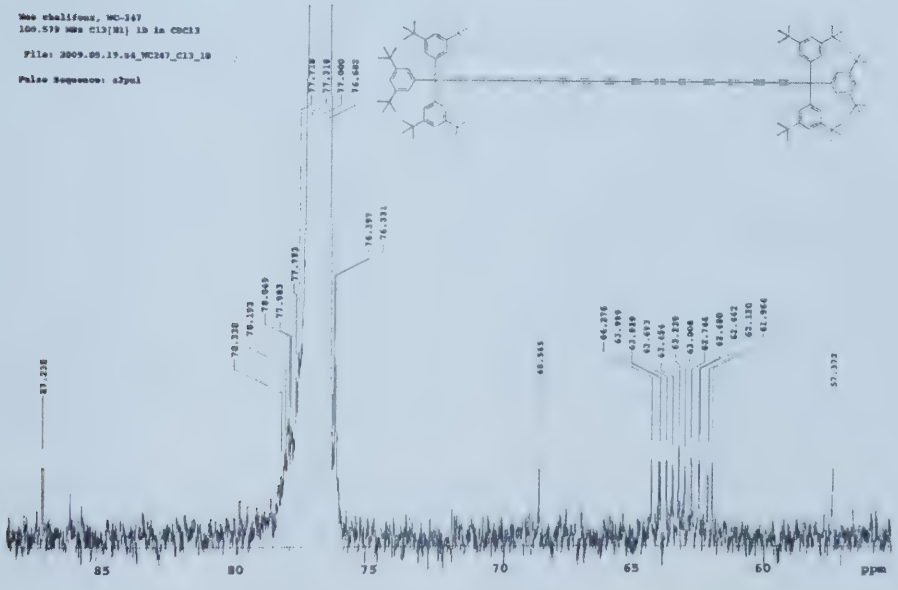


**Figure C-179.** $^{13}C$ NMR expanded spectrum of **5.f**.

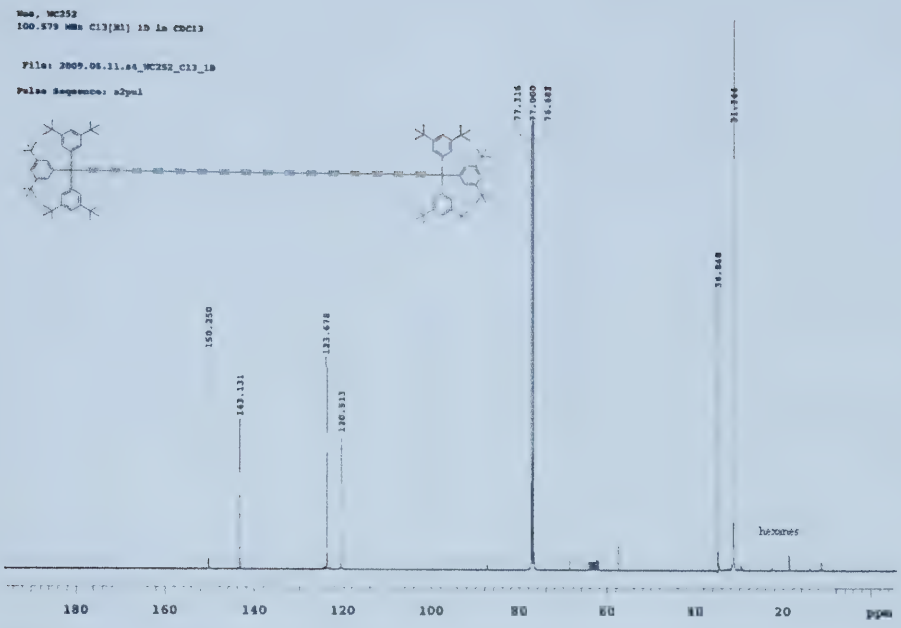


**Figure C-180.** $^{13}C$ NMR spectrum of **5.1g**.

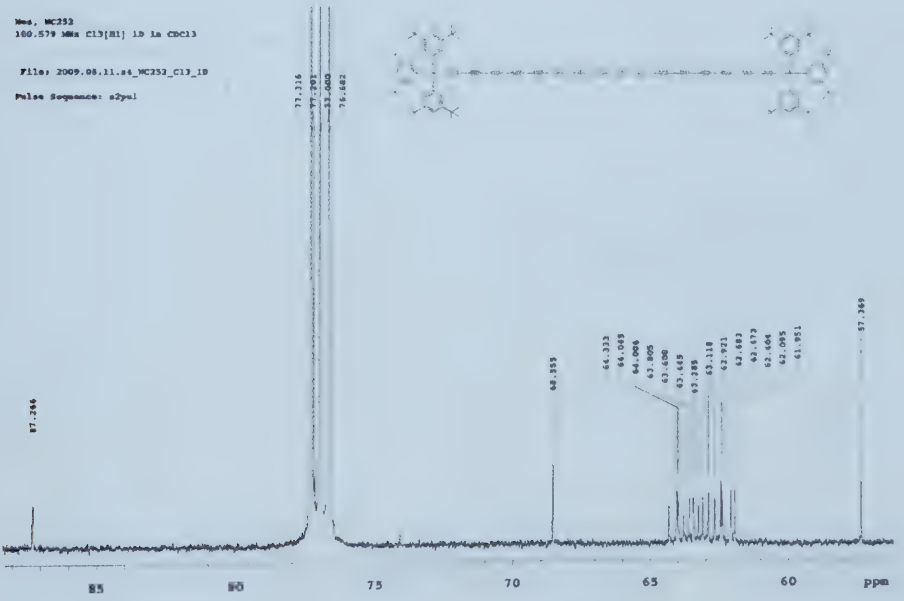


**Figure C-181.** $^{13}C$ NMR expanded spectrum of **5.1g**.

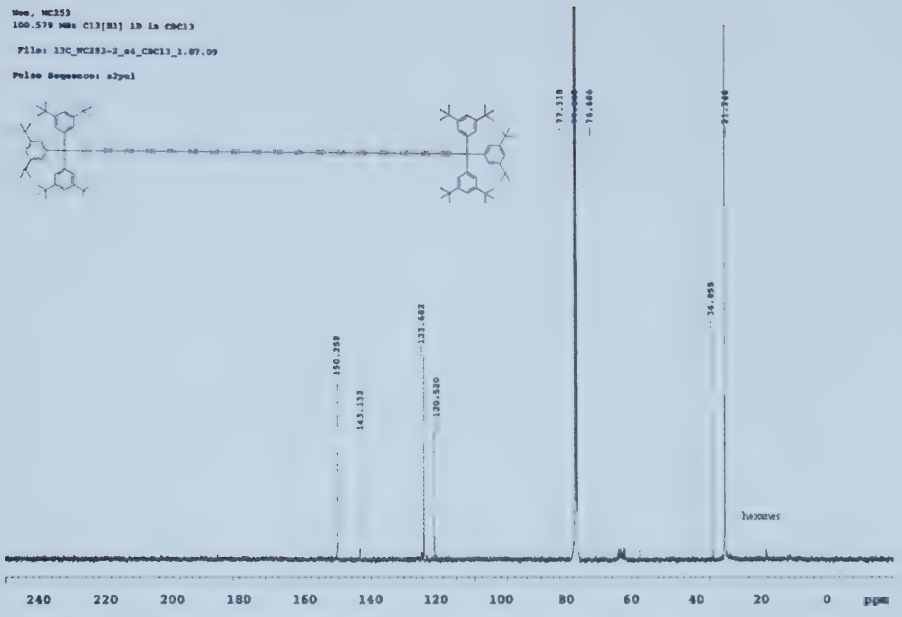


**Figure C-182.** $^{13}$C NMR spectrum of **5.1h**.

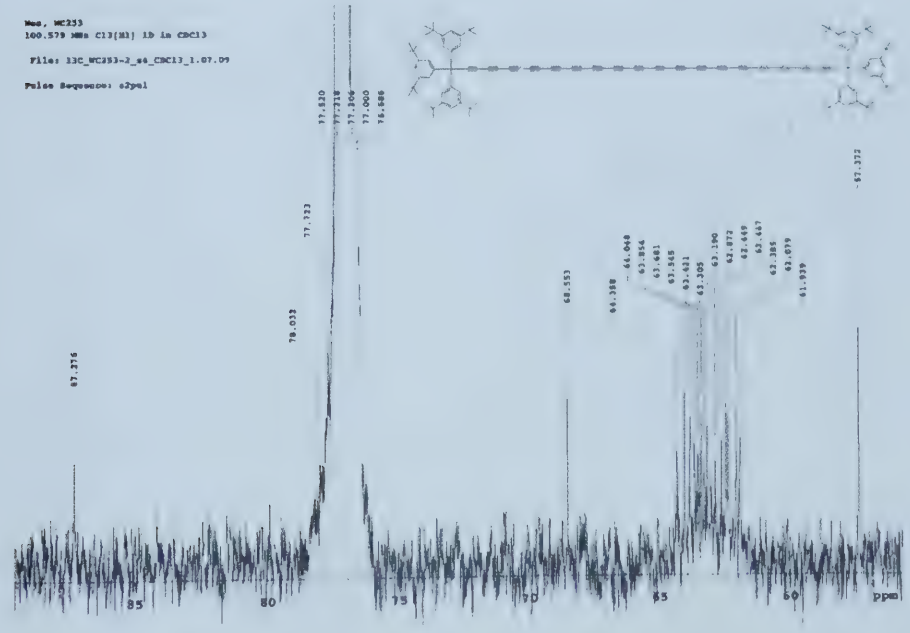


**Figure C-183.** $^{13}$C NMR expanded spectrum of **5.1h**.

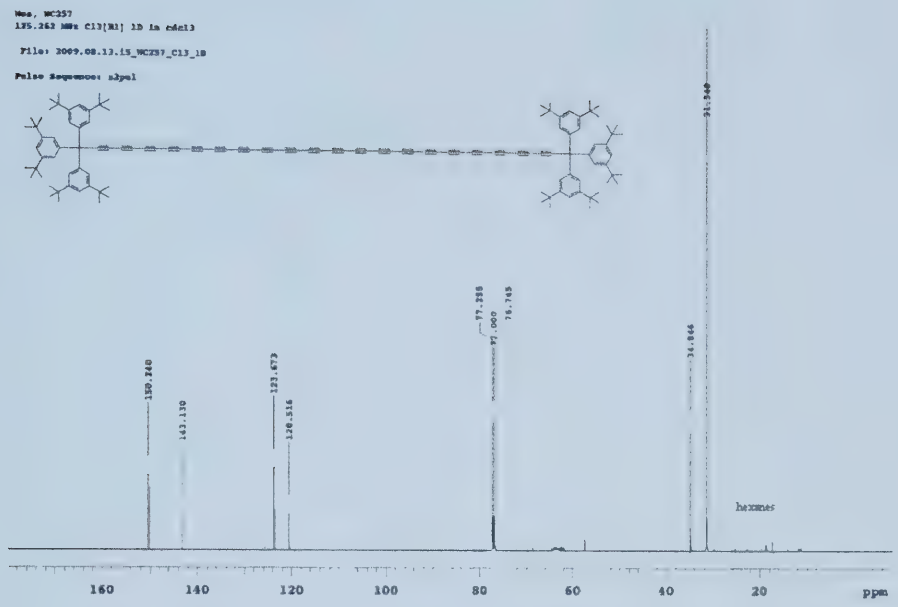


**Figure C-184.** $^{13}C$ NMR spectrum of **5.1j**.

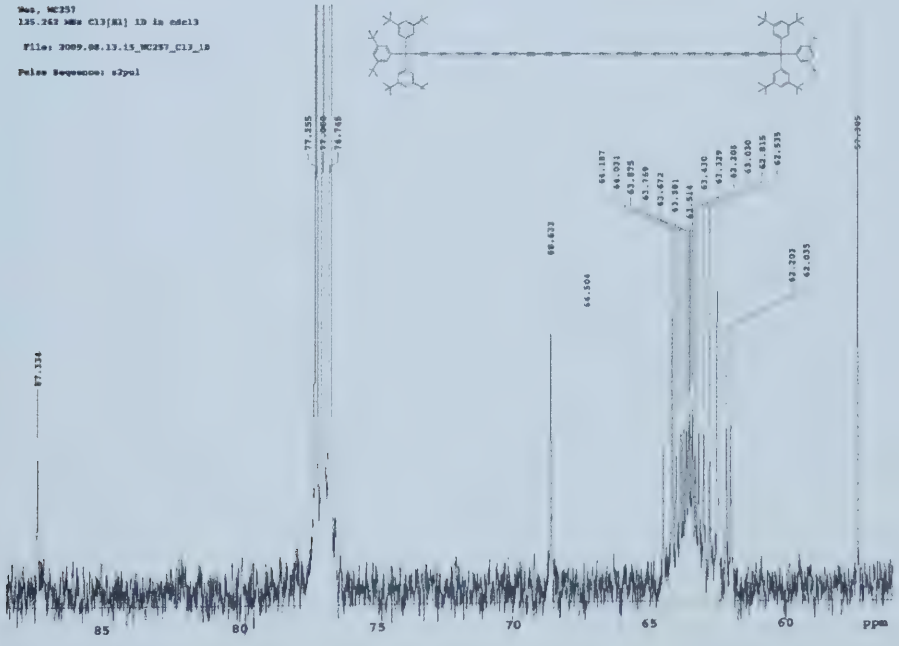


**Figure C-185.** $^{13}C$ NMR expanded spectrum of **5.1j**.

C12458